# MAPPING THE STRUCTURAL PROPERTIES OF THE LUMBOSACRAL VERTEBRAL ENDPLATES

by

Jenifer Pamela Grant

B.Eng.Sc., The University of Western Ontario, 1997

THESIS SUBMITTED IN PARTIAL FULFILLMENT OF

THE REQUIREMENTS FOR THE DEGREE OF

MASTER OF APPLIED SCIENCE

in

THE FACULTY OF GRADUATE STUDIES
(Department of Mechanical Engineering)

We accept this thesis as conforming to the required standard:

THE UNIVERSITY OF BRITISH COLUMBIA

November 2000

In presenting this thesis in partial fulfillment of the requirements for an advanced degree at the University of British Columbia, I agree that the Library shall make it freely available for reference and study. I further agree that permission for extensive copying of this thesis for scholarly purposes may be granted by the head of my department or by his or her representatives. It is understood that copying or publication of this thesis for financial gain shall not be allowed without my written permission.

Department of Mechanical Engineering

The University of British Columbia
Vancouver, Canada

Date Oct. 11, 2000

## Abstract

**Problem**:

Interbody fusion is a surgical technique in which a bone or synthetic implant is inserted between two vertebrae to support the spine following removal of diseased or damaged tissue. One failure mode of these implants is subsidence, in which the implant sinks into the adjacent vertebrae. This can lead to pain, deformity and nerve damage and can only be corrected through secondary surgery. Surgeons would like to know if there is some way to reduce the risk of subsidence, particularly in patients with low bone density, e.g. through implant design changes. This study looks for the bone regions which provide the most resistance to subsidence. The results could be used to improve upon current surgical techniques and may assist in the development of better spinal implants.

**Method**:

To identify the strongest and stiffest regions in the upper and lower surfaces of the vertebrae, indentation tests were done in fresh-frozen human vertebrae from the lower spine (L3-S1) using a 3 mm-diameter hemispherical indenter at 0.2 mm/s to a depth of 3 mm. The results were used to develop structural property maps. The effects of spinal level, bone density, disc degeneration and removal of the endplate (a thin shelf of bone covering the main load-bearing component of the vertebra) were considered.

**Results**:

The upper and lower L3-L5 surfaces were stronger around the periphery than centrally and stronger at the rear margin than in front. The rear half of the lower surface was stronger than the corresponding region of the upper surface. The S1 surface was strongest at the rear margin, with a steady decrease in strength from the back to the front and no lateral variation.

Bone density and disc degeneration had no effect on stiffness, however strength was proportional to bone density in L3-L5, and disc degeneration lowered the strength of the lower L3-L5 surfaces. Endplate removal reduced the strength and stiffness by about 2.5 times. The locations of the strongest bone were not affected by any of these secondary variables.

**Implications**:

Implant designs and/or placement could be altered to take advantage of the stronger bone regions in the vertebral surfaces. Since degeneration did not change the locations of the strongest bone regions, implants designed using the general structural property maps should perform well in patients with a wide range of bone and disc conditions. Sparing the endplate may reduce the risk of implant subsidence.

## Table of Contents

## List of Tables

## List of Figures

## Acknowledgements

I would like to begin by thanking my supervisor, Dr. Tom Oxland, for providing me with the opportunity to join his lab at its inception and to experience first-hand the excitement of its development. His enthusiastic support of this project has given me opportunities to attend international research meetings and speak before recognised experts in this field, and provided me with invaluable experience, from which I will benefit throughout my career.

Several other people made valuable contributions to this project: I gratefully acknowledge the assistance of Mr. Alston Bonamis and Dr. Jesse Chen in preparing and photographing the many specimens used in this study. I'd also like to thank Mr. Darrell Goertzen for his invaluable technical advice, and Dr. Kevin Wing for his tutelage on spine dissection.

I thank Dr. Marcel Dvorak and Dr. Charles Fisher for taking the time to offer their clinical perspective on the issue of subsidence and implant use in general, and Dr. Doug Romilly for his pointers on where to look for mechanical testing information.

Thanks also go to the other students and engineers in the DOER lab, in particular Andrew Speirs, Anthony Choo, Hanspeter Frei, and Chris Lane who have contributed time and suggestions to orchestrating the transfer of my thesis across the country, as well as providing advice throughout the course of this project.

I'd also like to thank Dr. Antony Hodgson, who first got me interested in the UBC engineering program and introduced me to Dr. Oxland.

I gratefully acknowledge the financial support of the George W. Bagby Research Fund and the National Science and Engineering Research Council, which made this project possible.

Finally, I'd like to thank my husband, Eric VanDerLoo, for his unwavering support and his hours of assistance with computer glitches and program interaction problems.

# Chapter 1

## An Overview of Current Issues in Interbody Fusion and the Role of Structural Property Maps

The purpose of this research is to answer some fundamental questions in the area of interbody fusion, a surgical procedure used to stabilise the spine following the removal of diseased or damaged tissue. A spine surgeon was consulted on the major design aspects of the project to ensure that the questions being posed were clinically relevant. The results of this study will be used to improve upon current surgical techniques, may assist in the development of better spinal implants, and will provide fundamental information on spine biomechanics.

### 1.1 Overview of Chapters

In the first chapter, the importance of this study is addressed in relation to the clinical and engineering fields. Basic spinal anatomy is reviewed for readers with limited background in this area. This is followed by a review of relevant literature in the anatomy, biomechanics, and materials engineering literature as it pertains to this study.

The experimental methods are described in detail in the second chapter. Programs and equipment details are provided in appendices for readers who require additional details. A brief introduction to the statistics used in the analysis and correct interpretation of the results is provided for readers with limited background in statistics.

The experiment results are presented in the third chapter. Graphs are used to demonstrate the relationships between the variables.

Chapter four contains a discussion of the results and ties them back to the questions posed in chapter one.

The final chapter presents conclusions and recommendations based on the discussion.

### 1.2 Clinical Questions

As the population ages, the prevalence of spinal surgery also rises. Cancer, disc degeneration, fracture (traumatic or osteoporotic, Figure 1.1 a) and other clinical conditions may require removal of tissue from the spine. To provide support for the spine while it heals, an interbody fusion (in which a bone or synthetic "spacer" is placed between two vertebrae to maintain the space once occupied by a vertebra and/or intervertebral disc) is often performed (Figure 1.1 b). This surgery is usually very successful, with clinical success rates of 68 to 90% reported in the literature (Hammerburg 1996). Unfortunately, more and more frequently the patients requiring such surgery are older individuals who have naturally diminished bone mass and are at greater risk of complications.

There are several possible failure modes for interbody fusion (An 1999):

1. The implant may subside into one or both of the adjacent vertebrae (Figure 1.1 c), leading to impingement (pinching) of the nerve roots, which emerge between the posterior elements of the vertebrae (Figure 1.2). This can cause spinal instability, deformity, pain or loss of sensory or motor function in the nerve groups associated with the affected nerve roots.
2. The implant may migrate anteriorly or posteriorly, resulting in loss of fixation and potentially damage to blood vessels, which run along the front of the vertebral bodies, or the spinal cord, which runs behind them.
3. The implant itself may fracture, which again may lead to loss of implant height, nerve root impingement, spinal instability, etc. Synthetic implant fracture is rare, generally occurring through fatigue loading when fusion of the bone has not been achieved. Fractures of bone implants are more common.

Any one of these failure modes may require correction through secondary surgery, with all of the inherent complications associated with a surgical procedure.

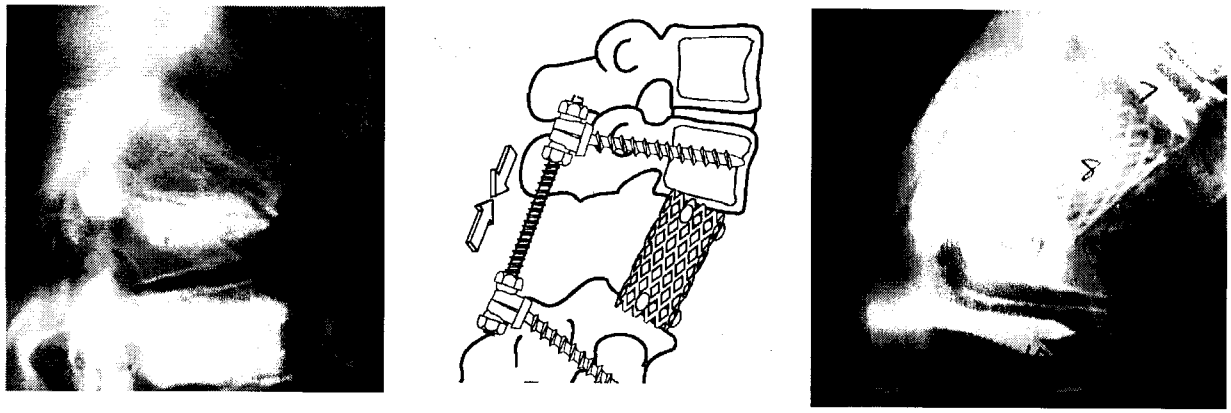

Figure 1.1: Subsidence of an interbody cage: a) lateral x-ray showing a wedge fracture of the T8 vertebral body; b) interbody fusion using a Harm's cage (and posterior rods and screws) to replace the damaged vertebra and restore spinal alignment (from Harms et al. (1996): p. 537); c) lateral x-ray showing subsidence of a Harm's cage into the vertebra below, leading to a loss of spinal alignment.

## 1.3 Engineering Solutions

Surgeons want to know what can be done to minimise the risk of subsidence, whether it be using only certain implant designs in older people, modifying the placement of implants, or using implants designed specifically for use in patients with poor bone stock (which have yet to be developed). For answers to their questions they turn to the engineering community.

The mechanical engineer can address the subsidence issue from several perspectives:

1. Mechanical testing can be done to study the resistance of different implant designs to subsidence. Factors such as age and bone density can be accounted for in such studies, to see if some implant designs perform better in patients with less than ideal bone stock. Many studies have been conducted in this area, but the implants have not been found to differ significantly in terms of their performance (Oxland and Lund 2000).

2. Existing implant designs can be modified to increase the contact area between the implant and the bone, thus distributing the load more evenly over the vertebra and increasing the load required to cause failure. The problem with this solution is that a large bone area must be left uncovered so that bone will grow through the implant, fusing the spinal level. If this fusion does not occur then the implant will fail under fatigue loading and revision surgery will be required.
3. New designs accounting for regional strength differences in the vertebra could be developed, which would reduce the incidence of subsidence in all patients. This seems like a reasonable solution, but there is a dearth of information on the subject of regional bone strength in vertebrae, both general and density-specific. This lack of information leads to the final role of engineers in addressing the problem of subsidence.
4. By doing regional property tests in a large series of vertebrae, it is possible to identify stronger regions in the bone and differences related to bone density, disc degeneration, etc. Tests of this nature have been done in various other bones and have been used to optimise implant designs. Generating such a database would provide valuable information to aid in modifying existing designs and developing new designs for use in all patients, but especially the growing elderly population. It may also help researchers to address other basic research questions such as the effects of disc degeneration on the underlying bone, reasons for common spinal fracture patterns, how osteoporosis affects vertebral strength, etc.

## 1.4 Basic Clinical Terminology and Spinal Anatomy

This section is included for readers who have limited knowledge of clinical terminology or spinal anatomy. The clinical and anatomical terminology required for a complete understanding of this study is contained in this section. Readers who are well versed in this area may prefer to move on to Section 1.5.

### 1.4.1 Basic Terminology

***Types of Tissue:***

*cartilage:* a flexible tissue which covers the articulating surfaces of joints, including those in the spine. It acts as a "shock absorber" and smooth articulating surface.

*cortical bone:* the hard, dense bone that makes up the outer surfaces of bones.

*trabecular, cancellous or spongy bone:* matrix-like bone made up of thin rods and plates of bone called trabeculae. Trabecular bone fills the interior of bones (Figure 1.7), providing strength while minimising the bone weight and allowing the access of blood vessels. The spaces between the trabeculae are filled with blood, bone marrow and blood vessels.

*subchondral bone:* the trabecular bone that underlies a cartilaginous surface. Subchondral bone has small holes in it through which blood vessels grow to supply the cartilage.

***Parts of the Vertebra (Figure 1.2):***

*endplate (bony endplate):* the thin layer of subchondral bone which covers the superior and inferior surfaces of the vertebral body. The bony endplate is covered by a layer of cartilage which is called the cartilaginous endplate. Alternative spellings include *end-plate* and *end plate*.

*intervertebral foramen:* the gap between the posterior elements of two vertebrae through which the nerve roots of the spinal cord exit the spine.

*pedicles:* the two spicules of bone which connect the posterior elements to the vertebral body.

*posterior elements:* projecting spines of bone which provide interfaces between adjacent vertebrae, attachment sites for muscles and protect the spinal cord.

*ring apophysis:* a ridge of thicker bone which runs around the periphery of each bony endplate. Alternate names include *ring epiphysis*.

*vertebral body:* approximately cylindrical portion of the vertebra which transmits the majority of spinal loads.

*vertebral foramen:* the arch formed by the posterior elements through which the spinal cord runs.

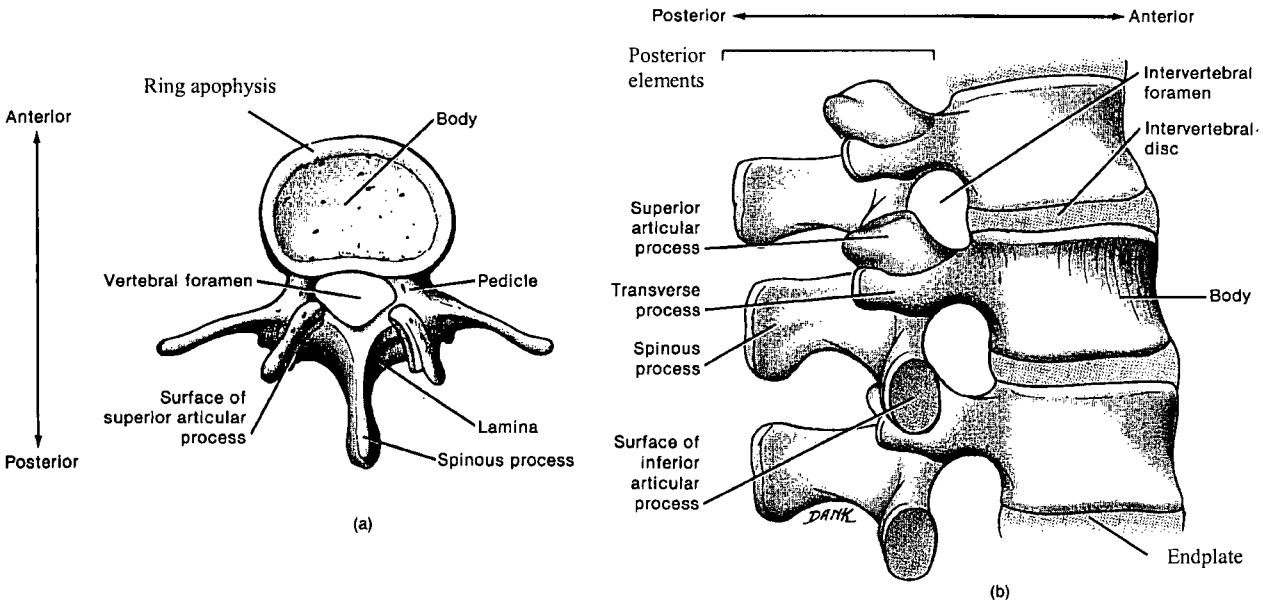


Figure 1.2: Parts of the vertebra: a) top view of a lumbar vertebra, b) side view of a section of the lumbar spine (Tortura & Anagstakos 1984, p. 157).

***Parts of the Intervertebral Disc:***

*intervertebral disc (disc):* the compressible tissue which separates the vertebral bodies. The intervertebral discs give the spine its mobility, cushion the spine from shock loading, and help to distribute spinal loads more evenly over the vertebral body.

*annulus fibrosus (annulus):* fibrous tissue arranged in concentric rings around the axis of the spine which makes up the majority of the intervertebral disc.

*nucleus pulposus (nucleus):* a gelatinous core which is situated near the centre of the intervertebral disc.

***Parts of the Spine (Figure 1.3):***

*cervical (C1-C7):* 7 vertebrae which make up the neck and support the head

*thoracic (T1-T12):* 12 vertebrae which make up the thorax, each with a pair of ribs attached to it

*lumbar (L1-L5):* 5 vertebrae which make up the lower back

*sacral (S1-S5):* 5 fused vertebrae which interface with the pelvic bones to transmit load from the torso to the legs

*coccygeal:* 4 fused vestigial vertebrae at the base of the spine which serve no functional purpose

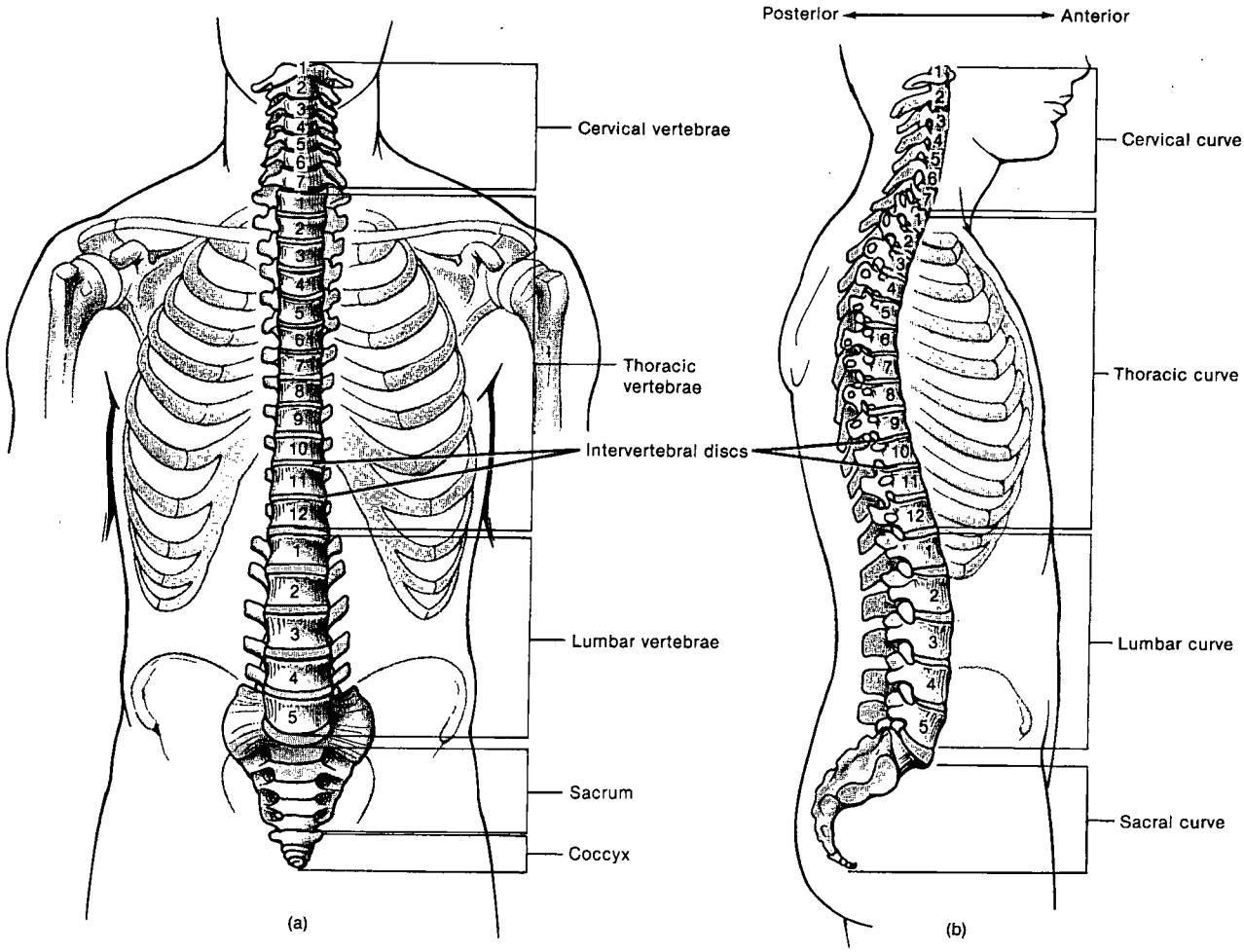


Figure 1.3: Regions of the spine: a) anterior view, b) right lateral view (Tortura & Anagnostakos 1984, p. 153).

***Descriptive Terms (Anatomical Positions):***

*anterior:* nearer the front of the body (e.g. the anterior part of the vertebral body is the part of the vertebra closest to the front of the torso)

*posterior:* nearer the back of the body (e.g. the posterior elements of the vertebra are the part of the vertebra closest to the back of the torso)

*lateral:* situated on one side or the other of the body (or component of the body) (e.g. the left lateral endplate is the left half of the endplate); can be combined: anterolateral, posterolateral

*superior:* nearer to the head (e.g. the superior endplate of the vertebral body is the top endplate: the endplate closer to the top of the spine)

*inferior:* farther from the head (e.g. the inferior endplate of the vertebral body is the bottom endplate: the endplate closer to the base of the spine)

*cranial:* nearer the head

*caudal:* nearer the base of the spine

*proximal:* the part of an extremity or bone closest to the torso; may also be used to describe the position of one body part or anatomical feature relative to another (e.g. the proximal femur; the elbow is proximal to the wrist)

*distal:* the part of an extremity or bone furthest from the torso; may also be used to describe the position of one body part or anatomical feature relative to another (e.g. the distal femur; the knee is distal to the hip)

***Anatomical Planes (Figure 1.4):***

*coronal (a.k.a. frontal):* the anatomical plane which divides the body into front and back regions

*sagittal:* the anatomical plane which divides the body into left and right regions

*transverse:* the anatomical plane which divides the body into top and bottom regions

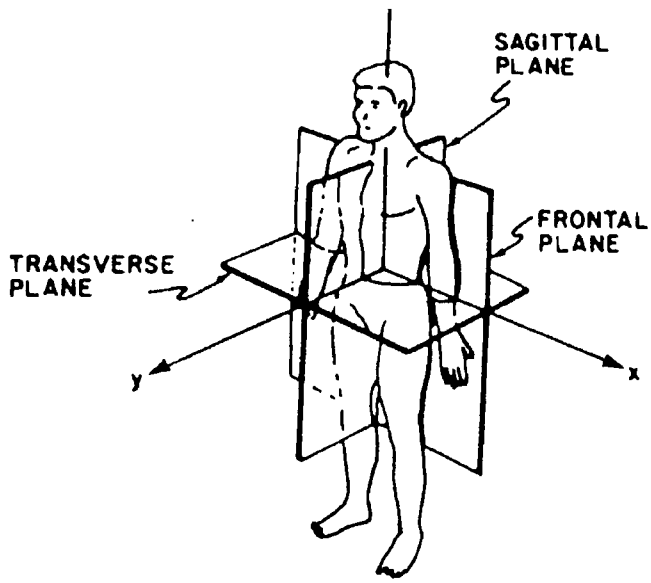


Figure 1.4: The three anatomical planes. From Alici et al. (1990): pg. 805.

***Clinical Terms:***

*DEXA (dual-energy x-ray absorpsiometry):* a technique used to estimate the bone density of a patient, usually by scanning the hip, lumbar spine or wrist. The DEXA scanner returns a bone mineral density in grams per square centimetre (since x-rays give a two-dimensional representation of the three-dimensional bone). By comparing this value with a population average the radiologist can judge whether the patient is at risk of osteoporotic fracture.

*QCT (quantitative computed tomography):* a method in which small "slices" of scanning are used to obtain a three-dimensional representation of a bone or tissue within the body. This method can be also be used to approximate bone density or, using more modern equipment, to look at the microarchitecture of the trabeculae in a bone to identify the characteristic structural changes of osteoporosis.

*radiograph (x-ray):* a method of looking at the human skeleton using x-rays captured on film. Radiographs can be used to identify and diagnose spinal fractures or degenerative changes in the discs (e.g. osteophyte formation or disc thinning (see definitions below)).

*disc degeneration:* changes in the disc which result in loss of moisture in the intervertebral disc, formation of fissures and altered load transmission. The disc height decreases as the disc loses moisture. This is visible on lateral x-rays in the form of dissimilar disc heights in adjacent levels or wedging of the disc.

*osteophyte:* a bony projection which forms at the periphery of the endplate in response to degenerative changes in the disc. Osteophytes can be used to help identify disc degeneration on x-rays. On lateral radiographs they make the margins of the bone appear jagged or look like thin shelves of bone protruding from the anterior portion of the endplate.

*osteoporosis:* a loss of bone density accompanied by changes in the trabecular architecture of the vertebral body (and other bones) leading to loss of strength. Osteoporotic patients are at much greater risk of fracture and can experience spinal fractures under loads encountered during normal daily activities.

*osteoporotic fracture:* any fracture occurring under loads considered to be normal anatomical loads (i.e. loads encountered during normal daily activities) as a result of bone strength loss associated with osteoporosis. On a lateral x-ray the vertebra will have a wedge-shape or decreased height. Usually only one or two vertebrae show evidence of fracture, but they tend to indicate a low density throughout the spine.

*burst fracture:* a fracture in which the vertebral body is broken into several pieces. This is normally a result of trauma, but can occur in osteoporotic individuals.

*comminuted:* broken into many small pieces

*compression fracture:* a fracture of the vertebral body which causes loss of vertebral height. This can be caused by either trauma or osteoporosis (loss of bone strength leading to an inability to support normal spinal loads).

*wedge fracture:* a fracture in which the anterior portion of the vertebral body collapses more than the posterior portion, causing a wedge-like profile in the vertebra when viewed on a lateral x-ray

*wedge fracture:* a fracture in which the anterior portion of the vertebral body collapses more than the posterior portion, causing a wedge-like profile in the vertebra when viewed on a lateral x-ray (Figure 1.1 a). This can be caused by either trauma or osteoporosis (loss of bone strength leading to an inability to support normal spinal loads).

*interbody fusion:* a surgical procedure in which a bone or synthetic spacer is placed between two vertebrae to provide support and maintain the desired anatomical distance between them while the spine heals or "fuses" after removal of diseased or damaged tissue (Figure 1.5)

*bone graft:* bone taken from tissue donors and used during surgery to replace diseased or damaged bone or to promote healing. Bone graft is used in interbody fusion surgery to act as the spacer or to supplement a synthetic spacer by providing an appropriate biological environment for promoting bone growth.

*allograft:* bone graft taken from a tissue donor other than the person receiving it

*autograft:* bone graft removed from a patient at the time of surgery and used in another site. Autograft is usually taken from the pelvis, a rib, or the fibula (a small bone in the shin).

*interbody cage:* a synthetic implant used as a spacer in interbody fusion surgery (Figure 1.5). Interbody cages are always supplemented with bone graft, which provides the appropriate biological environment for bone growth. Most cages are designed to be packed with bone graft. Graft is usually packed around the implant as well. Interbody cages are stronger than graft alone and are less likely to collapse under physiologic loads.

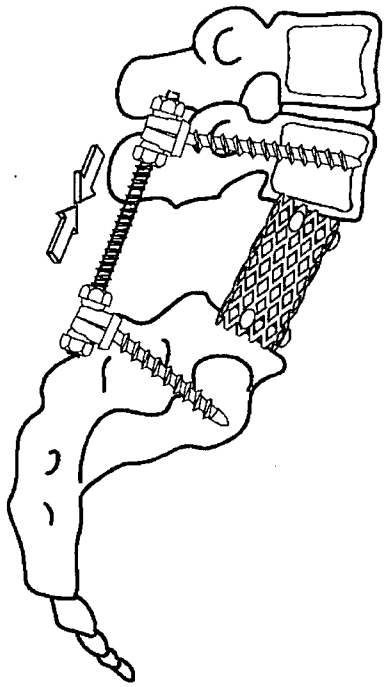

Figure 1.5: Interbody fusion using a Harms cage to replace a vertebra and the two adjacent discs. This patient has also been fitted with posterior instrumentation (rods and screws) to provide additional stability. From Harms et al. (1996): p. 537.

*in vivo:* in a living creature (e.g. an *in vivo* study to compare the performance of two implants in patients or animals)

*in vitro:* in cadaver tissue (e.g. an *in vitro* experiment to compare spinal implants might be done using spinal segments taken from a human cadaver)

### 1.4.2 Spinal Anatomy

The spine is divided into 5 distinct regions: the cervical spine, the thoracic spine, the lumbar spine, the sacrum and the coccyx (Figure 1.3). The cervical spine is made up of 7 vertebrae (C1-C7) which support the skull and make up the neck. The thoracic spine contains 12 vertebrae (T1-T12), each with a pair of ribs attached to it, forming the torso. The lumbar spine has 5 vertebrae (L1-L5) which make up the lower back, and the sacrum contains 5 fused vertebrae (S1-S5) which interface with the pelvic bones to transmit load from the torso to the legs. The coccyx is made up of 4 fused vestigial vertebrae that serve no functional purpose.

The cervical, thoracic and lumbar vertebrae share several characteristics. Each is made up of a vertebral body (an approximately cylindrical column of cancellous bone covered by a thin shell of cortical and subchondral bone) which transmits the majority of the spinal loads, and the posterior elements (an arch of bone with several bony projections) which interface with the vertebrae above and below, provide attachment sites for muscles and protect the spinal cord (Figure 1.2).

The vertebral body is filled with a matrix of strut-like trabeculae running mainly in the horizontal and vertical directions. The spaces between the trabeculae are filled with blood and bone marrow. The trabeculae are not equally spaced, but rather are distributed to provide optimal load transmission while minimising the weight of the bone and allowing blood vessels to penetrate the bone. Anatomical studies (Amstutz et al. 1969; Jayasinghe et al. 1994) have shown that the trabeculae are more widely spaced near the middle of the vertebral body where the basivertebral veins run, and become more closely packed near the upper and lower surfaces of the vertebra.

The circumference of the vertebral body is covered with a thin shell of denser cortical bone. It holds the bone marrow in place, provides a framework to which the trabeculae are attached and transmits part of the spinal load. The literature is unclear on the relative load-bearing role of the cortical shell. Rockoff et al. (1969) tested both cored and decorticated lumbar vertebral bodies in compression and found that the cortical bone provided 45-75% of the vertebral body strength, depending on the bone density (which decreases with age). In younger donors the cortex supported about 45% of the load, while in donors over 40 it supported about 65% of the load. McBroom et al. (1985) did a similar study using bones from older donors (63–99 years) and concluded that the cortical shell provides only about 10% of the vertebra's ultimate compressive strength. It is unclear why the findings of these two studies differ.

The upper and lower surfaces of the vertebral body are capped with subchondral bone. This bone is referred to as the "bony endplates". There is some disagreement over the exact composition of this bone. It was originally thought to be cortical bone (Coventry et al. 1945, Whitehouse et al. 1971), but more recent studies have suggested that it is actually made up of denser cancellous bone (Ritchie et al. 1970, Mosekilde 1993, Silva et al. 1994). The average thickness of this bone varies from about 0.4 to 0.5 mm in younger people to 0.2 to 0.3 mm in older individuals (Vesterby et al. 1991). A slightly thicker rim of bone, called the ring apophysis, runs around the periphery of each endplate. Overlying the subchondral bone is a layer of cartilage that helps to cushion the bone (protects it from shock loading).

Separating the unfused vertebrae are intervertebral discs, which provide flexibility to the spine, act as shock absorbers, and distribute load evenly over the endplates. The discs have two distinct regions: the annulus fibrosus (concentric rings of fibrous tissue) and the nucleus pulposus (the gelatinous centre which acts as a shock absorber and helps to distribute the load transmitted through the spine).

The spinal cord runs through the vertebral foramen, a protective arch of bone formed by the posterior elements, just behind the vertebral body (Figure 1.2). The nerve roots, which branch off of the

spinal cord to provide motor control to the muscles and sensory feedback to the skin, emerge between the vertebrae through gaps between the posterior elements called the intervertebral foramen. The aorta (the largest artery in the body) runs along the front of the vertebral bodies. The proximity of these delicate and crucial pieces of anatomy to the intervertebral space has important implications for interbody fusion surgery and for any recommendations for design changes that may arise from this research.

## 1.5 Implant Subsidence: A Review of the Literature

The implants currently used for interbody fusions have reported clinical success rates of 68 to 95% (Hammerburg, 1996), however the increasing number of older patients receiving interbody fusions may lead to an increase in the incidence of subsidence, since bone density and bone strength decrease with age (Martin, 1993). It may be that implant design changes are required to reduce the risk of subsidence in patients with diminished bone density. If some regions of the bone remain strong longer than others, engaging these sections of the endplate may reduce the incidence of subsidence in older patients.

There are many different implant designs available, raising the question "do some implants resist subsidence better than others?" Currently, the answer appears to be "no". Many biomechanics studies have been conducted looking at the loads at which different implants subside. Most involve inserting the implant between two vertebrae, loading the construct at a fixed rate and measuring the load at failure (the point at which the load transmitted by the implant-bone interface drops). These studies have shown that subsidence occurs at lower loads in specimens with low bone density (Oxland and Lund 2000).

Jost et al. (1998) tested the Brantigan cage (a rectangular, porous carbon-fibre implant), Ray cage (a cylindrical, threaded, porous titanium implant), and Stratec cage (a porous titanium implant designed to fit the contours of the endplate) in compression. They found no significant difference in load at failure (all medians about 5000 N, range: 1700 to 9900 N), although at 3 mm of subsidence the Brantigan and Ray cages (means of about 2300 N) were found to perform significantly better than the Stratec cage (mean about 1700 N). The overall mean at 3 mm of subsidence was about 2000 N, range: 800 to 3700 N.

They also found a strong correlation between failure load and bone density: the loads at 3 mm of displacement were higher in bones with higher bone density. Many other studies have shown the same direct relationship between bone density and compressive strength (Bell et al. 1967; Hansson et al. 1980, 1981, 1986; Biggemann et al. 1988; Closkey et al. 1993; Holte et al. 1994, Hollowell et al. 1996, Hoshijima et al. 1997, Steffen et al. 2000).

Hollowell et al. (1996) tested seven different surgical constructs (one synthetic implant and six bone graft options) to failure, each in an average of eight human superior thoracic vertebral surfaces. Five had mean failure loads which were not significantly different, ranging from 959-1473 N. Only the smallest bone graft implant (single rib with or without the endplate) was significantly weaker (262-537N).

The most likely explanation for the similarities in failure load is that the implants are all placed in the centre of the vertebral endplate. Because the upper and lower surface of the vertebra are rarely flat (and most often are concave), implants which nominally have a larger area in contact with the bone (e.g. the BAK cage) actually engage about the same area as those with narrower walls (e.g the Harms cage).

The mode of compressive failure seen in the Jost study was fracture of one or both endplates. Brantigan et al. (1991) also noted that the cancellous bone directly superior and inferior to the cages fractured during compression tests using carbon fibre cages.

Several researchers have measured the intradiscal pressure *in vitro* (Nachemson 1960; Andersson and Schultz 1979; Adams et al. 1979; Panjabi et al. 1988) and in *vivo* (Nachemson et al. 1964, 1970; Andersson et al. 1974; Quinell and Stockdale 1983; Wilke et al. 1999; Sato et al. 1999) and used these results to determine the loads on the spine in various postures, all with similar findings. To give some indication of how likely an implant is to subside or to fail itself, a graph and table showing typical spinal loads during daily activities are provided below (Figure 1.6, Table 1.1). Note that the failure loads found in the implant studies (the loads at which subsidence occurred) lie within the normal range of loads encountered during daily activities (e.g. in Jost et al.'s 1998 study the median failure loads were about 5000 N, range 1700 to 9900 N).

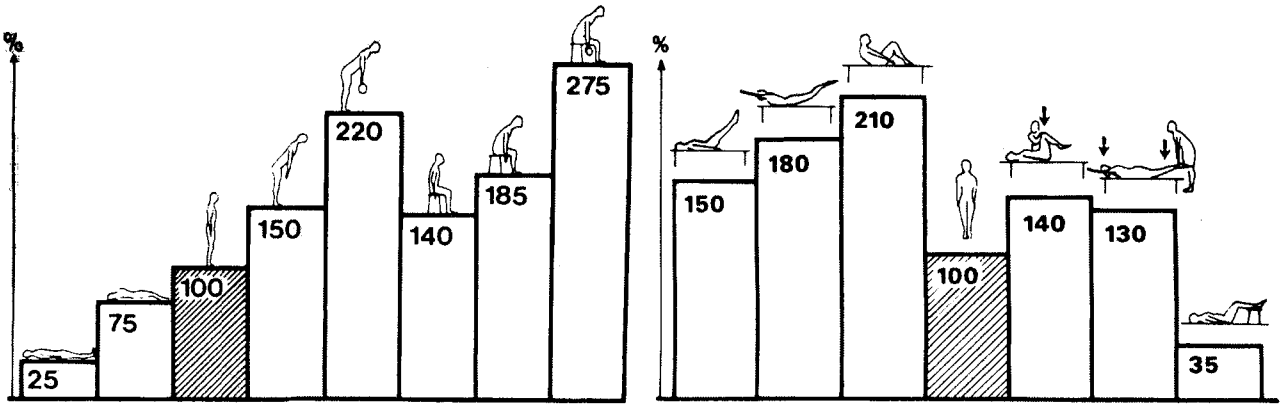


Figure 1.6: Typical spinal loads encountered during daily activities – a comparison of disc pressures in the third lumbar disc during various activities. From Nachemson 1976.

Table 1.1: Loads in the lumbar spine (L3) during typical daily activities. From Nachemson 1963, 1965, 1975.

| Activity | Load (N) |
|---|---|
| Supine in traction | 100 |
| Supine | 300 |
| Standing | 700 |
| Walking | 850 |
| Twisting | 900 |
| Bending sideways | 950 |
| Upright sitting, no support | 1000 |
| Coughing | 1100 |
| Isometric abdominal muscle exercise | 1100 |
| Jumping | 1100 |

| Activity | Load (N) |
|---|---|
| Straining | 1200 |
| Laughing | 1200 |
| Bending forward 20° | 1200 |
| Bilateral straight leg raising | 1200 |
| Active back hyperextension, prone | 1500 |
| Sit-up exercise with knees extended | 1750 |
| Sit-up exercise with knees bent | 1800 |
| Bending forward 20° with 10 kg in each hand | 1850 |
| Lifting 20 kg, back straight, knees bent | 2100 |
| Lifting 20 kg, back bent, knees straight | 3400 |

Several researchers have also looked at the effects of implant size on subsidence. Closkey et al. (1993) found that to prevent subsidence in the thoracic vertebrae a minimum of between 30 and 40% of the vertebral cross-sectional area must be in contact with the implant. Pearcy et al. (1983) also suggested a minimum of 40% coverage of the endplate. Gill (1989) suggested between 50 and 80% coverage of the endplate. This percentage criteria may be too simplistic, however, since the actual implant-bone interface area is affected by the relative profiles of the implant and the vertebral body, and underlying bone properties, such as bone density, affect the required area.

Clinically, in order to achieve a bony fusion across the spinal level, a large area of the endplate must be left exposed. The actual area required is unknown, however existing implants attempt to maximise the endplate exposure while providing sufficient contact with the endplate to prevent subsidence.

### 1.6.1. Regional variation in vertebral structure and properties

The vertebral body structure is very much affected by its environment, and adapts to minimise weight by eliminating unnecessary bone, while maximising strength by laying down new bone where stresses are high (Atkinson 1967). For this reason, the endplates do not have a uniform thickness, nor is the trabecular structure uniform throughout the vertebral body.

Silva et al. (1994) measured the central thickness of 16 superior and inferior L1 endplates in specimens aged 43 to 89 and found that the superior endplate thickness ranged from a mean and standard deviation of 0.25 mm (0.12 mm) to 0.37 mm (0.18 mm), while the inferior endplate thickness ranged from 0.29 mm (0.15 mm) to 0.52 mm (0.25 mm). The inferior endplate was not significantly thicker than the superior endplate, although it was nominally thicker. Due to the limited number of specimens used they were unsure if age or gender had an effect on the thickness. The endplate is surrounded by a slightly thicker, often raised, ring of bone called the ring apophysis.

Roberts et al. (1997) measured the thickness of 83 cadaveric lumbar vertebral endplates from donors aged 17-93 years using microfocal x-ray. They found that the endplates were thicker adjacent to the annulus (around the periphery) than below the nucleus, and that the inferior endplates were thicker than the superior endplates.

The internal structure also has significant structural variation. It is filled with a series of primarily vertical and horizontal strut-like trabeculae. Mosekilde (1993) found that the horizontal trabeculae are about 90-180 μm thick, while the vertical trabeculae are 200-220 μm thick. Bergot et al. (1988) found similar values (horizontal trabeculae 110-180 μm thick). In both cases, the lower horizontal thickness values were found in older specimens.

The arrangement of the trabeculae within the bone appears to be at least partially dictated by anatomical in addition to mechanical considerations. The alignment of the trabeculae along horizontal and vertical axes is the most efficient arrangement for transmission of the loads supported by the spine, but this pattern is broken in the middle of the bone. Here, the trabeculae are more widely spaced and the vertical trabeculae become more plate-like (Atkinson 1967, Amstutz et al. 1969, Mosekilde 1993). This break in the regular arrangement of the trabeculae is thought to be caused by the large blood vessels which run through the central region of the vertebral body, in particular the basivertebral vein (Gray 1980).

Figure 1.7 shows a cross-section through the vertebral body taken from Jayasinghe et al. (1994). Here the differences in trabecular spacing are clearly shown. Note the gap in the centre of the vertebra where the blood vessels which supply the vertebra run into the centre of the bone.

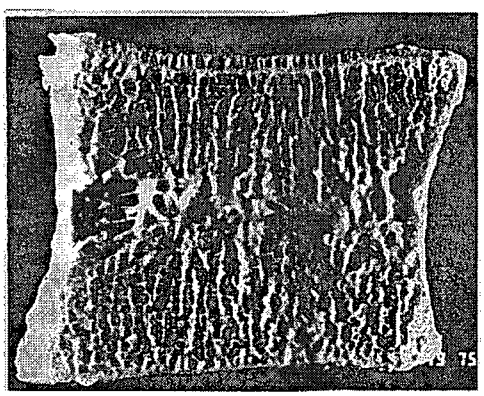

Figure 1.7: Central sagittal cross-section through a healthy vertebra from Jayasinghe et al. (1994): p. 261.

### 1.6.2 Population variation

#### *1.6.2.1 Geometry*

Many studies have been done looking at the dimensions of the lumbar vertebrae (Cotterill et al. 1986; Gilad and Nissan 1986; Krag et al. 1986, 1988; Berry et al. 1987; Zindrick et al. 1987; Scoles et al. 1988; Panjabi et al. 1991). The values found in these studies are very similar, so for clarity, only the endplate dimensions given in Panjabi's study are included in Table 1.2, in the format: mean (standard error of the mean). These values are based on measurements of 8 male and 4 female subjects with an average age of 46.3 years (range: 19-59 years). The average subject weight was 67.8 kg (range 54-85 kg), and average height was 167.8 cm (range: 157-178 cm). Note that the mean endplate width appears to increase at lower lumbar levels, while the depth appears to decrease.

Table 1.2: Dimensions of the lumbar vertebral endplates (Panjabi et al.1991). Values are given in the form: mean (standard error of the mean).

| | | | Vertebra | | |
|---|---|---|---|---|---|
| **Dimension** | **Units** | **Endplate** | **L3** | **L4** | **L5** |
| Endplate Width (LAT) (side-to-side) | mm | superior | 44.1 (0.88) | 46.6 (1.20) | 47.3 (1.20) |
| | | inferior | 48.0 (1.24) | 49.5 (1.38) | 49.4 (1.41) |
| Endplate Depth (AP) (front to back) | mm | superior | 35.2 (1.10) | 35.5 (0.88) | 34.7 (1.17) |
| | | inferior | 34.8 (1.24) | 33.9 (0.85) | 33.2 (0.92) |
| Endplate Inclination (transverse plane) | degrees | superior | 1.7 (0.43) | 4.7 (1.1) | 2.2 (0.54) |
| | | inferior | 2.7 (1.1) | 2.7 (0.69) | 1.8 (0.42) |

#### *1.6.2.2 Gender*

According to Schmorl et al. (1971) the peak bone mass in men is 20-30% higher than in women, with this difference being solely a result of size, since the density and structure of the bone are identical, however, Nottestad et al. (1987) examined the proportion of trabecular bone in human vertebrae and found a significant difference between males and females in the percentages of trabecular bone (trabecular mass / entire body mass x 100%). In females the trabecular bone in the vertebral body accounted for 41.8% (standard deviation 7.5%) of the vertebral body bone mass. In males, the percentage was 33.5% (standard deviation 8.1%). This difference was found to be significant ($p < 0.005$).

Brandner (1970) found that female vertebrae are narrower for a given height in the sagittal plane (front-to-back) than male vertebrae. Taylor and Twomey (1984) demonstrated that they are also narrower in the coronal plane (side-to-side).

Hansson and Roos (1980) found that males and females both experience a linear decrease in bone mineral content with age, and that the rate of loss is the same in both genders. They also showed that there is a high correlation between bone strength and bone mineral content. Since men started out with higher bone mineral content, their bone was stronger relative to the female specimens despite the equal bone loss in each group.

According to An and Draughn (2000: p. 68), in general, the differences between male and female bone are caused by bone quantity rather than bone quality, i.e. they arise from the fact that men have larger skeletons rather than denser bone. After menopause, women tend to experience accelerated bone resorption rates, which result in a more rapid strength decline than men experience with ageing.

### *1.6.2.3 Age*

Many changes occur in the vertebra as part of the natural aging process. Peak bone mass is reached between the ages of 18 and 25 years (Schmorl et al. 1971). At this age the load bearing capacity of a lumbar vertebral body is 9800 N, or more (Mosekilde 1990).

Atkinson (1967) looked at a series of vertebral cross-sections and observed several changes in the trabecular structure with age. He found that young vertebral bodies have a closely woven network of cancellous bone, with the upper and lower thirds having a closely-spaced, grid-like arrangement of trabeculae, while the central third is less evenly organised, with wider spacing around the central blood vessels. In older bones the trabeculae become thinner, are often discontinuous, and decrease in number with age. The transverse trabeculae in the centre of the vertebral body are the first to be resorbed. In the oldest spines the grid-like trabecular organisation is lost due to thinning and loss of trabeculae. Atkinson also noted an apparent thickening of some of the remaining vertical trabeculae, particularly in the central region of the vertebra, although he did not measure their thickness. This observation was also reported by Cassucio (1962) and Jayasinghe et al. (1994).

Oda et al. (1998) found that midsagittal sections of the second lumbar vertebrae in middle aged humans had rod-like trabeculae in the superior and inferior thirds of the vertebral body, arranged in a lattice pattern. Horizontal sections showed a homogenous honeycomb pattern throughout the vertebral body. Trabecular atrophy was not prominent and few trabeculae with free ends were evident.

In elderly patients they found that the rod-like trabeculae of the superior and inferior thirds of the midsagittal section were thinner and often more discontinuous. The plate-like trabeculae in the middle third developed perforations, transforming the plates into rods. Loss of trabeculae, reduction in number of trabeculae, and increased spacing between trabeculae were seen in all regions of the vertebral body, but were not homogenous and were more prominent in the anterior vertical third of the vertebral body. Atrophy of the horizontal trabeculae was more pronounced and tended to occur with increasing age.

Mosekilde (1988) and Jayasinghe et al. (1994) also found that age-related changes begin in the vascular region at the centre of the vertebral body, spreading superiorly and inferiorly, and Mosekilde measured a gradual thinning of the horizontal trabeculae, from about 180 μm in young individuals to 90 μm in the elderly. Perforation and fracture of thin struts occured in some bones, with these changes being more pronounced in women than in men. Mosekilde also measured the thickness of the vertical trabeculae using polarised light with a lambda filter and did not find evidence that the vertical trabecular thickness increases with age, instead concluding that the width of the vertical trabeculae is almost constant at approximately 200 μm.

The trabeculae are not the only part of the bone which changes with age. The endplates thin to 200–300 μm in the elderly (Vesterby et al. 1991), compared with a thickness of 400-500 μm in the young, and the cross-sectional area of the vertebral body increases due to the formation of periosteal bone and osteophytes (Schmorl et al. 1971; Mosekilde et al. 1990). These changes result in vastly decreased bone strength (in the order of 785 – 1470 N in an elderly individual) (Schmorl et al. 1971).

Twomey et al. (1983, 1987) studied the effect of age on bone density and bone structure in the embalmed lumbar vertebra of 93 adult subjects. They found that there is a significant decrease in bone density with age, accompanied by progressive concavity of the endplates, beginning earlier in females than in males. The main structural change accounting for these results was a decrease in the number of horizontal trabeculae.

It has been shown by many authors that the compressive failure load of bone decreases as the bone density drops (Bell et al, 1967, Hansson and Roos 1980). It has also been demonstrated that the density of bone decreases naturally with age (Hansson et al. 1980). It is not surprising then to find that there is a gradual decline in failure load with ageing (Perey 1957, Mosekilde et al, 1986, Oxland 1992).

Bell et al. (1967) used Euler's theory (an engineering concept which predicts the critical load at which a vertical column loaded in compression will buckle) to demonstrate that the rigidity of bone is enhanced more by the incorporation of a series of "reinforcing ties" (horizontal trabeculae) than it would be by an increase in the diameter of the vertical trabeculae of an equivalent amount of material. This would explain the fact that the strength loss in older vertebrae is much greater than would be predicted based on the relative amount of bone loss (a 25% decrease in bone tissue results in a more than 50% decrease in the vertebral strength) (Figure 1.8).

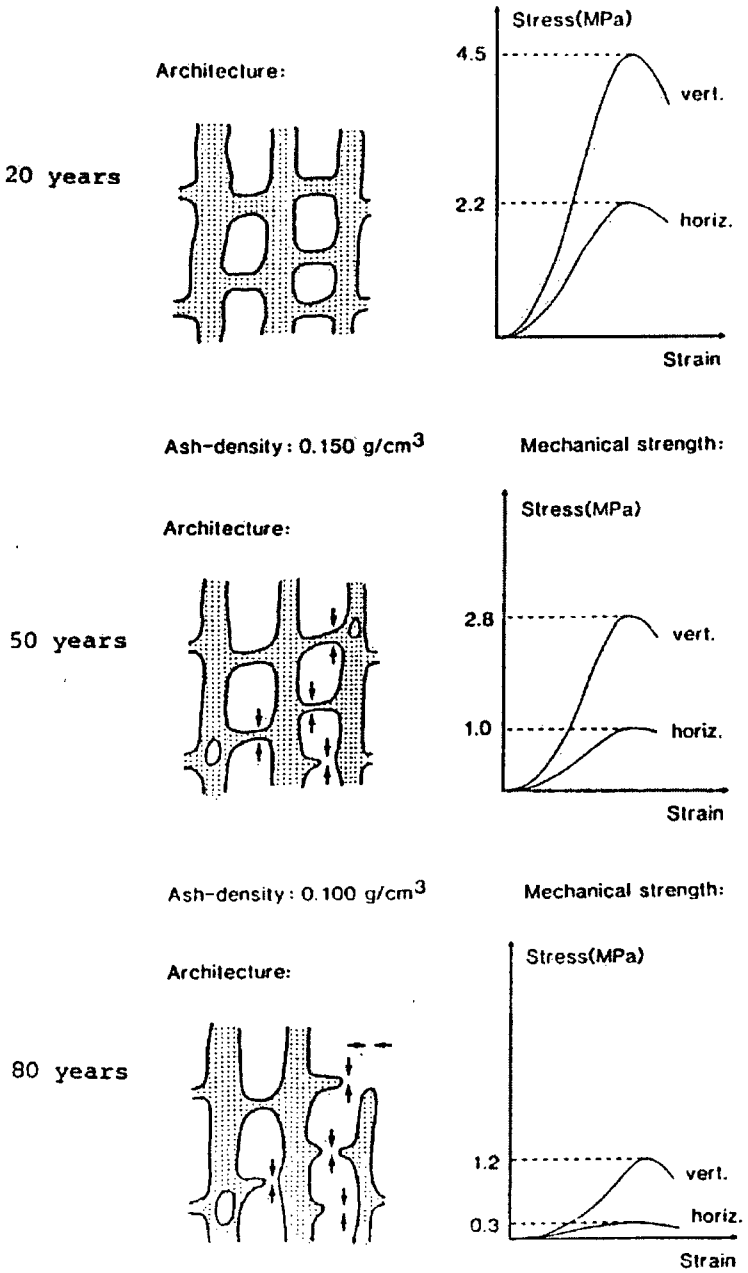


Figure 1.8: Age-related changes in bone architecture and stress-strain curves for horizontal and vertical trabeculae. Figure 5 from Mosekilde (1993).

### 1.6.3 Effects of degenerative changes

#### *1.6.3.1 Effects of osteoporosis*

Ten million people in the United States have osteoporosis, 80% of whom are women. Eighteen million have low bone mass, placing them at increased risk of osteoporosis. One in two women and one in eight men over age 50 will have an osteoporosis-related fracture in their lifetime. Osteoporosis is responsible for more than 1.5 million fractures annually in the United States alone (700,000 vertebral fractures, 300,000 hip fractures, 250,000 wrist fractures, and 300,000 fractures at other sites). Treatment and care costs related to osteoporotic fractures in the United States are currently at US$13.8 billion annually (US$38 million each day) (National Osteoporosis Foundation 2000).

At age 65, x-ray comparison with a "standard" suggests that 65.8% of females and 21.5% of males have osteoporosis. In women, the incidence increases by about 8% for each additional decade, whereas in men, a large increase does not occur until after age 76 (Gitman and Kamholtz 1965). This difference stems from the increased rate of bone loss caused by the hormonal changes of menopause.

Nottesad et al. (1987) compared the trabecular bone content of a single female osteoporotic spine to the average content found in 10 "normal" female spines. Their results showed that, although the osteoporotic spine's overall bone mass was lower (63.5% of the mass of the average "normal" female vertebra), the percentage of trabeculae (trabecular mass / entire body mass x 100%) in the osteoporotic vertebral body (46.41%, standard deviation of 4.3%) was not significantly different from the "normal" female vertebral body (41.8%, standard deviation 7.5%). The fact that these values were not found to be different led the researchers to conclude that the bone loss in osteoporotic individuals occurs evenly over the bone. The limited sample size seriously undermines this argument, however. Their method also does not account for regional trabecular variation.

Most researchers believe that the trabeculae are affected more by osteoporosis than is the cortex. This belief is based partially on anatomical studies showing loss of horizontal trabeculae in osteoporotic vertebrae. Figure 1.9 shows a "healthy" vertebra next to an osteoporotic specimen (Jayasinghe et al. 1994). Note the reduction in horizontal trabeculae in the osteoporotic specimen. While it may be true that there is a general decline in bone over the entire vertebra, the loss of these supporting struts is likely to have a far greater impact on the overall strength of the bone than a thinning of the cortex would (Bell et al. (1967), see section 1.6.2.3).

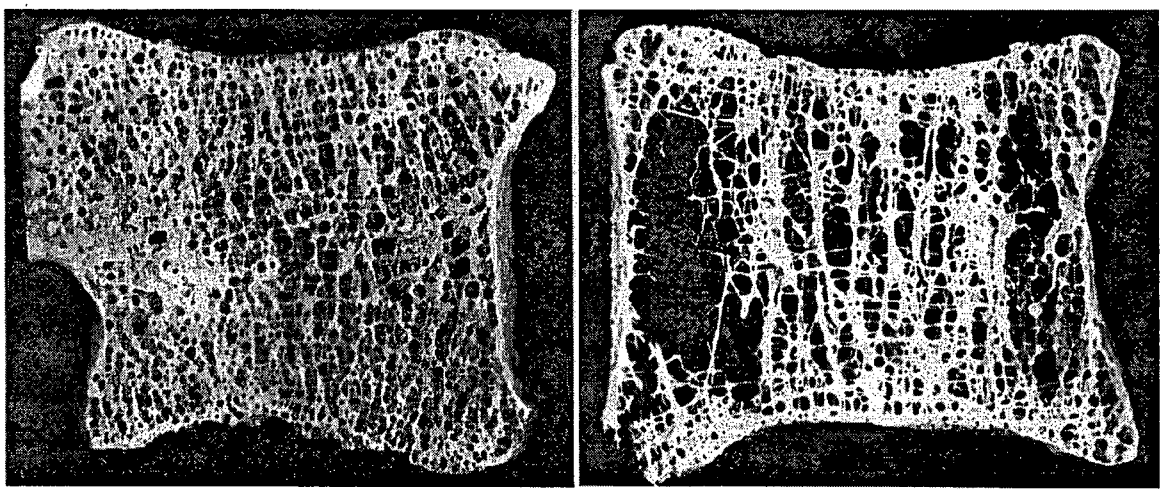

Figure 1.9: Normal and osteoporotic trabecular architecture (posterior to the left). From Figures 10 and 12, Jayasinghe, et al. (1994).

The most interesting feature of Figure 1.9, for the purpose of this study, is the non-uniform loss of trabeculae. Note that the gaps between trabeculae are larger in some regions of the bone than in others. One aspect of this study will seek to identify patterns in strength loss that can be associated with declining bone density. If this bone loss occurs in a predictable manner, designing an implant to take advantage of these trends could dramatically reduce the risk of subsidence in people with low bone density.

Though the majority of the changes associated with osteoporosis are generally attributed to the trabeculae, Wenger et al. (1998) have shown that there is also a change in the material properties of the bony endplates in osteoporotics. They tested 8 mm-wide frontal-plane strips taken from the central region of the superior and inferior endplates of 29 vertebrae from 10 donors in 3-point bending and tension to failure. They found that the Young's modulus (median and range) for normal specimens was 380 (121-955) MPa (n=26), for specimens with disc degeneration it was 342 (96-891) MPa (n=9), and for osteoporotic specimens it was 214 (48-459) MPa (n=12), which was significantly lower than the other groups. The median failure loads of the three groups were similar (global median: 12.7 MPa), as were the median failure strains (global median ~ 2%).

### *1.6.3.2 Effects of disc degeneration*

Disc degeneration may be a natural consequence of ageing. Miller et al. (1988) studied 600 lumbar discs sectioned in the transverse plane and graded the disc degeneration on a scale of 1 to 4. They found that disc degeneration began sooner in men than in women (men: second decade, women: third decade). By age 50, 97% of the discs showed some sign of degeneration, with the L3-L4, L4-L5, and L5-S1 discs being the most degenerated. Based on these results, it appears that load may have something to do with the degeneration, since men would tend to be heavier than women, and the lowest discs would support more load than those higher up in the spine.

Panjabi et al. (1988) also found that disc degeneration was greater in the lower lumbar spine than in the upper lumbar spine. In this study of 84 cadaveric lumbar disc spaces they found that the pressure required to inject a fluid into the disc and the maximum pressure that the disc could hold both decreased as the disc degenerated. This seems to indicate that the structural integrity of the disc is compromised by disc degeneration, i.e. it cannot hold fluid as effectively as it could when it was healthier. The abilities of the disc to distribute loads over the endplate and act as a shock absorber are at least partially dependent upon its fluid content, thus this finding suggests that the disc will not perform these functions as well once it has begun to degenerate.

Nachemson showed, in 1960, that the nucleus pulposus loses pressure as the disc degenerates, which means that the annulus fibrosus must support more of the spinal load. In a healthy, young spine (up to age 25 – 30) the nucleus pulposus is moist and acts like a gelatinous mass (Beadle 1931, Naylor 1955). When subjected to a compressive load, the central portions of the vertebral endplates are pushed away from one another (Brinckmann et al. 1983, Rolander et al. 1975), and the annular ring is pushed radially outward (Brinckmann et al. 1985, Brown et al. 1957, Reuber et al. 1982). In older spines, in which the water content of the nucleus has decreased, the endplates are subjected to less central pressure and the loads are distributed more around the periphery (White and Panjabi, 1990, p. 13-15).

Using Wolff's theorem (Wolff 1892), which states that bone subjected to load becomes stronger through remodelling, while bone that is not loaded loses strength, one would theorise that the strength distribution in the vertebra would change as the disc degenerates. More specifically, one would expect to

find that the centre of the vertebral body becomes weaker, while the periphery increases in strength. Part of this study looks at the effects of disc degeneration on the endplate property distribution.

### 1.6.4. Differences between vertebrae

The size and mass of the vertebrae increase from the first cervical to the last lumbar vertebra to support the increasing compressive loads to which they are subjected (White and Panjabi, 1990, p. 29). Compression tests done by various authors, including Perey (1957) and Bell et al. (1967), have shown that the strengths of the vertebrae increase in a similar manner, getting stronger moving from the head to the base of the spine. Weaver (1966 a) showed that this strength increase was most likely due to the increase in cross-sectional area alone, rather than an increased local bone strength by doing compression tests on cubes of cancellous bone from the L3-L5 vertebrae; they did not have significantly different strengths.

### 1.6.5 Differences between endplates

It has been well documented in the literature that the superior and inferior endplates demonstrate different failure modes under similar loading (e.g. in pure compressive loading). Magerl et al. (1994) showed that in the majority of burst-type fractures of the vertebral body, the superior portion of the vertebra is far more comminuted than the inferior portion. Hashimoto et al. (1988) did a clinical study of 120 burst fractures and found that the superior endplates had fractured in 100%, while the inferior endplate was fractured in only 85%. Oxland (1992) found that in a series of 10 specimens in which a burst fracture was produced experimentally, all had fractures of the superior endplate, while only 7 had inferior endplate fractures.

This study will investigate the differences between the superior and inferior lumbar endplates in terms of overall strength and stiffness, as well as differences in the structural property distributions in an attempt to better understand these findings.

### 1.6.6 Effects of endplate removal

There are two different surgical perspectives regarding the best method of endplate preparation prior to the insertion of interbody implants. The first believes that the endplate must be left intact in order to preserve the strength of the vertebra and minimise the risk of subsidence occurring. The second believes that the endplate should be punctured or removed entirely in order to promote fusion (bone growth).

Some researchers have done studies to look at the effects of endplate removal on the strength of the surgical construct. All of these have been done on cadaveric specimens, thus the effects of healing have not been addressed, only the initial strength of the bone-implant interface.

An (1999) did a study in cervical vertebrae (C3-C7) looking at the effect of removing the endplate on the failure load using an 8 mm-diameter indenter. He found that the vertebra was significantly stronger when the endplate was left intact ($p < 0.05$). However, studies looking at *in vitro* implant performance in the lumbar spine have not shown any difference between the failure loads in specimens with and without the endplate (Hollowell et al 1996, Jost et al. 1998, Steffen et al. 2000).

Part of this study will look at the effect of removing the endplate on the mean local structural properties in the vertebrae, as well as effects on the property distributions.

### 1.7.1 Basic Engineering Terminology

***load:*** application or measurement of a force or moment. A load can be compressive (pushing) or tensile (pulling): metric unit = Newton (N); e.g. by pressing on a table, one is applying a compressive load to it

***displacement:*** amount of deformation from a point of origin: metric unit = metre (m)

***load-displacement curve:*** a graph showing the relationship between the load applied to a structure and the amount of deformation caused by that load (Figure 1.10)

***failure load (strength):*** the load at which a material or structure loses integrity: metric unit = Newton (N) This value is indicated by the initial peak on the load-displacement curve. (Figure 1.10)

***stiffness:*** the amount of resistance a structure has to applied loads prior to failure (load / deformation): metric unit = Newton/millimetre (N/mm). The stiffness is given by the linear slope of the load-displacement curve. (Figure 1.10)

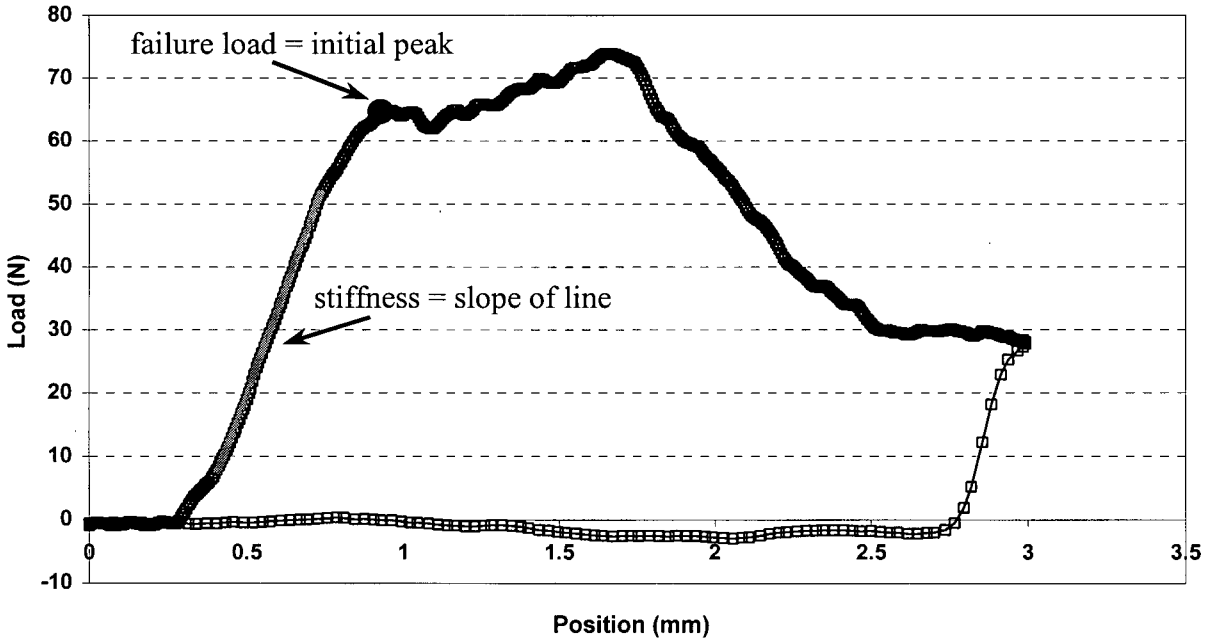


Figure 1.10: Load-displacement curve generated during an indentation test. The slope of the linear portion of the curve gives the stiffness of the bone at this point, and the first peak gives the failure load.

***stress:*** force per unit area, this is a measurement of the intensity of a force (force / area): metric unit = Newton/metre$^2$

***strain:*** deformation in a material or object under load (change in length / original length): no units

***stress-strain curve:*** graph showing the relationship between the stress and strain in a structure or material (Figure 1.11)

***strain rate:*** the rate of change of strain with time (rate of deformation / original length): unit = 1/second

***homogenous:*** having the same properties throughout

***anisotropic:*** having different mechanical properties along different axes, e.g. wood is anisotropic: it is easier to split a log using a hatchet by cutting along the grain rather than across the grain.

***material properties:*** physical properties (strength, stiffness) which are material dependent, e.g steel has different material properties than copper

***structural properties:*** physical properties (strength, stiffness) which are dependent upon the geometric characteristics as well as the material properties of a structure, e.g. a lattice made of wood has different structural properties than a solid sheet of wood, but they have the same material properties; a lattice made of wood also has different structural properties than a lattice made of iron, in addition to their different material properties

### 1.7.2 Structural and Material Properties of Cancellous Bone: A Natural Foam

As stated earlier, the vertebral body has an outer shell of cortical and subchondral bone surrounding an approximately cylindrical core of cancellous (a.k.a. trabecular) bone. This structure enables the bone to support the large anatomical loads it is subjected to while minimising its own weight. The resulting composite can be likened to an inhomogenous, anisotropic foam covered by a solid shell of varying thickness.

The mechanical behaviour of cancellous bone is typical of a cellular material. Its modulus and strength vary with density and its compressive stress-strain curve has the three distinct regions characteristic of all cellular solids (Figure 1.11, Gibson and Ashby 1988, pp. 316-323). The three regions of the curve are the:

1. Linear elastic region: a linear increase in stress as the strain is applied. If the stress is removed, the bone will return to its original height. This recoverable deformation results from elastic bending of the cell walls.

2. Plastic collapse region: a gradual decline in the slope of the stress-strain curve followed by a drop in stress and a levelling off of the curve. This indicates that permanent deformation has occurred as the cell walls begin to buckle.

3. Densification region: an exponential increase in stress as the strain is increased. This dramatic rise in stress is the result of cellular collapse which causes the walls of opposing cells to meet.

As stated above, cancellous bone is anisotropic, meaning its structural properties depend upon the axis along which it is loaded. In vertebrae the principal stresses are directed along the central axis of the approximately cylindrical vertebral body, thus the bone is strongest if loaded parallel to this line. The strain rate also affects the properties of the bone. The ultimate strength (failure load) and elastic modulus are approximately proportional to the strain rate raised to the power 0.06 (Mow and Hayes 1997, p. 84). Finally, the cancellous bone is filled with marrow, but according to Carter and Hayes (1977) this does not affect its behaviour below strain rates of about 10/s (compression rate in mm/s divided by the length being strained in mm). The strength of cancellous bone is also affected by its density, as expected for a foam.

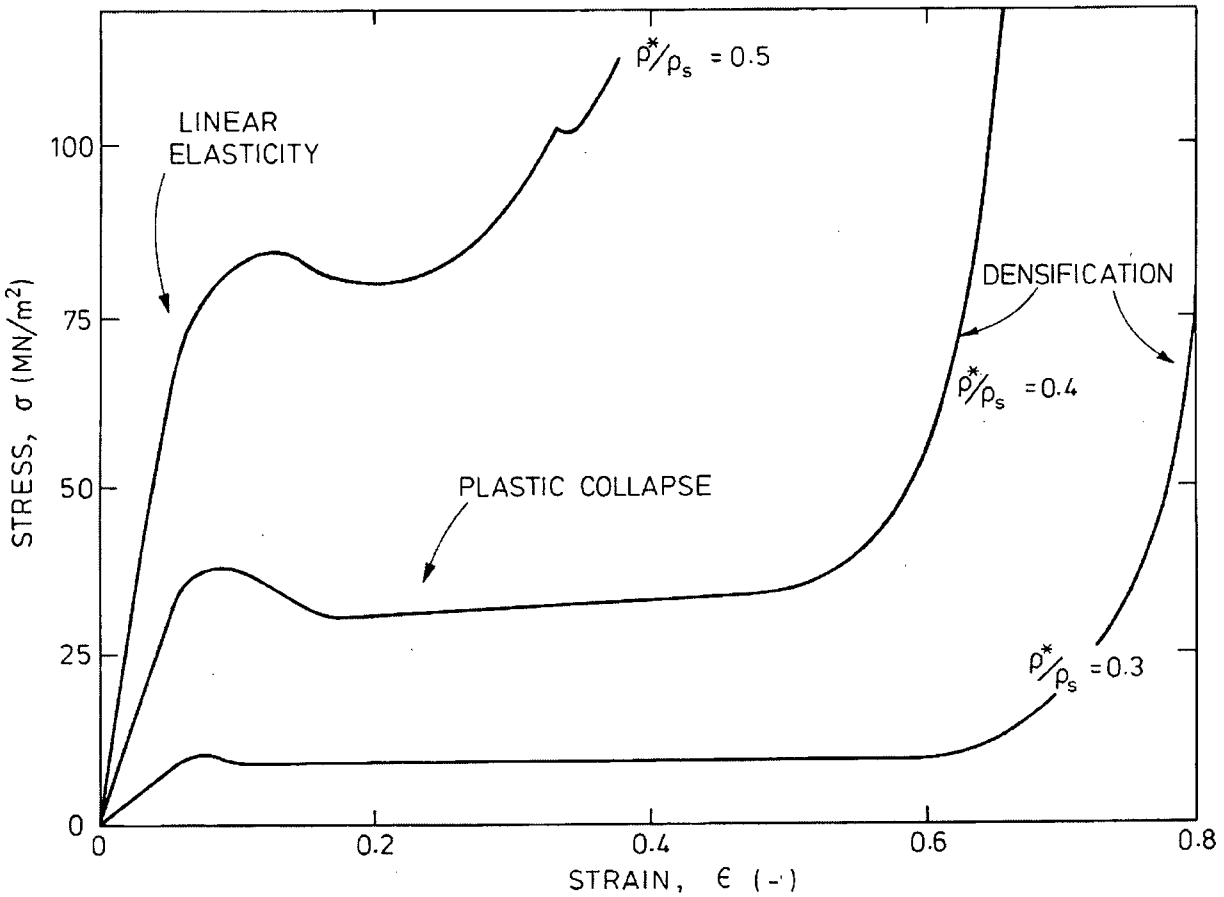


Figure 1.11: Compressive stress-strain curves for several relative densities of wet cancellous bone. Hayes and Canter 1976.

Bone is classified as cortical or cancellous based on its relative density (the specimen's density divided by 1.8 g/cm$^3$, the density of fully dense cortical bone) with cancellous bone ranging from 0.05 to 0.7, and cortical bone ranging from 0.7 to 0.95 (Mow and Hayes 1997, p. 72).

The compositions of cortical and cancellous bone are very similar. Both are composed of approximately 35% organic matrix (by wet weight), 45% calcium compounds and 20% water. The density of cortical bone is about 1800-2000 kg/m$^3$, while the density of the individual trabeculae in cancellous bone averages 1820 kg/m$^3$ (Gibson and Ashby 1988, pp. 320, 321).

### 1.7.3 Indentation Testing in Bone

Indentation testing is an accepted engineering method for studying the material or structural properties of an item, be it concrete, wood, foam, or bone. There are many examples in the literature of indentation tests being done in bones from various skeletal sites, generally with the intention of improving the design or performance of implants. A brief overview of this literature is provided here.

Some of the bones that have been tested using indentation include the tibia (shinbone – Behrens et al. 1974, Hvid et al. 1983 (proximal); Aitken et al. 1985 (distal)), the patella (knee cap - Weaver 1966), the femur (thighbone – Hardinge 1949 (proximal); Nakabayashi et al. 1994 (distal)), the glenoid (shoulder socket – Frish et al. 1997; Anglin et al. 1999) and the vertebrae (Perey 1957, Kumar et al. 1993, An 1999).

A variety of indenter shapes and sizes have been employed, including flat-faced cylindrical indenters, conical indenters and spherical indenters. There were also variations in indenter size, indentation depth and test rate. In most cases the overlying cortical or subchondral bone was removed, leaving only the trabecular bone to be tested. This was done either to provide access to the bone that would be in contact with the implant being studied, or to provide a level surface for indentation.

Indentation tests done in bone provide information on the local structural properties (i.e. those at the test site) by generating a load-displacement curve, from which the failure load and stiffness can be extracted (Figure 1.10). The structural, rather than material, properties are measured, since the indenter is deforming the bony shell and/or underlying trabeculae, rather than a uniform piece of bone, thus, in the vertebra the resulting load-displacement curve represents the combined structural responses of the endplate and trabecular components.

Since trabecular bone is, in essence, an open-celled foam, one would expect its general behaviour to match that given in the material testing literature for such foams. Gibson and Ashby (1988, pp. 146-153) provide a comprehensive overview of indentation testing in foams, from which the following information was extracted:

> Since the foam cells collapse when a foam is compressed, there is very little lateral spreading of the material under the indenter (typically the ratio of lateral spreading to axial compression is 0.04). This lack of lateral expansion means that the material in the plastic zone is not constrained by the surrounding material, thus the indentation test becomes equivalent to a direct compression test for foams with relative densities of less than about 0.3, when using a flat-faced punch.
>
> An open-celled foam can be idealised as a network of rods. During an indentation test the rods fracture one after the other as they are deflected by the indenter. If the space between the rods is large enough, the broken pieces fall between the remaining rods, away from the contact area. Otherwise, the broken pieces build up below the indenter and help to distribute the load, thus increasing the compressive strength of the foam.

In this study the endplate was left intact for the majority of the tests, thus there is the added complexity of a shell covering the underlying core of foam. This shell would tend to distribute the load more evenly over the underlying cells until the shell itself fails.

## 1.8 Objectives

### 1.8.1 General

This study attempts to provide information that will help spine surgeons and engineers to improve the outcomes of interbody fusion surgery by reducing the incidence of subsidence. The information gathered may also prove useful for improving our understanding of spinal fracture, and bone and disc degeneration.

### 1.8.2 Specific Hypotheses

This study tests the following hypotheses:

a) There are regional variations in the structural properties of the lower lumbosacral endplates (L3-S1).

b) These variations are different in the superior and inferior lumbar endplates.

c) The variations are affected by spinal level.

d) Bone mineral density (as measured by a lateral DEXA scan) affects the structural properties and their distribution.

e) Disc degeneration (graded using the Nachemson scale) affects the structural properties and their distribution.

f) Endplate removal affects the structural properties and their distribution.

## 1.9 Scope

This study identifies variations in the structural properties (failure load and stiffness) of the bony endplates in the lower lumbosacral spine (L3-S1), and the effects of bone density, disc degeneration and endplate removal on those properties. Further tests are required to determine if the results are applicable to other regions in the spine. The clinical and design implications of the results are discussed, along with recommendations for future studies that would increase the usefulness of the data.

# Chapter 2

# Experimental Methods

## 2.1 Materials

Seventy-seven endplates from the lower lumbar spine (L3-S1) of eleven human cadaveric specimens were chosen for inclusion in this study. The spines were selected based on lateral radiographs to represent a range of degenerative states, from "healthy" (good delineation of vertebrae, large disc spaces of approximately uniform height, no osteophytes, no osteoporotic fractures) to badly degenerated (osteophytes, decreased disc height, and/or osteoporotic fractures elsewhere in the spine (not in L3-S1)) (Clinical Terms, p. 7). The radiographs were taken using a Techmobile mobile x-ray machine [Picker Dunlee Corp., Bellwood, Illinois] at a distance of 1 m from the table with 60 kV at 5 mAs. Based on the x-rays, three spines were considered healthy, three showed signs of disc degeneration, two showed evidence of osteoporosis, and three showed evidence of both disc degeneration and osteoporosis (Table A.2, Appendix A).

The age of ten of the eleven donors was known. The ages ranged from 48 to 90 years, with a mean age of 74.6. Three donors were female and eight were male. Additional specimen information is provided in Table 2.1, and more detailed information is provided in Appendix A.

**Table 2.1: Specimen Information**

Specimen #: The laboratory inventory number assigned to the donor from whom the specimen was taken.

DD: Disc degeneration based on Nachemson's macroscopic grading scale (1 through 4) (section 2.3.4). A lower grade indicates a healthier disc.

DEXA: Dual energy x-ray absorptiometry, a measurement of bone mineral density in $g/cm^2$ (section 2.3.2). A higher DEXA value indicates stronger bone. DEXA is low in osteoporotic individuals.

NA: not available

| Specimen # | Age (years) | Gender | Height (cm) | Weight (kg) | Mean DD | Mean DEXA | Cause of Death |
|---|---|---|---|---|---|---|---|
| 1004 | NA | M | NA | NA | 2.9 | 0.616 | NA |
| 1007 | 83 | M | 190.5 | 68.0 | 4.0 | 0.619 | Coronary artery disease |
| 1008 | 58 | F | 162.6 | 52.1 | 2.1 | 1.117 | End-stage liver disease |
| 1010 | 84 | M | 177.8 | 61.2 | 3.6 | 0.650 | Sepsis, pneumonia, lung cancer (metastasis) |
| 1012 | 62 | M | 167.6 | 54.4 | 2.4 | 0.638 | Liver cancer (metastasis) |
| 1014 | 48 | M | 167.6 | 77.1 | 2.0 | 0.735 | Head injury (motor vehicle accident) |
| 1017 | 84 | M | 190.5 | 59.0 | 3.7 | 0.709 | Alzheimer's disease |
| 1018 | 72 | F | 157.5 | 54.4 | 3.4 | 1.021 | Leukemia |
| 1019 | 85 | M | 167.6 | 73.5 | 3.6 | 0.613 | Unknown |
| 1021 | 90 | M | 167.0 | 69.9 | 4.0 | 0.719 | Myocardial infarction |
| 1023 | 80 | F | 158.0 | 60.0 | 2.9 | 0.299 | Second cerebrovascular accident |

Of the 77 endplates originally selected for inclusion in this study, five were too badly degenerated to be tested. Level L3 of specimen 1012 contained an undetected crush fracture which affected the test results for both endplates, and the S1 vertebra of specimen 1012 had degenerated to the point that very little of the endplate remained. The anterior third of the S1 vertebra in specimen 1023 had detached from the specimen, and the inferior endplate of the L5 vertebra in the same specimen had degenerated to the point that none of the endplate remained. These five endplates were removed from the study.

When the endplates were being cleaned, a mistake was made with one specimen, resulting in the majority of the endplate being removed prior to testing. Later tests showing that removal of the endplate affected bone strength resulted in the exclusion of this endplate (the superior L5 endplate of specimen 1019) from the analysis.

Nine specimens were used to study the effects of removing the endplate on bone strength, leaving 62 endplates from 11 donors in the endplate mapping study. One of the nine specimens used in the endplate effect study (the S1 endplate of specimen 1008) was excluded due to problems encountered during testing (the indenter was found to be slipping in the chuck). The second S1 endplate (from specimen 1018) was also removed from the study due to the very different shapes of the lumbar and sacral endplate maps. This left seven endplates in the study addressing the effects of endplate removal.

All specimens were stored fresh frozen in heat-sealed bags at –20°C.

## 2.2 Experimental Protocol

The experimental protocol is summarised in Table 2.2. The specimens were dissected and appropriately prepared for the mechanical testing procedures using standard surgical and woodworking tools. The structural properties of the specimens were determined using a custom-made uni-axial testing machine to perform indentation tests at standardised test sites. An in-house C program was used to determine the failure load and stiffness of the bone at each test site. The test results were analysed using the Statistica 5.1 H software package [StatSoft, Inc., Tulsa, Oklahoma], to look for differences in failure load and stiffness in the different endplate regions tested, and examine the effects of several variables on the test results. The experimental protocol is presented in more detail in the remainder of this chapter.

**Table 2.2: Experimental Protocol Summary**

***1. Select and Prepare Spines for Testing***

Use lateral x-rays of spines to look for evidence of osteoporosis and/or disc degeneration
Select spines ranging from healthy to badly degenerated (disc degeneration, osteoporosis) based on lateral x-rays
Section spines between L2 and L3 to separate the segment used in this study (L3-S) from the rest of the spine
Bag L3-S spine segments with rice for DEXA scanning
Take lateral DEXA scans of spine segments to record bone density of the top and bottom half of each vertebra
Section spines into individual vertebrae by making central transverse cuts through the intervertebral discs

***2. Test Individual Endplates***

Photograph cut surfaces of the disc for use in grading disc degeneration
Grade disc degeneration using Nachemson's scale (Nachemson 1960)
Clean the disc and cartilage material off the endplate using a scalpel
Photograph the clean endplate to record any pre-test anomalies
Measure the anterior-posterior and lateral-lateral dimensions of the endplate
Calculate the correct locations of the test sites based on the endplate dimensions
Mount the vertebra in the orienter with the endplate to be tested facing up
Level the endplate on the x-y table using a tripod bubble level
Locate the centre of the endplate using the posterior longitudinal ligament and endplate dimensions
Test the endplate
Photograph the tested endplate as a record of test results and the location of test sites relative to any anomalies
Remove the vertebra from the orienter
Return the specimen to the freezer in a heat-sealed bag

## 2.3 Specimen Preparation

### 2.3.1 Section the Spine

Once the specimens had been selected for inclusion in the study based on their radiographic appearance, they were sectioned to separate the lower lumbar spine (L3-S, Figure 1.3) from the rest of the spine. The lower spine was cleaned of any remaining muscle tissue using a scalpel, then the L2-L3 intervertebral disc was sectioned transversely thorough the middle using a knife with a 7 cm-long blade. The lower lumbar spine (L3-S) was then wrapped in plastic wrap (Saran Wrap) which was tied in place with strips of plastic wrap, then bagged with 9 cups of long-grained rice in a 28.4 cm wide plastic bag heat-sealed to a length of 33 cm. The rice was used to simulate soft tissue in the DEXA scan. The plastic wrap was used to keep the spine from becoming dehydrated by the rice. The rest of the spine (C1-L2) was placed in a heat-sealed bag and returned to the freezer. Only the L3-S1 vertebrae were used in this study.

### 2.3.2 Lateral DEXA Scan

The specimens (L3-S1) were DEXA scanned in order to determine the bone mineral density (BMD) of the endplates and underlying bone. The bone mineral density has been shown to correlate strongly with bone strength (Oxland and Lund 2000, section 1.5) and it is known to decrease in individuals with osteoporosis (Mosekilde 1993, Figure 1.8).

Lateral DEXA scans were chosen rather than anterior scans because the vertebral body is not obscured by the posterior elements in this view. Using an anterior scan would include the BMD of the posterior elements in the results, which would tend to artificially inflate the BMD of the superior endplate (Figure 1.2). The lateral scan results in more inflated BMD results in the S1 vertebra than an anterior scan would produce due to the additional bone of the sacrum on either side of the spine (Figure 1.3), however the greater accuracy in the lumbar spine seemed to justify this.

The spine segments were placed atop two bags of long-grained white rice in order to simulate soft tissue. The DEXA scanner requires a minimum amount of soft tissue in order to calibrate the scanner. Clinically, the technician will use a bag of wheat seed or rice placed beneath the patient being scanned if the patient is slender. The two bags used in this case were each 28.4 cm wide. The first contained 14 cups of rice and was sealed to give a length of 35.4 cm. The second contained 12.25 cups of rice and was sealed to give a length of 34.6 cm. Together they provided the recommended minimum soft tissue thickness of 7 cm. Each spine segment was also bagged with 9 cups of rice (section 2.3.1) in order to help support the spine segment in a lateral position and to eliminate air gaps between the spine and the underlying rice bags.

The DEXA technician scanned the entire spine segment, then manually selected the regions to be summed. Each vertebra was divided into a top and a bottom half (Figure 2.1). The BMD for each half of the vertebra was the BMD value used for the corresponding endplate. In each case the BMD of the top and bottom half of the vertebra and, in fact, throughout each entire specimen, were close in magnitude (Table A.1, Appendix A), which indicates that the method is robust (one would expect the two halves of a single vertebra to have very similar values). Each of the specimens was scanned by the same technician, using the same DEXA scanner and supporting rice bags.

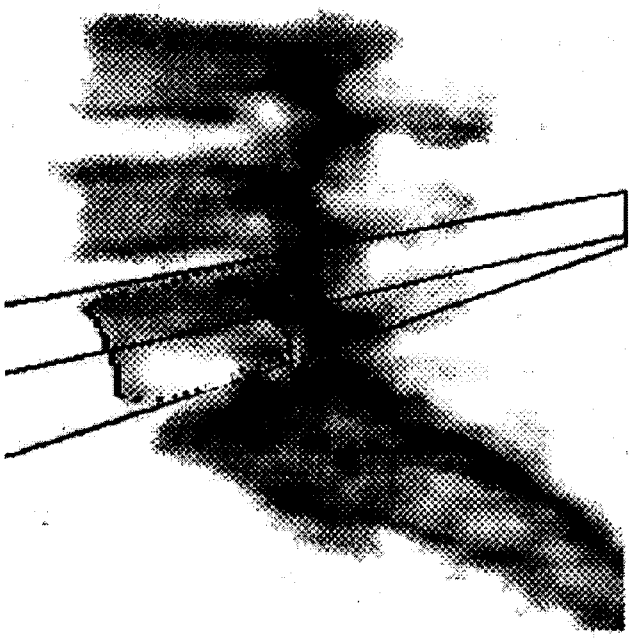

Figure 2.1: DEXA scan of specimen 1004 showing the L5 superior and inferior halves of the vertebra selected for DEXA value calculation. The dots surrounding the vertebral body show the area which was used in the calculation. The lines mark the limits of the regions which were calculated independently.

### 2.3.3 Separate Vertebrae

Once the spines had been DEXA scanned, the specimens were separated into individual vertebrae. The S1 vertebra segment was removed from the rest of the sacrum using a standard carpentry handsaw. The cut was made parallel to the S1 endplate such that the endplate would sit horizontally when potted. A knife with a 7 cm-blade was used to cut transversely through the middle of the L3-L4, L4-L5 and L5-S1 discs. A knife was used rather than a scalpel since it enabled the disc to be halved in a single cut, leaving a smooth disc surface. Each disc surface was then photographed using a Nikon Coolpix 950 digital camera [Nikon Corp., Tokyo, Japan] set to "Fine" (pixel count: 1600 x 1200) (Figure 2.2). A custom-made "unipod" (Figure 2.3) was used to hold the camera steady for these photographs. The photographs were used to grade the disc health using Nachemson's grading scale (section 2.3.4).

Figure 2.2: Photograph of the 1012 L3 superior disc used to grade disc condition. (grade 3).

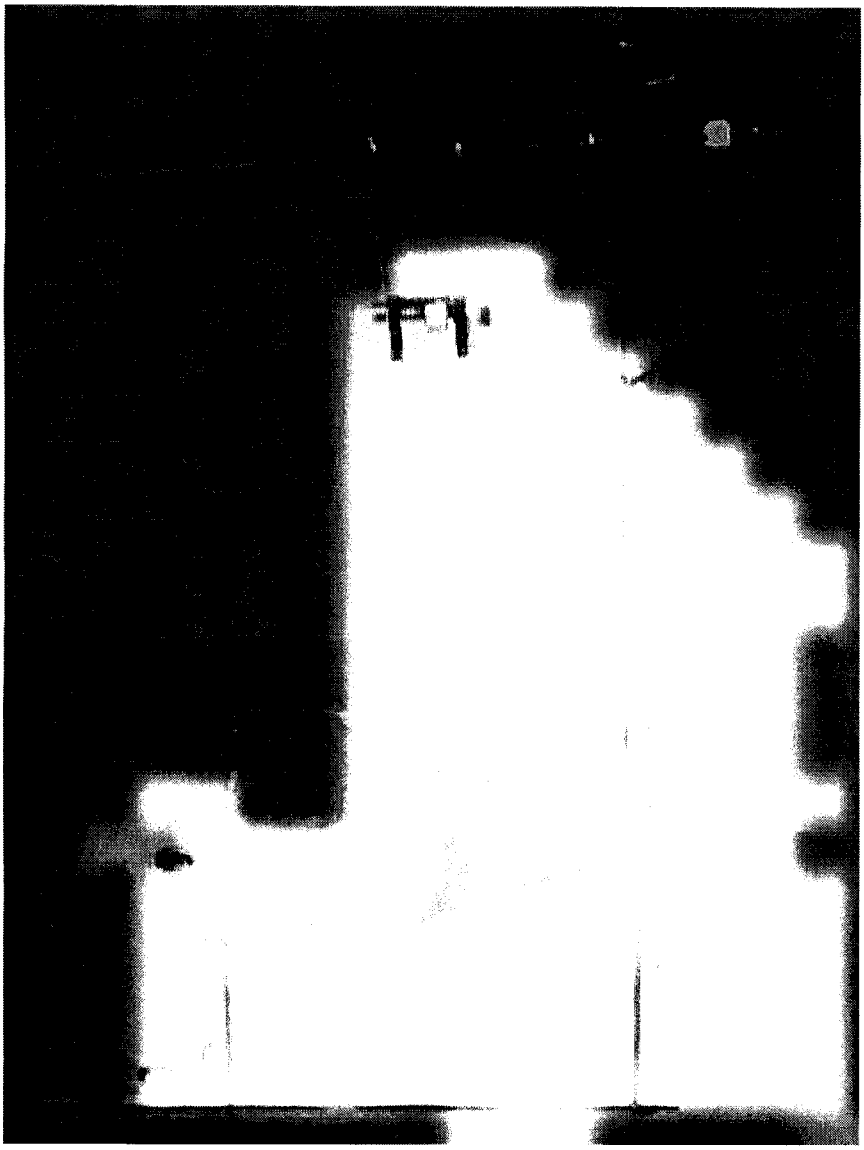

Figure 2.3: "Unipod" used to hold the camera steady while photographing the discs and the endplates.

### 2.3.4 Grade Discs

Disc condition was determined using a macroscopic grading system developed by Nachemson (Nachemson 1960) (Table 2.3). The photographs were viewed on a personal computer (with a 17 inch monitor. Both halves of the L3-L4, L4-L5 and L5-S1 discs were used to rank these discs, and only the lower half of the L2-L3 disc was used to grade this disc. Three people graded the discs, following a training session designed to equalise the rankings. The three graders were Dr. Thomas Oxland, an Associate Professor of Orthopaedic and Mechanical Engineering who did his PhD in spine biomechanics, Dr. Marcel Dvorak, a Clinical Assistant Professor and the Academic Head of the Spine Division at UBC, and Pamela Grant, the Master of Applied Science student working on this project. In no case did the ratings differ by more than one point. The disc grade used for the study was the majority ranking from among the three rankings. The rankings of each grader and the pooled rankings are given in Table A.4, Appendix A. Due to the advanced age of most specimens, only one disc was given a grade of 1. For the purpose of analysis, this specimen was included in the grade 2 disc group, since a single specimen provides insufficient statistical power to make any valid observations.

**Table 2.3: Nachemson's Disc Grading Scale (Nachemson 1960)**

**Grade 1:**

- shiny, gelatinous nucleus pulposus
- nucleus easily delimited from annulus
- annulus free of macroscopic ruptures or discolouration

**Grade 2:**

- macroscopic changes present only in nucleus
- nucleus somewhat more fibrous
- nucleus still distinct from annulus
- annulus fibrosus intact

**Grade 3:**

- macroscopic changes in nucleus and annulus
- nucleus more fibrotic but still soft
- boundary between nucleus and annulus not distinct
- isolated fissures in annulus fibrosus

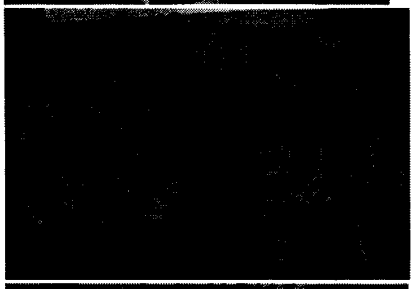

**Grade 4:**

- severe macroscopic changes in nucleus and annulus
- fissures and cavities in nucleus and annulus
- marginal osteophytes often found on vertebrae

### 2.3.5 Clean Endplates

After the discs had been photographed, the endplates were cleaned. The disc material and cartilage covering the bony endplate were removed using a scalpel. Care was taken to avoid damaging the endplate during the cleaning process (Figure 2.4).

Figure 2.4: Cleaned endplate

The anterior-posterior and lateral-lateral dimensions of each cleaned endplate were measured using Vernier callipers. These measurements were used to locate the centre of the endplate and to define the locations of the test sites (section 2.4). The anterior-posterior dimension (AP) was defined as the distance between the most anterior point of the vertebral foramen (above the centre of the posterior longitudinal ligament) and the most anterior point on the vertebral body (the point lying on the line perpendicular to the posterior border of the endplate, running through the centre of the posterior longitudinal ligament (PLL) (Figure 2.5). The centre of the endplate is the midpoint of this line.

The lateral-lateral dimension (LAT) was defined as the length of the line perpendicular to AP, joining the two most lateral points on the endplate (i.e. the line through the widest part of the endplate).

These two dimensions were defined using the landmarks described above in order to make the measurements repeatable and to ensure that they were consistent between specimens.

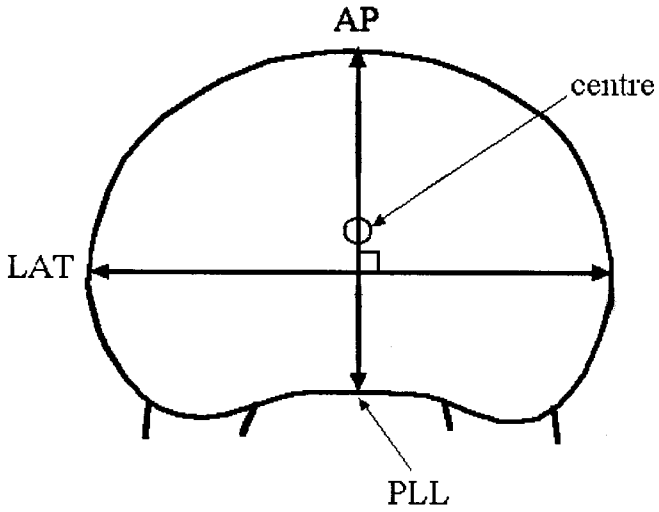


Figure 2.5: Endplate dimensions:
AP = anterior-posterior dimension (mm)
LAT = lateral-lateral dimension (mm)
PLL = posterior longitudinal ligament
centre = location of test site (0% AP,0% LAT)

### 2.3.6 Photograph Endplates

When each endplate had been cleaned, it was photographed, again using a Nikon Coolpix 950 digital camera [Nikon Corp., Tokyo, Japan] set to "Fine" (pixel count: 1600 x 1200) (Figure 2.4). These photographs were taken to record any anomalies in the endplate that might affect the test outcomes.

### 2.3.7 Pot Specimen

In order to hold each specimen securely during the testing procedure, the aluminium potting device used to attach the specimen to the testing machine and to level the endplate (section B.1, Appendix B) was filled with plaster of Paris (about 125 mL plaster and 50 mL water) and the vertebra was placed within, with the endplate to be tested uppermost. Before placing the vertebra in the plaster it was wrapped in plastic wrap (a piece about 30 cm long by 30 cm wide) to protect the lower endplate from infiltration by the plaster (Figure 2.6). An elastic band was used to secure the plastic wrap tightly around the anterior body and posterior elements of the vertebra such that no gaps would be left between the vertebra and the plaster. Any gaps would increase the likelihood that the vertebra would move within the plaster cast, thus giving erroneous stiffness values. This potting method was found to be a reliable way of holding the specimen securely without damaging the vertebral body or the endplate not being tested.

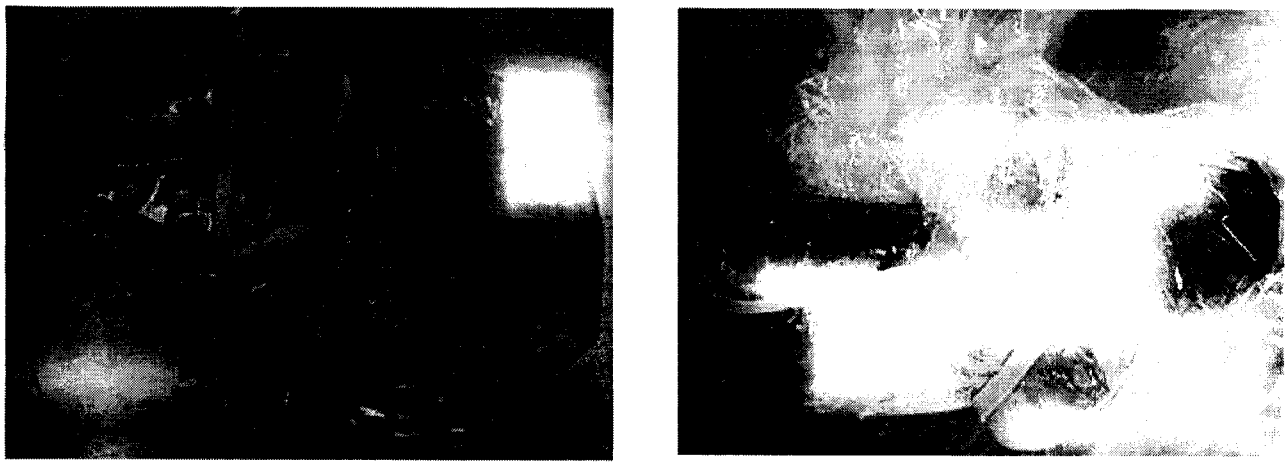

Figure 2.6: A vertebra wrapped in plastic secured with an elastic band: a) endplate which will be in the plaster, b) lateral view, endplate to be tested upright.

A chisel was used to aid in visually orienting the vertebra such that the posterior margin of the endplate would be perpendicular to the side of the potting device. The chisel was held with the cutting edge parallel to the side of the rectangular potting device and the vertebra's position within the potting device was adjusted until it was parallel with the side of the chisel (perpendicular to the potting device wall) (Figure 2.7).

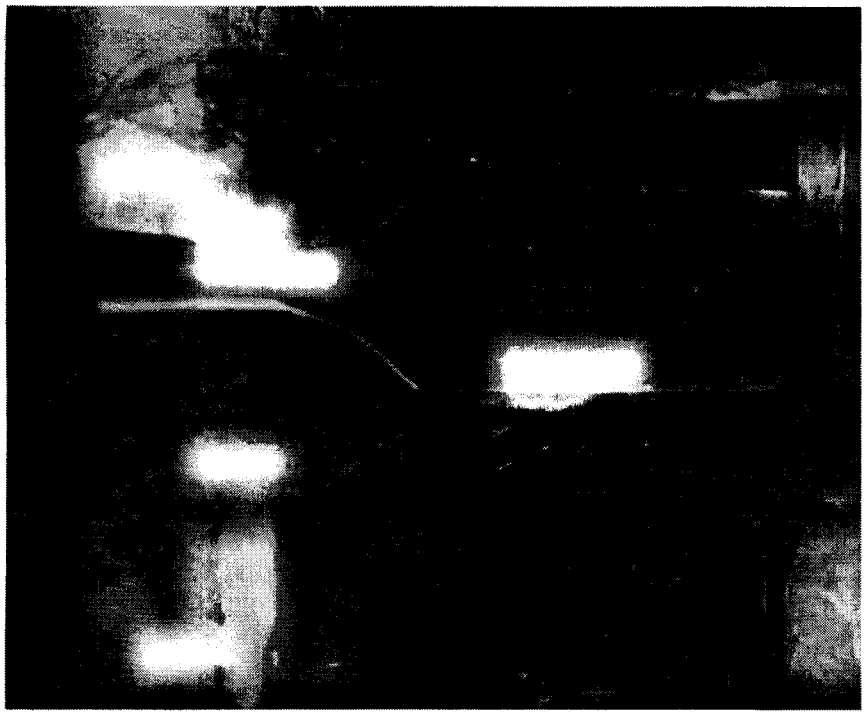

Figure 2.7: Using a chisel to position the vertebra within the orienter such that the posterior margin of the endplate is perpendicular to the orienter wall.

The plaster covered approximately half of the vertebral body and posterior elements when the vertebra was placed in the orienter. A small paddle was used to cover the posterior elements and the flared base of the vertebral body with plaster anywhere that they were visible above the plaster. This closed any gaps formed as a result of repositioning the vertebra and ensured that there would be resistance to any tensile forces placed on the vertebra during indenter retraction.

The exposed endplate was sprayed with distilled water and the Saran Wrap was closed over the top of the vertebra to keep it from drying out. Care was taken to ensure that the vertebra was not moved when the Saran Wrap was closed. The plaster was left to dry for a minimum of 1 hour prior to testing.

After the plaster had dried, the snugness of the casting was tested by manually attempting to move the vertebra within the cast. If the vertebra could be moved (very rare), it was broken out of the potting device using a chisel and the potting procedure was repeated.

To give an indication of the amount of contact between the lower endplate and the plaster, the cast remaining after a specimen was removed from the orienter is shown in Figure 2.8.

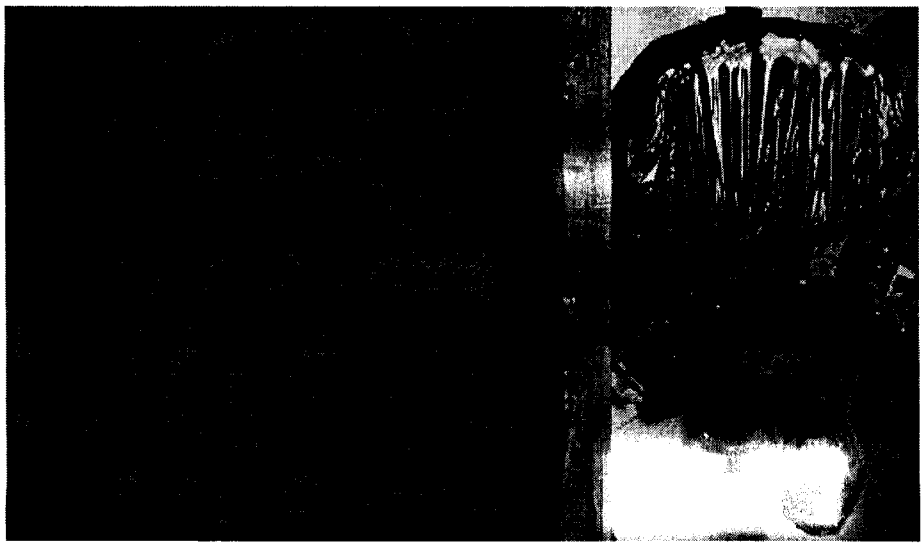

Figure 2.8: Plaster cast showing imprint left by a specimen. This shows that the loads applied during testing were well distributed over the lower endplate.

### 2.3.8 Level the Endplate on the Test Machine

Once the specimen had been successfully potted it was taken to the test machine and placed on three adjustable legs attached to the xy-translating table (Figure 2.9). The leg length was adjusted until the endplate appeared to be level. At this point a tripod bubble level (section B.2, Appendix B) was used to refine the orientation of the endplate. The bubble level was placed in the centre of the endplate and the leg length adjusted until the bubble was centred (Figure 2.10). Locking nuts were then placed on the legs and tightened using a wrench. The orienter was checked manually to ensure there was no play in the system.

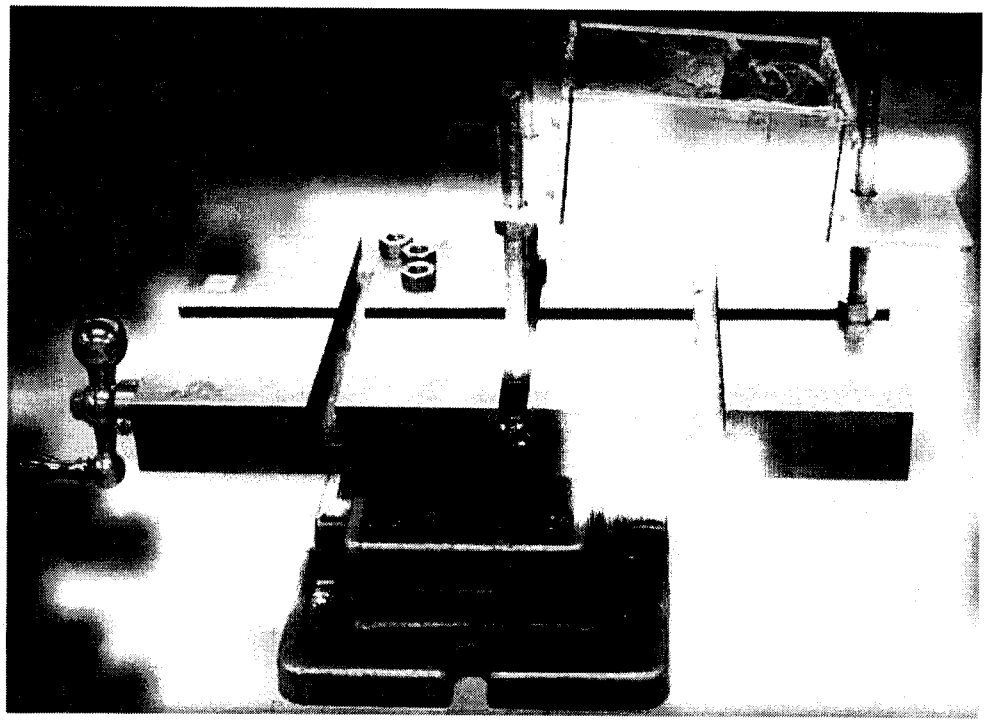

Figure 2.9: Orienter mounted on the xy-translating table, ready to be levelled

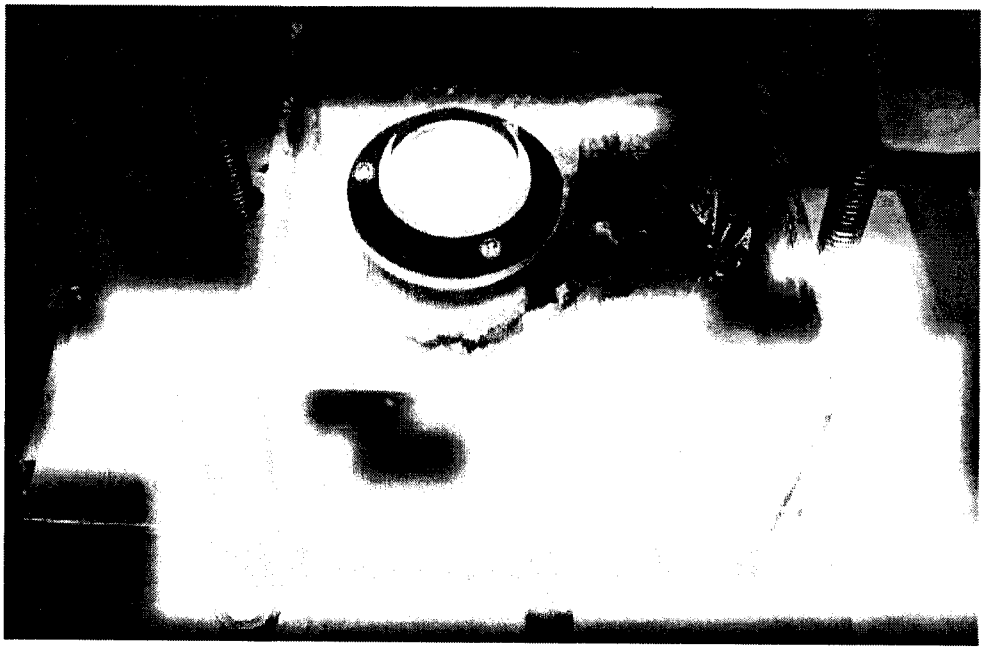

Figure 2.10: Tripod bubble-level on an endplate ready to be levelled

### 2.3.9 Half-Endplate Specimens

The nine specimens that were used to look at the effects of endplate removal had two additional preparatory steps. Once the specimen had been potted it was taken to the test machine and the endplate was levelled in the manner described above. The specimen was then taken from the test machine and half of the endplate was removed using a Model 395 variable speed Dremel rotary tool, with a flex-shaft extension and #191 (3.175 mm-diameter spherical) engraving bit [Dremel, Racine, Wisconsin] (Figure 2.11; section B.5, Appendix B). Care was taken to remove the minimum amount of material necessary to expose the trabeculae underlying the bony endplate (approximately 0.5 to 1 mm). A toothbrush and distilled water were used to remove the marrow and bone particles from between the exposed trabeculae.

The specimen was photographed when the endplate had been removed, then returned to the test machine for testing.

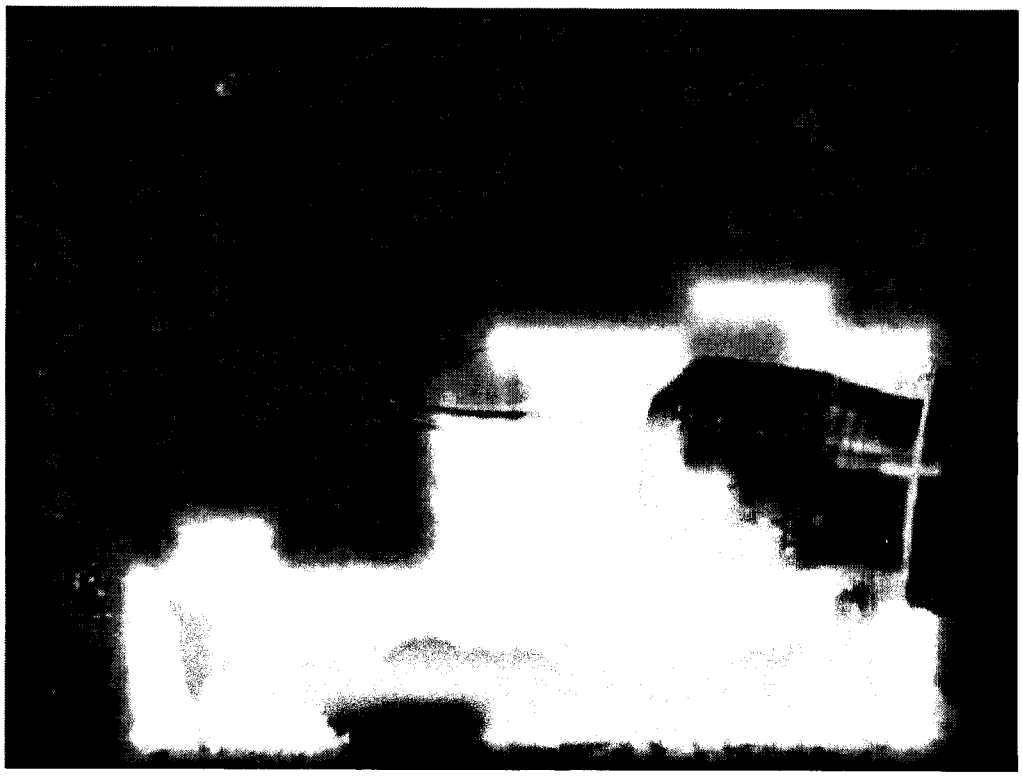

Figure 2.11: Half of the endplate removed using a Dremel rotary tool

## 2.4 Endplate Testing

### 2.4.1 Test Layout and Indenter Selection

The layout of test sites was chosen to maximise the number of tests per endplate while leaving enough space between test sites to avoid interaction. A grid pattern superimposed on the ovoid endplate. was chosen for two reasons: a rectangular grid (test sites defined by their AP and LAT distance from the centre) could be defined more repeatably on the endplate surface than a polar grid (test sites defined by their distance from the centre and their angle relative to a base line), and the rectangular grid was more

intuitive for interpreting the results. The grid defining the test locations was scaled based on the endplate dimensions in order to standardise the test sites for comparison between specimens (section 2.4.1.4).

Once the rectangular grid had been settled upon as the layout of choice, it was necessary to determine the appropriate spacing of the test sites, based on the endplate dimensions. Before the spacing could be set, an indenter size had to be chosen. A series of tests were done in embalmed bone to determine the best indenter shape, how small the indenter could be made, and how close the holes could be to one another.

### *2.4.1.1 Indenter Shape*

The four indenter shapes considered were a flat-faced cylinder, a hemisphere, a cone, and a sharp "pin". After examining the endplates of several vertebrae, it became obvious that most endplates are not simply a flat surface, but are rather a concave "bowl", with or without a raised peripheral ring. Since the vertebra surface is not level, a flat-faced indenter would not contact the surface evenly and would tend to break through at one edge before the other in an unpredictable fashion (Figure 2.12). This ruled out the use of a flat-faced cylindrical indenter.

The internal structure of the vertebra was considered next. The vertebra is not a continuous solid. It is actually a shell of denser bone surrounding a core of strut-like trabeculae. A sharp indenter would tend to give imprecise results, since it could intersect more struts at one test site than another. This eliminated pin and cone-shaped indenters, leaving the hemispherical indenter as the shape of choice.

A hemispherical indenter would tend to have a more uniform contact profile, contact area and contact volume than either a flat-faced cylindrical or conical indenter, when being pressed into a sloping surface (Figure 2.12). It would also have more uniform contact with the trabeculae underlying the endplate than either a conical or pin-shaped indenter.

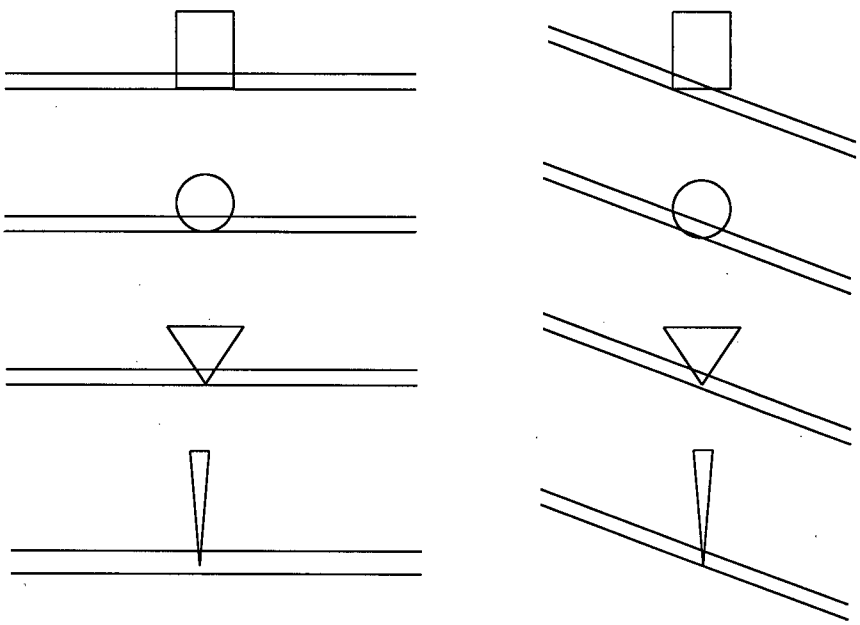

Figure 2.12: Possible indenter shapes and their interactions with level and inclined surfaces

### *2.4.1.2 Indenter Size*

The final consideration was indenter size. As stated previously, bones are not composed of a continuous material, thus an indenter large enough to overlap several trabecular cells is required to obtain consistent results (i.e. results that are not biased by the position of the indentation site relative to the underlying trabeculae). On the other hand, in order to maximise the amount of data obtained on the property distributions of the endplate, the indenter size had to be minimised so that a large number of tests could be performed on each endplate. For this reason, the maximum acceptable indenter size was set at 4 mm. A search of the literature was used to get a basic idea of the distance between the trabeculae.

Goulet et al. (1994) found that the distance between trabeculae in cubes of bone taken from various bones, including vertebrae, ranged from 0.32-1.67 mm, with a mean value of 0.64 mm and standard deviation of 0.24 mm.

Since the spacing varies with bone region (within and between bones), individual, pathology (e.g. osteoporosis) and possibly spinal level, to get a better indication of the trabecular spacing in the vertebral body adjacent to the endplates, journal figures showing sections through both normal and osteoporotic vertebrae (Amstutz and Sissons 1969, Jayasinghe et al. 1994, Silva, et al. 1994, Amling et al. 1996, Oda et al. 1998, Peretz et al. 1998) were examined, and a series of embalmed vertebrae were sectioned using a rotary-blade diamond saw, then examined using a stereomicroscope. Based on these observations it was estimated that an indenter of approximately 2 mm diameter would be required to give adequate trabecular coverage (several trabeculae under the indenter, regardless of indenter placement) (Figure 1.7).

A series of indenters made of chrome steel balls [Small Parts Inc., Miami Lakes, Florida] from 1 mm to 4 mm in diameter, in half-millimetre increments, and hollow stainless steel tubes [Small Parts Inc., Miami Lakes, Florida] were assembled using either epoxy or Loctite Weld. These were used to perform a series of tests in embalmed vertebrae (treated with preservatives, such as formaldehyde, to preserve the tissue and kill pathogens) at 0.2 mm/s to a depth of 3 mm (section 2.4.4). Embalmed bone was used for these preliminary tests in order to save the fresh frozen specimens for inclusion in the study. The 2 mm-diameter indenters appeared to produce repeatable results, based on failure load comparisons in test sites equidistant from the central sagittal plane. In addition, cross-sections through the bone at these sites using a rotary-blade diamond saw showed that several trabecular cells were contacted at each site, thus 2 mm-diameter indenters could have been selected.

After looking at photographs of osteoporotic bone, however, it was decided that a larger indenter size might be required to obtain repeatable results in osteoporotic specimens (osteoporosis causes a loss of vertical trabeculae, thus making the distance between consecutive trabeculae greater) (Figure 1.9). The embalmed specimens tested did not show signs of osteoporotic changes, thus they would tend to favour a smaller indenter size than could be used in osteoporotic bone. A compromise was made between ensuring adequate trabecular coverage of test sites and maximising the number of test sites by choosing a 3 mm-diameter indenter.

The same indenter was used for all tests. It was constructed by silver-soldering a 3 mm-diameter chrome steel ball bearing with sphericity 0.0006 mm and Rockwell C hardness of 60-67 to a 2.77 mm-diameter, 40 mm-long stainless steel tube [Small Parts Inc., Miami Lakes, Florida; section B.4, Appendix B]. The silver-soldering was performed by a skilled individual working for an independent company.

#### *2.4.1.3 Test Spacing*

Tests were also done in embalmed lumbar vertebrae to determine the minimum distance required between test sites. It was observed that the holes produced by the indenter were the same diameter as the indenter used. A rotary diamond saw was used to section several vertebrae to look at the underlying damage to the trabeculae using a stereomicroscope. Again, only the trabeculae in the region of the hole showed signs of damage. This suggested that the "crush zone" is limited to the indentation site, with little or no peripheral damage being produced during the test.

A series of tests were done to determine how close together the holes could be before interactions were observed. After looking at the results of these tests, 3 mm was selected as the minimum separation distance. The holes could be placed closer than this, but 3 mm was chosen to incorporate a margin of error based on the fact that the trabecular structure varies between people, particularly between "normal" and "osteoporotic" individuals.

#### *2.4.1.4 Test Layout*

Once the test site distribution (grid-like), indenter shape (hemisphere), indenter size (3 mm), and minimum test site separation (3 mm) had been determined, it was possible to decide on an appropriate definition of test site locations, based on the endplate dimensions.

To ensure that the specimens could be compared to one another, the test sites were defined using percentages of the AP and LAT endplate dimensions (Figure 2.5) rather than selecting an arbitrary fixed distance between test sites. This approach accounted for the fact that each individual has different endplate dimensions but the basic transmission of load through the vertebra is relatively similar. In other words, setting the test sites a fixed number of millimetres apart would not actually test the same regions of the bone in different people

Panjabi et al.'s 1991 paper on the morphology of the lumbar vertebrae provides information on the mean and standard error of the mean of the two dimensions used to define the test sites (AP and LAT) (Table 1.1). These values were used to help select appropriate percentages such that the test sites would not interact or overlap the edges of the endplates, and to maximise the number of tests per endplate. Based on the chosen indenter size (3 mm) and minimum distance between test sites (3 mm), it was found that by dividing the AP dimension into increments of 20% and the LAT dimension 15%, it was possible to leave at least 3 mm between test sites (6 mm centre-to-centre) and 4.5 mm between the centres of the outermost holes and the edge of the endplate (Figure 2.13). This layout gave approximately 27 tests per endplate; the actual number varied due to slight variations in endplate shape (Table A.1, Appendix A). For these values to work, the endplates needed minimum dimensions of 30 mm AP and 42 mm LAT. All specimens used in the study met these minimum dimension requirements (Table A.1, Appendix A).

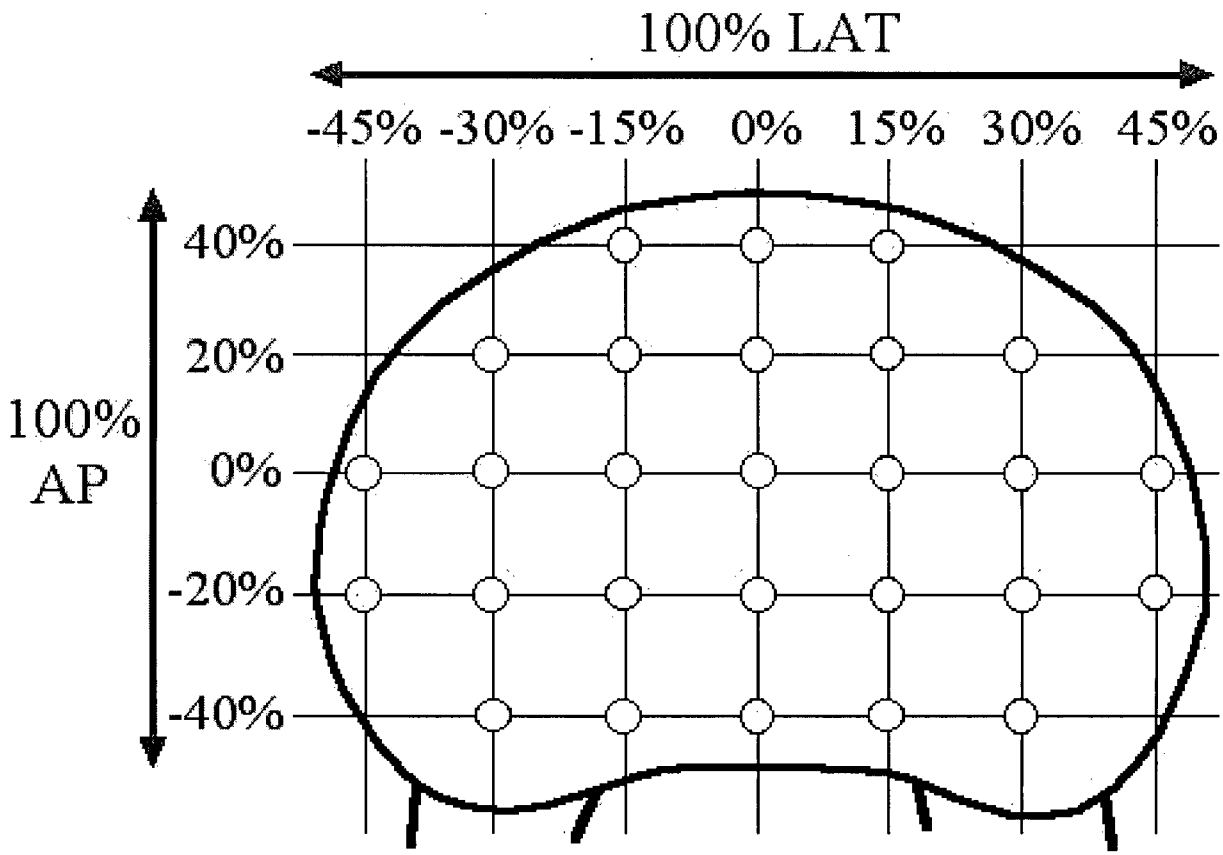


Figure 2.13: Test site layout based on endplate dimensions.

### 2.4.2 Find the Centre of the Endplate

Once the vertebra had been mounted in the test machine (as described in section 2.3.8), the xy-translating table was used to position the indenter over the centre of the posterior longitudinal ligament at the posterior margin of the endplate (Figure 2.14). A dental mirror was used to accurately view the indenter position relative to the specimen. Both the x- and y-axes of the translating table were set to zero and the y-axis was then advanced to the reading calculated to be the centre of the endplate, based on the AP measurement. A visual check was used to confirm that the correct number of revolutions had been input. If the indenter did not appear to be centred, then the centring procedure was repeated. The y-axis was then re-zeroed.

The posterior longitudinal ligament was chosen as the centre of the LAT dimension because not all vertebrae are symmetric and this was found to be the most consistent method of defining the centreline.

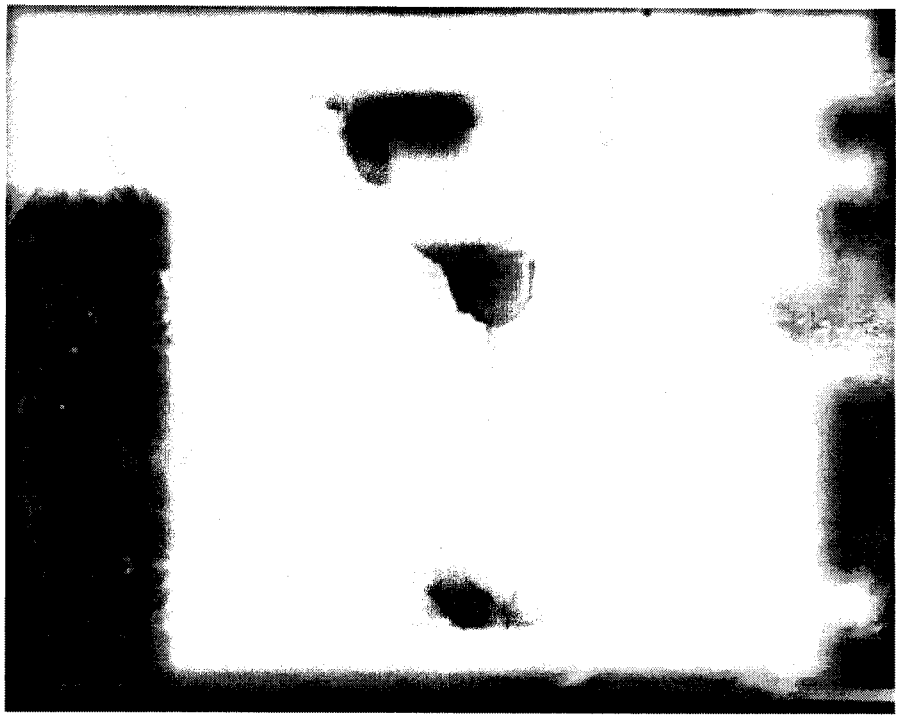

Figure 2.14: Indenter over the centre of the posterior longitudinal ligament and the posterior margin of the endplate.

### 2.4.3 Calibrate the Machine

The uni-axial test apparatus consisted of a step motor mounted on a rigid metal frame, a step motor driver, a 222 N load cell connected to a load signal amplifier, and a 3 mm-diameter hemispherical indenter held in a drill-type chuck (Figure 2.15; section B.3, Appendix B). The 222 N load cell was replaced with a 1000 N load cell for the strongest endplates (those with the highest BMD values, Table A.1, Appendix A) because there was concern that the 222 N load cell could be damaged by the anticipated higher loads.

The load and indenter position data was collected using a Galil DMC-1010 motor control card in a 486 PC at 35 Hz. The testing program was written in the Galil Motor Controller language required by the card. A copy of the program is included in section C.1, Appendix C.

Before each endplate was tested, the load cell was calibrated. A digital voltmeter was connected between the load cell amplifier output and ground and set to a sensitivity of 1 mV. The amplifier's balance was set to 0 mV. The gain was then adjusted to an appropriate value, based on the specimen BMD, and the corresponding conversion factor (N/V) was recorded on the test record sheet (section A.1, Appendix A). The conversion factor was used to convert the voltage signal of the load cell into the load transmitted through the indenter in Newtons (calibration curve shown in section B.3 Appendix B). The calibration was checked using weights.

Endplates with low BMD had lower failure loads, resulting in smaller signal-to-noise ratios than in higher BMD specimens (section B.3, Appendix B). Increasing the gain increased the signal-to-noise ratio. In specimens with higher BMD values, the range of the load cell was exceeded if the gain was set too high, thus the gain was decreased. Although this slightly increased the amplitude of the noise signal and thus artificially inflated the failure load in the higher BMD specimens, the actual difference between failure load values was such that the noise contribution had negligible effects on the BMD failure load comparisons (section B.3, Appendix B). These differences were consistent within endplates, thus the specimens acted as their own internal controls for all other comparisons.

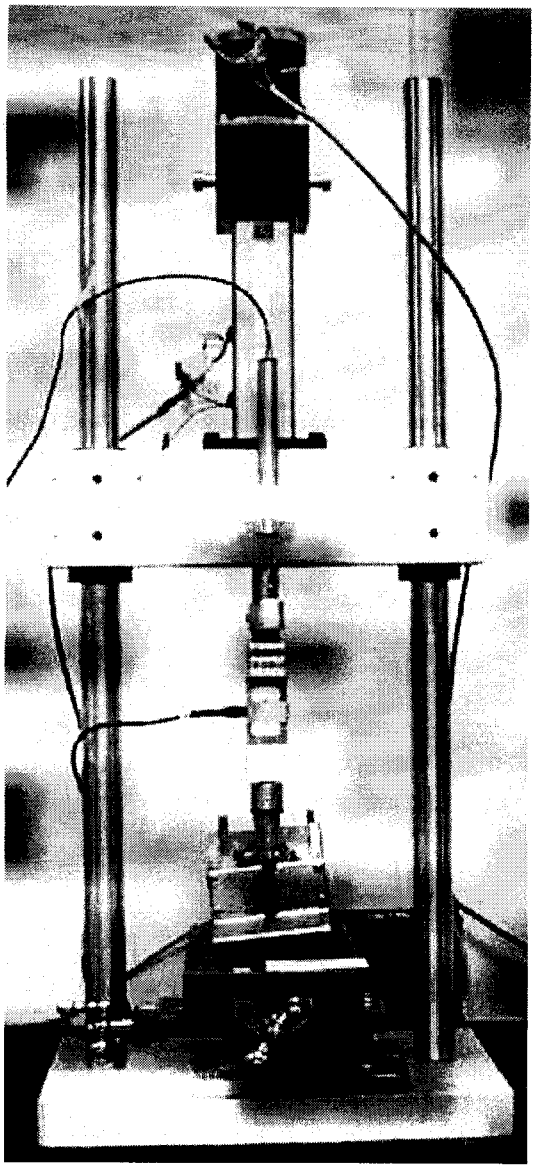

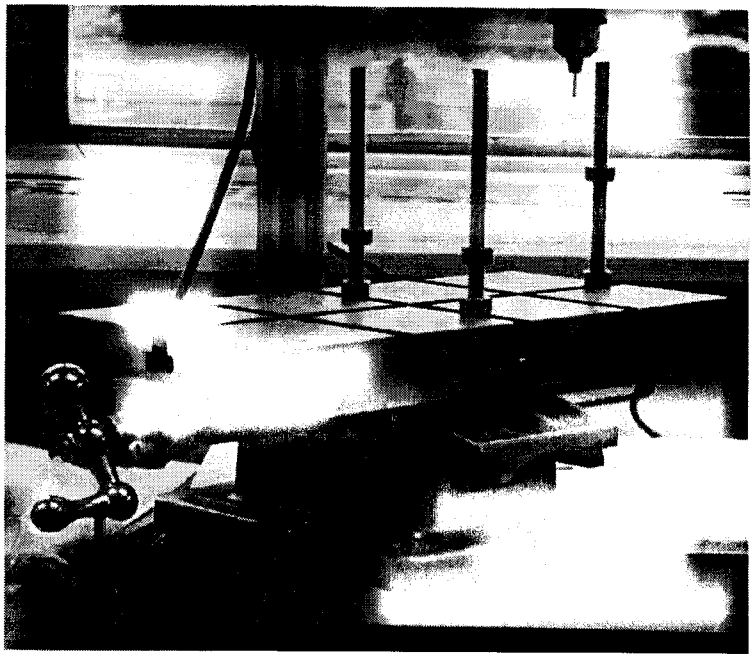

Figure 2.15: a) Entire test machine, b) Close-up showing xy-translating table (note the adjustable legs, which were used to position the orienter such that the endplate was level for testing by moving nuts up or down along the threaded legs).

### 2.4.4 Testing Procedure

#### *2.4.4.1 Test Rate*

A test rate of 0.2 mm/s was chosen as a compromise between a very slow test speed and a very rapid speed for several reasons. The large number of test sites per bone meant that test time had to be minimised to allow the tests to be completed in a reasonable amount of time, however, the subsidence of implants does not occur instantaneously, arguing for a low test rate. The rate of 0.2 mm/s was low enough to allow some gradual deformation of the bone, while making the testing time short enough to complete the tests in a timely fashion.

It should be noted that bone's deformation rate has only a small effect on the actual values of failure load and stiffness (approximately proportional to the strain rate raised to the power 0.06 (Mow and Hayes 1997, p. 84)). In addition, the same rate was used for each test. Since this study is addressing the *relative* strength values, rather than the actual values, testing rate is not crucial so long as it is consistent and slow enough to allow gradual failure of the structures.

#### *2.4.4.2 Test Depth*

A test depth of 3 mm was used for all tests. This depth was chosen in order to identify any effects based on the indenter shape, particularly the radius of the sphere used for the indenter tip. This required that the indenter penetrate the bone to a depth of greater than 1.5 mm. In addition, in a very few cases failure was not reached until almost 3 mm of displacement had been reached, thus 3 mm was chosen to ensure that each indentation test could be included in the study.

#### *2.4.4.3 Running a Test*

Once the specimen to be tested had been mounted in the machine, its centre had been located and the machine had been calibrated, the process of testing the endplate could begin. The xy-translating table was used to position the indenter over the test site. Notes were made on the specimen's test record sheet including the test site location, the name of the raw data file, and any characteristics of the test site that might cause anomalous results (e.g. a flaw in the endplate). The indenter was then lowered to within less than 0.3 mm of the endplate. A dental mirror was used to see how close the indenter was to the endplate.

The test was observed using the dental mirror and direct line of sight. Any anomalous occurrences observed during the test were recorded on the test record sheet. An Excel macro was used to convert the indenter position from motor steps to mm and the load cell output from volts to Newtons. A linear variable differential transformer (LVDT) was originally tried for recording the indenter position, but tests showed that using the step motor position was just as accurate (section B.3, Appendix B), so the LVDT was removed from the system.

The macro then plotted the load-displacement curve for the test. This curve was later used to select the curve region used for the stiffness calculation and to double-check the failure load value selected by the analysis program (see section 2.5). It also served as a check that the load cell's range had not been exceeded, and that the signal-to-noise ratio was appropriate.

The indenter was then raised a short distance, so as not to intercept the endplate during repositioning, and the xy-translating table was used to move to the next test site. This process was repeated until the entire endplate had been tested.

The endplate was sprayed intermittently with distilled water to prevent it from drying out.

When the entire endplate had been tested, it was re-photographed to provide a record of any anomalous features of the endplate and their location relative to test sites, as well as any unusual tests (e.g. larger hole than usual).

In the majority of endplates, the first test site was the central point. Testing this site first meant that the centre of the endplate could always be found, even if one lost track of the indenter's position. In the endplates not tested in the centre first the same strength profiles were seen, indicating that this did not have an effect of the results. In addition, the central point was found to have the lowest failure load and stiffness. It can be assumed that, if there was an interaction between test sites, the first site tested would be stronger than subsequent test sites. Since the central test site was found to be weaker than surrounding sites, it is therefore safe to say that this testing order did not bias the results. As well, regardless of the testing order (front-to-back, back-to-front, left-to-right, random, etc.) the same endplate profiles were found, and the specimens had laterally symmetric results (section A.5, Appendix A). This indicates that the testing order did not affect the results and that there was no interaction between the test sites using the minimum separation distance of 3 mm. It also supports the choice of a 3 mm indenter diameter (i.e. the test results were not unduly influenced by the relative position of the underlying trabeculae).

## 2.5 Data Extraction

Once all of the tests had been completed in a given endplate, the failure load and stiffness data were extracted from the raw data files. This was done using a series of in-house C programs (code and details of use provided in Appendix C).

The raw data files contained the load and displacement values describing the load-displacement curves of the test sites. In a load-displacement curve the slope of the initial (linear) region of the curve gives the stiffness, while the peak load reached prior to a load decrease gives the failure load (Figure 2.16). It was found, during the initial programming phase, that the amount of variability between tests made it difficult to automate the process of locating the appropriate curve segment for use in the stiffness calculation. For this reason, the curve segments used for calculating stiffness were chosen manually. Identifying the failure load was relatively easy to automate, however each value was checked against the corresponding graph to ensure that no mistakes were made by the program.

Each of the load-displacement curves generated during the testing process (one per test site) was reviewed by the researcher at 100% magnification on a fifteen-inch computer monitor. The linear segment of the load-displacement curve to be used for the stiffness calculation was identified using a ruler held against the monitor. The cursor was used to highlight the points corresponding to the ends of this linear segment, displaying the co-ordinates (displacement and failure load). These values were recorded for use in the data analysis program. The failure load value (the initial peak in the data) was also recorded, for use in verifying the output of the C program.

The test record sheet, used to record any anomalies related to the test, was referred to prior to analysis of the graph. Any anomalies were taken into account during the analysis process (e.g. slipping between the indenter and the endplate prior to indentation). Tests that were compromised as a result of anomalies, such as tests too close to the edge of the vertebra, were rejected.

Three C programs were used to analyse the data. All of the programs were written using CodeWarrior IDE 3.0 [Metrowerks Inc., Austin, Texas]. The first program, PALstiffness.c (section C.2, Appendix C), took as input a data file containing the names of the files containing the test results for a single endplate, along with the associated conversion factors (Newtons/Volt), and the load values bracketing the linear regions of the curves to be used for the stiffness calculations. This program returned the failure load values, the stiffness values, and the correlation coefficients ($r^2$, indicating "goodness-of-fit" of the stiffness values).

The second program, MapEndplate.c (section C.3, Appendix C), placed the failure loads, stiffnesses, and correlation coefficients in arrays based on the x- and y-values of the test sites and output this data in the form of maps (see section A.5, Appendix A). These maps were used as a way of visually analysing the results to get a basic impression of which regions of the endplate appeared to be stronger and to give some insight into the data. The statistics described in chapter 3 were used to obtain actual relationships between the endplate regions.

The third program , GenerateStatsFiles&Maps+Norm.c (section C.4, Appendix C), put the data into a format appropriate for statistical analysis using the Statistica software package. This program simply reorganised the values and output them into a series of files in the appropriate formats for the various desired analyses.

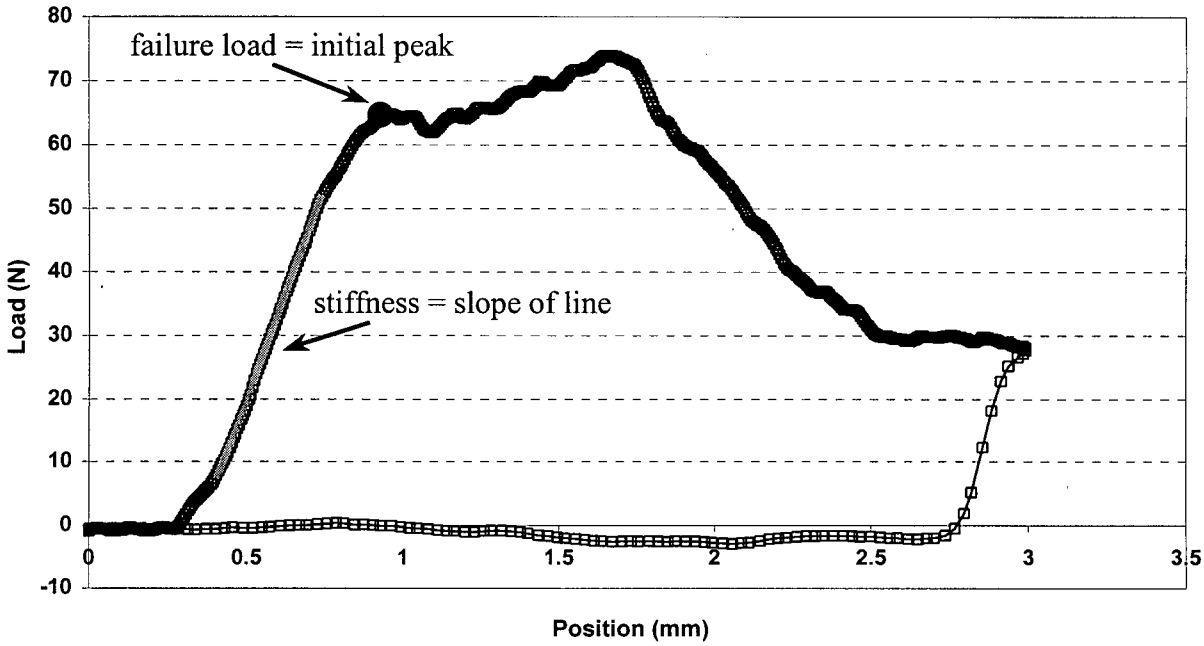


Figure 2.16: Sample load-displacement curve. The slope of the initial linear region gives the stiffness of the endplate at this test site. The initial peak gives the failure load.

## 2.6 Statistics

The Statistica 5.1 H software package [StatSoft, Inc., Tulsa, Oklahoma] was used for all statistical analysis. Separate analyses were done on the full endplate and half endplate specimens.

Linear regression was used to look at the effects of bone mineral density on failure load and stiffness.

Analysis of variance (ANOVA) was used to generate maps of the strength profiles for both stiffness and strength and to look at the effects of the different variables on these profiles. The test site AP and LAT values were used as repeated measures so that each endplate acted as its own control.

The statistics used for each analysis are described in greater detail below.

### General Notes on Interpreting Graphs, Tables and Endplate Maps

Unlike the majority of mechanical engineering studies, the material used in this research does not have standardised properties. Bone, like other biological tissues, is strongly affected by its environment and the loading conditions to which it is subjected. For this reason, there is a great deal of variation between the specimens that cannot be entirely explained by the variables that the study considered. To control for this variability, statistics were used extensively in the interpretation of the results. This section describes the statistics that were used and how to interpret the results. Readers who are familiar with analysis of variance and linear regression analysis may wish to move directly to chapter 3, where the study results are presented.

### 2.6.1 Basic Definitions

**mean:** average value
**standard deviation (SD)**: an indicator of the variability of the data, assuming it has a normal distribution
**standard error of the mean (SEM)**: range of possible means based on the uncertainty due to the standard deviation

### 2.6.2 Correct Interpretation of the p-Value

For the purposes of this study an ANOVA or a *post hoc* p-value of less than 0.05 is considered significant (i.e. there is a statistically significant difference between the means being compared). **Please note: A *non*-significant p-value does not necessarily imply that there is no difference between the means, only that no difference can be shown based on the available data.**

The actual meaning of the p-value can be summarised as follows: it is the percent probability of being wrong if one states that the factor being considered has an effect on the variable (failure load or stiffness), divided by 100, based on the available data. That is, for a p-value of 0.0080, there is a 0.8% chance of being wrong if one states that the factor had an effect on the variable.

### 2.6.3 Accounting for Variability: Repeated Measures

There was a wide range of strengths in the specimens used in this study, which introduces additional variability into the data. In order to account for these differences, the AP and LAT test site co-ordinates were used as "repeated measures" in the ANOVAs. This means that the tests within each specimen were compared to the corresponding tests in each other specimen to determine the p-values.

### 2.6.4 Analysis of Variance (ANOVA):

Analysis of variance (ANOVA) was the primary statistical tool employed in this study. In essence, an ANOVA compares the means of a set of data and indicates the likelihood that they are different. Each of the ANOVAs used in this study was a three-way ANOVA, i.e. three factors were considered. Two of the factors were the AP and LAT test site co-ordinates, which were included as repeated measures (section 2.6.3). The third factor was the primary one being considered in the comparison, for example spinal level or bone density. The variable was either failure load or stiffness.

An ANOVA returns information about the data in two forms: p-values, which indicate the probability that there are differences between the means, and graphs showing the means which were compared. For the purposes of this study, an ANOVA p-value of less than 0.05 was considered statistically significant (i.e. the primary factor had an effect on the variable).

In the study results (Chapter 3), two p-values are given for each ANOVA. The first is for the overall mean comparison, and the second is for the map shape comparison.

### *2.6.4.1 Overall Mean Comparison*

A significant p-value (< 0.05) for the overall mean comparison indicates that the primary factor (e.g. lumbar endplate) has a significant effect on the mean magnitude of the variable being considered (failure load or stiffness). To generate the means used in this comparison, the values of all of the tests done in specimens with the same primary factor (e.g superior lumbar endplate or inferior lumbar endplate) were averaged together and the resulting means were compared. If one group was significantly stronger (or stiffer) than the other, a p-value of less than 0.05 was returned.

Figure 2.17 shows the graphical results of an overall mean comparison of failure load in the superior and inferior lumbar endplates. The test sites marked in black on the endplate picture were averaged together to generate the points on the graph. Note that on the graph the inferior lumbar endplates appear to have a higher mean failure load than do the superior lumbar endplates. This difference was significant at $p < 0.0080$, thus the inferior endplates are significantly stronger than the superior endplates.

In cases where more than two points appear on the graph, a *post hoc* comparison (section 2.6.5) was required to determine which points were significantly different if a significant p-value was returned.

The overall mean comparison graphs are not shown in chapter 3, since they do not add much to the interpretation of the p-value. The means are provided in tables at the end of each section for readers who require this additional information.

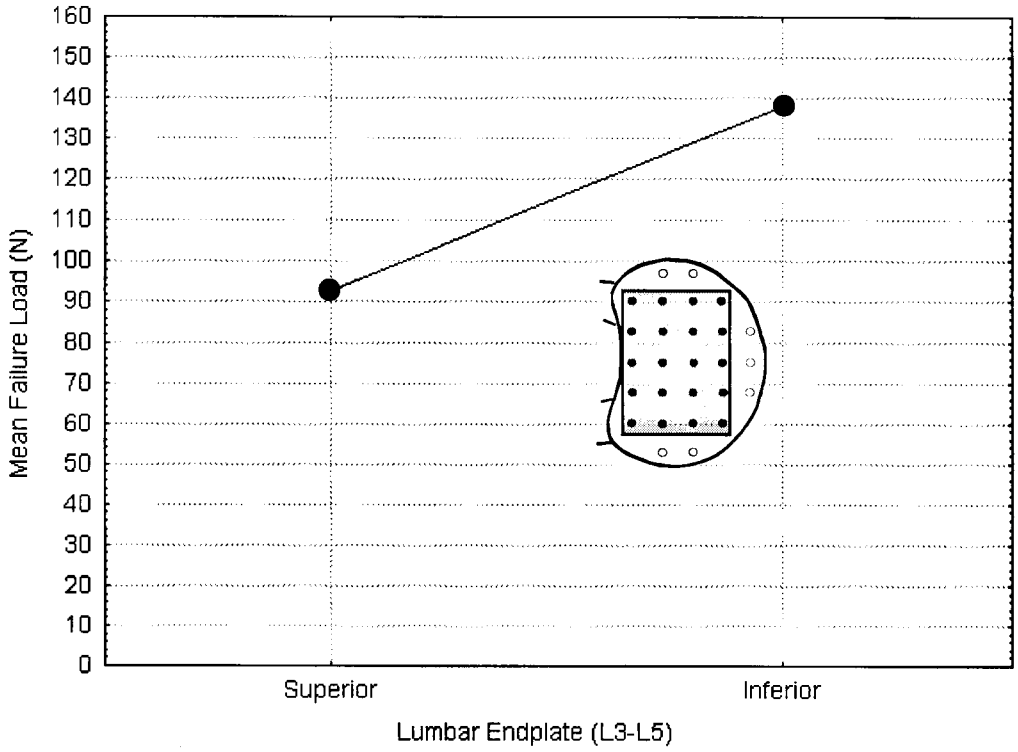


Figure 2.17: Overall mean comparison of the superior and inferior lumbar endplate failure loads in the maximum AP, LAT test site region. The test sites marked in black indicate the values which were averaged together to generate the mean failure loads shown on the graph. In this case the inferior endplates were found to be significantly stronger than the superior endplates at $p < 0.0080$.

### *2.6.4.2 Map Shape Comparison*

The ANOVA graphs shown in chapter 3 are from the ANOVAs comparing the map shapes. A significant p-value (< 0.05) for the map comparison indicates that the primary factor (e.g. lumbar endplate) has a significant effect on the AP, LAT distribution of the variable being considered (failure load or stiffness). The test site means shown in the graphs were generated by averaging the values of the variable at each test site in each map.

Figure 2.18 shows the graphical results of a failure load map shape comparison in the superior and inferior lumbar endplates. The test site marked in black on the endplate picture indicates the site from which the failure load values were taken on each endplate to generate the corresponding means marked in the graphs. Note that the shapes of the two graphs appear to be different. This difference was significant at $p < 0.0001$, thus the failure load distributions in the superior and inferior lumbar endplates were significantly different. Note that sometimes graphs that appear to have different shapes are *not* significantly different.

A *post hoc* comparison (section 2.6.5) was required to determine which points in the graphs were significantly different. These values are provided in Appendix D for most graphs.

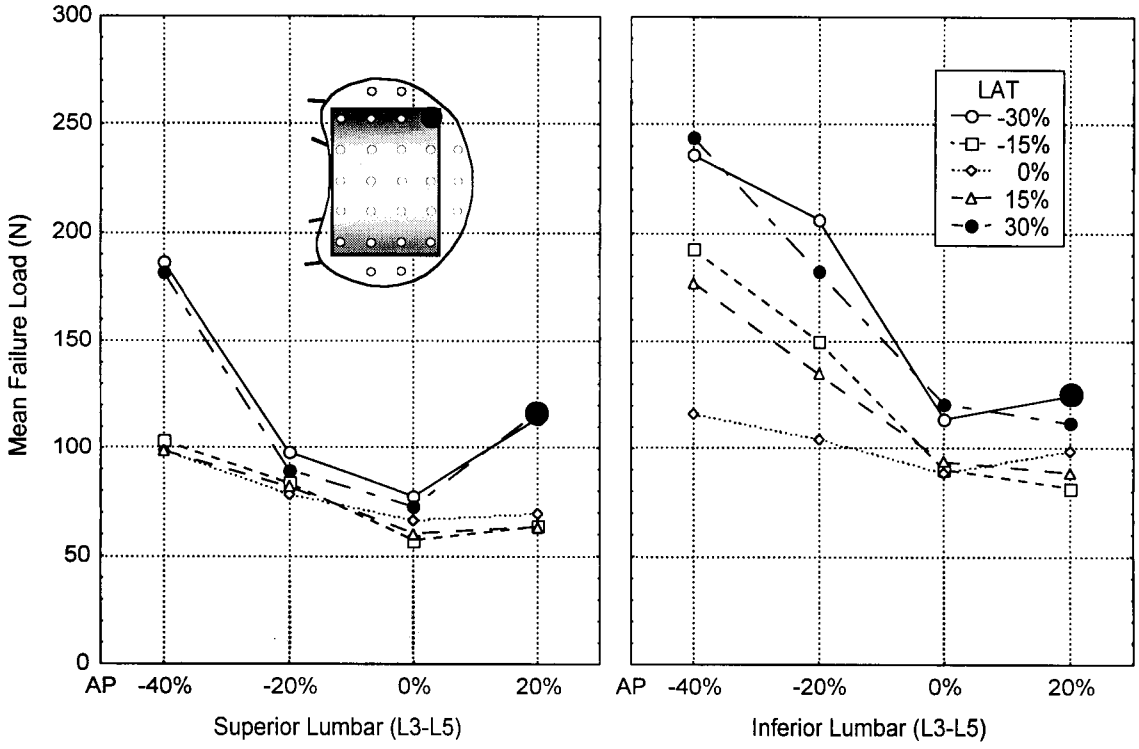


Figure 2.18: Failure load map shape comparison of the superior and inferior lumbar endplate maximum AP, LAT test site regions. The test site marked in black indicates the values which were averaged together to generate the mean failure loads marked on the graphs. In this case the map shapes were significantly different at $p < 0.0001$.

### 2.6.5 *Post Hoc* Newman-Keuls Mean Comparisons

Newman-Keuls (also known as Student-Newman-Keuls or SNK) *post hoc* comparisons were used to determine which means generated in an ANOVA were actually significantly different. The tables generated by such comparisons are given in Appendix B, where appropriate. The only exception to this is the endplate removal study, which contains the *post hoc* tables in the text for ease of comparison.

Due to the large size of each *post hoc* comparison table, they were broken into their component pieces in order to meet the thesis formatting requirements of the library, thus the "within map" comparisons (i.e. comparisons of the points in a single graph) are given separately from the "between map" comparisons (i.e. comparisons of the points in two different maps). To aid in interpretation, the ANOVA graphs associated with each *post hoc* comparison are provided with the table.

Table 2.4 shows half of the "between map" comparison table for Figure 2.18. The AP and LAT test site co-ordinates are given as percentages of the endplate dimensions. The mean values of the failure loads (FL) are shown in bold. The body of the table contains p-values indicating whether the means differ; significant p-values are shaded. The cell at the intersection of the co-ordinates for two points contains the p-value indicating whether they differ. For example, (-40% AP, 30% LAT) in the superior endplate and (-20% AP, -15% LAT) in the inferior lumbar endplate are significantly different at $p = 0.0116$ ($p < 0.05$).

Table 2.4: The first half of the Newman-Keuls *post hoc* comparison of the means in the superior and inferior lumbar endplate maximum AP, LAT failure load distributions (Figure 2.18). The full table is given in Table D.19, Appendix D. The "within endplate" comparisons for the superior and inferior lumbar endplate maximum AP, LAT failure load maps can be found in Tables D.1 and D.7, respectively.

| inferior | | AP | -40% | | | | | -20% | | | | |
|---|---|---|---|---|---|---|---|---|---|---|---|---|
| superior | | LAT | -30% | -15% | 0% | 15% | 30% | -30% | -15% | 0% | 15% | 30% |
| AP | LAT | Mean FL | **235.8** | **192.4** | **116.0** | **177.1** | **243.9** | **206.3** | **150.1** | **104.6** | **134.7** | **182.1** |
| -40% | -30% | **186.4** | 0.0000 | 0.5798 | 0.0000 | 0.8309 | 0.0000 | 0.1618 | 0.0080 | 0.0000 | 0.0001 | 0.6960 |
| | -15% | **103.1** | 0.0000 | 0.0000 | 0.8484 | 0.0000 | 0.0000 | 0.0000 | 0.0009 | 0.8936 | 0.1075 | 0.0000 |
| | 0% | **98.8** | 0.0000 | 0.0000 | 0.7016 | 0.0000 | 0.0000 | 0.0000 | 0.0002 | 0.8577 | 0.0405 | 0.0000 |
| | 15% | **98.5** | 0.0000 | 0.0000 | 0.7509 | 0.0000 | 0.0000 | 0.0000 | 0.0002 | 0.9447 | 0.0430 | 0.0000 |
| | 30% | **181.4** | 0.0000 | 0.7452 | 0.0000 | 0.6924 | 0.0000 | 0.1523 | 0.0116 | 0.0000 | 0.0001 | 0.9500 |
| -20% | -30% | **97.9** | 0.0000 | 0.0000 | 0.8216 | 0.0000 | 0.0000 | 0.0000 | 0.0002 | 0.9903 | 0.0475 | 0.0000 |
| | -15% | **83.5** | 0.0000 | 0.0000 | 0.1809 | 0.0000 | 0.0000 | 0.0000 | 0.0000 | 0.7409 | 0.0005 | 0.0000 |
| | 0% | **78.4** | 0.0000 | 0.0000 | 0.0642 | 0.0000 | 0.0000 | 0.0000 | 0.0000 | 0.5177 | 0.0001 | 0.0000 |
| | 15% | **81.8** | 0.0000 | 0.0000 | 0.1338 | 0.0000 | 0.0000 | 0.0000 | 0.0000 | 0.6771 | 0.0003 | 0.0000 |
| | 30% | **89.6** | 0.0000 | 0.0000 | 0.4313 | 0.0000 | 0.0000 | 0.0000 | 0.0000 | 0.9074 | 0.0042 | 0.0000 |
| 0% | -30% | **77.4** | 0.0000 | 0.0000 | 0.0523 | 0.0000 | 0.0000 | 0.0000 | 0.0000 | 0.4808 | 0.0001 | 0.0000 |
| | -15% | **57.2** | 0.0000 | 0.0000 | 0.0000 | 0.0000 | 0.0000 | 0.0000 | 0.0000 | 0.0032 | 0.0000 | 0.0000 |
| | 0% | **66.0** | 0.0000 | 0.0000 | 0.0011 | 0.0000 | 0.0000 | 0.0000 | 0.0000 | 0.0476 | 0.0000 | 0.0000 |
| | 15% | **60.3** | 0.0000 | 0.0000 | 0.0001 | 0.0000 | 0.0000 | 0.0000 | 0.0000 | 0.0094 | 0.0000 | 0.0000 |
| | 30% | **72.5** | 0.0000 | 0.0000 | 0.0118 | 0.0000 | 0.0000 | 0.0000 | 0.0000 | 0.2173 | 0.0000 | 0.0000 |
| 20% | -30% | **113.8** | 0.0000 | 0.0000 | 0.8445 | 0.0000 | 0.0000 | 0.0000 | 0.0159 | 0.8323 | 0.3942 | 0.0000 |
| | -15% | **63.6** | 0.0000 | 0.0000 | 0.0005 | 0.0000 | 0.0000 | 0.0000 | 0.0000 | 0.0247 | 0.0000 | 0.0000 |
| | 0% | **69.1** | 0.0000 | 0.0000 | 0.0036 | 0.0000 | 0.0000 | 0.0000 | 0.0000 | 0.1044 | 0.0000 | 0.0000 |
| | 15% | **63.4** | 0.0000 | 0.0000 | 0.0005 | 0.0000 | 0.0000 | 0.0000 | 0.0000 | 0.0253 | 0.0000 | 0.0000 |
| | 30% | **116.9** | 0.0000 | 0.0000 | 0.9330 | 0.0000 | 0.0000 | 0.0000 | 0.0202 | 0.8706 | 0.3602 | 0.0000 |

### 2.6.6 Linear Regression Analysis (Correlation):

To look at the effects of bone density on the failure load and stiffness values, correlation graphs were used. These graphs are essentially a plot of the DEXA value on the x-axis and the failure load or stiffness values on the y-axis, with a line-of-best fit through them. A correlation coefficient ($r^2$) is generated, which gives an indication of how closely the line approximates the data. A correlation coefficient of 1 indicates that every point lies on the line (i.e. the effect of bone density on the stiffness or failure load describes 100% (100 x $r^2$) of the variability in the data). The correlation coefficients for the data sets in this study are very low (in the order of $r^2 = 0.17$ to 0.39). This was expected, since the other variables in the study (e.g. AP and LAT locations of test sites) have a strong effect on the outcome of the test.

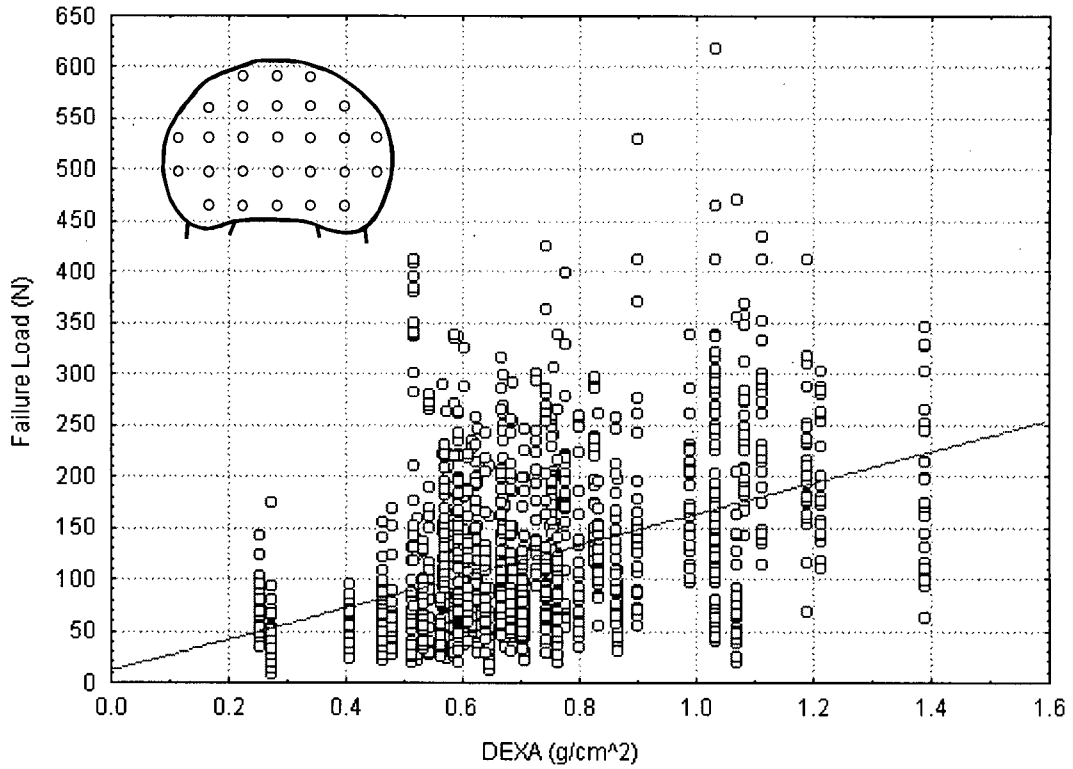


Figure 2.19: Correlation between failure load and bone density (all test sites) in all of the intact endplate specimens. Each vertical line represents the tests in a single endplate. The line is the "line-of-best-fit" generated by the linear regression analysis. Note the large amount of scatter in the data. The low correlation coefficient ($r^2 = 0.1726$) reflects the large amount of variability in the data.

### 2.6.7 Data Grouping – Test Sites:

Due to the shape of the endplate (semi-ovoid) the design of the statistical analyses is incomplete (i.e. a full 2-way analysis of the data, looking at the AP and LAT test co-ordinates of all test sites simultaneously is not possible). For the design to be complete, each AP co-ordinate must have the full complement of LAT co-ordinates, and *vice versa*. Figure 2.20, shows the test sites which would have been required to make the design complete. The circles show tests which were done and the crosses show missing tests. To get around this problem the data was analysed in several ways. The method used is indicated using a picture inset in the ANOVA graph.

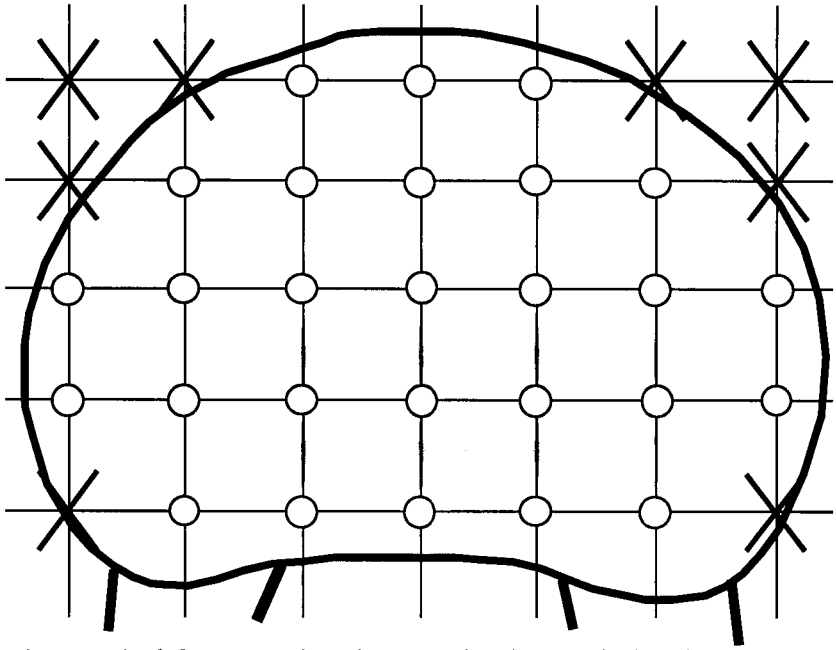

Figure 2.20: Test sites required for a complete design. The sites marked with crosses show the missing tests. Circles show the tests which were done.

#### *2.6.7.1 Maximum AP and LAT Analysis*

The largest area of the endplate which can be used as a complete design for a combined analysis of the AP and LAT effects of failure load and stiffness runs from AP = -40% through AP = 20% and from LAT = -30% through LAT = 30%. This region is illustrated pictorially in Figure 2.21. This region allows for the largest possible analysis containing equal numbers of test sites in each group. Unfortunately it does not allow for a complete analysis from front-to-back or side-to-side. This was accomplished by analysing smaller regions of the endplate.

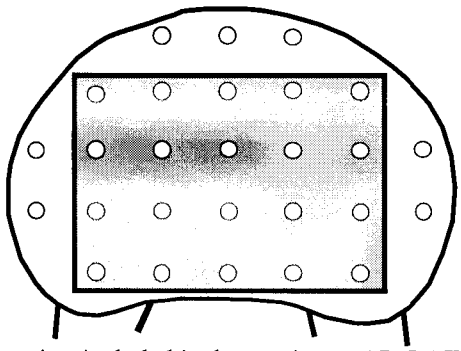

Figure 2.21: Test sites included in the maximum AP, LAT analyses.

### *2.6.7.2 Full AP Analysis*

The largest area of the endplate which can be used as a complete design for a full analysis of the AP effects of failure load and stiffness runs from AP = -40% through AP = 40% and from LAT = -15% through LAT = 15%. This region is illustrated pictorially in Figure 2.22.

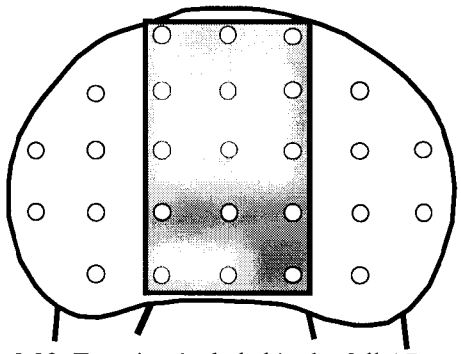

Figure 2.22: Test sites included in the full AP analyses.

### *2.6.7.3 Full LAT Analysis*

The largest area of the endplate which can be used as a complete design for a full analysis of the LAT effects of failure load and stiffness runs from AP = -20% through AP = 0% and from LAT = -45% through LAT = 45%. This region is illustrated pictorially in Figure 2.23

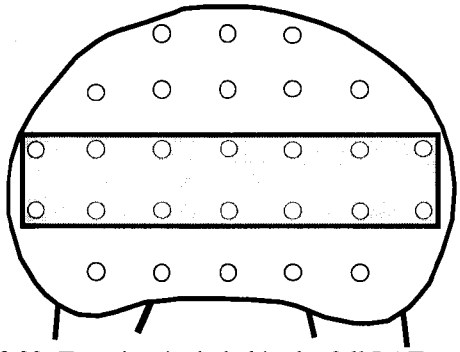

Figure 2.23: Test sites included in the full LAT analyses.

### 2.6.8 Interpretation of Maps:

The majority of the results are presented in the form of endplate maps. For the purposes of this document, the term "endplate map" refers to a representation of the strength distribution (failure load or stiffness) over the surface of the endplate based on the test sites used in the study.

Each test site was defined based on the geometry specific to the endplate in which the test was conducted. This enabled the results to be compared across endplates. Each of the maps uses the AP or LAT test site co-ordinates on the lower axis. The lines joining the points indicating failure load or stiffness correspond to the other set of test site co-ordinates, as indicated by the graph legend.

Each point on the graph is the average of the points on the endplates, i.e. each (AP, LAT) point on the graph represents the average value at that point over all of the endplates included in the analysis. Thus for an AP and LAT failure load analysis, the test at (AP,LAT) = (-40%,-30%) in each endplate would be combined to generate the average plotted at (-40%,-30%) on the ANOVA graph (Figure 2.24).

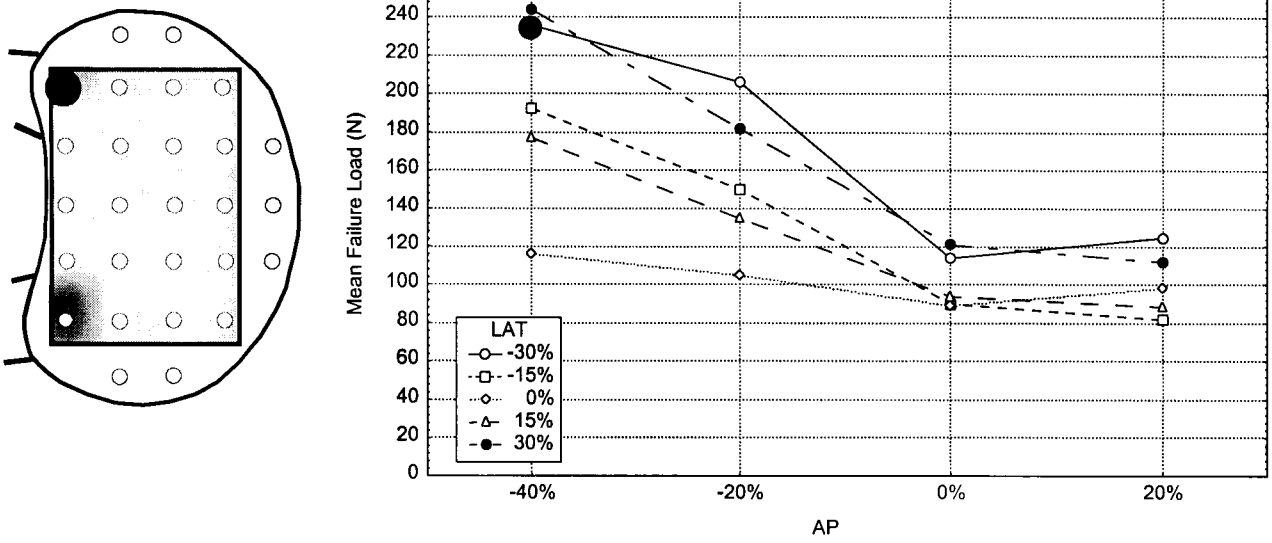


Figure 2.24: Inferior lumbar endplate maximum AP, LAT failure load map. The test site marked in black indicates the values which were averaged together to generate the mean failure load marked on the graph.

# Chapter 3

# Results

## 3.1 General Trends

Before beginning a rigorous analysis of the data, the general characteristics of the data were examined. The relationship between bone strength and bone density was studied, as was the general distribution of the structural properties over the endplate. A more rigorous examination of the structural property distributions, broken down by spinal section, is given in section 3.2.

### 3.1.1 Effect of Bone Density on Bone Properties

It is well known that bone strength is related to bone density. To see if this relationship held true in the results of this study, linear regression analyses were used to look at the effects of bone density on the failure load and stiffness of the bone.

Figure 3.1 shows the results of the linear regression analysis on the bone density and failure loads at all test sites in each of the 62 endplates tested. The correlation coefficient of 0.1726 indicates that the bone density accounted for about 17% of the variability in failure load. Each of the vertical lines of points in this graph represents the failure loads obtained in testing a single endplate. The large spread in the data for each endplate indicates that there was a wide range of failure loads found in each endplate.

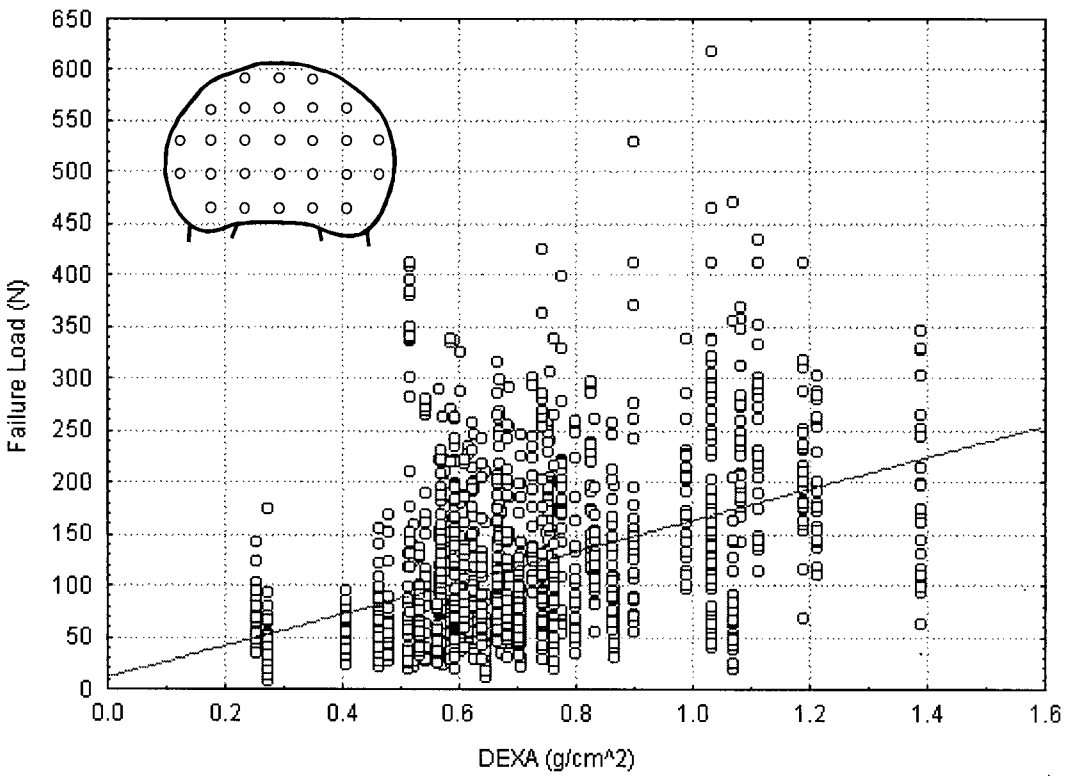


Figure 3.1: Relationship between bone density and failure load in all full endplate specimens. Each vertical line of points represents the failure loads recorded in a single endplate. Note that there was approximately 17% correlation between the failure load and the endplate bone density recorded using a lateral DEXA scan.

Most studies showing a strong correlation between vertebral bone density and failure load of the implant-bone interface are based on compression of bone-implant-bone specimens (Hollowell et al. 1996, Jost et al. 1998, Steffen 2000), thus a large endplate area would bear the load. This would be more closely approximated by using the mean failure loads in the endplates rather than the discrete test values for the bone density and failure load correlation, thus a second regression analysis was done on the mean endplate failure loads and the endplate bone density. Figure 3.2 shows the results of this analysis. The correlation coefficient was higher ($r^2 = 0.3962$) showing stronger correlation, as expected since the spread in the data was smaller when the values were averaged together within each endplate specimen. Note that the specimens with lower DEXA values (bone density) had lower failure loads.

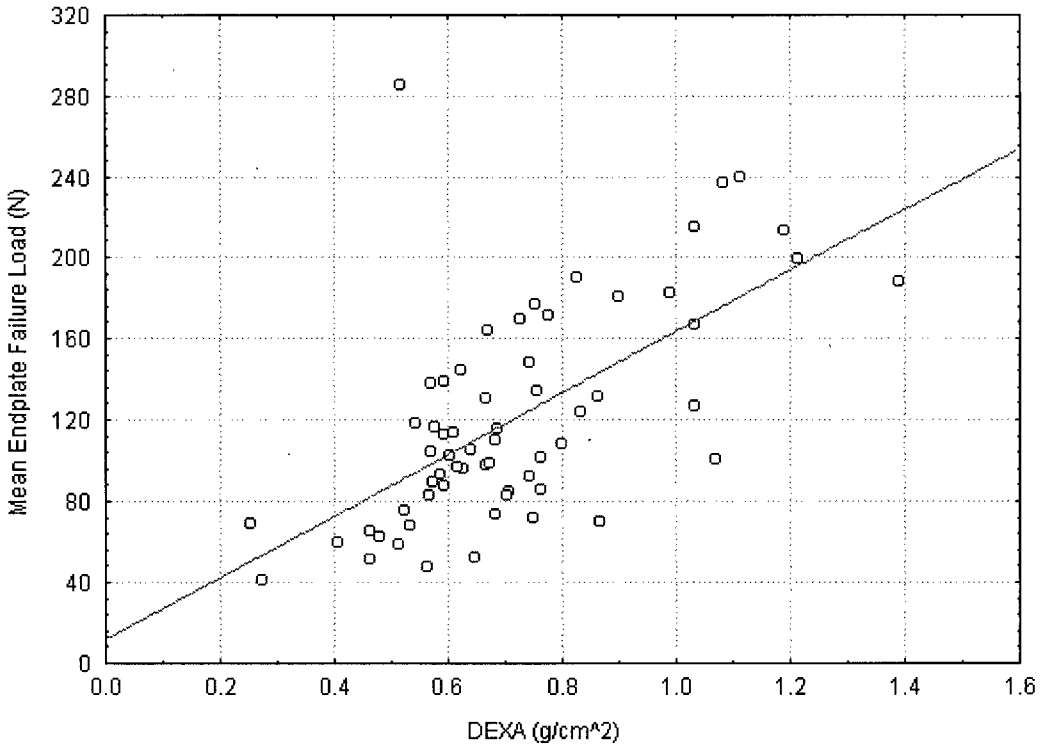


Figure 3.2: Relationship between bone density and mean endplate failure load. Each point on this graph shows the mean value of the failure loads recorded in one of the 62 endplates that were tested. Note that there was approximately 39% correlation between the mean endplate failure load and the endplate bone density recorded using a lateral DEXA scan.

Failure load is more commonly discussed than stiffness in relation to bone density in the literature, however one would expect both structural properties to be related to bone density. To examine the effect of bone density on the local endplate stiffness, a third linear regression was performed. Figure 3.3 shows the results of the linear regression analysis on the bone density and stiffness. Each of the vertical lines of points in this graph represents the stiffnesses obtained in testing a single endplate. The large spread in the data for each endplate indicates that there was a wide range of stiffnesses found in each endplate, just as there was in the failure load. The correlation coefficient of 0.0514 indicates that the bone density of an endplate accounted for about 5% of the variability in stiffness between the specimens. This value is very small, thus there was little correlation between the vertebral bone density and the local endplate stiffness.

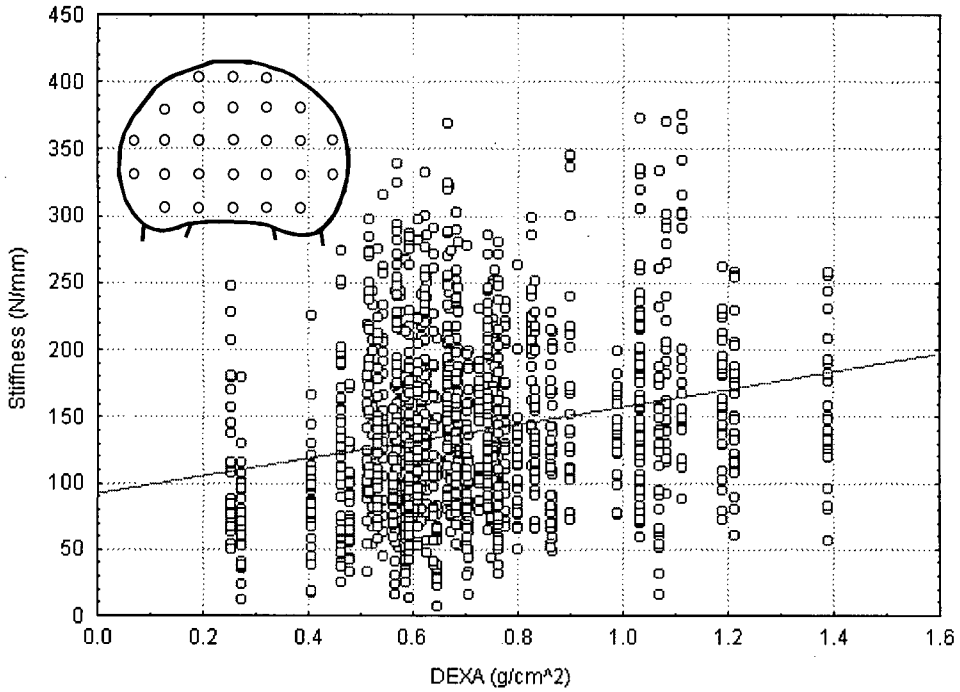


Figure 3.3: Relationship between bone density and stiffness in all specimens. Each vertical line of points represents the stiffnesses recorded in a single endplate. Note that there was negligible correlation (approximately 5%) between the stiffness and the endplate bone density recorded using a lateral DEXA scan.

To see if the mean endplate stiffness had a significant correlation with bone density, a fourth linear regression analysis was done. The results of this analysis are shown in Figure 3.4. The correlation coefficient was still very small ($r^2 = 0.1673$). Based on this result it appears that the endplate stiffness and bone density had a very weak correlation.

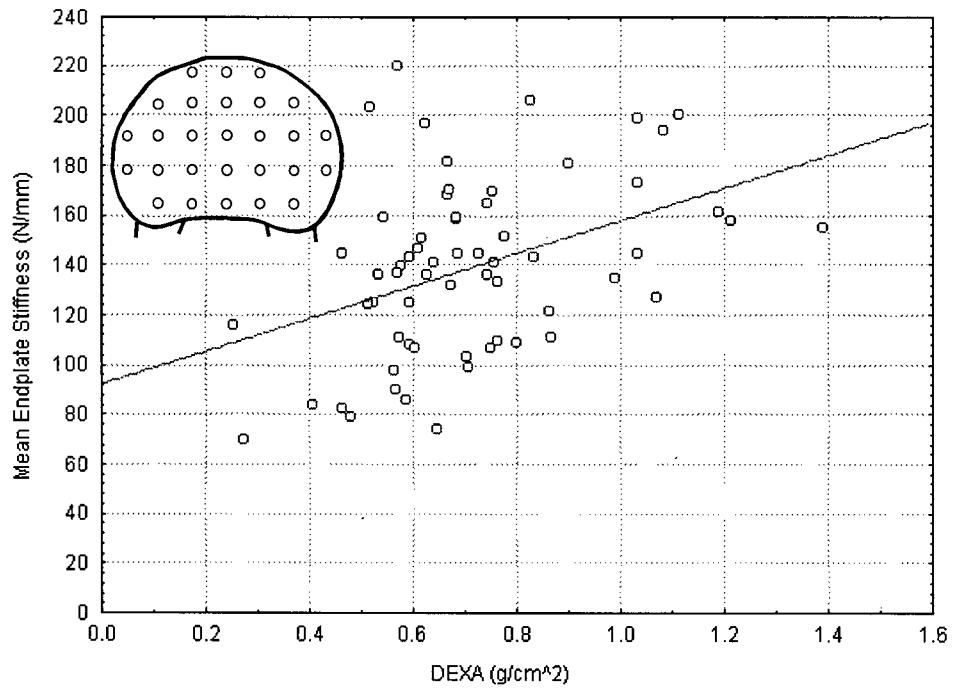


Figure 3.4: Relationship between bone density and mean endplate stiffness. Each point on this graph shows the mean value of the stiffnesses recorded in one of the 62 endplates that were tested. Note that there was a very weak correlation (approximately 17%) between the mean endplate stiffness and the endplate bone density recorded using a lateral DEXA scan.

### 3.1.2 Relationship Between Failure Load and Stiffness

Each test produced both a failure load and a stiffness value. To see how closely these values were related a linear regression analysis was performed. Figure 3.5, a plot of stiffness versus failure load, shows the results of this analysis. The correlation coefficient of 0.4510 indicates that about 45% of the variability in the stiffness values was explained by the variability in the failure load.

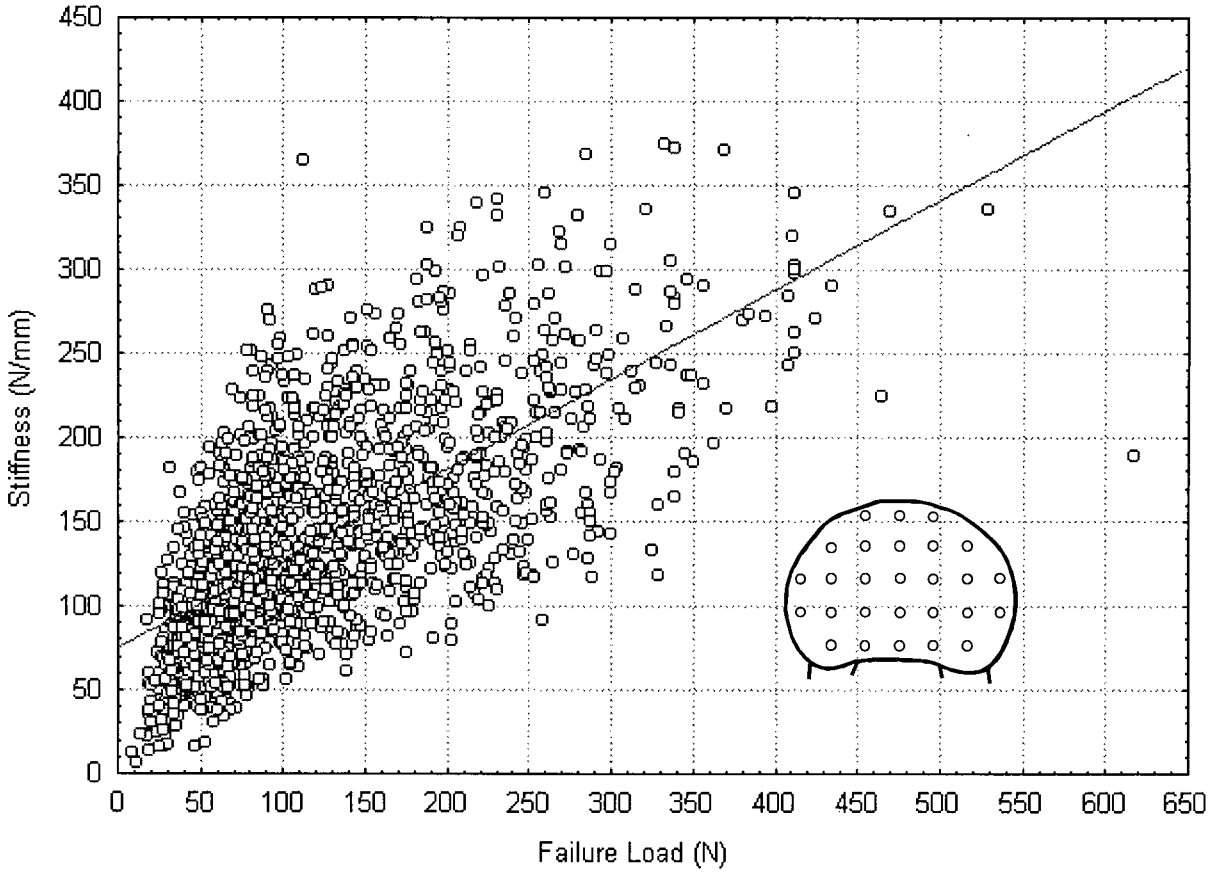


Figure 3.5: Relationship between failure load and stiffness in all specimens. Note that test sites with a low failure load also tended to have a low stiffness value.

A second linear regression analysis compared the mean endplate failure load and the mean endplate stiffness (Figure 3.6), giving a correlation coefficient of 0.5728. This indicates that there was a relatively strong relationship between the mean endplate failure load and stiffness.

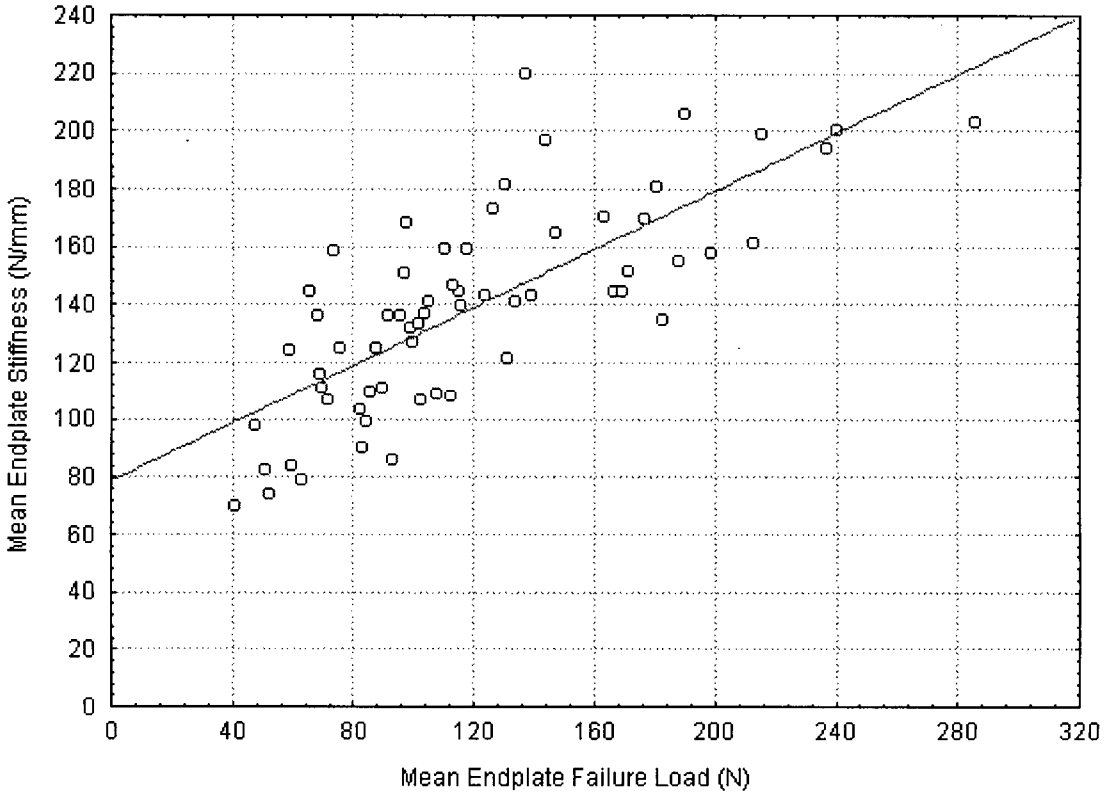


Figure 3.6: Relationship between the mean endplate failure load and mean endplate stiffness in all specimens. Note that there was a relatively strong correlation between the failure load and stiffness ($r^2 = 0.5728$).

### 3.1.3 Summary of General Trends

In sections 3.1.1 and 3.1.2 it was shown that the endplate bone density, measured using a lateral DEXA scan, was more accurate at predicting the mean structural properties in the endplate than the structural properties at a given test site, due to the variability in values within a single endplate. This finding was unsurprising, since reducing the variability within a data set should increase the correlation coefficient (there was a large amount of variation in the local structural properties in each endplate). As well, the DEXA scan measures the overall bone density, and the mean structural properties give an overall indication of the endplate structural properties, while the local structural properties may reflect local bone density to some extent. The remainder of this chapter gives the results of ANOVAs used to look for patterns in the variability found within the endplates to see if the structural properties vary in a predictable fashion, rather than being randomly variable.

## 3.2 Identifying the Basic Structural Property Maps

This section seeks to identify basic patterns in the distribution of the structural properties in the endplates. Two questions are addressed in this section: are there differences between the spinal levels (L3-S1) and are there differences between the superior and inferior endplates? Three-way ANOVAs were used to compare the structural property maps and overall failure load and stiffness to identify discrete groups sharing equivalent structural property maps. Subsequent sections examine the effects of bone density and disc degeneration on the general maps.

### 3.2.1 Effect of Spinal Level on the Lumbar Endplate Properties

Although the lumbar vertebrae are similar in size and shape, this does not necessarily mean that the structural property distributions are the same in different lumbar levels since the internal architecture may differ between levels. This sub-section looks for any differences in mean structural properties or property distributions between the lumbar endplates based on spinal level. The superior and inferior endplates were analysed separately in order to account for any potential differences between them.

#### *3.2.1.1 L3-L5 Superior Lumbar Endplate Comparisons*

To establish whether the maps in the three superior lumbar endplates (L3, L4 and L5) were different, and thus should be analysed separately, the distributions of the structural properties in the superior lumbar endplates were compared using 3-way ANOVAs on spinal level, and the AP and LAT test site locations (included as repeated measures). Neither the shapes of the failure load maps ($p < 0.5806$), nor the stiffness maps ($p < 0.9579$) were found to be significantly different in the three superior lumbar endplates when the maximum AP and LAT analysis was used (Figure 3.7 a). The mean endplate failure loads ($p < 0.6583$) and stiffnesses ($p < 0.4220$) were also not significantly different between levels.

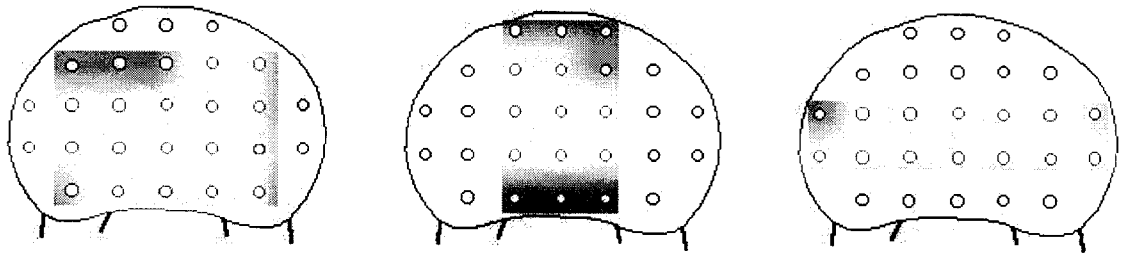

Figure 3.7: Test sites included in the three different ANOVAs: a) Maximum AP, LAT, b) Full AP, and c) Full LAT.

**Table 3.0: Effect of Lumbar Level on Failure Load and Stiffness:** P-values showing the probability of being wrong if one states that the overall means or maps of the L3, L4 and L5 superior or inferior endplates are different. Significant p-values ($p < 0.05$) are highlighted in grey. The AP, LAT columns correspond to ANOVAs using the test sites shown in Figure 3.7 a, the AP columns to Figure 3.7 b, and the LAT columns to Figure 3.7 c.

| | | Comparison of | | | | | |
|---|---|---|---|---|---|---|---|
| | | AP, LAT Means | AP Means | LAT Means | AP, LAT Maps | AP Maps | LAT Maps |
| L3-L5 superior | Failure Load | 0.6583 | 0.8570 | 0.2189 | 0.5806 | 0.3204 | 0.8074 |
| | Stiffness | 0.4220 | 0.6328 | 0.8824 | 0.9579 | 0.3177 | 0.5231 |
| L3-L5 inferior | Failure Load | 0.5280 | 0.6958 | 0.6461 | 0.5245 | 0.8151 | 0.9565 |
| | Stiffness | 0.3259 | 0.4590 | 0.7604 | 0.2402 | 0.0256 | 0.5090 |

Full AP and full LAT analyses (Figure 3.7 b, c) were also done to check that no significant differences were found if the outermost test sites were included in the maps. The results of these analyses are shown in Table 3.0. Note that none of the p-values showed a significant difference between the three superior lumbar endplates in either map shape or mean endplate properties. This means that the superior lumbar endplate maps are not significantly different and can be grouped together for comparison with other endplate maps.

#### *3.2.1.2 L3-L5 Inferior Lumbar Endplate Comparisons*

The three inferior lumbar endplates were compared using the same analyses applied to the superior lumbar endplates. The maximum AP and LAT analysis (Figure 3.7 a) found that the shapes of the failure load maps were not significantly different in the three inferior lumbar endplates ($p < 0.5245$), nor were the stiffness maps ($p < 0.2402$). The mean endplate failure loads ($p < 0.5280$) and stiffnesses ($p < 0.3259$) were also not significantly different.

Full AP and full LAT analyses (Figure 3.7 b, c) were done to check that no significant differences were found if the outermost test sites were included in the maps. The p-values for these comparisons are also shown in Table 3.0. Only the full AP stiffness map comparison showed a significant difference between the levels.

The fact that the full AP stiffness map had a significant p-value should not prevent the pooling of the inferior lumbar endplate results. A *post hoc* Newman-Keuls mean comparison (not shown) was done to look at the differences between the maps and found that in the L4 inferior 15% LAT curve there was a significant increase in stiffness between 20% AP and 40% AP. This difference was not significant in any of the other maps. The difference is very slight and does not seem to justify generating separate maps for the three inferior lumbar endplates. This means that the inferior lumbar endplate maps can be grouped together for comparison with other endplate maps.

### 3.2.2 Effect of Endplate - Superior and Inferior Lumbar Endplate Comparisons

To look for differences between the superior and inferior lumbar endplates the maps were compared using three-way ANOVAs, with endplate, AP and LAT test site co-ordinates as the factors. The AP and LAT test sites were included as repeated measures so that each specimen acted as its own control. After each analysis a *post hoc* Newman-Keuls mean comparison was done to look at the specific differences within and between the two maps. The results of these *post hoc* comparisons, including the values of the means shown in the graphs and p-values for the comparisons of each pair of points, are provided in Appendix D in the form of *post hoc* Newman-Keuls mean comparison tables.

#### *3.2.2.1 Maximum AP, LAT Analysis - Failure Load*

The first comparison looked at the largest complete set of AP, LAT test co-ordinates (as shown in the inset endplate pictures in Figure 3.8). The inferior lumbar endplates were significantly stronger than the superior lumbar endplates ($p < 0.0080$, Table 3.1) and the map shapes in the superior and inferior endplates were found to be significantly different ($p < 0.0001$).

A closer examination of the data using a *post hoc* Newman-Keuls mean comparison (Table D.19, Appendix D) shows that the differences were primarily in the posterior portion of the endplate (-40% AP and -20% AP). The differences are clearest in Figure 3.8 b. Note the U-shaped posterior curves in the superior endplate map, versus the V-shape of the same curves in the inferior endplate map. The results of this comparison indicate that the mean endplate failure load was higher in the inferior endplates due to the higher posterior strength of the inferior lumbar endplates, not to an evenly distributed strength difference. Note that, despite the differences in the maps, the strongest test sites in both endplates were the postero-lateral sites, in front of the pedicles.

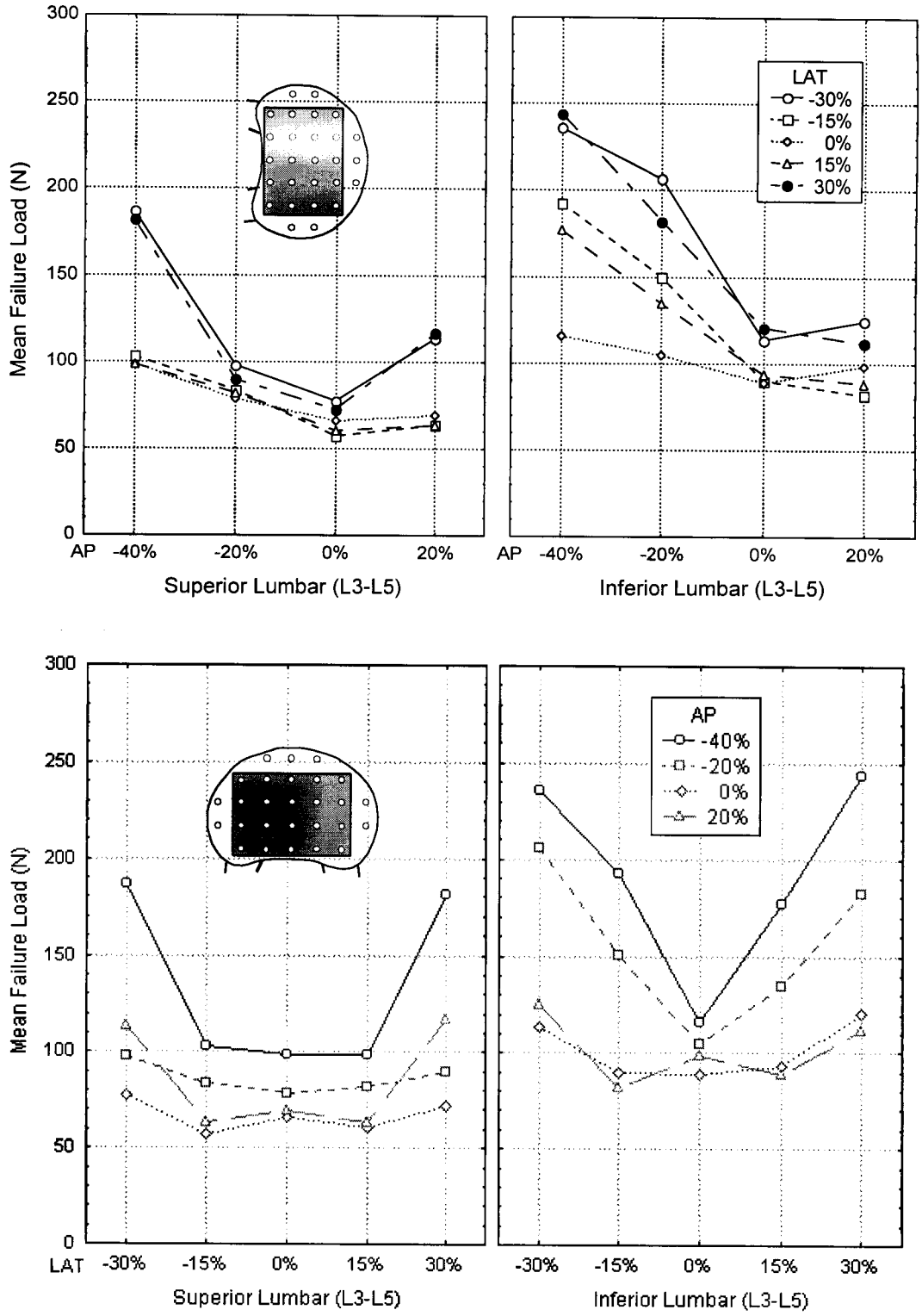


Figure 3.8: Comparison of the superior and inferior lumbar endplate maximum AP, LAT failure load distributions. Figures a and b show the same maps with the AP and LAT axes interchanged. The p-value of $< 0.0001$ indicates that there were significant differences between the shapes of the superior and inferior lumbar endplate maps. These differences were mainly in the posterior half of the endplate. In both endplate groups the strongest test sites were located postero-laterally (+/- 40% AP, +/- 30% LAT), in front of the pedicles. The *post hoc* Newman-Keuls comparison of these graphs is given in Table D.19, Appendix D.

### *3.2.2.2 Full AP Analysis – Failure Load*

To look at the effect of including the most anterior test sites in the analysis, a second ANOVA was done using the largest complete AP data set (Figure 3.9). The shapes of the superior and inferior failure load maps were again found to be different ($p < 0.0001$), but in this analysis the inferior endplates were not significantly stronger than the superior endplates ($p < 0.0666$ Table 3.1).

A *post hoc* Newman-Keuls mean comparison was done to look at the specific differences within and between the two maps (Table D.20, Appendix D). The most interesting difference between the two graphs is in the relative failure load between the most posterior and most anterior test sites. In the superior endplates the most posterior test sites were weaker than the most anterior sites, except at 0% LAT, where they were not significantly different ($p = 0.9072$). The inferior endplates were found to be stronger posteriorly than anteriorly, except at 0% LAT, where they were stronger anteriorly.

A direct comparison of equivalent test sites in the two endplates showed that there were no significant differences between the two 0% LAT curves, the 20% AP, or the 40% AP points in the superior and inferior lumbar endplates.

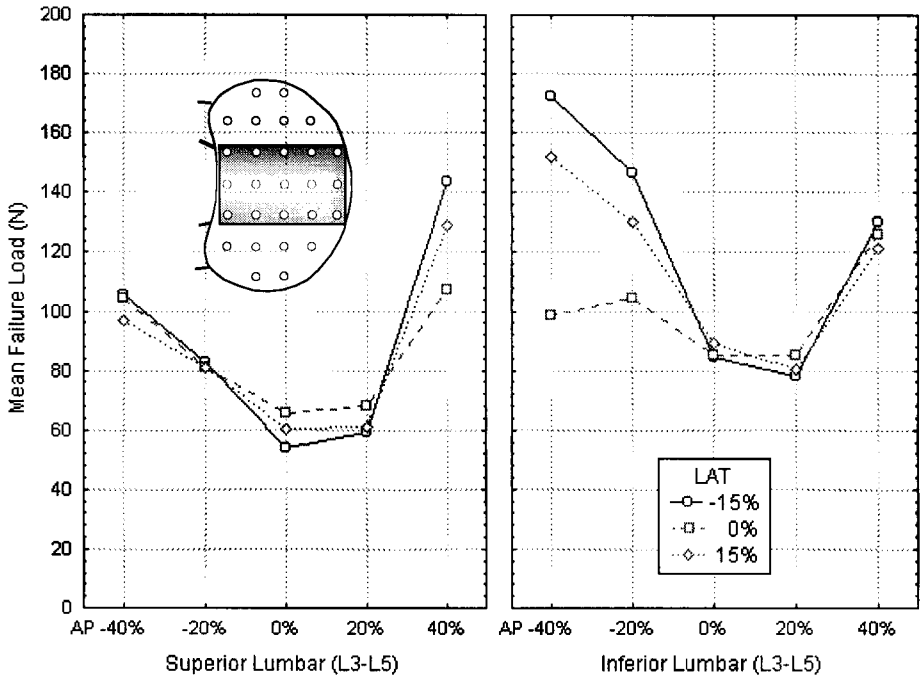


Figure 3.9: Comparison of the superior and inferior lumbar endplate full AP failure load distributions. The p-value of $< 0.0001$ indicates that there were significant differences in the shapes of the maps. Note that the inferior lumbar endplates were stronger posteriorly than anteriorly, while the reverse was true in the superior endplates. The *post hoc* Newman-Keuls comparison of these graphs is given in Table D.20, Appendix D.

### *3.2.2.3 Full LAT Analysis – Failure Load*

To look at the effect of including the most lateral test sites in the analysis, a third ANOVA was done using the largest complete LAT data set (Figure 3.10). Again, the shapes of the superior and inferior failure load maps were found to be different ($p < 0.0271$). The inferior endplate was not significantly stronger than the superior endplate in this analysis ($p < 0.0640$, Table 3.1).

A *post hoc* Newman-Keuls mean comparison was done to look at the specific differences within and between the two maps (Table D.21, Appendix D). A direct comparison of equivalent test sites in the two endplates showed that there were no significant differences between the two 0% AP curves. In the –20% AP curves, however, all points were significantly different except for the 0%, 15% ($p = 0.0592$) and 45% LAT ($p = 0.1616$) points. This means that the main difference between the two endplate maps stems from the fact that the inferior endplates were stronger posteriorly, as was demonstrated in the previous ANOVAs.

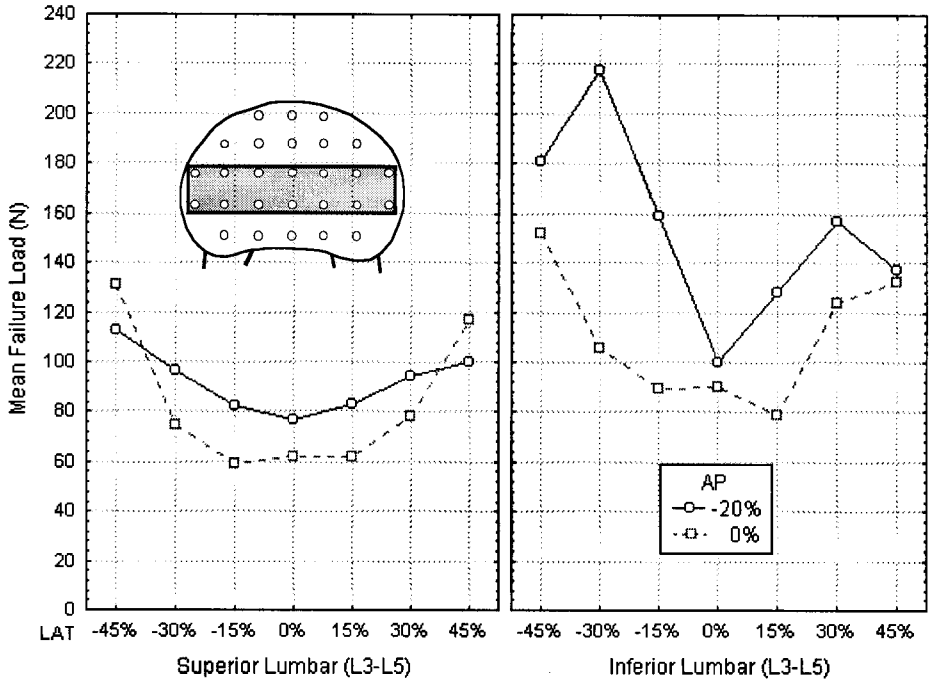


Figure 3.10: Comparison of the superior and inferior endplate full LAT failure load distributions. The p-value of < 0.0271 indicates that there were significant differences between the shapes of the superior and inferior lumbar endplate maps. This difference was mainly due to the larger posterior failure loads in the inferior endplate map. The *post hoc* Newman-Keuls comparison of these graphs is given in Table D.21, Appendix D.

### *3.2.2.4 Maximum AP, LAT Analysis – Stiffness*

Once the failure load data had been compared, the same analyses were used to look at the stiffness results, beginning with the maximum AP, LAT map comparison (Figure 3.11). Note the similarities between these stiffness maps and the corresponding failure load maps (Figure 3.8). As in the failure load comparison, the shapes of the maximum AP, LAT superior and inferior endplate stiffness maps were found to be significantly different ($p < 0.0248$), and the inferior endplate was significantly stiffer than the superior endplate ($p < 0.0027$, Table 3.1).

The *post hoc* Newman-Keuls mean comparison (Table D.22, Appendix D) showed that these differences were all in the posterior portion of the endplate (-40% AP and -20% AP). A direct comparison of equivalent test sites in the two endplates showed that there were no significant differences between the two 0% AP curves or the two 20% AP curves, nor between the 0% LAT test sites. Here again, note the U-shaped posterior curves in the superior endplate map versus the V-shape of the same curves in the inferior endplate map (Figure 3.11 b). The results of this comparison indicate that the mean endplate stiffness was higher in the inferior endplates due to the higher posterior stiffness of the inferior

lumbar endplates, not to an evenly distributed stiffness difference. Note that, despite the differences in the maps, the stiffest test sites in both endplates were the postero-lateral sites, in front of the pedicles, where the strongest tests were found (Figure 3.8).

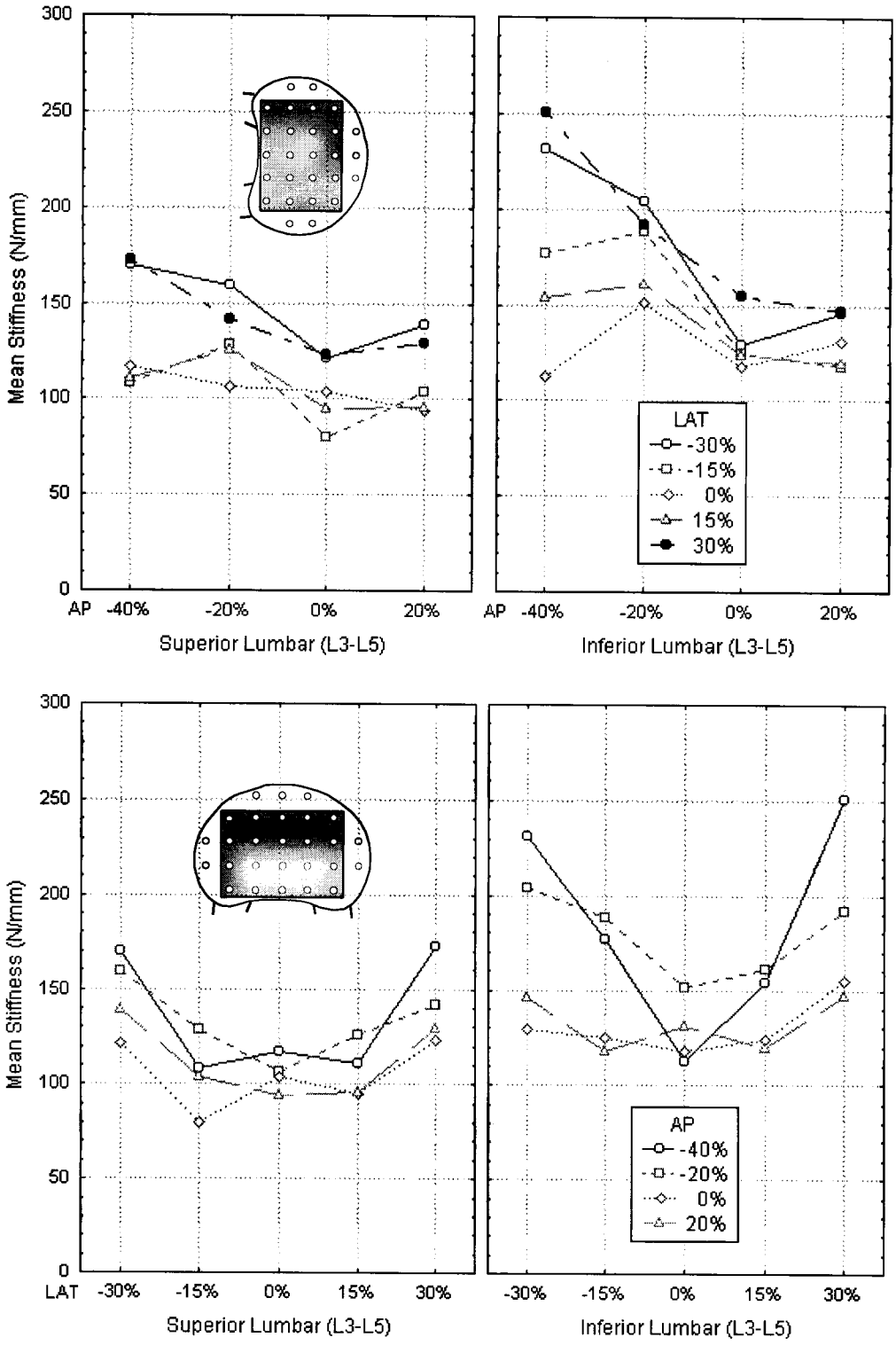


Figure 3.11: Comparison of the superior and inferior lumbar endplate maximum AP, LAT stiffness distributions. Figures a and b show the same maps with the AP and LAT axes interchanged. The p-value of $< 0.0248$ indicates that there were significant differences between the shapes of the superior and inferior lumbar endplate stiffness maps. In both endplate groups the stiffest test sites were located postero-laterally (+/- 40% AP, +/- 30% LAT), in front of the pedicles. The *post hoc* Newman-Keuls comparison of these graphs is given in Table D.22, Appendix D.

### *3.2.2.5 Full AP Analysis – Stiffness*

Using the full AP data set, the shapes of the superior and inferior stiffness maps were again found to be significantly different ($p < 0.0068$, Figure 3.12), and the inferior endplate was significantly stiffer than the superior endplate ($p < 0.0012$, Table 3.1).

A *post hoc* Newman-Keuls mean comparison was done to look at the specific differences within and between the two maps (Table D.23, Appendix D). A direct comparison of equivalent test sites in the two endplates showed that there were no significant differences between the 0% AP points, nor the 20% AP points. All of the -20% AP points were significantly stiffer in the inferior endplates. Of the most posterior test sites, only the (-40% AP, -15% LAT) point was significantly stiffer in the inferior endplates. Overall, the inferior endplate had a less uniform AP stiffness distribution than did the superior endplate.

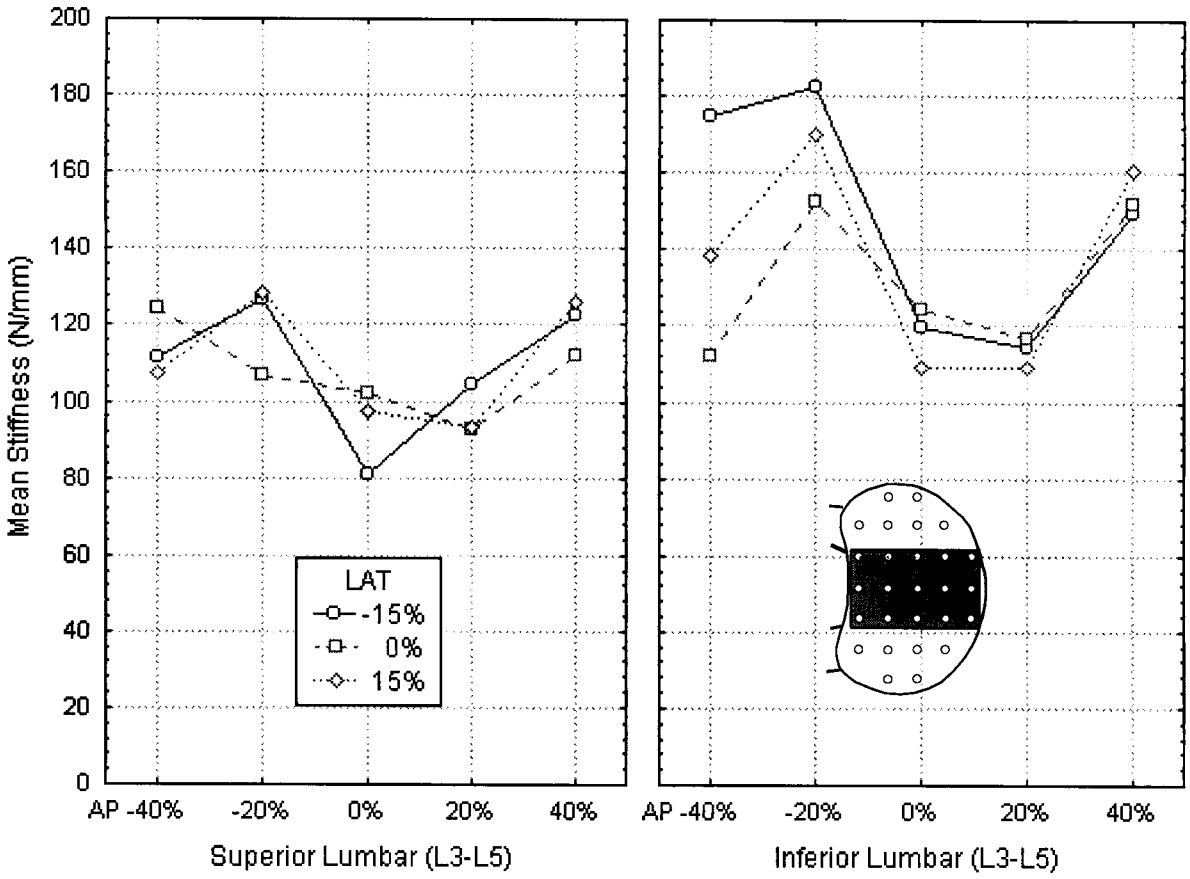


Figure 3.12: Comparison of the superior and inferior lumbar endplate full AP stiffness distributions. The p-value of $< 0.0068$ indicates that there were significant differences in the shapes of the superior and inferior lumbar endplate stiffness maps. The *post hoc* Newman-Keuls comparison of these graphs is given in Table D.23, Appendix D.

### *3.2.2.6 Full LAT Analysis – Stiffness*

No significant differences were found between the superior and inferior endplate means ($p < 0.2040$, Table 3.1) or stiffness map shapes ($p < 0.7113$, Figure 3.13) using the full LAT data set.

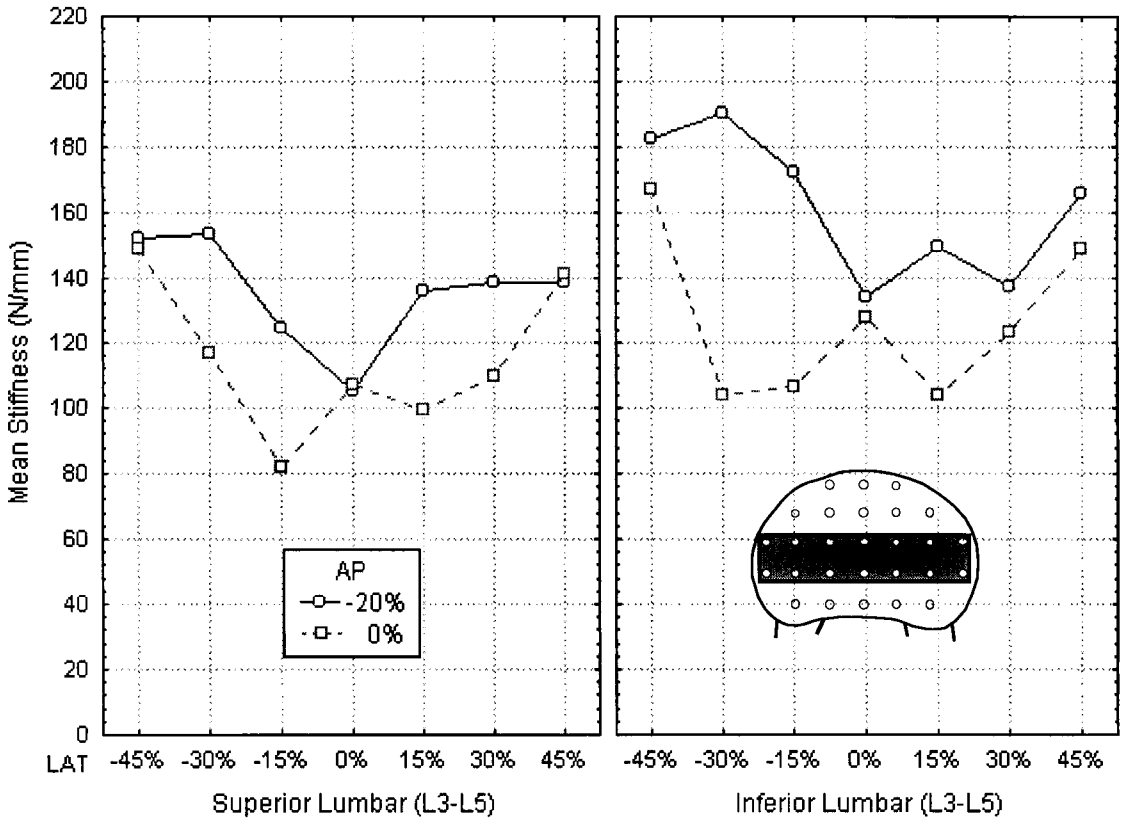


Figure 3.13: Comparison of the superior and inferior lumbar endplate full LAT stiffness distributions. The p-value of < 0.7113 indicates that there were no significant differences in the shapes of the superior and inferior lumbar endplate stiffness maps. The *post hoc* Newman-Keuls comparison of these graphs is in Table D.24, Appendix D.

**Table 3.1: Effect of Endplate (Superior vs. Inferior Lumbar) on Failure Load and Stiffness.** This table shows the mean overall endplate failure loads (FL) in Newtons and stiffnesses (ST) in Newtons/millimetre for the superior and inferior lumbar endplates using the test sites included in the three test site groupings discussed in section 3.2.2. The p-values for the mean comparisons (Means) and map shape comparisons (Maps) are also given. Significant p-values are shaded. Based on these p-values it was concluded that the superior and inferior endplate maps were significantly different.

| | Max. AP, LAT | | Full AP | | Full LAT | |
|---|---|---|---|---|---|---|
| | Mean FL | Mean ST | Mean FL | Mean ST | Mean FL | Mean ST |
| Superior Mean | 93.0 | 121.3 | 86.7 | 109.1 | 87.7 | 125.3 |
| Inferior Mean | 137.7 | 156.7 | 112.2 | 139.0 | 132.3 | 143.9 |
| p-value: Means | 0.0080 | 0.0027 | 0.0666 | 0.0012 | 0.0640 | 0.2040 |
| p-value: Maps | 0.0001 | 0.0248 | 0.0001 | 0.0068 | 0.0271 | 0.7113 |

### 3.2.3 Superior Lumbar and Sacral Endplate Comparisons

The different shapes of the lumbar and sacral vertebrae raise questions as to whether the two types of vertebrae share the same strength profiles, or if underlying structural differences lead to different profiles. In order to determine whether or not the superior lumbar and sacral endplates should be grouped together, a series of ANOVAs were used to compare the mean structural properties and property distributions of the two groups.

As in the comparison of the superior and inferior lumbar endplates (section 3.2.2), the maps were compared using three-way ANOVAs, with endplate, AP and LAT test site co-ordinates as the factors. The AP and LAT test sites were included as repeated measures such that each specimen acted as its own control. After each analysis, a *post hoc* Newman-Keuls mean comparison was done to look at the specific differences within and between the two maps. The results of these *post hoc* comparisons, including the values of the means shown in the graphs and p-values for the comparisons of each pair of points, are provided in Appendix D in the form of *post hoc* Newman-Keuls mean comparison tables.

#### *3.2.3.1 Maximum AP, LAT Analysis – Failure Load*

The first comparison looked at the largest complete set of AP, LAT test co-ordinates (as shown in the inset endplate pictures in Figure 3.14). The shapes of the superior lumbar and sacral endplate maps were found to be significantly different in this comparison ($p < 0.0077$), and the mean failure loads were also significantly different ($p < 0.0541$, Table 3.2), with the sacrum being stronger than the superior lumbar endplates.

A closer examination of the data was done using a *post hoc* Newman-Keuls mean comparison (Table D.25, Appendix D). The posterior test sites in the sacrum (-40% AP) were all found to be significantly stronger than the corresponding superior lumbar endplate test sites. No lateral variation was found in the sacrum, while both the anterior (20% AP) and posterior (-40% AP) superior lumbar endplate failure loads varied in the lateral direction. Finally, there was a steady decline in failure load from the posterior to the anterior test sites in the sacrum, while the superior lumbar endplate failure load dropped from the posterior test sites to the centre of the endplate, then increased again anteriorly.

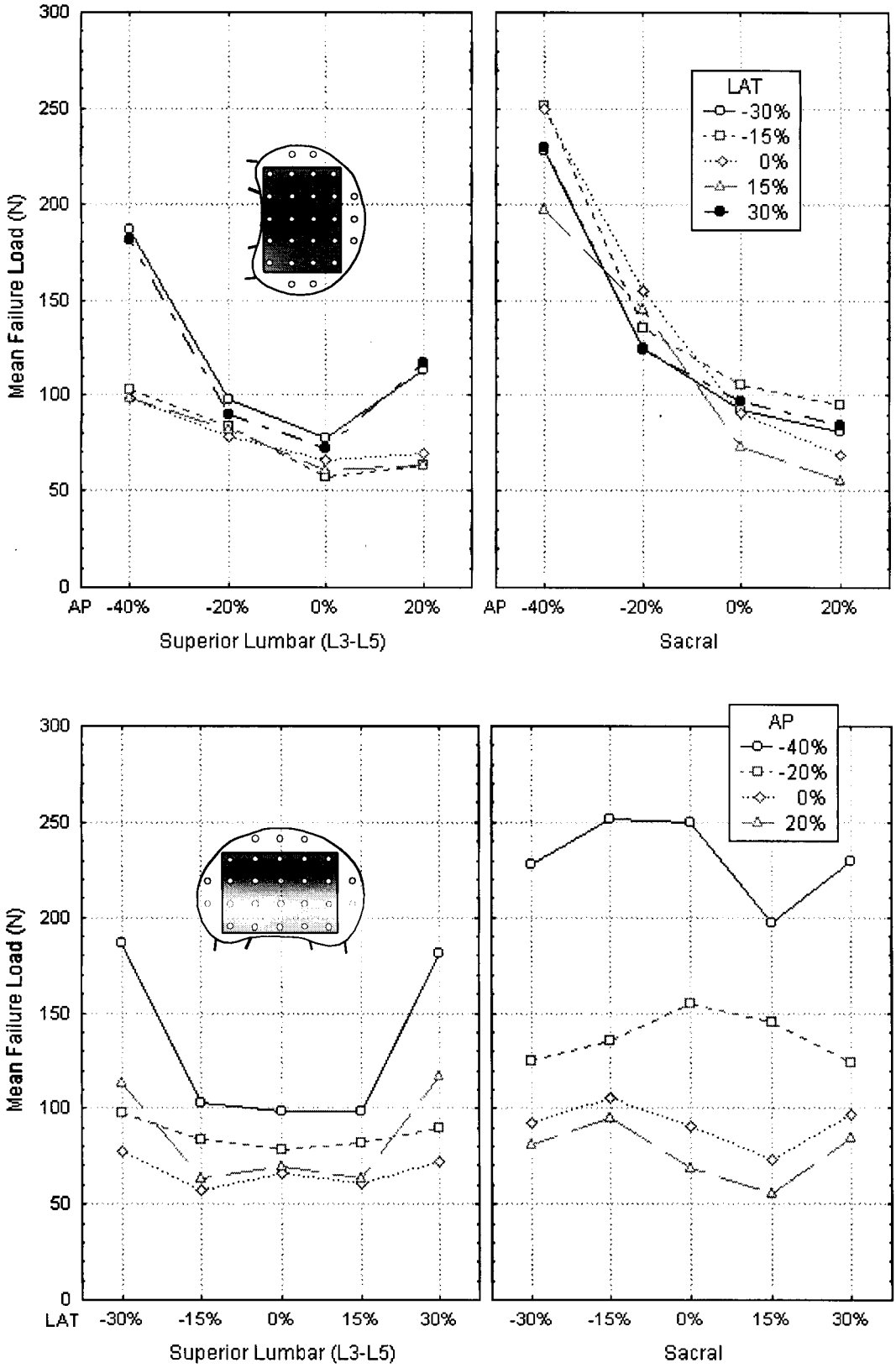


Figure 3.14: Comparison of the superior lumbar and sacral endplate maximum AP, LAT failure load distributions. Figures a and b show the same maps with the AP and LAT axes interchanged. The p-value of < 0.0077 indicates that there were significant shape differences between the two failure load maps. The *post hoc* Newman-Keuls results for this comparison are given in Table D.25, Appendix D.

### *3.2.3.2 Full AP Analysis - Failure Load*

To look at the effect of including the most anterior test sites in the analysis, a second ANOVA was done using the largest complete AP data set (Figure 3.15). The shapes of the superior lumbar and sacral failure load maps were again found to be different ($p < 0.0482$), and the sacral endplate was significantly stronger than the superior lumbar endplates ($p < 0.0335$, Table 3.2).

The results of the *post hoc* Newman-Keuls mean comparison of these maps is given in Table D.26, Appendix D. Looking at the most anterior test sites, in the superior lumbar endplates there was a significant increase in failure load from 20% AP to 40% AP, while there was no significant difference between these test sites in the sacral endplates. The posterior test sites in the sacral endplates were significantly stronger than the same sites in the superior lumbar endplates.

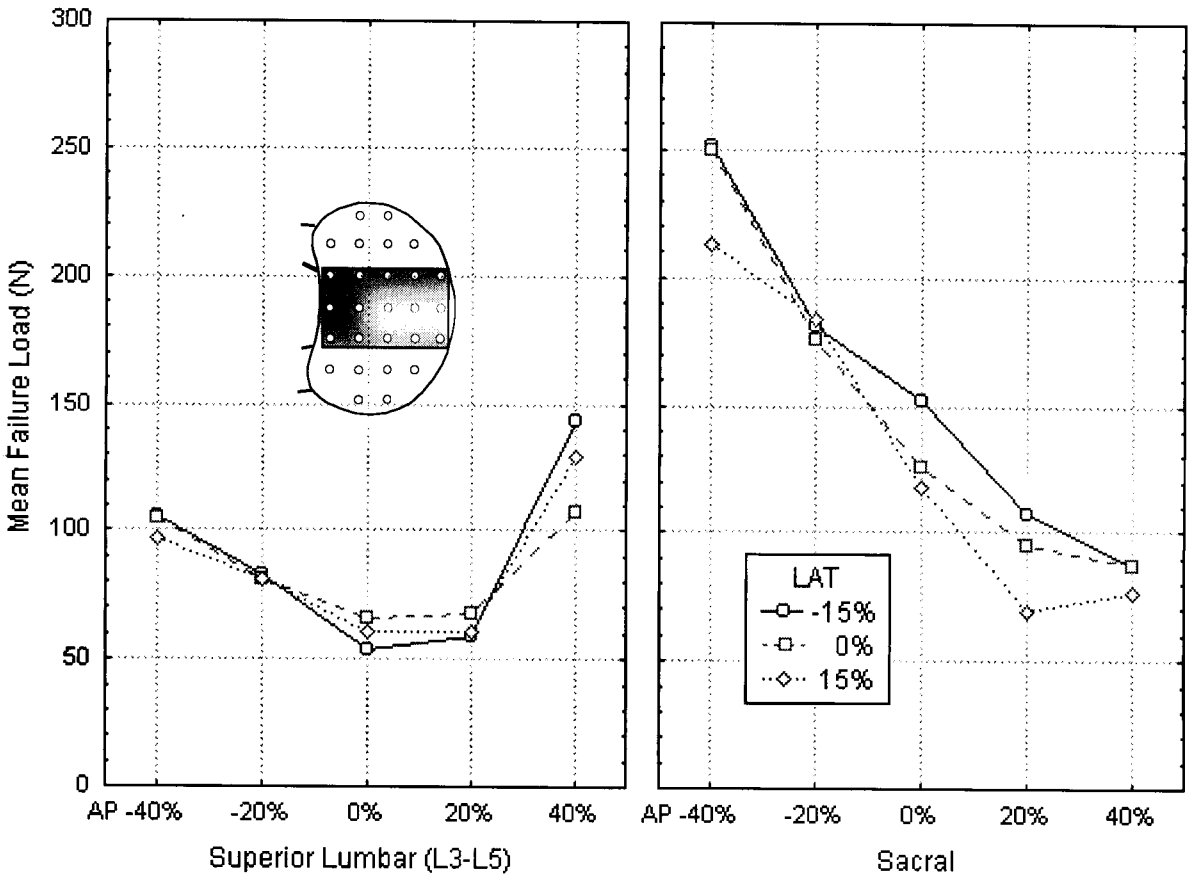


Figure 3.15: Comparison of the full AP failure load distribution in the superior lumbar and sacral endplates. The p-value of $< 0.0482$ indicates that there were significant differences between the shapes of these two failure load maps. The *post hoc* Newman-Keuls results for this comparison are given in Table D.26, Appendix D.

### *3.2.3.3 Full LAT Analysis – Failure Load*

To look at the effect of including the most lateral test sites in the analysis, a third ANOVA was done using the largest complete LAT data set (Figure 3.16). In this analysis the superior lumbar and sacral endplate map shapes were not found to be significantly different ($p = 0.3303$), nor were the mean endplate failure loads ($p < 0.3206$, Table 3.2).

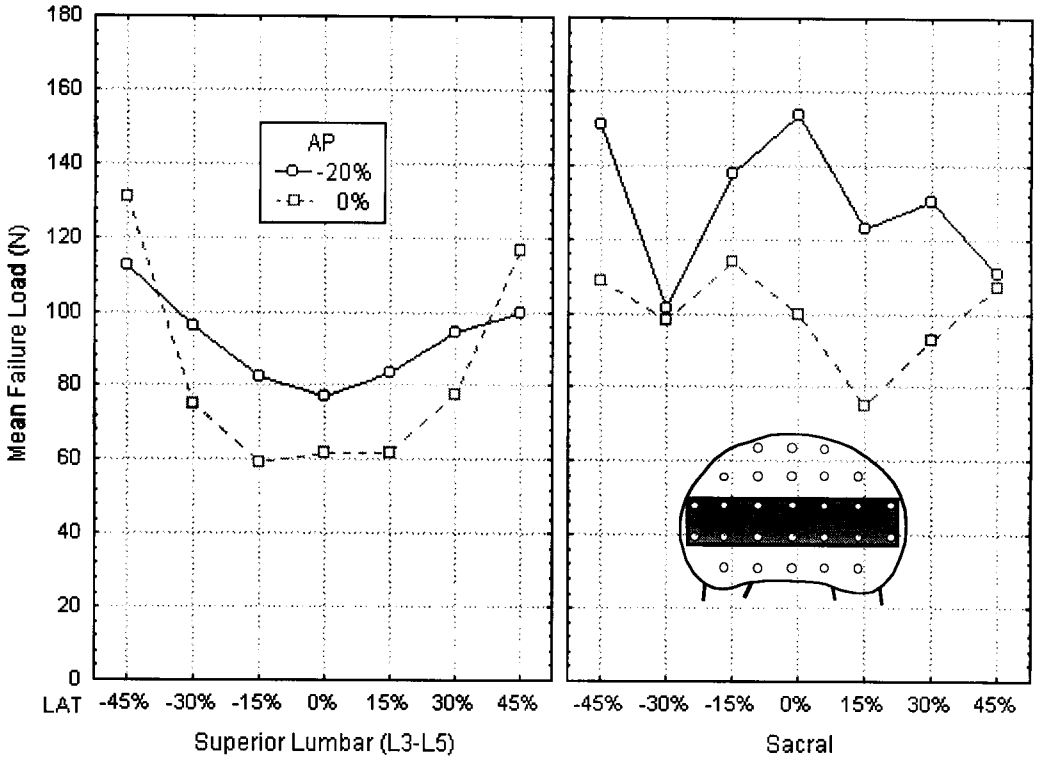


Figure 3.16: Comparison of the full LAT failure load distribution in the superior lumbar and sacral endplates. The p-value of < 0.3303 indicates that there were no significant shape differences between these two failure load maps. The *post hoc* Newman-Keuls results for this comparison are given in Table D.27, Appendix D.

### *3.2.3.4 Maximum AP, LAT Analysis – Stiffness*

The stiffness data was analysed using the same procedure as was used for the failure load data, beginning with an ANOVA on the maximum AP, LAT test sites (Figure 3.17). Note the similarities between these maps and the corresponding failure load maps (Figure 3.14). In this analysis, the shapes of the superior lumbar and sacral endplate maps were not found to be significantly different ($p = 0.0702$), although the p-value was very close to significant (significant p-values being arbitrarily set as less than 0.05). Neither group was significantly stiffer than the other ($p < 0.2697$, Table 3.2).

A closer examination of the data was done using a *post hoc* Newman-Keuls mean comparison (Table D.28, Appendix D). A direct comparison of equivalent test sites in the two endplates showed that there were no significant differences between the two –20% AP curves, the two 0% AP curves, or the two 20% AP curves, however there were significant differences between the –15%, 0% and 15% LAT test sites on the two –40% AP curves at $p < 0.01$.

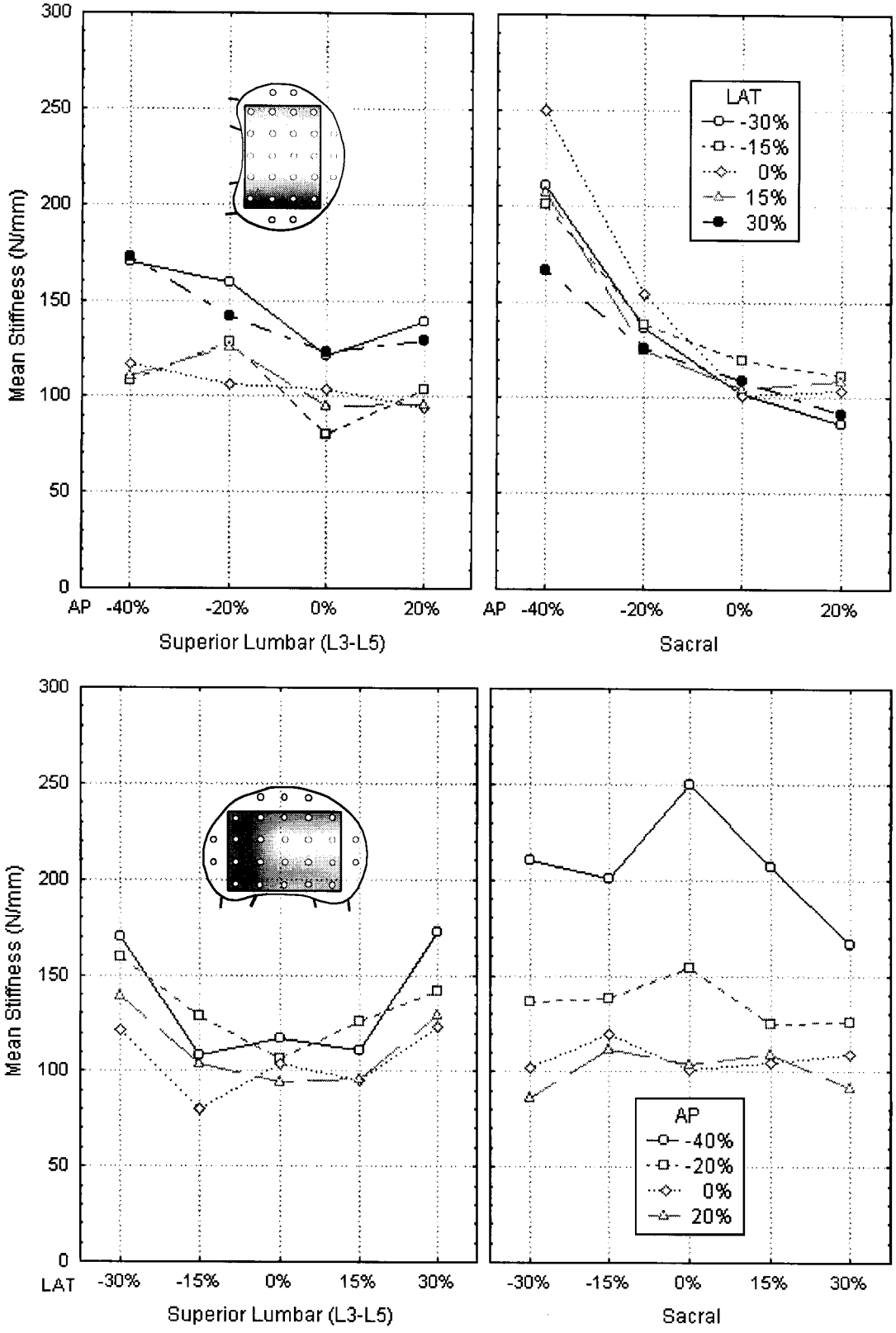


Figure 3.17: Comparison of the maximum AP, LAT stiffness distribution in the superior lumbar and sacral endplates. Figures a and b show the same maps with the AP and LAT axes interchanged. The p-value of < 0.0702 indicates that the superior and inferior lumbar endplate stiffness maps were not significantly different. The *post hoc* Newman-Keuls results for this comparison are given in Table D.28, Appendix D.

### *3.2.3.5 Full AP Analysis - Stiffness*

To look at the effect of including the most anterior test sites in the analysis, a second ANOVA was done using the largest complete AP data set (Figure 3.29). The superior lumbar and sacral stiffness maps were again not found to be significantly different ($p = 0.2888$), nor was the sacrum significantly stiffer than the superior lumbar endplates ($p < 0.0989$, Table 3.2).

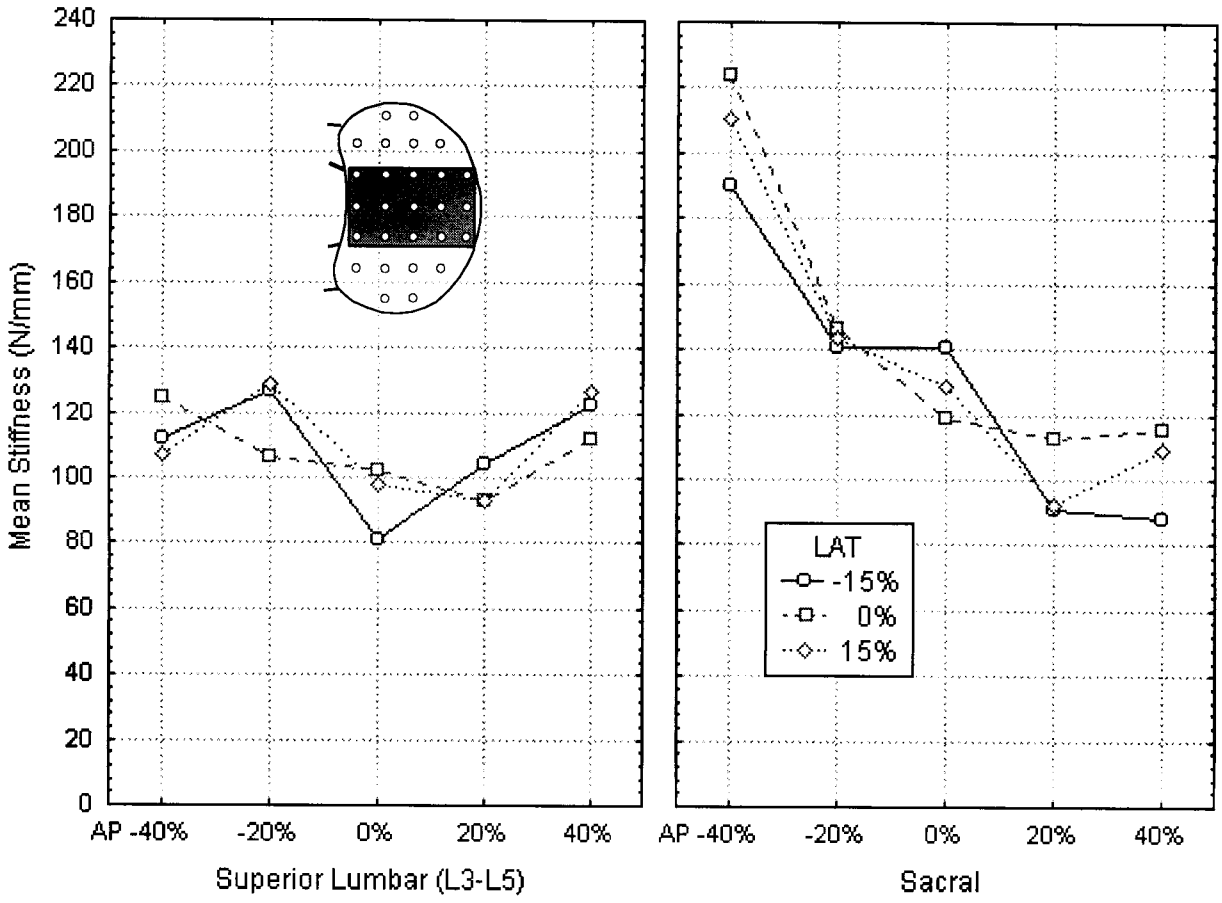


Figure 3.18: Comparison of the full AP stiffness distribution in the superior lumbar and sacral endplates. The p-value of $< 0.2888$ indicates that the shapes of the two maps were not significantly different. The *post hoc* Newman-Keuls results for this comparison are given in Table D.29, Appendix D.

### *3.2.3.6 Full LAT Analysis – Stiffness*

To look at the effect of including the most lateral test sites in the analysis, a third ANOVA was done using the largest complete LAT data set (Figure 3.30). No significant differences were found between the shapes of the superior lumbar and sacral complete LAT analysis stiffness maps ($p < 0.4651$), or the mean endplate stiffnesses ($p < 0.8890$, Table 3.2).

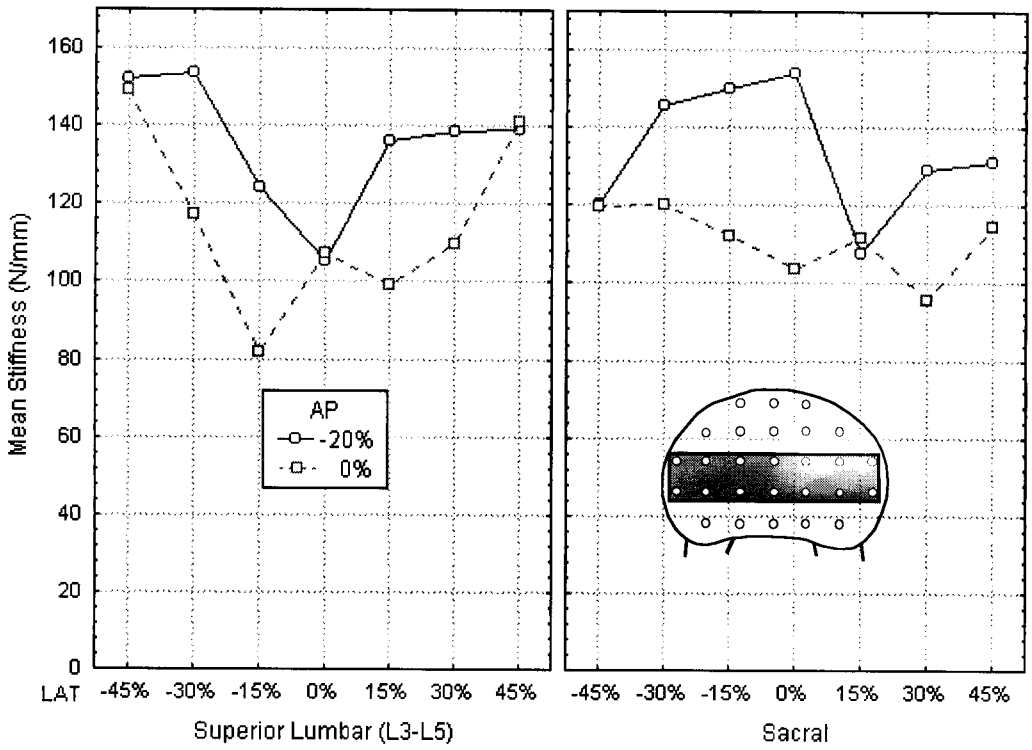


Figure 3.19: Comparison of the full LAT stiffness distribution in the superior lumbar and sacral lumbar endplates. The p-value of $< 0.4651$ indicates that there were no significant differences between the shapes of the maps. The *post hoc* Newman-Keuls results for this comparison are given in Table D.30, Appendix D.

**Table 3.2: Effect of Level on Failure Load and Stiffness in the Superior Endplates.** This table shows the mean overall endplate failure loads (FL) in Newtons, and stiffnesses (ST) in Newtons/millimetre for the lumbar and sacral endplates using the test sites included in the three test site groupings discussed in section 3.2.3. The p-values for the mean comparisons (Means) and map shape comparisons (Maps) are also given. Significant p-values are shaded. Based on these p-values it was concluded that the superior lumbar and sacral endplate failure load maps were significantly different. The p-value of 0.0702 was considered close enough to significant to make the assumption that the stiffness maps should also not be grouped together.

| | Max. AP, LAT | | Full AP | | Full LAT | |
|---|---|---|---|---|---|---|
| | Mean FL | Mean ST | Mean FL | Mean ST | Mean FL | Mean ST |
| Sup. Lumbar Mean | 93.0 | 121.3 | 86.7 | 109.1 | 87.7 | 125.3 |
| Sacral Mean | 134.1 | 137.6 | 144.9 | 136.3 | 114.5 | 122.6 |
| p-value: Means | 0.0541 | 0.2697 | 0.0335 | 0.0989 | 0.3206 | 0.8890 |
| p-value: Maps | 0.0077 | 0.0702 | 0.0482 | 0.2888 | 0.3303 | 0.4651 |

### 3.2.4 Inferior Lumbar and Sacral Endplate Comparisons

To determine whether or not the inferior lumbar and sacral endplates share the same structural property profiles, the maps were compared using three-way ANOVAs, with endplate, AP and LAT test site co-ordinates as the factors. The AP and LAT test sites were included as repeated measures so that each endplate acted as its own control. After each analysis a *post hoc* Newman-Keuls mean comparison was done to look at the specific differences within and between the two maps. The results of these *post hoc* comparisons, including the values of the means shown in the graphs and p-values for the comparisons of each pair of points, are provided in Appendix D in the form of *post hoc* Newman-Keuls mean comparison tables.

#### *3.2.4.1 Maximum AP, LAT Analysis – Failure Load*

The first comparison (Figure 3.20) looked at the largest complete set of AP, LAT test co-ordinates (as shown in the inset endplate pictures). The shapes of the inferior lumbar and sacral endplates maps were found to be significantly different in this comparison ($p = 0.0014$). The overall endplate strengths were not significantly different ($p < 0.8901$, Table 3.3).

A closer examination of the data was done using a *post hoc* Newman-Keuls mean comparison (Table D.31, Appendix D). A direct comparison of equivalent test sites in the two endplates found that there were no significant differences between the anterior test sites (0% AP, or 20% AP), however there were significant differences between the more posterior test sites. The reason for this difference can be seen most clearly in Figure 3.20 b: there is no significant lateral variation in the sacral endplate failure loads (flat distribution), however there is in the posterior half of the inferior lumbar endplates (V-shaped curves).

#### *3.2.4.2 Full AP Analysis – Failure Load*

To look at the effect of including the most anterior test sites in the analysis, a second ANOVA was done using the largest complete AP data set (Figure 3.21). The shapes of the inferior lumbar and sacral failure load maps were again found to be different ($p < 0.0127$), but neither was significantly stronger than the other ($p < 0.1952$, Table 3.3).

A *post hoc* Newman-Keuls mean comparison was done to look at the specific differences between the two maps (Table D.32, Appendix D). This analysis showed significant lateral variation in the posterior region of the inferior lumbar endplates (Table D.8, Appendix D), while the sacrum had no significant lateral variation (Table D.13, Appendix D). The inferior lumbar endplates also had a significant increase in failure load in the most anterior test sites, while the sacral specimens had a steady decrease in failure load from the posterior to anterior test sites.

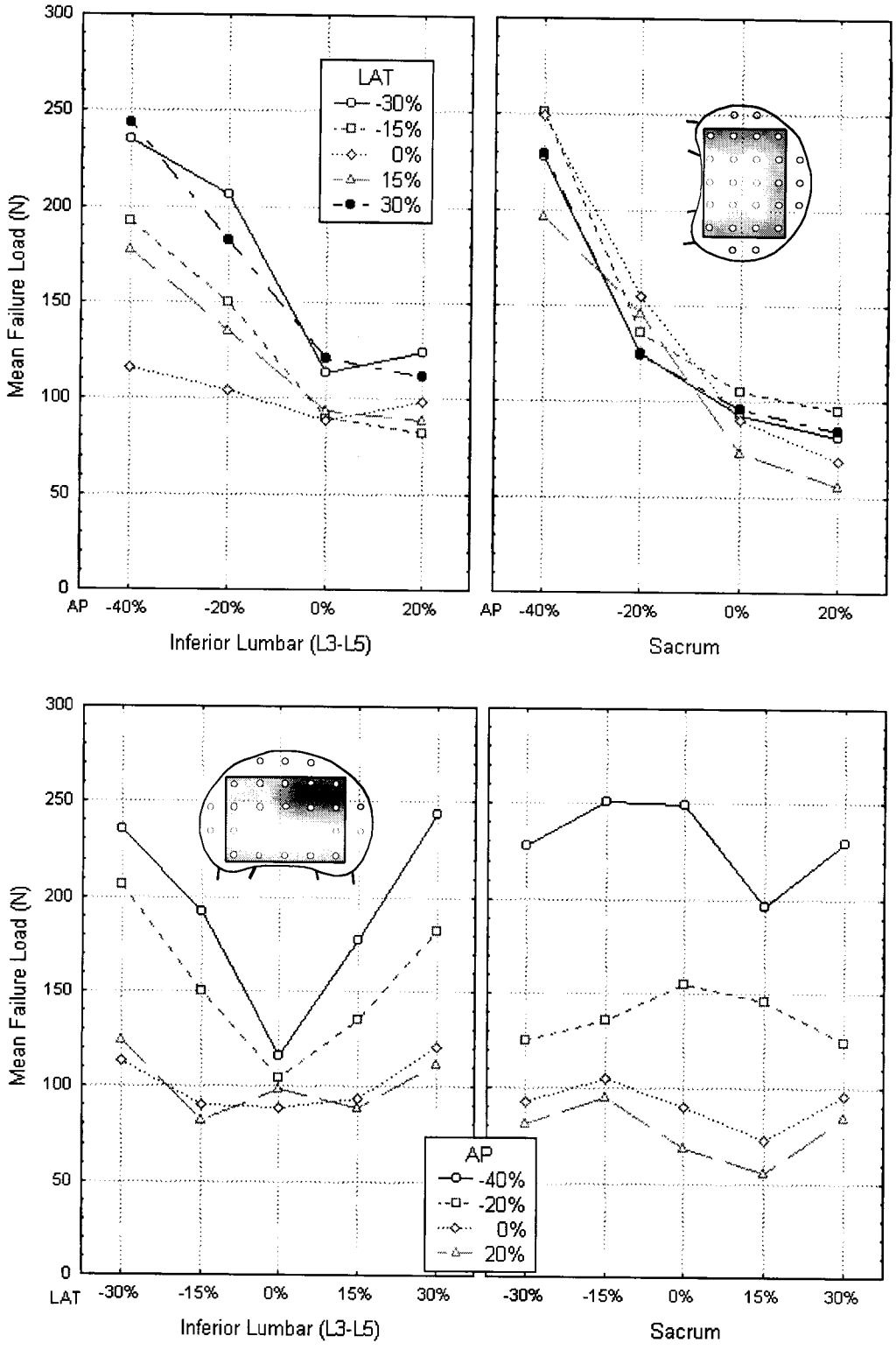


Figure 3.20: Comparison of the maximum AP, LAT failure load distribution in the inferior lumbar and sacral endplates. Figures a and b show the same maps with the AP and LAT axes reversed. The p-value of $< 0.0014$ indicates that there were significant differences between the shapes of the two failure load maps. The *post hoc* Newman-Keuls comparison of these maps is given in Table D.31, Appendix D.

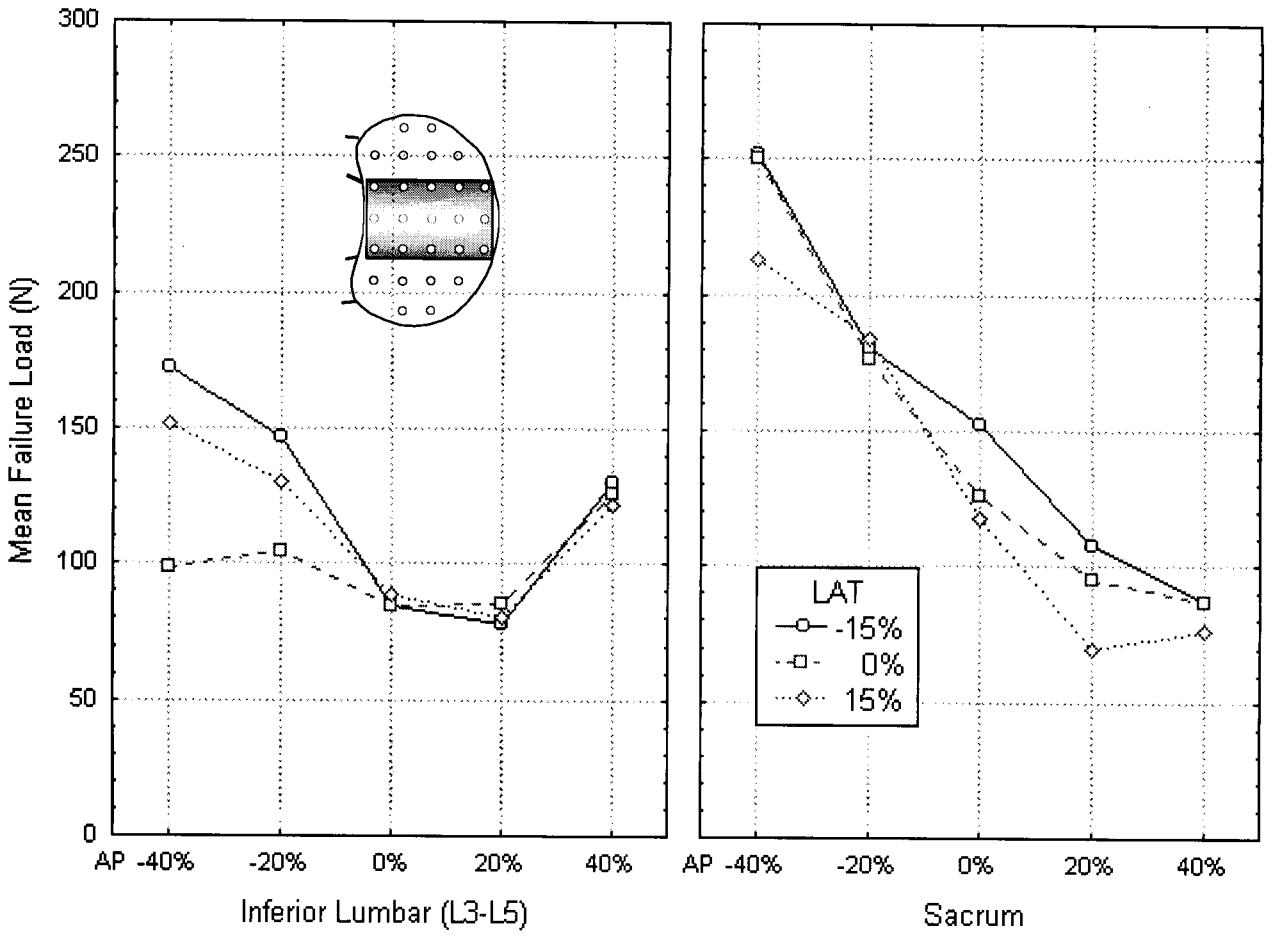


Figure 3.21: Comparison of the full AP failure load distribution in the inferior lumbar and sacral endplates. The p-value of < 0.0127 indicates that there were significant shape differences between these two failure load maps. The *post hoc* Newman-Keuls comparison of these graphs is given in Table D.32, Appendix D.

### *3.2.4.3 Full LAT Analysis – Failure Load*

To look at the effect of including the most lateral test sites in the analysis, a third ANOVA was done using the largest complete LAT data set (Figure 3.22). In this analysis the inferior lumbar and sacral endplate map shapes were again found to be significantly different ($p < 0.0128$). The mean endplate failure loads were not significantly different ($p < 0.6760$, Table 3.3).

Using a *post hoc* Newman-Keuls mean comparison to look at the specific differences within and between the two maps, it was found that the inferior lumbar endplates had significant lateral variation in failure load (Table D.9, Appendix D), while the superior endplates did not (Table D.15, Appendix D).

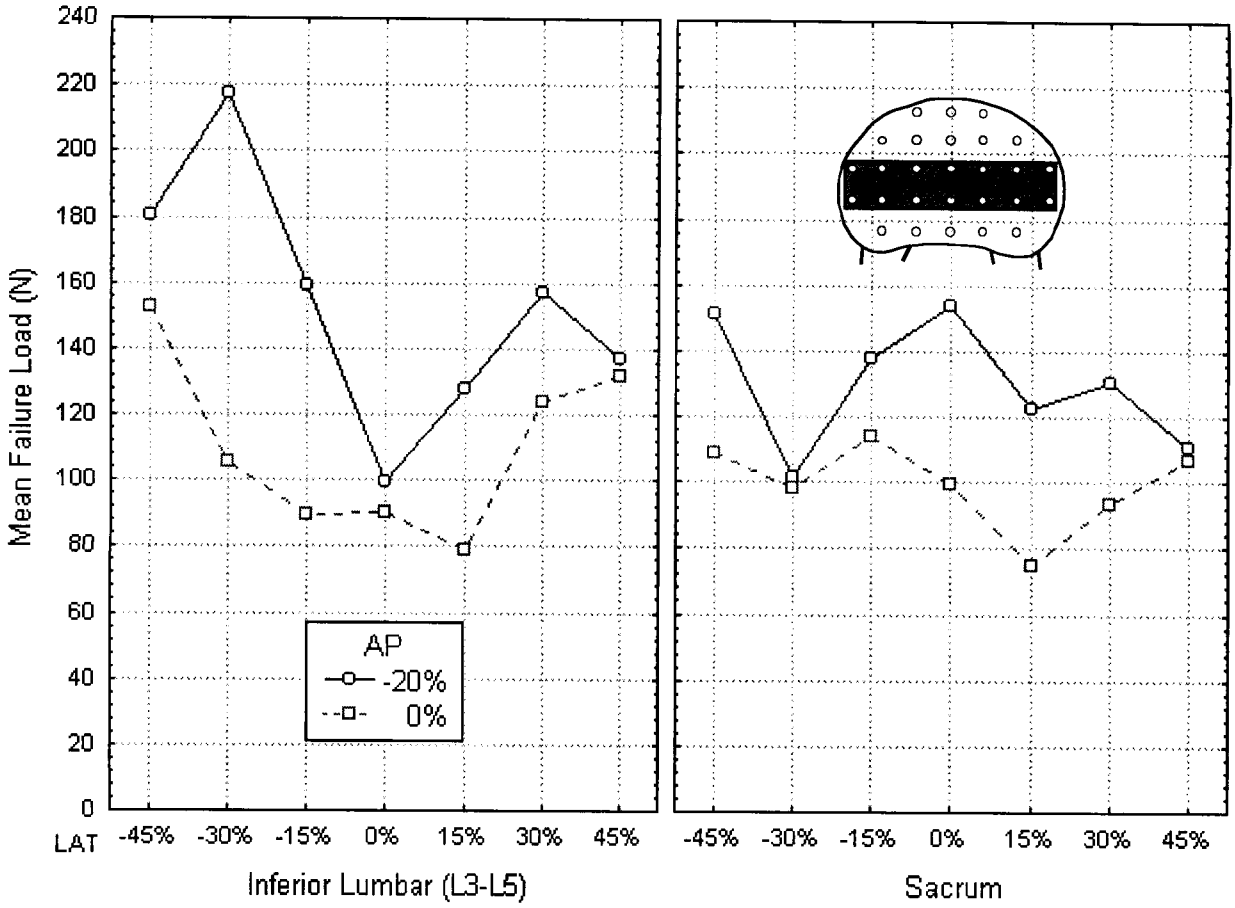


Figure 3.22: Comparison of the full LAT failure load distribution in the inferior lumbar and sacral endplates. The p-value of < 0.0128 indicates that the shapes of these two failure load maps are significantly different. The *post hoc* Newman-Keuls comparison of these two maps is given in Table D.33, Appendix D.

### *3.2.4.4 Maximum AP, LAT Analysis - Stiffness*

The stiffness data was compared using the same analyses used for the failure load data, beginning with the largest complete set of AP, LAT tests (Figure 3.23). Note the similarities between these plots and the corresponding failure load maps (Figure 3.20). In this analysis, the inferior lumbar and sacral endplate stiffness map shapes were found to be significantly different ($p = 0.0017$), but the overall endplate stiffnesses were not ($p < 0.3235$, Table 3.3).

A closer examination of the data was done using a *post hoc* Newman-Keuls mean comparison. A direct comparison of equivalent test sites in the two endplates showed that the differences were all in the posterior region of the endplate. The lateral variation in the stiffness of the posterior half of the inferior endplate (Table D.10, Appendix D) contrasts strongly with the sacral endplate, which has no significant lateral stiffness variation (Table D.16, Appendix D).

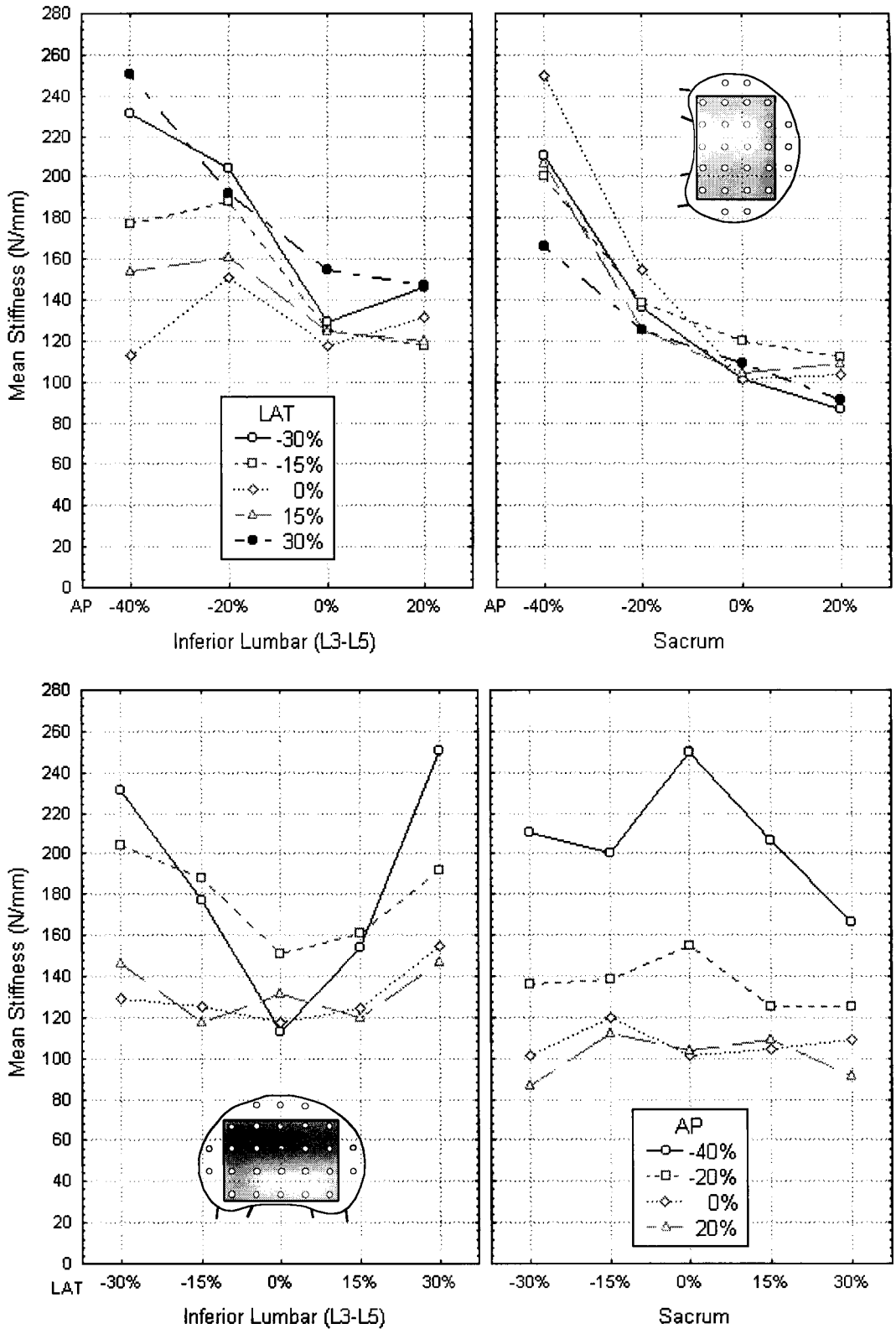


Figure 3.23: Comparison of the maximum AP, LAT stiffness distribution in the inferior lumbar and sacral endplates. Figures a and b show the same maps with the AP and LAT axes interchanged. The p-value of $< 0.0017$ indicates that the shapes of the superior and inferior lumbar endplate stiffness maps were significantly different. The Newman-Keuls *post hoc* comparison of these two graphs is given in Table D.34, Appendix D.

### *3.2.4.5 Full AP Analysis - Stiffness*

To look at the effect of including the most anterior test sites in the analysis, a second ANOVA was done using the largest complete AP data set (Figure 3.24). In this case the shapes of the inferior lumbar and sacral stiffness maps were not found to be significantly different ($p < 0.2237$), nor were the mean endplate stiffnesses different ($p < 0.8784$, Table 3.3).

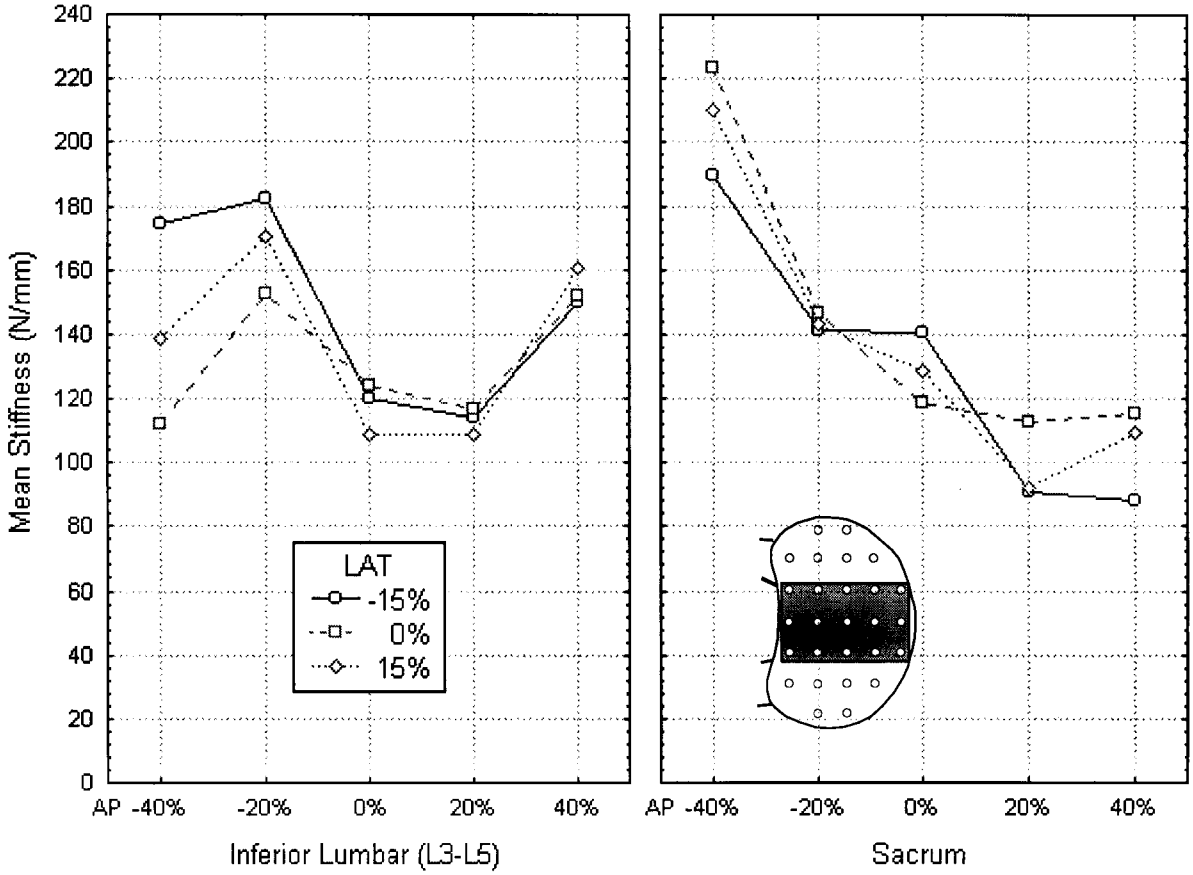


Figure 3.24: Comparison of the full AP stiffness distribution in the inferior lumbar and sacral endplates. The p-value of < 0.2237 indicates that the shapes of the two maps were not significantly different. The *post hoc* comparison of the two maps is given in Table D.35, Appendix D.

### *3.2.4.6 Full LAT Analysis - Stiffness*

To look at the effect of including the most lateral test sites in the stiffness analysis, a third ANOVA was done using the largest complete LAT data set (Figure 3.25). No significant shape differences were found between the inferior lumbar and sacral complete LAT analysis stiffness maps ($p < 0.4778$), or between the mean endplate stiffnesses ($p < 0.3941$, Table 3.3).

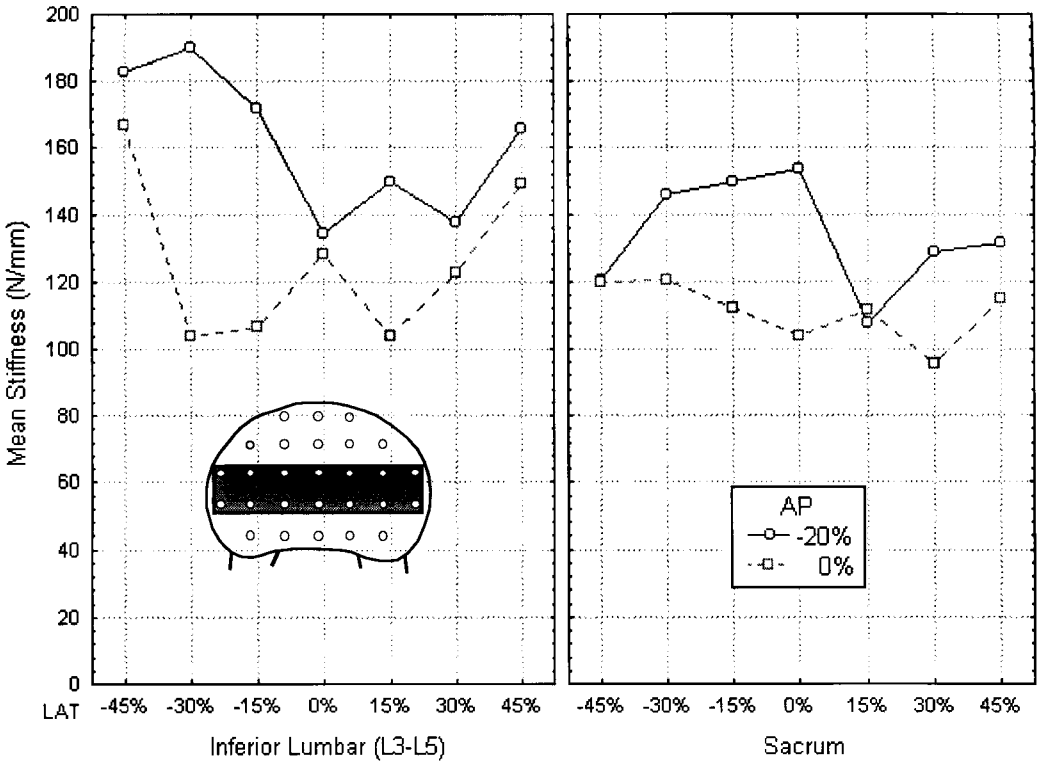


Figure 3.25: Comparison of the full LAT stiffness distribution in the inferior lumbar and sacral lumbar endplates. The p-value of < 0.4778 indicates that there were no significant shape differences between the inferior lumbar and sacral lumbar endplate stiffness maps. The *post hoc* Newman-Keuls comparison of the two maps is given in Table D.36, Appendix D.

**Table 3.3: Effect of Level on Failure Load and Stiffness in the Inferior Lumbar and Sacral Endplates.** This table shows the mean overall endplate failure loads (FL) in Newtons and stiffnesses (ST) in Newtons/millimetre for the inferior lumbar and sacral endplates using the test sites included in the three test site groupings discussed in section 3.2.4. The p-values for the mean comparisons (Means) and map shape comparisons (Maps) are also given. Significant p-values are shaded. Based on these p-values it was concluded that the inferior lumbar and sacral endplate maps were significantly different.

| | Max. AP, LAT | | Full AP | | Full LAT | |
|---|---|---|---|---|---|---|
| | Mean FL | Mean ST | Mean FL | Mean ST | Mean FL | Mean ST |
| Inf. Lumbar Mean | 137.7 | 156.7 | 112.2 | 139.0 | 132.3 | 143.9 |
| Sacral Mean | 134.1 | 137.6 | 144.9 | 136.7 | 114.5 | 122.6 |
| p-value: Means | 0.8901 | 0.3235 | 0.1952 | 0.8784 | 0.6760 | 0.3941 |
| p-value: Maps | 0.0014 | 0.0017 | 0.0127 | 0.2237 | 0.0128 | 0.4778 |

### 3.2.5 Check for Confounding Variables

To check that the results observed in the superior lumbar, inferior lumbar, and sacral specimens were not the result of differences in bone properties, two ANOVAs were done. The first used the endplate as the independent factor and the DEXA value as the dependent variable; the mean DEXA values were not found to be significantly different in the three endplate groups ($p < 0.4589$). The second used disc degeneration grade as the dependent variable. Again, the mean disc degeneration values were not found to differ significantly between the three endplate groups ($p < 0.5055$).

This means that the differences observed between endplate groups were not the result of differences in bone density or disc degeneration.

### 3.2.6 Summary: The Basic Structural Property Maps

It has been shown that the superior lumbar, inferior lumbar and sacral endplates have different structural property distributions (sections 3.2.2-4). The basic maps are summarised here in the form of tables (Table 3.4-3.9) containing the means, standard errors of mean and standard deviations of the failure load or stiffness at each of the test sites included in the analyses.

Careful readers will notice that there are slight discrepancies between the means given in the ANOVA graphs and the means shown in the maps below. The means given in the tables are the simple means calculated directly from the raw data. Note that the number of tests used to generate the means is not constant. This is because some of the tests had to be rejected due to problems encountered during the test. The ANOVA means were weighted by the Statistica program using Type IV hypotheses to account for the missing data. The means generated using this method differ slightly from the simple means generated using the raw data.

#### *3.2.6.1 Superior Lumbar Endplate Basic Structural Property Maps*

**Table 3.4: Superior lumbar endplate failure load (FL) map (L3-L5).** Mean failure load (Mean), standard error of the mean (SEM) and standard deviation (SD) are given in Newtons. The number of tests (n) has no units. The AP and LAT test site co-ordinates are given as percentages of the corresponding endplate dimensions (Figure 2.13).

| LAT | -45% | -30% | -15% | 0% | 15% | 30% | 45% |
|---|---|---|---|---|---|---|---|
| AP | | | | | | | |
| 40% | | | **142.5** | **107.4** | **125.4** | | *Mean FL* |
| | | | 15.6 | 12.6 | 16.7 | | *SEM FL* |
| | | | 77.8 | 64.5 | 78.4 | | *SD FL* |
| | | | 25 | 26 | 22 | | *n* |
| 20% | | **108.5** | **63.4** | **65.4** | **65.8** | **116.4** | |
| | | 15.4 | 7.1 | 9.1 | 7.3 | 14.4 | |
| | | 77.1 | 36.4 | 45.3 | 37.9 | 73.5 | |
| | | 25 | 26 | 25 | 26 | 26 | |
| 0% | **116.1** | **72.0** | **55.3** | **61.8** | **58.5** | **70.6** | **128.7** |
| | 15.2 | 8.3 | 5.9 | 7.9 | 5.4 | 8.2 | 19.0 |
| | 64.3 | 42.3 | 30.7 | 41.0 | 28.3 | 42.4 | 94.9 |
| | 18 | 26 | 27 | 27 | 27 | 27 | 25 |
| -20% | **108.8** | **89.5** | **77.9** | **74.7** | **84.7** | **87.0** | **111.8** |
| | 12.3 | 9.2 | 7.0 | 8.9 | 8.1 | 7.1 | 15.0 |
| | 61.7 | 47.1 | 36.5 | 45.2 | 41.2 | 36.9 | 73.3 |
| | 25 | 26 | 27 | 26 | 26 | 27 | 24 |
| -40% | | **174.3** | **96.9** | **90.6** | **103.0** | **173.5** | |
| | | 18.2 | 11.7 | 14.2 | 13.0 | 16.1 | |
| | | 92.8 | 60.6 | 73.8 | 67.5 | 82.1 | |
| | | 26 | 27 | 27 | 27 | 26 | |

**Table 3.5: Superior lumbar endplate stiffness (ST) map (L3-L5).** Mean stiffness (Mean), standard error of the mean (SEM) and standard deviation (SD) are given in Newtons / millimetre. The number of tests (n) has no units. The AP and LAT test site co-ordinates are given as percentages of the corresponding endplate dimensions (Figure 2.13).

| LAT | -45% | -30% | -15% | 0% | 15% | 30% | 45% |
|---|---|---|---|---|---|---|---|
| AP | | | | | | | |
| 40% | | | **130.5** | **108.0** | **125.6** | | *Mean ST* |
| | | | 12.1 | 8.1 | 11.6 | | *SEM ST* |
| | | | 60.6 | 41.2 | 54.3 | | *SD ST* |
| | | | 25 | 26 | 22 | | *n* |
| 20% | | **141.1** | **104.3** | **88.5** | **95.3** | **132.9** | |
| | | 10.2 | 8.4 | 7.3 | 7.1 | 10.4 | |
| | | 50.9 | 42.7 | 36.3 | 36.4 | 53.1 | |
| | | 25 | 26 | 25 | 26 | 26 | |
| 0% | **136.4** | **115.8** | **79.8** | **101.1** | **92.7** | **114.1** | **140.8** |
| | 15.0 | 9.8 | 6.2 | 6.7 | 7.2 | 12.0 | 12.6 |
| | 63.5 | 49.7 | 31.9 | 34.9 | 37.3 | 62.6 | 63.1 |
| | 18 | 26 | 27 | 27 | 27 | 27 | 25 |
| -20% | **143.9** | **146.8** | **118.4** | **104.1** | **122.8** | **131.0** | **137.7** |
| | 11.2 | 11.5 | 9.3 | 7.0 | 8.9 | 9.1 | 12.7 |
| | 56.0 | 58.6 | 48.2 | 35.7 | 45.4 | 47.5 | 62.1 |
| | 25 | 26 | 27 | 26 | 26 | 27 | 24 |
| -40% | | **160.7** | **101.7** | **112.3** | **103.7** | **164.0** | |
| | | 12.1 | 8.6 | 10.7 | 9.6 | 9.6 | |
| | | 61.6 | 44.9 | 55.3 | 50.1 | 48.8 | |
| | | 26 | 27 | 27 | 27 | 26 | |

The superior lumbar endplate failure load and stiffness maps had very similar shapes. The posterior region was stronger and stiffer than the anterior region. The weakest region was the centre of the endplate and the strongest points were the postero-lateral sites, in front of the pedicles.

### *3.2.6.2 Inferior Lumbar Endplate Basic Structural Property Maps*

**Table 3.6: Inferior lumbar endplate failure load (FL) map (L3-L5).** Mean failure load (Mean), standard error of the mean (SEM) and standard deviation (SD) are given in Newtons. The number of tests (n) has no units. The AP and LAT test site co-ordinates are given as percentages of the corresponding endplate dimensions (Figure 2.13).

| LAT | -45% | -30% | -15% | 0% | 15% | 30% | 45% |
|---|---|---|---|---|---|---|---|
| AP | | | | | | | |
| 40% | | | **130.6** | **131.9** | **124.5** | | *Mean FL* |
| | | | 14.0 | 13.8 | 11.2 | | *SEM FL* |
| | | | 68.6 | 71.5 | 53.7 | | *SD FL* |
| | | | 24 | 27 | 23 | | *n* |
| 20% | | **123.1** | **83.6** | **93.2** | **81.9** | **115.9** | |
| | | 12.8 | 7.3 | 10.5 | 7.4 | 12.4 | |
| | | 67.7 | 38.7 | 54.6 | 39.1 | 65.5 | |
| | | 28 | 28 | 27 | 28 | 28 | |
| 0% | **152.4** | **115.2** | **94.3** | **88.7** | **100.1** | **127.1** | **142.8** |
| | 16.7 | 10.8 | 8.3 | 8.6 | 9.2 | 10.6 | 19.8 |
| | 83.6 | 56.0 | 43.7 | 45.6 | 47.7 | 55.2 | 92.8 |
| | 25 | 27 | 28 | 28 | 27 | 27 | 22 |
| -20% | **186.4** | **201.8** | **155.0** | **113.2** | **144.6** | **174.4** | **180.9** |
| | 21.3 | 14.9 | 12.6 | 12.2 | 13.4 | 15.8 | 28.4 |
| | 85.1 | 77.7 | 66.6 | 64.6 | 69.8 | 82.2 | 127.0 |
| | 16 | 27 | 28 | 28 | 27 | 27 | 20 |
| -40% | | **226.5** | **182.4** | **115.9** | **156.0** | **237.6** | |
| | | 16.9 | 17.7 | 16.8 | 14.8 | 16.5 | |
| | | 77.6 | 93.4 | 87.3 | 74.2 | 75.8 | |
| | | 21 | 28 | 27 | 25 | 21 | |

**Table 3.7: Inferior lumbar endplate stiffness (ST) map (L3-L5).** Mean stiffness (Mean), standard error of the mean (SEM) and standard deviation (SD) are given in Newtons / millimetre. The number of tests (n) has no units. The AP and LAT test site co-ordinates are given as percentages of the corresponding endplate dimensions (Figure 2.13).

| LAT | -45% | -30% | -15% | 0% | 15% | 30% | 45% |
|---|---|---|---|---|---|---|---|
| AP | | | | | | | |
| 40% | | | **145.5** | **144.8** | **157.0** | | *Mean ST* |
| | | | 12.3 | 11.0 | 12.6 | | *SEM ST* |
| | | | 60.0 | 56.9 | 60.5 | | *SD ST* |
| | | | 24 | 27 | 23 | | *n* |
| 20% | | **150.2** | **116.6** | **122.0** | **108.8** | **146.8** | |
| | | 11.9 | 8.2 | 9.6 | 7.4 | 10.5 | |
| | | 62.7 | 43.2 | 50.1 | 38.9 | 55.4 | |
| | | 28 | 28 | 27 | 28 | 28 | |
| 0% | **176.8** | **134.4** | **131.3** | **130.4** | **126.4** | **146.4** | **157.6** |
| | 10.8 | 9.4 | 7.7 | 9.0 | 9.5 | 11.7 | 11.0 |
| | 54.1 | 48.8 | 40.8 | 47.4 | 49.4 | 60.7 | 51.4 |
| | 25 | 27 | 28 | 28 | 27 | 27 | 22 |
| -20% | **191.1** | **196.4** | **189.7** | **165.0** | **186.0** | **180.2** | **170.8** |
| | 19.7 | 10.4 | 10.9 | 13.2 | 13.9 | 15.1 | 15.0 |
| | 78.9 | 54.0 | 57.9 | 70.0 | 72.0 | 78.4 | 67.1 |
| | 16 | 27 | 28 | 28 | 27 | 27 | 20 |
| -40% | | **238.3** | **178.6** | **116.8** | **149.0** | **238.7** | |
| | | 17.1 | 12.8 | 10.6 | 14.1 | 15.4 | |
| | | 78.2 | 67.9 | 55.2 | 70.3 | 70.5 | |
| | | 21 | 28 | 27 | 25 | 21 | |

The basic shapes of the inferior lumbar endplate failure load and stiffness maps were similar to each other and to the superior lumbar endplate maps. The periphery was stronger than the centre and the posterior region was stronger than the anterior margin. The strongest regions were the posterolateral sites, in front of the pedicles. The main difference between the inferior lumbar endplate maps and the superior lumbar endplate maps was the higher failure load and stiffness values in the posterior half of the inferior lumbar endplate maps.

### *3.2.6.3 Sacral Endplate Basic Structural Property Maps*

**Table 3.8: Sacral endplate failure load (FL) map.** Mean failure load (Mean), standard error of the mean (SEM) and standard deviation (SD) are given in Newtons. The number of tests (n) has no units. The AP and LAT test site co-ordinates are given as percentages of the corresponding endplate dimensions (Figure 2.13).

| LAT | -45% | -30% | -15% | 0% | 15% | 30% | 45% | |
|---|---|---|---|---|---|---|---|---|
| AP | | | | | | | | |
| 40% | | | **86.7** | **84.51** | **76.48** | | | *Mean FL* |
| | | | 22.5 | 15.49 | 14.13 | | | *SEM FL* |
| | | | 55.0 | 40.98 | 37.39 | | | *SD FL* |
| | | | 6 | 7 | 7 | | | *n* |
| 20% | | **90.3** | **106.4** | **88.6** | **67.6** | **94.2** | | |
| | | 18.3 | 37.8 | 28.0 | 16.4 | 23.9 | | |
| | | 48.4 | 100.1 | 74.2 | 43.3 | 63.1 | | |
| | | 7 | 7 | 7 | 7 | 7 | | |
| 0% | **136.6** | **119.7** | **144.6** | **126.0** | **111.9** | **131.4** | **142.6** | |
| | 42.8 | 31.7 | 47.9 | 38.1 | 41.4 | 41.8 | 52.0 | |
| | 113.2 | 83.7 | 126.6 | 100.9 | 109.6 | 110.6 | 137.5 | |
| | 7 | 7 | 7 | 7 | 7 | 7 | 7 | |
| -20% | **147.2** | **162.2** | **174.8** | **191.0** | **183.5** | **156.1** | **103.4** | |
| | 42.5 | 42.0 | 47.7 | 46.5 | 48.2 | 41.4 | 39.8 | |
| | 95.0 | 111.1 | 126.1 | 122.9 | 127.6 | 109.6 | 89.0 | |
| | 5 | 7 | 7 | 7 | 7 | 7 | 5 | |
| -40% | | **227.7** | **258.2** | **262.7** | **227.5** | **229.4** | | |
| | | 66.8 | 39.9 | 40.7 | 45.6 | 50.5 | | |
| | | 163.7 | 105.6 | 107.7 | 120.7 | 123.7 | | |
| | | 6 | 7 | 7 | 7 | 6 | | |

**Table 3.9: Sacral endplate stiffness (ST) map.** Mean stiffness (Mean), standard error of the mean (SEM) and standard deviation (SD) are given in Newtons / millimetre. The number of tests (n) has no units. The AP and LAT test site co-ordinates are given as percentages of the corresponding endplate dimensions (Figure 2.13).

| LAT | -45% | -30% | -15% | 0% | 15% | 30% | 45% |
|---|---|---|---|---|---|---|---|
| AP | | | | | | | |
| 40% | | | **88.1** | **116.0** | **116.6** | | *Mean ST* |
| | | | 14.1 | 17.2 | 24.9 | | *SEM ST* |
| | | | 34.4 | 45.5 | 65.9 | | *SD ST* |
| | | | 6 | 7 | 7 | | *n* |
| 20% | | **87.1** | **111.7** | **115.7** | **107.0** | **100.2** | |
| | | 12.6 | 27.0 | 14.7 | 27.4 | 16.3 | |
| | | 33.2 | 71.4 | 38.9 | 72.4 | 43.0 | |
| | | 7 | 7 | 7 | 7 | 7 | |
| 0% | **147.8** | **114.6** | **141.1** | **127.6** | **123.2** | **123.9** | **148.9** |
| | 27.0 | 20.1 | 27.7 | 30.9 | 34.0 | 29.2 | 32.3 |
| | 71.4 | 53.2 | 73.2 | 81.7 | 89.9 | 77.2 | 85.5 |
| | 7 | 7 | 7 | 7 | 7 | 7 | 7 |
| -20% | **120.9** | **156.0** | **153.2** | **172.9** | **149.8** | **141.3** | **126.6** |
| | 21.4 | 24.5 | 34.7 | 37.9 | 33.5 | 22.8 | 26.0 |
| | 47.9 | 64.8 | 91.9 | 100.3 | 88.7 | 60.3 | 58.2 |
| | 5 | 7 | 7 | 7 | 7 | 7 | 5 |
| -40% | | **210.4** | **196.7** | **244.9** | **212.9** | **166.7** | |
| | | 29.0 | 30.4 | 24.2 | 27.6 | 30.1 | |
| | | 71.0 | 80.4 | 64.0 | 72.9 | 73.6 | |
| | | 6 | 7 | 7 | 7 | 6 | |

The sacral endplate maps had very different shapes than the lumbar endplate maps. Both the failure load and stiffness maps had no significant lateral variation. The highest values were found at the posterior margin of the endplate and there was a steady decrease in failure load and stiffness from the posterior to anterior margin of the endplate.

### 3.3 Effects of Bone Density on Property Distribution

To determine the effects of bone density on the failure load and stiffness maps, the specimens were divided into groups based on their DEXA values (as recorded using a lateral DEXA scan, section 2.3.2). This grouping was necessary because an ANOVA requires discrete values for comparisons between groups (i.e., values divided into discrete groups, e.g. A, B, and C, can be compared, but a continuous variable, such as DEXA = 0.50, 0.61, 0.77, 0.78 and 1.03, cannot).

To decide how best to group the values, two scatterplots were generated, one showing the failure load values at all test sites plotted versus DEXA (Figure 3.26 a) and the second showing the stiffness values plotted versus DEXA (Figure 3.26 b). These plots were examined to identify groups of data with similar ranges in failure load and stiffness. Based on these comparisons, the specimens were grouped into three categories: Low (DEXA < 0.65 g/cm$^2$), Mid, and High (DEXA > 0.90 g/cm$^2$).

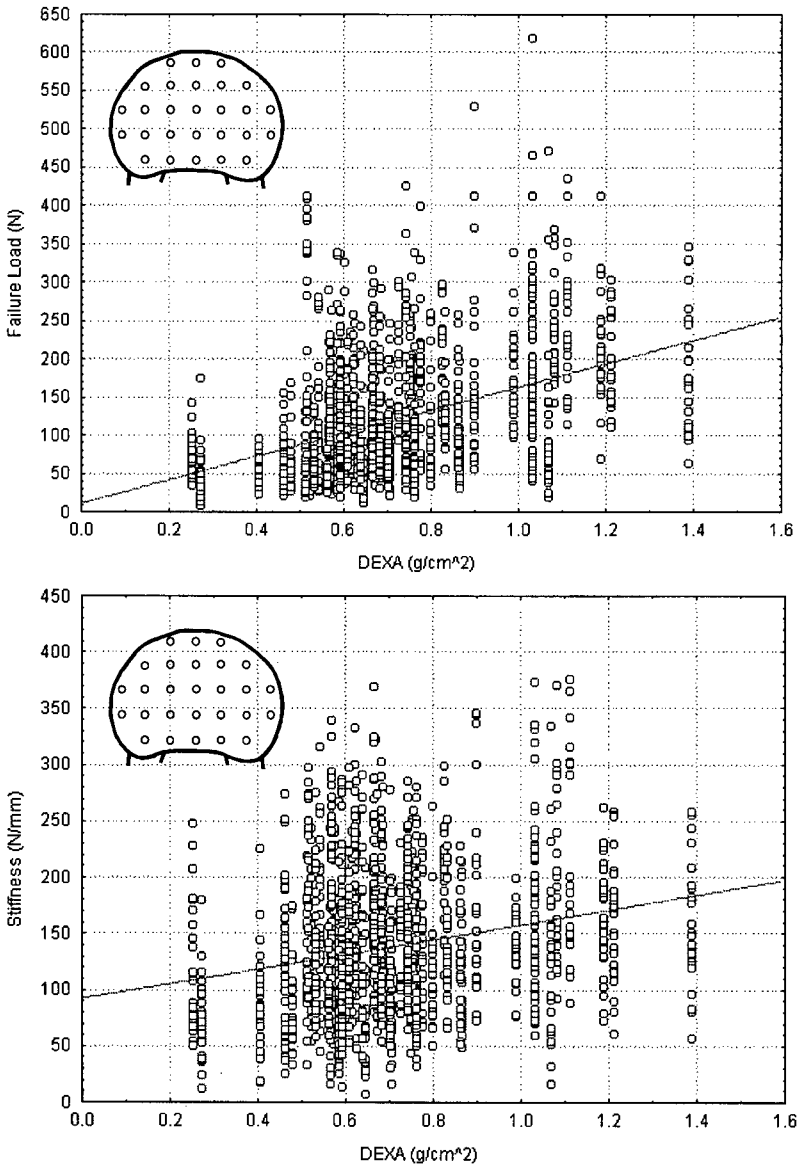


Figure 3.26: Effect of bone density on a) failure load and b) stiffness. These graphs were used to get a basic idea of how best to group the endplates based on their DEXA values. Based on these "back-of-the-envelope" comparisons, the specimens were grouped into three categories: Low (DEXA < 0.65 g/cm$^2$), Mid, and High (DEXA >0.90 g/cm$^2$).

To check that these groupings were reasonable, a statistical comparison of the groups was done. A one-way ANOVA on the failure loads using the DEXA groups as factors showed that there was a significant difference in the mean failure loads of the groups ($p < 0.0001$). A second ANOVA, on the stiffness values, showed that the mean stiffnesses in the groups were also significantly different ($p < 0.0001$). *Post hoc* Newman-Keuls comparisons of the mean failure loads showed that all three means differed significantly from one another at $p < 0.0001$. The same was found for the mean stiffnesses of the three groups. A summary of the characteristics of the three groups is given in Table 3.10.

**Table 3.10: Characteristics of the three DEXA groups.** DEXA values are given in g/cm$^2$, failure load means, standard errors of mean (SEM), and standard deviations (SD) are given in Newtons, and the number of tests (n) has no units. Stiffness values are given in Newtons per millimetre. Note that fewer of the specimens fell into the "High" DEXA group, thus the standard errors of the means are larger in this group.

| Variable | DEXA Group | Mean | SEM | SD | n |
|---|---|---|---|---|---|
| Failure Load | Low (< 0.65) | 94.7 | 2.6 | 69.7 | 708 |
| | Mid | 121.1 | 3.0 | 72.8 | 601 |
| | High (> 0.90) | 186.5 | 5.7 | 92.1 | 266 |
| Stiffness | Low (< 0.65) | 125.7 | 2.4 | 64.2 | 708 |
| | Mid | 143.6 | 2.5 | 60.8 | 601 |
| | High (> 0.90) | 164.3 | 4.0 | 65.9 | 266 |

A look at the contents of Table 3.10 reveals that there were far fewer specimens falling into the "High" DEXA group than into the other two groups. This will tend to reduce the power of the analysis to detect significant differences between the maps, since the means in the "High" DEXA group are less well defined (note the larger standard errors of mean in the "High" DEXA groups).

A linear regression analysis was done to look at how closely related the bone density and disc degeneration were, with the DEXA value being the dependent variable. The correlation coefficient of $r^2 = 0.0001$ indicated that the two variables were not interrelated.

Once the DEXA groups had been established, the effects of bone density on the strength distributions could be examined. Since significant differences were identified between the superior lumbar, inferior lumbar and sacral endplate maps (section 3.2) these groups were examined separately.

### 3.3.1 Effect of Bone Density on the Superior Lumbar Endplate Failure Load Map

#### *3.3.1.1 Maximum AP, LAT Analysis*

To get more detailed information on the differences between the Low, Mid, and High bone density failure load distributions, three-way ANOVAs were used to generate failure load maps grouped by bone density. The bone density maps were significantly different ($p < 0.0052$) with an interesting pattern of change illustrated by the curves. Looking at the AP failure load distributions (Figure 3.27) it can be seen that the High bone density group had high posterior and anterior failure loads in all five LAT curves. The three central LAT curves (-15, 0, and 15% LAT) levelled out in the Mid density group due to a drop in both anterior and posterior failure load values, with the largest decrease being posterior. The posterior failure loads in the –30 and 30% LAT curves also decreased, but less dramatically. The Low density group showed a further levelling of the LAT curves.

Looking at the magnitude of the failure load, rather than the distribution, it was found that there were significant differences between the mean failure loads in the three DEXA groups in the superior lumbar endplate ($p < 0.0001$). A *post hoc* Newman-Keuls test showed that the mean failure load in the High density group was significantly higher than the mean failure load in either the Mid ($p = 0.0006$) or the Low ($p = 0.0002$) density groups, and the Mid density group was significantly stronger than the Low density group ($p = 0.0341$). To see if the map shapes in the Low and Mid density groups were significantly different, a second ANOVA was done comparing the Low and Mid density groups. It confirmed that the shape differences in these two more similar maps were significant ($p < 0.0054$).

To summarise, the failure load in the superior lumbar endplates decreased more rapidly posteriorly than anteriorly as the bone density dropped, resulting in a flatter failure load profile. The overall endplate strength also decreased as the bone density dropped.

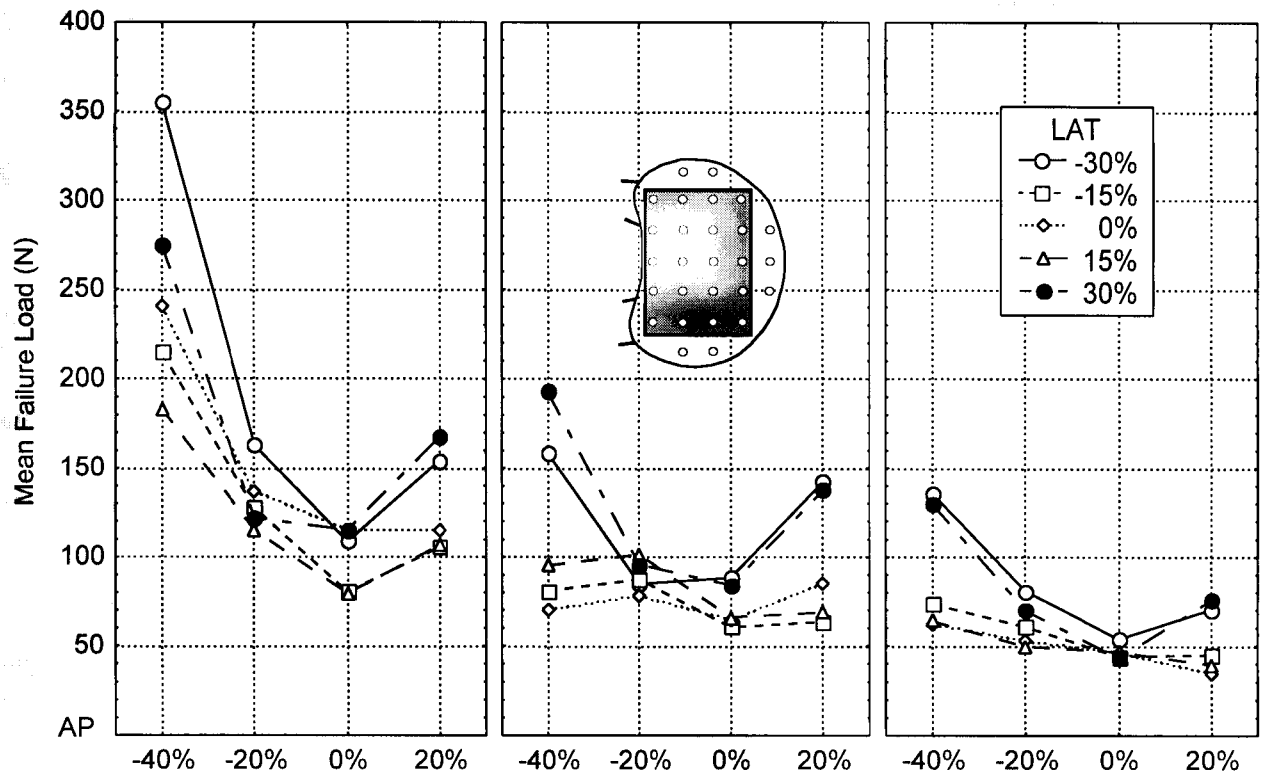


Figure 3.27: Effect of bone density on the superior endplate AP, LAT failure load map. The p-value of $< 0.0052$ indicates that the map shape did change significantly as the bone density decreased. The failure load decreased more rapidly posteriorly than anteriorly as the bone density dropped, resulting in a flatter AP failure load profile.

### *3.3.1.2 Full AP Analysis*

The full AP analysis was done to see if the inclusion of the most anterior test sites had an effect on the bone density failure load map comparison in the superior lumbar endplates. Note the high failure loads at the most anterior test sites (40% AP) (Figure 3.28), which were not included in the maximum area analysis (Figure 3.27).

Significant differences were found between the map shapes ($p < 0.0189$). Again, similar trends were observed: the High density group had a U-shaped AP profile; the failure load decreased more posteriorly than anteriorly moving from the High to Mid density groups, and finally the anterior failure load decreased in the Low density group, leading to a more uniform failure load distribution.

The mean endplate failure load was also significantly different in the three groups ($p < 0.0001$). A *post hoc* Newman-Keuls test showed that the High density group was significantly stronger than either the Mid ($p = 0.0013$) or Low ($p = 0.0002$) density groups, and the Mid density group was significantly stronger than the Low density group ($p = 0.0167$).

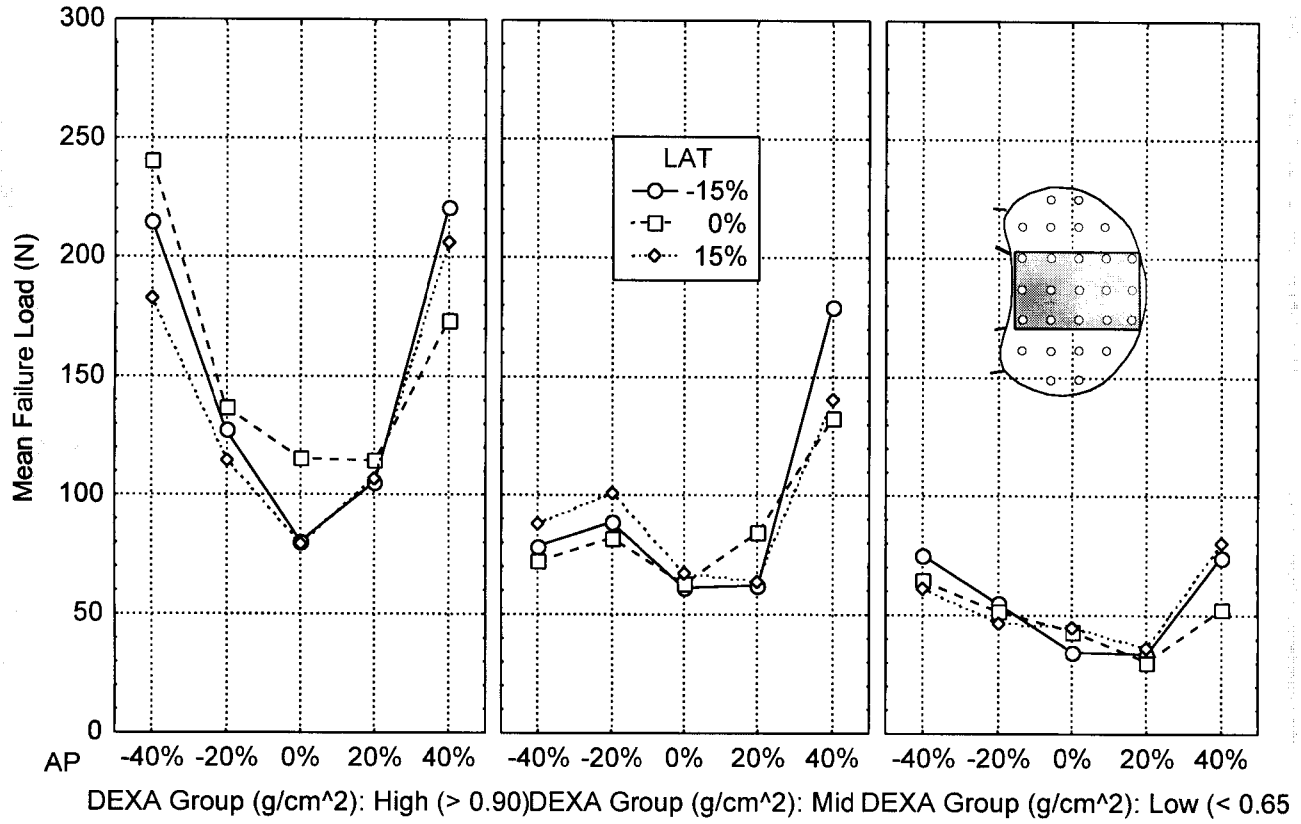


Figure 3.28: Effect of bone density on the shape of the superior endplate full AP failure load map. The p-value of < 0.0189 indicates that the map shape did change significantly as the bone density decreased. Notice again the flattening of the AP failure load curve profile with progressively lower bone density.

### *3.3.1.3 Full LAT Analysis*

The full LAT analysis was used to look at the effects of AP test location on the most lateral test sites. No significant difference was found between the map shapes in the three bone density groups ($p < 0.7993$), however the mean endplate failure load did show a significant decrease with lower bone density ($p < 0.0485$).

### *3.3.1.4 Summary*

The overall magnitude of the superior lumbar endplate failure load decreased as the bone density decreased, and the superior lumbar endplate failure load map flattened out as the bone density decreased, resulting in a more uniform endplate strength.

### 3.3.2 Effect of Bone Density on the Superior Lumbar Endplate Stiffness Map

#### *3.3.2.1 Maximum AP, LAT Analysis*

No significant differences were found between the shapes of the superior lumbar endplate stiffness maps in the three bone density groups ($p < 0.7636$), nor were the mean stiffness magnitudes significantly different ($p < 0.0835$) (Figure 3.29).

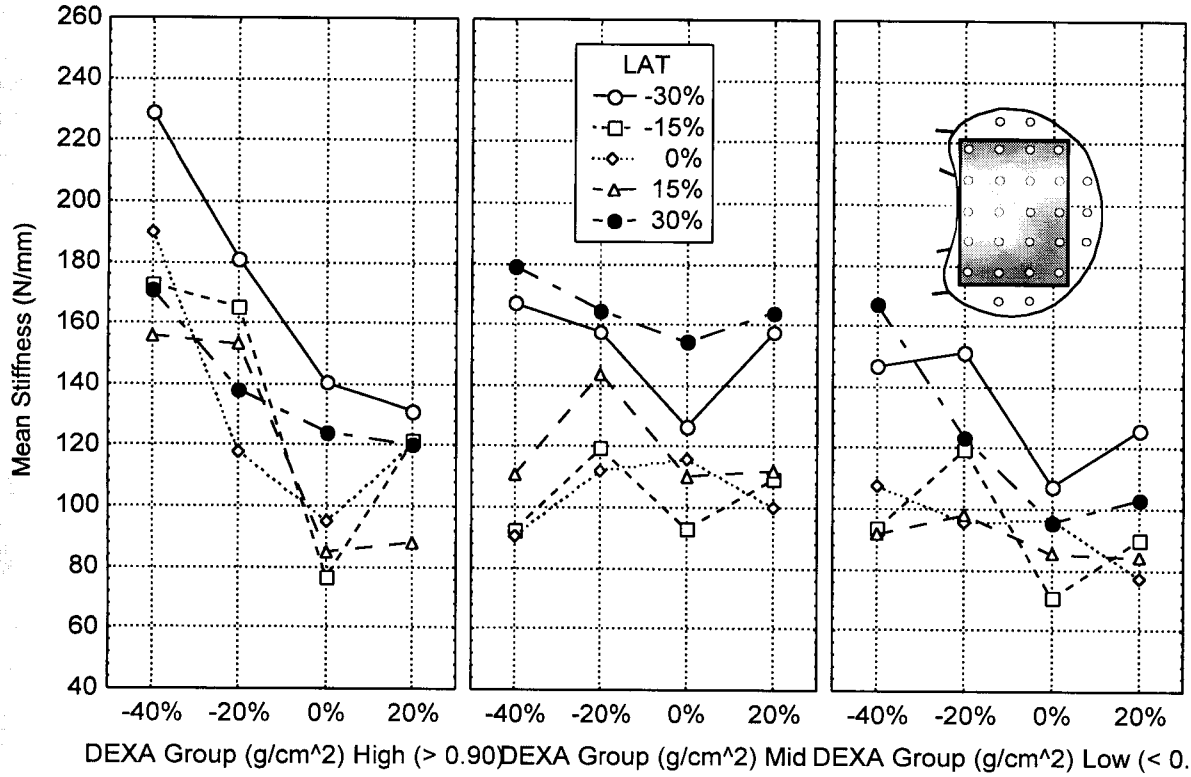


Figure 3.29: Effect of bone density on the superior endplate AP, LAT stiffness map. The p-value of $< 0.7636$ indicates that the map shape did not change significantly as the bone density decreased.

#### *3.3.2.2 Full AP Analysis*

The three-way ANOVA on the full AP stiffness data set (the complete analysis which included the most anterior test sites) also found that there was no significant difference between the superior endplate stiffness map shapes in the three bone density groups ($p < 0.9100$). It did, however, show that the mean endplate stiffness differed in the three DEXA groups ($p < 0.0153$). A Newman-Keuls *post hoc* comparison showed that the Low and Mid density means ($p = 0.0394$), and the Low and High density means ($p = 0.0188$) were significantly different, but the Mid and High means were not ($p = 0.4173$).

#### *3.3.2.3 Full LAT Analysis*

The three-way ANOVA on the full LAT stiffness data set (the complete analysis which included the most lateral test sites) again found that there was no significant difference between the superior endplate stiffness map shapes in the three bone density groups ($p < 0.5764$). It also found that there was no significant difference between the mean endplate stiffness in the three DEXA groups ($p < 0.7292$).

### *3.3.2.4 Summary*

Bone density did not appear to have a significant effect on the shape of the superior lumbar endplate stiffness maps, and had only a mild effect on the magnitude of the overall endplate stiffness, mainly in the central strip of the endplate (-15 through 15% LAT).

## 3.3.3 Effect of Bone Density on the Inferior Lumbar Endplate Failure Load Map

### *3.3.3.1 Maximum AP, LAT Analysis*

No significant change in map shape was found in the inferior lumbar endplates using the maximum AP, LAT data set ($p < 0.9013$, Figure 3.30). The overall strength of the endplate was, however, affected by the DEXA value ($p < 0.0112$). A *post hoc* Newman-Keuls test showed that the failure loads in the High density group were significantly higher than either the Mid ($p = 0.0038$) or Low ($p = 0.0073$) density group failure loads. There was no significant difference between the failure load magnitudes in the Mid and Low density groups ($p = 0.8765$).

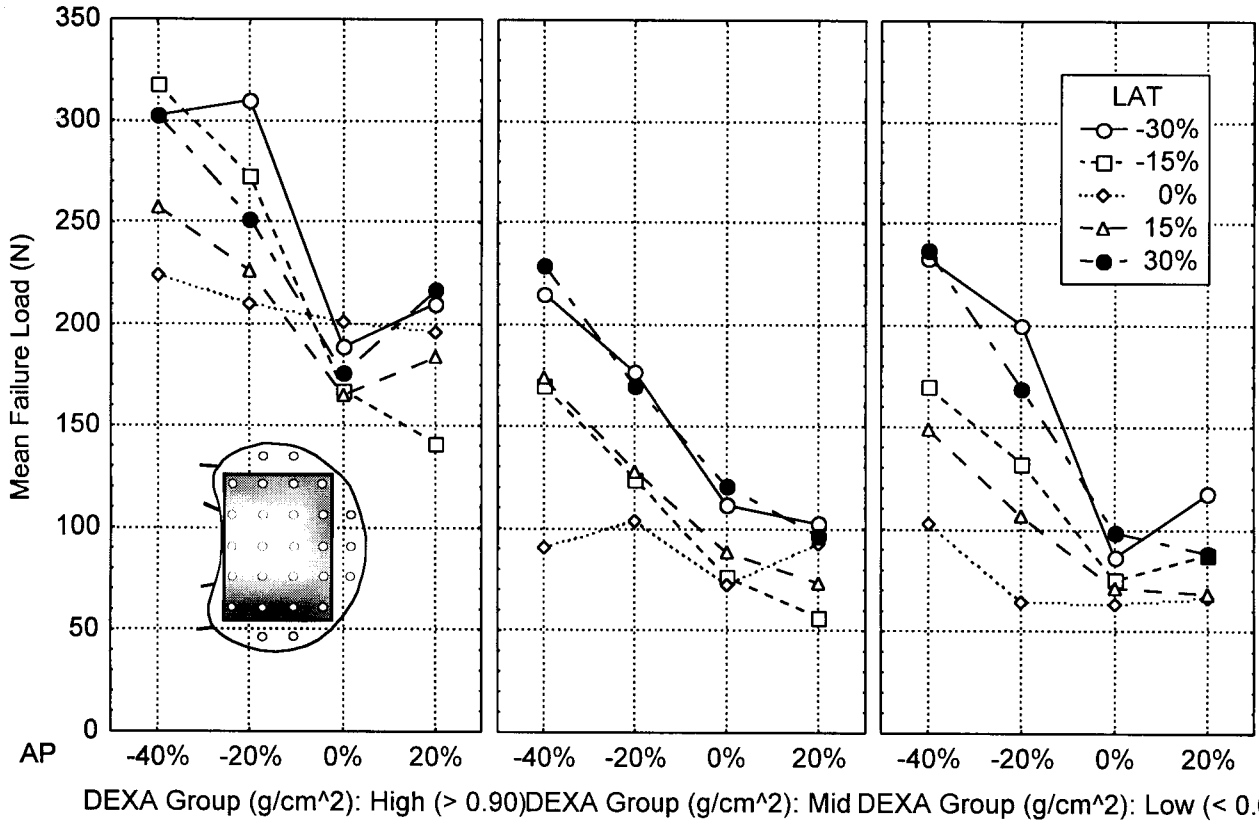


Figure 3.30: Effect of bone density on the inferior lumbar endplate AP, LAT failure load map. The p-value of < 0.9013 indicates that the map shape did not change significantly as the bone density decreased. Note, however, that the High density group was significantly stronger than either the Mid ($p = 0.0038$) or Low ($p = 0.0073$) density groups. The Mid density group was not significantly stronger than the Low density group ($p = 0.8765$).

### *3.3.3.2 Full AP Analysis*

The three-way analysis of variance using the full AP data set found again that there was no significant difference between the inferior endplate failure load map shapes when grouped by bone density ($p < 0.3996$). There was, however, a significant difference in the failure load magnitudes ($p < 0.0011$). A *post hoc* Newman-Keuls test showed that the High density group was significantly stronger than either the Mid ($p = 0.0004$) or Low ($p = 0.0008$) density groups, while the failure load magnitudes in the Mid and Low density groups were not significantly different ($p = 0.7909$).

### *3.3.3.3 Full LAT Analysis*

The three-way ANOVA on the full LAT data set found that there *was* a significant difference between the inferior endplate failure load map shapes when grouped by bone density ($p < 0.0245$). There was also a significant difference in the failure load magnitudes ($p < 0.0017$). A *post hoc* Newman-Keuls test showed that the High density group was significantly stronger than either the Mid ($p = 0.0020$) or Low ($p = 0.0014$) density groups, while the failure load magnitudes in the Mid and Low density groups were not significantly different ($p = 0.5653$). Looking at the maps, one sees that the High density group had higher failure loads posteriorly than anteriorly. This was not the case in either the Mid or Low density groups.

A second ANOVA comparing the Mid and Low density maps found that the map shapes ($p < 0.3699$) were not significantly different in these two groups.

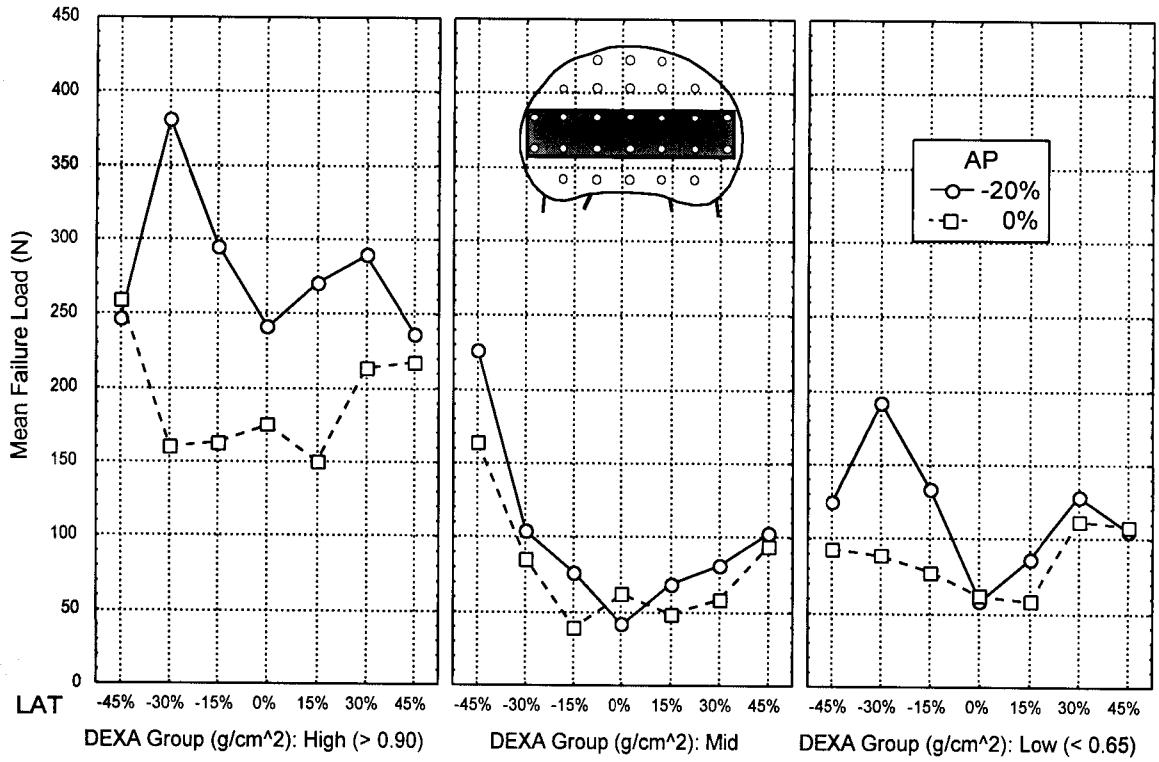


Figure 3.31: Effect of bone density on the inferior endplate full LAT failure load map. The p-value of $< 0.0245$ indicates that the map shape changed significantly as the bone density decreased. A *post hoc* Newman-Keuls mean comparison showed that the High density map differed from the Mid and Low density maps.

### *3.3.3.4 Summary*

There was a significant strength decrease in the inferior lumbar endplates as the bone density dropped. This loss of strength was essentially uniform over the endplate since bone density did not appear to have much effect on the failure load distribution (i.e. the relative strength of only the most lateral points was affected by bone density).

## 3.3.4 Effects of Bone Density on the Inferior Lumbar Endplate Stiffness Map

### *3.3.4.1 Maximum AP, LAT Analysis*

The shape of the maximum AP, LAT inferior lumbar endplate stiffness map was not significantly affected by bone density ($p < 0.9669$), nor was the mean endplate stiffness affected by density ($p < 0.6320$).

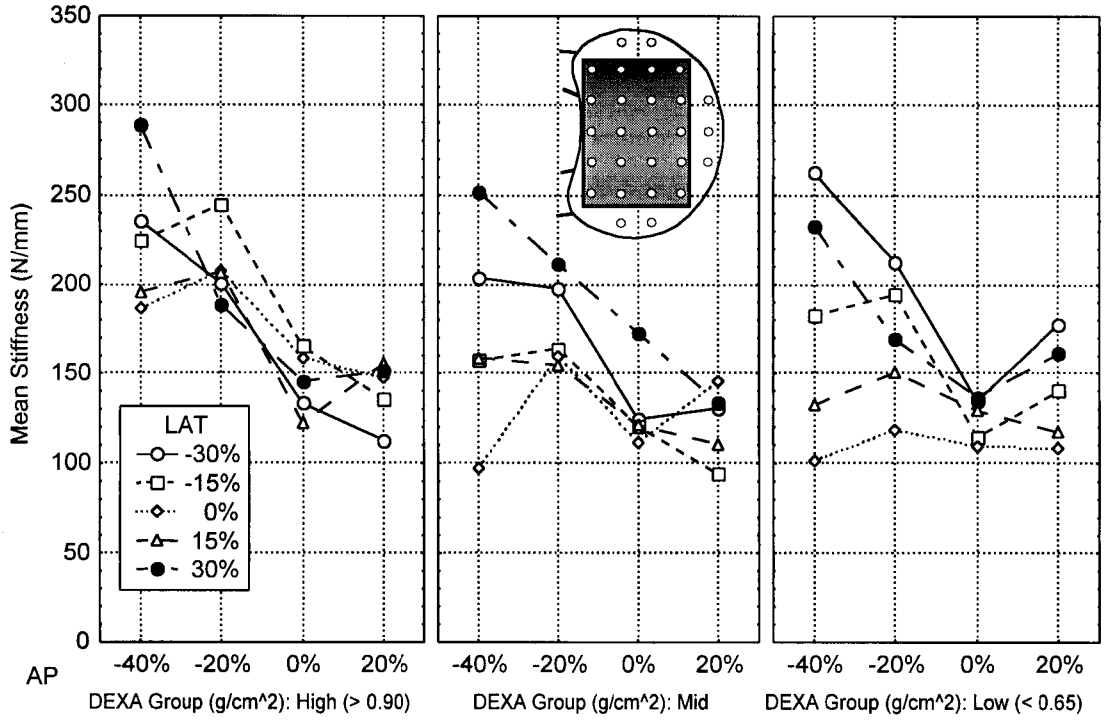


Figure 3.32: Effect of bone density on the inferior lumbar endplate AP, LAT stiffness map. The p-value of $< 0.9669$ indicates that the map shape did not change significantly as the bone density decreased.

### *3.3.4.2 Full AP Analysis*

The full AP analysis also found that bone density did not affect either the stiffness distribution ($p < 0.3616$) or the mean endplate stiffness ($p < 0.1733$) in the inferior lumbar endplates.

### *3.3.4.3 Full LAT Analysis*

The full LAT analysis of the inferior lumbar endplates showed that bone density had no significant effect on the shape of the stiffness map ($p < 0.5846$), however there was a difference between the mean endplate stiffnesses ($p < 0.0048$). A *post hoc* Newman-Keuls comparison showed that the High density group was significantly stiffer than both the Mid ($p = 0.0030$) and Low ($p = 0.0094$) density groups, however the Mid and Low group stiffnesses were not significantly different ($p = 0.0565$).

### *3.3.4.4 Summary*

The shape of the inferior lumbar endplate stiffness map was unaffected by bone density. Only the full LAT analysis showed a difference in the mean endplate stiffness. This appeared to be the result of larger stiffness differences in the –20 and 0% AP test sites rather than just the inclusion of the most lateral test sites, although the most lateral values in the High density group were significantly greater than those in the Mid and Low density groups.

## 3.3.5 Effect of Bone Density on the Sacral Endplate Failure Load Map

Neither the failure load map shape, nor the mean failure load were significantly affected by bone density in the sacral endplates in the maximum AP, LAT analysis ($p < 0.2451$; $p < 0.5829$, Figure 3.33), the full AP analysis ($p < 0.3242$; $p < 0.7781$), or the full LAT analysis ($p < 0.4661$; $p < 0.6043$).

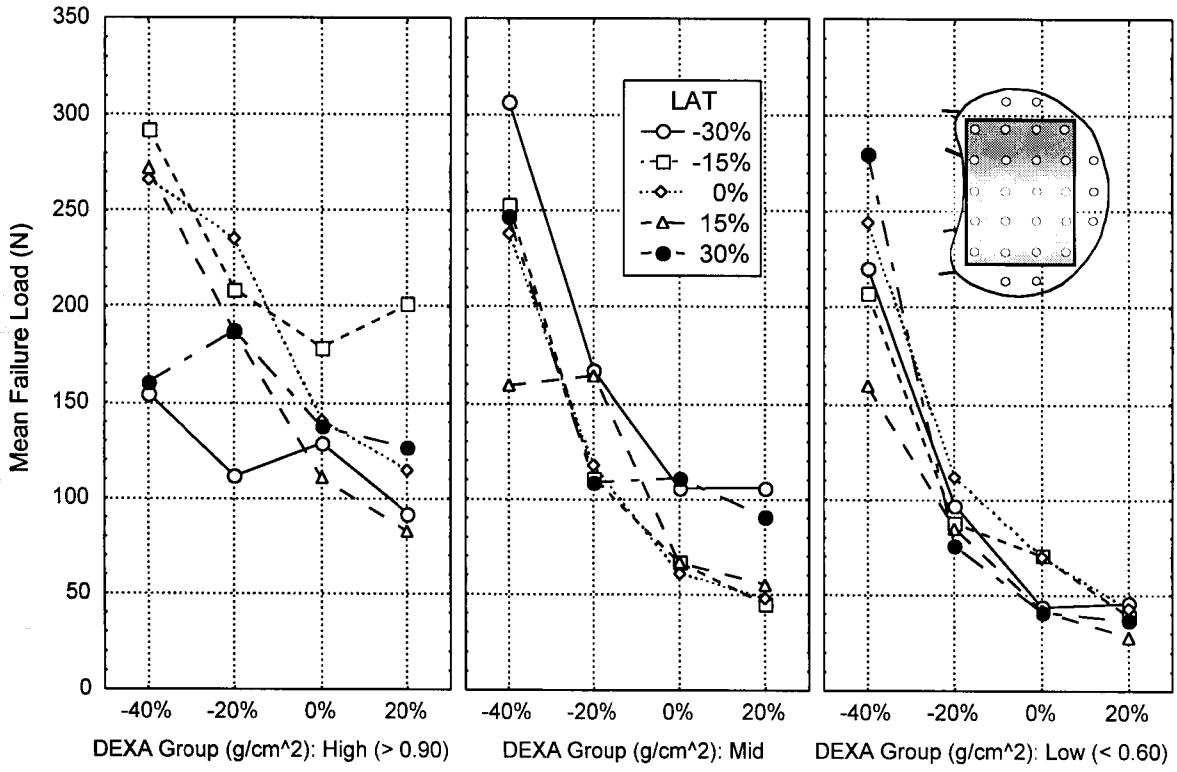


Figure 3.33: Effect of bone density on the sacral endplate AP, LAT failure load map. The p-value of < 0.2451 indicates that the map shape did not change significantly as the bone density decreased.

### 3.3.6 Effect of Bone Density on the Stiffness Map: Sacral Endplates

#### *3.3.6.1 Maximum AP, LAT Analysis*

The sacral stiffness map shape was not significantly affected by bone density ($p < 0.2436$), nor was the mean sacral endplate stiffness ($p < 0.2465$) in the maximum AP, LAT analysis.

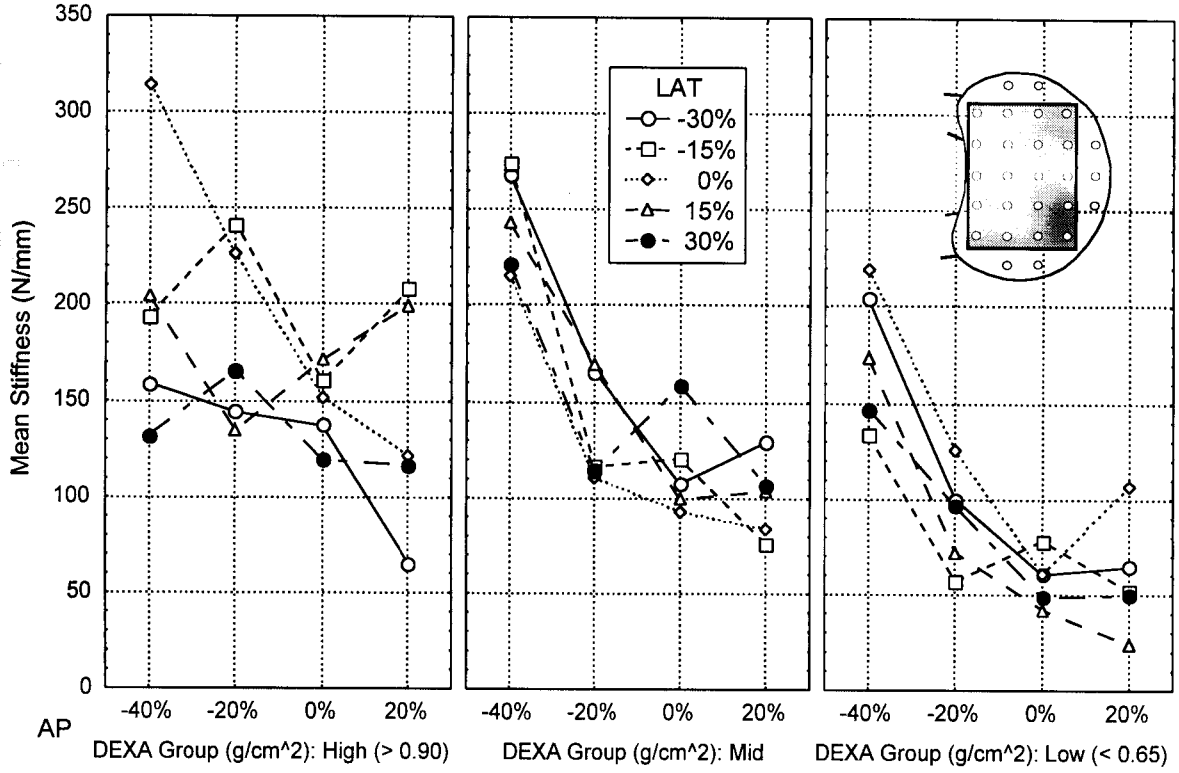


Figure 3.34: Effect of bone density on the sacral endplate AP, LAT stiffness map. The p-value of < 0.2436 indicates that the map shape did not change significantly as the bone density decreased.

#### *3.3.6.2 Full AP Analysis*

In the full AP analysis, the sacral stiffness map shape was affected by bone density ($p < 0.0025$), however the mean endplate stiffness was not ($p < 0.8051$).

A closer look at the map shapes revealed that the High density group had quite a skewed map, while both the Mid and Low density groups had maps more like the characteristic sacral endplate map presented in section 3.2.9. This is most likely a result of the small number of specimens in the High density group.

Additional ANOVAs comparing map shapes in the Mid and Low density groups ($p < 0.1186$), the High and Mid density groups ($p < 0.1262$), and the High and Low density groups found that only the map shapes of the High and Low density groups were significantly different ($p < 0.0001$).

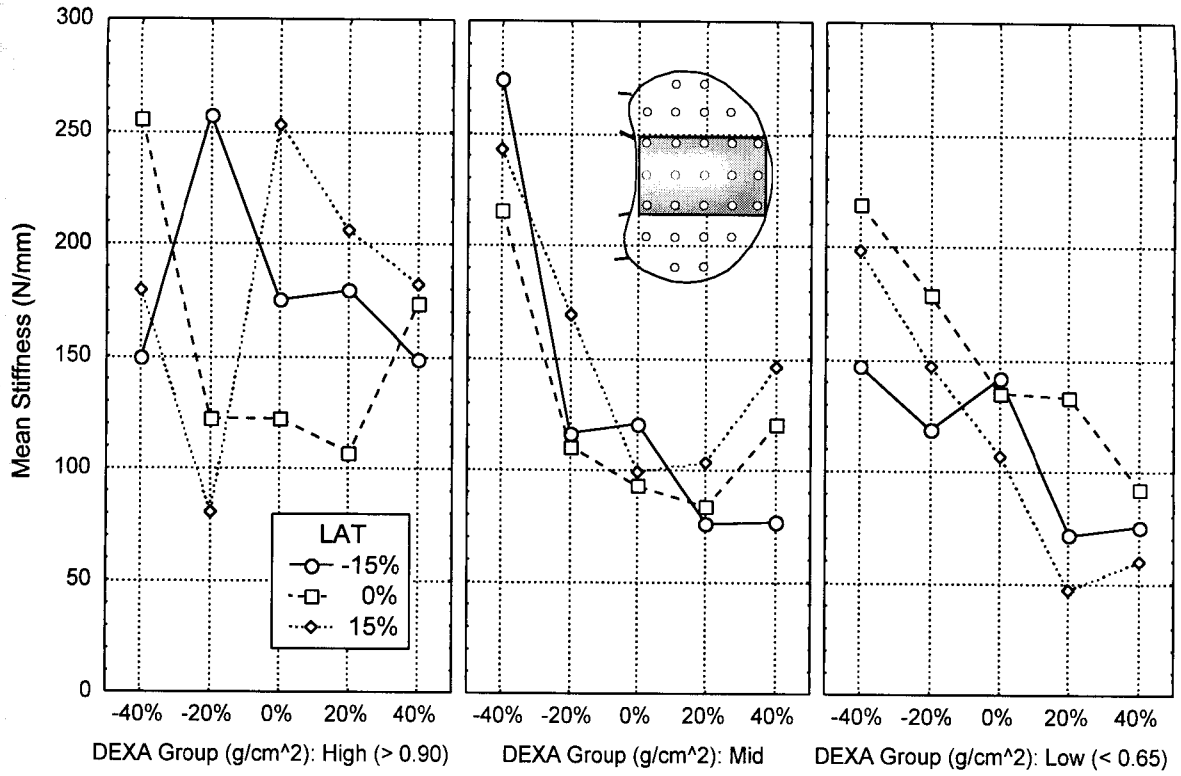


Figure 3.35: Effect of bone density on the sacral endplate full AP stiffness map. The p-value of $< 0.0025$ indicates that the map shape changed significantly as the bone density decreased.

### *3.3.6.3 Full LAT Analysis*

The full LAT analysis of the sacral endplate stiffness maps found no significant differences in map shape in the different bone density groups ($p < 0.8484$), however there was a significant decrease in mean endplate stiffness with decreasing density ($p < 0.0192$). A *post hoc* Newman-Keuls test showed that the High density group was stiffer than both the Mid ($p = 0.0210$) and Low ($p = 0.0207$) density groups, and the Mid density group was significantly stiffer than the Low density group ($p = 0.0403$).

### *3.3.6.4 Summary*

Bone density had little effect on the sacral endplate stiffness. Only the full AP analysis had significantly different map shapes at different bone densities, and only the full LAT analysis showed a significant decrease in mean endplate stiffness as the bone density decreased.

### 3.3.7 Effects of Bone Density: Summary

#### *3.3.7.1 Mean Endplate Properties*

The mean failure load was lower in specimens with lower bone density in the superior and inferior lumbar endplates, but the sacral specimens showed no significant difference in failure load at different densities.

Bone density had very little effect on stiffness in any of the three endplate groups (differences were only found in the full AP or full LAT maps, where fewer test sites were included in the comparison).

#### *3.3.7.2 Map Shape*

Only the superior lumbar endplate had significant differences in map shape in the three bone density groups in the maximum AP, LAT analysis. The inferior lumbar endplate had significantly different map shapes in the full LAT analysis. The sacral failure load map showed no variation in shape related to bone density. In general, this demonstrates that, while there were some more localised changes, particularly in the superior lumbar endplate, the loss of strength related to lower bone density was uniform over the endplate.

Bone density had almost no effect on the stiffness map shape. Only the full AP sacral map had significant shape differences based on the bone density.

## 3.4 Effects of Disc Degeneration

To look at the effects of disc degeneration on the endplate maps, the specimens were divided into groups by disc grade. The disc condition was graded using the four-point Nachemson scale (Nachemson, 1960), as discussed in chapter 2 (section 2.3.4), with "1" being healthy and "4" being in an advanced state of degeneration. Due to the advanced age of the specimens used in this study, only discs of grades 2 through 4 were found.

To give some indication of the general characteristics of the specimens in the three disc grade groups, one-way ANOVAs were done looking at the effect of disc condition on the mean failure load and mean stiffness in the specimens. The three disc condition groups were found to have significantly different failure loads ($p < 0.0001$), but the stiffnesses were not significantly different ($p < 0.0792$). Some general information on the groups is provided in Table 3.11. Note that there were fewer specimens with grade 3 discs, which will reduce the statistical power of the ANOVA, making it more difficult to detect changes in the grade 3 specimens.

To look at the effects of disc condition on the map shapes and mean structural properties of the three endplate groups, three-way ANOVAs were done using disc grade and the AP and LAT co-ordinates (as repeated measures) as the three factors. Since significant differences were identified between the lumbar and sacral maps, and the superior and inferior lumbar endplate maps (section 3.2), these groups were examined separately.

**Table 3.11: Characteristics of the three disc groups.** Disc grade values are the Nachemson grade of the disc (Nachemson, 1960), failure load means, standard errors of mean (SEM), and standard deviations (SD) are given in Newtons, and the number of tests (n) has no units. Stiffness values are given in Newtons per millimetre. Note that fewer of the specimens fell into the grade 3 group, thus the standard errors of the means are larger in this group.

| Variable | Disc Grade | Mean | SEM | SD | n |
|---|---|---|---|---|---|
| Failure Load | 2 | 134.7 | 3.7 | 82.7 | 508 |
| | 3 | 121.3 | 5.1 | 84.1 | 275 |
| | 4 | 110.7 | 2.8 | 78.8 | 792 |
| Stiffness | 2 | 136.1 | 2.6 | 59.4 | 508 |
| | 3 | 146.7 | 4.1 | 67.8 | 275 |
| | 4 | 138.3 | 2.4 | 66.7 | 792 |

### 3.4.1 Effect of Disc Degeneration on the Superior Lumbar Endplate Failure Load Map

#### *3.4.1.1 Maximum AP, LAT Analysis*

The shape of the superior lumbar endplate failure load map was significantly different at the three disc conditions ($p < 0.0012$), but the mean endplate failure load did not change with disc degeneration ($p < 0.7352$). Looking at the maps (Figure 3.36), one can see that the centre of the endplate weakened, while the periphery remained strong as the disc degenerated, resulting in a less uniform failure load profile.

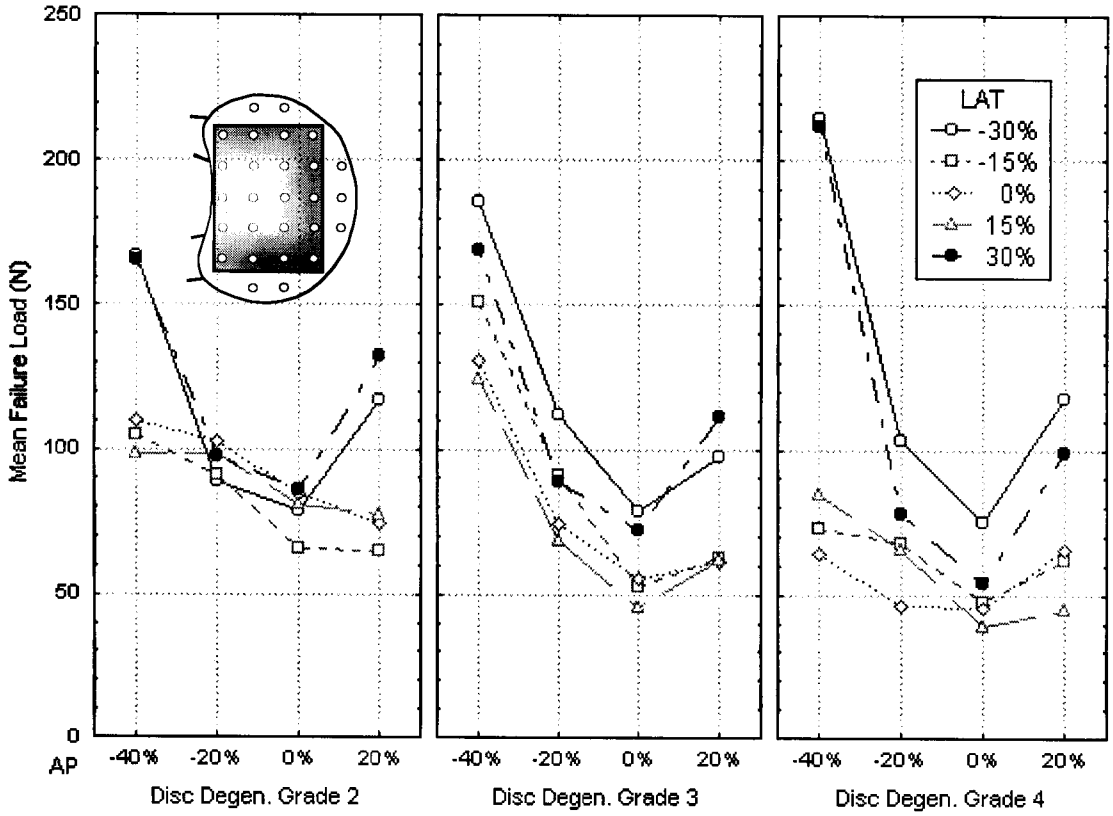


Figure 3.36: Effect of disc degeneration on the superior endplate AP, LAT failure load map. The p-value of < 0.0012 indicates that the map shape changed significantly as the disc degenerated. The centre of the endplate weakened, while the periphery remained strong, resulting in a less uniform failure load profile.

### *3.4.1.2 Full AP Analysis*

The full AP analysis found no significant changes in the shape of the failure load map with disc degeneration ($p < 0.2784$), nor were the mean endplate failure loads significantly different ($p < 0.4686$).

### *3.4.1.3 Full LAT Analysis*

The full LAT analysis also found no significant differences between the map shapes in the three disc conditions ($p < 0.1935$), nor were the mean endplate failure loads different ($p < 0.3045$).

### *3.4.1.4 Summary*

The superior lumbar endplate map shape underwent significant changes as the disc degenerated. The centre of the endplate became weaker while the peripheral test sites remained strong. The mean failure load was unaffected by disc grade.

## 3.4.2 Effect of Disc Degeneration on the Superior Lumbar Endplate Stiffness Map

Disc degeneration had no significant effect on map shape or mean endplate stiffness in the superior lumbar endplates in the maximum AP, LAT analysis ($p < 0.2299$, $p < 0.3907$; Figure 3.37), the full AP analysis ($p < 0.3822$, $p < 0.2902$), or the full LAT analysis ($p < 0.0524$, $p < 0.1392$).

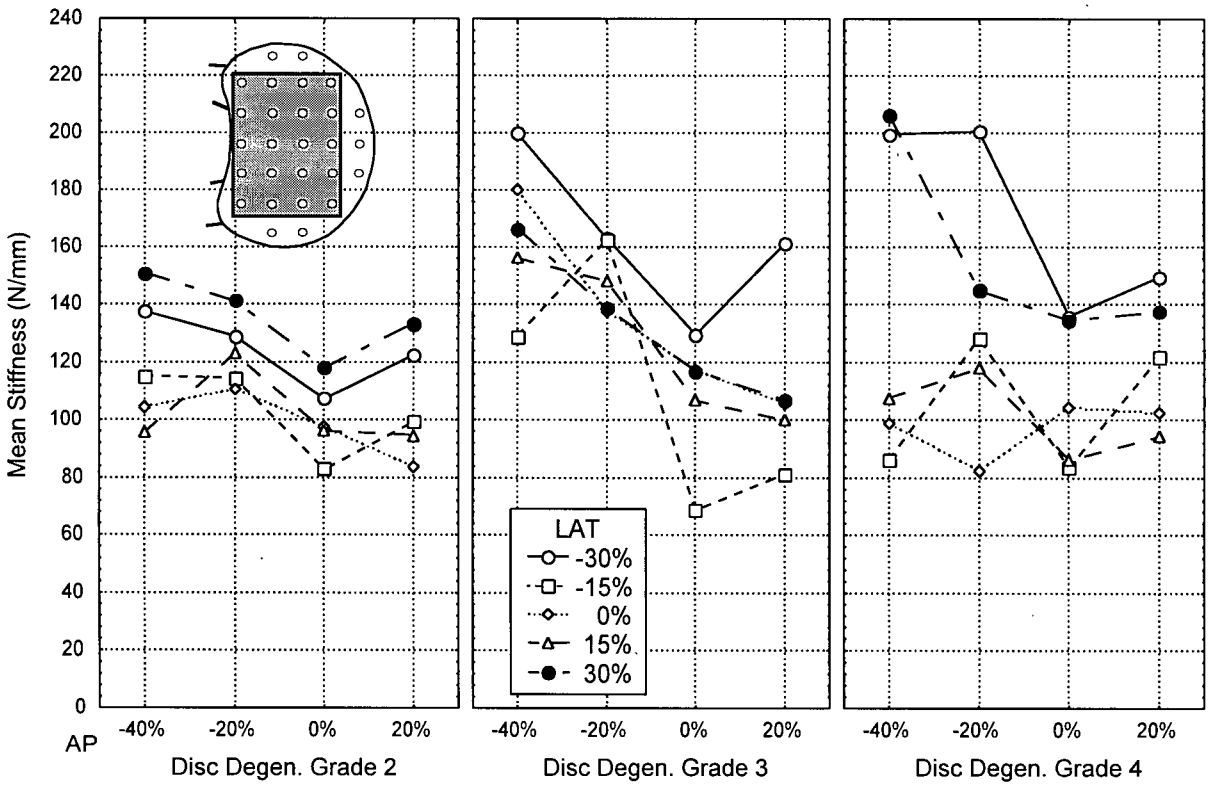


Figure 3.37: Effect of disc degeneration on the superior endplate AP, LAT stiffness map. The p-value of $< 0.2299$ indicates that the map shape did not change significantly as the disc degenerated.

### 3.4.3 Effect of Disc Degeneration on the Inferior Lumbar Endplate Failure Load Map

#### *3.4.3.1 Maximum AP, LAT Analysis*

In the maximum AP, LAT analysis, the inferior lumbar endplate failure load map shape was not significantly affected by disc degeneration ($p < 0.4531$, Figure 3.38), however the mean endplate failure load was ($p < 0.0023$). A *post hoc* Newman-Keuls mean comparison showed that the endplates with grade 2 discs were significantly stronger than endplates with either grade 3 ($p = 0.0111$) or grade 4 ($p = 0.0208$) discs. Endplates with grade 3 and grade 4 discs did not have significantly different strengths ($p = 0.8738$).

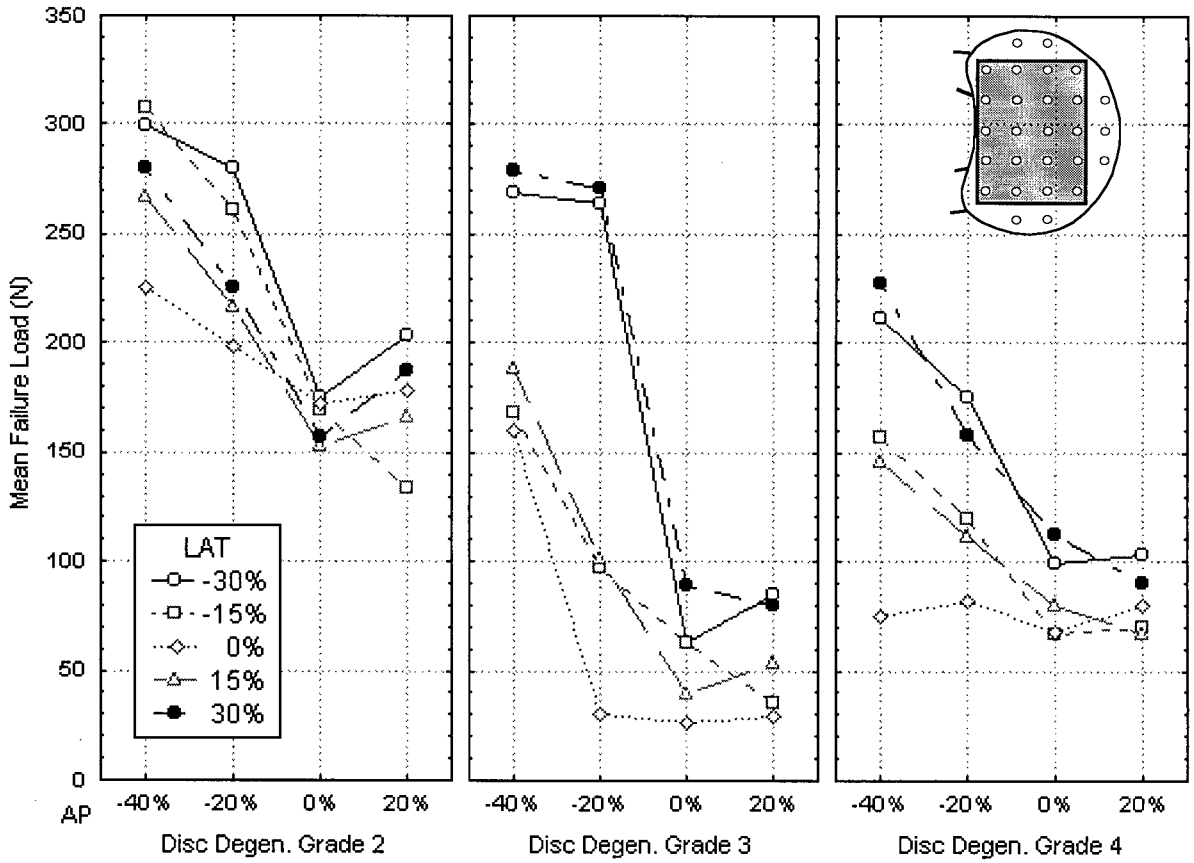


Figure 3.38: Effect of disc degeneration on the shape of the inferior endplate AP, LAT failure load map. The p-value of < 0.4531 indicates that the map shape did not change significantly with disc degeneration.

#### *3.4.3.2 Full AP Analysis*

Neither the failure load map shape ($p < 0.3365$) nor the mean endplate failure load ($p < 0.0963$) were found to be significantly affected by disc degeneration in the full AP analysis of the inferior lumbar endplates.

### *3.4.3.3 Full LAT Analysis*

The full LAT analysis of the inferior lumbar endplate failure load maps found that both the map shape ($p < 0.0304$) and the mean endplate failure load ($p < 0.0021$) were significantly affected by disc degeneration (Figure 3.39). A *post hoc* Newman-Keuls comparison showed that the endplates with grade 2 ($p = 0.0044$) and grade 3 ($p = 0.0095$) discs were significantly stronger than the endplates with grade 4 discs. The strengths of the endplates with grade 2 and grade 3 discs were not significantly different ($p = 0.9744$).

Additional ANOVAs comparing pairs of maps showed that the shapes of the grade 2 and grade 4 maps were significantly different ($p < 0.0170$), but the grade 3 and grade 4 map shapes were not ($p < 0.1134$). A p-value could not be generated for the grade 2, grade 3 map comparison due to the incomplete data set.

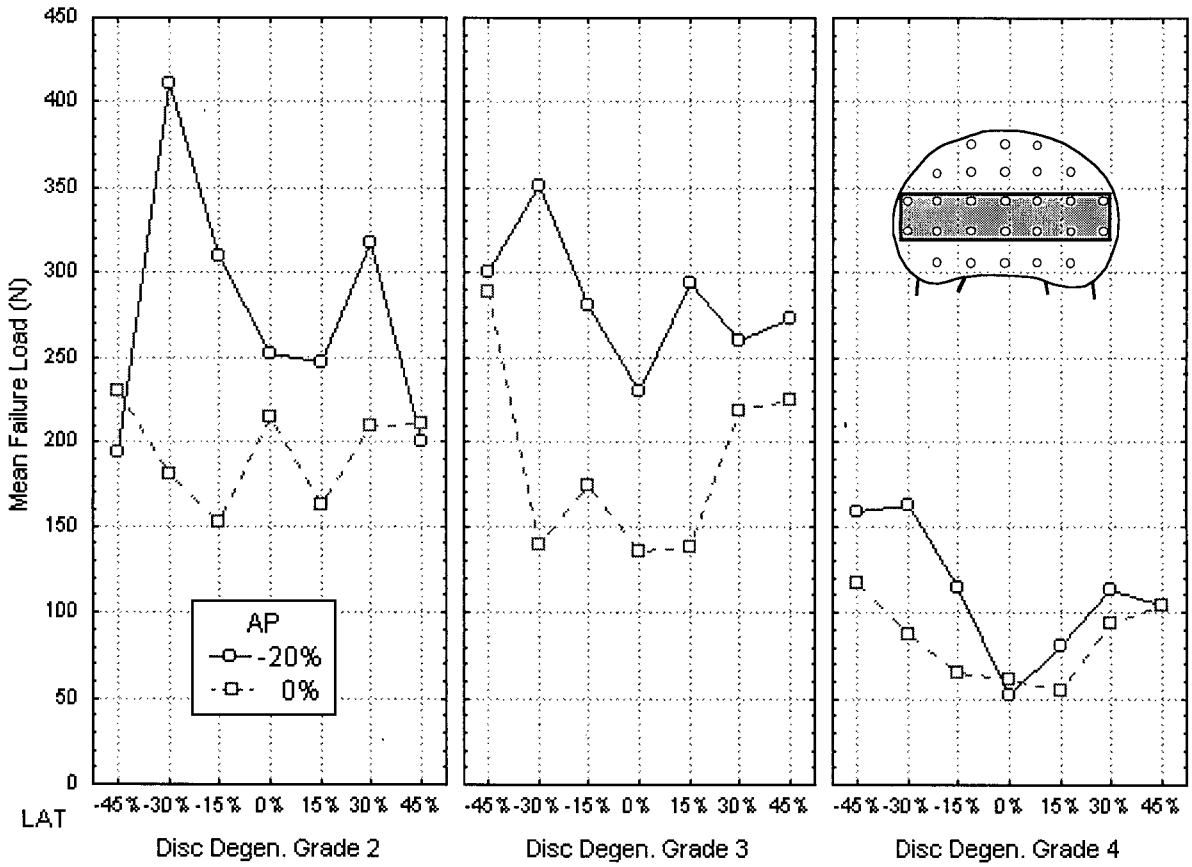


Figure 3.39: Effect of disc degeneration on the shape of the inferior endplate full LAT failure load map. The p-value of < 0.0304 indicates that the map shape changed significantly with disc degeneration.

### *3.4.3.4 Summary*

The failure load of the inferior lumbar endplate decreased as the disc degenerated, but the map shape did not appear to be strongly affected by disc degeneration (only the full LAT analysis had significant changes in map shape).

### 3.4.4 Effect of Disc Degeneration on the Inferior Lumbar Endplate Stiffness Map

#### *3.4.4.1 Maximum AP, LAT Analysis*

Neither the shape of the stiffness map ($p < 0.8675$) nor the mean endplate stiffness ($p < 0.1832$) was significantly affected by disc degeneration in the inferior lumbar endplate maximum AP, LAT analysis.

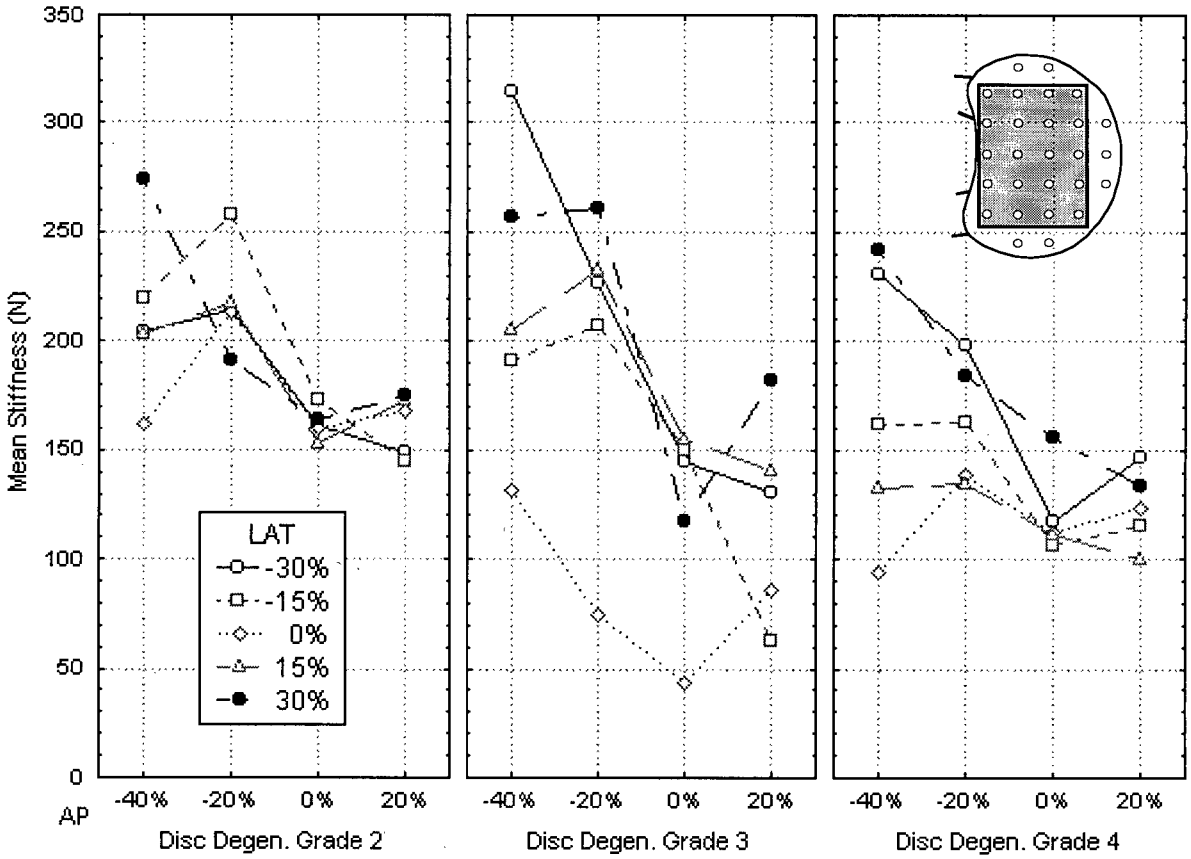


Figure 3.40: Effect of disc degeneration on the shape of the inferior endplate AP, LAT stiffness map. The p-value of < 0.8675 indicates that the map shape did not change significantly with disc degeneration.

#### *3.4.4.2 Full AP Analysis*

In the full AP analysis of the inferior lumbar endplates, the shape of the stiffness map ($p < 0.5326$) and the mean endplate stiffness ($p < 0.8828$) were again not found to be significantly affected by disc degeneration.

### *3.4.4.3 Full LAT Analysis*

The full LAT analysis found that disc degeneration did affect both the stiffness map shape ($p < 0.0448$, Figure 3.40) and the mean endplate stiffness ($p < 0.0369$) in the inferior lumbar endplates. Additional ANOVAs comparing map pairs showed that the endplates with grade 3 and grade 4 discs had significantly different map shapes ($p < 0.0055$) and stiffness magnitudes ($p < 0.0273$). The endplates with grade 2 and grade 4 discs were not significantly different in either map shape ($p < 0.9526$) or stiffness magnitude ($p < 0.0567$). P-values could not be generated for the grade 2, grade 3 disc comparison due to the incomplete data set.

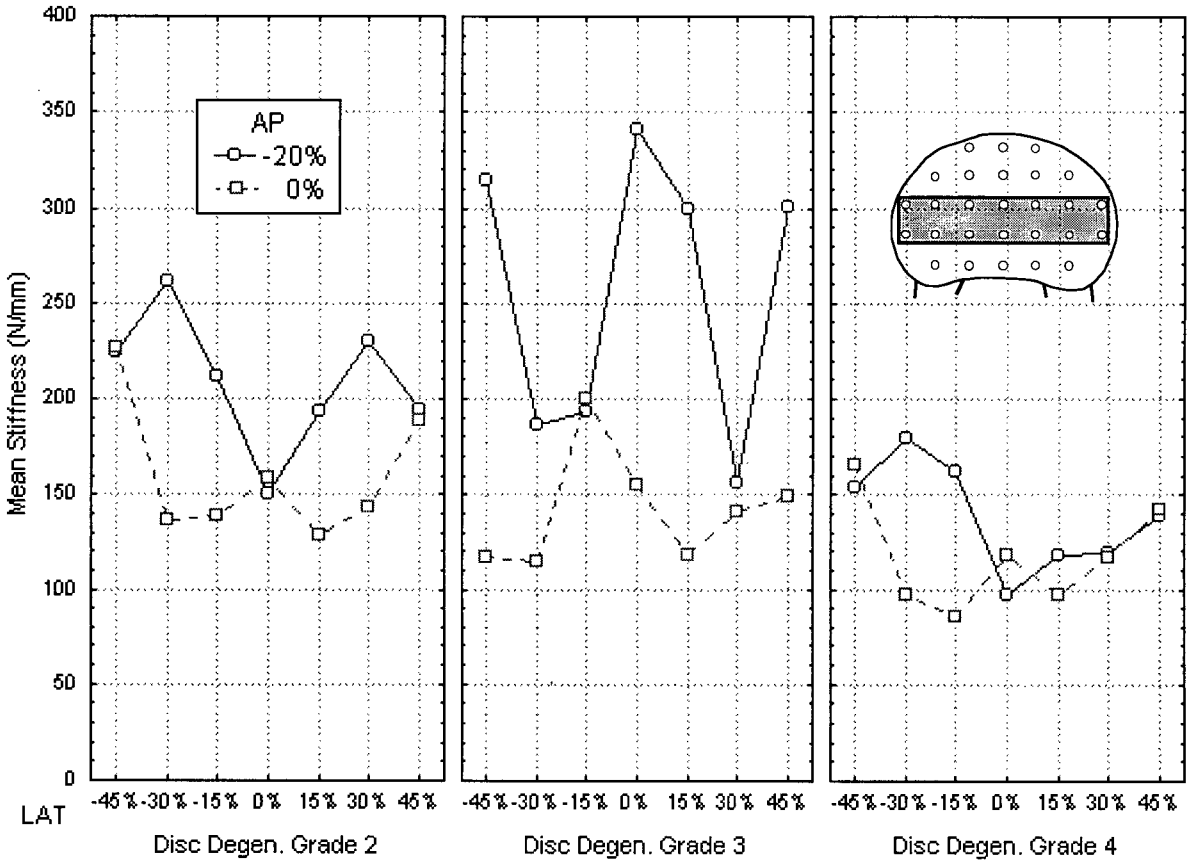


Figure 3.41: Effect of disc degeneration on the shape of the inferior endplate full LAT stiffness map. The p-value of $< 0.0448$ indicates that the map shape changed significantly with disc degeneration.

### *3.4.4.4 Summary*

Disc degeneration appears to have little effect on the stiffness map or magnitude in the inferior lumbar endplates (only the full LAT analysis found significant differences between the three disc conditions).

### 3.4.5 Effect of Disc Degeneration on the Sacral Endplate Failure Load Map

Only one of the sacral specimens had a disc grade of 2 and that specimen was missing tests, thus the grade 2 specimen could only be included in the full AP analysis, for which it had a complete data set.

There were no significant differences in map shape or failure load magnitude in the sacral endplates in the maximum AP, LAT (Figure 3.42: $p < 0.2392$; $p < 0.8606$), full AP ($p < 0.3207$; $p < 0.2192$), or full LAT analysis ($p < 0.2773$; $p < 0.5583$).

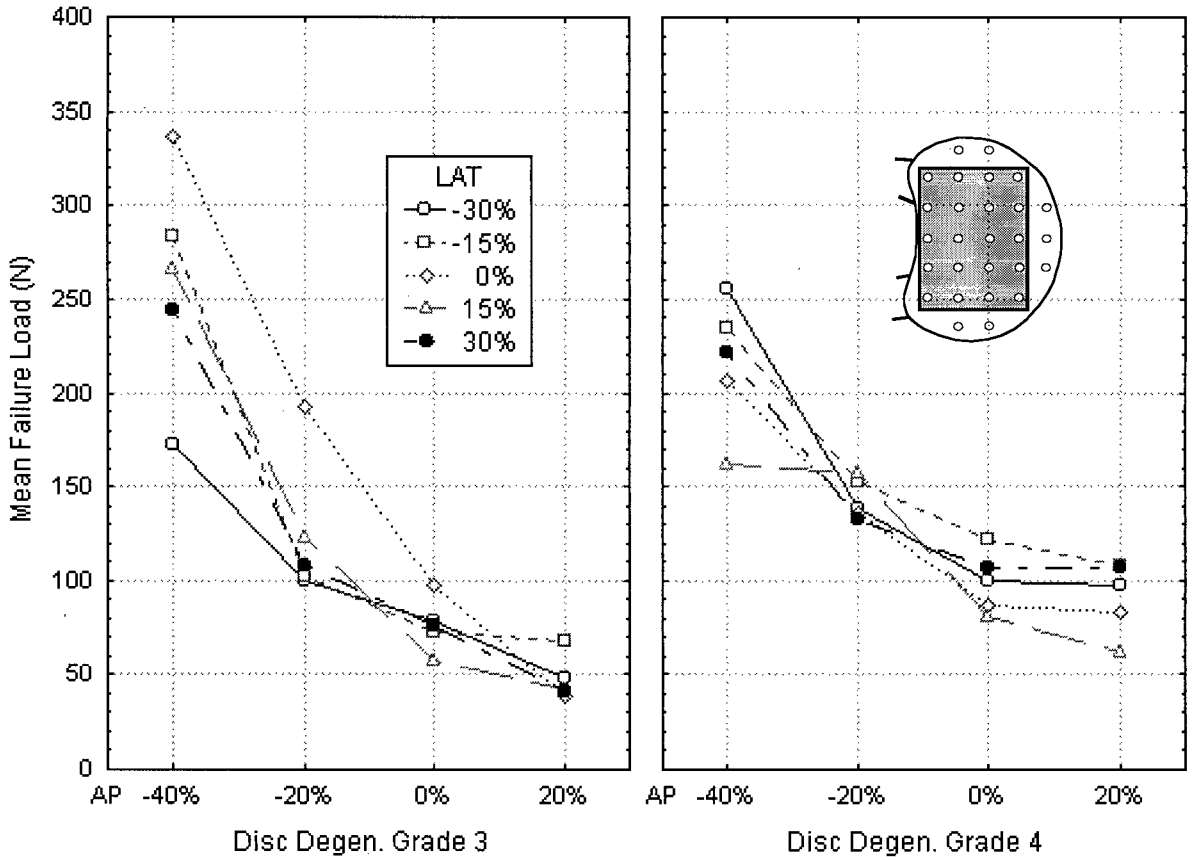


Figure 3.42: Effect of disc degeneration on the shape of the sacral endplate AP, LAT failure load map. The p-value of < 0.2392 indicates that the map shape did not change significantly with disc degeneration.

### 3.4.6 Effect of Disc Degeneration on the Sacral Endplate Stiffness Map

Again, only one of the sacral specimens had a disc grade of 2 and that specimen was missing tests, thus the grade 2 specimen could only be included in the full AP analysis, for which it had a complete data set.

There were no significant differences in map shape or stiffness magnitude in the sacral endplates in the maximum AP, LAT (Figure 3.43: $p < 0.3865$; $p < 0.8351$), full AP ($p < 0.9828$; $p < 0.3495$), or full LAT analysis ($p < 0.5498$; $p < 0.8163$).

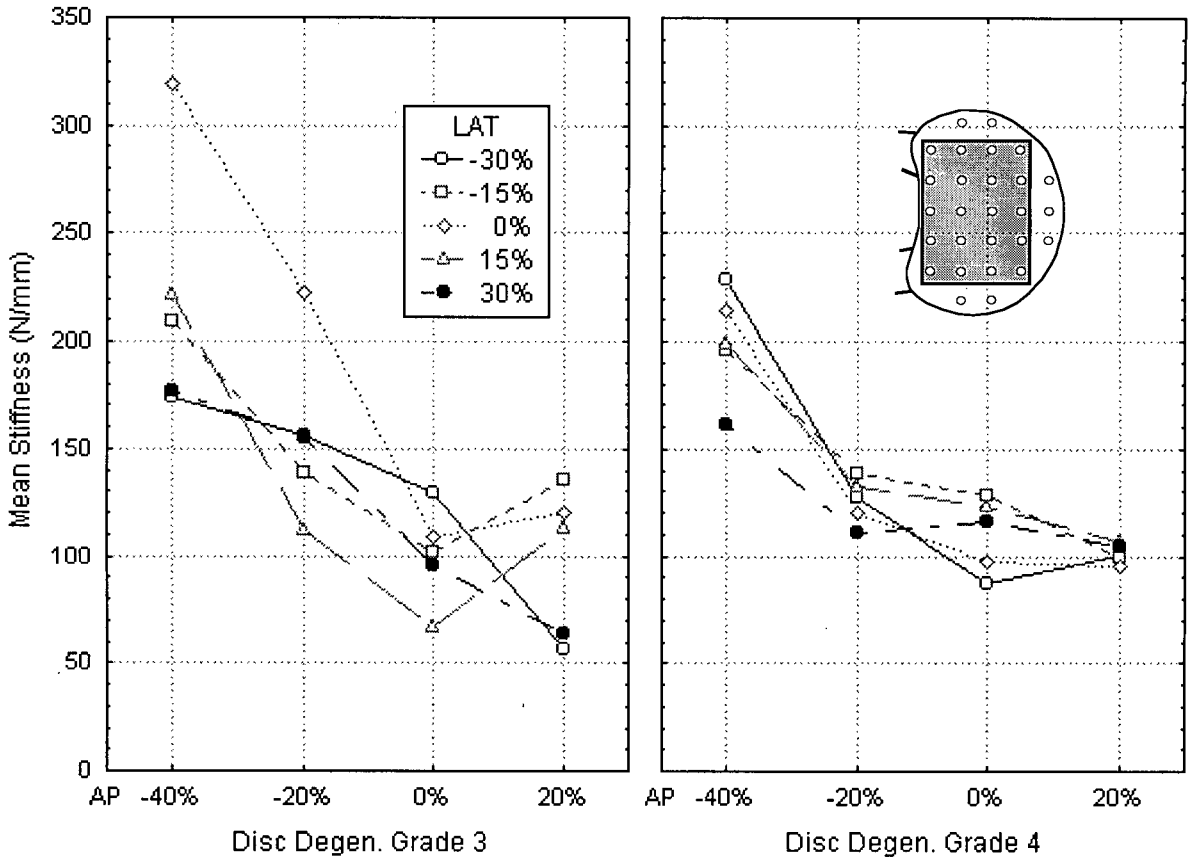


Figure 3.43: Effect of disc degeneration on the shape of the sacral endplate AP, LAT stiffness map. The p-value of $< 0.3865$ indicates that the map shape did not change significantly with disc degeneration.

### 3.4.7 Effects of Disc Degeneration: Summary

#### *3.4.7.1 Mean Endplate Properties*

Only the inferior lumbar endplate mean failure load was significantly affected by disc degeneration, experiencing a decrease in strength with disc degeneration.

Disc degeneration had essentially no effect on mean endplate stiffness in any of the three endplate groups (only the inferior lumbar endplate full LAT analysis had a significant p-value).

#### *3.4.7.2 Map Shape*

The superior lumbar endplate maximum AP, LAT map changed significantly with disc degeneration: the centre of the endplate became weaker while the peripheral test sites remained strong. In the inferior lumbar endplate full LAT analysis, the most lateral test sites became stronger relative to the centre as the disc degenerated. None of the other failure load maps showed significant changes with disc degeneration..

Disc degeneration had almost no effect on the stiffness maps (only the superior and inferior lumbar full LAT analyses had significant shape changes with disc degeneration).

## 3.5 Effects of Removing the Endplate

It has been shown that there is significant variation in the structural properties over the surface of the endplates and that they are somewhat affected by bone density and disc health. This section looks at the effect of removing the endplate on the structural properties.

In this secondary study each specimen acted as its own control. One half of the endplate was removed (the left or right side was chosen randomly) and the other was left intact. Unlike in the full endplate specimens, the lateral test co-ordinate was assigned only in terms of its distance from the centre of the endplate; negative values were not used, i.e. only 15, 30 and 45% LAT were used. This means that 15% LAT in the intact endplate maps corresponds to 15% LAT in the endplate-removed maps, and so on. The results of the tests were then compared using ANOVAs with three repeated measures: endplate condition (intact or removed), and AP and LAT test co-ordinates.

In section 3.2.2 it was seen that the superior and inferior lumbar endplate structural property maps were all laterally symmetric. This means that if the removal of the endplate does not have an effect one would expect to see no significant differences between the properties or the maps in the two halves of the endplates. If they are significantly different then the endplate removal had a significant effect on the structural properties. Note that there could be a significant strength or stiffness difference without the map shape being altered (i.e. an evenly distributed change in strength or stiffness).

Due to the small number of specimens used in this study (4 superior and 3 inferior lumbar endplates) all of the values were combined. This means that the results given here can only be considered in terms of the endplate condition (intact or removed) and cannot be compared directly to the maps presented in section 3.2.2.

### 3.5.1 Effects of Removing the Endplate on the Failure Load Maps

Table 3.12 shows the mean, standard error of the mean and standard deviation of the failure load at each of the test sites, calculated using the raw data. Note the large standard errors of mean and standard deviations. The small number of specimens is partially responsible for this result, along with the fact that some of the specimens were weaker than others, however the fact that the superior and inferior endplates were combined may also contribute to this result. The standard deviation and standard error of mean appear to be somewhat larger posteriorly. This is the region of the endplate where the superior and inferior endplate maps differed the most (section 3.2.2), thus one would expect to find a larger spread in the data.

Comparing the intact endplate data with the endplate removed data in Table 3.12, it appears that the failure loads were higher in the intact endplate test sites, but that there was more variability in the results (i.e. the standard deviations were larger, both in base value and as a percentage of the mean failure load).

Note that, unlike in section 3.2.5, the ANOVA means in all graphs except the full AP analysis graph (Figure 3.45) match the means in the table generated using the raw data (Table 3.12). This is because there was a complete data set (i.e. no missing values) for all of these analyses except for the full AP analysis, so Statistica did not use Type IV hypotheses to generate the means.

**Table 3.12: Half-endplate failure load (FL) map (L3-L5 superior and inferior specimens).** The left side of the table shows the results of the tests with the endplate removed, while the right side shows the corresponding intact endplate results. Mean failure load (Mean), standard error of the mean (SEM) and standard deviation (SD) are given in Newtons. The number of tests (n) has no units. The AP and LAT test site co-ordinates are given as percentages of the corresponding endplate dimensions (see Figure 2.13 for a diagram of the test site layout).

| | Endplate Removed | | | | Endplate Intact | | |
|---|---|---|---|---|---|---|---|
| LAT | 45% | 30% | 15% | 0% | 15% | 30% | 45% |
| AP | | | | | | | |
| 40% | | | **86.3** | | **187.4** | | *Mean FL* |
| | | | 36.4 | | 98.9 | | *SEM FL* |
| | | | 89.0 | | 242.1 | | *SD FL* |
| | | | 6 | | 6 | | *n* |
| 20% | | **40.7** | **47.9** | | **84.9** | **119.9** | |
| | | 10.9 | 7.6 | | 40.9 | 59.2 | |
| | | 28.9 | 20.1 | | 108.1 | 156.7 | |
| | | 7 | 7 | | 7 | 7 | |
| 0% | **36.4** | **30.9** | **42.5** | | **61.0** | **109.6** | **104.7** |
| | 3.3 | 2.9 | 5.6 | | 8.6 | 32.2 | 23.3 |
| | 8.7 | 7.8 | 14.9 | | 22.8 | 85.3 | 61.7 |
| | 7 | 7 | 7 | | 7 | 7 | 7 |
| -20% | **46.8** | **39.9** | **66.5** | | **120.0** | **170.3** | **125.0** |
| | 7.9 | 4.5 | 8.5 | | 21.1 | 41.7 | 26.9 |
| | 20.9 | 12.0 | 22.5 | | 55.8 | 110.2 | 69.0 |
| | 7 | 7 | 7 | | 7 | 7 | 7 |
| -40% | | **89.3** | **69.1** | | **188.2** | **259.8** | |
| | | 15.1 | 14.2 | | 49.8 | 89.2 | |
| | | 40.0 | 37.6 | | 131.9 | 236.0 | |
| | | 7 | 7 | | 7 | 7 | |

### *3.5.1.1 Maximum AP, LAT Analysis*

The first three-way ANOVA looked at the largest complete AP, LAT analysis area (Figure 3.44). Although no significant shape differences were found between the two maps ($p < 0.9091$), there was a significant decrease in the mean endplate failure load when the endplate was removed ($p < 0.0437$). The mean endplate failure load in the intact endplate (139.2 N) was about 2.5 times the size of the value in the area where the endplate had been removed (53.3 N). Looking at Figure 3.44 and Table 3.13 one sees that that this difference in magnitude arises primarily as a result of the higher posterior strength in the intact endplate specimens.

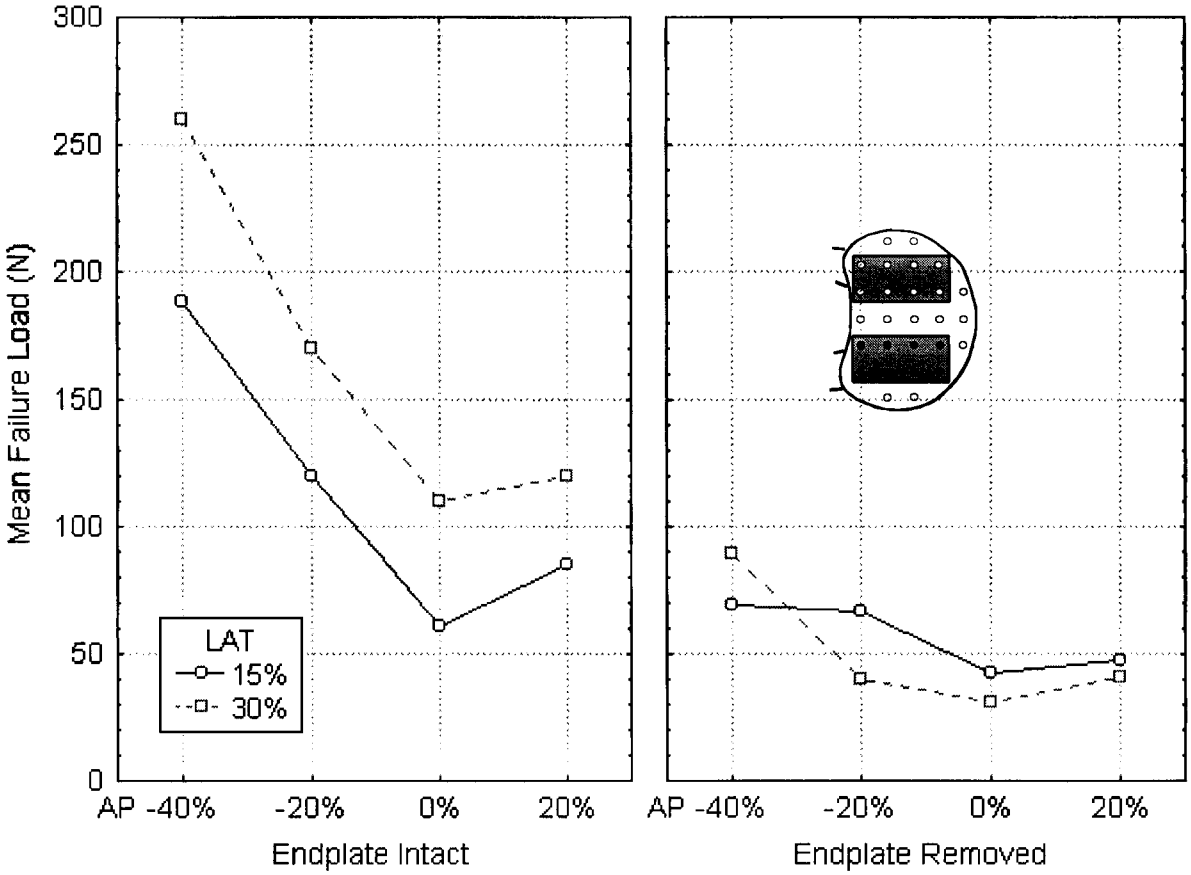


Figure 3.44: Comparison of the maximum AP, LAT failure load distributions in the intact and removed lumbar endplate specimens. The p-value of < 0.9091 indicates that there were no significant differences between the shapes of the two failure load maps. The intact endplate test sites were, however, significantly stronger than the sites where the endplate had been removed ($p = 0.0437$).

A Newman-Keuls *post hoc* mean comparison was done on the 3-way ANOVA shown in Figure 3.44 to look at the intra- and intermap relationships (Table 3.13). Readers interested in knowing precisely which pairs of means in Figure 3.44 were significantly different can refer to this table. It showed that there were no significant differences between any of the points in the "Endplate Removed" curves (i.e. all of the points effectively had the same strength), while there was significant strength variation over the "Endplate Intact" surface. The anterior points in the intact endplate were not significantly stronger than those without the endplate, however the posterior points were.

**Table 3.13: Newman-Keuls *post hoc* comparison of the means in the intact and removed lumbar endplate AP, LAT failure load maps** (Figure 3.44). The p-values indicating the probability that each pair of means was different are given in the body of the table to four decimal places. The significant p-values ($p < 0.05$) are highlighted in grey (i.e. less than 5% chance of being wrong if one states that the two means are significantly different). The top three rows and left columns show the endplate condition (EP: intact, no EP: removed) and the AP and LAT test site co-ordinates as percentages of the endplate dimensions. The mean failure loads being compared are given in the fourth row and column in Newtons (bold).

| | | | Endplate Intact | | | | | | | | |
|---|---|---|---|---|---|---|---|---|---|---|---|
| | | AP | -40% | | -20% | | 0% | | 20% | | |
| | | LAT | 15% | 30% | 15% | 30% | 15% | 30% | 15% | 30% | |
| | AP | LAT | **Mean FL** | **188.2** | **259.8** | **120.0** | **170.3** | **61.0** | **109.6** | **84.9** | **119.9** |
| EP | -40% | 15% | **188.2** | | 0.0096 | 0.0326 | 0.4759 | 0.0022 | 0.0362 | 0.0083 | 0.0560 |
| | | 30% | **259.8** | 0.0096 | | 0.0003 | 0.0053 | 0.0002 | 0.0003 | 0.0002 | 0.0003 |
| | -20% | 15% | **120.0** | 0.0326 | 0.0003 | | 0.0567 | 0.3019 | 0.9075 | 0.6213 | 0.9970 |
| | | 30% | **170.3** | 0.4759 | 0.0053 | 0.0567 | | 0.0077 | 0.1015 | 0.0284 | 0.1311 |
| | 0% | 15% | **61.0** | 0.0022 | 0.0002 | 0.3019 | 0.0077 | | 0.3951 | 0.7689 | 0.2588 |
| | | 30% | **109.6** | 0.0362 | 0.0003 | 0.9075 | 0.1015 | 0.3951 | | 0.5848 | 0.6816 |
| | 20% | 15% | **84.9** | 0.0083 | 0.0002 | 0.6213 | 0.0284 | 0.7689 | 0.5848 | | 0.5039 |
| | | 30% | **119.9** | 0.0560 | 0.0003 | 0.9970 | 0.1311 | 0.2588 | 0.6816 | 0.5039 | |
| no EP | -40% | 15% | **69.1** | 0.0028 | 0.0002 | 0.3476 | 0.0099 | 0.9428 | 0.3810 | 0.5300 | 0.2790 |
| | | 30% | **89.2** | 0.0090 | 0.0002 | 0.6059 | 0.0296 | 0.7816 | 0.4193 | 0.8626 | 0.4438 |
| | -20% | 15% | **66.5** | 0.0028 | 0.0002 | 0.3563 | 0.0100 | 0.8284 | 0.4303 | 0.7386 | 0.2991 |
| | | 30% | **39.9** | 0.0008 | 0.0002 | 0.1211 | 0.0025 | 0.9084 | 0.1983 | 0.6120 | 0.1087 |
| | 0% | 15% | **42.5** | 0.0007 | 0.0002 | 0.1151 | 0.0024 | 0.7371 | 0.1785 | 0.5375 | 0.1002 |
| | | 30% | **30.9** | 0.0005 | 0.0002 | 0.0692 | 0.0014 | 0.8207 | 0.1196 | 0.4503 | 0.0623 |
| | 20% | 15% | **47.9** | 0.0010 | 0.0002 | 0.1467 | 0.0031 | 0.6000 | 0.2148 | 0.5741 | 0.1258 |
| | | 30% | **40.7** | 0.0007 | 0.0002 | 0.1150 | 0.0024 | 0.8431 | 0.1842 | 0.5698 | 0.1017 |

| | | | Endplate Removed | | | | | | | |
|---|---|---|---|---|---|---|---|---|---|---|
| | | AP | -40% | | -20% | | 0% | | 20% | |
| | | LAT | 15% | 30% | 15% | 30% | 15% | 30% | 15% | 30% |
| | AP | LAT | **Mean FL** | **69.1** | **89.2** | **66.5** | **39.9** | **42.5** | **30.9** | **47.9** | **40.7** |
| EP | -40% | 15% | **188.2** | 0.0028 | 0.0090 | 0.0028 | 0.0008 | 0.0007 | 0.0005 | 0.0010 | 0.0007 |
| | | 30% | **259.8** | 0.0002 | 0.0002 | 0.0002 | 0.0002 | 0.0002 | 0.0002 | 0.0002 | 0.0002 |
| | -20% | 15% | **120.0** | 0.3476 | 0.6059 | 0.3563 | 0.1211 | 0.1151 | 0.0692 | 0.1467 | 0.1150 |
| | | 30% | **170.3** | 0.0099 | 0.0296 | 0.0100 | 0.0025 | 0.0024 | 0.0014 | 0.0031 | 0.0024 |
| | 0% | 15% | **61.0** | 0.9428 | 0.7816 | 0.8284 | 0.9084 | 0.7371 | 0.8207 | 0.6000 | 0.8431 |
| | | 30% | **109.6** | 0.3810 | 0.4193 | 0.4303 | 0.1983 | 0.1785 | 0.1196 | 0.2148 | 0.1842 |
| | 20% | 15% | **84.9** | 0.5300 | 0.8626 | 0.7386 | 0.6120 | 0.5375 | 0.4503 | 0.5741 | 0.5698 |
| | | 30% | **119.9** | 0.2790 | 0.4438 | 0.2991 | 0.1087 | 0.1002 | 0.0623 | 0.1258 | 0.1017 |
| no EP | -40% | 15% | **69.1** | | 0.6980 | 0.9156 | 0.8907 | 0.8151 | 0.7721 | 0.8243 | 0.8539 |
| | | 30% | **89.2** | 0.6980 | | 0.7926 | 0.5606 | 0.5080 | 0.3975 | 0.5620 | 0.5278 |
| | -20% | 15% | **66.5** | 0.9156 | 0.7926 | | 0.8838 | 0.7675 | 0.7730 | 0.7352 | 0.8324 |
| | | 30% | **39.9** | 0.8907 | 0.5606 | 0.8838 | | 0.9938 | 0.7202 | 0.9879 | 0.9722 |
| | 0% | 15% | **42.5** | 0.8151 | 0.5080 | 0.7675 | 0.9938 | | 0.9645 | 0.8310 | 0.9436 |
| | | 30% | **30.9** | 0.7721 | 0.3975 | 0.7730 | 0.7202 | 0.9645 | | 0.9566 | 0.9163 |
| | 20% | 15% | **47.9** | 0.8243 | 0.5620 | 0.7352 | 0.9879 | 0.8310 | 0.9566 | | 0.9553 |
| | | 30% | **40.7** | 0.8539 | 0.5278 | 0.8324 | 0.9722 | 0.9436 | 0.9163 | 0.9553 | |

### *3.5.1.2 Full AP Analysis*

The full AP analysis in the half-endplate specimens was only a 2-way analysis since there was only a single LAT co-ordinate (15%) in each endplate condition map. The results of this ANOVA are shown in Figure 3.45 and the corresponding Newman-Keuls *post hoc* comparisons are given in Table 3.14. Again, the maps were not quite significantly different ($p < 0.0960$). In this case the mean endplate failure loads were also not quite significantly different ($p < 0.0701$).

The *post hoc* comparison indicates that there was no significant variation in failure load along the 15% LAT full AP curve where the endplates had been removed (i.e. the curve should be interpreted as level). In contrast, the most anterior ($p = 0.0129$) and most posterior ($p = 0.0216$) test sites in the intact endplates were stronger than the central points in the same curve.

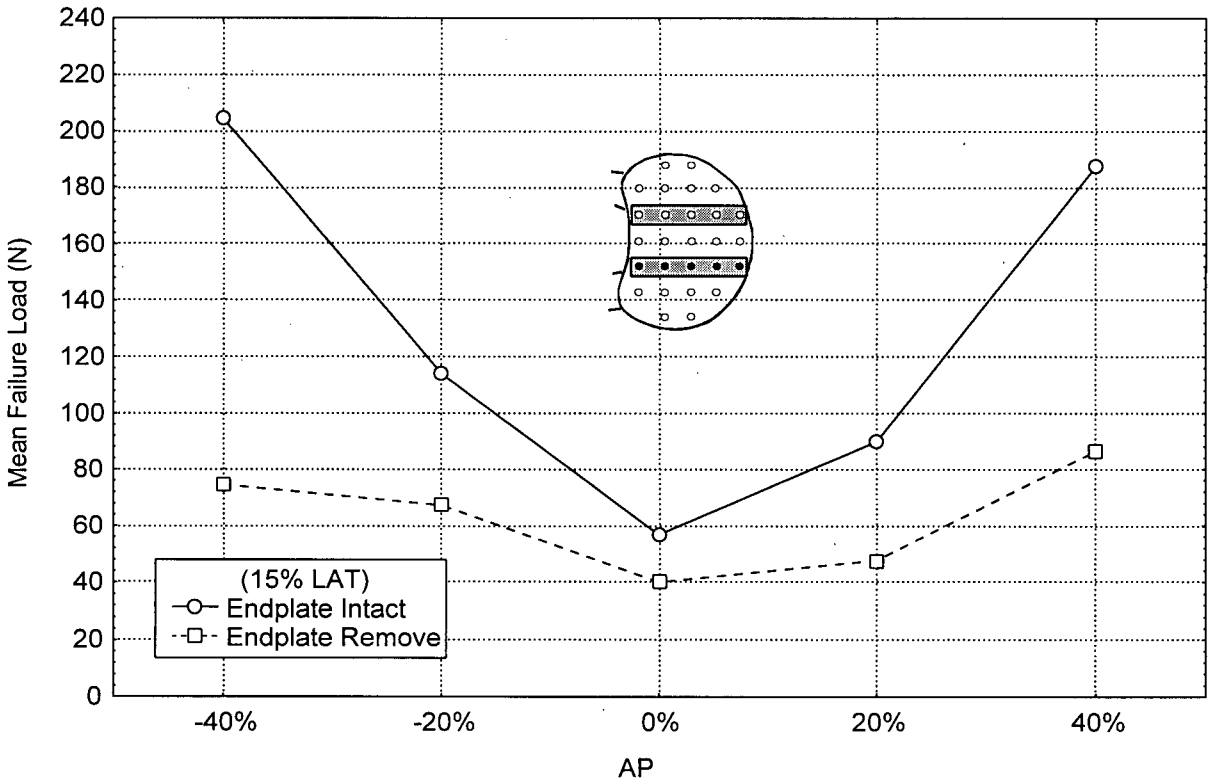


Figure 3.45: Comparison of the full AP failure load distributions in the intact and removed lumbar endplate specimens. The p-value of $< 0.0960$ indicates that there were no significant differences between the shapes of the two failure load curves, nor was the intact endplate significantly stronger than the exposed trabeculae ($p = 0.0701$).

### *3.5.1.3 Full LAT Analysis*

The full LAT analysis in the half endplate specimens also found that there was no significant difference between the failure load maps for the two endplate conditions ($p < 0.2986$, Figure 3.46). Again, the mean endplate failure load was significantly higher in the intact endplate than where the endplate was removed ($p < 0.0127$). The results of the *post hoc* Newman-Keuls test for this analysis are given in Table 3.15.

Again, the "Endplate Removed" curves had no significant strength variation (i.e. all points in the map were essentially equal), while the "Endplate Intact" map did show significant strength variation. All points in the "Endplate Intact" map were significantly stronger than those in the "Endplate Removed" map, with the exception of 15% LAT, 0% AP, which was not significantly different from any of the points in the "Endplate Removed" map.

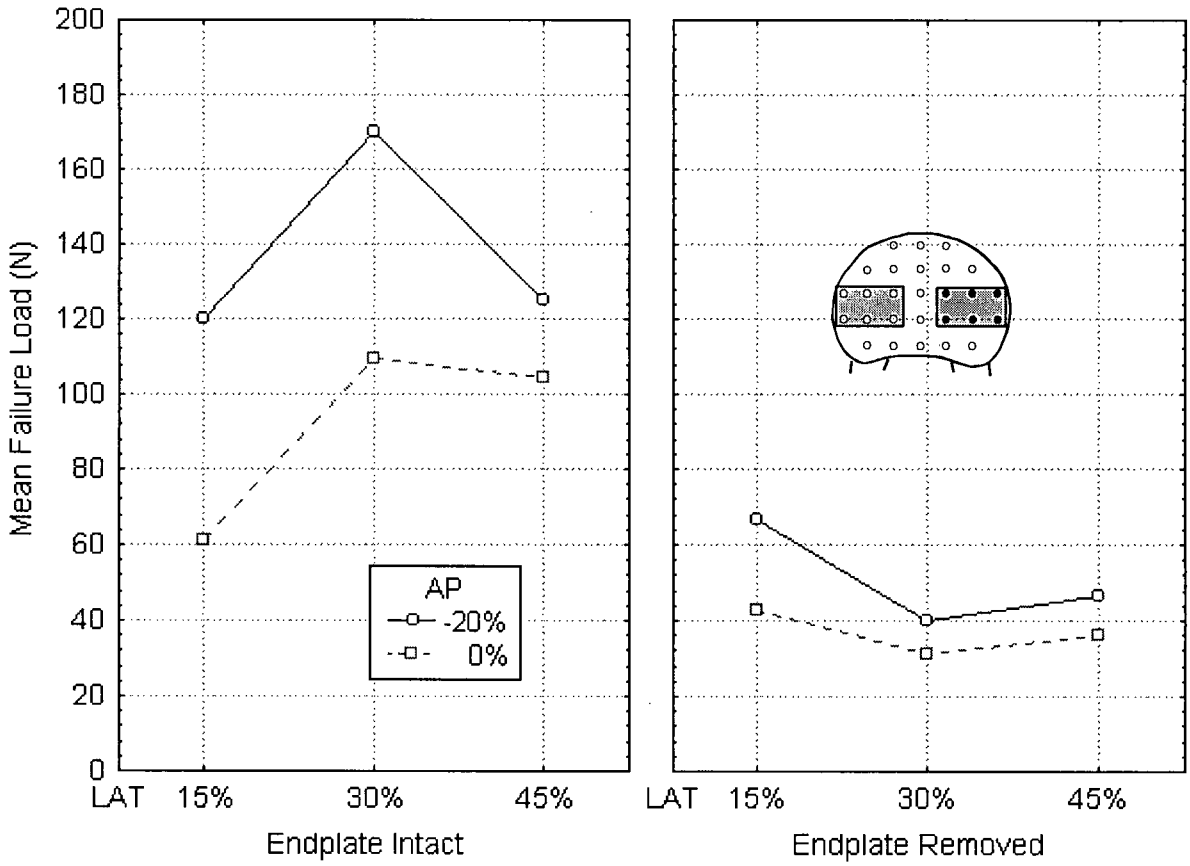


Figure 3.46: Comparison of the full LAT failure load distributions in the intact and removed lumbar endplate specimens. The p-value of $< 0.2986$ indicates that there were no significant differences between the shapes of the two failure load curves, however the intact endplate was significantly stronger than the exposed trabeculae ($p < 0.0127$).

**Table 3.14: Newman-Keuls *post hoc* comparison of the means in the intact and removed lumbar endplate full AP failure load maps** (Figure 3.45). The p-values indicating the probability that each pair of means was different are given in the body of the table to four decimal places. The significant p-values ($p < 0.05$) are highlighted in grey (i.e. less than 5% chance of being wrong if one states that the two means are significantly different). The top three rows and left columns show the endplate condition (EP: intact, no EP: removed) and the AP and LAT test site co-ordinates as percentages of the endplate dimensions. The mean failure loads being compared are given in the fourth row and column in Newtons (bold).

| | | | | Endplate Intact | | | | | Endplate Removed | | | | |
|---|---|---|---|---|---|---|---|---|---|---|---|---|---|
| | | | AP | -40% | -20% | 0% | 20% | 40% | -40% | -20% | 0% | 20% | 40% |
| | | | LAT | 15% | 15% | 15% | 15% | 15% | 15% | 15% | 15% | 15% | 15% |
| | AP | LAT | **Mean FL** | **204.4** | **114.1** | **56.7** | **89.7** | **187.4** | **74.4** | **67.1** | **40.0** | **47.6** | **86.3** |
| EP | -40% | 15% | **204.4** | | 0.0216 | 0.0024 | 0.0069 | 0.5879 | 0.0050 | 0.0039 | 0.0012 | 0.0016 | 0.0083 |
| | -20% | 15% | **114.1** | 0.0216 | | 0.4528 | 0.4388 | 0.0275 | 0.5811 | 0.5602 | 0.2912 | 0.3596 | 0.6468 |
| | 0% | 15% | **56.7** | 0.0024 | 0.4528 | | 0.8194 | 0.0063 | 0.8359 | 0.7396 | 0.8506 | 0.7697 | 0.7728 |
| | 20% | 15% | **89.7** | 0.0069 | 0.4388 | 0.8194 | | 0.0129 | 0.8736 | 0.8828 | 0.6752 | 0.7452 | 0.9141 |
| | 40% | 15% | **187.4** | 0.5879 | 0.0275 | 0.0063 | 0.0129 | | 0.0119 | 0.0099 | 0.0030 | 0.0042 | 0.0181 |
| no EP | -40% | 15% | **74.4** | 0.0050 | 0.5811 | 0.8359 | 0.8736 | 0.0119 | | 0.8161 | 0.7956 | 0.8202 | 0.7024 |
| | -20% | 15% | **67.1** | 0.0039 | 0.5602 | 0.7396 | 0.8828 | 0.0099 | 0.8161 | | 0.8143 | 0.8033 | 0.8091 |
| | 0% | 15% | **40.0** | 0.0012 | 0.2912 | 0.8506 | 0.6752 | 0.0030 | 0.7956 | 0.8143 | | 0.8072 | 0.6651 |
| | 20% | 15% | **47.6** | 0.0016 | 0.3596 | 0.7697 | 0.7452 | 0.0042 | 0.8202 | 0.8033 | 0.8072 | | 0.7188 |
| | 40% | 15% | **86.3** | 0.0083 | 0.6468 | 0.7728 | 0.9141 | 0.0181 | 0.7024 | 0.8091 | 0.6651 | 0.7188 | |

**Table 3.15: Newman-Keuls *post hoc* comparison of the means in the intact and removed lumbar endplate full LAT failure load maps** (Figure 3.46). The p-values indicating the probability that each pair of means was different are given in the body of the table to four decimal places. The significant p-values ($p < 0.05$) are highlighted in grey (i.e. less than 5% chance of being wrong if one states that the two means are significantly different). The top three rows and left columns show the endplate condition (EP: intact, no EP: removed) and the AP and LAT test site co-ordinates as percentages of the endplate dimensions. The mean failure loads being compared are given in the fourth row in Newtons (bold).

| | | | Endplate Intact | | | | | | Endplate Removed | | | | | |
|---|---|---|---|---|---|---|---|---|---|---|---|---|---|---|
| | | AP | -20% | | | 0% | | | -20% | | | 0% | | |
| | | LAT | 15% | 30% | 45% | 15% | 30% | 45% | 15% | 30% | 45% | 15% | 30% | 45% |
| | AP | LAT | **120.0** | **170.3** | **125.0** | **61.0** | **109.6** | **104.7** | **66.5** | **39.9** | **46.8** | **42.5** | **30.9** | **36.4** |
| EP | -20% | 15% | | 0.0055 | 0.7027 | 0.0046 | 0.4338 | 0.4778 | 0.0062 | 0.0009 | 0.0012 | 0.0010 | 0.0006 | 0.0008 |
| | | 30% | 0.0055 | | 0.0043 | 0.0002 | 0.0025 | 0.0020 | 0.0002 | 0.0002 | 0.0002 | 0.0002 | 0.0002 | 0.0002 |
| | | 45% | 0.7027 | 0.0043 | | 0.0034 | 0.4749 | 0.4212 | 0.0048 | 0.0007 | 0.0009 | 0.0007 | 0.0005 | 0.0006 |
| | 0% | 15% | 0.0046 | 0.0002 | 0.0034 | | 0.0120 | 0.0135 | 0.6796 | 0.3891 | 0.2874 | 0.3507 | 0.2469 | 0.3575 |
| | | 30% | 0.4338 | 0.0025 | 0.4749 | 0.0120 | | 0.7065 | 0.0144 | 0.0022 | 0.0028 | 0.0023 | 0.0012 | 0.0019 |
| | | 45% | 0.4778 | 0.0020 | 0.4212 | 0.0135 | 0.7065 | | 0.0116 | 0.0031 | 0.0035 | 0.0031 | 0.0017 | 0.0026 |
| no EP | -20% | 15% | 0.0062 | 0.0002 | 0.0048 | 0.6796 | 0.0144 | 0.0116 | | 0.2912 | 0.3093 | 0.2914 | 0.1602 | 0.2491 |
| | | 30% | 0.0009 | 0.0002 | 0.0007 | 0.3891 | 0.0022 | 0.0031 | 0.2912 | | 0.8548 | 0.8401 | 0.7680 | 0.7913 |
| | | 45% | 0.0012 | 0.0002 | 0.0009 | 0.2874 | 0.0028 | 0.0035 | 0.3093 | 0.8548 | | 0.7466 | 0.7312 | 0.8495 |
| | 0% | 15% | 0.0010 | 0.0002 | 0.0007 | 0.3507 | 0.0023 | 0.0031 | 0.2914 | 0.8401 | 0.7466 | | 0.8018 | 0.8833 |
| | | 30% | 0.0006 | 0.0002 | 0.0005 | 0.2469 | 0.0012 | 0.0017 | 0.1602 | 0.7680 | 0.7312 | 0.8018 | | 0.6753 |
| | | 45% | 0.0008 | 0.0002 | 0.0006 | 0.3575 | 0.0019 | 0.0026 | 0.2491 | 0.7913 | 0.8495 | 0.8833 | 0.6753 | |

### 3.5.2 Effects of Removing the Endplate on the Stiffness Maps

Table 3.16 shows the mean, standard error of the mean and standard deviation of the stiffness at each of the test sites calculated using the raw data. The comments made regarding the corresponding failure load map (Table 3.12) apply equally to this map.

**Table 3.16: Half-endplate stiffness (ST) map (L3-L5 superior and inferior specimens).** The left side of the table shows the results of the tests with the endplate removed, while the right side shows the corresponding intact endplate results. Mean stiffness (Mean), standard error of the mean (SEM) and standard deviation (SD) are given in Newtons/mm. The number of tests (n) has no units. The AP and LAT test site co-ordinates are given as percentages of the corresponding endplate dimensions (see Figure 2.13 for a diagram of the test site layout).

| | Endplate Removed | | | | Endplate Intact | | |
|---|---|---|---|---|---|---|---|
| LAT | 45% | 30% | 15% | 0% | 15% | 30% | 45% |
| AP | | | | | | | |
| 40% | | | **116.6** | | **164.5** | | *Mean ST* |
| | | | 39.5 | | 41.4 | | *SEM ST* |
| | | | 96.9 | | 101.3 | | *SD ST* |
| | | | 6 | | 6 | | *n* |
| 20% | | **49.5** | **54.6** | | **115.1** | **178.0** | |
| | | 12.5 | 9.6 | | 38.5 | 58.9 | |
| | | 33.2 | 25.4 | | 101.8 | 155.8 | |
| | | 7 | 7 | | 7 | 7 | |
| 0% | **77.5** | **43.8** | **53.6** | | **91.7** | **171.1** | **230.8** |
| | 12.8 | 9.2 | 9.8 | | 12.4 | 41.4 | 32.5 |
| | 33.9 | 24.3 | 25.9 | | 32.7 | 109.6 | 86.0 |
| | 7 | 7 | 7 | | 7 | 7 | 7 |
| -20% | **95.1** | **60.3** | **114.2** | | **205.1** | **257.8** | **273.0** |
| | 24.6 | 11.2 | 12.0 | | 33.0 | 41.6 | 48.5 |
| | 65.1 | 29.7 | 31.7 | | 87.3 | 110.0 | 128.2 |
| | 7 | 7 | 7 | | 7 | 7 | 7 |
| -40% | | **87.6** | **95.9** | | **209.7** | **302.4** | |
| | | 9.9 | 19.8 | | 55.8 | 66.2 | |
| | | 26.3 | 52.4 | | 147.6 | 175.2 | |
| | | 7 | 7 | | 7 | 7 | |

Three-way ANOVAs, using endplate condition (EP) and AP and LAT test co-ordinates as repeated measures, were done to look for differences between the regions where the endplate was intact and where it had been removed.

### *3.5.2.1 Maximum AP, LAT Analysis*

As before, the first ANOVA looked at the largest complete AP, LAT test area (Figure 3.47). This ANOVA showed that the specimens were significantly stiffer (about 2.7 times as stiff) where the endplate had been left intact ($p < 0.0117$) based on a comparison of the overall means of the stiffnesses in the two regions (intact: 191.4 N/mm, removed: 69.9 N/mm).

The shape of the map was not found to be significantly different in the intact and removed endplate regions ($p < 0.9178$). This means that, while there was a significant decrease in stiffness when the endplate was removed, the loss in stiffness was uniform over the vertebral surface. Note the similarities in the curve shapes but the difference in magnitude in Figure 3.47.

A *post hoc* Newman-Keuls mean comparison (Table 3.17) has been included here for readers who would like to know precisely which pairs of the means shown in Figure 3.47 were significantly different.

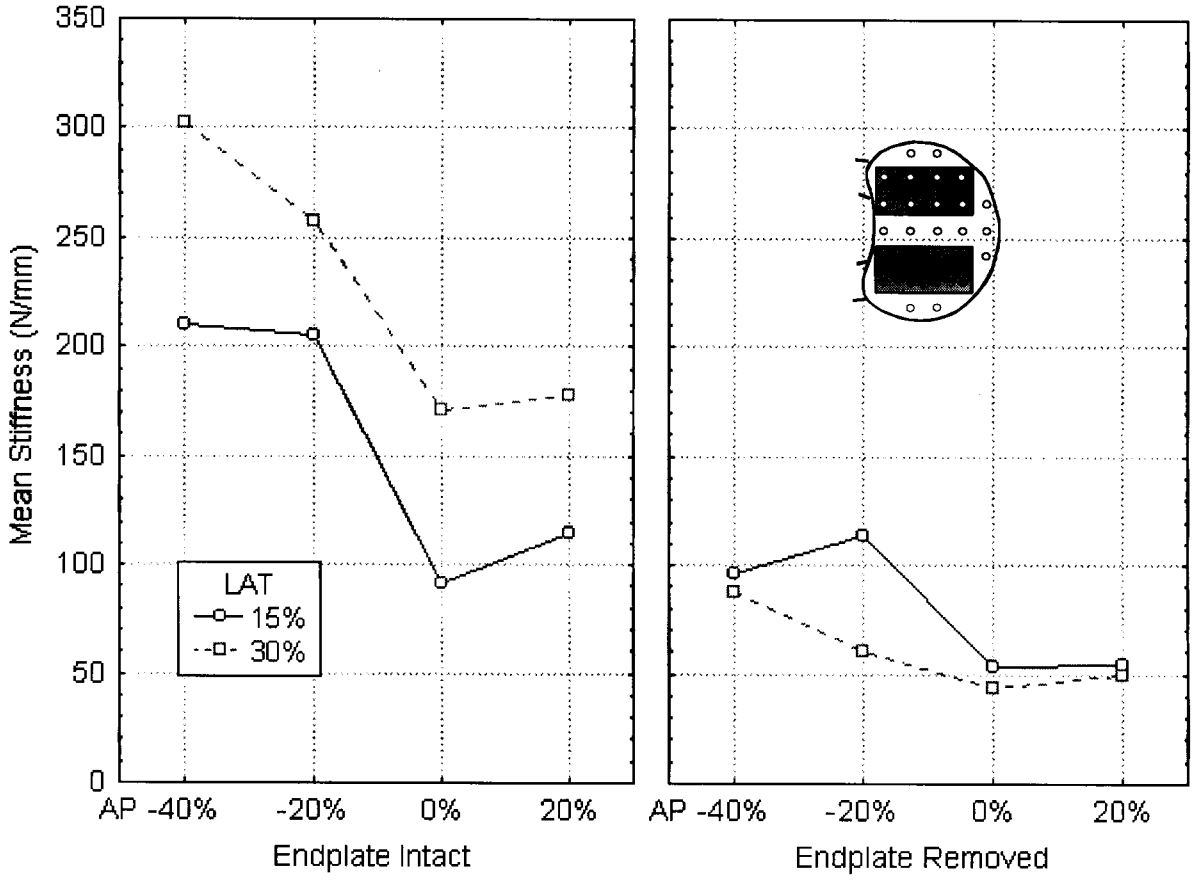


Figure 3.47: Comparison of the maximum AP, LAT stiffness distributions in the intact and removed lumbar endplate specimens. The p-value of $< 0.9178$ indicates that there were no significant differences between the shapes of the two stiffness maps. The intact endplate test sites were, however, significantly stiffer than the sites where the endplate had been removed ($p < 0.0117$).

**Table 3.17: Newman-Keuls *post hoc* comparison of the means in the intact and removed lumbar endplate maximum AP, LAT stiffness maps** (Figure 3.47). The p-values indicating the probability that each pair of means was different are given in the body of the table to four decimal places. The significant p-values ($p < 0.05$) are highlighted in grey (i.e. less than 5% chance of being wrong if one states that the two means are significantly different). The top three rows and left columns show the endplate condition (EP: intact, no EP: removed) and the AP and LAT test site co-ordinates as percentages of the endplate dimensions. The mean stiffnesses being compared are given in the fourth row and column in Newtons per millimetre (bold).

| | | | Endplate Intact | | | | | | | |
|---|---|---|---|---|---|---|---|---|---|---|
| | | AP | -40% | | -20% | | 0% | | 20% | |
| | | LAT | 15% | 30% | 15% | 30% | 15% | 30% | 15% | 30% |
| | AP | LAT | **Mean ST** | **209.7** | **302.4** | **205.1** | **257.8** | **91.7** | **171.1** | **115.1** | **178.0** |
| EP | -40% | 15% | **209.7** | | 0.0152 | 0.8802 | 0.1217 | 0.0159 | 0.5733 | 0.0357 | 0.5439 |
| | | 30% | **302.4** | 0.0152 | | 0.0197 | 0.1494 | 0.0002 | 0.0038 | 0.0002 | 0.0044 |
| | -20% | 15% | **205.1** | 0.8802 | 0.0197 | | 0.2052 | 0.0174 | 0.4974 | 0.0326 | 0.3712 |
| | | 30% | **257.8** | 0.1217 | 0.1494 | 0.2052 | | 0.0008 | 0.0605 | 0.0017 | 0.0648 |
| | 0% | 15% | **91.7** | 0.0159 | 0.0002 | 0.0174 | 0.0008 | | 0.0971 | 0.8587 | 0.0838 |
| | | 30% | **171.1** | 0.5733 | 0.0038 | 0.4974 | 0.0605 | 0.0971 | | 0.0750 | 0.8194 |
| | 20% | 15% | **115.1** | 0.0357 | 0.0002 | 0.0326 | 0.0017 | 0.8587 | 0.0750 | | 0.1133 |
| | | 30% | **178.0** | 0.5439 | 0.0044 | 0.3712 | 0.0648 | 0.0838 | 0.8194 | 0.1133 | |
| no EP | -40% | 15% | **95.9** | 0.0169 | 0.0002 | 0.0178 | 0.0008 | 0.8902 | 0.0873 | 0.7957 | 0.0817 |
| | | 30% | **87.6** | 0.0145 | 0.0002 | 0.0164 | 0.0008 | 0.8911 | 0.0997 | 0.8825 | 0.0817 |
| | -20% | 15% | **114.2** | 0.0458 | 0.0003 | 0.0456 | 0.0022 | 0.7328 | 0.1615 | 0.9761 | 0.1745 |
| | | 30% | **60.3** | 0.0027 | 0.0002 | 0.0031 | 0.0003 | 0.5499 | 0.0209 | 0.4619 | 0.0162 |
| | 0% | 15% | **53.6** | 0.0023 | 0.0002 | 0.0028 | 0.0002 | 0.7026 | 0.0199 | 0.4647 | 0.0148 |
| | | 30% | **43.8** | 0.0016 | 0.0002 | 0.0019 | 0.0002 | 0.6730 | 0.0140 | 0.3758 | 0.0101 |
| | 20% | 15% | **54.6** | 0.0022 | 0.0002 | 0.0025 | 0.0002 | 0.6034 | 0.0176 | 0.4249 | 0.0133 |
| | | 30% | **49.5** | 0.0020 | 0.0002 | 0.0024 | 0.0002 | 0.7128 | 0.0178 | 0.4377 | 0.0130 |

| | | | Endplate Removed | | | | | | | |
|---|---|---|---|---|---|---|---|---|---|---|
| | | AP | -40% | | -20% | | 0% | | 20% | |
| | | LAT | 15% | 30% | 15% | 30% | 15% | 30% | 15% | 30% |
| | AP | LAT | **Mean ST** | **95.9** | **87.6** | **114.2** | **60.3** | **53.6** | **43.8** | **54.6** | **49.5** |
| EP | -40% | 15% | **209.7** | 0.0169 | 0.0145 | 0.0458 | 0.0027 | 0.0023 | 0.0016 | 0.0022 | 0.0020 |
| | | 30% | **302.4** | 0.0002 | 0.0002 | 0.0003 | 0.0002 | 0.0002 | 0.0002 | 0.0002 | 0.0002 |
| | -20% | 15% | **205.1** | 0.0178 | 0.0164 | 0.0456 | 0.0031 | 0.0028 | 0.0019 | 0.0025 | 0.0024 |
| | | 30% | **257.8** | 0.0008 | 0.0008 | 0.0022 | 0.0003 | 0.0002 | 0.0002 | 0.0002 | 0.0002 |
| | 0% | 15% | **91.7** | 0.8902 | 0.8911 | 0.7328 | 0.5499 | 0.7026 | 0.6730 | 0.6034 | 0.7128 |
| | | 30% | **171.1** | 0.0873 | 0.0997 | 0.1615 | 0.0209 | 0.0199 | 0.0140 | 0.0176 | 0.0178 |
| | 20% | 15% | **115.1** | 0.7957 | 0.8825 | 0.9761 | 0.4619 | 0.4647 | 0.3758 | 0.4249 | 0.4377 |
| | | 30% | **178.0** | 0.0817 | 0.0817 | 0.1745 | 0.0162 | 0.0148 | 0.0101 | 0.0133 | 0.0130 |
| no EP | -40% | 15% | **95.9** | | 0.9581 | 0.5444 | 0.6344 | 0.7116 | 0.6525 | 0.6401 | 0.7049 |
| | | 30% | **87.6** | 0.9581 | | 0.8065 | 0.3692 | 0.6662 | 0.6806 | 0.5187 | 0.7032 |
| | -20% | 15% | **114.2** | 0.5444 | 0.8065 | | 0.3939 | 0.4229 | 0.3514 | 0.3746 | 0.4051 |
| | | 30% | **60.3** | 0.6344 | 0.3692 | 0.3939 | | 0.9724 | 0.9795 | 0.8503 | 0.9831 |
| | 0% | 15% | **53.6** | 0.7116 | 0.6662 | 0.4229 | 0.9724 | | 0.9412 | 0.9732 | 0.8919 |
| | | 30% | **43.8** | 0.6525 | 0.6806 | 0.3514 | 0.9795 | 0.9412 | | 0.9827 | 0.8480 |
| | 20% | 15% | **54.6** | 0.6401 | 0.5187 | 0.3746 | 0.8503 | 0.9732 | 0.9827 | | 0.9839 |
| | | 30% | **49.5** | 0.7049 | 0.7032 | 0.4051 | 0.9831 | 0.8919 | 0.8480 | 0.9839 | |

### *3.5.2.2 Full AP Analysis*

A second and third ANOVA were done to examine the effects of including the most anterior and most lateral test sites. Note that the full AP analysis in the half-endplate specimens was only a 2-way analysis since there was only a single LAT co-ordinate (15%) in each endplate condition map.

The full AP analysis (Figure 3.48) found again that, while the intact endplate was significantly stiffer ($p < 0.0319$; mean intact stiffness = 162.6 N/mm; mean removed stiffness = 84.7 N/mm), the shapes of the curves were not significantly different ($p < 0.2717$). The results of the *post hoc* Newman-Keuls analysis are provided in Table 3.18 for readers interested in the specific differences between the two endplate conditions.

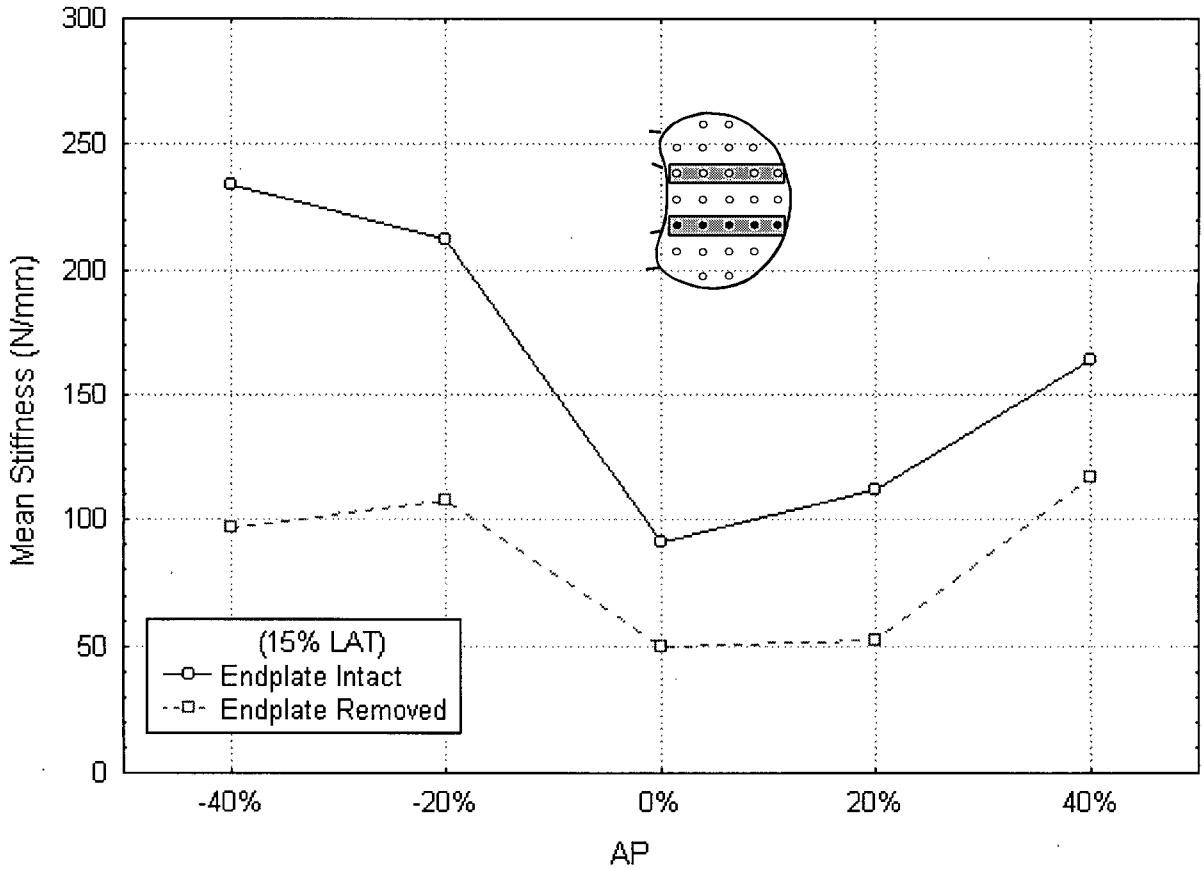


Figure 3.48: Comparison of the full AP stiffness distributions in the intact and removed lumbar endplate specimens. The p-value of $< 0.2717$ indicates that there were no significant differences between the shapes of the two stiffness curves. The intact endplate test sites were, however, significantly stiffer than the sites where the endplate had been removed ($p < 0.0319$).

### *3.5.2.3 Full LAT Analysis*

The full LAT analysis (Figure 3.49) also found that the intact endplate was significantly stiffer ($p < 0.0051$; mean intact stiffness = 204.9 N/mm; mean removed stiffness = 74.1 N/mm), while the shapes of the maps were not significantly different ($p < 0.6407$). The results of the *post hoc* Newman-Keuls mean comparison (Table 3.19) has been included here for readers who would like to know precisely which pairs of the means shown in Figure 3.49 were significantly different.

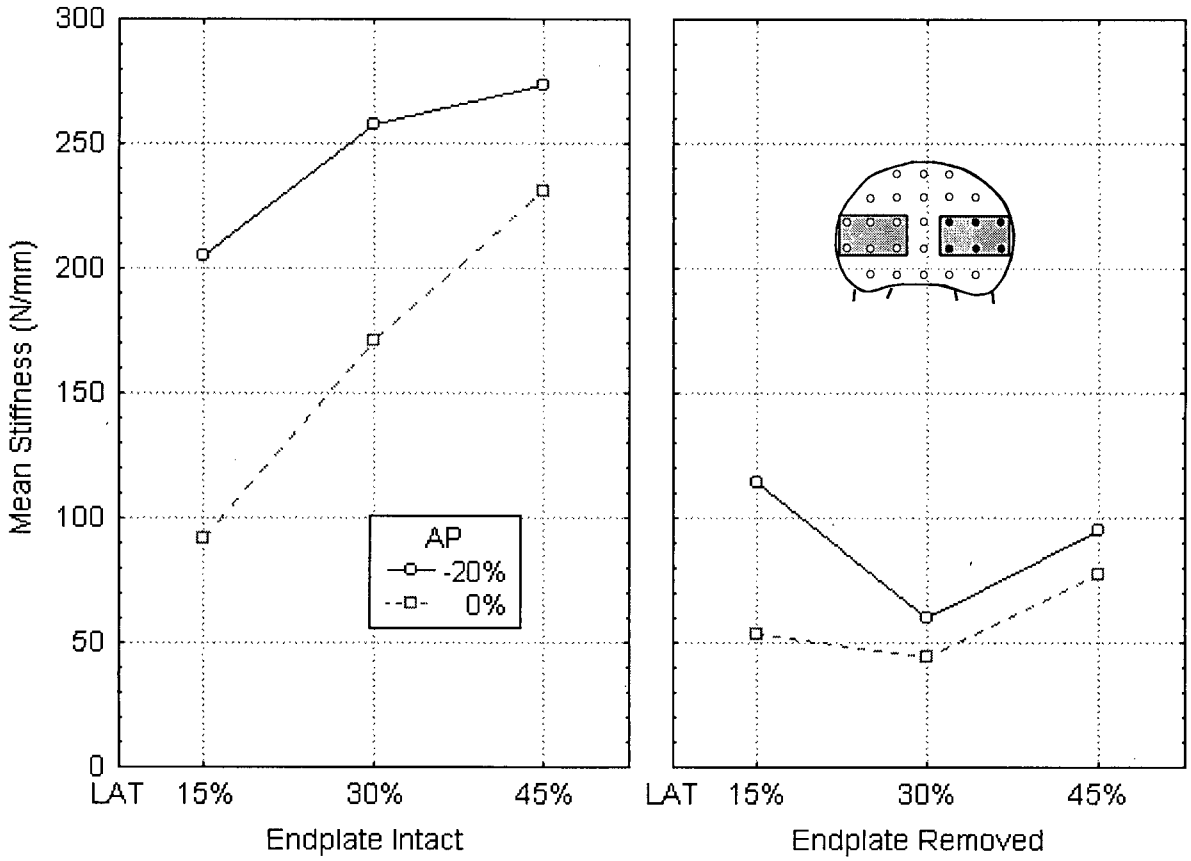


Figure 3.49: Comparison of the full LAT stiffness distributions in the intact and removed lumbar endplate specimens. The p-value of $< 0.6407$ indicates that there were no significant differences between the shapes of the two stiffness maps. The intact endplate test sites were, however, significantly stiffer than the sites where the endplate had been removed ($p < 0.0051$).

### 3.5.3 Summary

The vertebral surface was significantly stronger and stiffer when the endplate was left intact, however removing the endplate did not have a significant effect on the failure load or stiffness distribution, i.e. there was a uniform loss in strength over the vertebral surface when the endplate was removed.

**Table 3.18: Newman-Keuls *post hoc* comparison of the means in the intact and removed lumbar endplate full AP stiffness maps** (Figure 3.48). The p-values indicating the probability that each pair of means was different are given in the body of the table to four decimal places. The significant p-values ($p < 0.05$) are highlighted in grey (i.e. less than 5% chance of being wrong if one states that the two means are significantly different). The top three rows and left columns show the endplate condition (EP: intact, no EP: removed) and the AP and LAT test site co-ordinates as percentages of the endplate dimensions. The mean stiffnesses being compared are given in the fourth row in Newtons per millimetre (bold).

| | | | | Endplate Intact | | | | | Endplate Removed | | | | |
|---|---|---|---|---|---|---|---|---|---|---|---|---|---|
| | | | AP | -40% | -20% | 0% | 20% | 40% | -40% | -20% | 0% | 20% | 40% |
| | | | LAT | 15% | 15% | 15% | 15% | 15% | 15% | 15% | 15% | 15% | 15% |
| | AP | LAT | **Mean ST** | **233.9** | **211.9** | **90.9** | **111.9** | **164.5** | **97.2** | **108.1** | **49.3** | **52.0** | **116.6** |
| EP | -40% | 15% | **233.9** | | 0.5321 | 0.0100 | 0.0162 | 0.1368 | 0.0118 | 0.0177 | 0.0012 | 0.0011 | 0.0143 |
| | -20% | 15% | **211.9** | 0.5321 | | 0.0311 | 0.0416 | 0.1861 | 0.0352 | 0.0493 | 0.0036 | 0.0035 | 0.0316 |
| | 0% | 15% | **90.9** | 0.0100 | 0.0311 | | 0.9285 | 0.3134 | 0.8566 | 0.8735 | 0.4672 | 0.2755 | 0.9434 |
| | 20% | 15% | **111.9** | 0.0162 | 0.0416 | 0.9285 | | 0.3032 | 0.9059 | 0.9133 | 0.4835 | 0.4397 | 0.8932 |
| | 40% | 15% | **164.5** | 0.1368 | 0.1861 | 0.3134 | 0.3032 | | 0.3275 | 0.3851 | 0.0548 | 0.0519 | 0.1818 |
| no | -40% | 15% | **97.2** | 0.0118 | 0.0352 | 0.8566 | 0.9059 | 0.3275 | | 0.7568 | 0.5241 | 0.4091 | 0.9426 |
| EP | -20% | 15% | **108.1** | 0.0177 | 0.0493 | 0.8735 | 0.9133 | 0.3851 | 0.7568 | | 0.4580 | 0.3912 | 0.9672 |
| | 0% | 15% | **49.3** | 0.0012 | 0.0036 | 0.4672 | 0.4835 | 0.0548 | 0.5241 | 0.4580 | | 0.9387 | 0.4772 |
| | 20% | 15% | **52.0** | 0.0011 | 0.0035 | 0.2755 | 0.4397 | 0.0519 | 0.4091 | 0.3912 | 0.9387 | | 0.4500 |
| | 40% | 15% | **116.6** | 0.0143 | 0.0316 | 0.9434 | 0.8932 | 0.1818 | 0.9426 | 0.9672 | 0.4772 | 0.4500 | |

**Table 3.19: Newman-Keuls *post hoc* comparison of the means in the intact and removed lumbar endplate full LAT stiffness maps** (Figure 3.49). The p-values indicating the probability that each pair of means was different are given in the body of the table to four decimal places. The significant p-values ($p < 0.05$) are highlighted in grey (i.e. less than 5% chance of being wrong if one states that the two means are significantly different). The top three rows and left columns show the endplate condition (EP: intact, no EP: removed) and the AP and LAT test site co-ordinates as percentages of the endplate dimensions. The mean stiffnesses being compared are given in the fourth row in Newtons per millimetre (bold).

| | | | Endplate Intact | | | | | | Endplate Removed | | | | | |
|---|---|---|---|---|---|---|---|---|---|---|---|---|---|---|
| | AP | | -20% | | | 0% | | | -20% | | | 0% | | |
| | | LAT | 15% | 30% | 45% | 15% | 30% | 45% | 15% | 30% | 45% | 15% | 30% | 45% |
| | AP | LAT | **205.1** | **257.8** | **273.0** | **91.7** | **171.1** | **230.8** | **114.2** | **60.3** | **95.1** | **53.6** | **43.8** | **77.5** |
| EP | -20% | 15% | | 0.1114 | 0.0629 | 0.0037 | 0.1803 | 0.3049 | 0.0067 | 0.0010 | 0.0031 | 0.0008 | 0.0006 | 0.0020 |
| | | 30% | 0.1114 | | 0.5378 | 0.0004 | 0.0160 | 0.2810 | 0.0006 | 0.0002 | 0.0003 | 0.0002 | 0.0002 | 0.0003 |
| | | 45% | 0.0629 | 0.5378 | | 0.0003 | 0.0081 | 0.2230 | 0.0004 | 0.0002 | 0.0003 | 0.0002 | 0.0002 | 0.0002 |
| | 0% | 15% | 0.0037 | 0.0004 | 0.0003 | | 0.0273 | 0.0010 | 0.6274 | 0.4152 | 0.8891 | 0.4184 | 0.3204 | 0.5646 |
| | | 30% | 0.1803 | 0.0160 | 0.0081 | 0.0273 | | 0.0677 | 0.0350 | 0.0060 | 0.0204 | 0.0050 | 0.0033 | 0.0146 |
| | | 45% | 0.3049 | 0.2810 | 0.2230 | 0.0010 | 0.0677 | | 0.0020 | 0.0004 | 0.0009 | 0.0003 | 0.0003 | 0.0006 |
| no | -20% | 15% | 0.0067 | 0.0006 | 0.0004 | 0.6274 | 0.0350 | 0.0020 | | 0.2260 | 0.4417 | 0.1895 | 0.1234 | 0.4505 |
| EP | | 30% | 0.0010 | 0.0002 | 0.0002 | 0.4152 | 0.0060 | 0.0004 | 0.2260 | | 0.4916 | 0.7846 | 0.7730 | 0.4853 |
| | | 45% | 0.0031 | 0.0003 | 0.0003 | 0.8891 | 0.0204 | 0.0009 | 0.4417 | 0.4916 | | 0.4503 | 0.3274 | 0.7480 |
| | 0% | 15% | 0.0008 | 0.0002 | 0.0002 | 0.4184 | 0.0050 | 0.0003 | 0.1895 | 0.7846 | 0.4503 | | 0.6880 | 0.5908 |
| | | 30% | 0.0006 | 0.0002 | 0.0002 | 0.3204 | 0.0033 | 0.0003 | 0.1234 | 0.7730 | 0.3274 | 0.6880 | | 0.5161 |
| | | 45% | 0.0020 | 0.0003 | 0.0002 | 0.5646 | 0.0146 | 0.0006 | 0.4505 | 0.4853 | 0.7480 | 0.5908 | 0.5161 | |

# Chapter 4

# Discussion

In this chapter, the methods used in this study and the results described in chapter 3 are reviewed. Implications for current surgical practice and interbody implant design are discussed.

## 4.1 Methods

### 4.1.1 Effects of Freezing on Bone Properties

All of the specimens used in this study were fresh frozen (i.e. removed from donors and placed in the freezer with no chemical or other preservation). Sedlin (1965) showed that the strength and elastic modulus of cortical bone are not affected by deep freezing, and according to Gibson and Ashby (1988, pp. 320, 321) the biochemical compositions of cortical and cancellous bone are very similar (section 1.7.2). Even if this were not the case, the results presented here are meant to represent the *relative* properties of the bone rather than absolute properties. Since all of the specimens were frozen at the same temperature for approximately the same amount of time, one can assume that any effects of freezing would be uniform across the specimens, thus the relative property comparisons would be unaffected.

### 4.1.2 Specimen Age

The specimen donors for this study were mainly older individuals (mean age: 74.6 years, range: 48 to 90 years). This is a typical problem in studies relying on cadaveric material. The fact that some of the specimens were selected based on advanced states of degeneration in the discs and/or bone may also have increased the average donor age, since these degenerative changes tend to occur later in life.

In some ways this may be advantageous, since implant studies show increased risk of subsidence in lower density bones (lower load to failure) (Oxland and Lund 2000) and bone density tends to decrease with age (Martin 1993). This implies that these specimens may be more representative of the "high risk" patients than would be specimens supplied by younger donors.

### 4.1.3 Use of DEXA Rather than QCT

The bone density of the specimens was recorded using lateral DEXA scans. It may be argued that, since DEXA gives only a 2-dimensional representation of bone density (grams per square centimetre), quantitative computed tomography (QCT), which gives a three-dimensional representation of bone density, would be a better choice. Unfortunately the vastly greater expense of QCT makes it less clinically relevant than DEXA. For this reason, DEXA was used as the bone density indicator in this study to make the results more clinically relevant.

### 4.1.4 Use of a Hemispherical Indenter

If one looks in the literature, one will find that most indentation studies use either flat-faced cylindrical indenters, or conical indenters, such as the osteopenetrometer employed by Hvid et al. As was mentioned in section 2.4.1.1, these studies were conducted almost exclusively on bones which had been cut or machined to produce a flat, cancellous bone surface. Perey (1957), who used a flat-faced cylindrical indenter in unmachined endplates, was unable to test all sites in all specimens due to difficulties achieving appropriate contact. The non-planar endplate surface can be more repeatably engaged using a hemispherical indenter.

The use of a hemispherical indenter makes interpretation of the results somewhat more complex, since the indenter area changes with depth, however since this study looks at the *relative* failure load and stiffness values rather than absolute values, this should not affect the results. Specifically, the effects of the changing indenter area are constant across all sites and specimens, thus the failure load and stiffness values were equally influenced in each test.

### 4.1.5 Choice of Indenter Size

The indenter used in this study was 3 mm in diameter. The reasons for this choice are discussed in section 2.4.1.2. It should be noted that the author does not advocate this size as being necessarily better than other possible choices. For the study outlined here it proved to meet the requirements of being large enough to produce repeatable results, yet small enough to provide a reasonably detailed surface map. Investigators working in different bones, or even different levels of the spine, are encouraged to do some preliminary work to determine a suitable indenter size for their own application.

To give some basis for comparison, McKoy et al. (2000) report using flat-faced cylindrical indenters of between 1.3 and 5 mm in diameter for indentation tests in rat, rabbit, dog and cow bone, while Hvid et al. (1983) used a 2.5 mm-diameter conical indenter for penetration tests in human tibia, and Anglin et al. (1999) used a 2.95 mm-diameter flat-faced cylindrical indenter in the human glenoid.

### 4.1.6 Choice of Indentation Rate

The indentation rate of 0.2 mm/s used in this study was chosen as a compromise between a low rate to model the clinical failure conditions of implants, and a high rate to allow the tests to be completed in a reasonable amount of time, as discussed in section 2.4.4.1. Although a slower indentation rate might have been preferable, the fact that over 2000 tests were run means that the test time had to be minimised as much as possible. It should be noted that the rate dependency of bone's ultimate strength and elastic modulus are relatively weak, being approximately proportional to the strain rate raised to the power 0.06 (Mow and Hayes 1997, p. 84).

It is recommended that other investigators choose a test rate appropriate to their application, or base their test rate on the work of other researchers to which they hope to compare their results in order to minimise sources of error.

Some rates reported in the literature include 1 mm/min (Hvid et al. 1983, McKoy et al. 2000), 2 mm/min (Anglin et al. 1999), and 10 mm/min (An 1999).

### 4.1.7 Decision To Not Consider Gender as a Variable

There may be differences between the architecture in male and female vertebrae, however there doesn't seem to be clear agreement in the scientific community that differences exist or that they are significant (section 1.6.2.2). While it would have been interesting, and no doubt valuable, to look at gender as a variable in this study, the number of specimens required made this prohibitive.

Two points that are clear are that females' bones tend to be smaller than males' and women tend to experience diminished bone mass sooner as a result of the hormonal changes accompanying menopause. These factors were accounted for by using a test layout scaled using the dimensions of the endplate and by considering bone density as a variable.

Additional research looking specifically at the effects of gender would be very valuable and is encouraged as an additional avenue to pursue in future research.

### 4.1.8 Interpreting the Results - A Word on Failure Load and Stiffness

The main purpose of this study was to identify methods by which the risk of interbody implant subsidence might be reduced. The failure load has the most direct implications for implant subsidence since failure of the bone tends to result in more complications than deflection of the bone, thus the failure load results are likely of greater importance in terms of implant performance than are the stiffness results. Stiffness does, however, have implications for the amount of motion at the bone-implant interface during the initial healing phase. A certain amount of motion may be desirable to promote healing, but too much deflection of the bone can have negative effects on the fusion rate or prevent fusion altogether.

In general, the stiffness distributions and comparisons were not as clear as those for failure load (higher p-values) though they had similar shapes. This may have been due to the complications of measuring stiffness with the methods used in the study. Since a hemispherical indenter was used for the tests, the indenter area changed with penetration depth. This would tend to result in a non-linear load-displacement curve. Although this would be consistent over all tests, it might increase the uncertainty of the slope used to measure stiffness.

The structure of cancellous bone also tends to make stiffness measurement difficult, since the number of trabeculae in contact with the indenter at any one time is not constant. In widely-spaced trabecular regions, as trabeculae fracture they fall away from the contact area, leaving a smaller number of trabeculae bearing the load until deeper trabeculae are contacted. In more densely-packed regions, the trabecular fragments collect under the indenter, distributing the load more evenly over the remaining trabeculae. In each case, the stiffness varies with depth, adding additional "noise" into the load-displacement curve.

## 4.2 General Maps

### 4.2.1 Similarities Between the Lumbar Vertebrae

The literature contains many studies supporting "Wolff's Law" (Wolff 1892), which postulates that a bone adapts to its loading conditions by becoming stronger if subjected to load (Koch 1917; Hayes and Snyder 1981). Based on this theory it would be reasonable to assume that successively lower levels

of the spine would be stronger than those above since they must support larger loads. This may be partially accounted for by the fact that the vertebrae increase in size from the head to the base of the spine, thus providing a larger cross-sectional area for load transmission, however there may also be an increase in the local bone strength. Section 3.2.1 presented the results of ANOVA comparisons of the three superior lumbar endplates and of the three inferior lumbar endplates. The superior and inferior endplates were analysed separately in order to account for any potential differences between them.

No differences were found between the superior or inferior endplates of the three lumbar levels that were studied, either in mean structural properties or in property distribution. Weaver et al. (1966 a) showed that there was no difference between the material properties of cancellous bone cubes taken from the L3 through L5 lumbar vertebrae. This suggests that, although the overall compressive failure load differs in these three vertebrae (Bell et al. 1967; Perey 1957), the differences arise from the unequal cross-sectional areas of the vertebrae rather than from the properties of the bone. For the purposes of this study it meant that the lumbar specimens could be combined for the remaining comparisons.

The basic geometric similarities between the five lumbar vertebrae and the lack of structural property differences between the L3 through L5 vertebrae suggest that it may be possible to extrapolate the results obtained in this study to include the L1 and L2 vertebrae, however further research is required to confirm this.

### 4.2.2 Similarities Between the Superior and Inferior Lumbar Endplates

Section 3.2.2 showed the results of a series of ANOVAs used to compare the structural properties in the superior and inferior lumbar endplates. In both endplates the posterolateral test sites (in front of the pedicles) had the highest structural properties, the posterior was stronger than the anterior, and the centre was weaker than the periphery (Figure 4.1). The stiffness maps (Figure 3.11) were similar to the failure load maps (Figure 4.1).

The basic pattern of the lumbar structural property maps may be explained, at least in part, by the load transmission patterns imposed on the vertebrae by their geometry (Figure 1.1). White and Panjabi (1990, p. 112) report that the instantaneous axis of rotation for the lumbar vertebrae is located in the anterior third of the disc for flexion, between the posterior margin of the disc and the facet (articular process) joints for extension, and in the left third and right third of the disc, respectively, for right and left lateral bending. It is near the centre of the disc for left and right axial rotation. This means that the anterior and posterior margins of the disc would transmit the highest compressive or tensile loads in flexion and extension, while the lateral margins would bear the largest loads in lateral bending, since the load increases with distance from the centre of rotation. In axial rotation the shear stresses would increase with distance from the centre of the endplate. In addition, the pedicles transmit large bending loads to the vertebral body, particularly during extension, when the inferior articular processes of the upper vertebra press against the superior articular processes of the vertebra below (Figure 4.2). This would tend to put large loads on the posterior region of the vertebral body.

The fact that the postero-lateral test sites were the strongest tends to imply that the pedicles are at least partially responsible for the patterns which were observed, however the pedicles are closer to the superior endplate, and this endplate was the weaker of the two. This seems to indicate that the pedicles may not be responsible for the higher posterior strength.

Wenger et al. (1999) used pQCT to look at the regional bone density in 8 mm-wide frontal-plane strips cut from the widest portion of 30 normal, 15 osteoporotic, and 13 degenerate human endplates,

retaining 5 mm if the underlying trabecular bone. In each group, the bone density was higher at the lateral margins than in the centre and there were no significant differences between the groups in either density magnitude or curve shape. In general, the lateral margin had a density of 600-700 mg/cm$^3$, and the middle had a density of 350-450 mg/cm$^3$. This matches the results seen in this study, that the periphery of the lumbar endplates is stronger than the centre. Further research is required to determine if this variation is due to differences in the trabecular structure, endplate structure, or to material differences.

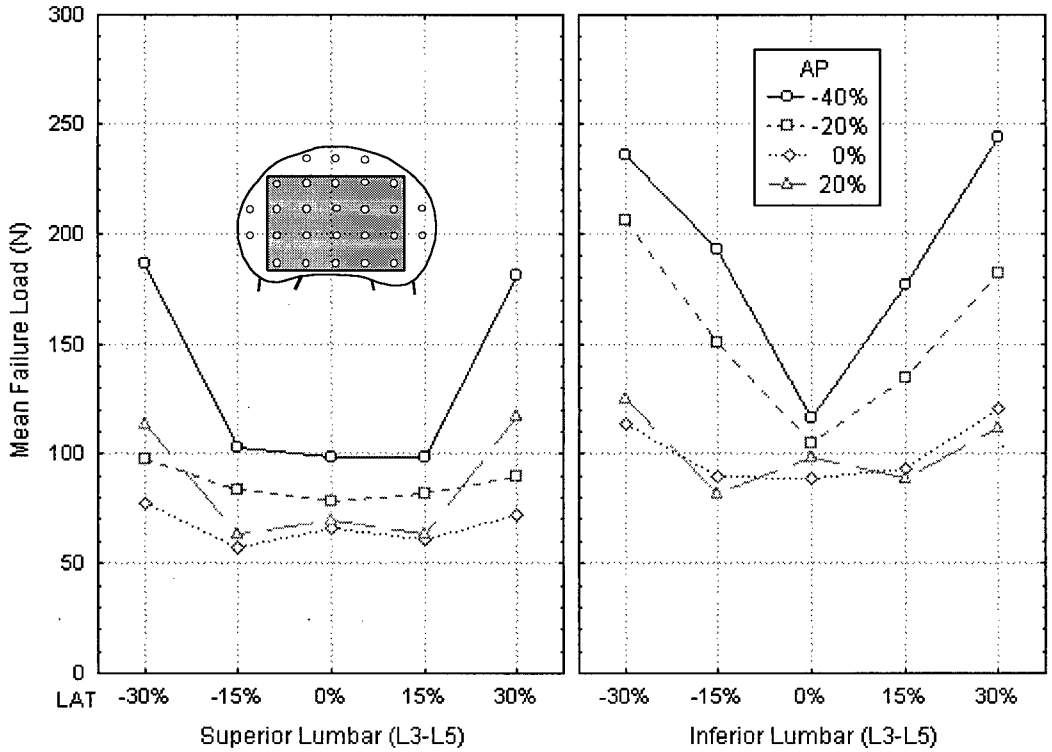


Figure 4.1: Superior and inferior lumbar endplate maximum AP, LAT failure load maps. Note the differences in the curve shapes in the posterior region of the endplates (-40 and –20% AP). In both maps the posterolateral test sites, in front of the pedicles, were the strongest sites (-40% AP, ±30% LAT).

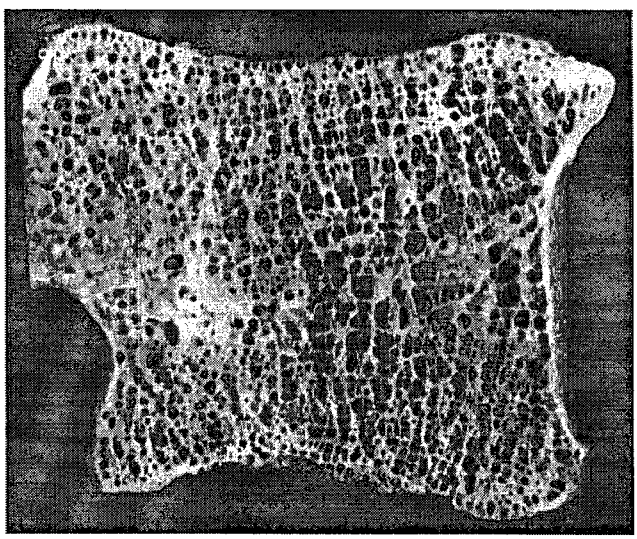

Figure 4.2: Cross-section through the vertebral body and a small part of one pedicle (posterior to the left). Note that the trabeculae appear to be thicker and closer together in the pedicle and adjacent to the pedicle than they are in the anterior two-thirds of the vertebral body. From Figure 12, Jayasinghe, et al. (1994).

### 4.2.3 Differences Between the Superior and Inferior Lumbar Endplates

The inferior lumbar endplates were significantly stronger and stiffer than the superior lumbar endplates. The failure load and stiffness distributions were also significantly different. This indicates that, while the inferior endplate was stronger, the property difference was not uniformly distributed over the endplate surface. A closer look at the maps (Figure 4.1) indicated that the posterior region was significantly stronger and stiffer in the inferior endplate, while the anterior portion had about the same strength and stiffness as was found in the superior endplate.

It is unclear why this shape difference was observed, however it has been well documented in the literature that the superior and inferior endplates demonstrate different failure modes under similar loading (e.g. in pure compressive loading). Magerl et al. (1994) reviewed 1445 consecutive clinical thoracolumbar injuries at five institutions and showed that in the majority of burst-type injuries to the vertebral body the superior portion of the vertebra is far more comminuted than the inferior portion. Willén et al. (1992) looked at ten acute thoracolumbar burst fractures (T11-L3) sustained as a result of fatal trauma (7 in falls, 3 in motor vehicle accidents) and also found that in every case the upper half of the vertebral body was far more comminuted than was the lower half. Other studies have produced similar findings (Hashimoto et al. (1988), Oxland (1992): section 1.6.5).

Oxland (1992) also observed that the anterior portion of the lumbar vertebral body sustained more damage in burst fracture injuries than did the posterior portion, which matches the finding of this study that the anterior region is weaker than the posterior region.

Underlying anatomical differences (e.g. differences in endplate thickness or trabecular spacing) and the locations of the intervertebral disc nutritional pathways may have some bearing on the locations of the stronger bone regions. Further research is required to better understand the reasons for the differences between the superior and inferior lumbar endplates.

### 4.2.4 Differences Between the Lumbar and Sacral Endplates

Unlike the lumbar endplates, the sacral endplate was not weakest in the middle, but rather had a steady decline in strength from the posterior to the anterior test sites, with no lateral variation. The results of the ANOVAs comparing the superior lumbar and sacral endplates are given in section 3.2.3. Comparisons of the inferior lumbar and sacral endplates are given in section 3.2.4. The stiffness maps were very similar to the failure load maps. It was found that the sacral endplate was significantly stronger than the superior lumbar endplate but not the inferior lumbar endplate. It was not significantly stiffer than either of the lumbar endplates.

The sacral failure load distribution was significantly different from both the superior (Figure 4.3) and inferior (Figure 4.4) lumbar distributions, but only the inferior lumbar stiffness distribution was significantly different from the sacral stiffness distribution. The most likely reason for the lack of significance in the superior lumbar stiffness comparison was the relatively small number of sacral specimens used in the tests (7 sacral specimens versus 28 superior lumbar specimens), which reduced the power of the test to detect differences.

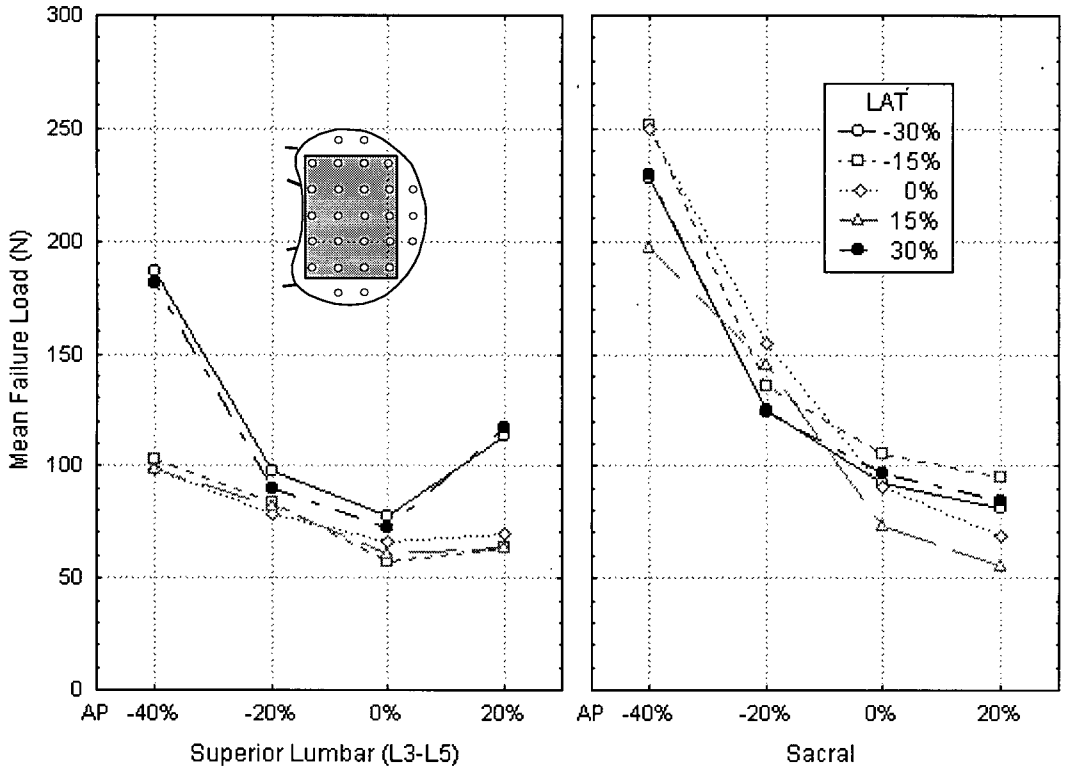


Figure 4.3: Superior lumbar and sacral endplate maximum AP, LAT failure load maps. Note that the lumbar specimens have significant lateral variation in failure load, while the sacral specimens do not.

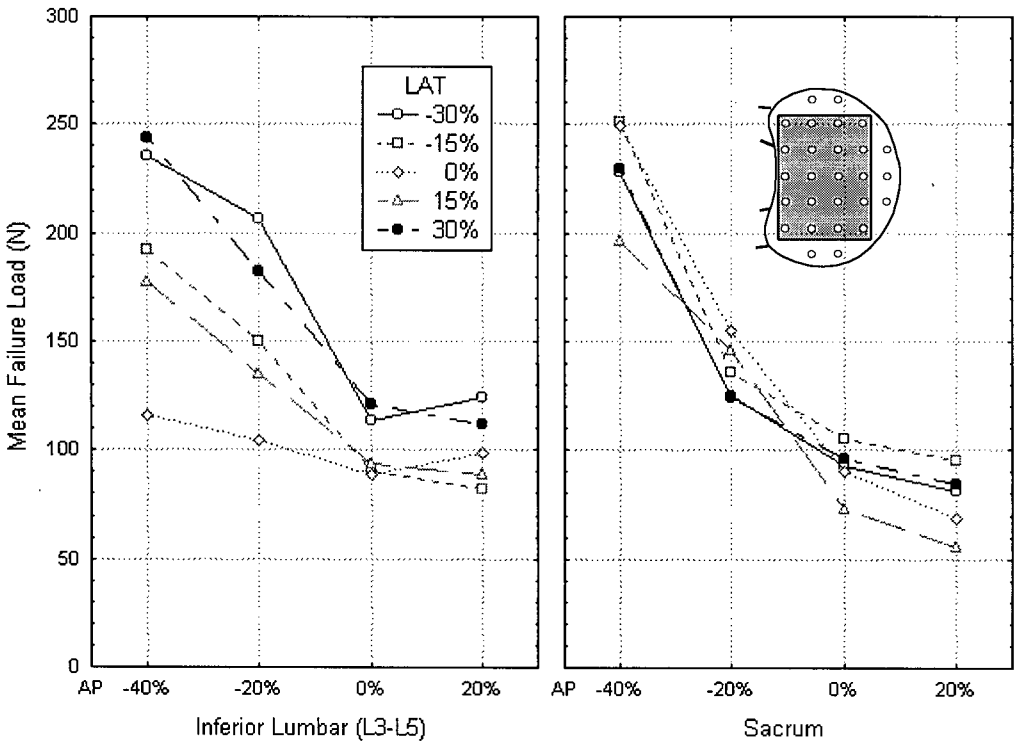


Figure 4.4: Inferior lumbar and sacral endplate maximum AP, LAT failure load maps. Note that the lumbar specimens have significant lateral variation in failure load, while the sacral specimens do not.

Peretz et al. (1998) studied the cortical and trabecular anatomy of the sacrum using radiographs and cross-sections. Though it is not commented upon in the paper, the figures showing sagittal sections through the sacrum show denser trabecular structure in the posterior region of the endplate, which becomes gradually less dense moving anteriorly. This correlates well with the shapes of the sacral structural property maps.

It is interesting to note that the sacral maps do not show a peripheral increase in value, while both the superior and inferior lumbar maps do. This may be a result of loading differences, specifically those related to the kinematics of the intervertebral discs. All of the lumbar vertebrae have a disc attached to both the superior and inferior endplates. During motion, the discs deform, allowing the vertebra to move relative to the bones above and below it. This would tend to compress the vertebra on the side toward which the individual was bending (i.e. the front if bending forward, the right if bending right, etc.). The sacral vertebrae are fused, reducing this "sandwiching" effect at the S1 level. As well, the L5-S1 disc tends to be more inclined than the other lumbar discs (Figure 1.2), thus the loads it supports have a larger shearing component and comparatively more load may be transmitted via the posterior elements.

## 4.3 Effects of Bone Density

### 4.3.1 General Effects of Bone Density

It has been shown time and again in the literature that vertebral strength is directly related to bone density (Bell et al. 1967; Hansson et al. 1980, 1981, 1986; Biggemann et al. 1988; Closkey et al. 1993; Holte et al. 1994; Hoshijima et al. 1997; Jost et al. 1998; An 1999; Oxland and Lund 2000). To determine whether this was also true for local bone failure loads, and what affect density had on stiffness, the structural properties of the test sites were plotted against the bone density of the endplates and linear regression analysis was used to look for relationships (section 3.1).

It was found that the local and mean failure loads were higher in specimens with greater bone density. This was not as evident in the stiffness values, but there was a similar trend. In both cases the relationship was rather weak, however the basic trend toward increased strength with higher bone density matches that shown in the literature. It is possible that the relationships between the local structural properties and the bone density were not as strong as those shown in the literature because the densities used in this study were taken from the entire upper or lower half of the vertebra, while the structural properties were measured locally.

The finding that the local bone strength and stiffness decrease as the bone density drops tends to suggest that older patients, osteoporotic patients, or those with unusually low bone density, are at higher risk of subsidence following interbody fusion. This is supported by *in vitro* implant performance studies (Jost et al. 1998, Oxland and Lund 2000).

### 4.3.2 Regional Effects of Bone Density

Bone density decreases naturally with age, reduction in loading (reduced activity) and menopause, as well as in some medical conditions, such as hormonal imbalances. There is some question as to whether the density (and, thus, failure load) decreases uniformly over the vertebra or whether some regions weaken faster.

Section 3.3 shows the results of the ANOVAs done to look at the effects of bone density on the structural property maps. Both the superior and inferior endplates became weaker as the bone density dropped, but the sacrum did not show a significant drop in strength. This may be due to the fact that fewer sacral specimens were used, resulting in insufficient statistical power to detect existing differences in failure load between the bone density groups. It may also be because lateral DEXA scans were used to measure the bone density. The shape of the sacrum makes lateral scans of this level more prone to error, since the sacrum flares on either side of the endplate to provide a stable interface with the pelvic girdle. This means that a smaller percentage of the bone measured with the DEXA scan is actually below the endplate, differing based on anatomical variation in the size and density of the sacral flares.

Only the superior endplate failure load map shape was significantly affected by a decline in bone density, with a more rapid drop in the posterior failure loads leading to a flatter failure load profile (Figure 3.27). Stiffness (overall means and distributions) was not significantly affected by bone density in any of the three endplate groups.

These results suggest that while there was an overall loss of strength associated with a decrease in bone density in the lumbar endplates, it was relatively evenly distributed over the inferior lumbar endplate, while the superior endplate had a more unequal strength loss. It is possible that this result was found because the specimens tested in this study had decreased bone mass due to the natural ageing process, rather than osteoporosis. It is reasonable to theorise that the decline in bone density which occurs as a natural part of ageing could be evenly distributed over the bone, while osteoporotic changes might be more region-specific. It may also be that the change to osteoporotic architecture occurs sooner in the superior half of the lumbar vertebral body.

Jayasinghe et al.'s 1994 study of the L4 trabecular structure found that, while there is a general thinning of the trabeculae in older patients, the normal pattern of trabecular architecture is maintained, but sections from osteoporotic donors showed a change in architecture resulting in large spaces within the bone (Figure 1.8).

Magerl et al. (1994) found that burst fractures causing minor anterior wedging of up to 5 degrees, loss of vertebral body height without extensive comminution, and/or a central collapse of the vertebral body leading to an "hourglass-shaped" lateral profile were most often seen in osteoporotic individuals.

Oda et al. (1998) looked at the effects of age on the three-dimensional structure of 25 L2 vertebra then correlated the structural changes with L2 deformity in 99 patients with involutional osteoporosis. They found that the space between trabeculae in the anterosuperior ninth of the midsagittal section of the vertebral body increased severely with age. This matched their clinical finding that 81% of the 52% with wedge-shaped deformities of L2 had anterosuperior deformity with good preservation of the anteroinferior region of the bone. Also, in 67% of the 36% with biconcave vertebrae the concavity was more prominent in the superior portion of the vertebra and in many patients with flat vertebrae the upper part of the vertebral body was more compressed than the lower surface. No patients had inferior collapse without superior collapse. This again supports this study's finding that the superior endplate is weaker than the inferior endplate, and the posterior is stronger than the anterior bone. Oda et al. also found significant increases in trabecular spacing in the midanterior, anteroinferior, and central ninths of the midsagittal section of the vertebral body, though these did not have a significant correlation with age.

Future studies may want to look more specifically at the effects of osteoporosis, rather than just bone density, by testing bone with known osteoporotic architecture, particularly in light of the literature which suggests that osteoporosis affects some regions of the bone more than others.

## 4.4 Effects of Disc Degeneration

Many researchers have studied the effects of disc degeneration on the behaviour and properties of the intervertebral discs. It has been demonstrated that, as the disc degenerates, the centre of the disc (the nucleus) transmits less of the load and the periphery (the annulus) supports this additional load (Shirazi-Adl et al.1984). Using Wolff's theorem (Wolff 1892) that bone is remodelled based on the load it supports (i.e. becoming stronger if supporting more load, and weaker if bearing less load), this suggests that the centre of the endplate should become weaker and the periphery stronger as the disc degenerates. To test this hypothesis, the effects of disc degeneration on the general map shapes was studied using ANOVAs (section 3.4).

It was found that the inferior endplates became weaker as disc degeneration increased, but neither the superior lumbar nor sacral endplates showed a significant change in strength. Only the superior endplate map shape was significantly affected by disc degeneration, with a decline in the central failure loads and a corresponding increase in peripheral failure loads. Stiffness was not significantly affected by disc degeneration in any of the three endplate groups.

The changes in the superior lumbar endplate map match the predictions of Shirazi-Adl et al. (1984) with surprising accuracy. Their computer simulations of the L2-L3 intervertebral disc predicted that as the disc degenerates (as the nucleus dries out), more of the spinal load is transmitted by the periphery of the disc. Nachemson (1960) showed experimentally that the nucleus pulposus loses pressure as the disc degenerates and therefore transfers somewhat less load centrally. This was also shown by Frei, et al (1998), who did a series of *in vitro* tests in lumbar functional spinal units (vertebra-disc-vertebra spinal segments) to look at the effects of simulating mild degenerative disc changes on endplate strain.

The predictions based on Wolff's theorem (Wolff 1892), that the centre of the vertebral body will become weaker, while the periphery increases in strength as the disc degenerates, were supported in the superior lumbar endplates. The fact that the other endplates did not demonstrate similar changes was surprising, however it may have something to do with the load transmission through the cranial and caudal surfaces of the disc or the internal structure of the disc. Disc nutrition and changes in the nutritional pathways may also have some effect (i.e. the relative contributions of the superior and inferior endplates in supplying nutrients to the discs may change with age or degeneration). In the case of the sacral endplate maps it may also be the result of insufficient statistical power to detect differences due to the small number of specimens used.

## 4.5 Effects of Endplate Removal

In the surgical setting it is often considered advantageous to remove the endplate in order to promote bone growth. The argument has been made, however, that removal of the endplate may weaken the bone, leading to an increased risk of implant subsidence. The endplate is a very thin shelf of bone (usually less than 0.5 mm thick), thus it may inherently provide little additional strength, however it may serve to distribute the load more evenly over the underlying strut-like trabecular bone.

This small secondary study (section 3.5) looked at the effect of endplate removal on the local structural properties. Only a small number of specimens was used (4 superior and 3 inferior lumbar endplates), thus the superior and inferior lumbar endplate results were not examined independently. The

only question being addressed in this secondary study was whether removing the endplate had any effect on the structural properties or the structural property maps. It was not possible to make direct comparisons with the general superior and inferior lumbar endplate structural property maps presented in section 3.2.2, since there were too few specimens to separate the superior and inferior endplate results.

There was a significant decrease in both the failure load and stiffness when the endplate was removed, but the shapes of the maps did not change significantly. This suggests that the decreases in failure load and stiffness were uniform across the vertebral surface. This finding supports the long-held theory that removing the endplate has a negative impact on the vertebral bone strength and thus increases the risk of implant subsidence.

Recent *in vitro* biomechanical studies in which implants were pressed into lumbar vertebrae with and without the endplate have found no difference between the bone failure loads under axial compressive loads (Hollowell et al. 1996; Jost et al. 1998; Steffen et al. 2000). However, An (1999) found that removing the endplate resulted in significantly lower compressive failure loads in 27 cervical vertebrae (C3-C7). He tested the upper and lower halves of the vertebrae separately using an 8 mm flat-faced cylindrical indenter running at 10 mm/min to a depth of 2 mm. The specimens with intact endplates had a mean failure load of 634.40 ± 524.2 N standard deviation, while the specimens with the endplate removed had a mean failure load of 419.32 ± 291.1 N.

This current study is limited in that it does not consider differences based on endplate (superior/inferior), spinal level, bone density, or disc condition and few specimens were used. Nevertheless, the apparent contradiction between these results and previous studies may be explained by the inherent differences between the local bone properties and the overall structural interaction of a complete vertebra and implant. Alternatively, the previous studies may not have found a difference due to the presence of confounding variables and the resultant lack of statistical power in detecting the effect of endplate removal.

It may also be because an indenter achieves better initial contact with the bone than do implants. The main advantage of retaining the endplate is that it distributes load more evenly over the underlying trabeculae. The endplate tends to be curved and often concave, thus in many cases only the periphery of the implant is initially in contact with the bone. When it is loaded, it punches through the endplate and subsides to some degree before it achieves better contact with the bone. If the endplate has been removed then the implant also has this initial subsidence before good contact is established. At this point, the implant itself acts as the endplate, distributing load over the trabeculae. In theory, if better initial contact could be achieved then the intact endplate should provide more strength to the construct.

Additional structural map studies looking at more specimens and correlating the results with tests in whole vertebrae using implants designed to take advantage of the stronger bone regions and contrasting them with existing implants may help to clarify this issue.

## 4.6 Implications for Implant Design and Surgical Use

Significant regional structural property variation was found in all three endplate groups, suggesting that implant placement may affect the risk of subsidence. The centre of the lumbar endplates was the weakest part of the bone and was one of the weaker sacral endplate regions, yet this is where the majority of implants are currently placed.

To minimise the risk of subsidence, several changes to the typical implant design should be considered, based on the endplate maps discussed in section 3.2. The locations of the strongest endplate regions were not affected by bone density, disc degeneration or endplate removal, thus implants designed using the features of the basic structural property maps should perform well in patients with a wide range of bone and disc conditions.

All three of the basic endplate maps were laterally symmetric (i.e. the left and right halves of the maps were the same), meaning that implants can be made symmetric about the sagittal plane, however, symmetry about the transverse plane may not be ideal, since the superior and inferior map shapes differ.

### 4.6.1 Current Implant Features

The synthetic implants currently used for interbody fusion are generally symmetric, designed to be placed at or near the centre of the endplate, and may or may not require endplate removal prior to insertion. The same design is used at all spinal levels, with the implant size selected to fit the space.

### 4.6.2 Recommendations for Implants Inserted Between Two Lumbar Vertebrae

Implants used between two lumbar vertebrae should ideally engage the peripheral endplate as much as possible, particularly the strong posterior and posterolateral regions. Implants symmetric about the transverse plane may work well in this part of the spine since the strongest regions of the superior and inferior endplates are located in similar areas. The centre of the endplate should be avoided, since this is the weakest area, and is a good area for bone growth.

Implants should be designed to spare the endplate, since the bone strength decreased significantly when the endplate was removed.

### 4.6.3 Recommendations for Implants Inserted Between a Lumbar Vertebra and the Sacrum

Implants which rest against the sacral endplate may require an entirely different shape than those used between two lumbar vertebrae, due to the large differences between the inferior lumbar and sacral structural property maps. Up until this point the majority of implants have been symmetric for ease of insertion, ease of production, etc. Asymmetric designs may be required at this level to provide optimum resistance to subsidence.

The posterior region of the sacral endplate provides the best support, with the anterior margin being significantly weaker. This makes implant design more complex, since clearly the posterior region cannot be supported without some corresponding anterior support, particularly at this level where the strong incline of the sacral endplate would tend to put a large anterior bending moment on the level. A horseshoe- or asymmetric, O-shaped implant (wider at the front than at the back, i.e. a wedged disc with an off-centre hole, closer to the back than the front) might serve the purpose by providing posterior and anterior support to the sacrum while engaging the strongest regions of the inferior endplate, however a

more radically asymmetric implant may perform better (i.e. with extensive asymmetry about the transverse plane).

### 4.6.4 Surgical Considerations

Based on the mechanical results of this study the endplate should be spared whenever possible to provide optimal initial implant support and implants should be selected to engage the posterior margin of the endplate and as much of the periphery as possible (based on the available implants and the manufacturer's instructions). Note, however, that *in vitro* studies have not shown that retaining the endplate provides significant additional strength (section 4.5).

Clearly this is not a clinical study, thus the recommendations given here should not supercede any clinical considerations or the recommended use of an implant.

### 4.6.5 Summary

There are evidently more considerations than the strictly mechanical concern of avoiding subsidence following this type of surgical procedure, including the proximity of the spinal cord and large blood vessels to the vertebral body. There is no argument that the overall safety of the surgical procedure must take precedence over any proposed implant design changes, however if the more peripheral regions of the endplate could be safely engaged, the incidence of subsidence could potentially be markedly decreased. Researchers working on future implant designs should at least consider the potential advantage of engaging the posterior and peripheral portions of the endplate.

## 4.7 Study Limitations

The specimens used in this study were all taken from the lower lumbar spine (L3-S1), thus the results are not necessarily applicable to other spinal levels. It would be unwise to extrapolate these results to other spinal levels without doing additional tests to ensure that the structural properties and their distributions are actually the same.

All of the specimens used in this study were from older donors (mean age 74.6) thus the possibility should be considered that the findings may be at least partially age-related. Oda et al. (1998) looked at age-related changes in the trabecular structure of 25 L2 vertebra and found that there were significant increases in trabecular spacing in the anterosuperior, midanterior, anteroinferior, and central ninths of the midsagittal section of the vertebral body, though only the anterosuperior changes had a significant correlation with age. The weaker regions in the lumbar endplate maps seem to match the age-related changes described by Oda et al. quite well.

Gender was not addressed as a variable due to the limitations imposed by the number of specimens available and the amount of time allotted to the study. It is possible that there may be gender-related differences which were not considered in this study.

The DEXA values used in this study are not necessarily directly comparable with clinical values, since only the vertebral bodies were used for the calculation; they merely represent a range from high to low density.

The small number of sacral specimens (7) limited the power of the statistics, thus existing differences may not have been detected. This is also true for the additional variables considered in this

study (bone density and disc degeneration) which reduced the number of specimens being considered by dividing each set of specimens into smaller groups.

The smaller study looking at the effects of endplate removal showed that removing the endplate decreased both the strength and stiffness of the bone, but there were insufficient specimens to look at the superior and inferior lumbar endplates separately, and the sacral endplate was not addressed. The small number of specimens also made it impossible to detect changes in the map shape based on endplate removal (i.e. whether removing the endplate has more effect in some parts of the vertebral surface than in others). In addition, studies conducted by other authors using implants in cadaveric specimens have shown that endplate removal does not have a significant effect on implant subsidence. It may be that the implant-bone interface is too complex to make direct comparisons between the local property tests conducted in this study and the overall surgical construct.

The indentation tests done in this study provide information on the structural, rather than material, properties of the vertebra at each test site. This is because the indenter is deforming the endplate and underlying trabeculae (shell and supporting struts) rather than a uniform piece of bone. The resulting load-displacement curve represents the combined structural responses of the endplate and trabecular components. The values should not be used to represent material properties, for example in a finite element study of the vertebra.

# Chapter 5

# Conclusions and Recommendations

## 5.1 Conclusions

Based upon the results given in chapter 3 the following conclusions can be drawn:

1. There are significant regional variations in the structural properties of the lower lumbosacral endplates (L3-S1).

2. The inferior lumbar endplates are stronger and stiffer than the superior lumbar endplates. Most of this difference is in the posterior half of the endplates. Their structural property maps also differ, again in the posterior region of the endplate.

3. The L3-L5 vertebrae do not have significantly different overall structural properties, or structural property distributions, therefore they can be treated as equivalent in terms of implant design.

4. The sacral endplates are stronger, but not stiffer, than the superior lumbar endplates. Their structural property profiles are very different.

5. The inferior lumbar and sacral endplates did not have significantly different mean structural properties, but their property maps were very different.

6. The failure load and stiffness of the endplates decrease as bone density drops.

7. Bone density (grouped by range) had a significant effect of the strength of the superior and inferior lumbar endplates, but not on the sacral endplates. Only the superior endplate failure load map was affected by bone density.

8. Stiffness was not affected by bone density when grouped by density range (High, Mid, Low).

9. Disc degeneration had a significant effect on the inferior lumbar endplate's strength, but did not affect the superior lumbar or sacral strength. Only the superior endplate failure load map was affected by disc degeneration.

10. Stiffness was not affected by disc degeneration.

11. Both the mean failure load and the mean stiffness decreased when the endplate was removed. These decreases were uniform across the surface (i.e. the map shapes were unaffected).

## 5.2 Recommendations

The fact that significant regional variation exists in all of the endplates studied suggests that it may be possible to design an implant that would resist subsidence better than existing implants do. The current footprint of the majority of implants lies at or near the centre of the vertebral body, where the bone was found to be weakest. Implant designers should consider the possible advantages of making major design changes to take advantage of the stronger bone in the posterior and peripheral regions of the bone.

The lack of significant changes in the positions of the strongest bone regions with either bone density or disc degeneration suggest that implants designed using the general structural property maps should perform well in a wide range of bone densities and disc conditions.

The large differences between the inferior lumbar and sacral endplate maps indicate that an asymmetric design may be required for optimal performance at the L5-S1 space. The superior and inferior map shapes were not quite as different as far as the positions of their strongest regions, thus a symmetric design could be acceptable at the L3-L4 and L4-L5 spaces.

## 5.3 Future Research

In order to answer some of the questions raised by the results of this study or clarify the findings, several areas of research could be pursued.

1. It would be illuminating to test more sacral specimens to see if statistical significance can be achieved for the comparisons done in this study or whether there truly is no difference, e.g. superior lumbar vs. sacral endplate comparisons.

2. None of the specimens tested in this study were known to have osteoporotic architecture. It would be interesting to test specimens with osteoporotic architecture paired with specimens of similar bone density but "normal" architecture to see if there is a difference in the property distributions. It could be that few changes with bone density were detected in the spines tested in this study because the decreased bone density was a result of the natural ageing process, leading to a relatively uniform decline in bone strength. Osteoporotic changes may be more region-specific.

3. *In vitro* studies comparing different implant designs have found that there was no significant difference in their resistance to subsidence. It would be interesting to see if the results obtained in this study can be extrapolated to the "whole body" situation, i.e. test to see if implants designed to engage the stronger regions of the bone actually perform better than those which are more centrally seated. It may be that the bone-implant interface is too complex to make that simple extrapolation.

4. The effects of endplate removal should be addressed in more detail. Additional tests looking at the effects of endplate removal and including more variables such as those used in this study (superior vs. inferior endplate, lumbar vs. sacral vertebra, bone density, disc degeneration) would be very valuable.

5. The findings of this study and the findings of *in vitro* studies using implants differ regarding the effects of removing the endplate. This study found a significant strength and stiffness decrease with endplate removal, but *in vitro* studies have found that removing the endplate did not have a significant effect on the load required to cause implant subsidence. It would be interesting to study whether this is a result of trying to make an extrapolation from the local properties to the more complex situation of a bone-implant interface by looking at the effects of the actual bone-implant contact area and load distribution with and without the endplate (e.g. using pressure-sensitive film). Use of a larger sample size might also prove to be valuable, since there may be additional variables affecting the results.

6. To establish whether bone density is the main source of the differences between male and female specimens, a study similar to this conducted using matched male and female specimens (age, disc degeneration) would be interesting.

7. Tests should be done in cervical and thoracic vertebrae to determine how closely the property maps in these spinal regions match the lumbar maps. Tests looking at the L1 and L2 vertebrae should also be done to see if they differ from the lower lumbar specimens tested in this study.

## Bibliography


Adams MA, Dolan P, Hutton WC: The stages of disc degeneration as revealed by discograms. Journal of Bone and Joint Surgery **68B**: 36-41, 1986.

Aitken GK, Bourne RB, Finlay JP, Rorabeck CH, Andreae PR: Indentation stiffness of the cancellous bone in the distal human tibia. Clinical Orthopaedics **201**: 264-270, 1985.

Alici E, Alku OZ, Dost S: Prosthesis designed for vertebral body replacement. Journal of Biomechanics **23 (8)**: 799-809, 1990.

Amling M, Herden S, Pösl M, Hahn M, Ritzel H, Delling G. Heterogeneity of the skeleton: comparison of the trabecular microarchitecture of the spine, the iliac crest, the femur, and the calcaneus. Journal of Bone and Mineral Research **11 (1)**: 36-45, 1996.

Amstutz HC, Sissons HA: The structure of the vertebral spongiosa. Journal of Bone Joint Surgery, British Edition **51(3)**: 540-50, 1969.

An HS: Effect of endplate conditions and bone mineral density on the compressive strength of the graft-endplate interface in the cervical spine. Paper #82, 27th Annual Meeting of the Cervical Spine Research Society, Seattle, Washington, December 16-18, 1999: pp. 192-195.

An YH, Draughn RA. *Mechanical Testing of Bone and the Bone-Implant Interface.* CRC Press, London, 2000.

Andersson G, Ortengren R, Nachemson A, Elfstrom G: Lumbar disc pressure and myoelectric back muscle activity during sitting. Scandinavian Journal of Rehabilitation Medicine **6**: 104-144, 1974.

Andersson G, Schultz A: Effects of fluid injection on mechanical properties of the intervertebral discs. Journal of Biomechanics **12**: 453-458, 1979.

Anglin C, Tolhurst P, Wyss UP, Pichora DR: Glenoid cancellous bone strength and modulus. Journal of Biomechanics **32 (10)**: 1091-1097, 1999.

Atkinson PJ. Variation in trabecular structure of vertebrae with age. Calcified Tissue Research **1**: 24-32, 1967.

Beadle OA: The intervertebral disc. Observations on their normal and morbid anatomy in relation to certain spinal deformities. Medical Research Council Special Report Service (London), No. 161, 1931.

Behrens JC, Walker PS, Shoji H: Variations in strength and structure of cancellous bone at the knee. Journal of Biomechanics **7 (3)**: 201-207, 1974.

Bell GH, Cohn SH, Ostuni JA, Cane R, Ellis K: Variations in strength of vertebrae with age and their relation to osteoporosis. Calcified Tissue Research **1**, 75-86, 1967.

Bergot C, Laval-Jeantet A-M, Pretêux F, Meunier A. Measurement if anisotropic trabecular bone loss during aging by quantitative image analysis. Calcified Tissue International **43**: 143-149, 1988.

Bernick S, Cailliet R: Vertebral end-plate changes with aging of human vertebrae. Spine **7(2)**: 97-102, 1982.

Berry JL, Moran JM, Berg WS, Steffee AD: A morphometric study of human lumbar and selected thoracic vertebrae. Spine **12**: 362-367, 1987.

Biggemann M, Hilweg D, Brinckmann P: Prediction of the compressive strength of vertebral bodies of the lumbar spine by quantitative computed tomography. Skeletal Radiology **17**: 264-269, 1988.

Brandner ME: Normal values of the vertebral body and intervertebral disc index during growth. American Journal of Roentgenology **110**: 618-627, 1970.

Brantigan JW, Steffee AD: A carbon fibre implant to aid interbody fusion. Two-year clinical results in the first 26 patients. Spine **26**: 277-282, 1991.

Brinckmann P, Frobin W, Hierholzer E, Horst M: Deformation of the vertebral end-plate under axial loading of the spine. Spine **8 (8)**: 851-856, 1983.

Brinckmann P, Horst M: The influence of vertebral body fracture, intradiscal injection, and partial discectomy on the radial bulge and height of human lumbar discs. Spine **10 (2)**: 138-145, 1985.

Brown T, Hanson R, Yorra A: Some mechanical tests on the lumbo-sacral spine with particular reference to the intervertebral discs. Journal of Bone and Joint Surgery [American] **39A**: 1135, 1957.

Carter DR, Hayes WC: The compressive behaviour of bone as a two-phase porous structure. Journal of Bone and Joint Surgery (American) **59A (7)**: 954-962, 1977.

Cassucio C. An introduction to the study of osteoporosis. Proc. Roy. Society of Medicine. **55**: 663-668, 1962.

Closkey RF, Parsons JR, Lee KC, Blacksin MF, Zimmermann MC: Mechanics of interbody spinal fusion. Analysis of critical bone graft area. Spine **18**: 1011-1015, 1993.

Cotterill PC, Kostuik JP, D'Angelo G, Fernie GR, Maki BE: An anatomical comparison of the human and bovine thoracolumbar spine. Journal of Orthopaedic Research **4**: 298-303, 1986.

Frei H, Oxland TR, Rathonyi GC, Nolte L-P. The effect of mild degeneration on lumbar spine mechanics in compression and shear loading. Submitted for publication, 1998.

Frish LH, Jensen NC, Odgaard A, Pedersen CM, Sojbjerg JO, Dalstra M: Bone strength and material properties of the glenoid. Journal of Shoulder and Elbow Surgery **6 (2)**: 97-104, 1997.

Gibson LJ, Ashby MF. Cellular Solids: Structure and Properties. Pergamon Press, Oxford, 1988.

Gilad I, Nissan M: A study of vertebra and disc geometric relations of the human cervical and lumbar spine. Spine **11**: 154-157, 1986.

Gill K: Introduction to interbody fusion. In: Lumbar interbody fusion. Lin MP, Gill K, Rockville, Aspen, Maryland, 1989, pp. 3-7.

Gitman L, Kamholtz T: Incidence of radiographic osteoporosis in a large series of aged individuals. Journal of Gerontology **20**: 32-33. 1960.

Goulet RW, Goldstein SA, Ciarelli MJ, Kuhn JL, Brown MB, Feldkamp LA: The relationship between the structural and orthogonal compressive properties of trabecular bone. Journal of Biomechanics **27 (4)**: 375-389, 1994.

Gray H. In: Gray's Anatomy, 36th Edition, Williams PL, Warwich R, Churchill Livingstone, London, 1980, pp. 756-757.

Hammerburg KW: Anterior lumbar interbody fusion. Chapter 39. In: Lumbosacral and Spinopelvic Fixation, Margulies JY, et al., Lippincott-Raven, Philadelphia, 1996, pp. 495-505.

Hansson TH, Keller TS, Panjabi MM: A study of the compressive properties of lumbar vertebral trabeculae: effects of tissue characteristics. Spine **11**: 56-62, 1986.

Hansson T, Roos B: The relation between bone mineral content, experimental compression fractures, and disc degeneration in lumbar vertebrae. Spine **6**: 147-153, 1981.

Hansson T, Roos B, Nachemson A: The bone mineral content and ultimate compressive strength of lumbar vertebrae. Spine **5 (1)**: 46-55, 1980.

Hansson T, Roos B: The effects of age, height, and weight on the bone mineral content of lumbar vertebrae. Spine **5 (6)**: 545 - 551, 1980.

Hardinge MG: Determination of the strength of the cancellous bone in the head and neck of the femur. Surgical Gynecology and Obstetrics **89**: 439, 1949.

Harms J, Beele B, Böhm H, Jeszensky DJ, Stoltze D. Lumbosacral fusion with Harms instrumentation. Chapter 41: *Lumbosacral and Spinopelvic Fixation.* Edited by Margulies JY, et al. Lippincott-Raven Publishers, Philadelphia, 1996. pp. 529-538: p. 537.

Hashimoto T, Kaneda K, Abumi K: Relationship between traumatic spinal canal stenosis and neurologic deficits in thoracolumbar burst fractures. Spine **13 (11)**: 1268-1272, 1988.

Hayes WC, Snyder B. Toward a quantitative formulation on Wolff's law in trabecular bone. Mechanical Properties of Bone. (ed. Cowin SC) AMD Vol. **45**: 43-65. ASME, New York, 1981.

Hollowell JP, Vollmer DG, Wilson CR, Pintar FA, Yoganandan N: Biomechanical analysis of thoracolumbar interbody constructs. How important is the endplate? Spine **21 (9)**: 1032-36, 1996.

Holte DC, O'Brien JP, Renton P: Anterior lumbar fusion using a hybrid interbody graft. A preliminary radiographic report. European Spine Journal **3**: 32-38, 1994.

Hoshijima K, Nigtingale RW, Yu Jr, Richardson WJ, Harper KD, Yamamoto H, Myers BS: Strength and stability of posterior lumbar interbody fusion. Comparison of titanium fiber mesh implant and tricortical bone graft. Spine **22 (11)**: 1181-1188, 1997.

Hvid I, Christensen P, Soondergaard J, Christensen PB, Larsen CG: Compressive strength of tibial cancellous bone. Instron and osteopenetrometer measurements in an autopsy material. Acta Orthop Scand **54 (6)**: 819-25, 1983.

Jayasinghe JAP, Jones SJ, Boyde A: Three-dimensional photographic study of cancellous bone in human fourth lumbar vertebral bodies. Anatomy and Embryology **189**: 259-274, 1994.

Jost B, Cripton PA, Lund T, Oxland TR, Lippuner K, Jaeger P, Nolte LP: Compressive strength of interbody cages in the lumbar spine: the effect of cage shape, posterior instrumentation and bone density. European Spine Journal **7 (2)**: 132-141, 1998.

Khosla H, Lufkin EG, Hodgson SF, Fitzpatrick LA, Melton III, LJ. Epidemiology and clinical features of osteoporosis in young individuals. Bone **15 (5)**: 551-555, 1994.

Koch JC. The laws of bone architecture. American Journal of Anatomy **21**: 177-298, 1971.

Krag MH, Weaver DL, Beynnon BD, Haugh LD: Morphometry of the thoracic and lumbar spine related to transpedicular screw placement for surgical spinal fixation. Spine **13**: 27-32, 1988.

Krag MH, Beynnon BD, Pope MH, Frymoyer JW, Haugh LD, Weaver DL. An internal fixator for posterior application to short segments of the thoracic, lumbar, or lumbosacral spine: Design and testing. Clinical Orthopaedics and Related Research **203**: 75-98, 1986.

Kumar A, Memphis TN, Doherty BJ, Houston TX: Biomechanical testing of vertebral endplate strength: A cadaver study (Paper 87). 8th Annual Meeting NASS, San Diego, California, October 14-16, 1993: 89.

Lang SM, Moyle DD, Berg EW, Detoria N, Gilpin AT, Pappas NJ, Reynolds JC, Tkacik M: Correlation of mechanical properties of vertebral trabecular bone with equivalent mineral density as measured by computed tomography. Journal of Bone and Joint Surgery [American] **70A (10)**: 1531-1538, 1988.

Magerl F, Aebi M, Gertzbein SD, Harms J, Nazarian S: A comprehensive classification of thoracic and lumbar injuries. European Spine Journal **3**: 184-201, 1994.

Martin B: Aging and strength of bone as a structural material. Calcified Tissue International **53 (Suppl 1)**: S34-S40, 1993.

McBroom RJ, Hayes WC, Edwards WT, Goldberg RP, White III AA. Prediction of vertebral body compressive fracture using quantitative computed tomography. Journal of Bone and Joint Surgery **67A (8)**: 1206-1214, 1985.

McKoy BE, Kang Q, An YH. Indentation testing of bone. *Mechanical Testing of Bone and the Bone-Implant Interface.* (ed. An YH, Draughn RA) CRC Press, London, 2000. Chapter 14: 233-239.

Miller JAA, Schmatz C, Schultz AB: Lumbar disc degeneration: correlation with age, sex, and spine level in 600 autopsy specimens. Spine **13 (2)**: 173-178, 1988.

Mosekilde L and Mosekilde L: Normal vertebral body size and compressive strength: relations to age and to vertebral and iliac trabecular bone compressive strength. Bone **7**: 207-212, 1986.

Mosekilde L, Mosekilde L: Sex differences in age-related changes in vertebral size, density, and biomechanical competence in normal individuals. Bone **11**: 67-73, 1990.

Mosekilde L: Vertebral structure and strength *in vivo* and *in vitro*. Calcified Tissue International **53 (Suppl 1)**: S121-S126, 1993.

Mow VC, Hayes WC. Basic Orthopaedic Biomechanics 2nd edition. Lippincott-Raven, Philadelphia, 1997.

Nachemson A: Lumbar intradiscal pressure: Experimental studies on post-mortem material. Acta Orthopaedics Scandinavica Supplementum: **43**: 21-105, 1960.

Nachemson AL: The influence of spinal movement on the lumbar intradiscal pressure and on the tensile stresses in the annulus fibrosus. Acta Orthopaedica Scandinavica **33**: 183, 1963.

Nachemson A, Morris J: In vivo measurements of intra-discal pressure. Journal of Bone and Joint Surgery **46**: 1077, 1964.

Nachemson AL: In vivo discometry in lumbar discs with irregular radiograms. Acta Orthopaedica Scandinavica **36**: 418, 1965.

Nachemson A, Elfstrom G: Intravital dynamic pressure measurements in lumbar discs. Scandinavian Journal of Rehabilitation Medicine Suppl: 1-40, 1970.

Nachemson AL: A critical look at the treatment for low back pain. The research status of spinal manipulative therapy. DHEW Publication No. (NIH) 76-998: 21B, Bethesda, MD, 1975.

Nachemson AL: The lumbar spine, an orthopaedic challenge. Spine **1**: 59, 1976.

Nakabayashi Y, Wevers HW, Cooke TD, Griffin M: Bone strength and histomorphometry of the distal femur. Journal of Arthroplasty **9 (3)**: 307-315, 1994.

National Osteoporosis Foundation: National Institutes of Health – Osteoporosis and Related Bone Diseases ~ National Resource Centre. Fast facts on Osteoporosis. http://www.osteo.org /osteofastfact.html, April 2000.

Naylor A, Happey F, MacRae T: Changes in the human intervertebral dic with age: a biophysical study. Journal of the American Geriatric Society **3**: 964, 1955.
Nottestad SY, Baumel JJ, Kimmel DB,Recker RR, Heaney RP: The proportion of trabecular bone in human vertebrae. Journal of Bone and Mineral Research **2 (3)**: 221-229, 1987.

Oda K, Shibayama Y, Abe M, Onomura T: Morphogenesis of vertebral deformities in involutional osteoporosis: Age-related, three-dimensional trabecular structure. Spine **23 (9)**: 1050-1056, 1998.

Oxland TR. *Burst fractures of the human thoracolumbar spine: a biomechanical investigation.* Yale University, PhD dissertation, 1992.

Oxland TR, Kuslich SD, Kohrs DW, Bagby GW. The BAK interbody fusion system: Biomechanical rationale and early clinical results. Chapter 43: *Lumbosacral and Spinopelvic Fixation.* Edited by Margulies JY, et al. Lippincott-Raven Publishers, Philadelphia, 1996. pp. 545-561.

Oxland TR, Lund T. Biomechanics of stand-alone cages and cages in combination with posterior fixation: a literature review. European Spine Journal **9 Suppl 1**:S95-101, 2000.

Panjabi M, Brown M, Lindahl S, Irsttam L, Hermens M: Intrinsic disc pressure as a measure of integrity of the lumbar spine. Spine **13 (8)**: 913-917, 1988.

Panjabi MM, Goel V, Oxland T, Takata K, Duranceau J, Krag M, Price M: Human lumbar vertebrae: quantitative three-dimensional anatomy. Spine **17 (3)**: 299-306, 1991.

Pearcy MJ, Evans JH, O'Brien JP: The load bearing capacity of vertebral cancellous bone in interbody fusion of the lumbar spine. Engineering in Medicine **12 (4)**: 183-185, 1983.

Peretz AM, Hipp JA, Heggeness MH. The internal bony architecture of the sacrum. Spine **23 (9)**: 971-974, 1998.

Perey O. Fracture of the vertebral end-plate in the lumbar spine: An experimental biomechanical investigation. Acta Orthopaedica Scandinavica Supplementum **XXV**: 1-101, 1957.

Perey O. Resistance and compression of the lumbar vertebral endplate. Encyclopedia of Medical Radiology. Springer-Verlag, New York, 1974.

Quinnell R, Stockdale H: The use of in vivo lumbar discography to assess the clinical significance of the position of the intercrestal line. Spine **8 (3)**: 305-307, 1983.

Reuber M, Schultz A, Denis F, Spencer D: Bulging of lumbar intervertebral disks. Journal of Biomechanical Engineering **104 (3)**: 187-192, 1982.

Roberts S, McCall IW, Menage J, Haddaway MJ, Eisenstein SM: Does the thickness of the vertebral subchondral bone reflect the composition of the intervertebral disc? European Spine Journal **6 (6)**: 385-389, 1997.

Rockoff SD, Sweet E, Bleustein J. The relative contribution of trabecular and cortical bone to the strength of human lumbar vertebrae. Calcified Tissue Research **3 (2)**: 163-175, 1969.

Rolander SD, Blair WE: Deformation and fracture of the lumbar vertebral end-plate. Orthop. Clinics of North America **6**: 75-81, 1975.

Sato K, Kikuchi S, Yonezawa T: *In vivo* intradiscal pressure measurement in healthy individuals and in patients with ongoing back problems. Spine **24 (23)**: 2468-2474, 1999.

Schmorl G, Junghanns H: Development, growth, anatomy and function of the spine. In: The human spine in health and disease II. Basemann EF. Grune & Stratton, New York, 1971, pp. 6-9.

Scoles PV, Linton AE, Latimer B, Levy ME, Diovanni BF: Vertebral body and posterior element morphology: The normal spine in middle life. Spine **13**: 1082-1086, 1988.

Shigley JE, Mischke CR. Mechanical Engineering Design: 5th Edition. McGraw-Hill, New York, 1989, p. 122.

Shirazi-Adl SA, Shrivastava SC, Ahmed AM: Stress analysis of the lumbar disc-body unit in compression. A three-dimensional nonlinear finite element study. Spine **9 (2)**: 120-134, 1984

Silva MJ, Wang C, Keaveny TM, Hayes WC. Direct and computed tomography thickness measurements of the human, lumbar vertebral shell and endplate. Bone **15 (4)**: 409-414, 1994.

Steffen T, Tsantrizos A, Aebi M: Effect of implant design and endplate preparation on the compressive strength of interbody fusion constructs. Spine **25 (9)**: 1077-84, 2000.

Taylor JR, Twomey LT: Sexual dimorphism in human vertebral body shape. Journal of Anatomy **138**: 281-286, 1984.

Tortura GJ, Anagnostakos NP. Principles of Anatomy and Physiology, 4th edition. Harper & Row, Publishers, New York, 1984.

Twomey L, Taylor J, Furniss B: Age changes in the bone density and structure of the lumbar vertebral column. Journal of Anatomy **136 (1)**: 15-25, 1983.

Twomey LT, Taylor JR: Age changes in lumbar vertebrae and intervertebral discs. Clinical Orthopaedics and Related Research **224**: 97-104, 1987.

Vesterby A, Mosekilde L, Gunderson JHG, Melsen F, Mosekilde L, Holme K, Sϕrensen S: Biologically meaningful determinants of the in vitro strength of the lumbar vertebrae. Bone **12**: 219-224, 1991.

Weaver JK: Bone: its strength and changes with aging and an evaluation of some methods for measuring its mineral content. Journal of Bone and Joint Surgery **41A**: 935, 1966.

Weaver JK: The microscopic hardness of bone. Journal of Bone Joint Surgery [American] **48 (2)**: 273-288, 1966.

Wenger KH, Wilke H-J, Pross A, Haid C, Claes LE: Vertebral osseous endplate mechanical properties. A comparison of normals, degeneratives, and osteoporotics. International Society for the Study of the Lumbar Spine: Abstract 189. Brussels: June 9-13, 1998.

Wenger KH, Pross A, Wilke HJ, Gossee F, Vahldiek M, Claes LE: Bone mineral density of the vertebral endplate: an in vitro comparison of normals, degeneratives, and osteoporotics. International Society for the Study of the Lumbar Spine: Abstract 21. Hawaii: June 21-25, 1999.

White III AA, Panjabi MM. *Clinical Biomechanics of the Spine, 2nd edition.* J.B. Lippincott Company, Philadelphia, 1990.

Wilke HJ, Neef P, Caimi M, Hoogland T, Claes LE: New *in vivo* measurements of pressures in the intervertebral disc in daily life. Spine **24 (8)**: 755-762, 1999.

Willén JAG, Gaekwad UH, Kakulas BA. Acute burst fractures: A comparative analysis of a modern fracture classification and pathologic findings. Clinical Orthopaedics and Related Research **276**: 169-175, 1992.

Wolff J. *Das Gesetz der Transformation der Knochen.* Hirschwald, Berlin, 1892.

Zindrick MR, Wiltse LL, Doornik A, Widell EH, Knight GW, Patwardhan AG, Thomas JC, Rothman SL, Fields BT. Analysis of morphometric characteristics of the thoracic and lumbar pedicles. Spine **12 (2)**: 160-66, 1987.

# Appendices

# Appendix A

## Specimen Details

**Table A.1 Specimen Details:** Specimens with half of the endplate removed are shaded.

Specimen #: The laboratory inventory number assigned to the donor from whom the specimen was taken.
DD: Disc degeneration based on Nachemson's macroscopic grading scale (1 through 4) (section 2.3.4). A lower grade indicates a healthier disc.
DEXA: Dual energy x-ray absorptiometry, a measurement of bone mineral density in g/cm$^2$ (section 2.3.2). A higher DEXA value indicates stronger bone. DEXA is low in osteoporotic individuals.
# Tests Done: Total # tests done in the endplate Conversion Factor: used to convert load cell voltage to Newtons (based on amp. gain)
# Tests Used: # tests used in the statistical analysis after bad tests were rejected (max. 27 for whole, 22 for half-endplate specimens)
AP: anterior-posterior endplate dimension; LAT: lateral-lateral endplate dimension
Testing Order: order in which the endplates were tested. Numeric for whole endplate specimens, alphabetical for half-endplate specimens
NA: not applicable (i.e. rejected or not testable due to excessive degeneration); s = superior endplate, i = inferior endplate

| Specimen # | Spinal Level | Endplate | DEXA (g/cm^2) | DD (grade) | # Tests Done | # Tests Used | AP (mm) | LAT (mm) | Conversion Factor (N/V) | Testing Order |
|---|---|---|---|---|---|---|---|---|---|---|
| 1004 | L3 | s | 0.480 | 2 | 28 | 26 | 35.3 | 52.8 | 31.516 | 4 |
| | | i | 0.523 | 2 | 27 | 21 | 36.2 | 55.2 | 31.516 | 6 |
| | L4 | s | 0.574 | 2 | 28 | 27 | 34.2 | 54.6 | 31.516 | 9 |
| | | i | 0.543 | 3 | 26 | 25 | 35.0 | 57.3 | 31.516 | 7 |
| | L5 | s | 0.750 | 3 | 26 | 25 | 36.8 | 54.9 | 31.516 | 10 |
| | | i | 0.576 | 4 | 27 | 26 | 35.9 | 54.2 | 31.516 | 8 |
| | S1 | s | 0.867 | 4 | 27 | 27 | 34.7 | 53.5 | 33.385 | 37 |
| 1007 | L3 | s | 0.462 | 4 | 26 | 26 | 38.4 | 53.0 | 33.385 | 25 |
| | | i | 0.627 | 4 | 27 | 27 | 40.2 | 56.4 | 40.519 | 23 |
| | L4 | s | 0.706 | 4 | 27 | 27 | 36.5 | 54.6 | 33.385 | 26 |
| | | i | 0.618 | 4 | 27 | 27 | 38.8 | 56.1 | 33.385 | 29 |
| | L5 | s | 0.648 | 4 | 25 | 25 | 37.9 | 51.0 | 33.385 | 27 |
| | | i | 0.705 | 4 | 27 | 27 | 36.9 | 58.4 | 33.385 | 28 |
| | S1 | s | 0.568 | 4 | 26 | 26 | 36.0 | 57.0 | 33.385 | 38 |
| 1008 | L3 | s | 0.990 | 1 | 27 | 26 | 36.2 | 52.4 | 60.779 | 22 |
| | | i | 1.082 | 2 | 26 | 26 | 36.2 | 52.4 | 60.779 | 24 |
| | L4 | s | 1.035 | 2 | 27 | 27 | 37 | 54.5 | 60.779 | 21 |
| | | i | 1.114 | 3 | 27 | 26 | 35 | 52 | 40.519 | 19 |
| | L5 | s | 1.391 | 3 | 27 | 27 | 37.6 | 54.0 | 60.779 | 20 |
| | | i | 1.191 | 2 | 27 | 27 | 35.7 | 50.6 | 40.519 | 18 |
| | S1 | s | 2.009 | 2 | 24 | NA | 33.0 | 50.3 | 74.388 | 39 /d |
| 1010 | L3 | s | 0.462 | 3 | 27 | 27 | 32 | 47.8 | 33.385 | 32 |
| | | i | 0.571 | 4 | 27 | 22 | 32 | 50.5 | 33.385 | 30 |
| | L4 | s | 0.515 | 4 | 27 | 26 | 32.2 | 49.3 | 33.385 | 33 |
| | | i | 0.622 | 4 | 26 | 24 | 33.7 | 51.4 | 33.385 | 31 |
| | L5 | s | 0.682 | 4 | 26 | 26 | 33.8 | 51.9 | 33.385 | 34 |
| | | i | 0.667 | 3 | 23 | 23 | 35.1 | 52.8 | 33.385 | 36 |
| | S1 | s | 1.032 | 3 | 27 | 26 | 32.6 | 52.6 | 33.385 | 35 |
| 1012 | L3 | s | 0.453 | 3 | 29 | NA | 33.8 | 55.0 | | 0 |
| | | i | 0.542 | 2 | | NA | | | | NA |
| | L4 | s | 0.674 | 2 | 27 | 27 | 33.8 | 52.5 | 25.128 | 1 |
| | | i | 0.671 | 2 | 25 | 23 | 34.1 | 55.3 | 31.516 | 2 |
| | L5 | s | 0.765 | 2 | 27 | 21 | 34.9 | 50.9 | 31.516 | 3 |
| | | i | 0.725 | 3 | 25 | 19 | 34.3 | 57.2 | 31.516 | 5 |
| | S1 | s | 0.634 | 3 | | | | | | NA |

**Table A.1: Specimen Details** continued

| Specimen # | Spinal Level | Endplate | DEXA (g/cm^2) | DD (grade) | # Tests Done | # Tests Used | AP (mm) | LAT (mm) | Conversion Factor (N/V) | Testing Order |
|---|---|---|---|---|---|---|---|---|---|---|
| 1014 | L3 | s | 0.757 | 2 | 27 | 26 | 34.6 | 50.7 | 31.516 | 11 |
| | | i | 0.827 | 2 | 27 | 25 | 32.1 | 52.4 | 31.516 | 12 |
| | L4 | s | 0.832 | 2 | 27 | 27 | 33.4 | 49.2 | 33.385 | 14 |
| | | i | 0.752 | 2 | 25 | 25 | 32.3 | 48.8 | 33.385 | 16 |
| | L5 | s | 0.865 | 2 | 27 | 25 | 32.9 | 49.3 | 33.385 | 13 |
| | | i | 0.592 | 2 | 23 | 23 | 32.9 | 46.1 | 33.385 | 15 |
| | S1 | s | 0.517 | 2 | 23 | 23 | 32.3 | 42.7 | 40.519 | 17 |
| 1017 | L3 | s | 0.406 | 2 | 28 | 26 | 39.8 | 51.0 | 33.385 | 42 |
| | | i | 0.57 | 4 | 27 | 26 | 39 | 57.4 | 33.385 | 40 |
| | L4 | s | 0.603 | 4 | 29 | 24 | 37.6 | 53.8 | 33.385 | 47 |
| | | i | 0.593 | 4 | 27 | 27 | 34.2 | 56.3 | 33.385 | 45 |
| | L5 | s | 0.801 | 4 | 25 | 23 | 38 | 61.2 | 33.385 | 49 |
| | | i | 0.777 | 4 | 26 | 26 | 36.3 | 61.5 | 33.385 | 52 |
| | S1 | s | 1.214 | 4 | 27 | 27 | 36.9 | 58.2 | 33.385 | 43 |
| 1018 | L3 | s | 0.860 | 4 | 23 | 22 | 32.1 | 43.9 | 74.388 | f |
| | | i | 0.797 | 2 | 23 | 22 | 31.2 | 45.2 | 74.388 | h |
| | L4 | s | 0.809 | 2 | 23 | 22 | 31.9 | 44.6 | 74.388 | g |
| | | i | 0.946 | 4 | 23 | 22 | 30.4 | 48.2 | 74.388 | e |
| | L5 | s | 1.07 | 4 | 27 | 27 | 30.5 | 48.4 | 60.779 | 41 |
| | | i | 1.032 | 4 | 27 | 26 | 30.9 | 49.6 | 60.779 | 44 |
| | S1 | s | 1.631 | 4 | 23 | NA | 31.7 | 50.3 | 74.388 | i |
| 1019 | L3 | s | 0.535 | 3 | 28 | 27 | 32.8 | 49.9 | 33.385 | 57 |
| | | i | 0.667 | 4 | 27 | 26 | 33.3 | 54.5 | 60.779 | 59 |
| | L4 | s | 0.564 | 4 | 27 | 20 | 30.2 | 51.9 | 33.385 | 62 |
| | | i | 0.688 | 4 | 27 | 23 | 33.6 | 56.9 | 60.779 | 60 |
| | L5 | s | 0.608 | 4 | 27 | NA | 34.6 | 53.9 | 33.385 | 54 |
| | | i | 0.641 | 3 | 23 | 22 | 33.9 | 52.9 | 33.385 | 55 |
| | S1 | s | 0.588 | 3 | 27 | 27 | 31.2 | 42.3 | 33.385 | 61 |
| 1021 | L3 | s | 0.592 | 4 | 27 | 26 | 33.3 | 52.9 | 33.385 | 48 |
| | | i | 0.682 | 4 | 27 | 25 | 33.5 | 54.4 | 33.385 | 46 |
| | L4 | s | 0.611 | 4 | 26 | 25 | 33 | 54.7 | 33.385 | 50 |
| | | i | 0.764 | 4 | 27 | 27 | 32.7 | 56.4 | 33.385 | 51 |
| | L5 | s | 0.743 | 4 | 27 | 26 | 35.3 | 61.0 | 60.779 | 58 |
| | | i | 0.742 | 4 | 25 | 26 | 34 | 54.1 | 60.779 | 56 |
| | S1 | s | 0.9 | 4 | 26 | 26 | 33.1 | 54.8 | 40.519 | 53 |
| 1023 | L3 | s | 0.272 | 2 | 28 | 27 | 31.8 | 43.0 | 33.385 | 63 |
| | | i | 0.29 | 3 | 23 | 20 | 31.7 | 47.6 | 24.482 | a |
| | L4 | s | 0.331 | 3 | 23 | 22 | 32.1 | 44.2 | 24.482 | b |
| | | i | 0.254 | 2 | 25 | 25 | 33.7 | 46.9 | 24.482 | 64 |
| | L5 | s | 0.395 | 2 | 23 | 22 | 30.4 | 44.0 | 24.482 | c |
| | | i | 0.254 | 4 | | | | | | NA |
| | S1 | s | 0.299 | 4 | | | | | | NA |

**Table A.2: X-ray Comments.** This table gives a summary of the observations used to select the eleven spines included in this study based on their radiographic appearance.

| Specimen | Condition | Comments |
|---|---|---|
| 1004 | healthy | no evidence of osteophytes or crush fractures; good disc height; well defined margins to each vertebral body |
| 1007 | disc degeneration | osteophytes; some variation in disc height; no crush fractures |
| 1008 | healthy | no evidence of osteophytes or crush fractures; good disc height; well defined margins to each vertebral body |
| 1010 | osteoporosis | crush fracture in L1; even disc height, no evidence of osteophytes |
| 1012 | osteoporosis | several crush fractures; no evidence of osteophytes |
| 1014 | healthy | no osteophytes, good disc height, no fractures |
| 1017 | osteoporosis and disc degeneration | crush fracture and small osteophytes; thin discs |
| 1018 | disc degeneration | osteophytes and variation in disc height |
| 1019 | disc degeneration | small osteophytes and variation in disc height |
| 1021 | osteoporosis and disc degeneration | crush fractures, large osteophytes and variation in disc height |
| 1023 | osteoporosis and disc degeneration | crush fracture and variation in disc height |

**Table A.3: Pooled Disc Grade.** These grades are the pooled results of the three graders (Tables A.4 -A.6: grade assigned by the majority gave the pooled value). This grading sheet matches the one used by the three disc graders.

| Disc Grade Scoring Sheet | |
|---|---|
| Graded by: All (Pooled Results) | Date: 99.12.02 |
| Scoring System Used: Nachemson | |
| Description of Scoring System: classifies disc degeneration into four grades (see below) | |

| Spec. | Lvl. | E.P. | Score |
|---|---|---|---|
| 1004 | L3 | s | 2 |
| 1004 | L3 | i | 2 |
| 1004 | L4 | s | 2 |
| 1004 | L4 | i | 3 |
| 1004 | L5 | s | 3 |
| 1004 | L5 | i | 4 |
| 1004 | S1 | s | 4 |

| Spec. | Lvl. | E.P. | Score |
|---|---|---|---|
| 1014 | L3 | s | 2 |
| 1014 | L3 | i | 2 |
| 1014 | L4 | s | 2 |
| 1014 | L4 | i | 2 |
| 1014 | L5 | s | 2 |
| 1014 | L5 | i | 2 |
| 1014 | S1 | s | 2 |

| Spec. | Lvl. | E.P. | Score |
|---|---|---|---|
| 1023 | L3 | s | 2 |
| 1023 | L3 | i | 3 |
| 1023 | L4 | s | 3 |
| 1023 | L4 | i | 2 |
| 1023 | L5 | s | 2 |
| 1023 | L5 | i | 4 |
| 1023 | S1 | s | 4 |

| Spec. | Lvl. | E.P. | Score |
|---|---|---|---|
| 1007 | L3 | s | 4 |
| 1007 | L3 | i | 4 |
| 1007 | L4 | s | 4 |
| 1007 | L4 | i | 4 |
| 1007 | L5 | s | 4 |
| 1007 | L5 | i | 4 |
| 1007 | S1 | s | 4 |

| Spec. | Lvl. | E.P. | Score |
|---|---|---|---|
| 1017 | [redacted] | | 2 |
| 1017 | L3 | i | 4 |
| 1017 | L4 | s | 4 |
| 1017 | L4 | i | 4 |
| 1017 | L5 | s | 4 |
| 1017 | L5 | i | 4 |
| 1017 | S1 | s | 4 |

**LEGEND**

Spec.= Specimen
Lvl. = Spinal Level
E.P.= Endplate
Score = Nachemson Grade

| Spec. | Lvl. | E.P. | Score |
|---|---|---|---|
| 1008 | L3 | s | 1 |
| 1008 | L3 | i | 2 |
| 1008 | L4 | s | 2 |
| 1008 | L4 | i | 3 |
| 1008 | L5 | s | 3 |
| 1008 | L5 | i | 2 |
| 1008 | S1 | s | 2 |

| Spec. | Lvl. | E.P. | Score |
|---|---|---|---|
| 1018 | L3 | s | 4 |
| 1018 | L3 | i | 2 |
| 1018 | L4 | s | 2 |
| 1018 | L4 | i | 4 |
| 1018 | L5 | s | 4 |
| 1018 | L5 | i | 4 |
| 1018 | S1 | s | 4 |

**Grade 1:**

- shiny, gelatinous nucleus pulposus
- nucleus easily delimited from annulus
- annulus free of macroscopic ruptures or discolouration

| Spec. | Lvl. | E.P. | Score |
|---|---|---|---|
| 1010 | L3 | s | 3 |
| 1010 | L3 | i | 4 |
| 1010 | L4 | s | 4 |
| 1010 | L4 | i | 4 |
| 1010 | L5 | s | 4 |
| 1010 | L5 | i | 3 |
| 1010 | S1 | s | 3 |

| Spec. | Lvl. | E.P. | Score |
|---|---|---|---|
| 1019 | L3 | s | 3 |
| 1019 | L3 | i | 4 |
| 1019 | L4 | s | 4 |
| 1019 | L4 | i | 4 |
| 1019 | L5 | s | 4 |
| 1019 | L5 | i | 3 |
| 1019 | S1 | s | 3 |

**Grade 2:**

- macroscopic changes present only in nucleus
- nucleus somewhat more fibrous
- nucleus still distinct from annulus
- annulus fibrosus intact

| Spec. | Lvl. | E.P. | Score |
|---|---|---|---|
| 1012 | L3 | s | 3 |
| 1012 | L3 | i | 2 |
| 1012 | L4 | s | 2 |
| 1012 | L4 | i | 2 |
| 1012 | L5 | s | 2 |
| 1012 | L5 | i | 3 |
| 1012 | S1 | s | 3 |

| Spec. | Lvl. | E.P. | Score |
|---|---|---|---|
| 1021 | L3 | s | 4 |
| 1021 | L3 | i | 4 |
| 1021 | L4 | s | 4 |
| 1021 | L4 | i | 4 |
| 1021 | L5 | s | 4 |
| 1021 | L5 | i | 4 |
| 1021 | S1 | s | 4 |

**Grade 3:**

- macroscopic changes in nucleus & annulus
- nucleus more fibrotic but still soft
- boundary btwn nucleus & annulus not distinct
- isolated fissures in annulus fibrosus

**Grade 4:**

- severe macroscopic changes in nucleus & annulus
- fissures and cavities in nucleus & annulus
- marginal osteophytes often found on vertebrae

**Table A.4:** Disc grade assigned using Nachemson's grading scale (section 2.4.3; Table A.3).

| | | | Disc Grade | | | |
|---|---|---|---|---|---|---|
| Spec. | Lvl. | E.P. | Pool | M.D. | T.O. | P.G. |
| 1004 | L3 | s | 2 | 2 | 3 | 2 |
| 1004 | L3 | i | 2 | 2 | 3 | 2 |
| 1004 | L4 | s | 2 | 2 | 3 | 2 |
| 1004 | L4 | i | 3 | 3 | 3 | 3 |
| 1004 | L5 | s | 3 | 3 | 3 | 3 |
| 1004 | L5 | i | 4 | 4 | 4 | 4 |
| 1004 | S1 | s | 4 | 4 | 4 | 4 |
| 1007 | L3 | s | 4 | 4 | 4 | 4 |
| 1007 | L3 | i | 4 | 4 | 4 | 4 |
| 1007 | L4 | s | 4 | 4 | 4 | 4 |
| 1007 | L4 | i | 4 | 4 | 4 | 4 |
| 1007 | L5 | s | 4 | 4 | 4 | 4 |
| 1007 | L5 | i | 4 | 4 | 4 | 4 |
| 1007 | S1 | s | 4 | 4 | 4 | 4 |
| 1008 | L3 | s | 1 | 1 | 1 | 1 |
| 1008 | L3 | i | 2 | 2 | 2 | 1 |
| 1008 | L4 | s | 2 | 2 | 2 | 1 |
| 1008 | L4 | i | 3 | 3 | 2 | 3 |
| 1008 | L5 | s | 3 | 3 | 2 | 3 |
| 1008 | L5 | i | 2 | 2 | 2 | 2 |
| 1008 | S1 | s | 2 | 2 | 2 | 2 |
| 1010 | L3 | s | 3 | 3 | 3 | 3 |
| 1010 | L3 | i | 4 | 4 | 4 | 4 |
| 1010 | L4 | s | 4 | 4 | 4 | 4 |
| 1010 | L4 | i | 4 | 4 | 4 | 3 |
| 1010 | L5 | s | 4 | 4 | 4 | 3 |
| 1010 | L5 | i | 3 | 3 | 3 | 3 |
| 1010 | S1 | s | 3 | 3 | 3 | 3 |
| 1012 | L3 | s | 3 | 3 | 2 | 3 |
| 1012 | L3 | i | 2 | 2 | 2 | 2 |
| 1012 | L4 | s | 2 | 2 | 2 | 2 |
| 1012 | L4 | i | 2 | 2 | 2 | 2 |
| 1012 | L5 | s | 2 | 2 | 2 | 2 |
| 1012 | L5 | i | 3 | 3 | 3 | 3 |
| 1012 | S1 | s | 3 | 3 | 3 | 3 |
| 1014 | L3 | s | 2 | 2 | 2 | 2 |
| 1014 | L3 | i | 2 | 2 | 2 | 2 |
| 1014 | L4 | s | 2 | 2 | 2 | 2 |
| 1014 | L4 | i | 2 | 3 | 2 | 2 |
| 1014 | L5 | s | 2 | 3 | 2 | 2 |
| 1014 | L5 | i | 2 | 3 | 2 | 2 |
| 1014 | S1 | s | 2 | 3 | 2 | 2 |

| | | | Disc Grade | | | |
|---|---|---|---|---|---|---|
| Spec. | Lvl. | E.P. | Pool | M.D. | T.O. | P.G. |
| 1017 | L3 | s | 2 | 2 | 3 | 2 |
| 1017 | L3 | i | 4 | 4 | 4 | 4 |
| 1017 | L4 | s | 4 | 4 | 4 | 4 |
| 1017 | L4 | i | 4 | 4 | 4 | 4 |
| 1017 | L5 | s | 4 | 4 | 4 | 4 |
| 1017 | L5 | i | 4 | 4 | 4 | 4 |
| 1017 | S1 | s | 4 | 4 | 4 | 4 |
| 1018 | L3 | s | 4 | 4 | 4 | 4 |
| 1018 | L3 | i | 2 | 2 | 2 | 2 |
| 1018 | L4 | s | 2 | 2 | 2 | 2 |
| 1018 | L4 | i | 4 | 3 | 4 | 4 |
| 1018 | L5 | s | 4 | 3 | 4 | 4 |
| 1018 | L5 | i | 4 | 4 | 4 | 3 |
| 1018 | S1 | s | 4 | 4 | 4 | 3 |
| 1019 | L3 | s | 3 | 4 | 3 | 3 |
| 1019 | L3 | i | 4 | 4 | 4 | 4 |
| 1019 | L4 | s | 4 | 4 | 4 | 4 |
| 1019 | L4 | i | 4 | 4 | 4 | 4 |
| 1019 | L5 | s | 4 | 4 | 4 | 4 |
| 1019 | L5 | i | 3 | 3 | 3 | 4 |
| 1019 | S1 | s | 3 | 3 | 3 | 4 |
| 1021 | L3 | s | 4 | 4 | 4 | 4 |
| 1021 | L3 | i | 4 | 4 | 4 | 4 |
| 1021 | L4 | s | 4 | 4 | 4 | 4 |
| 1021 | L4 | i | 4 | 4 | 4 | 4 |
| 1021 | L5 | s | 4 | 4 | 4 | 4 |
| 1021 | L5 | i | 4 | 4 | 4 | 4 |
| 1021 | S1 | s | 4 | 4 | 4 | 4 |
| 1023 | L3 | s | 2 | 2 | 2 | 2 |
| 1023 | L3 | i | 3 | 3 | 3 | 3 |
| 1023 | L4 | s | 3 | 3 | 3 | 3 |
| 1023 | L4 | i | 2 | 3 | 2 | 2 |
| 1023 | L5 | s | 2 | 3 | 2 | 2 |
| 1023 | L5 | i | 4 | 4 | 4 | 4 |
| 1023 | S1 | s | 4 | 4 | 4 | 4 |

Pool: pooled result used for the study:
the grade assigned by the majority of graders

M.D.: grade assigned by Dr. Marcel Dvorak

T.O.: grade assigned by Dr. Tom Oxland

P.G.: grade assigned by J. Pamela Grant

**Table A.5: Endplate Maps.** These maps show the results of the indentation tests (local structural property values) in each endplate which remained after bad test values were removed (i.e. tests which had to be rejected due to problems encountered during the test, such as indenter slippage). Tests which were not included in the statistics because they lay outside of the region included in the statistical analysis are shaded. The values are shown in terms of their AP and LAT positions on the endplate. The failure load map is given first (in Newtons), followed by stiffness map and the correlation coefficient map. (The correlation coefficients indicate how well the lines used to calculate the stiffnesses fit the points on the load-displacement curve. A correlation coefficient of 1 indicates that all of the points lay on the line. A coefficient > 0.95 indicates excellent fit.)

To make the maps easy to compare, the superior endplates are all on the left, while the corresponding inferior endplates are on the right. If an endplate was not tested, or was included in the "endplate removal" study, then a space is left where that endplate would have been placed.

The figure below shows an endplate with the test sites labelled. The maps correspond to these test sites.

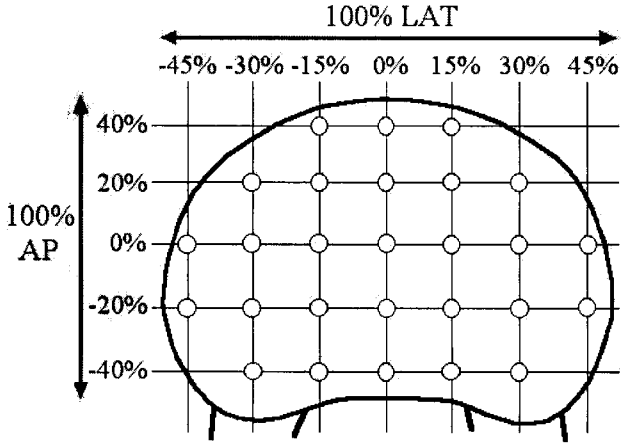


**Specimen 1004_L3_s**

Failure Load (N)

| AP \ LAT | -45% | -30% | -15% | 0% | 15% | 30% | 45% |
|---|---|---|---|---|---|---|---|
| 40% | | | 63.2 | 77.7 | 58.5 | 53.5 | |
| 20% | | 56.6 | 35.2 | 31.6 | 34.2 | 31.7 | |
| 0% | 89.3 | 37.4 | 25.9 | 43.4 | 50.0 | 27.0 | 63.0 |
| -20% | 168.7 | 55.2 | 36.8 | 66.5 | 39.6 | 63.7 | |
| -40% | | 123.2 | 68.9 | 68.7 | 63.3 | 150.4 | |

Stiffness (N/mm)

| AP \ LAT | -45% | -30% | -15% | 0% | 15% | 30% | 45% |
|---|---|---|---|---|---|---|---|
| 40% | | | 67.8 | 71.3 | 90.0 | 130.2 | |
| 20% | | 99.0 | 63.6 | 55.1 | 55.6 | 42.4 | |
| 0% | 74.9 | 68.9 | 32.6 | 59.2 | 41.9 | 42.2 | 64.6 |
| -20% | 171.7 | 104.7 | 66.5 | 107.2 | 69.1 | 173.7 | |
| -40% | | 86.1 | 91.7 | 85.1 | 42.7 | 125.9 | |

r-Squared

| AP \ LAT | -45% | -30% | -15% | 0% | 15% | 30% | 45% |
|---|---|---|---|---|---|---|---|
| 40% | | | 0.996 | 0.996 | 0.998 | 0.999 | |
| 20% | | 0.998 | 0.998 | 0.993 | 0.990 | 0.990 | |
| 0% | 0.997 | 0.988 | 0.975 | | 0.994 | 0.996 | 0.999 |
| -20% | 0.999 | 0.998 | 0.998 | 0.996 | 0.993 | 0.998 | |
| -40% | | 0.999 | 0.995 | 0.997 | 0.996 | 0.998 | |

**Specimen 1004_L3_i**

Failure Load (N)

| AP \ LAT | -45% | -30% | -15% | 0% | 15% | 30% | 45% |
|---|---|---|---|---|---|---|---|
| 40% | | | | 58.4 | | | |
| 20% | | 56.0 | 73.9 | 49.3 | 27.4 | 55.5 | |
| 0% | | 60.9 | 40.6 | 20.5 | | | 33.7 |
| -20% | 76.3 | 123.7 | 133.6 | 82.2 | 93.8 | 47.6 | 45.0 |
| -40% | | 159.6 | 78.4 | | 136.4 | 138.5 | 90.6 |

Stiffness (N/mm)

| AP \ LAT | -45% | -30% | -15% | 0% | 15% | 30% | 45% |
|---|---|---|---|---|---|---|---|
| 40% | | | | 93.8 | | | |
| 20% | | 71.9 | 136.1 | 96.0 | 75.0 | 73.1 | |
| 0% | | 119.8 | 111.4 | 53.7 | | | 67.3 |
| -20% | 108.1 | 157.8 | 233.0 | 199.2 | 243.0 | 80.8 | 94.8 |
| -40% | | 207.2 | 107.2 | | 144.4 | 156.6 | 120.8 |

r-Squared

| AP \ LAT | -45% | -30% | -15% | 0% | 15% | 30% | 45% |
|---|---|---|---|---|---|---|---|
| 40% | | | | 0.996 | | | |
| 20% | | 0.999 | 1.000 | 0.999 | 0.998 | 0.998 | |
| 0% | | 0.996 | 0.999 | 0.999 | | | 0.995 |
| -20% | 0.999 | 0.999 | 0.999 | 1.000 | 1.000 | 0.998 | 0.997 |
| -40% | | 0.999 | 0.996 | | 0.998 | 0.996 | 0.999 |

Table A.5: Endplate Maps continued

**Specimen 1004_L4_s**

Failure Load (N)

| | LAT | | | | | | |
|---|---|---|---|---|---|---|---|
| AP | -45% | -30% | -15% | 0% | 15% | 30% | 45% |
| 40% | | | 152.1 | 117.0 | 263.1 | | |
| 20% | | 129.0 | 32.2 | 23.4 | 45.6 | 217.2 | |
| 0% | 180.2 | 44.6 | 36.8 | 34.9 | 42.8 | 98.4 | 70.3 |
| -20% | 93.3 | 42.5 | 42.4 | 30.5 | 52.5 | 70.8 | 142.7 |
| -40% | | 87.0 | 71.9 | 66.1 | 64.7 | 164.3 | |

Stiffness (N/mm)

| | LAT | | | | | | |
|---|---|---|---|---|---|---|---|
| AP | -45% | -30% | -15% | 0% | 15% | 30% | 45% |
| 40% | | | 79.4 | 92.0 | 152.1 | | |
| 20% | | 175.3 | 73.9 | 71.7 | 153.2 | 106.7 | |
| 0% | 103.7 | 128.9 | 84.3 | 91.2 | 95.1 | 149.6 | 59.0 |
| -20% | 117.2 | 88.0 | 137.9 | 51.3 | 148.0 | 150.4 | 114.4 |
| -40% | | 150.7 | 119.1 | 77.6 | 54.5 | 170.0 | |

r-Squared

| | LAT | | | | | | |
|---|---|---|---|---|---|---|---|
| AP | -45% | -30% | -15% | 0% | 15% | 30% | 45% |
| 40% | | | 0.999 | 0.999 | 0.999 | | |
| 20% | | 0.999 | 0.997 | 0.996 | 0.999 | 0.998 | |
| 0% | 0.998 | 0.998 | 0.994 | 0.997 | 0.998 | 0.998 | 0.998 |
| -20% | 0.999 | 0.998 | 0.991 | 0.991 | 0.999 | 0.999 | 0.999 |
| -40% | | 0.999 | 1.000 | 0.997 | 0.998 | 0.999 | |

**Specimen 1004_L4_i**

Failure Load (N)

| | LAT | | | | | | |
|---|---|---|---|---|---|---|---|
| AP | -45% | -30% | -15% | 0% | 15% | 30% | 45% |
| 40% | | | 94.8 | 86.4 | 148.7 | | |
| 20% | | 84.7 | 35.2 | 28.9 | 53.7 | 80.2 | |
| 0% | | 63.0 | 63.1 | 26.3 | 39.8 | 88.6 | 108.4 |
| -20% | | 263.9 | 97.6 | 30.2 | 101.0 | 271.6 | 114.7 |
| -40% | | 269.1 | 168.1 | 160.0 | 188.4 | 279.1 | |

Stiffness (N/mm)

| | LAT | | | | | | |
|---|---|---|---|---|---|---|---|
| AP | -45% | -30% | -15% | 0% | 15% | 30% | 45% |
| 40% | | | 125.5 | 166.1 | 197.6 | | |
| 20% | | 131.0 | 62.7 | 85.8 | 140.6 | 182.2 | |
| 0% | | 144.4 | 149.6 | 44.0 | 154.5 | 117.7 | 104.4 |
| -20% | | 227.0 | 207.5 | 75.1 | 232.3 | 261.4 | 74.7 |
| -40% | | 314.9 | 191.4 | 131.5 | 205.4 | 257.0 | |

r-Squared

| | LAT | | | | | | |
|---|---|---|---|---|---|---|---|
| AP | -45% | -30% | -15% | 0% | 15% | 30% | 45% |
| 40% | | | 0.999 | 1.000 | 1.000 | | |
| 20% | | 1.000 | 0.998 | 0.995 | 1.000 | 0.999 | |
| 0% | | 0.998 | 0.998 | 0.992 | 0.998 | 0.999 | 0.999 |
| -20% | | 1.000 | 0.999 | 0.994 | 0.999 | 1.000 | 0.999 |
| -40% | | 1.000 | 0.999 | 0.998 | 0.998 | 0.999 | |

**Specimen 1004_L5_s**

Failure Load (N)

| | LAT | | | | | | |
|---|---|---|---|---|---|---|---|
| AP | -45% | -30% | -15% | 0% | 15% | 30% | 45% |
| 40% | | | 106.2 | 80.9 | | | |
| 20% | | 112.8 | 62.4 | 52.4 | 66.4 | 118.7 | |
| 0% | 102.8 | 32.2 | 28.7 | 34.8 | 34.7 | 35.1 | |
| -20% | 87.2 | 47.4 | 58.5 | 51.0 | 56.7 | 47.6 | 74.5 |
| -40% | | 106.6 | 80.5 | 57.9 | 96.8 | 150.9 | |

Stiffness (N/mm)

| | LAT | | | | | | |
|---|---|---|---|---|---|---|---|
| AP | -45% | -30% | -15% | 0% | 15% | 30% | 45% |
| 40% | | | 135.9 | 89.8 | | | |
| 20% | | 196.5 | 68.3 | 98.2 | 98.9 | 116.2 | |
| 0% | 98.7 | 73.2 | 42.6 | 101.3 | 65.0 | 96.0 | |
| -20% | 96.3 | 113.5 | 107.0 | 122.6 | 99.2 | 117.8 | 80.6 |
| -40% | | 192.8 | 73.6 | 90.5 | 104.1 | 194.4 | |

r-Squared

| | LAT | | | | | | |
|---|---|---|---|---|---|---|---|
| AP | -45% | -30% | -15% | 0% | 15% | 30% | 45% |
| 40% | | | 0.999 | 0.998 | | | |
| 20% | | 0.999 | 0.998 | 0.996 | 0.999 | 1.000 | |
| 0% | 0.998 | 0.998 | 0.996 | 0.999 | 0.997 | 0.999 | |
| -20% | 0.998 | 1.000 | 0.999 | 0.999 | 0.999 | 0.999 | 0.999 |
| -40% | | 1.000 | 0.986 | 0.999 | 0.999 | 0.999 | |

**Specimen 1004_L5_i**

Failure Load (N)

| | LAT | | | | | | |
|---|---|---|---|---|---|---|---|
| AP | -45% | -30% | -15% | 0% | 15% | 30% | 45% |
| 40% | | | 112.0 | 108.4 | 112.3 | | |
| 20% | | 102.9 | 73.3 | 72.7 | 63.8 | 97.3 | |
| 0% | 96.0 | 93.0 | 77.4 | 59.2 | 41.2 | 209.8 | 209.7 |
| -20% | 175.0 | 220.7 | 139.2 | 88.0 | 129.6 | 198.5 | 132.6 |
| -40% | | 144.8 | 57.7 | 76.3 | 120.1 | | |

Stiffness (N/mm)

| | LAT | | | | | | |
|---|---|---|---|---|---|---|---|
| AP | -45% | -30% | -15% | 0% | 15% | 30% | 45% |
| 40% | | | 126.3 | 109.6 | 123.7 | | |
| 20% | | 140.6 | 72.5 | 113.8 | 108.6 | 116.3 | |
| 0% | 141.0 | 104.9 | 123.4 | 119.7 | 79.7 | 130.9 | 161.4 |
| -20% | 144.3 | 215.1 | 227.9 | 152.3 | 243.3 | 122.9 | 162.6 |
| -40% | | 238.8 | 142.5 | 94.6 | 108.1 | | |

r-Squared

| | LAT | | | | | | |
|---|---|---|---|---|---|---|---|
| AP | -45% | -30% | -15% | 0% | 15% | 30% | 45% |
| 40% | | | 0.998 | 0.997 | 0.999 | | |
| 20% | | 0.999 | 0.998 | 0.998 | 0.997 | 0.999 | |
| 0% | 0.999 | 0.997 | 0.999 | 0.998 | 0.998 | 0.999 | 0.999 |
| -20% | 0.998 | 0.999 | 0.999 | 0.999 | 0.999 | 0.996 | 1.000 |
| -40% | | 0.999 | 0.999 | 0.992 | 0.996 | | |

Table A.5: Endplate Maps continued

**Specimen 1004_S1_s**

Failure Load (N)

| | LAT | | | | | | |
|---|---|---|---|---|---|---|---|
| AP | -45% | -30% | -15% | 0% | 15% | 30% | 45% |
| 40% | | | 77.5 | 74.7 | 85.0 | | |
| 20% | | 71.8 | 34.9 | 31.0 | 39.7 | 70.1 | |
| 0% | 66.1 | 78.3 | 49.1 | 50.0 | 43.6 | 43.9 | 52.5 |
| -20% | 197.0 | 92.9 | 66.8 | 40.1 | 53.8 | 53.1 | 77.1 |
| -40% | | 85.6 | 95.7 | 106.9 | 58.6 | 82.6 | |

Stiffness (N/mm)

| | LAT | | | | | | |
|---|---|---|---|---|---|---|---|
| AP | -45% | -30% | -15% | 0% | 15% | 30% | 45% |
| 40% | | | 81.7 | 88.6 | 90.8 | | |
| 20% | | 121.2 | 74.1 | 57.1 | 105.4 | 87.1 | |
| 0% | 128.9 | 109.0 | 71.0 | 74.7 | 59.0 | 77.8 | 76.5 |
| -20% | 168.6 | 158.9 | 65.3 | 48.2 | 127.9 | 88.7 | 137.0 |
| -40% | | 200.7 | 203.9 | 213.2 | 140.6 | 142.4 | |

r-Squared

| | LAT | | | | | | |
|---|---|---|---|---|---|---|---|
| AP | -45% | -30% | -15% | 0% | 15% | 30% | 45% |
| 40% | | | 0.999 | 0.994 | 0.998 | | |
| 20% | | 0.996 | 0.990 | 0.991 | 0.996 | 0.999 | |
| 0% | 0.999 | 0.997 | 0.998 | 0.991 | 0.995 | 0.997 | 0.990 |
| -20% | 0.998 | 0.999 | 0.997 | 0.994 | 0.990 | 0.996 | 0.997 |
| -40% | | 0.996 | 0.997 | 0.999 | 0.996 | 0.995 | |

**Specimen 1007_L3_s**

Failure Load (N)

| | LAT | | | | | | |
|---|---|---|---|---|---|---|---|
| AP | -45% | -30% | -15% | 0% | 15% | 30% | 45% |
| 40% | | | 72.2 | 55.8 | 139.8 | | |
| 20% | | 59.0 | 45.8 | 30.4 | 31.0 | 67.6 | |
| 0% | 43.4 | 28.1 | 20.1 | 32.4 | 33.7 | 26.4 | 61.5 |
| -20% | 40.6 | 34.3 | 40.9 | 46.7 | | 34.8 | 33.3 |
| -40% | | 93.0 | 68.6 | 29.4 | 79.5 | 81.5 | |

Stiffness (N/mm)

| | LAT | | | | | | |
|---|---|---|---|---|---|---|---|
| AP | -45% | -30% | -15% | 0% | 15% | 30% | 45% |
| 40% | | | 188.7 | 62.9 | 190.8 | | |
| 20% | | 118.5 | 113.1 | 48.6 | 74.4 | 162.1 | |
| 0% | 47.5 | 36.5 | 39.9 | 71.0 | 37.3 | 24.7 | 98.4 |
| -20% | 74.8 | 56.2 | 51.7 | 59.4 | | 47.3 | 63.4 |
| -40% | | 195.8 | 41.0 | 37.3 | 51.5 | 147.2 | |

r-Squared

| | LAT | | | | | | |
|---|---|---|---|---|---|---|---|
| AP | -45% | -30% | -15% | 0% | 15% | 30% | 45% |
| 40% | | | 0.997 | 0.995 | 0.998 | | |
| 20% | | 0.988 | 0.993 | 0.985 | 0.966 | 0.998 | |
| 0% | 0.959 | 0.985 | 0.938 | 0.982 | 0.970 | 0.972 | 0.993 |
| -20% | 0.997 | 0.987 | 0.981 | 0.988 | | 0.990 | 0.993 |
| -40% | | 0.996 | 0.990 | 0.970 | 0.996 | 0.994 | |

**Specimen 1007_L3_i**

Failure Load (N)

| | LAT | | | | | | |
|---|---|---|---|---|---|---|---|
| AP | -45% | -30% | -15% | 0% | 15% | 30% | 45% |
| 40% | | | 151.5 | 201.2 | 193.7 | | |
| 20% | | 106.6 | 72.5 | 69.1 | 54.1 | 65.5 | |
| 0% | 64.6 | 47.0 | 67.3 | 33.8 | 27.8 | 69.2 | 73.1 |
| -20% | 36.6 | 132.2 | 100.8 | 38.5 | 60.2 | 103.8 | 102.5 |
| -40% | | 194.1 | 133.8 | 65.0 | 78.0 | 246.0 | |

Stiffness (N/mm)

| | LAT | | | | | | |
|---|---|---|---|---|---|---|---|
| AP | -45% | -30% | -15% | 0% | 15% | 30% | 45% |
| 40% | | | 254.1 | 285.2 | 249.9 | | |
| 20% | | 173.7 | 113.6 | 119.0 | 104.9 | 127.6 | |
| 0% | 181.9 | 74.5 | 93.7 | 113.2 | 56.1 | 149.4 | 104.9 |
| -20% | 76.7 | 220.9 | 121.1 | 106.3 | 83.6 | 107.6 | 136.4 |
| -40% | | 162.6 | 133.6 | 47.1 | 46.7 | 238.1 | |

r-Squared

| | LAT | | | | | | |
|---|---|---|---|---|---|---|---|
| AP | -45% | -30% | -15% | 0% | 15% | 30% | 45% |
| 40% | | | 0.999 | 0.998 | 0.999 | | |
| 20% | | 0.998 | 0.996 | 0.994 | 0.997 | 0.994 | |
| 0% | 0.995 | 0.993 | 0.994 | 0.991 | 0.967 | 0.987 | 0.995 |
| -20% | 0.984 | 0.999 | 0.998 | 0.986 | 0.995 | 0.993 | 0.999 |
| -40% | | 0.997 | 0.998 | 0.989 | 0.992 | 0.996 | |

Table A.5: Endplate Maps continued

**Specimen 1007_L4_s**

Failure Load (N)

| AP \ LAT | -45% | -30% | -15% | 0% | 15% | 30% | 45% |
|---|---|---|---|---|---|---|---|
| 40% | | | 225.7 | 184.6 | 55.0 | | |
| 20% | | 97.2 | 49.7 | 198.8 | 25.0 | 70.0 | |
| 0% | 53.5 | 74.3 | 48.1 | 68.6 | 27.0 | 19.9 | 66.3 |
| -20% | 246.4 | 52.8 | 78.4 | 60.5 | 85.7 | 42.9 | 30.7 |
| -40% | | 141.9 | 46.6 | 46.8 | 54.3 | 129.8 | |

Stiffness (N/mm)

| AP \ LAT | -45% | -30% | -15% | 0% | 15% | 30% | 45% |
|---|---|---|---|---|---|---|---|
| 40% | | | 99.4 | 188.3 | 62.9 | | |
| 20% | | 169.5 | 81.7 | 198.8 | 50.3 | 160.9 | |
| 0% | 86.9 | 64.5 | 100.1 | 115.5 | 69.1 | 43.2 | 100.5 |
| -20% | 118.2 | 159.1 | 66.3 | 47.1 | 115.0 | 71.2 | 32.2 |
| -40% | | 135.6 | 15.5 | 81.1 | 64.1 | 185.6 | |

r-Squared

| AP \ LAT | -45% | -30% | -15% | 0% | 15% | 30% | 45% |
|---|---|---|---|---|---|---|---|
| 40% | | | 0.995 | 0.997 | 0.984 | | |
| 20% | | 0.989 | 0.991 | 0.998 | 0.965 | 0.997 | |
| 0% | 0.978 | 0.990 | 0.991 | 0.990 | 0.969 | 0.977 | 0.994 |
| -20% | 0.999 | 0.992 | 0.995 | 0.986 | 0.997 | 0.993 | 0.978 |
| -40% | | 0.994 | 0.940 | 0.987 | 0.983 | 0.997 | |

**Specimen 1007_L4_i**

Failure Load (N)

| AP \ LAT | -45% | -30% | -15% | 0% | 15% | 30% | 45% |
|---|---|---|---|---|---|---|---|
| 40% | | | 77.2 | 64.0 | 54.5 | | |
| 20% | | 98.6 | 47.5 | 78.8 | 87.8 | 81.5 | |
| 0% | 73.8 | 74.0 | 56.3 | 83.3 | 91.8 | 81.2 | 72.3 |
| -20% | 138.3 | 234.4 | 127.4 | 48.7 | 53.0 | 110.3 | 94.0 |
| -40% | | 135.4 | 127.1 | 87.3 | 108.4 | 227.3 | |

Stiffness (N/mm)

| AP \ LAT | -45% | -30% | -15% | 0% | 15% | 30% | 45% |
|---|---|---|---|---|---|---|---|
| 40% | | | 150.7 | 132.9 | 147.5 | | |
| 20% | | 186.6 | 179.7 | 148.8 | 110.0 | 147.6 | |
| 0% | 159.6 | 137.4 | 79.6 | 170.3 | 161.9 | 154.7 | 176.5 |
| -20% | 139.4 | 209.0 | 240.5 | 96.1 | 108.3 | 120.4 | 173.5 |
| -40% | | 217.8 | 121.1 | 101.0 | 70.8 | 220.8 | |

r-Squared

| AP \ LAT | -45% | -30% | -15% | 0% | 15% | 30% | 45% |
|---|---|---|---|---|---|---|---|
| 40% | | | 0.998 | 0.997 | 0.991 | | |
| 20% | | 0.997 | 0.995 | 0.992 | 0.997 | 0.995 | |
| 0% | 0.999 | 0.997 | 0.995 | 0.998 | 0.997 | 0.994 | 0.995 |
| -20% | 0.996 | 0.998 | 0.999 | 0.985 | 0.995 | 0.996 | 0.990 |
| -40% | | 0.998 | 0.996 | 0.998 | 0.993 | 0.997 | |

**Specimen 1007_L5_s**

Failure Load (N)

| AP \ LAT | -45% | -30% | -15% | 0% | 15% | 30% | 45% |
|---|---|---|---|---|---|---|---|
| 40% | | | 36.6 | 22.2 | 40.8 | | |
| 20% | | 18.9 | 21.0 | 11.1 | 17.8 | 35.6 | |
| 0% | | 18.5 | 32.7 | 52.9 | 32.2 | 17.3 | |
| -20% | 32.3 | 86.8 | 49.6 | 32.7 | 29.5 | 85.0 | 90.0 |
| -40% | | 209.8 | 68.4 | 44.8 | 62.9 | 160.0 | |

Stiffness (N/mm)

| AP \ LAT | -45% | -30% | -15% | 0% | 15% | 30% | 45% |
|---|---|---|---|---|---|---|---|
| 40% | | | 34.2 | 38.0 | 109.3 | | |
| 20% | | 35.4 | 28.8 | 6.1 | 22.6 | 28.0 | |
| 0% | | 60.0 | 75.7 | 82.4 | 64.8 | 21.8 | |
| -20% | 61.3 | 163.9 | 57.9 | 57.8 | 56.4 | 149.0 | 104.6 |
| -40% | | 148.1 | 57.3 | 117.4 | 66.1 | 207.9 | |

r-Squared

| AP \ LAT | -45% | -30% | -15% | 0% | 15% | 30% | 45% |
|---|---|---|---|---|---|---|---|
| 40% | | | 0.979 | 0.919 | 0.995 | | |
| 20% | | 0.928 | 0.931 | 0.440 | 0.937 | 0.961 | |
| 0% | | 0.991 | 0.991 | 0.992 | 0.990 | 0.863 | |
| -20% | 0.980 | 0.993 | 0.986 | 0.987 | 0.991 | 0.995 | 0.989 |
| -40% | | 0.998 | 0.989 | 0.995 | 0.991 | 0.996 | |

**Specimen 1007_L5_i**

Failure Load (N)

| AP \ LAT | -45% | -30% | -15% | 0% | 15% | 30% | 45% |
|---|---|---|---|---|---|---|---|
| 40% | | | 50.4 | 92.7 | 57.6 | | |
| 20% | | 86.7 | 36.7 | 99.6 | 52.6 | 65.8 | |
| 0% | 62.5 | 110.0 | 42.6 | 97.3 | 53.6 | 49.9 | 127.2 |
| -20% | 114.3 | 87.4 | 91.7 | 33.3 | 76.6 | 44.7 | 119.6 |
| -40% | | 169.9 | 79.5 | 32.6 | 98.0 | 197.8 | |

Stiffness (N/mm)

| AP \ LAT | -45% | -30% | -15% | 0% | 15% | 30% | 45% |
|---|---|---|---|---|---|---|---|
| 40% | | | 109.4 | 144.4 | 30.7 | | |
| 20% | | 87.1 | 79.2 | 77.3 | 65.5 | 50.0 | |
| 0% | 196.2 | 82.8 | 50.5 | 159.8 | 79.3 | 79.9 | 140.3 |
| -20% | 121.9 | 104.8 | 88.9 | 54.2 | 59.1 | 104.1 | 125.9 |
| -40% | | 154.4 | 107.7 | 68.4 | 92.1 | 277.5 | |

r-Squared

| AP \ LAT | -45% | -30% | -15% | 0% | 15% | 30% | 45% |
|---|---|---|---|---|---|---|---|
| 40% | | | 0.991 | 0.995 | 0.973 | | |
| 20% | | 0.978 | 0.980 | 0.996 | 0.990 | 0.986 | |
| 0% | 0.995 | 0.996 | 0.986 | 0.998 | 0.993 | 0.996 | 0.995 |
| -20% | 0.993 | 0.997 | 0.995 | 0.980 | 0.989 | 0.995 | 0.998 |
| -40% | | 0.991 | 0.988 | 0.998 | 0.992 | 0.994 | |

Table A.5: Endplate Maps continued

**Specimen 1007_S1_s**

Failure Load (N)

| AP \ LAT | -45% | -30% | -15% | 0% | 15% | 30% | 45% |
|---|---|---|---|---|---|---|---|
| 40% | | | 28.0 | 32.1 | 46.0 | | |
| 20% | | 40.7 | 40.6 | 56.2 | 27.5 | 44.8 | |
| 0% | 58.8 | 29.6 | 92.0 | 72.1 | 47.8 | 28.3 | 29.5 |
| -20% | | 104.5 | 109.3 | 118.8 | 106.3 | 57.8 | 74.4 |
| -40% | | 289.3 | 145.4 | 154.0 | 100.0 | 221.6 | |

Stiffness (N/mm)

| AP \ LAT | -45% | -30% | -15% | 0% | 15% | 30% | 45% |
|---|---|---|---|---|---|---|---|
| 40% | | | 54.8 | 75.6 | 62.6 | | |
| 20% | | 84.8 | 69.1 | 107.8 | 15.6 | 74.1 | |
| 0% | 96.9 | 23.0 | 98.7 | 84.3 | 40.1 | 30.6 | 100.3 |
| -20% | | 64.5 | 63.0 | 137.7 | 109.1 | 96.5 | 108.2 |
| -40% | | 242.7 | 86.7 | 172.8 | 132.6 | 115.3 | |

r-Squared

| AP \ LAT | -45% | -30% | -15% | 0% | 15% | 30% | 45% |
|---|---|---|---|---|---|---|---|
| 40% | | | 0.994 | 0.996 | 0.993 | | |
| 20% | | 0.993 | 0.991 | 0.999 | 0.970 | 0.996 | |
| 0% | 0.999 | 0.990 | 0.999 | 0.996 | 0.993 | 0.963 | 0.994 |
| -20% | | 0.996 | 0.995 | 0.995 | 0.999 | 0.995 | 0.996 |
| -40% | | 1.000 | 0.997 | 1.000 | 0.997 | 0.995 | |

**Specimen 1008_L3_s**

Failure Load (N)

| AP \ LAT | -45% | -30% | -15% | 0% | 15% | 30% | 45% |
|---|---|---|---|---|---|---|---|
| 40% | | | 214.3 | 205.6 | 225.0 | | |
| 20% | | 203.0 | 141.7 | 148.5 | 142.4 | 202.6 | |
| 0% | | 143.5 | 127.1 | 226.6 | 113.1 | 109.9 | 100.1 |
| -20% | 285.8 | 161.4 | 172.9 | 229.8 | 149.8 | 96.0 | 205.0 |
| -40% | | 338.4 | 224.8 | 260.0 | 132.7 | 191.4 | 168.2 |

Stiffness (N/mm)

| AP \ LAT | -45% | -30% | -15% | 0% | 15% | 30% | 45% |
|---|---|---|---|---|---|---|---|
| 40% | | | 148.3 | 137.8 | 122.6 | | |
| 20% | | 121.6 | 136.9 | 122.0 | 77.0 | 142.3 | |
| 0% | | 136.7 | 139.6 | 144.1 | 75.8 | 105.8 | 98.2 |
| -20% | 159.7 | 131.2 | 139.4 | 128.5 | 129.3 | 104.9 | 148.1 |
| -40% | | 164.1 | 182.4 | 199.4 | 139.7 | 168.2 | 172.9 |

r-Squared

| AP \ LAT | -45% | -30% | -15% | 0% | 15% | 30% | 45% |
|---|---|---|---|---|---|---|---|
| 40% | | | 0.998 | 0.999 | 0.999 | | |
| 20% | | 0.992 | 0.998 | 0.996 | 0.987 | 0.998 | |
| 0% | | 0.995 | 0.997 | 0.996 | 0.995 | 0.991 | 0.994 |
| -20% | 0.999 | 0.998 | 0.998 | 0.998 | 0.998 | 0.996 | 0.995 |
| -40% | | 0.998 | 0.994 | 0.996 | 0.994 | 0.997 | 0.993 |

**Specimen 1008_L3_i**

Failure Load (N)

| AP \ LAT | -45% | -30% | -15% | 0% | 15% | 30% | 45% |
|---|---|---|---|---|---|---|---|
| 40% | | | 258.4 | 312.1 | 224.2 | | |
| 20% | | 247.4 | 166.4 | 233.5 | 188.8 | 240.3 | |
| 0% | 282.2 | 196.7 | 182.2 | 187.8 | 167.1 | 142.4 | |
| -20% | 232.1 | 208.6 | 236.1 | 169.4 | 205.3 | 185.8 | 273.7 |
| -40% | | 356.5 | 347.1 | 273.1 | 283.5 | 369.1 | |

Stiffness (N/mm)

| AP \ LAT | -45% | -30% | -15% | 0% | 15% | 30% | 45% |
|---|---|---|---|---|---|---|---|
| 40% | | | 92.1 | 239.3 | 118.0 | | |
| 20% | | 123.0 | 162.9 | 199.8 | 181.9 | 139.1 | |
| 0% | 154.6 | 129.9 | 191.3 | 159.4 | 115.8 | 147.6 | |
| -20% | 301.2 | 139.4 | 278.3 | 264.3 | 220.9 | 146.6 | 190.6 |
| -40% | | 290.3 | 293.7 | 191.6 | 205.7 | 370.8 | |

r-Squared

| AP \ LAT | -45% | -30% | -15% | 0% | 15% | 30% | 45% |
|---|---|---|---|---|---|---|---|
| 40% | | | 0.993 | 0.999 | 0.998 | | |
| 20% | | 0.997 | 0.998 | 0.997 | 0.999 | 0.999 | |
| 0% | 0.997 | 0.997 | 0.992 | 0.997 | 0.997 | 0.997 | |
| -20% | 0.997 | 0.997 | 0.997 | 0.992 | 0.997 | 0.994 | 0.998 |
| -40% | | 0.999 | 0.999 | 0.994 | 0.998 | 0.999 | |

Table A.5: Endplate Maps continued

**Specimen 1008_L4_s**

Failure Load (N)

| | LAT | | | | | | |
|---|---|---|---|---|---|---|---|
| AP | -45% | -30% | -15% | 0% | 15% | 30% | 45% |
| 40% | | | 249.2 | 242.5 | 240.0 | | |
| 20% | | 178.6 | 106.0 | 117.0 | 129.6 | 175.7 | |
| 0% | 166.4 | 110.2 | 72.4 | 122.3 | 117.6 | 136.0 | 191.3 |
| -20% | 157.3 | 164.9 | 122.8 | 156.1 | 147.4 | 141.8 | 168.9 |
| -40% | | 269.3 | 187.8 | 230.8 | 172.4 | 224.1 | |

Stiffness (N/mm)

| | LAT | | | | | | |
|---|---|---|---|---|---|---|---|
| AP | -45% | -30% | -15% | 0% | 15% | 30% | 45% |
| 40% | | | 139.0 | 163.6 | 130.7 | | |
| 20% | | 142.2 | 139.3 | 97.8 | 120.0 | 156.9 | |
| 0% | 125.9 | 155.4 | 79.7 | 100.7 | 115.3 | 129.4 | 139.1 |
| -20% | 147.2 | 183.2 | 165.7 | 160.2 | 137.2 | 105.7 | 160.3 |
| -40% | | 228.7 | 214.3 | 158.9 | 133.1 | 165.8 | |

r-Squared

| | LAT | | | | | | |
|---|---|---|---|---|---|---|---|
| AP | -45% | -30% | -15% | 0% | 15% | 30% | 45% |
| 40% | | | 0.999 | 0.998 | 0.985 | | |
| 20% | | 0.999 | 0.984 | 0.989 | 0.992 | 0.998 | |
| 0% | 0.996 | 0.989 | 0.979 | 0.993 | 0.993 | 0.997 | 0.997 |
| -20% | 0.997 | 0.992 | 0.998 | 0.998 | 0.997 | 0.996 | 0.997 |
| -40% | | 0.996 | 0.996 | 0.998 | 0.997 | 0.994 | |

**Specimen 1008_L4_i**

Failure Load (N)

| | LAT | | | | | | |
|---|---|---|---|---|---|---|---|
| AP | -45% | -30% | -15% | 0% | 15% | 30% | 45% |
| 40% | | | 204.4 | 300.3 | 214.0 | | |
| 20% | | 221.9 | 146.9 | 188.4 | 143.5 | 224.1 | |
| 0% | 288.2 | 139.6 | 173.9 | 134.6 | 137.9 | 218.1 | 225.0 |
| -20% | 300.1 | 350.6 | 281.3 | 230.4 | 294.0 | 260.6 | 272.6 |
| -40% | | 112.7 | 411.5 | 434.7 | | 332.2 | |

Stiffness (N/mm)

| | LAT | | | | | | |
|---|---|---|---|---|---|---|---|
| AP | -45% | -30% | -15% | 0% | 15% | 30% | 45% |
| 40% | | | 167.0 | 143.1 | 111.4 | | |
| 20% | | 113.9 | 87.9 | 175.7 | 150.1 | 147.4 | |
| 0% | 116.9 | 114.5 | 200.3 | 154.9 | 118.1 | 140.5 | 149.4 |
| -20% | 315.0 | 186.0 | 192.8 | 341.0 | 299.0 | 155.6 | 300.6 |
| -40% | | 364.9 | 302.3 | 289.9 | | 374.9 | |

r-Squared

| | LAT | | | | | | |
|---|---|---|---|---|---|---|---|
| AP | -45% | -30% | -15% | 0% | 15% | 30% | 45% |
| 40% | | | 0.993 | 0.998 | 0.996 | | |
| 20% | | 0.997 | 0.994 | 0.997 | 0.995 | 0.996 | |
| 0% | 0.998 | 0.986 | 0.996 | 0.999 | 0.994 | 0.993 | 0.999 |
| -20% | 0.999 | 1.000 | 0.997 | 0.999 | 0.999 | 0.997 | 0.996 |
| -40% | | 0.998 | 0.999 | 0.999 | | 0.999 | |

**Specimen 1008_L5_s**

Failure Load (N)

| | LAT | | | | | | |
|---|---|---|---|---|---|---|---|
| AP | -45% | -30% | -15% | 0% | 15% | 30% | 45% |
| 40% | | | 213.9 | 196.6 | 245.5 | | |
| 20% | | 165.1 | 130.3 | 130.0 | 110.5 | 251.7 | |
| 0% | 171.1 | 143.8 | 102.0 | 93.4 | 62.0 | 173.5 | 244.6 |
| -20% | 171.3 | 198.2 | 161.2 | 115.1 | 98.7 | 165.1 | 160.5 |
| -40% | | 345.0 | 303.1 | 327.7 | 264.3 | 329.0 | |

Stiffness (N/mm)

| | LAT | | | | | | |
|---|---|---|---|---|---|---|---|
| AP | -45% | -30% | -15% | 0% | 15% | 30% | 45% |
| 40% | | | 125.1 | 139.6 | 148.2 | | |
| 20% | | 138.6 | 80.1 | 122.1 | 95.8 | 118.7 | |
| 0% | 131.1 | 176.5 | 56.3 | 82.4 | 133.3 | 182.0 | 131.9 |
| -20% | 254.8 | 149.9 | 230.5 | 130.3 | 207.4 | 192.8 | 158.4 |
| -40% | | 190.2 | 181.2 | 243.9 | 257.1 | 118.4 | |

r-Squared

| | LAT | | | | | | |
|---|---|---|---|---|---|---|---|
| AP | -45% | -30% | -15% | 0% | 15% | 30% | 45% |
| 40% | | | 0.994 | 0.994 | 0.993 | | |
| 20% | | 0.995 | 0.995 | 0.995 | 0.996 | 0.996 | |
| 0% | 0.996 | 0.994 | 0.996 | 0.990 | 0.993 | 0.998 | 0.996 |
| -20% | 0.994 | 0.992 | 0.998 | 0.992 | 0.991 | 0.999 | 0.996 |
| -40% | | 0.996 | 0.998 | 0.998 | 0.998 | 0.995 | |

**Specimen 1008_L5_i**

Failure Load (N)

| | LAT | | | | | | |
|---|---|---|---|---|---|---|---|
| AP | -45% | -30% | -15% | 0% | 15% | 30% | 45% |
| 40% | | | 205.5 | 174.9 | 67.7 | | |
| 20% | | 173.6 | 116.1 | 159.5 | 178.7 | 193.3 | |
| 0% | 230.4 | 180.7 | 152.6 | 215.2 | 162.9 | 209.1 | 210.1 |
| -20% | 194.4 | 411.5 | 309.1 | 251.7 | 247.4 | 318.0 | 200.9 |
| -40% | | 248.5 | 287.8 | 176.1 | 231.8 | 236.1 | |

Stiffness (N/mm)

| | LAT | | | | | | |
|---|---|---|---|---|---|---|---|
| AP | -45% | -30% | -15% | 0% | 15% | 30% | 45% |
| 40% | | | 102.4 | 72.5 | 78.4 | | |
| 20% | | 102.3 | 108.0 | 94.9 | 129.5 | 163.0 | |
| 0% | 226.2 | 136.2 | 138.9 | 158.6 | 128.7 | 143.5 | 187.9 |
| -20% | 224.0 | 261.7 | 211.6 | 150.7 | 193.4 | 230.1 | 194.4 |
| -40% | | 180.7 | 154.8 | 182.3 | 185.8 | 206.7 | |

r-Squared

| | LAT | | | | | | |
|---|---|---|---|---|---|---|---|
| AP | -45% | -30% | -15% | 0% | 15% | 30% | 45% |
| 40% | | | 0.995 | 0.996 | 0.995 | | |
| 20% | | 0.994 | 0.997 | 0.999 | 0.997 | 0.999 | |
| 0% | 0.997 | 0.999 | 0.997 | 0.999 | 0.988 | 0.998 | 0.999 |
| -20% | 0.999 | 0.998 | 0.998 | 0.998 | 0.999 | 0.996 | 0.997 |
| -40% | | 0.998 | 0.999 | 0.998 | 0.997 | 0.998 | |

Table A.5: Endplate Maps continued

**Specimen 1010_L3_s**

Failure Load (N)

| | LAT | | | | | | |
|---|---|---|---|---|---|---|---|
| AP | -45% | -30% | -15% | 0% | 15% | 30% | 45% |
| 40% | | | 64.7 | 55.2 | 50.0 | | |
| 20% | | 50.8 | 26.7 | 26.8 | 34.0 | 34.3 | |
| 0% | 61.4 | 72.9 | 32.2 | 52.9 | 44.6 | 38.6 | 66.4 |
| -20% | 80.9 | 108.3 | 79.9 | 84.8 | 69.3 | 87.6 | 39.7 |
| -40% | | 155.8 | 120.7 | 74.4 | 55.0 | 98.0 | |

Stiffness (N/mm)

| | LAT | | | | | | |
|---|---|---|---|---|---|---|---|
| AP | -45% | -30% | -15% | 0% | 15% | 30% | 45% |
| 40% | | | 101.3 | 104.5 | 155.0 | | |
| 20% | | 124.8 | 119.4 | 97.6 | 133.6 | 111.5 | |
| 0% | 190.0 | 128.4 | 89.1 | 138.8 | 129.7 | 124.5 | 127.6 |
| -20% | 250.8 | 249.1 | 171.5 | 164.2 | 155.8 | 148.1 | 63.9 |
| -40% | | 273.8 | 110.4 | 201.0 | 98.2 | 145.9 | |

r-Squared

| | LAT | | | | | | |
|---|---|---|---|---|---|---|---|
| AP | -45% | -30% | -15% | 0% | 15% | 30% | 45% |
| 40% | | | 0.990 | 0.997 | 0.995 | | |
| 20% | | 0.996 | 0.997 | 0.995 | 0.993 | 0.993 | |
| 0% | 0.999 | 0.998 | 0.984 | 0.987 | 0.979 | 0.998 | 0.993 |
| -20% | 0.998 | 0.998 | 0.998 | 0.999 | 0.999 | 0.997 | 0.986 |
| -40% | | 0.998 | 0.998 | 0.999 | 0.989 | 0.997 | |

**Specimen 1010_L3_i**

Failure Load (N)

| | LAT | | | | | | |
|---|---|---|---|---|---|---|---|
| AP | -45% | -30% | -15% | 0% | 15% | 30% | 45% |
| 40% | | | | | 95.7 | | |
| 20% | | 90.8 | 82.8 | | 61.4 | 86.9 | |
| 0% | 107.8 | | 102.5 | 103.8 | 142.8 | 126.7 | 130.0 |
| -20% | | 183.2 | 140.9 | 129.5 | 159.3 | 208.1 | 133.6 |
| -40% | | 218.4 | 193.9 | 153.1 | 181.2 | 186.7 | |

Stiffness (N/mm)

| | LAT | | | | | | |
|---|---|---|---|---|---|---|---|
| AP | -45% | -30% | -15% | 0% | 15% | 30% | 45% |
| 40% | | | | | 128.1 | | |
| 20% | | 239.4 | 158.5 | | 107.7 | 188.9 | |
| 0% | 174.0 | | 184.9 | 223.2 | 254.3 | 240.8 | 182.1 |
| -20% | | 280.8 | 271.2 | 246.8 | 193.1 | 324.3 | 215.7 |
| -40% | | 339.1 | 249.3 | 84.1 | 293.5 | 262.8 | |

r-Squared

| | LAT | | | | | | |
|---|---|---|---|---|---|---|---|
| AP | -45% | -30% | -15% | 0% | 15% | 30% | 45% |
| 40% | | | | | 0.993 | | |
| 20% | | 0.998 | 0.998 | | 0.990 | 0.998 | |
| 0% | 0.999 | | 0.997 | 0.999 | 0.999 | 0.999 | 0.999 |
| -20% | | 0.999 | 1.000 | 0.999 | 0.999 | 1.000 | 0.999 |
| -40% | | 0.999 | 0.998 | 0.997 | 0.999 | 1.000 | |

**Specimen 1010_L4_s**

Failure Load (N)

| | LAT | | | | | | |
|---|---|---|---|---|---|---|---|
| AP | -45% | -30% | -15% | 0% | 15% | 30% | 45% |
| 40% | | | 62.3 | 50.9 | 64.2 | | |
| 20% | | 38.3 | 18.1 | 25.4 | 25.8 | 56.1 | |
| 0% | | 27.5 | 22.7 | 31.6 | 56.8 | 35.3 | 86.0 |
| -20% | 81.9 | 68.9 | 60.6 | 40.2 | 58.8 | 80.5 | 70.8 |
| -40% | | 118.0 | 55.4 | 98.4 | 60.0 | 130.5 | |

Stiffness (N/mm)

| | LAT | | | | | | |
|---|---|---|---|---|---|---|---|
| AP | -45% | -30% | -15% | 0% | 15% | 30% | 45% |
| 40% | | | 71.1 | 122.9 | 53.7 | | |
| 20% | | 167.7 | 91.7 | 97.0 | 100.9 | 116.3 | |
| 0% | | 111.9 | 32.2 | 182.2 | 99.6 | 88.1 | 180.7 |
| -20% | 217.8 | 141.1 | 155.7 | 104.0 | 159.5 | 124.4 | 166.9 |
| -40% | | 155.6 | 111.1 | 99.2 | 96.5 | 177.8 | |

r-Squared

| | LAT | | | | | | |
|---|---|---|---|---|---|---|---|
| AP | -45% | -30% | -15% | 0% | 15% | 30% | 45% |
| 40% | | | 0.985 | 0.996 | 0.975 | | |
| 20% | | 0.994 | 0.995 | 0.997 | 0.990 | 0.992 | |
| 0% | | 0.995 | 0.976 | 0.992 | 0.993 | 0.992 | 0.998 |
| -20% | 0.998 | 0.992 | 0.997 | 0.995 | 0.996 | 0.996 | 0.998 |
| -40% | | 0.997 | 0.996 | 0.992 | 0.996 | 0.999 | |

**Specimen 1010_L4_i**

Failure Load (N)

| | LAT | | | | | | |
|---|---|---|---|---|---|---|---|
| AP | -45% | -30% | -15% | 0% | 15% | 30% | 45% |
| 40% | | | 89.6 | 175.0 | 79.5 | | |
| 20% | | 98.7 | 132.3 | 95.1 | 82.7 | 137.4 | |
| 0% | 94.8 | 108.4 | 78.4 | 103.7 | 125.9 | 167.1 | |
| -20% | | 191.3 | 170.8 | 144.3 | 214.5 | 257.5 | |
| -40% | | 231.0 | 198.2 | 141.4 | 150.0 | 193.2 | |

Stiffness (N/mm)

| | LAT | | | | | | |
|---|---|---|---|---|---|---|---|
| AP | -45% | -30% | -15% | 0% | 15% | 30% | 45% |
| 40% | | | 109.6 | 192.1 | 206.3 | | |
| 20% | | 258.8 | 165.3 | 119.9 | 128.7 | 219.3 | |
| 0% | 180.2 | 171.1 | 143.5 | 104.6 | 133.6 | 151.8 | |
| -20% | | 244.4 | 191.6 | 229.4 | 254.4 | 238.9 | |
| -40% | | 331.7 | 275.8 | 145.8 | 233.8 | 299.4 | |

r-Squared

| | LAT | | | | | | |
|---|---|---|---|---|---|---|---|
| AP | -45% | -30% | -15% | 0% | 15% | 30% | 45% |
| 40% | | | 0.996 | 0.998 | 0.999 | | |
| 20% | | 0.999 | 0.998 | 0.998 | 0.998 | 0.999 | |
| 0% | 0.998 | 0.998 | 0.997 | 0.998 | 0.995 | 0.996 | |
| -20% | | 0.995 | 0.996 | 0.999 | 0.997 | 0.996 | |
| -40% | | 0.999 | 0.998 | 0.998 | 0.996 | 0.999 | |

Table A.5: Endplate Maps continued

**Specimen 1010_L5_s**

Failure Load (N)

| | LAT | | | | | | |
|---|---|---|---|---|---|---|---|
| AP | -45% | -30% | -15% | 0% | 15% | 30% | 45% |
| 40% | | | 81.3 | 92.2 | 102.2 | | |
| 20% | | 51.8 | 50.9 | 40.0 | 49.7 | 92.9 | |
| 0% | 93.0 | 67.3 | 32.5 | 41.8 | 29.7 | 77.8 | 53.5 |
| -20% | 81.3 | 89.8 | 64.2 | 55.6 | 79.4 | 81.9 | |
| -40% | | 142.6 | 43.0 | 48.6 | 77.9 | 196.9 | |

Stiffness (N/mm)

| | LAT | | | | | | |
|---|---|---|---|---|---|---|---|
| AP | -45% | -30% | -15% | 0% | 15% | 30% | 45% |
| 40% | | | 110.5 | 121.3 | 171.5 | | |
| 20% | | 151.1 | 181.6 | 93.3 | 174.5 | 140.2 | |
| 0% | 145.4 | 198.4 | 105.1 | 113.0 | 126.9 | 251.6 | 137.5 |
| -20% | 186.0 | 234.9 | 201.9 | 101.4 | 154.6 | 239.1 | |
| -40% | | 208.2 | 115.6 | 116.5 | 127.1 | 217.6 | |

r-Squared

| | LAT | | | | | | |
|---|---|---|---|---|---|---|---|
| AP | -45% | -30% | -15% | 0% | 15% | 30% | 45% |
| 40% | | | 0.996 | 0.998 | 0.991 | | |
| 20% | | 0.997 | 0.998 | 0.977 | 0.994 | 0.998 | |
| 0% | 0.999 | 0.998 | 0.998 | 0.995 | 0.997 | 0.996 | 0.998 |
| -20% | 0.995 | 0.999 | 0.998 | 0.993 | 0.998 | 0.997 | |
| -40% | | 0.999 | 0.997 | 0.985 | 0.994 | 0.999 | |

**Specimen 1010_L5_i**

Failure Load (N)

| | LAT | | | | | | |
|---|---|---|---|---|---|---|---|
| AP | -45% | -30% | -15% | 0% | 15% | 30% | 45% |
| 40% | | | 75.2 | 89.8 | 61.3 | | |
| 20% | | 96.2 | 115.3 | 51.1 | 79.3 | 98.7 | |
| 0% | 64.7 | 91.4 | 62.9 | 100.6 | 97.4 | 176.1 | 93.5 |
| -20% | | 160.9 | 143.2 | 99.3 | 137.0 | 91.6 | |
| -40% | | | 54.9 | 118.3 | 90.1 | | |

Stiffness (N/mm)

| | LAT | | | | | | |
|---|---|---|---|---|---|---|---|
| AP | -45% | -30% | -15% | 0% | 15% | 30% | 45% |
| 40% | | | 116.2 | 140.0 | 80.3 | | |
| 20% | | 161.2 | 188.0 | 106.5 | 145.2 | 205.6 | |
| 0% | 139.1 | 193.2 | 159.4 | 185.5 | 105.8 | 203.9 | 212.4 |
| -20% | | 215.5 | 171.1 | 137.5 | 250.9 | 269.5 | |
| -40% | | | 177.7 | 216.6 | 88.4 | | |

r-Squared

| | LAT | | | | | | |
|---|---|---|---|---|---|---|---|
| AP | -45% | -30% | -15% | 0% | 15% | 30% | 45% |
| 40% | | | 0.999 | 0.998 | 0.998 | | |
| 20% | | 1.000 | 0.999 | 0.990 | 0.999 | 0.996 | |
| 0% | 0.999 | 0.999 | 0.998 | 0.999 | 1.000 | 0.997 | 1.000 |
| -20% | | 0.999 | 0.999 | 0.996 | 0.997 | 0.999 | |
| -40% | | | 0.998 | 1.000 | 0.993 | | |

**Specimen 1010_S1_s**

Failure Load (N)

| | LAT | | | | | | |
|---|---|---|---|---|---|---|---|
| AP | -45% | -30% | -15% | 0% | 15% | 30% | 45% |
| 40% | | | | 71.2 | 76.0 | | |
| 20% | | 46.3 | 99.6 | 48.2 | 55.9 | 52.9 | |
| 0% | 65.2 | 99.8 | 96.3 | 127.0 | 78.6 | 99.8 | 59.8 |
| -20% | 56.8 | 108.9 | 137.0 | 279.9 | 182.8 | 121.7 | 41.4 |
| -40% | | 191.9 | 297.6 | 339.1 | 314.9 | 149.9 | |

Stiffness (N/mm)

| | LAT | | | | | | |
|---|---|---|---|---|---|---|---|
| AP | -45% | -30% | -15% | 0% | 15% | 30% | 45% |
| 40% | | | | 120.4 | 161.4 | | |
| 20% | | 69.6 | 236.8 | 135.3 | 193.9 | 102.1 | |
| 0% | 125.3 | 161.8 | 145.3 | 179.9 | 89.4 | 124.1 | 93.7 |
| -20% | 82.8 | 176.6 | 226.1 | 331.4 | 188.7 | 214.3 | 143.0 |
| -40% | | 181.2 | 237.9 | 372.2 | 229.1 | 174.8 | |

r-Squared

| | LAT | | | | | | |
|---|---|---|---|---|---|---|---|
| AP | -45% | -30% | -15% | 0% | 15% | 30% | 45% |
| 40% | | | | 0.998 | 0.999 | | |
| 20% | | 0.998 | 1.000 | 0.999 | 0.996 | 0.998 | |
| 0% | 0.999 | 0.999 | 0.998 | 0.999 | 0.998 | 0.999 | 0.998 |
| -20% | 0.999 | 0.999 | 0.999 | 0.999 | 0.997 | 1.000 | 0.997 |
| -40% | | 0.997 | 1.000 | 1.000 | 0.999 | 0.999 | |

Table A.5: Endplate Maps continued

**Specimen 1012_L4_s**

Failure Load (N)

| AP \ LAT | -45% | -30% | -15% | 0% | 15% | 30% | 45% |
|---|---|---|---|---|---|---|---|
| 40% | | | 170.2 | 112.5 | 126.6 | | |
| 20% | | 66.1 | 39.6 | 63.5 | 79.6 | 117.4 | |
| 0% | 81.4 | 68.7 | 75.4 | 60.1 | 96.0 | 83.7 | 34.3 |
| -20% | 118.2 | 105.9 | 109.7 | 116.0 | 120.1 | 126.0 | 104.9 |
| -40% | | 171.9 | 75.3 | 84.4 | 73.3 | 189.8 | |

Stiffness (N/mm)

| AP \ LAT | -45% | -30% | -15% | 0% | 15% | 30% | 45% |
|---|---|---|---|---|---|---|---|
| 40% | | | 273.8 | 164.8 | 165.2 | | |
| 20% | | 105.8 | 63.4 | 85.6 | 109.5 | 129.4 | |
| 0% | 87.2 | 127.2 | 83.0 | 137.1 | 119.1 | 145.4 | 76.2 |
| -20% | 119.2 | 119.8 | 134.6 | 141.2 | 115.9 | 188.4 | 175.1 |
| -40% | | 184.1 | 75.1 | 154.5 | 102.1 | 181.9 | |

r-Squared

| AP \ LAT | -45% | -30% | -15% | 0% | 15% | 30% | 45% |
|---|---|---|---|---|---|---|---|
| 40% | | | 1.000 | 1.000 | 0.999 | | |
| 20% | | 0.998 | 0.995 | 0.997 | 0.998 | 0.999 | |
| 0% | 0.998 | 0.999 | 0.999 | 0.998 | 0.999 | 0.999 | 0.996 |
| -20% | 0.999 | 0.999 | 0.999 | 0.999 | 0.999 | 0.997 | 1.000 |
| -40% | | 1.000 | 0.999 | 0.996 | 0.995 | 0.999 | |

**Specimen 1012_L4_i**

Failure Load (N)

| AP \ LAT | -45% | -30% | -15% | 0% | 15% | 30% | 45% |
|---|---|---|---|---|---|---|---|
| 40% | | | | 243.9 | | | |
| 20% | | 150.6 | 115.3 | 218.0 | 84.8 | 81.8 | |
| 0% | 143.6 | 188.1 | 149.7 | 116.0 | 127.2 | 147.6 | 128.2 |
| -20% | 268.0 | 298.0 | 93.8 | 94.9 | | 260.2 | 127.1 |
| -40% | | 248.6 | 177.0 | 59.4 | | 234.3 | |

Stiffness (N/mm)

| AP \ LAT | -45% | -30% | -15% | 0% | 15% | 30% | 45% |
|---|---|---|---|---|---|---|---|
| 40% | | | | 184.3 | | | |
| 20% | | 172.6 | 139.8 | 187.7 | 92.9 | 90.2 | |
| 0% | 153.0 | 144.1 | 173.5 | 168.0 | 206.5 | 117.6 | 141.2 |
| -20% | 322.5 | 248.3 | 90.5 | 142.1 | | 242.0 | 229.7 |
| -40% | | 166.8 | 230.2 | 133.3 | | 132.4 | |

r-Squared

| AP \ LAT | -45% | -30% | -15% | 0% | 15% | 30% | 45% |
|---|---|---|---|---|---|---|---|
| 40% | | | | 1.000 | | | |
| 20% | | 0.999 | 0.998 | 0.999 | 0.996 | 0.997 | |
| 0% | 0.999 | 0.999 | 0.994 | 0.998 | 0.998 | 0.998 | 0.999 |
| -20% | 0.999 | 0.999 | 0.999 | 0.999 | | 1.000 | 0.999 |
| -40% | | 0.995 | 1.000 | 0.998 | | 0.998 | |

**Specimen 1012_L5_s**

Failure Load (N)

| AP \ LAT | -45% | -30% | -15% | 0% | 15% | 30% | 45% |
|---|---|---|---|---|---|---|---|
| 40% | | | 152.9 | 86.9 | 124.5 | | |
| 20% | | | 45.2 | 42.2 | 51.6 | 94.7 | |
| 0% | | | 44.1 | 56.8 | 79.1 | 101.6 | 96.5 |
| -20% | | | 88.0 | 88.3 | 110.9 | 108.1 | 86.3 |
| -40% | | | 70.8 | 69.4 | 78.5 | 121.1 | |

Stiffness (N/mm)

| AP \ LAT | -45% | -30% | -15% | 0% | 15% | 30% | 45% |
|---|---|---|---|---|---|---|---|
| 40% | | | 165.7 | 148.3 | 185.4 | | |
| 20% | | | 65.3 | 49.3 | 70.7 | 107.3 | |
| 0% | | | 79.4 | 98.8 | 126.7 | 92.8 | 175.1 |
| -20% | | | 83.3 | 154.5 | 127.5 | 89.5 | 118.6 |
| -40% | | | 100.8 | 104.9 | 52.1 | 98.7 | |

r-Squared

| AP \ LAT | -45% | -30% | -15% | 0% | 15% | 30% | 45% |
|---|---|---|---|---|---|---|---|
| 40% | | | 0.999 | 0.999 | 0.999 | | |
| 20% | | | 0.999 | 0.993 | 0.998 | 0.999 | |
| 0% | | | 0.998 | 1.000 | 0.999 | 0.999 | 0.999 |
| -20% | | | 0.998 | 0.999 | 0.999 | 0.999 | 0.999 |
| -40% | | | 0.999 | 0.999 | 0.995 | 0.998 | |

**Specimen 1012_L5_i**

Failure Load (N)

| AP \ LAT | -45% | -30% | -15% | 0% | 15% | 30% | 45% |
|---|---|---|---|---|---|---|---|
| 40% | | | | 92.2 | | | |
| 20% | | 135.8 | 109.7 | 104.3 | 123.2 | 223.6 | |
| 0% | 156.4 | 92.5 | 137.3 | 135.1 | 192.7 | 135.6 | |
| -20% | | 299.7 | 243.1 | 205.1 | 293.3 | | 234.6 |
| -40% | | | 175.9 | 128.7 | | | |

Stiffness (N/mm)

| AP \ LAT | -45% | -30% | -15% | 0% | 15% | 30% | 45% |
|---|---|---|---|---|---|---|---|
| 40% | | | | 78.6 | | | |
| 20% | | 155.8 | 99.3 | 111.8 | 86.9 | 176.8 | |
| 0% | 230.5 | 105.4 | 157.6 | 173.3 | 147.2 | 101.7 | |
| -20% | | 167.6 | 190.7 | 161.4 | 186.3 | | 155.8 |
| -40% | | | 152.4 | 109.9 | | | |

r-Squared

| AP \ LAT | -45% | -30% | -15% | 0% | 15% | 30% | 45% |
|---|---|---|---|---|---|---|---|
| 40% | | | | 0.998 | | | |
| 20% | | 0.999 | 0.999 | 0.997 | 0.999 | 1.000 | |
| 0% | 1.000 | 0.995 | 0.999 | 0.999 | 0.999 | 0.999 | |
| -20% | | 0.998 | 0.999 | 1.000 | 1.000 | | 1.000 |
| -40% | | | 1.000 | 0.998 | | | |

Table A.5: Endplate Maps continued

**Specimen 1014_L3_s**

Failure Load (N)

| AP \ LAT | -45% | -30% | -15% | 0% | 15% | 30% | 45% |
|---|---|---|---|---|---|---|---|
| 40% | | | 203.6 | 176.3 | 198.5 | | |
| 20% | | 199.9 | 80.8 | 88.7 | 79.2 | 172.5 | |
| 0% | | 78.4 | 75.4 | 91.2 | 85.1 | 93.6 | 239.9 |
| -20% | 170.4 | 76.4 | 104.2 | 110.1 | 122.7 | 91.9 | 307.0 |
| -40% | | 151.6 | 122.0 | 105.2 | 107.8 | 147.8 | |

Stiffness (N/mm)

| AP \ LAT | -45% | -30% | -15% | 0% | 15% | 30% | 45% |
|---|---|---|---|---|---|---|---|
| 40% | | | 176.0 | 132.8 | 124.3 | | |
| 20% | | 172.0 | 122.3 | 101.8 | 105.9 | 136.0 | |
| 0% | | 134.6 | 114.1 | 100.3 | 93.0 | 187.0 | 208.6 |
| -20% | 130.7 | 135.9 | 144.0 | 114.5 | 123.7 | 176.5 | 259.0 |
| -40% | | 141.6 | 121.7 | 97.7 | 108.9 | 200.4 | |

r-Squared

| AP \ LAT | -45% | -30% | -15% | 0% | 15% | 30% | 45% |
|---|---|---|---|---|---|---|---|
| 40% | | | 1.000 | 0.996 | 1.000 | | |
| 20% | | 0.999 | 0.999 | 0.999 | 0.999 | 0.999 | |
| 0% | | 0.998 | 0.998 | 0.996 | 0.998 | 1.000 | 0.999 |
| -20% | 0.999 | 0.999 | 0.999 | 0.999 | 1.000 | 1.000 | 0.999 |
| -40% | | 0.999 | 0.999 | 0.999 | 0.993 | 0.999 | |

**Specimen 1014_L3_i**

Failure Load (N)

| AP \ LAT | -45% | -30% | -15% | 0% | 15% | 30% | 45% |
|---|---|---|---|---|---|---|---|
| 40% | | | 140.8 | 149.7 | | | |
| 20% | | 190.4 | 119.7 | 141.7 | 130.5 | 126.4 | |
| 0% | | 147.6 | 173.0 | 114.4 | 126.8 | 118.1 | 218.6 |
| -20% | 226.0 | 220.7 | 237.6 | 174.8 | 196.5 | 172.1 | 296.8 |
| -40% | | 292.1 | 287.0 | 228.8 | 285.9 | 236.0 | |

Stiffness (N/mm)

| AP \ LAT | -45% | -30% | -15% | 0% | 15% | 30% | 45% |
|---|---|---|---|---|---|---|---|
| 40% | | | 140.5 | 176.5 | | | |
| 20% | | 221.5 | 162.6 | 209.1 | 206.4 | 224.0 | |
| 0% | | 215.3 | 187.5 | 162.1 | 213.2 | 200.4 | 200.1 |
| -20% | 202.8 | 241.5 | 285.0 | 224.7 | 239.0 | 196.1 | 298.7 |
| -40% | | 143.4 | 210.9 | 112.9 | 218.0 | 245.3 | |

r-Squared

| AP \ LAT | -45% | -30% | -15% | 0% | 15% | 30% | 45% |
|---|---|---|---|---|---|---|---|
| 40% | | | 1.000 | 0.998 | | | |
| 20% | | 0.998 | 0.999 | 0.997 | 0.999 | 0.997 | |
| 0% | | 0.998 | 1.000 | 0.999 | 0.999 | 0.999 | 0.999 |
| -20% | 1.000 | 0.999 | 0.999 | 0.999 | 0.999 | 1.000 | 0.999 |
| -40% | | 0.998 | 0.999 | 1.000 | 1.000 | 1.000 | |

**Specimen 1014_L4_s**

Failure Load (N)

| AP \ LAT | -45% | -30% | -15% | 0% | 15% | 30% | 45% |
|---|---|---|---|---|---|---|---|
| 40% | | | 143.3 | 98.2 | 108.3 | | |
| 20% | | 127.7 | 54.7 | 104.2 | 80.4 | 119.2 | |
| 0% | 261.4 | 119.4 | 95.2 | 82.3 | 109.6 | 105.0 | 151.9 |
| -20% | 109.3 | 121.7 | 110.8 | 115.6 | 120.1 | 128.3 | 153.4 |
| -40% | | 169.1 | 100.0 | 122.6 | 132.3 | 194.9 | |

Stiffness (N/mm)

| AP \ LAT | -45% | -30% | -15% | 0% | 15% | 30% | 45% |
|---|---|---|---|---|---|---|---|
| 40% | | | 107.0 | 128.4 | 123.7 | | |
| 20% | | 137.1 | 94.1 | 65.6 | 90.8 | 157.6 | |
| 0% | 159.8 | 136.2 | 112.0 | 122.1 | 200.7 | 164.1 | 227.5 |
| -20% | 170.0 | 212.8 | 112.1 | 133.0 | 217.0 | 199.4 | 251.0 |
| -40% | | 115.7 | 103.6 | 70.3 | 102.3 | 154.6 | |

r-Squared

| AP \ LAT | -45% | -30% | -15% | 0% | 15% | 30% | 45% |
|---|---|---|---|---|---|---|---|
| 40% | | | 0.997 | 0.999 | 0.999 | | |
| 20% | | 0.997 | 0.986 | 0.995 | 0.996 | 0.997 | |
| 0% | 0.999 | 0.998 | 0.997 | 0.997 | 0.998 | 0.996 | 0.995 |
| -20% | 0.983 | 0.998 | 0.999 | 0.996 | 0.998 | 0.998 | 0.999 |
| -40% | | 0.998 | 0.996 | 0.998 | 0.996 | 0.999 | |

**Specimen 1014_L4_i**

Failure Load (N)

| AP \ LAT | -45% | -30% | -15% | 0% | 15% | 30% | 45% |
|---|---|---|---|---|---|---|---|
| 40% | | | 199.7 | 191.6 | 195.3 | | |
| 20% | | 197.3 | 99.4 | 127.2 | 104.2 | 94.9 | |
| 0% | 255.1 | 164.9 | 157.8 | 132.4 | 177.7 | 129.0 | 171.2 |
| -20% | | 248.1 | 229.4 | 128.4 | 183.4 | 237.2 | 258.0 |
| -40% | | | 192.8 | 134.5 | 144.1 | 263.7 | |

Stiffness (N/mm)

| AP \ LAT | -45% | -30% | -15% | 0% | 15% | 30% | 45% |
|---|---|---|---|---|---|---|---|
| 40% | | | 250.7 | 173.3 | 134.9 | | |
| 20% | | 208.0 | 88.1 | 146.4 | 86.5 | 160.4 | |
| 0% | 214.4 | 124.6 | 139.8 | 119.0 | 169.0 | 101.9 | 217.3 |
| -20% | | 198.5 | 200.2 | 168.1 | 222.0 | 205.1 | 249.0 |
| -40% | | | 210.2 | 120.6 | 164.6 | 161.2 | |

r-Squared

| AP \ LAT | -45% | -30% | -15% | 0% | 15% | 30% | 45% |
|---|---|---|---|---|---|---|---|
| 40% | | | 0.996 | 0.999 | 0.998 | | |
| 20% | | 0.997 | 0.993 | 0.996 | 0.995 | 0.996 | |
| 0% | 0.998 | 0.999 | 0.999 | 0.999 | 0.999 | 0.998 | 1.000 |
| -20% | | 0.998 | 0.997 | 1.000 | 0.999 | 0.999 | 0.998 |
| -40% | | | 0.999 | 0.998 | 0.996 | 1.000 | |

Table A.5: Endplate Maps continued

**Specimen 1014_L5_s**

Failure Load (N)

| | LAT | | | | | | |
|---|---|---|---|---|---|---|---|
| AP | -45% | -30% | -15% | 0% | 15% | 30% | 45% |
| 40% | | | | 165.2 | | | |
| 20% | | 118.6 | 55.8 | 76.5 | 87.9 | 148.2 | |
| 0% | 212.2 | 103.4 | 70.7 | 93.8 | 104.5 | 145.5 | 257.1 |
| -20% | 136.1 | 76.2 | 107.6 | 89.8 | 158.7 | 166.3 | 201.8 |
| -40% | | 183.5 | 86.1 | 64.4 | 128.6 | 245.1 | |

Stiffness (N/mm)

| | LAT | | | | | | |
|---|---|---|---|---|---|---|---|
| AP | -45% | -30% | -15% | 0% | 15% | 30% | 45% |
| 40% | | | | 108.7 | | | |
| 20% | | 130.2 | 53.8 | 69.6 | 111.2 | 188.6 | |
| 0% | 124.8 | 77.6 | 65.6 | 142.3 | 90.6 | 111.8 | 215.2 |
| -20% | 82.9 | 120.8 | 83.0 | 131.5 | 176.8 | 167.2 | 227.7 |
| -40% | | 113.2 | 111.2 | 51.7 | 109.2 | 169.7 | |

r-Squared

| | LAT | | | | | | |
|---|---|---|---|---|---|---|---|
| AP | -45% | -30% | -15% | 0% | 15% | 30% | 45% |
| 40% | | | | 0.996 | | | |
| 20% | | 0.996 | 0.996 | 0.995 | 0.996 | 0.999 | |
| 0% | 0.998 | 0.996 | 0.997 | 0.992 | 0.991 | 0.998 | 0.999 |
| -20% | 0.994 | 0.999 | 0.998 | 0.996 | 0.999 | 0.999 | 0.999 |
| -40% | | 0.999 | 0.994 | 0.996 | 0.999 | 0.998 | |

**Specimen 1014_L5_i**

Failure Load (N)

| | LAT | | | | | | |
|---|---|---|---|---|---|---|---|
| AP | -45% | -30% | -15% | 0% | 15% | 30% | 45% |
| 40% | | | 104.2 | 103.0 | 126.1 | | |
| 20% | | 154.1 | 87.5 | 99.1 | 88.8 | 102.8 | |
| 0% | 260.2 | 131.7 | 93.2 | 84.0 | 113.9 | 116.6 | 175.0 |
| -20% | | 147.8 | 99.2 | 78.3 | 82.2 | 133.9 | |
| -40% | | | 91.5 | 35.2 | 71.7 | | |

Stiffness (N/mm)

| | LAT | | | | | | |
|---|---|---|---|---|---|---|---|
| AP | -45% | -30% | -15% | 0% | 15% | 30% | 45% |
| 40% | | | 129.4 | 130.9 | 113.8 | | |
| 20% | | 123.9 | 82.4 | 77.5 | 56.1 | 99.4 | |
| 0% | 197.9 | 109.7 | 110.6 | 159.6 | 81.7 | 88.4 | 216.6 |
| -20% | | 114.0 | 83.4 | 97.6 | 87.4 | 84.4 | |
| -40% | | | 65.1 | 89.8 | 84.3 | | |

r-Squared

| | LAT | | | | | | |
|---|---|---|---|---|---|---|---|
| AP | -45% | -30% | -15% | 0% | 15% | 30% | 45% |
| 40% | | | 0.993 | 0.997 | 0.996 | | |
| 20% | | 0.998 | 0.998 | 0.987 | 0.996 | 0.998 | |
| 0% | 0.999 | 0.996 | 0.999 | 0.998 | 0.997 | 0.992 | 0.999 |
| -20% | | 0.999 | 0.996 | 0.993 | 0.995 | 0.990 | |
| -40% | | | 0.995 | 0.998 | 0.994 | | |

**Specimen 1014_S1_s**

Failure Load (N)

| | LAT | | | | | | |
|---|---|---|---|---|---|---|---|
| AP | -45% | -30% | -15% | 0% | 15% | 30% | 45% |
| 40% | | | 118.0 | 129.6 | 74.5 | | |
| 20% | | 144.9 | 175.2 | 209.3 | 141.3 | 152.1 | |
| 0% | 336.7 | 282.0 | 380.1 | 339.1 | 346.3 | 341.1 | 394.0 |
| -20% | | 384.0 | 408.6 | 408.2 | 411.5 | 348.9 | |
| -40% | | | 300.0 | 341.7 | 411.4 | | |

Stiffness (N/mm)

| | LAT | | | | | | |
|---|---|---|---|---|---|---|---|
| AP | -45% | -30% | -15% | 0% | 15% | 30% | 45% |
| 40% | | | 106.6 | 151.4 | 93.3 | | |
| 20% | | 91.7 | 110.8 | 186.5 | 94.0 | 154.2 | |
| 0% | 243.1 | 192.0 | 269.4 | 283.5 | 237.0 | 214.2 | 272.5 |
| -20% | | 273.0 | 242.4 | 284.1 | 297.2 | 236.6 | |
| -40% | | | 173.2 | 217.0 | 249.5 | | |

r-Squared

| | LAT | | | | | | |
|---|---|---|---|---|---|---|---|
| AP | -45% | -30% | -15% | 0% | 15% | 30% | 45% |
| 40% | | | 0.999 | 0.997 | 0.994 | | |
| 20% | | 0.997 | 0.997 | 0.998 | 0.997 | 0.996 | |
| 0% | 0.999 | 0.999 | 0.999 | 0.999 | 0.998 | 0.999 | 0.998 |
| -20% | | 1.000 | 0.999 | 0.999 | 1.000 | 0.999 | |
| -40% | | | 0.999 | 0.999 | 0.999 | | |

Table A.5: Endplate Maps continued

**Specimen 1017_L3_s**

Failure Load (N)

| AP \ LAT | -45% | -30% | -15% | 0% | 15% | 30% | 45% |
|---|---|---|---|---|---|---|---|
| 40% | | | 81.9 | 22.6 | 53.1 | | |
| 20% | | 59.6 | 79.0 | 57.6 | 66.6 | 68.4 | 85.7 |
| 0% | | 57.0 | 29.8 | 56.6 | 45.7 | 38.5 | 54.2 |
| -20% | 68.8 | 38.0 | 52.7 | 70.2 | 50.9 | 53.4 | 78.7 |
| -40% | | 95.2 | 78.3 | 47.9 | 68.8 | 74.7 | |

Stiffness (N/mm)

| AP \ LAT | -45% | -30% | -15% | 0% | 15% | 30% | 45% |
|---|---|---|---|---|---|---|---|
| 40% | | | 120.7 | 37.7 | 17.9 | | |
| 20% | | 79.9 | 165.6 | 101.4 | 83.2 | 144.3 | 224.8 |
| 0% | | 51.7 | 17.2 | 41.3 | 58.1 | 108.2 | 97.7 |
| -20% | 106.7 | 86.1 | 93.6 | 84.8 | 75.5 | 44.7 | 129.8 |
| -40% | | 97.1 | 71.8 | 111.9 | 66.2 | 76.6 | |

r-Squared

| AP \ LAT | -45% | -30% | -15% | 0% | 15% | 30% | 45% |
|---|---|---|---|---|---|---|---|
| 40% | | | 0.996 | 0.991 | 0.977 | | |
| 20% | | 0.998 | 0.998 | 0.999 | 0.999 | 0.999 | 0.999 |
| 0% | | 0.993 | 0.898 | 0.985 | 0.998 | 0.997 | 0.999 |
| -20% | 0.996 | 0.999 | 0.993 | 0.998 | 0.997 | 0.995 | 0.998 |
| -40% | | 0.994 | 0.993 | 0.999 | 0.998 | 0.998 | |

**Specimen 1017_L3_i**

Failure Load (N)

| AP \ LAT | -45% | -30% | -15% | 0% | 15% | 30% | 45% |
|---|---|---|---|---|---|---|---|
| 40% | | | 76.0 | 95.9 | 80.4 | | |
| 20% | | 55.1 | 82.7 | 70.8 | 87.6 | 63.3 | |
| 0% | 120.3 | 64.5 | 90.6 | 55.2 | 61.8 | 43.9 | 74.7 |
| -20% | | 113.3 | 167.3 | 221.6 | 113.7 | 73.2 | 120.7 |
| -40% | | 143.3 | 224.4 | 66.8 | 230.2 | | |

Stiffness (N/mm)

| AP \ LAT | -45% | -30% | -15% | 0% | 15% | 30% | 45% |
|---|---|---|---|---|---|---|---|
| 40% | | | 160.0 | 149.1 | 159.7 | | |
| 20% | | 145.7 | 175.5 | 154.9 | 145.1 | 76.6 | |
| 0% | 288.4 | 144.2 | 106.3 | 124.8 | 90.2 | 71.4 | 86.6 |
| -20% | | 138.8 | 132.2 | 227.3 | 95.4 | 78.8 | 145.0 |
| -40% | | 81.8 | 219.6 | 116.2 | 110.3 | | |

r-Squared

| AP \ LAT | -45% | -30% | -15% | 0% | 15% | 30% | 45% |
|---|---|---|---|---|---|---|---|
| 40% | | | 0.999 | 0.998 | 0.999 | | |
| 20% | | 0.997 | 1.000 | 0.997 | 0.998 | 0.998 | |
| 0% | 0.999 | 0.998 | 0.991 | 0.996 | 0.997 | 0.997 | 0.998 |
| -20% | | 0.999 | 0.999 | 0.999 | 0.997 | 0.999 | 0.999 |
| -40% | | 0.998 | 1.000 | 0.998 | 0.997 | | |

**Specimen 1017_L4_s**

Failure Load (N)

| AP \ LAT | -45% | -30% | -15% | 0% | 15% | 30% | 45% |
|---|---|---|---|---|---|---|---|
| 40% | | | 67.5 | 62.3 | 93.7 | 96.5 | |
| 20% | | 53.0 | 78.4 | 83.7 | 88.8 | 44.4 | |
| 0% | | 36.8 | 75.0 | 46.2 | 46.7 | 61.3 | 110.1 |
| -20% | | 62.7 | 91.6 | | 146.7 | 67.1 | 72.3 |
| -40% | | 178.8 | 133.0 | 140.1 | 286.9 | 325.0 | |

Stiffness (N/mm)

| AP \ LAT | -45% | -30% | -15% | 0% | 15% | 30% | 45% |
|---|---|---|---|---|---|---|---|
| 40% | | | 80.1 | 118.8 | 119.6 | 120.9 | |
| 20% | | 91.1 | 117.1 | 68.3 | 107.7 | 77.0 | |
| 0% | | 94.4 | 103.4 | 96.3 | 81.8 | 67.9 | 101.9 |
| -20% | | 123.7 | 139.1 | | 150.3 | 85.4 | 79.6 |
| -40% | | 96.8 | 111.2 | 183.8 | 142.1 | 132.8 | |

r-Squared

| AP \ LAT | -45% | -30% | -15% | 0% | 15% | 30% | 45% |
|---|---|---|---|---|---|---|---|
| 40% | | | 0.992 | 0.999 | 0.996 | 0.999 | |
| 20% | | 0.999 | 0.997 | 0.998 | 0.999 | 0.999 | |
| 0% | | 0.997 | 0.995 | 0.999 | 0.991 | 0.999 | 0.995 |
| -20% | | 0.990 | 0.997 | | 0.999 | 0.996 | 0.997 |
| -40% | | 0.999 | 0.999 | 0.999 | 0.999 | 0.999 | |

**Specimen 1017_L4_i**

Failure Load (N)

| AP \ LAT | -45% | -30% | -15% | 0% | 15% | 30% | 45% |
|---|---|---|---|---|---|---|---|
| 40% | | | 77.5 | 74.7 | 85.0 | | |
| 20% | | 71.8 | 34.9 | 31.0 | 39.7 | 70.1 | |
| 0% | 66.1 | 78.3 | 49.1 | 50.0 | 43.6 | 43.9 | 52.5 |
| -20% | 197.0 | 92.9 | 66.8 | 40.1 | 53.8 | 53.1 | 77.1 |
| -40% | | 85.6 | 95.7 | 106.9 | 58.6 | 82.6 | |

Stiffness (N/mm)

| AP \ LAT | -45% | -30% | -15% | 0% | 15% | 30% | 45% |
|---|---|---|---|---|---|---|---|
| 40% | | | 81.7 | 88.6 | 90.8 | | |
| 20% | | 121.2 | 74.1 | 57.1 | 105.4 | 87.1 | |
| 0% | 128.9 | 109.0 | 71.0 | 74.7 | 59.0 | 77.8 | 76.5 |
| -20% | 168.6 | 158.9 | 65.3 | 48.2 | 127.9 | 88.7 | 137.0 |
| -40% | | 200.7 | 203.9 | 213.2 | 140.6 | 142.4 | |

r-Squared

| AP \ LAT | -45% | -30% | -15% | 0% | 15% | 30% | 45% |
|---|---|---|---|---|---|---|---|
| 40% | | | 0.999 | 0.994 | 0.998 | | |
| 20% | | 0.996 | 0.990 | 0.991 | 0.996 | 0.999 | |
| 0% | 0.999 | 0.997 | 0.998 | 0.991 | 0.995 | 0.997 | 0.990 |
| -20% | 0.998 | 0.999 | 0.997 | 0.994 | 0.990 | 0.996 | 0.997 |
| -40% | | 0.996 | 0.997 | 0.999 | 0.996 | 0.995 | |

Table A.5: Endplate Maps continued

**Specimen 1017_L5_s**

Failure Load (N)

| | LAT | | | | | | |
|---|---|---|---|---|---|---|---|
| AP | -45% | -30% | -15% | 0% | 15% | 30% | 45% |
| 40% | | | 101.5 | 184.4 | | 259.7 | |
| 20% | | 59.3 | 90.9 | | 161.8 | 254.5 | |
| 0% | | 68.6 | 33.5 | 49.8 | 68.7 | 83.0 | 248.1 |
| -20% | 78.8 | 59.5 | 42.8 | 61.3 | 131.7 | 137.9 | 115.1 |
| -40% | | 105.1 | 63.3 | 55.8 | 222.3 | | |

Stiffness (N/mm)

| | LAT | | | | | | |
|---|---|---|---|---|---|---|---|
| AP | -45% | -30% | -15% | 0% | 15% | 30% | 45% |
| 40% | | | 135.6 | 141.6 | | 263.6 | |
| 20% | | 124.8 | 131.6 | | 136.1 | 200.3 | |
| 0% | | 98.8 | 66.7 | 65.3 | 112.5 | 114.1 | 119.6 |
| -20% | 138.8 | 82.4 | 50.3 | 86.9 | 77.0 | 100.6 | 101.8 |
| -40% | | 102.1 | 75.7 | 95.1 | 148.8 | | |

r-Squared

| | LAT | | | | | | |
|---|---|---|---|---|---|---|---|
| AP | -45% | -30% | -15% | 0% | 15% | 30% | 45% |
| 40% | | | 0.987 | 0.999 | | 0.999 | |
| 20% | | 0.998 | 0.997 | | 0.996 | 1.000 | |
| 0% | | 0.997 | 0.997 | 0.998 | 0.999 | 0.996 | 0.999 |
| -20% | 0.998 | 0.996 | 0.998 | 0.999 | 0.999 | 0.995 | 0.999 |
| -40% | | 0.998 | 0.998 | 0.999 | 0.998 | | |

**Specimen 1017_L5_i**

Failure Load (N)

| | LAT | | | | | | |
|---|---|---|---|---|---|---|---|
| AP | -45% | -30% | -15% | 0% | 15% | 30% | 45% |
| 40% | | | 142.1 | 175.9 | 169.8 | | |
| 20% | | 106.9 | 62.2 | 53.5 | 76.2 | 202.8 | |
| 0% | 328.6 | 168.1 | 70.6 | 76.5 | 155.4 | 217.2 | 195.3 |
| -20% | 218.4 | 221.3 | 107.5 | 196.3 | 180.8 | 211.0 | |
| -40% | | 199.1 | 277.1 | 61.2 | 183.5 | 397.8 | |

Stiffness (N/mm)

| | LAT | | | | | | |
|---|---|---|---|---|---|---|---|
| AP | -45% | -30% | -15% | 0% | 15% | 30% | 45% |
| 40% | | | 235.0 | 174.1 | 124.9 | | |
| 20% | | 110.5 | 70.8 | 67.2 | 91.8 | 79.1 | |
| 0% | 160.3 | 155.9 | 124.9 | 126.8 | 113.8 | 175.9 | 139.8 |
| -20% | 203.7 | 152.7 | 219.3 | 230.2 | 206.7 | 153.9 | |
| -40% | | 221.4 | 130.1 | 97.3 | 145.2 | 217.8 | |

r-Squared

| | LAT | | | | | | |
|---|---|---|---|---|---|---|---|
| AP | -45% | -30% | -15% | 0% | 15% | 30% | 45% |
| 40% | | | 0.999 | 0.999 | 0.998 | | |
| 20% | | 0.999 | 0.995 | 0.996 | 0.999 | 0.995 | |
| 0% | 0.999 | 0.998 | 0.996 | 0.996 | 1.000 | 0.998 | 0.999 |
| -20% | 1.000 | 0.997 | 0.999 | 1.000 | 0.999 | 1.000 | |
| -40% | | 0.998 | 0.997 | 0.998 | 0.999 | 1.000 | |

**Specimen 1017_S1_s**

Failure Load (N)

| | LAT | | | | | | |
|---|---|---|---|---|---|---|---|
| AP | -45% | -30% | -15% | 0% | 15% | 30% | 45% |
| 40% | | | 176.4 | 136.4 | 143.7 | | |
| 20% | | 138.0 | 302.4 | 180.4 | 109.6 | 199.7 | |
| 0% | 252.3 | 157.5 | 261.6 | 153.7 | 141.9 | 175.2 | 262.8 |
| -20% | 284.1 | 113.9 | 280.4 | 190.0 | 191.1 | 253.2 | 260.6 |
| -40% | | 118.0 | 287.5 | 193.0 | 228.7 | 171.5 | |

Stiffness (N/mm)

| | LAT | | | | | | |
|---|---|---|---|---|---|---|---|
| AP | -45% | -30% | -15% | 0% | 15% | 30% | 45% |
| 40% | | | 148.4 | 173.1 | 181.8 | | |
| 20% | | 60.5 | 179.3 | 107.3 | 205.7 | 131.6 | |
| 0% | 187.0 | 112.5 | 175.1 | 122.3 | 253.2 | 114.8 | 228.5 |
| -20% | 166.8 | 111.7 | 257.4 | 122.3 | 80.4 | 116.8 | 202.5 |
| -40% | | 136.7 | 149.9 | 255.7 | 179.4 | 89.2 | |

r-Squared

| | LAT | | | | | | |
|---|---|---|---|---|---|---|---|
| AP | -45% | -30% | -15% | 0% | 15% | 30% | 45% |
| 40% | | | 1.000 | 0.999 | 0.999 | | |
| 20% | | 0.994 | 0.999 | 0.998 | 0.999 | 0.999 | |
| 0% | 0.999 | 0.995 | 0.999 | 0.998 | 1.000 | 0.999 | 1.000 |
| -20% | 0.999 | 0.999 | 0.999 | 1.000 | 0.999 | 0.999 | 1.000 |
| -40% | | 0.997 | 0.999 | 0.998 | 0.999 | 0.996 | |

Table A.5: Endplate Maps continued

**Specimen 1018_L5_s**

Failure Load (N)

| | LAT | | | | | | |
|---|---|---|---|---|---|---|---|
| AP | -45% | -30% | -15% | 0% | 15% | 30% | 45% |
| 40% | | | 203.8 | 48.9 | 112.5 | | |
| 20% | | 71.2 | 44.0 | 62.5 | 45.1 | 41.8 | |
| 0% | 75.1 | 37.2 | 20.1 | 19.0 | 25.2 | 41.1 | 48.1 |
| -20% | 90.5 | 127.2 | 52.1 | 46.7 | 64.0 | 83.7 | 66.6 |
| -40% | | 470.0 | 142.0 | 143.8 | 163.0 | 356.1 | |

Stiffness (N/mm)

| | LAT | | | | | | |
|---|---|---|---|---|---|---|---|
| AP | -45% | -30% | -15% | 0% | 15% | 30% | 45% |
| 40% | | | 157.3 | 90.8 | 178.8 | | |
| 20% | | 122.8 | 129.1 | 139.8 | 59.9 | 62.3 | |
| 0% | 174.6 | 92.4 | 31.1 | 53.4 | 15.8 | 80.0 | 65.1 |
| -20% | 187.3 | 259.8 | 125.3 | 51.7 | 137.9 | 148.5 | 129.8 |
| -40% | | 334.0 | 112.9 | 156.3 | 93.7 | 231.8 | |

r-Squared

| | LAT | | | | | | |
|---|---|---|---|---|---|---|---|
| AP | -45% | -30% | -15% | 0% | 15% | 30% | 45% |
| 40% | | | 0.999 | 0.995 | 0.990 | | |
| 20% | | 0.997 | 0.996 | 0.988 | 0.980 | 0.995 | |
| 0% | 0.998 | 0.997 | 0.902 | 0.963 | 0.746 | 0.992 | 0.982 |
| -20% | 0.992 | 0.999 | 0.992 | 0.962 | 0.997 | 0.999 | 0.996 |
| -40% | | 0.999 | 0.995 | 0.997 | 0.996 | 0.999 | |

**Specimen 1018_L5_i**

Failure Load (N)

| | LAT | | | | | | |
|---|---|---|---|---|---|---|---|
| AP | -45% | -30% | -15% | 0% | 15% | 30% | 45% |
| 40% | | | 202.0 | 43.7 | 161.4 | | |
| 20% | | 321.5 | 79.8 | 40.1 | 61.6 | 291.0 | |
| 0% | 164.7 | 285.0 | 66.8 | 106.2 | 58.4 | 201.3 | 464.8 |
| -20% | 245.1 | | 260.2 | 153.5 | 230.6 | 304.6 | 617.3 |
| -40% | | 411.2 | 184.0 | 138.7 | 169.8 | 336.1 | |

Stiffness (N/mm)

| | LAT | | | | | | |
|---|---|---|---|---|---|---|---|
| AP | -45% | -30% | -15% | 0% | 15% | 30% | 45% |
| 40% | | | 196.9 | 71.5 | 202.1 | | |
| 20% | | 335.2 | 162.7 | 102.0 | 147.7 | 263.0 | |
| 0% | 258.5 | 228.1 | 77.8 | 222.7 | 58.3 | 241.7 | 224.6 |
| -20% | 194.9 | | 235.7 | 218.8 | 222.4 | 216.9 | 189.0 |
| -40% | | 319.1 | 215.8 | 70.3 | 193.4 | 305.4 | |

r-Squared

| | LAT | | | | | | |
|---|---|---|---|---|---|---|---|
| AP | -45% | -30% | -15% | 0% | 15% | 30% | 45% |
| 40% | | | 0.997 | 0.988 | 0.999 | | |
| 20% | | 1.000 | 0.999 | 0.996 | 0.997 | 0.998 | |
| 0% | 0.998 | 0.999 | 0.992 | 0.996 | 0.989 | 0.999 | 1.000 |
| -20% | 0.998 | | 0.999 | 0.993 | 0.999 | 0.996 | 0.999 |
| -40% | | 1.000 | 1.000 | 0.993 | 0.998 | 1.000 | |

**Specimen 1019_L3_s**

Failure Load (N)

| | LAT | | | | | | |
|---|---|---|---|---|---|---|---|
| AP | -45% | -30% | -15% | 0% | 15% | 30% | 45% |
| 40% | | | 126.2 | 59.7 | 80.6 | | |
| 20% | | 62.6 | 31.3 | 37.0 | 36.6 | 39.7 | |
| 0% | 91.1 | 65.5 | 47.7 | 40.7 | 42.0 | 40.7 | 90.8 |
| -20% | 81.9 | 94.9 | 65.3 | 46.0 | 49.4 | 55.5 | 75.0 |
| -40% | | 135.9 | 100.8 | 63.4 | 80.8 | 98.3 | 127.8 |

Stiffness (N/mm)

| | LAT | | | | | | |
|---|---|---|---|---|---|---|---|
| AP | -45% | -30% | -15% | 0% | 15% | 30% | 45% |
| 40% | | | 110.1 | 123.5 | 77.9 | | |
| 20% | | 185.3 | 58.1 | 104.2 | 71.5 | 81.4 | |
| 0% | 275.2 | 139.9 | 86.7 | 146.8 | 98.9 | 66.3 | 211.9 |
| -20% | 224.3 | 140.6 | 141.3 | 133.8 | 130.1 | 96.0 | 121.7 |
| -40% | | 142.2 | 150.9 | 185.7 | 164.8 | 207.3 | 177.6 |

r-Squared

| | LAT | | | | | | |
|---|---|---|---|---|---|---|---|
| AP | -45% | -30% | -15% | 0% | 15% | 30% | 45% |
| 40% | | | 0.998 | 0.997 | 0.998 | | |
| 20% | | 0.999 | 0.994 | 0.998 | 0.998 | 0.994 | |
| 0% | 1.000 | 0.999 | 0.990 | 0.995 | 0.995 | 0.996 | 0.999 |
| -20% | 0.999 | 0.998 | 0.998 | 0.999 | 0.999 | 0.998 | 0.999 |
| -40% | | 0.999 | 0.998 | 0.999 | 0.999 | 1.000 | 0.999 |

**Specimen 1019_L3_i**

Failure Load (N)

| | LAT | | | | | | |
|---|---|---|---|---|---|---|---|
| AP | -45% | -30% | -15% | 0% | 15% | 30% | 45% |
| 40% | | | 75.5 | 83.0 | 113.1 | | |
| 20% | | 65.1 | 44.5 | 97.6 | 56.5 | 46.2 | |
| 0% | 89.8 | 92.2 | 83.6 | 71.3 | 99.9 | 187.3 | 107.3 |
| -20% | | 197.9 | 103.5 | 96.7 | 174.8 | 285.3 | 202.9 |
| -40% | | 163.1 | 206.7 | 127.5 | 315.2 | 206.8 | 265.1 |

Stiffness (N/mm)

| | LAT | | | | | | |
|---|---|---|---|---|---|---|---|
| AP | -45% | -30% | -15% | 0% | 15% | 30% | 45% |
| 40% | | | 91.2 | 127.9 | 165.4 | | |
| 20% | | 113.1 | 90.9 | 255.2 | 89.9 | 86.0 | |
| 0% | 176.8 | 93.8 | 150.3 | 94.5 | 146.4 | 324.9 | 217.5 |
| -20% | | 286.6 | 154.7 | 246.8 | 232.2 | 368.4 | 89.2 |
| -40% | | 149.9 | 180.5 | 173.9 | 287.5 | 319.1 | 125.1 |

r-Squared

| | LAT | | | | | | |
|---|---|---|---|---|---|---|---|
| AP | -45% | -30% | -15% | 0% | 15% | 30% | 45% |
| 40% | | | 0.993 | 0.998 | 0.999 | | |
| 20% | | 0.999 | 0.983 | 0.999 | 0.995 | 0.998 | |
| 0% | 0.998 | 0.982 | 0.998 | 0.998 | 0.985 | 0.999 | 0.999 |
| -20% | | 0.999 | 0.999 | 1.000 | 0.999 | 1.000 | 0.997 |
| -40% | | 0.998 | 0.999 | 0.996 | 1.000 | 0.999 | 0.998 |

Table A.5: Endplate Maps continued

**Specimen 1019_L4_s**

Failure Load (N)

| | LAT | | | | | | |
|---|---|---|---|---|---|---|---|
| AP | -45% | -30% | -15% | 0% | 15% | 30% | 45% |
| 40% | | | | | | | |
| 20% | | | | 28.0 | | | |
| 0% | 59.6 | 33.4 | 36.0 | 25.6 | 35.8 | 44.7 | 80.9 |
| -20% | 49.5 | 35.6 | 43.1 | 45.3 | 43.1 | 50.5 | 56.6 |
| -40% | | 75.2 | 59.4 | 45.2 | 24.8 | 77.5 | |

Stiffness (N/mm)

| | LAT | | | | | | |
|---|---|---|---|---|---|---|---|
| AP | -45% | -30% | -15% | 0% | 15% | 30% | 45% |
| 40% | | | | | | | |
| 20% | | | | 68.2 | | | |
| 0% | 83.0 | 88.5 | 75.2 | 95.4 | 87.7 | 69.8 | 155.4 |
| -20% | 135.9 | 91.0 | 118.5 | 92.4 | 86.0 | 141.1 | 117.0 |
| -40% | | 82.2 | 103.1 | 105.2 | 59.5 | 98.4 | |

r-Squared

| | LAT | | | | | | |
|---|---|---|---|---|---|---|---|
| AP | -45% | -30% | -15% | 0% | 15% | 30% | 45% |
| 40% | | | | | | | |
| 20% | | | | 0.994 | | | |
| 0% | 0.998 | 0.996 | 0.997 | 0.998 | 0.996 | 0.999 | 0.998 |
| -20% | 0.998 | 0.998 | 0.999 | 0.998 | 0.998 | 0.998 | 0.997 |
| -40% | | 0.999 | 0.996 | 0.998 | 0.989 | 0.997 | |

**Specimen 1019_L4_i**

Failure Load (N)

| | LAT | | | | | | |
|---|---|---|---|---|---|---|---|
| AP | -45% | -30% | -15% | 0% | 15% | 30% | 45% |
| 40% | | | 78.1 | 113.9 | 98.2 | | |
| 20% | | 90.0 | 33.2 | 103.1 | 56.6 | 72.9 | |
| 0% | 151.0 | 94.0 | 97.2 | 79.8 | 101.7 | 107.3 | |
| -20% | | 110.0 | 144.7 | 81.5 | 118.0 | 120.0 | |
| -40% | | 253.1 | 290.9 | 75.4 | 184.9 | | |

Stiffness (N/mm)

| | LAT | | | | | | |
|---|---|---|---|---|---|---|---|
| AP | -45% | -30% | -15% | 0% | 15% | 30% | 45% |
| 40% | | | 89.8 | 176.0 | 167.1 | | |
| 20% | | 75.0 | 52.3 | 97.1 | 67.7 | 78.8 | |
| 0% | 144.6 | 95.0 | 131.2 | 110.7 | 114.8 | 181.9 | |
| -20% | | 105.5 | 229.2 | 187.3 | 200.0 | 155.4 | |
| -40% | | 279.8 | 245.9 | 116.9 | 227.4 | | |

r-Squared

| | LAT | | | | | | |
|---|---|---|---|---|---|---|---|
| AP | -45% | -30% | -15% | 0% | 15% | 30% | 45% |
| 40% | | | 0.998 | 0.999 | 0.999 | | |
| 20% | | 0.996 | 0.992 | 0.999 | 0.991 | 0.998 | |
| 0% | 0.999 | 0.998 | 0.997 | 0.998 | 0.998 | 0.999 | |
| -20% | | 0.999 | 1.000 | 0.998 | 0.999 | 0.998 | |
| -40% | | 1.000 | 0.999 | 0.993 | 0.999 | | |

**Specimen 1019_L5_i**

Failure Load (N)

| | LAT | | | | | | |
|---|---|---|---|---|---|---|---|
| AP | -45% | -30% | -15% | 0% | 15% | 30% | 45% |
| 40% | | | 56.7 | 72.1 | | | |
| 20% | | 56.3 | 51.2 | 28.7 | 40.7 | 107.0 | |
| 0% | 66.0 | 118.9 | 91.7 | 79.3 | 109.0 | 116.9 | |
| -20% | | 242.3 | 131.7 | 56.0 | 126.7 | 217.6 | |
| -40% | | | 163.8 | 58.1 | 111.7 | 203.8 | |

Stiffness (N/mm)

| | LAT | | | | | | |
|---|---|---|---|---|---|---|---|
| AP | -45% | -30% | -15% | 0% | 15% | 30% | 45% |
| 40% | | | 39.3 | 38.5 | | | |
| 20% | | 141.2 | 80.0 | 56.7 | 40.7 | 120.4 | |
| 0% | 111.0 | 260.4 | 143.4 | 105.1 | 187.2 | 165.4 | |
| -20% | | 271.2 | 213.7 | 97.4 | 289.8 | 188.5 | |
| -40% | | | 81.7 | 74.1 | 166.0 | 226.3 | |

r-Squared

| | LAT | | | | | | |
|---|---|---|---|---|---|---|---|
| AP | -45% | -30% | -15% | 0% | 15% | 30% | 45% |
| 40% | | | 0.993 | 0.997 | | | |
| 20% | | 0.999 | 0.999 | 0.995 | 0.995 | 0.999 | |
| 0% | 0.998 | 1.000 | 1.000 | 0.998 | 0.999 | 0.999 | |
| -20% | | 0.999 | 0.998 | 0.999 | 0.996 | 1.000 | |
| -40% | | | 0.998 | 0.991 | 0.998 | 0.999 | |

Table A.5: Endplate Maps continued

**Specimen 1019_S1_s**

Failure Load (N)

| | LAT | | | | | | |
|---|---|---|---|---|---|---|---|
| AP | -45% | -30% | -15% | 0% | 15% | 30% | 45% |
| 40% | | | 35.8 | 41.4 | 23.9 | | |
| 20% | | 50.5 | 37.1 | 30.0 | 28.9 | 28.3 | |
| 0% | 51.6 | 57.5 | 48.9 | 68.1 | 35.8 | 53.7 | 52.8 |
| -20% | 67.0 | 89.8 | 66.3 | 104.2 | 63.7 | 93.7 | 63.4 |
| -40% | | 152.1 | 269.7 | 333.9 | 218.6 | 339.1 | |

Stiffness (N/mm)

| | LAT | | | | | | |
|---|---|---|---|---|---|---|---|
| AP | -45% | -30% | -15% | 0% | 15% | 30% | 45% |
| 40% | | | 65.2 | 50.9 | 24.6 | | |
| 20% | | 44.0 | 34.5 | 105.7 | 32.1 | 25.1 | |
| 0% | 38.3 | 97.8 | 57.9 | 37.7 | 44.2 | 66.3 | 60.3 |
| -20% | 63.3 | 135.2 | 50.8 | 113.5 | 34.6 | 96.2 | 42.5 |
| -40% | | 165.2 | 180.5 | 266.2 | 213.9 | 178.8 | |

r-Squared

| | LAT | | | | | | |
|---|---|---|---|---|---|---|---|
| AP | -45% | -30% | -15% | 0% | 15% | 30% | 45% |
| 40% | | | 0.998 | 0.994 | 0.982 | | |
| 20% | | 0.995 | 0.996 | 0.999 | 0.988 | 0.991 | |
| 0% | 0.996 | 0.998 | 0.997 | 0.993 | 0.983 | 0.998 | 0.996 |
| -20% | 0.995 | 0.999 | 0.990 | 0.998 | 0.995 | 0.998 | 0.995 |
| -40% | | 0.999 | 0.998 | 0.999 | 0.999 | 0.999 | |

**Specimen 1021_L3_s**

Failure Load (N)

| | LAT | | | | | | |
|---|---|---|---|---|---|---|---|
| AP | -45% | -30% | -15% | 0% | 15% | 30% | 45% |
| 40% | | | 262.2 | 75.6 | 74.8 | | |
| 20% | | 150.8 | 51.8 | | 46.9 | 110.5 | |
| 0% | 194.9 | 78.6 | 84.5 | 73.0 | 49.8 | 65.6 | 184.1 |
| -20% | 63.6 | 78.9 | 42.8 | 53.3 | 51.9 | 69.4 | 68.4 |
| -40% | | 165.5 | 33.4 | 30.3 | 19.5 | 96.9 | |

Stiffness (N/mm)

| | LAT | | | | | | |
|---|---|---|---|---|---|---|---|
| AP | -45% | -30% | -15% | 0% | 15% | 30% | 45% |
| 40% | | | 229.5 | 70.5 | 51.9 | | |
| 20% | | 275.3 | 111.7 | | 83.0 | 185.3 | |
| 0% | 283.4 | 151.3 | 102.2 | 129.8 | 66.4 | 119.0 | 262.6 |
| -20% | 97.9 | 116.5 | 60.3 | 80.6 | 103.8 | 94.3 | 176.9 |
| -40% | | 130.1 | 42.1 | 48.0 | 12.9 | 167.6 | |

r-Squared

| | LAT | | | | | | |
|---|---|---|---|---|---|---|---|
| AP | -45% | -30% | -15% | 0% | 15% | 30% | 45% |
| 40% | | | 1.000 | 0.998 | 0.997 | | |
| 20% | | 1.000 | 0.998 | | 0.997 | 0.999 | |
| 0% | 1.000 | 0.999 | 1.000 | 0.999 | 0.998 | 0.999 | 0.999 |
| -20% | 0.997 | 0.996 | 0.995 | 0.995 | 0.996 | 0.997 | 0.999 |
| -40% | | 0.998 | 0.992 | 0.991 | 0.964 | 1.000 | |

**Specimen 1021_L3_i**

Failure Load (N)

| | LAT | | | | | | |
|---|---|---|---|---|---|---|---|
| AP | -45% | -30% | -15% | 0% | 15% | 30% | 45% |
| 40% | | | 117.2 | 151.9 | 77.8 | | |
| 20% | | 76.3 | 30.3 | 83.9 | 75.8 | 75.3 | |
| 0% | 124.0 | 90.2 | 52.8 | 47.1 | 50.3 | 85.5 | |
| -20% | 201.4 | 211.9 | 143.5 | 68.1 | 78.4 | 187.7 | |
| -40% | | 255.3 | 60.7 | 75.6 | 91.4 | 241.2 | |

Stiffness (N/mm)

| | LAT | | | | | | |
|---|---|---|---|---|---|---|---|
| AP | -45% | -30% | -15% | 0% | 15% | 30% | 45% |
| 40% | | | 138.4 | 151.0 | 132.6 | | |
| 20% | | 198.2 | 68.6 | 163.4 | 137.5 | 176.2 | |
| 0% | 289.1 | 159.5 | 149.4 | 91.2 | 104.5 | 181.8 | |
| -20% | 160.0 | 238.7 | 152.9 | 111.1 | 53.1 | 302.2 | |
| -40% | | 301.9 | 77.7 | 82.1 | 100.0 | 259.5 | |

r-Squared

| | LAT | | | | | | |
|---|---|---|---|---|---|---|---|
| AP | -45% | -30% | -15% | 0% | 15% | 30% | 45% |
| 40% | | | 0.989 | 0.999 | 0.998 | | |
| 20% | | 0.999 | 0.996 | 0.999 | 0.987 | 0.997 | |
| 0% | 0.999 | 0.997 | 0.999 | 0.998 | 0.996 | 0.999 | |
| -20% | 0.997 | 0.999 | 0.999 | 0.999 | 0.998 | 1.000 | |
| -40% | | 1.000 | 0.996 | 0.999 | 0.995 | 1.000 | |

Table A.5: Endplate Maps continued

**Specimen 1021_L4_s**

Failure Load (N)

| AP \ LAT | -45% | -30% | -15% | 0% | 15% | 30% | 45% |
|---|---|---|---|---|---|---|---|
| 40% | | | 221.1 | 128.7 | | | |
| 20% | | 186.0 | 134.5 | 70.2 | 67.8 | 133.4 | |
| 0% | 60.0 | 138.4 | 120.0 | 66.1 | 58.9 | 74.6 | 161.1 |
| -20% | 66.0 | 187.7 | 105.9 | 58.6 | 76.4 | 91.7 | |
| -40% | | 217.3 | 60.4 | 40.4 | 82.5 | 221.1 | |

Stiffness (N/mm)

| AP \ LAT | -45% | -30% | -15% | 0% | 15% | 30% | 45% |
|---|---|---|---|---|---|---|---|
| 40% | | | 166.7 | 90.4 | | | |
| 20% | | 203.6 | 130.5 | 97.2 | 95.6 | 168.8 | |
| 0% | 147.3 | 224.2 | 118.8 | 86.9 | 108.5 | 222.7 | 133.6 |
| -20% | 190.0 | 281.2 | 183.7 | 107.4 | 52.3 | 123.9 | |
| -40% | | 172.4 | 66.9 | 55.2 | 138.6 | 296.8 | |

r-Squared

| AP \ LAT | -45% | -30% | -15% | 0% | 15% | 30% | 45% |
|---|---|---|---|---|---|---|---|
| 40% | | | 1.000 | 0.999 | | | |
| 20% | | 0.999 | 0.999 | 0.990 | 0.998 | 0.999 | |
| 0% | 0.998 | 1.000 | 0.999 | 0.999 | 0.999 | 0.999 | 0.999 |
| -20% | 0.998 | 1.000 | 1.000 | 0.996 | 0.996 | 0.998 | |
| -40% | | 0.999 | 0.997 | 0.998 | 0.997 | 0.999 | |

**Specimen 1021_L4_i**

Failure Load (N)

| AP \ LAT | -45% | -30% | -15% | 0% | 15% | 30% | 45% |
|---|---|---|---|---|---|---|---|
| 40% | | | 265.3 | 102.9 | 139.1 | | |
| 20% | | 87.9 | 47.5 | 80.9 | 49.0 | 61.7 | |
| 0% | 265.5 | 61.1 | 36.3 | 26.6 | 44.0 | 67.4 | 61.1 |
| -20% | 339.1 | 120.1 | 60.7 | 49.5 | 60.9 | 117.6 | 85.8 |
| -40% | | 214.6 | 107.7 | 19.6 | 68.6 | 99.2 | |

Stiffness (N/mm)

| AP \ LAT | -45% | -30% | -15% | 0% | 15% | 30% | 45% |
|---|---|---|---|---|---|---|---|
| 40% | | | 270.6 | 247.4 | 202.9 | | |
| 20% | | 52.8 | 90.7 | 97.3 | 71.4 | 182.5 | |
| 0% | 215.1 | 38.4 | 59.5 | 31.4 | 68.4 | 74.5 | 96.8 |
| -20% | 279.6 | 161.6 | 82.6 | 90.1 | 137.5 | 143.4 | 55.8 |
| -40% | | 251.2 | 236.9 | 52.0 | 110.3 | 194.1 | |

r-Squared

| AP \ LAT | -45% | -30% | -15% | 0% | 15% | 30% | 45% |
|---|---|---|---|---|---|---|---|
| 40% | | | 0.999 | 0.998 | 0.998 | | |
| 20% | | 0.977 | 0.999 | 0.993 | 0.999 | 0.999 | |
| 0% | 0.999 | 0.997 | 0.985 | 0.993 | 0.999 | 0.999 | 0.996 |
| -20% | 1.000 | 0.999 | 0.993 | 0.993 | 0.996 | 0.998 | 0.994 |
| -40% | | 0.999 | 0.999 | 0.984 | 0.998 | 0.999 | |

**Specimen 1021_L5_s**

Failure Load (N)

| AP \ LAT | -45% | -30% | -15% | 0% | 15% | 30% | 45% |
|---|---|---|---|---|---|---|---|
| 40% | | | 278.9 | 175.8 | 269.2 | | |
| 20% | | 363.0 | 114.6 | 54.4 | 81.2 | 261.4 | |
| 0% | | 162.6 | 57.5 | 38.3 | 42.3 | 113.0 | 424.6 |
| -20% | 94.5 | 108.3 | 65.3 | 28.3 | 67.6 | 81.4 | 253.1 |
| -40% | | 201.8 | 93.9 | 28.4 | 90.1 | 285.7 | |

Stiffness (N/mm)

| AP \ LAT | -45% | -30% | -15% | 0% | 15% | 30% | 45% |
|---|---|---|---|---|---|---|---|
| 40% | | | 227.4 | 96.4 | 244.2 | | |
| 20% | | 196.5 | 209.9 | 85.9 | 155.3 | 284.9 | |
| 0% | | 200.2 | 121.9 | 96.5 | 119.1 | 234.0 | 270.2 |
| -20% | 85.0 | 164.0 | 106.7 | 107.7 | 149.7 | 157.8 | 245.6 |
| -40% | | 243.4 | 124.5 | 64.6 | 167.6 | 128.0 | |

r-Squared

| AP \ LAT | -45% | -30% | -15% | 0% | 15% | 30% | 45% |
|---|---|---|---|---|---|---|---|
| 40% | | | 1.000 | 0.998 | 1.000 | | |
| 20% | | 1.000 | 0.999 | 0.997 | 0.998 | 0.999 | |
| 0% | | 0.999 | 0.995 | 0.997 | 0.998 | 1.000 | 1.000 |
| -20% | 0.999 | 0.999 | 0.997 | 0.996 | 0.998 | 0.999 | 1.000 |
| -40% | | 0.999 | 0.998 | 0.993 | 0.997 | 0.999 | |

**Specimen 1021_L5_i**

Failure Load (N)

| AP \ LAT | -45% | -30% | -15% | 0% | 15% | 30% | 45% |
|---|---|---|---|---|---|---|---|
| 40% | | | 82.4 | 61.9 | 109.6 | | |
| 20% | | 62.7 | 81.8 | 41.1 | 64.8 | 123.7 | |
| 0% | 115.5 | 68.6 | 61.5 | 53.0 | 50.3 | 86.1 | 130.2 |
| -20% | 70.3 | 126.0 | 92.3 | 65.4 | 89.1 | 109.3 | |
| -40% | | | 252.9 | 83.6 | 124.8 | | |

Stiffness (N/mm)

| AP \ LAT | -45% | -30% | -15% | 0% | 15% | 30% | 45% |
|---|---|---|---|---|---|---|---|
| 40% | | | 145.3 | 124.5 | 206.4 | | |
| 20% | | 79.2 | 131.8 | 81.1 | 111.8 | 179.2 | |
| 0% | 99.0 | 113.9 | 163.3 | 90.7 | 99.5 | 90.1 | 199.8 |
| -20% | 101.5 | 145.4 | 217.0 | 111.6 | 215.8 | 134.5 | |
| -40% | | | 221.7 | 116.3 | 90.2 | | |

r-Squared

| AP \ LAT | -45% | -30% | -15% | 0% | 15% | 30% | 45% |
|---|---|---|---|---|---|---|---|
| 40% | | | 0.997 | 0.996 | 0.996 | | |
| 20% | | 0.996 | 0.995 | 0.991 | 0.995 | 0.999 | |
| 0% | 0.997 | 0.993 | 0.986 | 0.998 | 0.996 | 0.992 | 0.999 |
| -20% | 0.998 | 0.998 | 0.998 | 0.998 | 0.997 | 0.998 | |
| -40% | | | 1.000 | 0.992 | 0.994 | | |

Table A.5: Endplate Maps continued

**Specimen 1021_S1_s**

Failure Load (N)

| | LAT | | | | | | |
|---|---|---|---|---|---|---|---|
| AP | -45% | -30% | -15% | 0% | 15% | 30% | 45% |
| 40% | | | 84.6 | 106.3 | 86.3 | | |
| 20% | | 140.2 | 55.0 | 64.9 | 70.6 | 111.4 | |
| 0% | 125.3 | 133.1 | 84.3 | 72.3 | 89.5 | 178.1 | 146.6 |
| -20% | 131.2 | 241.4 | 155.1 | 195.6 | 275.5 | 164.3 | |
| -40% | | 529.3 | 411.5 | 370.1 | 260.1 | 411.5 | |

Stiffness (N/mm)

| | LAT | | | | | | |
|---|---|---|---|---|---|---|---|
| AP | -45% | -30% | -15% | 0% | 15% | 30% | 45% |
| 40% | | | 71.8 | 151.8 | 201.5 | | |
| 20% | | 137.8 | 77.7 | 110.0 | 102.1 | 126.9 | |
| 0% | 215.3 | 106.1 | 170.5 | 110.9 | 139.8 | 239.5 | 210.6 |
| -20% | 123.0 | 172.1 | 167.6 | 173.1 | 210.6 | 140.1 | |
| -40% | | 335.8 | 344.7 | 217.4 | 345.1 | 299.5 | |

r-Squared

| | LAT | | | | | | |
|---|---|---|---|---|---|---|---|
| AP | -45% | -30% | -15% | 0% | 15% | 30% | 45% |
| 40% | | | 0.997 | 0.999 | 0.999 | | |
| 20% | | 1.000 | 0.994 | 0.998 | 0.999 | 0.999 | |
| 0% | 1.000 | 0.998 | 0.999 | 0.998 | 0.997 | 0.998 | 0.999 |
| -20% | 0.997 | 0.999 | 0.999 | 0.999 | 1.000 | 0.999 | |
| -40% | | 1.000 | 1.000 | 1.000 | 1.000 | 1.000 | |

**Specimen 1023_L3_s**

Failure Load (N)

| | LAT | | | | | | |
|---|---|---|---|---|---|---|---|
| AP | -45% | -30% | -15% | 0% | 15% | 30% | 45% |
| 40% | | | 8.4 | 13.9 | 33.5 | | |
| 20% | | 33.5 | 27.2 | 31.4 | 25.8 | 66.3 | |
| 0% | 92.8 | 22.4 | 48.0 | 34.3 | 46.4 | 18.8 | 32.6 |
| -20% | 64.9 | 43.6 | 52.5 | 42.1 | 21.0 | 39.3 | 26.8 |
| -40% | | 80.1 | 35.8 | 50.2 | 36.6 | 70.8 | 174.4 |

Stiffness (N/mm)

| | LAT | | | | | | |
|---|---|---|---|---|---|---|---|
| AP | -45% | -30% | -15% | 0% | 15% | 30% | 45% |
| 40% | | | 11.7 | 23.3 | 87.2 | | |
| 20% | | 62.6 | 80.0 | 67.3 | 40.4 | 129.8 | |
| 0% | 114.8 | 55.2 | 100.4 | 35.5 | 71.1 | 38.2 | 60.8 |
| -20% | 72.1 | 107.1 | 68.7 | 52.5 | 36.4 | 99.3 | 77.8 |
| -40% | | 93.7 | 62.0 | 38.3 | 97.4 | 95.5 | 178.7 |

r-Squared

| | LAT | | | | | | |
|---|---|---|---|---|---|---|---|
| AP | -45% | -30% | -15% | 0% | 15% | 30% | 45% |
| 40% | | | 0.912 | 0.942 | 0.995 | | |
| 20% | | 0.996 | 0.985 | 0.993 | 0.992 | 0.995 | |
| 0% | 0.999 | 0.988 | 0.999 | 0.989 | 0.993 | 0.996 | 0.995 |
| -20% | 0.997 | 0.995 | 0.995 | 0.994 | 0.991 | 0.996 | 0.988 |
| -40% | | 0.997 | 0.994 | 0.972 | 0.998 | 0.994 | 0.999 |

Table A.5: Endplate Maps continued

**Specimen 1023_L4_i**

Failure Load (N)

| | LAT | | | | | | |
|---|---|---|---|---|---|---|---|
| AP | -45% | -30% | -15% | 0% | 15% | 30% | 45% |
| 40% | | | 40.3 | 61.6 | 86.5 | | |
| 20% | | 36.6 | 45.2 | 41.9 | 55.6 | 68.8 | |
| 0% | 67.0 | 38.9 | 68.0 | 71.3 | 74.6 | 47.1 | 53.7 |
| -20% | | 141.1 | 88.6 | 96.3 | 101.3 | 79.1 | 93.6 |
| -40% | | | 55.2 | 58.8 | 33.2 | 122.3 | |

Stiffness (N/mm)

| | LAT | | | | | | |
|---|---|---|---|---|---|---|---|
| AP | -45% | -30% | -15% | 0% | 15% | 30% | 45% |
| 40% | | | 72.4 | 76.5 | 247.9 | | |
| 20% | | 144.6 | 75.8 | 80.6 | 64.5 | 228.3 | |
| 0% | 112.7 | 87.1 | 69.2 | 107.6 | 84.1 | 63.2 | 66.9 |
| -20% | | 206.5 | 179.0 | 170.1 | 180.5 | 115.3 | 156.4 |
| -40% | | | 74.3 | 54.2 | 49.4 | 137.2 | |

r-Squared

| | LAT | | | | | | |
|---|---|---|---|---|---|---|---|
| AP | -45% | -30% | -15% | 0% | 15% | 30% | 45% |
| 40% | | | 0.998 | 0.993 | 0.998 | | |
| 20% | | 0.998 | 0.999 | 0.997 | 0.998 | 0.999 | |
| 0% | 0.999 | 0.999 | 0.998 | 0.999 | 0.998 | 0.996 | 0.996 |
| -20% | | 0.999 | 0.998 | 1.000 | 0.999 | 0.999 | 0.998 |
| -40% | | | 0.997 | 0.995 | 0.996 | 0.999 | |

**Table A.6: Half-Endplate Maps.** These maps show the results of the indentation tests in the specimens with half of the endplate removed. The negative LAT values denote sites with no endplate, while the positive LAT values denote sites with the endplate intact. The 0% LAT sites were not tested in these endplates. The superior endplates are on the left, the inferior endplates on the right. Three maps are shown for each endplate: the failure load, stiffness, and correlation coefficient ($r^2$) map. (The correlation coefficient indicates how well the line used to calculate the stiffness fit the points on the load-displacement curve. A correlation coefficient of 1 indicates that all of the points lay on the line. A coefficient > 0.95 indicates excellent fit.)

In one endplate, one of the values had to be discarded due to a testing problem. The corresponding value (-LAT) was removed to avoid biasing the results. The good value which was discarded is crossed out in all three maps.

The figure below shows an endplate with the test sites corresponding to the maps labelled.

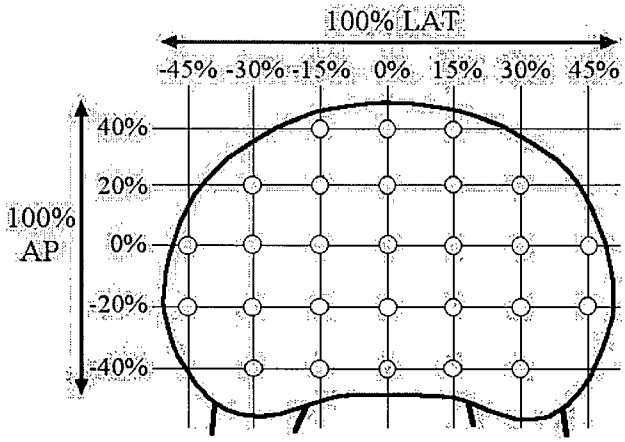


**Half-Endplate Specimen 1018_L3_s**

Failure Load (N)

| AP \ LAT | -45% | -30% | -15% | 0% | 15% | 30% | 45% |
|---|---|---|---|---|---|---|---|
| 40% | | | 262.3 | | 667.2 | | |
| 20% | | 101.2 | 86.7 | | 325.5 | 460.1 | |
| 0% | 41.5 | 22.9 | 25.3 | | 60.2 | 238.1 | 205.6 |
| -20% | 42.5 | 30.7 | 64.7 | | 106.6 | 258.0 | 264.9 |
| -40% | | 57.8 | 143.5 | | 380.2 | 755.5 | |

Stiffness (N/mm)

| AP \ LAT | -45% | -30% | -15% | 0% | 15% | 30% | 45% |
|---|---|---|---|---|---|---|---|
| 40% | | | 280.0 | | 279.5 | | |
| 20% | | 113.5 | 94.5 | | 304.1 | 414.4 | |
| 0% | 78.6 | 21.9 | 43.3 | | 130.2 | 311.9 | 375.5 |
| -20% | 75.1 | 26.3 | 114.9 | | 193.6 | 465.7 | 502.2 |
| -40% | | 63.7 | 211.7 | | 184.6 | 385.1 | |

r-Squared

| AP \ LAT | -45% | -30% | -15% | 0% | 15% | 30% | 45% |
|---|---|---|---|---|---|---|---|
| 40% | | | 0.992 | | 0.999 | | |
| 20% | | 0.986 | 0.848 | | 0.999 | 0.997 | |
| 0% | 0.957 | 0.836 | 0.879 | | 0.963 | 0.998 | 0.997 |
| -20% | 0.900 | 0.756 | 0.970 | | 0.994 | 0.996 | 0.998 |
| -40% | | 0.818 | 0.994 | | 0.998 | 0.998 | |

**Half-Endplate Specimen 1018_L3_i**

Failure Load (N)

| AP \ LAT | -45% | -30% | -15% | 0% | 15% | 30% | 45% |
|---|---|---|---|---|---|---|---|
| 40% | | | 21.7 | | 60.3 | | |
| 20% | | 51.9 | 47.1 | | 35.3 | 119.6 | |
| 0% | 21.2 | 25.5 | 49.0 | | 42.2 | 124.7 | 96.4 |
| -20% | 26.1 | 33.9 | 94.8 | | 142.9 | 240.0 | 104.8 |
| -40% | | 93.4 | 69.5 | | 251.7 | 243.1 | |

Stiffness (N/mm)

| AP \ LAT | -45% | -30% | -15% | 0% | 15% | 30% | 45% |
|---|---|---|---|---|---|---|---|
| 40% | | | 11.5 | | 85.4 | | |
| 20% | | 16.6 | 54.4 | | 51.8 | 323.0 | |
| 0% | 64.6 | 20.4 | 33.1 | | 69.3 | 221.1 | 237.4 |
| -20% | 11.8 | 58.1 | 141.4 | | 347.4 | 266.7 | 286.8 |
| -40% | | 76.4 | 86.0 | | 417.3 | 466.6 | |

r-Squared

| AP \ LAT | -45% | -30% | -15% | 0% | 15% | 30% | 45% |
|---|---|---|---|---|---|---|---|
| 40% | | | 0.535 | | 0.972 | | |
| 20% | | 0.857 | 0.845 | | 0.920 | 0.998 | |
| 0% | 0.838 | 0.578 | 0.945 | | 0.885 | 0.995 | 0.995 |
| -20% | 0.586 | 0.956 | 0.992 | | 0.996 | 0.995 | 0.998 |
| -40% | | 0.967 | 0.983 | | 0.997 | 0.992 | |

Table A.6: Half-Endplate Maps continued

**Half-Endplate Specimen 1018_L4_s**

Failure Load (N)

| AP \ LAT | -45% | -30% | -15% | 0% | 15% | 30% | 45% |
|---|---|---|---|---|---|---|---|
| 40% | | | 44.2 | | 80.6 | | |
| 20% | | 31.5 | 54.2 | | 23.8 | 38.3 | |
| 0% | 45.1 | 21.0 | 24.6 | | 37.5 | 32.6 | 40.0 |
| -20% | 36.8 | 39.7 | 58.7 | | 62.1 | 72.5 | 83.1 |
| -40% | | 145.3 | 81.5 | | 106.2 | 223.6 | |

Stiffness (N/mm)

| AP \ LAT | -45% | -30% | -15% | 0% | 15% | 30% | 45% |
|---|---|---|---|---|---|---|---|
| 40% | | | 170.4 | | 139.0 | | |
| 20% | | 26.1 | 27.8 | | 22.2 | 40.7 | |
| 0% | 128.8 | 27.8 | 15.0 | | 42.9 | 139.6 | 204.5 |
| -20% | 130.2 | 27.7 | 60.4 | | 146.4 | 225.9 | 276.4 |
| -40% | | 102.7 | 90.6 | | 135.5 | 309.9 | |

r-Squared

| AP \ LAT | -45% | -30% | -15% | 0% | 15% | 30% | 45% |
|---|---|---|---|---|---|---|---|
| 40% | | | 0.950 | | 0.995 | | |
| 20% | | 0.887 | 0.870 | | 0.843 | 0.948 | |
| 0% | 0.982 | 0.457 | 0.707 | | 0.922 | 0.980 | 0.997 |
| -20% | 0.988 | 0.939 | 0.935 | | 0.974 | 0.994 | 0.984 |
| -40% | | 0.986 | 0.965 | | 0.990 | 0.998 | |

**Half-Endplate Specimen 1018_L4_i**

Failure Load (N)

| AP \ LAT | -45% | -30% | -15% | 0% | 15% | 30% | 45% |
|---|---|---|---|---|---|---|---|
| 40% | | | 88.3 | | 205.6 | | |
| 20% | | 30.1 | 40.8 | | 85.7 | 133.2 | |
| 0% | 35.1 | 39.3 | 61.9 | | 71.1 | 203.4 | 166.1 |
| -20% | 79.0 | 51.5 | 98.0 | | 210.6 | 346.4 | 166.4 |
| -40% | | 116.8 | 72.6 | | 332.7 | 284.2 | |

Stiffness (N/mm)

| AP \ LAT | -45% | -30% | -15% | 0% | 15% | 30% | 45% |
|---|---|---|---|---|---|---|---|
| 40% | | | 107.1 | | 304.8 | | |
| 20% | | 52.5 | 19.0 | | 189.0 | 274.9 | |
| 0% | 64.5 | 66.8 | 84.2 | | 90.9 | 302.7 | 315.1 |
| -20% | 218.3 | 66.9 | 119.0 | | 288.6 | 270.3 | 352.6 |
| -40% | | 107.0 | 67.2 | | 411.8 | 536.2 | |

r-Squared

| AP \ LAT | -45% | -30% | -15% | 0% | 15% | 30% | 45% |
|---|---|---|---|---|---|---|---|
| 40% | | | 0.947 | | 0.999 | | |
| 20% | | 0.909 | 0.815 | | 0.983 | 0.996 | |
| 0% | 0.917 | 0.840 | 0.960 | | 0.994 | 0.999 | 0.993 |
| -20% | 0.993 | 0.954 | 0.983 | | 0.997 | 0.997 | 0.998 |
| -40% | | 0.977 | 0.917 | | 0.997 | 0.997 | |

**Half-Endplate Specimen 1023_L3_i**

Failure Load (N)

| AP \ LAT | -45% | -30% | -15% | 0% | 15% | 30% | 45% |
|---|---|---|---|---|---|---|---|
| 40% | | | ~~25.6~~ | | | | |
| 20% | | 19.5 | 49.4 | | 56.1 | 21.0 | |
| 0% | 30.5 | 38.4 | 57.7 | | 86.7 | 102.8 | 46.4 |
| -20% | 33.0 | 57.9 | 62.4 | | 155.8 | 119.9 | 83.7 |
| -40% | | 60.8 | 37.4 | | 91.4 | 198.5 | |

Stiffness (N/mm)

| AP \ LAT | -45% | -30% | -15% | 0% | 15% | 30% | 45% |
|---|---|---|---|---|---|---|---|
| 40% | | | ~~39.2~~ | | | | |
| 20% | | 41.9 | 70.2 | | 134.2 | 33.9 | |
| 0% | 19.2 | 77.8 | 79.3 | | 96.9 | 104.9 | 156.1 |
| -20% | 72.3 | 83.8 | 150.8 | | 164.6 | 287.9 | 215.9 |
| -40% | | 64.6 | 87.9 | | 64.3 | 242.9 | |

r-Squared

| AP \ LAT | -45% | -30% | -15% | 0% | 15% | 30% | 45% |
|---|---|---|---|---|---|---|---|
| 40% | | | ~~0.987~~ | | | | |
| 20% | | 0.971 | 0.996 | | 0.999 | 0.968 | |
| 0% | 0.973 | 0.999 | 0.999 | | 0.999 | 0.998 | 0.999 |
| -20% | 0.989 | 0.998 | 0.998 | | 1.000 | 0.999 | 0.999 |
| -40% | | 0.998 | 0.998 | | 0.999 | 0.999 | |

Table A.6: Half-Endplate Maps continued

**Half-Endplate Specimen 1023_L4_s**

Failure Load (N)

| | LAT | | | | | | |
|---|---|---|---|---|---|---|---|
| AP | -45% | -30% | -15% | 0% | 15% | 30% | 45% |
| 40% | | | 60.7 | | 63.2 | | |
| 20% | | 32.8 | 33.7 | | 37.4 | 24.6 | |
| 0% | 35.8 | 37.3 | 44.3 | | 38.2 | 18.8 | 70.0 |
| -20% | 35.9 | 23.1 | 50.2 | | 48.9 | 73.3 | 72.3 |
| -40% | | 33.6 | 44.2 | | 45.9 | 49.1 | |

Stiffness (N/mm)

| | LAT | | | | | | |
|---|---|---|---|---|---|---|---|
| AP | -45% | -30% | -15% | 0% | 15% | 30% | 45% |
| 40% | | | 86.6 | | 82.8 | | |
| 20% | | 68.3 | 62.2 | | 48.8 | 68.0 | |
| 0% | 94.5 | 29.1 | 47.2 | | 77.6 | 29.3 | 142.3 |
| -20% | 61.2 | 50.4 | 85.0 | | 89.8 | 170.3 | 146.2 |
| -40% | | 67.5 | 60.1 | | 73.1 | 75.8 | |

r-Squared

| | LAT | | | | | | |
|---|---|---|---|---|---|---|---|
| AP | -45% | -30% | -15% | 0% | 15% | 30% | 45% |
| 40% | | | 0.998 | | 0.994 | | |
| 20% | | 0.995 | 0.997 | | 0.996 | 0.996 | |
| 0% | 0.998 | 0.996 | 0.999 | | 0.995 | 0.986 | 0.999 |
| -20% | 0.998 | 0.995 | 0.995 | | 0.999 | 0.999 | 0.999 |
| -40% | | 0.995 | 0.999 | | 0.997 | 0.995 | |

**Half-Endplate Specimen 1023_L5_s**

Failure Load (N)

| | LAT | | | | | | |
|---|---|---|---|---|---|---|---|
| AP | -45% | -30% | -15% | 0% | 15% | 30% | 45% |
| 40% | | | 40.8 | | 47.5 | | |
| 20% | | 18.3 | 23.1 | | 30.7 | 42.8 | |
| 0% | 45.6 | 32.0 | 34.7 | | 91.3 | 47.2 | 108.2 |
| -20% | 73.8 | 42.3 | 36.5 | | 113.2 | 81.8 | 100.1 |
| -40% | | 117.1 | 35.1 | | 109.6 | 64.8 | |

Stiffness (N/mm)

| | LAT | | | | | | |
|---|---|---|---|---|---|---|---|
| AP | -45% | -30% | -15% | 0% | 15% | 30% | 45% |
| 40% | | | 44.0 | | 95.3 | | |
| 20% | | 27.8 | 54.4 | | 55.4 | 90.8 | |
| 0% | 92.6 | 62.5 | 73.2 | | 134.2 | 87.9 | 184.4 |
| -20% | 97.0 | 109.1 | 127.8 | | 205.5 | 117.7 | 130.7 |
| -40% | | 131.3 | 67.5 | | 181.1 | 100.4 | |

r-Squared

| | LAT | | | | | | |
|---|---|---|---|---|---|---|---|
| AP | -45% | -30% | -15% | 0% | 15% | 30% | 45% |
| 40% | | | 0.996 | | 0.999 | | |
| 20% | | 0.974 | 0.994 | | 0.999 | 0.999 | |
| 0% | 0.998 | 0.991 | 0.992 | | 0.995 | 0.991 | 0.998 |
| -20% | 0.998 | 0.999 | 0.998 | | 0.999 | 0.999 | 0.999 |
| -40% | | 0.999 | 0.997 | | 1.000 | 0.998 | |

## Appendix B

## Equipment

The equipment used in this study was partially designed and constructed by the investigator, and partially the work of fourth year and summer students. The testing machine frame was designed by a group of fourth year UBC engineering students (1999). The linear actuator and control components were selected and assembled by a summer student (1999). The investigator made modifications to the wiring to reduce the noise in the system and wrote software to run the equipment (Appendix C). The other custom equipment described in this appendix was designed by the investigator.

Since the equipment used in this study was designed with very specific applications in mind and had certain dimensions dictated by existing laboratory facilities, the drawings are not given with full details, since they would not be useful under other circumstances. Instead, basic details and dimensions are provided, such that other investigators can make use of the general design concepts to construct similar equipment using materials available in their own laboratories and make changes as dictated by their own infrastructure. Suppliers are provided, where applicable, to facilitate ordering of parts.

### B.1 Orienter

The orienter was used to hold the test specimen securely during testing, yet allowed the specimen to be levelled prior to testing. The specimen was mounted in the orienter using plaster of Paris. Once the plaster had set, the orienter was mounted on three adjustable legs (threaded rods with nuts which were raised or lowered until the appropriate length was reached) attached to an x-y translating table. The length of the legs was adjusted until the endplate was level, then locking nuts were used to secure the orienter in place on the legs.

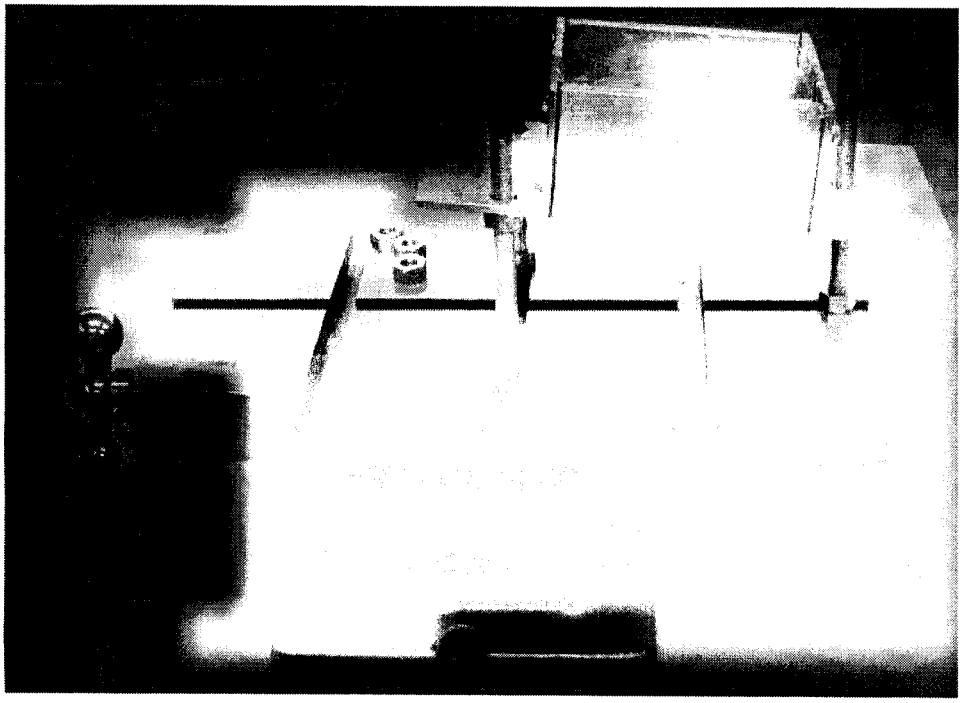

Orienter on the x-y table, ready to be leveled.

# Orienter

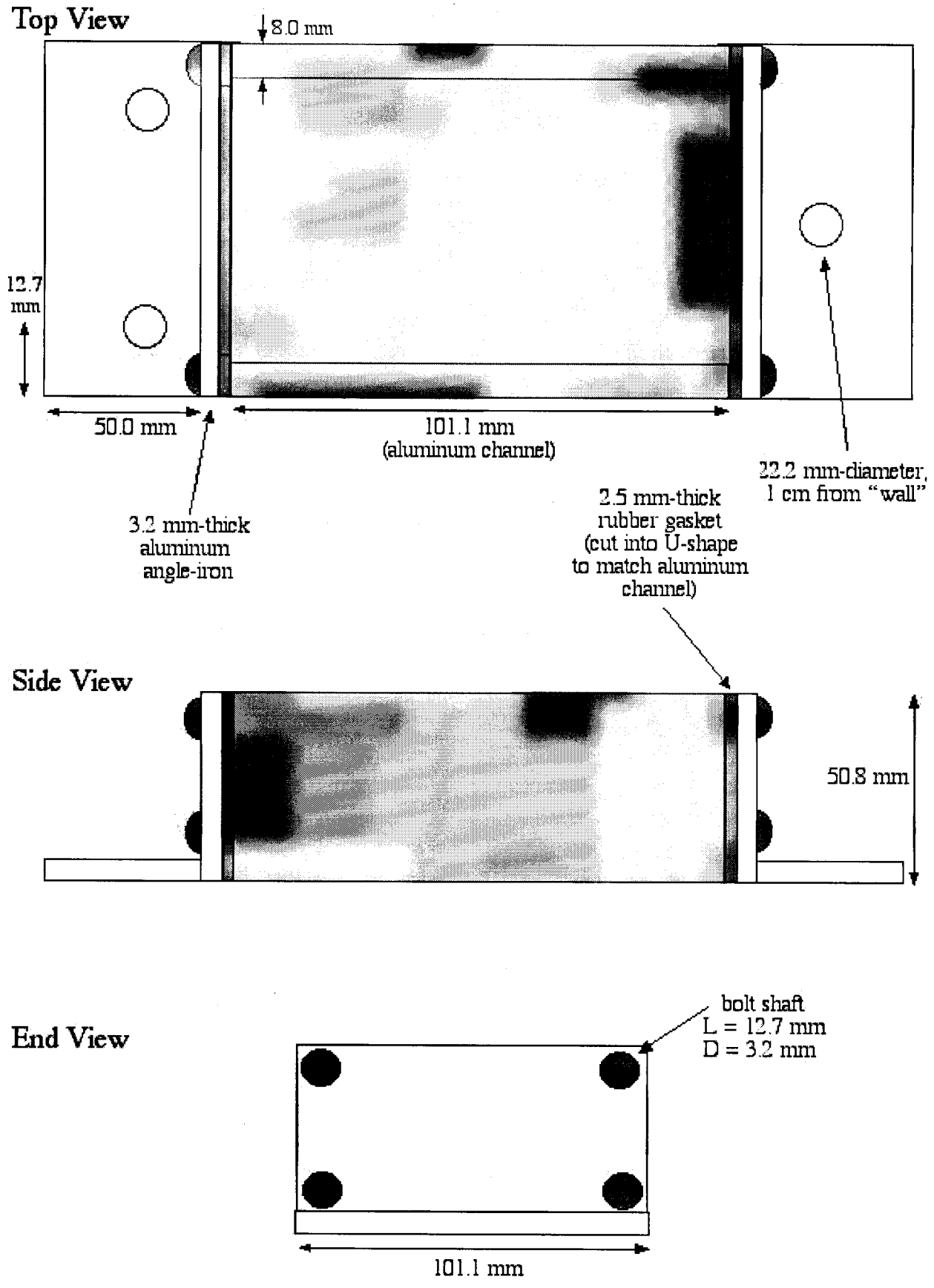
Top View
8.0 mm
12.7 mm
50.0 mm
101.1 mm
(aluminum channel)
22.2 mm-diameter,
1 cm from "wall"
3.2 mm-thick
aluminum
angle-iron
2.5 mm-thick
rubber gasket
(cut into U-shape
to match aluminum
channel)
Side View
50.8 mm
End View
bolt shaft
L = 12.7 mm
D = 3.2 mm
101.1 mm

## B.2 Tripod Bubble Level

The tripod bubble level used to level the endplate prior to testing was constructed from a standard "camping trailer level", a piece of aluminum plate, three nuts and six bolts. The lengths of the three legs could be adjusted by screwing them into the aluminum plate, then tightening the nuts to hold them securely at the selected length. This was done so that the leg length could be calibrated after the level was assembled, allowing the device to be calibrated.

Since it may be difficult to locate a level which exactly matches the dimensions of the one shown here, it is important to note that the only feature of the level which must be maintained, at least for use in the lumbar spine, is the distance between the legs. It may be necessary to place the legs closer together for tests in the thoracic or cervical spine due to the smaller endplate sizes in these spinal regions.

Tests done with the level used to construct the tripod bubble level showed that on an incline of 1 degree the bubble was half out of the centring circle, and at 5 degrees of inclination the bubble was against the side of the level. Indentation tests in polyurethane foams at angles of 0 and 5 degrees showed no significant effect angle on the failure load (0 degrees: mean 12.10 N, range 10.75-13.47 N; 5 degrees: mean 12.59 N, range: 11.45-14.03 N) or stiffness (0 degrees: mean 1.68 N/mm, range 0.72-3.02 N/mm; 5 degrees: mean 1.66 N/mm, range 0.74-2.68 N/mm) found using indentation tests.

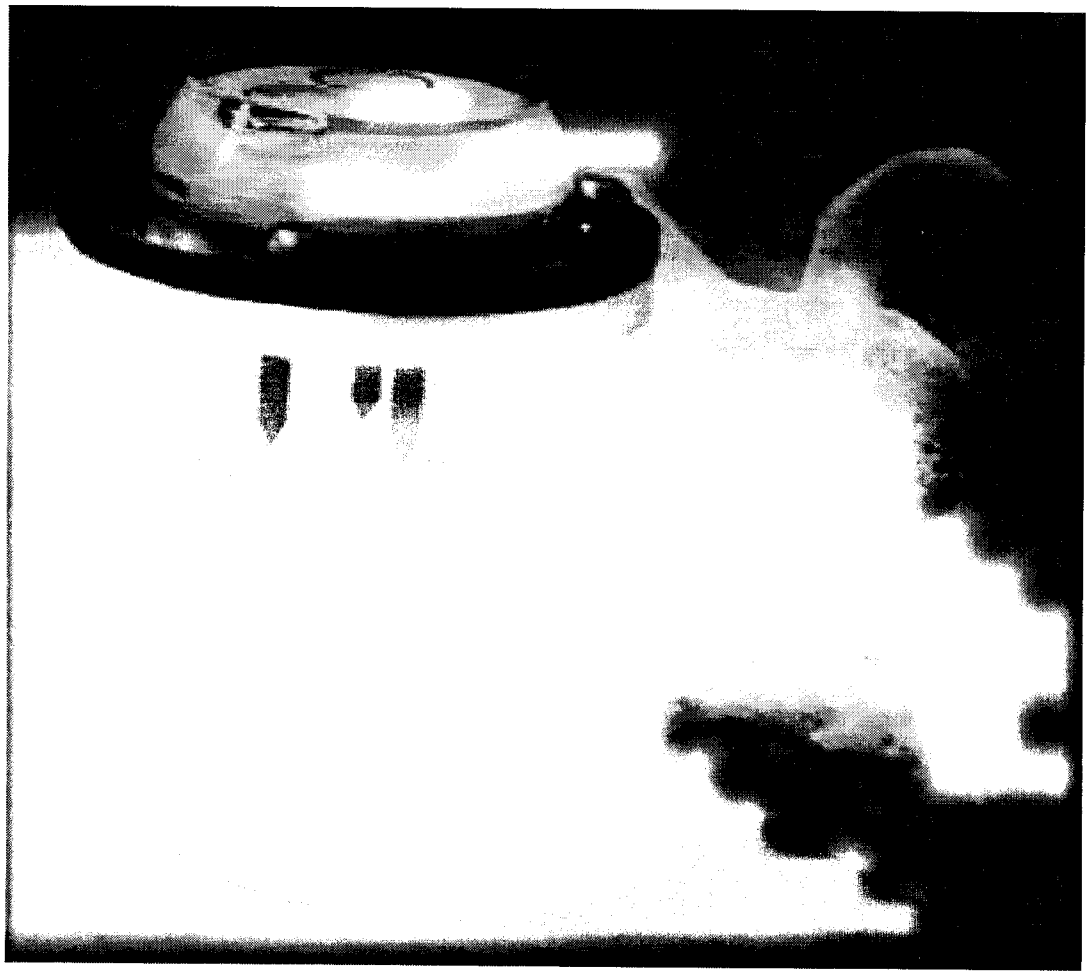

# Tripod Bubble Level

## Side View

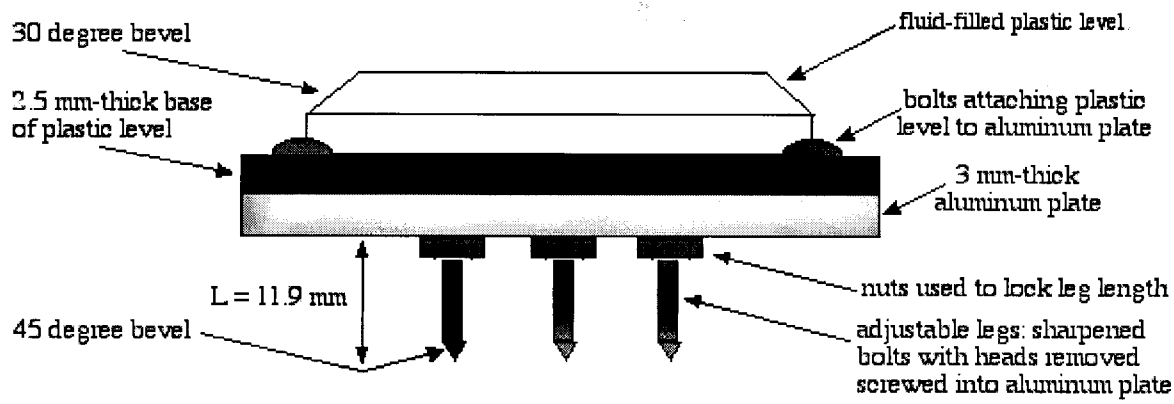


## Top View

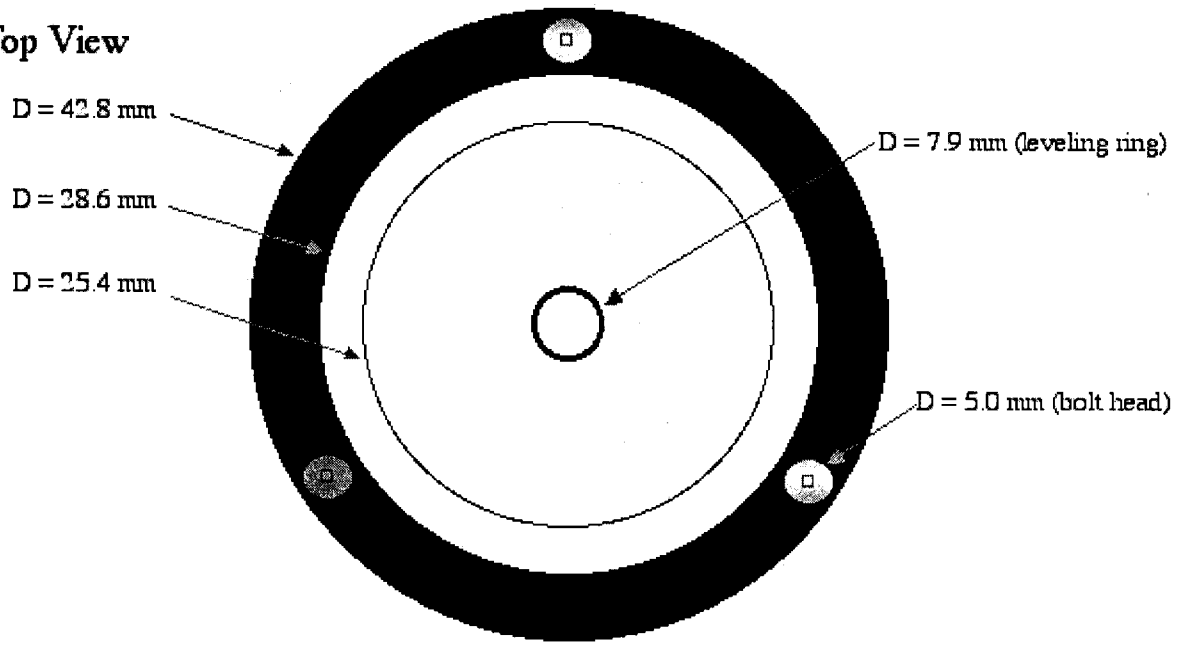


## Bottom View

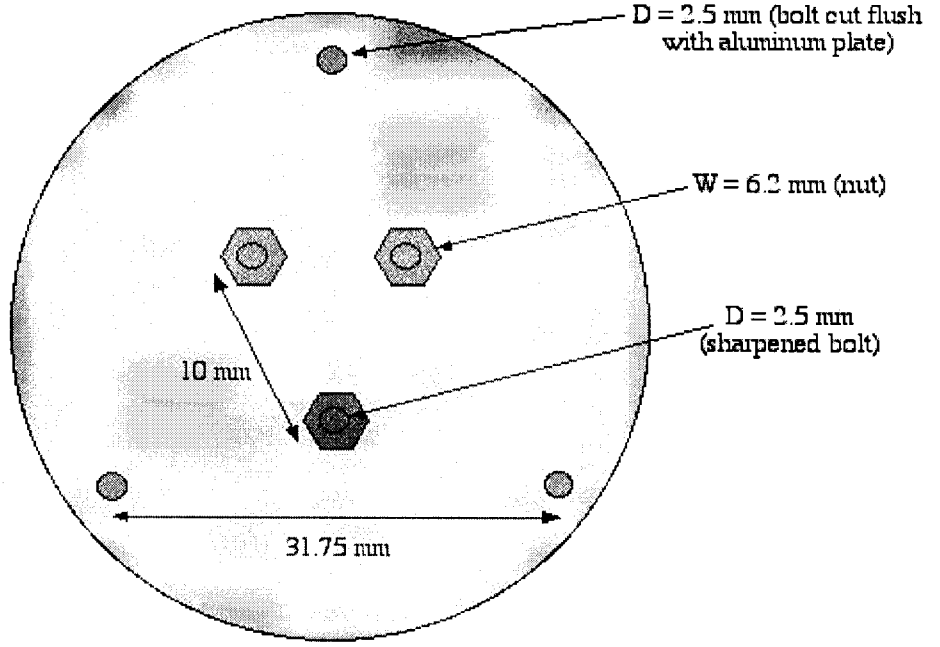

## B.3 Testing Machine

The basic components of the testing machine are listed here for investigators who would like to construct a similar device. It was designed for testing small specimens at low loads only, thus more robust equipment may be required for other applications than those described in this study. Few component details are given here, since they can be obtained from the suppliers listed here and specifications are likely to change.

**Linear Actuator:**

Supplier: Dynact Corp., Orchard Park, NY via Electromate Industrial Sales Ltd., Woodbridge, ON
http://www.dynact.com; http://www.electromate.com

Product: PPIII-B5-D1-3S

Pulse Power III Linear Actuator

- 5 pitch ball drive screw
- 4 inch stroke
- NEMA 34 step motor (Applied Motion Products 5023-124)
- direct coupled (in-line) drive

**Motion Controller:**

Supplier: Galil Motion Control, Rocklin, CA via Electromate Industrial Sales Ltd., Woodbridge, ON
http://www.galilmc.com; http://www.electromate.com

Product: DMC-1010-AF

Single-axis step motor controller

- analog feedback
- 7 AD input

Galil ICM 1100 Interconnect Module

Galil COM DISK Communication Software

**Step Motor Driver:**

Supplier: Applied Motion Products, Watsonville, CA via Electromate Industrial Sales Ltd., Woodbridge, ON http://applied-motion.com; http://www.electromate.com

Product: PD5580

**Signal Conditioner / Amplifier:**

Supplier: Measurements Group Inc., Raleigh, NC
http://www.measurementsgroup.com

Product: 2100 System

Components: Model 2110B Power Supply,
Model 2120B Strain Gage Conditioners/Amplifiers
http://www.measurementsgroup.com/guide/inst/2100/2100.htm
http://www.measurementsgroup.com/guide/inst/2100/2110.htm
http://www.measurementsgroup.com/guide/inst/2100/2120.htm

**Calibration Curve for the Step Motor:**

The step motor and LVDT accuracies were compared by measuring the displacement of the actuator and comparing it to the values output by the two devices. They were found to have similar values, however the noise on the LVDT made the reading slightly less repeatable, thus the step motor position was used to track the indenter displacement.

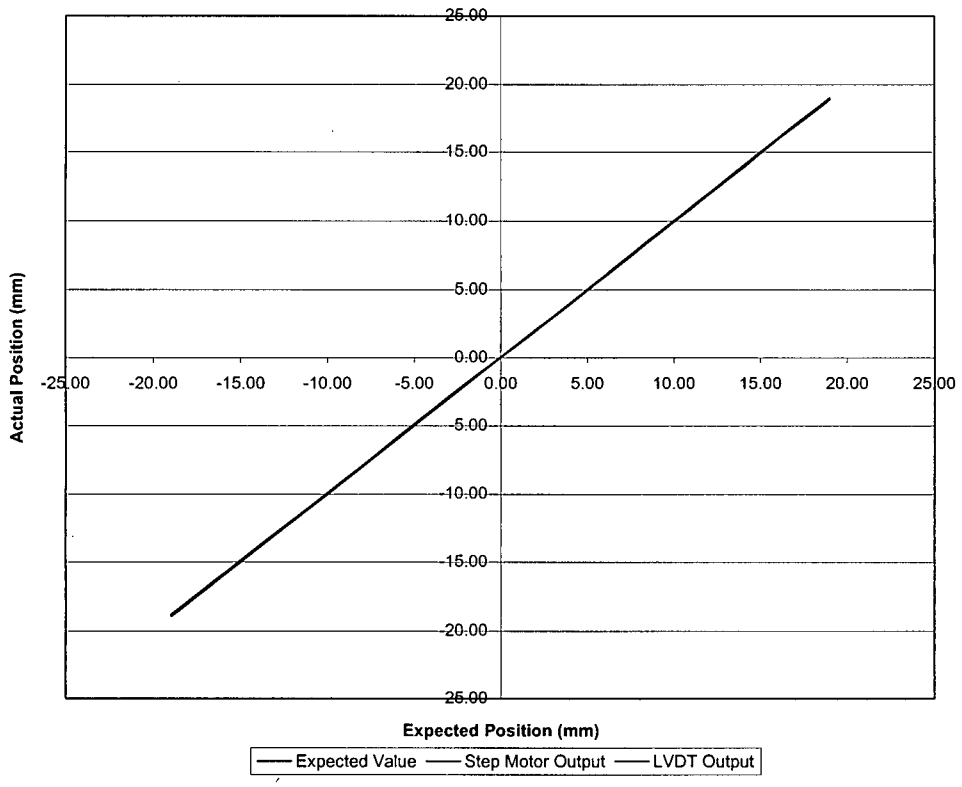


**Load Cell:**

Supplier: Omega Engineering, Inc., Stamford, Connecticut
http://www.omega.com

Product: LC 101-50 (50 lb-capacity stainless steel "S" beam load cell)

Specifications:

Excitation: 10 Vdc, 15 Vdc max
Output: 3 mV/V ±.0075 mV/V
Linearity: ±0.03% FSO (0.1% 40 K)
Hysteresis: ±0.02% FSO(0.1% 40 K)
Repeatability: ±0.01% FSO (0.05% 40 K)
Zero Balance: ±1% FSO
Agency Approval: FM Intrinsically Safe
IS/I.II.III/1/CDEFG - Standard
Operating Temp Range: -40 to +93°C (-40 to 200°F)
Compensated Temp Range: 17 to 71°C (60 to 160°F)
Thermal Effects: Zero: 0.001% FSO/°F Span: 0.001% FSO/°F

Safe Overload: 150% of Capacity
Ultimate Overload: 300% of Capacity
Input Resistance: 350 ±10 Ohms
Output Resistance: 350 ±10 Ohms
Full Scale Deflection: 0.010 to 0.020"
Construction: 17-4 PH Stainless Steel

**Factory Calibration of Load Cell: (Excitation 10 Vdc)**

| Force (lbs) (mVdc) | Unit Data |
|---|---|
| 0.00 | 0.000 |
| 25.00 | 14.974 |
| 50.00 | 29.986 |
| 25.00 | 14.980 |
| 0.00 | 0.005 |

Zero Balance: - 0.101
Sensitivity: 29.986

Input Resistance: 350.50 Ohms
Output Resistance: 352.30 Ohms

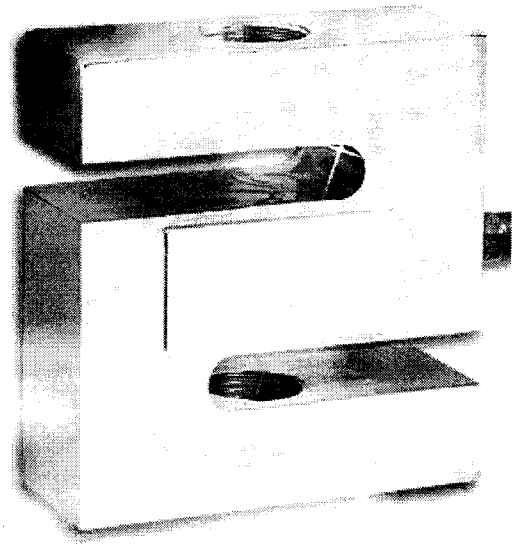

**Sample Laboratory Load Cell Calibration Curve**

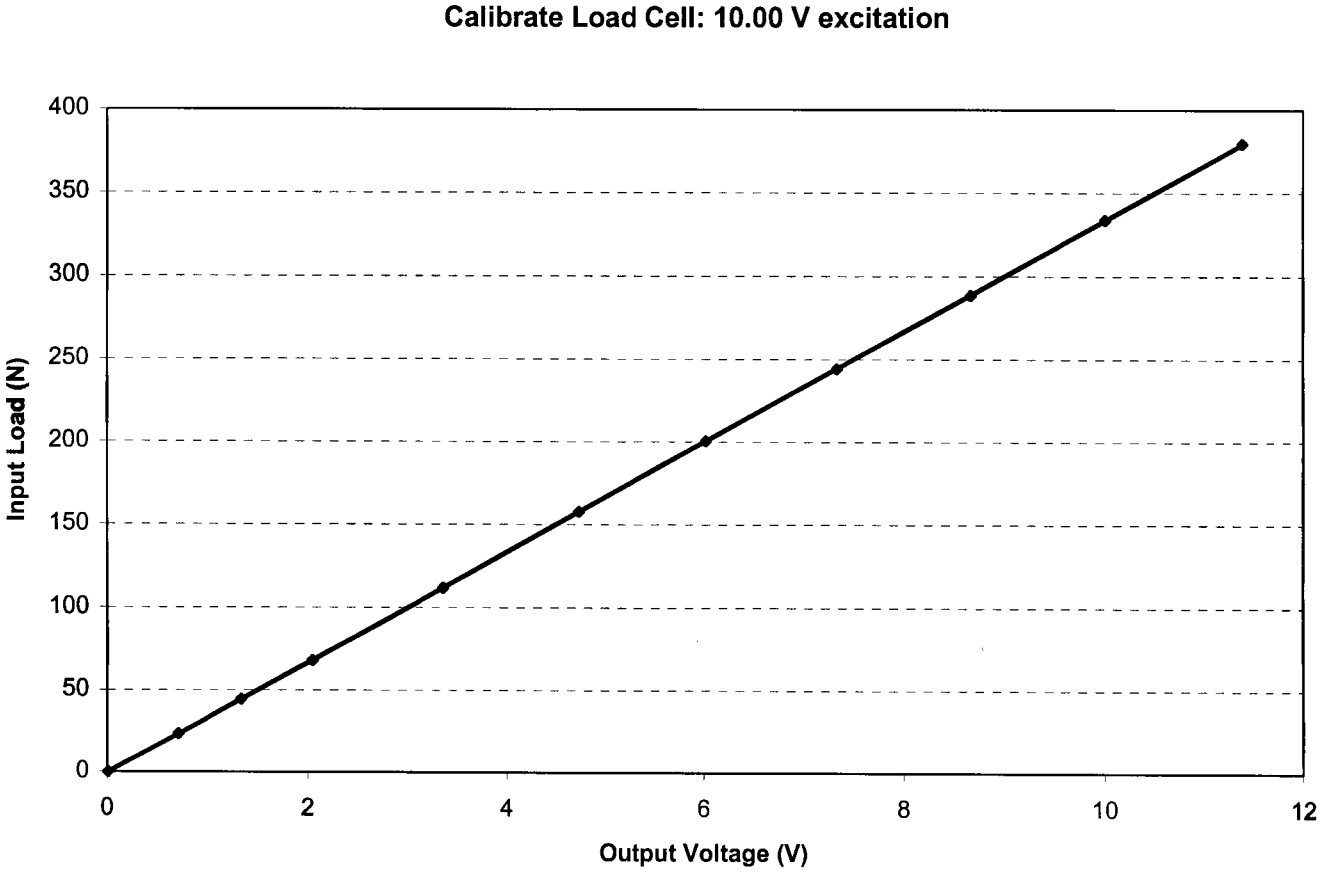


| Input Load (N) | 0.000 | 23.514 | 44.439 | 67.953 | 111.823 | 157.593 | 200.561 | 244.108 | 288.537 | 333.604 | 379.476 |
|---|---|---|---|---|---|---|---|---|---|---|---|
| Output Voltage (V) | 0.00 | 0.71 | 1.34 | 2.05 | 3.36 | 4.73 | 6.02 | 7.33 | 8.66 | 10.00 | 11.37 |

Conversion Factor (slope of line) = 33.385 N/V

**Noise on the Load Cell:**

The amplifier gain was set based on the DEXA value of the endplate being tested (Table A.1, Appendix A) to maximise the signal-to-noise ratio, while not exceeding the range of the load cell (maximum load which can be recorded = conversion factor * excitation voltage of 10 V). Specimens with lower bone density tended to have lower failure loads, and *vice versa*. For weaker specimens, the gain had to be set high to maximise the signal-to-noise ratio, in order to keep the noise below 1% of the failure load in most tests. For stronger specimens, the gain had to be lowered to avoid exceeding the range of the load cell (which would mean that the failure load would not be recorded), which decreased the signal-to-noise ratio, but still kept the noise below 1% of the failure load in most tests.

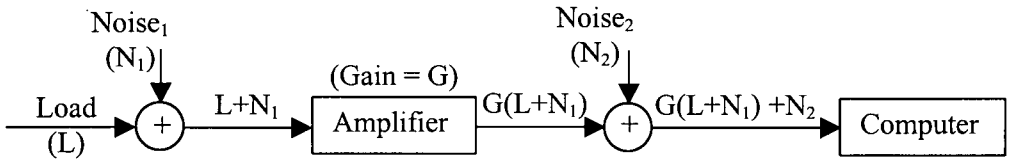


**Load to Computer = GL**

**Noise to Computer = $GN_1 + N_2$**

**Signal / Noise = Load to Computer / Noise to Computer**

**= GL / $GN_1 + N_2$**

**= L / ($N_1 + N_2/G$)**

**Therefore, as the gain increases, the signal to noise ratio increases.**

The table below shows the conversion factors (used to convert the load cell output voltage to Newtons) for each of the six gains used in the study, and the corresponding maximum levels of noise when the actuator was moving, but unloaded. The conversion factor is inversely proportional to the gain. Although the noise values were higher in the specimens with greater DEXA values (i.e. larger conversion factors), the actual amount of difference was negligible, considering the large differences in the failure load magnitudes observed in the two groups (i.e. 1 N of noise, versus 50-100 N difference in failure load). As well, the failure loads were averaged together, which will tend to cancel out the effects of noise. The stiffness values are found using a linear regression, so noise (at least of this relative magnitude) should not have a significant effect on the stiffness values.

| Conversion Factor (N/V) | Noise (N) |
|---|---|
| 24.2823 | 0.315 |
| 31.5162 | 0.400 |
| 33.3850 | 0.415 |
| 40.5190 | 0.545 |
| 60.7785 | 0.955 |
| 74.3880 | 1.550 |

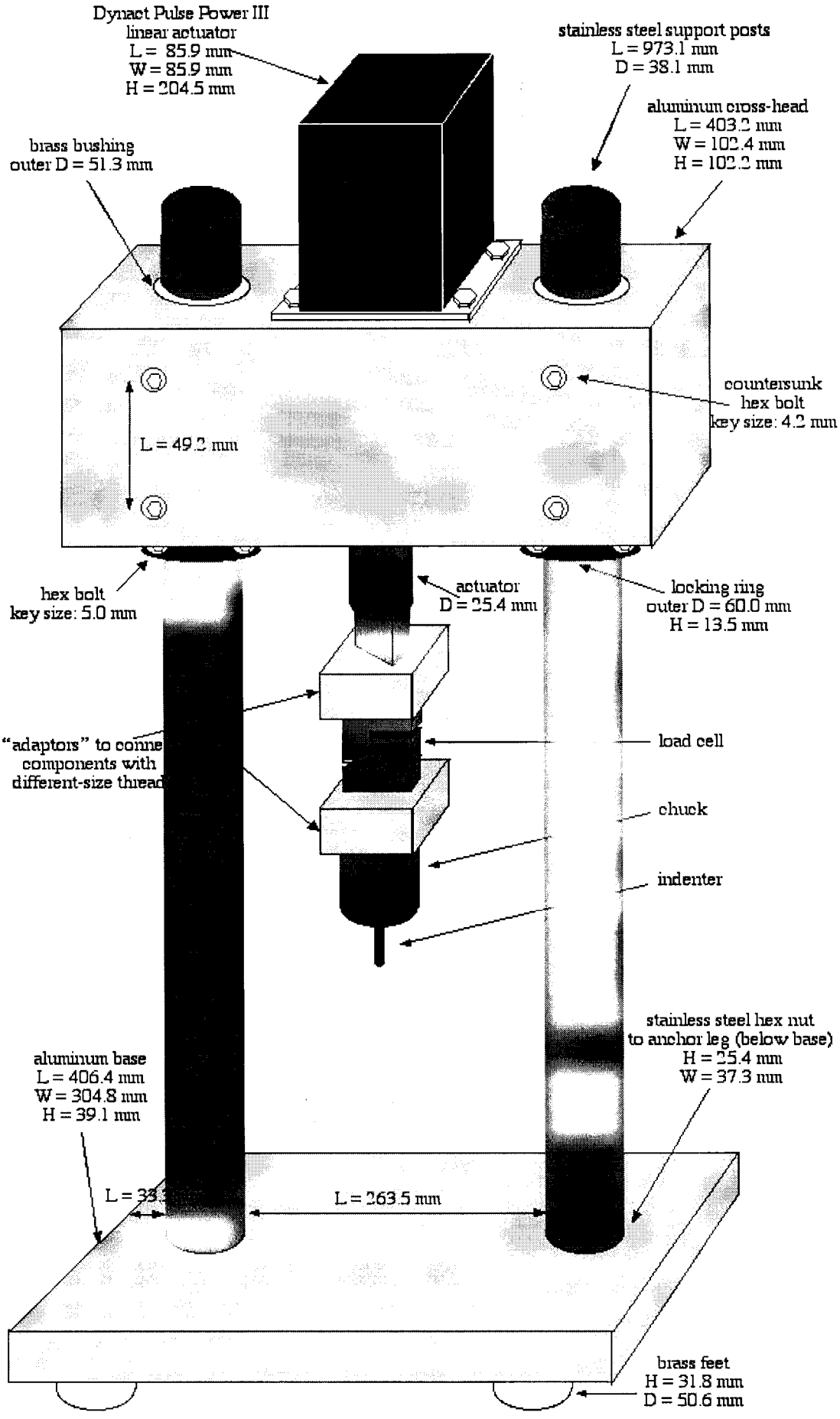
Dynact Pulse Power III
linear actuator
L = 85.9 mm
W = 85.9 mm
H = 204.5 mm
stainless steel support posts
L = 973.1 mm
D = 38.1 mm
aluminum cross-head
L = 403.2 mm
W = 102.4 mm
H = 102.2 mm
brass bushing
outer D = 51.3 mm
countersunk
hex bolt
key size: 4.2 mm
L = 49.2 mm
hex bolt
key size: 5.0 mm
actuator
D = 25.4 mm
locking ring
outer D = 60.0 mm
H = 13.5 mm
"adaptors" to conne
components with
different-size thread
load cell
chuck
indenter
stainless steel hex nut
to anchor leg (below base)
H = 25.4 mm
W = 37.3 mm
aluminum base
L = 406.4 mm
W = 304.8 mm
H = 39.1 mm
L = 263.5 mm
brass feet
H = 31.8 mm
D = 50.6 mm

Sample Load-Displacement Curves

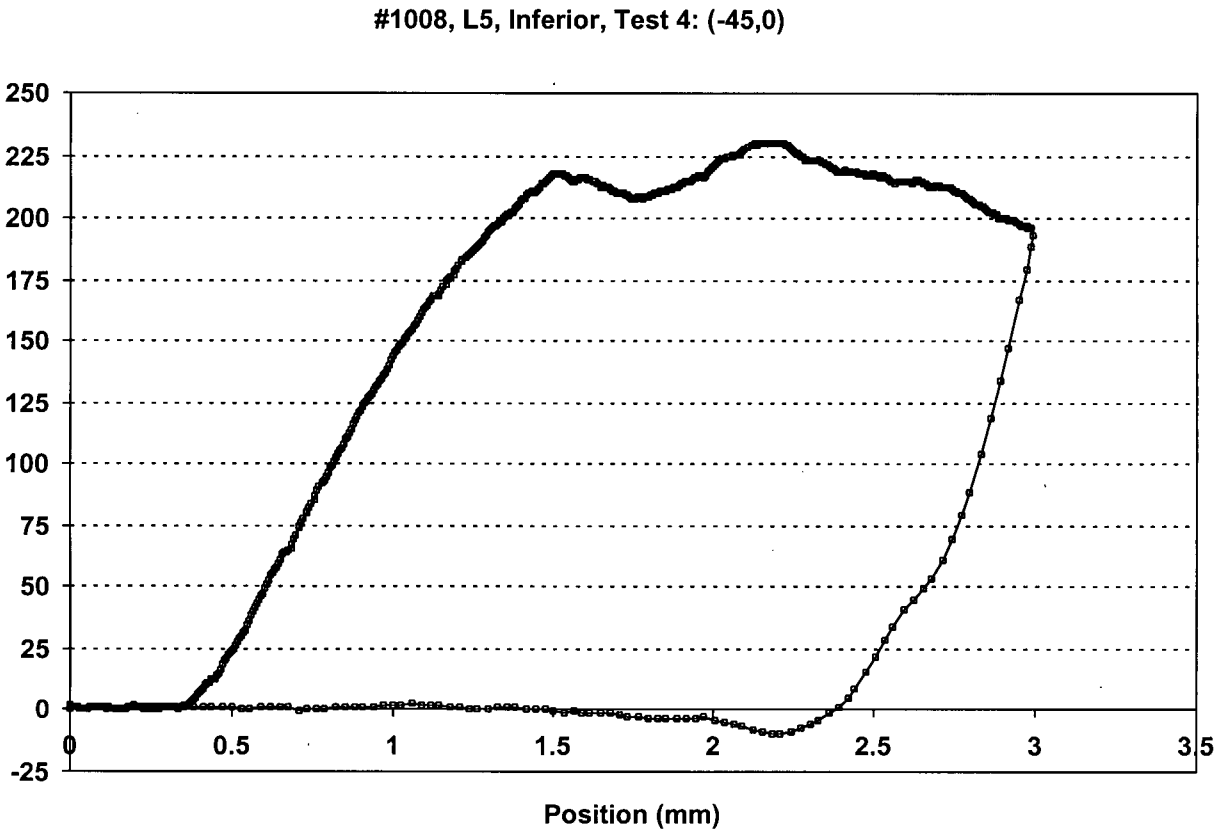


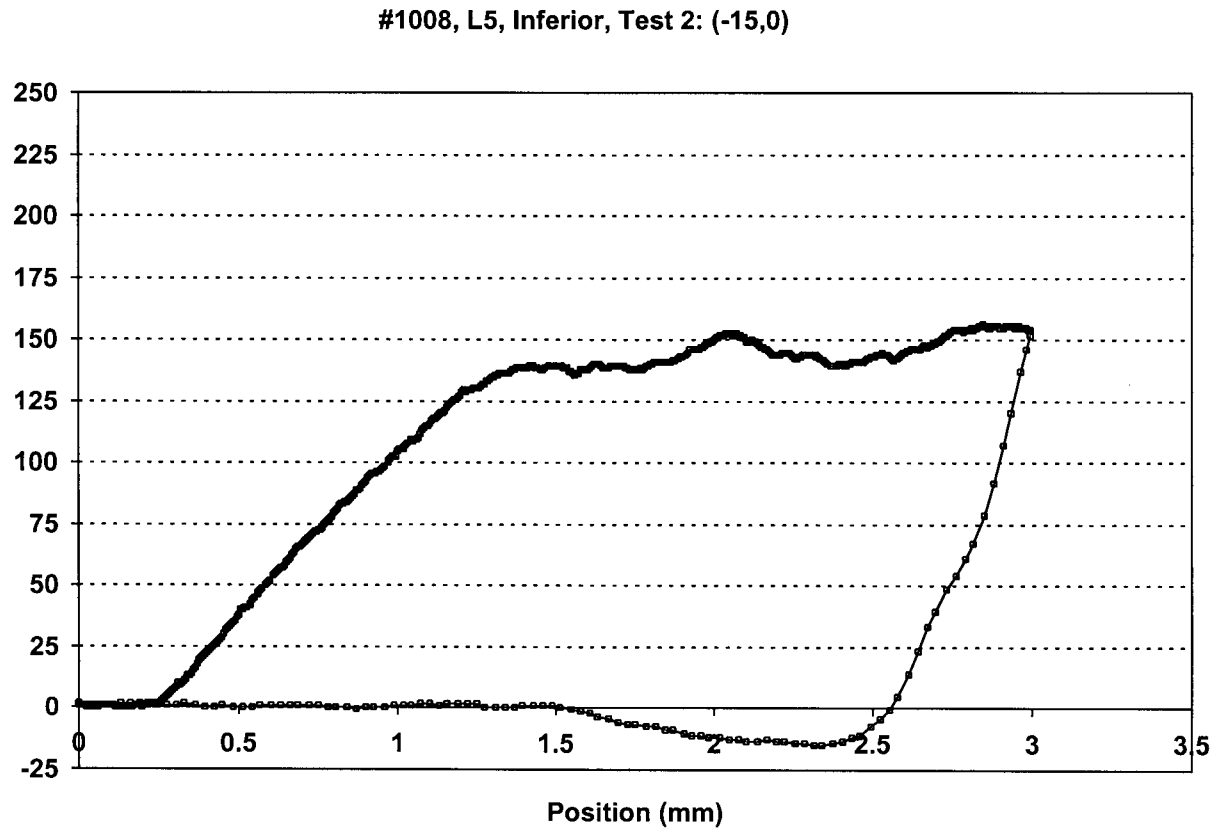

## B.4 Indenter

The hemispherical indenter used for this study was made from a 3 mm-diameter chrome steel ball bearing silver-soldered to a stainless steel tube. Preliminary studies found that epoxy, Loctite Weld, and crazy glue do not provide a sufficient degree of fixation for multiple tests, although they can be used for preliminary studies involving few tests.

**Ball Bearing:**

Supplier: Small Parts Inc., Miami Lakes, Florida http://www.smallparts.com
Part No.:R-BS-3M

| | |
|---|---|
| Material: | Chrome Steel |
| Diameter: | 3 mm |
| Sphericity: | 0.0006 mm |
| Rockwell C: | 60-67 |
| Grade: | 25 |

**Tube:**

Supplier: Small Parts Inc., Miami Lakes, Florida http://www.smallparts.com
Part No.: R-HTX-12HW

| | |
|---|---|
| Material: | Stainless Steel |
| Outer Diameter: | 0.109 inches = 2.77 mm |
| Inner Diameter: | 0.077 inches = 1.96 mm |
| Length: | 40 mm |

## B.5 Dremel Rotary Tool

Supplier: Dremel, Racine, WI http://www.dremel.com

Product Components: 395 Variable Speed Tool, 225 Flex-Shaft Attachment, 191 High Speed Cutting Tool (3.175 mm shank, 3.175 mm diameter spherical end)



**395 Variable Speed Tool :**

Variable speed: 5,000 to 30,000 rpm..

**225 Flex-Shaft Attachment:**

Allows fingertip control for polishing, carving, sanding and engraving. 36"-long cable with pencil-like, 1/2"-diameter handpiece.

**191 High Speed Engraving Bit:**

Made of high speed steel. Can be used for shaping, hollowing, grooving, slotting, inletting, and making tapered holes in soft metals, plastics and woods.

## Appendix C

## Programs

### C.1 Galil Controller Program

To run the test machine, a Galil motion controller was used to drive the uni-axial linear actuator on which the load cell and indenter were mounted. The program that ran the machine was written in the Galil controller language. The program is presented below, along with comments (in the right-hand column). There are three parts to this program. The first section initialises the software to prepare for data collection, the second drives the indenter, and the third collects the load and displacement data while the test is running.

**Part 1: Initialisation**

This part of the program initialises all array elements to zero, defines the arrays to be used for data collection, and collects the first set of load and displacement data prior to beginning the test (i.e. it stores the initial conditions of the load cell and step motor). LOADsum and POSsum are the values that are stored by the computer and used to generate the load-displacement curves. They are actually made up of 20 discrete readings from the load cell and step motor, respectively. This summing effectively acts as a box filter, removing some of the noise from the system. Part of the post-processing involved dividing each LOADsum and POSsum value by 20 to get the average value of that set of points, and provide the load-displacement data set used for the failure load and stiffness data extraction.

| | |
|---|---|
| #I | Galil program name – used to run the program |
| NO "Set up arrays for BoxFilter task" | Note to user |
| DA*[0] | Set all array elements to zero |
| DM LOADary[20], POSary[20] | Define 2 matrices of 20 elements each |
| LOADsum = 0 | Initialise LOADsum to zero |
| POSsum = 0 | Initialise POSsum to zero |
| I = 0 | Initialise counter to zero |
| SUMload = 0 | Initialise SUMload to zero |
| SUMpos = 0 | Initialise SUMpos to zero |
| #INITARY | Beginning of INITARY function |
| LOADary[I] = @AN[1] | Store load value on analog input 1 in element I |
| POSary[I] = _TDX | Store current motor position in element I |
| SUMload = SUMload + LOADary[I] | Add new load reading to SUMload |
| SUMpos = SUMpos + POSary[I] | Add new position reading to SUMpos |
| I = I + 1 | Increment loop counter |
| JP #INITARY, I < 20 | While counter < 20 repeat from #INITARY |
| LOADsum = SUMload | Store SUMload (20 load values) in LOADsum |
| POSsum = SUMpos | Store SUMpos (20 position values) in POSsum |
| XQ #BOXFILT, 1 | Begin running the BOXFILT function |
| WT 500 | Wait 500 ms before executing next command |
| SP 1969 | Set speed to 1969 steps/s (0.2 mm/s) |

**Part 2: Run a Test**

This segment of the program begins the data collection and then begins to drive the indenter. There is a short waiting period (500 ms) prior to commencing the indentation. This provided an indication of the amount of noise in the system and ensured that the computer had started collecting data prior to the crucial specimen contact phase.

Each step of the motor was equivalent to 0.000004 inches, thus for an indentation rate of 0.2 mm/s, the speed was set to 1969 steps/s and the displacement of 3 mm translated to 29528 steps. The indenter was driven down into the bone at 0.2 mm/s second, then retracted at 1 mm/s. The higher withdrawal rate was chosen because it reduced the size of the data set considerably and sped up the test. The retraction phase of the load-displacement curve is of little interest in this study, and this test rate provided adequate information to reveal any unusual conditions during the withdrawal of the indenter.

| | |
|---|---|
| PR -29528 | Move actuator down 29528 steps (3 mm) |
| BG | Begin moving actuator now |
| AM | After completing motion execute next command |
| SP 9843 | Set speed to 9843 steps/s (1 mm/s) |
| PR 29528 | Move actuator up 29528 steps (3 mm) |
| BG | Begin moving actuator now |
| AM | After completing motion execute next command |
| #END | End of BOXFILT function |
| HX | Halt execution of program |
| EN | End of program |
| #BOXFILT | Beginning of the BOXFILT function |
| #COLLECT | Beginning of the COLLECT sub-function |
| I = 0 | Initialise loop counter to zero |
| #LOOP | Beginning of the LOOP sub-function |
| LOAD = @AN[1] | Store the current load cell reading in LOAD |
| POS = _TDX | Store the current motor position in POS |

**Part 3: Collect Load and Displacement Data**

This part of the program is responsible for data collection in the form of the load cell reading (in Volts) and the step motor position (in steps). It runs continuously from the time the XQ #BOXFILT, 1 command is encountered in Part 2 until the HX command is reached.

This function stores the sums of 20 consecutive readings in the variables LOADsum and POSsum, updating the sums after each reading to reflect the 20 most recent readings. The values are output after every 5 readings. This is done continuously until the indenter motion has been completed.

| | |
|---|---|
| LOADsum = LOADsum - LOADary[I]+LOAD | Replace oldest load value in sum with LOAD |
| POSsum = POSsum - POSary[I] + POS | Replace oldest position value in sum with POS |
| LOADary[I] = LOAD | Update array of 20 load values to include LOAD |
| POSary[I] = POS | Update array of position values to include POS |
| I = I + 1 | Increment counter |
| JP #OUT, I = 4 | If counter = 4, go to #OUT |
| JP #OUT, I = 9 | If counter = 9, go to #OUT |
| JP #OUT, I = 14 | If counter = 14, go to #OUT |
| #RETURN | Note to user that program will start LOOP again |
| JP #LOOP, I < 20 | If I < 20, go to #LOOP |
| #OUT | Beginning of OUT (output) function |
| MG " X", TIME, POSsum, LOADsum {N} | Output "X", time, and position and load sums |
| JP #RETURN, I = 4 | If I = 4, go to #RETURN |
| JP #RETURN, I = 9 | If I = 9, go to #RETURN |
| JP #RETURN, I = 14 | If I = 14, go to #RETURN |
| JP #COLLECT | If I = 20, go to #COLLECT |

## C.2 Failure Load and Stiffness Extraction Program: PALstiffness.c

Once all of the tests had been completed in a given endplate, the failure load and stiffness data were extracted from the raw data files using a C program written by the investigator using CodeWarrior IDE 3.0 [Metrowerks Inc., Austin, Texas]. The program takes as input a data file containing the names of the files containing the test results for a single endplate, along with the associated conversion factors (Newtons/Volt), and the load values bracketing the linear regions of the curves to be used for the stiffness calculations. It returns the failure load value, the stiffness value, and the correlation coefficient ($r^2$, indicating "goodness-of-fit" of the stiffness values) for each test site.

The input text file serves three main purposes:

1) By including all of the raw data file names in a single file, the C program could be run once for each endplate, rather than being run for each discrete test.

2) Rather than recalibrate the program for each endplate by modifying the calibration factor used to convert the signal from volts to Newtons based on the amplifier gain used for that test, the calibration factor was incorporated into the text file.

3) It was found, during the initial programming phase, that the amount of variability between tests made it difficult to automate the process of locating the appropriate curve segment for use in the stiffness calculation. For this reason, the curve segments used for calculating stiffness were chosen manually. The curve segments were defined using the initial and final load in the linear segment of the load-displacement curve (section 2.5).

The input text file contains the following columns:

a) test site text file name, e.g. 1023_L3_s_-15,-20_9.txt
b) conversion factor (N/V), e.g. 33.385
c) load at the initial point in the linear segment defining the test site's stiffness (N), e.g. 7.6
d) load at the final point in the linear segment defining the test site's stiffness (N), e.g. 29.8

The data extraction program returns information about the tests in the form of two output files:

a) a general output file with a name in the format Specimen#_SpinalLevel_Endplate_DataOut_st, e.g. 1023_L3_s_DataOut_st, which is a summary of the data generated by the program. This file was used to assist in checking the results of the program. It contains the following columns:
   i. Data File Name: the name of the text file containing the raw data
   ii. Contact i-value: the point at which the indenter contacts the endplate
   iii. Failure i-value: the point at which failure occurs
   iv. n: the number of points (Failure – Contact)
   v. Failure Load (N): the load at which failure occurs (it is followed by a decrease in load > 5%)
   vi. Stiffness (N/mm): the stiffness of the manually selected linear region; the slope of the line as found using linear regression analysis

vii. Intercept (N): the point at which the linear regression line defining the stiffness would intercept the y-axis
viii. r-Squared: how closely the points defining the linear region of the graph align with the linear regression analysis line-of-best-fit. $r^2 = 1$ indicates that every point lies on the line (perfect fit)
ix. # Regression Points: number of points used in the linear regression to find the stiffness of the test site
x. Start Stiffness (N): load value defining beginning of linear region used to find stiffness
xi. End Stiffness (N): load value defining end of linear region used to find stiffness
xii. Start Stiffness i-value: point at which the linear region begins
xiii. End Stiffness i-value: point at which the linear region ends

b) a file used to continue the data extraction process with a name in the format Specimen#_ SpinalLevel_Endplate_ToMap_st, e.g. 1023_L3_s_ToMap_st. This file was used as input for the C programs which generated the endplate maps and Statistica input files (sections C.3 and C.4). It contains the following columns:
i. x-value of test site
ii. y-value of test site
iii. Failure Load (N)
iv. Stiffness (N/mm)
v. r-Squared (correlation coefficient)

The code for the data extraction program is provided below.

```
/********************** Beginning of Program **********************/

/* PALstiffness.c */
/* Last modified 99.09.23 */
/* Comments updated 00.08.29 */

/* This program is used to extract failure load and stiffness data from a series
        of load-displacement files generated from a single endplate specimen. It
        takes as input a text file containing the file names, initial and final loads
        defining the linear regions to be used for the stiffness calculations, and the
        conversion factors for the tests (Newtons/Volt).

The input text file must contain the following columns:
        a) test site text file name,  e.g. 1023_L3_s_-15,-20_9.txt (see note, below)
        b) conversion factor (N/V), e.g. 33.385
        c) load at the initial point in the linear segment defining the test site's stiffness (N), e.g. 7.6
        d) load at the final point in the linear segment defining the test site's stiffness (N), e.g. 208.8

NOTE: The files containing the data to be analysed must be named using the convention:
        Specimen#_SpinalLevel_Endplate_x,y_test#,
                where Specimen# is 4 digits long. Otherwise the program will not extract the
                x and y co-ordinates correctly.
```

*The data within the text files should consist of the time, indenter positions and loads during an indentation test run using the Galil motion controller. With the time in the form seconds * 1024; position in the form of 20 summed motor step readings; and load in the form of 20 summed voltage readings from a load cell.*

*The data is normalised by:*

*1) subtracting the initial time from each time value and dividing by 1024*
*- this gives the time in seconds*

*2) subtracting the initial contact position value from each position value and dividing by 20 then dividing by 9842.519685039 (steps/mm),*
*- this converts the indenter position from steps to mm*
*- Note: each position value is actually the sum of 20 discrete step readings, thus each value must be divided by 20*
*- this accounts for the fact that the indenter position is given in an absolute coordinate system and we want the initial contact position to be 0mm*

*3) dividing each load value by 20, then multiplying by ac onversion factor (N/V)*
*- this converts the indenter load from volts to Newtons (the conversion factor is based on the gain setting of the load cell during data sampling)*
*- Note: for some initial tests load = -(load/20 * 25.1275 - 5.0294)*
*- Note: each load value is actually the sum of 20 discrete load readings, thus each value must be divided by 20*

*4) multiplying each data point by -1*
*- this flips the data from the fourth quadrant into the first quadrant, which makes it easier to interpret and provides a traditional Load-Displacement curve shape*

*The data is processed by:*

*1) finding the initial peak in the load data (drop in load > 5%, 5N)*
*- this locates the failure load of the material being indented*
*- this will be the final point output to the new data file*

*2) finding the stiffness and r-squared values based on an initial and final load reading entered by the user (bracketing the region visually selected as being most linear)*

**/*

*/***** Libraries *****/*

```
#include <math.h>
#include <stdlib.h>
#include <stdio.h>
#include <string.h>
```

*/***** Functions *****/*

```
int ContactCheckingFunction (float *, float *, int);
```

```
int FailureLoadFunction (float*, float*, int, int);
void StiffnessCalculation (float*, float*, int, float, float, float *, float *, float *, int *, int *);

/***** Constants *****/

#define ARRAY_NUMBER 10000/* a number larger than the largest expected number of points */
#define NOISE 3                 /* difference in load of NOISE = contact */
#define TRUE 1
#define FALSE 0

/************************ Beginning of Main Program ************************/

int main() {

/***** define and initialise variables *****/

int i=0;                        /* array pointer */
int LastPoint=0;                /* i value of last data point */

float ConversionFactor=0;       /* conversion factor - from input file */
float StartStiffness=0;         /* load at point stiffness calculation will begin - from input file */
float EndStiffness=0;           /* load at point stiffness calculation will end - from input file */
int iStartStiffness=0;          /* i-value of first point used to calculate stiffness */
int iEndStiffness=0;            /* i-value of last point used to calculate stiffness */
int Contact=0;                  /* i-value at which indenter contacts bone */
int Failure=0;                  /* i-value at which bone fails */
int n=0;                        /* = Failure - Contact */
float Slope=0;                  /* slope of line which defines stiffness */
float Intercept=0;              /* y-intercept of line which defines stiffness */
float rSquared=0;               /* correlation coefficient of slope value */
int NumRegresPoints=0;          /* = iEndStiffness - iStartStiffness */

int x=0;                        /* LAT co-ordinate of test site */
int y=0;                        /* AP co-ordinate of test site */
int multiplyXby=0;              /* 1 if LAT co-ordinate is positive, else -1 */
int multiplyYby=0;              /* 1 if AP co-ordinate is positive, else -1 */
int NumDigitsX=0;               /* number of digits in the LAT test site co-ordinate */
int NumDigitsY=0;               /* number of digits in the AP test site co-ordinate */

char DataIn[90];                /* name of data file to be analysed */
char ListOfFileNames[70];       /* name of file listing the data files to be analysed */
char GetXY[90];                 /* name of file currently being analysed from which x and y will be extracted */

char DataOut[70];               /* name of file storing general data generated by this program */
char FileToMap[70];             /* name of the file containing data using by the endplate mapping program */
FILE *InFile;                   /* file pointer to the data file to be analysed */
FILE *pointerDataOut;           /* file pointer to the general data output file */
FILE *pointerFileToMap;         /* file pointer to the endplate mapping data */
FILE *pointerListOfFileNames;   /* file pointer to the file listing the data files to be analysed */
float PositionAtContact;        /* motor step value when indenter contacts bone */

int Time1=0;                    /* initial time value recorded in the data file (used to set initial time to 0) */
float Position1=0;              /* initial position value recorded in data file (used to set initial position to 0)*/
```

```
float *Time;                    /* pointer to array of time values */
float *Position;                /* pointer to array of position values */
float *Load;                    /* pointer to array of load values */

Time = (float *) malloc (sizeof(float) * ARRAY_NUMBER);      /* array for storing Time values */
Position = (float *) malloc (sizeof(float) * ARRAY_NUMBER);  /* array for storing Position values */
Load = (float *) malloc (sizeof(float) * ARRAY_NUMBER);      /* array for storing Load values */

/***** program description for user *****/
printf ("This is a data processing program designed to analyse data files \n");
printf ("generated during indentation tests.  It extracts the failure load \n");
printf ("and stiffness values from a load-displacement data set generated using \n");
printf ("a Galil motion controller running the program #I.  Data must be entered \n");
printf ("in text file format, with the file names, conversion factor, and initial and \n");
printf ("final failure loads in the linear region to be used for the stiffness calculation.\n");
printf ("For more information, please read the comments in this program. \n");

/* open the data file containing the names of all files to be processed by the program in read mode*/

printf ("Please enter the name of the text file containing the names of the data files to be processed: ");
scanf ("%s", &ListOfFileNames);  /* read in the name of the text file */
if ((pointerListOfFileNames = fopen (ListOfFileNames, "r")) = = NULL)
{       printf ("\nCould not open file %s", ListOfFileNames);
        exit(1);
}

printf ("Please enter the name of the combined data output file: ");
scanf ("%s", &DataOut);         /* read in the name of the detailed data file to be generated */

printf ("Please enter the name of the data output file to be used by the mapping program: ");
scanf ("%s", &FileToMap);       /* read in the name of the output file to be used by the mapping program */

/* open combined output file in write mode and check that file opened */
if ((pointerDataOut = fopen (DataOut,"w")) = = NULL)
{       printf ("\nCould not open file %s", DataOut);
        exit(1);
}

/* header for combined output file */
fprintf (pointerDataOut,"Data File\tContact i\tFailure i\tn\tFailureLoad\tStiffness\tIntercept\trSquared\t#RegresPts");
fprintf (pointerDataOut, "\tStartStiffness (N)\tEndStiffness (N)\tStartStiffness i\tEndStiffness i\n");


/* open output file to be used by the mapping program in write mode and check that the file opened */
if ((pointerFileToMap = fopen (FileToMap,"w")) = = NULL)
{       printf ("\nCould not open file %s", FileToMap);
        exit(1);
}

/* header for mapping program file */
fprintf (pointerFileToMap, "x\ty\tLoad\tStiffness\tr-Squared\t:\n");

/********** begin while loop that analyses each data file listed in the ListOfFileNames file **********/
```

```
while (fscanf
(pointerListOfFileNames,"%s\t%f\t%f\t%f",DataIn,&ConversionFactor,&StartStiffness,&EndStiffness)!=EOF)
{       if ((InFile = fopen(DataIn,"r")) = = NULL)  /* open file in read mode and check that file opened */
        {       printf ("\nCould not open file %s", DataIn);
                exit(1);
        }
        /****** read in the position and load values ******/
        /****** each data line is composed of Time (s * 1024), 20 * Position (V), 20 * Load (V) ******/
        i = 0;  /* initialise array pointer */
        while (fscanf(InFile, "%f%f%f", &Time[i], &Position[i], &Load[i]) != EOF) {i++;}
        LastPoint = i;  /* final data point */
        /****** finished reading in all data from InFile -> close the input file ******/
        fclose (InFile);
        /****** convert the values read in from the data file into seconds, mm, and Newtons ******/
        Time1 = Time[10];
        Position1 = Position[10];
        for (i = 0; i < LastPoint; i++)
        {       Time[i] = (Time[i] - Time1)/1024;                        /* convert time to seconds */
                Position[i] = - ((Position[i] - Position1)/20) / 9842.519685039;/* steps to mm */
                Load[i] = -(Load[i]/20) * ConversionFactor;              /* convert load from V to N */
        }
        /* call the function that finds the point at which the indenter contacts the endplate surface */
        Contact = ContactCheckingFunction (Load, Position, LastPoint);  /* find contact point */
        /****** normalise position data using contact point ******/
        PositionAtContact = Position[Contact];
        for (i = 0; i < LastPoint; i++) {Position[i] = (Position[i] - PositionAtContact);}
        /* call the function that finds the failure point */
        Failure = FailureLoadFunction (Load, Position, Contact, LastPoint);
        /* call the function that finds the stiffness through linear regression */
        StiffnessCalculation (Load, Position, Contact, StartStiffness, EndStiffness, &Slope, &Intercept, &rSquared,
&iStartStiffness, &iEndStiffness);
/***** extract x and y values using the known properties of the file names and convert them to integer values ****/
        /* copy the file name into variable GetXY to ensure that no modifications are made to it */
        strcpy(GetXY, DataIn);
        /***** find value of x *****/
        if (GetXY[10] = = '-')      /* x is negative */
        {       multiplyXby = -1;
                if (GetXY[12] = = ',')      /* x is 1 digit long */
                {       NumDigitsX = 1;
                        x = multiplyXby * (GetXY[11] - '0');
                }
                else                        /* x is 2 digits long */
                {       NumDigitsX = 2;
```

```
                x = multiplyXby * ((GetXY[11] - '0')*10 + (GetXY[12] - '0'));
        }
}
else                    /* x is positive */
{       multiplyXby = 1;

        if (GetXY[11] = = ',')      /* x is 1 digit long */
        {       NumDigitsX = 1;
                x = multiplyXby * (GetXY[10] - '0');
        }
        else                        /* x is 2 digits long */
        {       NumDigitsX = 2;
                x = multiplyXby * ((GetXY[10] - '0')*10 + (GetXY[11] - '0'));
        }
}

/* if x is negative add one to NumDigitsX */
if (multiplyXby = = -1) {NumDigitsX++;}

/***** find value of y *****/

if (GetXY[11+NumDigitsX] = = '-')       /* y is negative */
{       multiplyYby = -1;

        if (GetXY[13+NumDigitsX] = = '_')       /* y is 1 digit long */
        {       NumDigitsY = 1;
                y = multiplyYby * (GetXY[12+NumDigitsX] - '0');
        }
        else                                    /* y is 2 digits long */
        {       NumDigitsY = 2;
                y = multiplyYby * ((GetXY[12+NumDigitsX] - '0')*10 + (GetXY[13+NumDigitsX]-'0'));
        }
}
else                        /* y is positive */
{       multiplyYby = 1;

        if (GetXY[12+NumDigitsX] = = '_')       /* y is 1 digit long */
        {       NumDigitsY = 1;
                y = multiplyYby * (GetXY[11+NumDigitsX] - '0');
        }
        else                                    /* y is 2 digits long */
        {       NumDigitsY = 2;
                y = multiplyYby * ((GetXY[11+NumDigitsX] - '0')*10 + (GetXY[12+NumDigitsX]-'0'));
        }
}

/* output data for this indentation test to the output file to be used for mapping the endplate */
fprintf (pointerFileToMap, "%d\t%d\t%f\t%f\t%f\n", x, y, Load[Failure], Slope, rSquared);

/* print summary of results to combined output file */

n = Failure - Contact;
NumRegresPoints = iEndStiffness - iStartStiffness;
```

```
        fprintf (pointerDataOut, "%s\t%d\t%d\t%d\t%f\t%f\t%f\t%f\t%d\t%f\t%f\t%d\t%d\n", DataIn, Contact,
Failure, n, Load[Failure], Slope, Intercept, rSquared, NumRegresPoints, StartStiffness, EndStiffness, iStartStiffness,
iEndStiffness);

} /****************** end of first while loop ******************/

fclose (pointerDataOut);  /* close the combined output file */
return (1);

} /************************ End of Main Program ************************/

/******************* Function to find the contact point *******************/

int ContactCheckingFunction (float *Load, float *Position, int LastPoint)
{
/* loop to locate indenter's initial contact with material */
/* loop will be entered if the indenter has not yet contacted the material being tested */
/* |load change| > NOISE = surface contact */

   int i=0;                 /* initialise array counter */
   int NoContact;           /* loop checker; = 0 when the contact point is found */
   float ContactCheck;      /* difference in load values; if > NOISE N, contact has occurred */
   int Contact = 0;         /* stores i value at which contact occurs */

        NoContact = TRUE;       /* initialise loop checker to 1 */
        do
        {       ContactCheck = abs(Load[i]-Load[0]);       /* check to see if change in load > noise */
                if (ContactCheck > NOISE)                  /* if load change is > NOISE contact has occurred */
                {       printf ("Indenter contact at position %f mm, i = %d \n", Position[i], i);
                        Contact = i;                       /* store the i-value at which contact occurs */
                        NoContact = FALSE;
                }
                i++;
        } while (NoContact && (i<LastPoint));
        return Contact;

/****************** Function to find the failure load ******************/

int FailureLoadFunction (float *Load, float *Position, int Contact, int LastPoint)
{
/* Note: Contact is the i-value at which the indenter contacted the material */

int i;                                  /* array counter */
float MaxValue = -1000;         /* initialise */
int NoFailure;                  /* loop checker; = 0 when the failure point is found */
        /* MaxValue - Load[i] = difference in load values; if > 5% MaxValue, failure has occurred */
int MinimumDifference = 3;      /* minimum difference in Newtons which constitutes a 5% difference in load
        value => used to account for noise in signal */
int Failure;                    /* stores i value at which failure occurs */

i = Contact;
do
{       NoFailure = TRUE;  /* initialise loop checker */
```

```
        if (MaxValue < Load[i])
        {       MaxValue = Load[i];
                Failure = i;
        }

        else if ((MaxValue - Load[i] > 0.05*MaxValue) && (MaxValue - Load[i] > MinimumDifference))
        {       printf ("Failure at %f N, %f mm, i = %d.\n", Load[Failure], Position[Failure], Failure);
                NoFailure = FALSE;
        }
        i++;
    } while (NoFailure && i < LastPoint);

return Failure;
}
```

***/****************** Function to do linear regression analysis (find stiffness) ******************/***

```
void StiffnessCalculation (float *Load, float *Position, int Contact, float StartStiffness, float EndStiffness, float
*Slope, float *Intercept, float *rSquared, int *iStartStiffness, int *iEndStiffness)
    /* StartStiffness = load value of beginning of linear region (determined visually) */
    /* EndStiffness = load value of end of linear region (determined visually) */
{   int i;
    float SumLoad;                  /* sum Y */
    float SumPosition;              /* sum X */
    float SumSquaredPosition;       /* sum (X^2) */
    float SumLoadPosition;          /* sum (XY) */
    float SumSquaredLoad;           /* sum (Y^2) */
    int n;                          /* number of data points */
    int FoundStart;                 /* loop checker */
    int FoundEnd;                   /* loop checker */

    /* initialise variables */

    SumLoad = 0;
    SumPosition = 0;
    SumSquaredPosition = 0;
    SumLoadPosition = 0;
    SumSquaredLoad = 0;

    FoundStart = 0;         /* this loop checker will be set to the i value of the first point in the linear region */
    FoundEnd = 0;           /* this loop checker will be set to the i value of the last point in the linear region */

    /* find the i-value of the point at which the linear region begins */

    i = Contact;    /* start checking at Contact point */
    while (FoundStart = = 0)
    {   if (Load[i] > StartStiffness)
        {       FoundStart = i;
                *iStartStiffness = FoundStart;
        }
        i++;
    }
```

```
/* find the i-value of the point at which the linear region ends */
i = FoundStart;
while (FoundEnd = = 0
{       if (Load[i] > EndStiffness)
        {       FoundEnd = i;
                *iEndStiffness = FoundEnd;
        }
        i++;
}
n = FoundEnd - FoundStart;      /* number of data points in linear regression */
i = FoundStart;         /* start linear regression from the beginning of the linear region */
/* calculate values needed for linear regression calculations */
while (i < FoundEnd)
{       SumLoad = SumLoad + Load[i];
        SumPosition = SumPosition + Position[i];
        SumSquaredPosition = SumSquaredPosition + (Position[i] * Position[i]);
        SumLoadPosition = SumLoadPosition + (Load[i] * Position[i]);
        SumSquaredLoad += Load[i] * Load[i];
        i++;
}
/* Linear Regression Analysis */
/* y = mx + b; m = slope, b = intercept */
/* m = [(sum y)(sum x^2) - (sum x)(sum xy)] / [n(sum x^2) - (sum x)^2] */
   *Slope = ((n * SumLoadPosition) - (SumPosition * SumLoad)) / ((n * SumSquaredPosition) -
SumPosition*SumPosition);
/* b = [n(sum xy) - (sum x)(sum y)] / [n(sum x^2) - (sum x)^2] */
   *Intercept = ((SumLoad * SumSquaredPosition) - (SumPosition * SumLoadPosition)) / ((n *
SumSquaredPosition) - SumPosition*SumPosition);
/* r^2 = [sum (X-Xavg)(Y-Yavg)]^2 / [(sum (X-Xavg)^2) (sum (Y-Yavg)^2)]
        = [n(sum xy) - (sum x)(sum y)]^2 / [(n(sum x^2) - (sum x)^2) (n (sum y^2) - (sum y)^2)] */
   *rSquared = (n * SumLoadPosition) - (SumLoad * SumPosition);
   *rSquared *= *rSquared;
   *rSquared /= ((n * SumSquaredPosition) - SumPosition*SumPosition) * ((n * SumSquaredLoad) -
SumLoad*SumLoad);
return;
}
```

### C.3 Endplate Map Generator: MapEndplate.c

MapEndplate.c takes the second text file output by PALstiffness.c as input (section C.2). It places the failure loads, stiffnesses, and $r^2$-values in arrays based on the x- and y-values of the test sites and outputs this data in the form of maps (section A.5, Appendix A).

These maps were used as a way of visually analysing the results to get a basic impression of which regions of the endplate appeared to be stronger. The statistics described in chapter 3 were used to obtain actual relationships between the endplate regions.

Normalised failure loads and stiffnesses were also calculated and output in map form. The normalised values were calculated by dividing each failure load or stiffness by the failure load or stiffness at point (0,0) (the centre of the endplate). This provided an easy method of comparing between endplates for an initial, "back-of-the-envelope" type of comparison, by eliminating differences based on the overall strength of the different endplates. These values are not shown in this document due to space limitations.

```
/********************** Beginning of Program **********************/
/* MapEndplate.c */
/* 99.07.25 */

/* Reads in data from the output file produced by the Indentation data processing file:
   PALstiffness.c.
   The data is in the form: x        y        failure load      stiffness        r-squared
   for a single endplate, with failure load in Newtons and stiffness in N/mm.

   This program organises the data using the x,y coordinates of the test sites and normalises
   it using the values at (0,0).
                Normalised failure load = failure load (x,y) / failure load (0,0)
                Normalised stiffness = stiffness (x,y) / stiffness (0,0)
*/

#include <math.h>
#include <stdlib.h>
#include <stdio.h>
#include <string.h>

/***** Functions *****/

void InitialiseFloatArray (float [ ], int);
void InitialiseIntArray (int [ ], int);
int SortByX (int);
void SortByY (int, int , float , float);
void SendToFile (FILE *, float [ ], int, float);

/***** Global Variables *****/

float forty[14];                /* array of elements with y = 40 */
float twenty[14];           /* array of elements with y = 20 */
float zero[14];                 /* array of elements with y = 0 */
float minus_twenty[14];         /* array of elements with y = -20 */
float minus_forty[14];          /* array of elements with y = -40 */

/********************** Beginning of Main Program **********************/

int main()
{

char DataFile[70];              /* name of the data file containing the information to be processed */
char MappedData[70];            /* mapped data */
```

```
FILE *pointerDataFile;          /* file pointer to input file containing the information to be processed */
FILE *pointerMappedData;        /* file pointer to output file containing the mapped data */

char FindDataPoints;      /* used to find end of header information (x  y  Load  Stiffness  r-Squared  :) */
int AtDataPoints; /* 0 while still looking at header of DataFile, 1 when reach :
                                (indicates end of header) */

int i;                          /* array pointer to X, Y, FailureLoad and Stiffness */
int X[35];                      /* array containing all x-values from DataFile */
int Y[35];                      /* array containing all y-values from DataFile */
float FailureLoad[35];          /* array containing all failure loads from DataFile */
float Stiffness[35];            /* array containing all stiffnesses from DataFile */
float rSquared[35];             /* array containing all r-squared values from DataFile */
int NumPoints;                  /* number of data points in the arrays from DataFile */

int x_value;                    /* value of X[i] sent to SortByX function */
int y_value;                    /* value of Y[i] sent to SortByY function */
float ToSort;                   /* value of FailureLoad[i] or Stiffness[i] sent to SortByY function */
float rSq;                      /* value of r-Squared[i] sent to SortByY function (0 if sorting load) */

int x_el;                       /* array pointer to y-arrays */

float failure_0;                /* failure load at 0,0 */
float stiffness_0;        /* stiffness at 0,0 */
/* float failure_norm;          /* normalised failure load at the point being processed */
/* float stiffness_norm;        /* normalised stiffness at the point being processed */

/***** open the data file containing the information to be processed by this program *****/


printf ("Please enter the name of the text file containing the x,y coordinates, \n");
printf ("failure loads and stiffnesses for the endplate to be analysed: ");
scanf ("%s", &DataFile);

if ((pointerDataFile = fopen (DataFile, "r")) == NULL)
{       printf ("\nCould not open file %s", DataFile);
        exit(1);
}

printf ("Please enter the name of the mapped data output file: ");
scanf ("%s", &MappedData);   /* read in the name of the data file to be analysed */

/***** open file and check that file opened *****/
if ((pointerMappedData = fopen (MappedData,"w")) == NULL)  /* open the output file in write mode */
{       printf ("\nCould not open file %s", MappedData);
        exit(1);
}

/* header for mapped data output file */
fprintf (pointerMappedData, "This is the mapped data for %s.\n\n", DataFile);

/***** initialise arrays *****/
InitialiseIntArray (X, 35);
InitialiseIntArray (Y, 35);
InitialiseFloatArray (FailureLoad, 35);
```

```
InitialiseFloatArray (Stiffness, 35);
InitialiseFloatArray (rSquared, 35);
InitialiseFloatArray (forty, 14);
InitialiseFloatArray (twenty, 14);
InitialiseFloatArray (zero, 14);
InitialiseFloatArray (minus_twenty, 14);
InitialiseFloatArray (minus_forty, 14);

/***** read in x, y, failure load, and stiffness *****/

/* skip header information */
AtDataPoints = 0;
while (!AtDataPoints)
{       FindDataPoints = fgetc (pointerDataFile);
        AtDataPoints = (FindDataPoints ==':');
}

/***** read in values *****/

i = 0;    /* initialise array pointer */

while (fscanf(pointerDataFile,"%d %d %f %f %f", &X[i], &Y[i], &FailureLoad[i], &Stiffness[i], &rSquared[i]) !=
EOF)
{       printf ("%d\t%d\t%f\t%f\t%f\n", X[i], Y[i], FailureLoad[i], Stiffness[i], rSquared[i]);
        i++;
}
NumPoints = i;    /* number of data points read in from DataFile */

/* close the data file */
fclose (pointerDataFile);

/***** sort the failure loads by (x,y) *****/

i = 0;

while (i < NumPoints)
{       x_value = X[i];
        x_el = SortByX (x_value);
        printf ("Sorted by x.\n");

        y_value = Y[i];
        ToSort = FailureLoad[i];
        rSq = 0;

        SortByY (x_el, y_value, ToSort, rSq);
        printf ("Sorted by y.\n");

        i++;
}

/***** output the mapped failure loads to the mapped data output file *****/

fprintf (pointerMappedData, "Failure Load (N)\n\n");
fprintf (pointerMappedData, "x =\t -45\t -30\t -15\t 0\t 15\t 30\t 45\t\n\n");

fprintf (pointerMappedData, "y = 40");
```

```
SendToFile (pointerMappedData, forty, 0, 1);

fprintf (pointerMappedData, "y = 20");
SendToFile (pointerMappedData, twenty, 0, 1);

fprintf (pointerMappedData, "y = 0");
SendToFile (pointerMappedData, zero, 0, 1);

fprintf (pointerMappedData, "y = -20");
SendToFile (pointerMappedData, minus_twenty, 0, 1);

fprintf (pointerMappedData, "y = -40");
SendToFile (pointerMappedData, minus_forty, 0, 1);

/***** output the normalised mapped failure loads to the mapped data output file *****/

fprintf (pointerMappedData, "\n\nNormalised Failure Load (N)\n\n");
fprintf (pointerMappedData, "x =\t -45\t -30\t -15\t 0\t 15\t 30\t 45\t\n\n");

failure_0 = zero[3];

fprintf (pointerMappedData, "y = 40");
SendToFile (pointerMappedData, forty, 0, failure_0);

fprintf (pointerMappedData, "y = 20");
SendToFile (pointerMappedData, twenty, 0, failure_0);

fprintf (pointerMappedData, "y = 0");
SendToFile (pointerMappedData, zero, 0, failure_0);

fprintf (pointerMappedData, "y = -20");
SendToFile (pointerMappedData, minus_twenty, 0, failure_0);

fprintf (pointerMappedData, "y = -40");
SendToFile (pointerMappedData, minus_forty, 0, failure_0);

/***** sort the stiffnesses by (x,y) *****/

i = 0;

while (i < NumPoints)
{       x_value = X[i];
        x_el = SortByX (x_value);

        y_value = Y[i];
        ToSort = Stiffness[i];
        rSq = rSquared[i];

        SortByY (x_el, y_value, ToSort, rSq);

        i++;
}

/***** output the mapped stiffnesses values to the mapped data output file *****/

fprintf (pointerMappedData, "\n\nStiffness (N/mm)\n\n");
fprintf (pointerMappedData, "x =\t -45\t -30\t -15\t 0\t 15\t 30\t 45\t\n\n");

fprintf (pointerMappedData, "y = 40");
SendToFile (pointerMappedData, forty, 0, 1);
```

```
fprintf (pointerMappedData, "y = 20");
SendToFile (pointerMappedData, twenty, 0, 1);

fprintf (pointerMappedData, "y = 0");
SendToFile (pointerMappedData, zero, 0, 1);

fprintf (pointerMappedData, "y = -20");
SendToFile (pointerMappedData, minus_twenty, 0, 1);

fprintf (pointerMappedData, "y = -40");
SendToFile (pointerMappedData, minus_forty, 0, 1);
/***** output the mapped r-squared values to the mapped data output file *****/

fprintf (pointerMappedData, "\n\nr-Squared Values for Stiffness and Normalised Stiffness\n\n");
fprintf (pointerMappedData, "x =\t -45\t -30\t -15\t 0\t 15\t 30\t 45\t\n\n");

fprintf (pointerMappedData, "y = 40");
SendToFile (pointerMappedData, forty, 7, 1);

fprintf (pointerMappedData, "y = 20");
SendToFile (pointerMappedData, twenty, 7, 1);

fprintf (pointerMappedData, "y = 0");
SendToFile (pointerMappedData, zero, 7, 1);

fprintf (pointerMappedData, "y = -20");
SendToFile (pointerMappedData, minus_twenty, 7, 1);

fprintf (pointerMappedData, "y = -40");
SendToFile (pointerMappedData, minus_forty, 7, 1);

/***** output the normalised mapped stiffnesses to the mapped data output file *****/
fprintf (pointerMappedData, "\n\nNormalised Stiffness (N/mm)\n\n");
fprintf (pointerMappedData, "x =\t -45\t -30\t -15\t 0\t 15\t 30\t 45\t\n\n");

stiffness_0 = zero[3];

fprintf (pointerMappedData, "y = 40");
SendToFile (pointerMappedData, forty, 0, stiffness_0);

fprintf (pointerMappedData, "y = 20");
SendToFile (pointerMappedData, twenty, 0, stiffness_0);

fprintf (pointerMappedData, "y = 0");
SendToFile (pointerMappedData, zero, 0, stiffness_0);

fprintf (pointerMappedData, "y = -20");
SendToFile (pointerMappedData, minus_twenty, 0, stiffness_0);

fprintf (pointerMappedData, "y = -40");
SendToFile (pointerMappedData, minus_forty, 0, stiffness_0);

/* close output file */
fclose (pointerMappedData);

return (1);

} /********** End of Main Program **********/
```

```
/*************** Beginning of Functions ***************/
/***** function that initialises float arrays *****/

void InitialiseFloatArray (float array_name[], int number_elements)
{       int i;
        for (i = 0; i < number_elements; i++) {array_name[i] = 0;}
        return;
}

/***** function that initialises integer arrays *****/

void InitialiseIntArray (int array_name[], int number_elements)
{       int i;

        for (i = 0; i < number_elements; i++) {array_name[i] = 0;}
        return;
}

/***** function that determines the correct array location based on x value *****/

int SortByX (int x_value)
{       int x_el;

        switch (x_value)
        {       case -45:
                        x_el = 0;
                        break;
                case -30:
                        x_el = 1;
                        break;
                case -15:
                        x_el = 2;
                        break;
                case 0:
                        x_el = 3;
                        break;
                case 15:
                        x_el = 4;
                        break;
                case 30:
                        x_el = 5;
                        break;
                default: /* case 45 */
                        x_el = 6;
                        break;
        }

        return x_el;
}
/***** function that determines the correct array to store the failure load or stiffness value in
        based on y-value -> stores the value *****/

void SortByY (int x_el, int y_value, float ToSort, float rSq)
```

```
{       switch (y_value)
        {       case 40:
                        forty[x_el] = ToSort;
                        forty[x_el + 7] = rSq;
                        break;
                case 20:
                        twenty[x_el] = ToSort;
                        twenty[x_el + 7] = rSq;
                        break;
                case 0:
                        zero[x_el] = ToSort;
                        zero[x_el + 7] = rSq;
                        break;
                case -20:
                        minus_twenty[x_el] = ToSort;
                        minus_twenty[x_el + 7] = rSq;
                        break;
                default: /* case -40 */
                        minus_forty[x_el] = ToSort;
                        minus_forty[x_el + 7] = rSq;
                        break;
        }
        return;
}
```

***/***** function to output data to file ****/***

```
void SendToFile (FILE *file_pointer, float array[], int array_pointer, float divisor)
{       int i;
        for (i = array_pointer; i < (array_pointer + 7); i++) {fprintf (file_pointer, "\t%f", array[i]/divisor);}
        fprintf (file_pointer, "\n");
        return;
}
```

## C.4 Statistics Input File Generator: GenerateStatsFiles&Maps+Norm.c

GenerateStatsFiles&Maps+Norm.c takes as input a text file containing the combined contents of all of the "_ToMap_st" files output by PALstiffness.c (section C.2) along with some additional data about the endplates. The data in this file is arranged in the following manner:

| | | | | | |
|---|---|---|---|---|---|
| Specimen#_SpinalLevel_Endplate*(space)* | | | DEXA | DD | # Tests |
| x-value | y-value | Failure Load | Stiffness | $r^2$ | |
| … | … | … | … | … | |
| 1 | 1 | 1 | 1 | 1 | |
| Specimen#_SpinalLevel_Endplate*(space)* | | | DEXA | DD | # Tests |

| | | | | | |
|---|---|---|---|---|---|
| x-value | y-value | Failure Load | Stiffness | $r^2$ | |
| ... | ... | ... | ... | ... | |
| 1 | 1 | 1 | 1 | 1 | |
| ... | | | | | |
| Specimen#_SpinalLevel_Endplate*(space)* | | | DEXA | DD | # Tests |
| x-value | y-value | Failure Load | Stiffness | $r^2$ | |
| ... | ... | ... | ... | ... | |
| 1 | 1 | 1 | 1 | 1 | |

i.e. each endplate is listed by name (with a space after the name to ensure correct processing of the string), followed by the DEXA and DD values found for that endplate, and the number of tests that were not rejected. This line is followed by the contents of the "_ToMap_st" file for that endplate, generated by PALstiffness.c. Each endplate is followed by a row of 1's, separating it from the next endplate listing.

Two such files were created. The first contained the listing for each specimen tested with the entire endplate in place. The second contained the listings for each specimen tested with half of the endplate removed.

These input files were used to generate files for use in the Statistica software package for statistical analysis of the test results. The program simply reorganises the values and outputs them into a series of files in the appropriate formats for the various desired analyses.

```
/************************ Beginning of Program ************************/
/* Generate Files for Statistical Analysis and Map Revised Endplate Data */
/* GenerateStatsFilesAndMaps.c */
/* 99.09.24 */

/* Reads in data from a summary file of the data to be used in Statistica to generate
   statistics on the endplate data.
   The data file contains data for each endplate that has been tested to date.
   Modifications have been made to the data to correct errors in the initial processing phase
   (mainly errors in choosing the correct slope).
   The data is in the form:

                Specimen#_Level_Endplate        DEXA    #tests
                x       y       failure load    stiffness r-squared
                1       1       1       1       1

   with failure load in Newtons and stiffness in N/mm.

   This program organises the data using the x,y coordinates of the test sites and outputs them to
   data files (Specimen#_Level_Endplate_Revised.map).
                Normalised failure load = failure load (x,y) / failure load (0,0)
                Normalised stiffness = stiffness (x,y) / stiffness (0,0)
*/

#include <math.h>
#include <stdlib.h>
#include <stdio.h>
#include <string.h>
```

```
/***** Functions *****/

void InitialiseFloatArray (float [ ], int);
void InitialiseIntArray (int [ ], int);
int SortByX (int);
void SortByY (int, int , float , float);
void SendToFile (FILE *, float [ ], int, float);
void GeneralOutput (FILE *, float [ ], float [ ], float [ ], float [ ], float [ ], float);

/***** Global Variables *****/
float forty[14];                /* array of elements with y = 40 */
float twenty[14];               /* array of elements with y = 20 */
float zero[14];                 /* array of elements with y = 0 */
float minus_twenty[14];         /* array of elements with y = -20 */
float minus_forty[14];          /* array of elements with y = -40 */

/********************** Beginning of Main Program ********************/

int main()
{

char DataFile[70];              /* name of the data file containing the information to be processed */
char MappedData[70];            /* name of the output file containing the mapped data */
char CentrePointFL[70];   /* name of output file containing only centre point Failure Load data */
char CentrePointST[70];   /* name of output file containing only centre Stiffness data */
char AverageMiddle5FL[70];      /* output file containing Failure Load averages of central 5 points */
char AverageMiddle5ST[70];      /* output file containing Stiffness averages of central 5 points */
char AverageCornerFL[70];       /* output file containing Failure Load averages of 5 corner points */
char AverageCornerST[70];       /* output file containing Stiffness averages of the 5 corner points */
char DEXAfl[70];
char DEXAst[70];
char GeneralFL[70];
char GeneralST[70];
char DEXAfl_Norm[70];
char DEXAst_Norm[70];
char GeneralFL_Norm[70];
char GeneralST_Norm[70];
char Statistica[70];

FILE *pointerDataFile;          /* file pointer to the input file containing information to be processed */
FILE *pointerMappedData;        /* file pointer to the output file containing the mapped data */
FILE *pointerCentrePointFL;     /* pointer to name of the output file containing centre point FLs */
FILE *pointerCentrePointST;     /* pointer to name of the output containing centre point STs */
FILE *pointerAverageMiddle5FL; /*pointer to name of output file containing avrgs of central 5 FLs */
FILE *pointerAverageMiddle5ST; /*pointer to name of output file containing avrgs of central 5 STs */
FILE *pointerAverageCornerFL;  /*pointer to name of output file containing avrgs of corner FLs */
FILE *pointerAverageCornerST;  /*pointer to name of output file containing avrgs of corner STs */
FILE *pointerDEXAfl;
FILE *pointerDEXAst;
FILE *pointerGeneralFL;
FILE *pointerGeneralST;
```

```
FILE *pointerDEXAfl_Norm;
FILE *pointerDEXAst_Norm;
FILE *pointerGeneralFL_Norm;
FILE *pointerGeneralST_Norm;
FILE *pointerStatistica;

char MapThisData[70];    /* name of the endplate currently being analysed */
float DEXA;              /* DEXA value of the endplate being analysed */
int NumTests;            /* number of tests that are being used on the endplate being analysed */

char GetEndplate[11];          /* endplate identifier (e.g. 1007_L3_s ) */
char SpecimenNum[5]=" ";       /* specimen number (e.g. 1007) */
char SpinalLevel[3]=" ";       /* spinal level (e.g. L3) */
char Endplate[2]=" ";          /* endplate (e.g. s) */

float NormFailureLoad;
float NormStiffness;

float AverageMiddle;     /* average central failure load or stiffness:
                                average value of points (0,0), (15,0), (-15,0), (0,20), (0,-20) */
float AverageCorner;     /* average corner failure load or stiffness:
                                average value of points (-30,20), (30,20), (-30,40), (30,-40) */
int NumberNonZero;       /* number of non-zero values included in the average */

/* char FindDataPoints;  /* used to find end of header information (x y Load Stiffness r-Squared :) */
/* int AtDataPoints;     /* 0 while still looking at header of DataFile, 1 when reach :
                                (indicates end of header) */

int i;                   /* array pointer to X, Y, FailureLoad and Stiffness */
int LoopCheck;           /* holds the value of X[i] -> equal to 1 when the final data point for an endplate
                                is reached */
int X[35];               /* array containing all x-values from DataFile */
int Y[35];               /* array containing all y-values from DataFile */
float FailureLoad[35];   /* array containing all failure loads from DataFile */
float Stiffness[35];     /* array containing all stiffnesses from DataFile */
float rSquared[35];      /* array containing all r-squared values from DataFile */
int NumPoints;           /* number of data points in the arrays from DataFile */

int x_value;             /* value of X[i] sent to SortByX function */
int y_value;             /* value of Y[i] sent to SortByY function */
float ToSort;            /* value of FailureLoad[i] or Stiffness[i] sent to SortByY function */
float rSq;               /* value of r-Squared[i] sent to SortByY function (0 if sorting load) */

int x_el;                /* array pointer to y-arrays */

float failure_0;         /* failure load at 0,0 */
float stiffness_0; /* stiffness at 0,0 */

/***** open the data file containing the information to be processed by this program *****/

printf ("Please enter the name of the text file containing the x,y coordinates, \n");
printf ("failure loads and stiffnesses for the endplates to be analysed: ");
scanf ("%s", &DataFile);
```

```
if ((pointerDataFile = fopen (DataFile, "r")) == NULL)
{       printf ("\nCould not open file %s", DataFile);
        exit(1);
}

printf ("Please enter the name of the mapped data output file: ");
scanf ("%s", &MappedData);   /* read in the name of the data file that will contain the mapped data */

/* open map output file and check that file opened */
if ((pointerMappedData = fopen (MappedData,"w")) == NULL)  /* open the output file in write mode */
{       printf ("\nCould not open file %s", MappedData);
        exit(1);
}

printf ("Please enter the name of the centre point failure load data output file: ");
scanf ("%s", &CentrePointFL);

/* open file and check that file opened */
if ((pointerCentrePointFL = fopen (CentrePointFL,"w")) == NULL)  /* open output file in write mode */
{       printf ("\nCould not open file %s", CentrePointFL);
        exit(1);
}

fprintf (pointerCentrePointFL, "Specimen\tLevel\tEndplate\tCentral Failure Load (N)\n");

printf ("Please enter the name of the centre point stiffness data output file: ");
scanf ("%s", &CentrePointST);

/* open file and check that file opened */
if ((pointerCentrePointST = fopen (CentrePointST,"w")) == NULL)  /* open output file in write mode */
{       printf ("\nCould not open file %s", CentrePointST);
        exit(1);
}

fprintf (pointerCentrePointST, "Specimen\tLevel\tEndplate\tCentral Stiffness (N/mm)\n");

printf ("Please enter the name of the average middle 5 failure load data output file: ");
scanf ("%s", &AverageMiddle5FL);

/* open file and check that file opened */
if ((pointerAverageMiddle5FL = fopen (AverageMiddle5FL,"w"))==NULL) /* open output file in write mode */
{       printf ("\nCould not open file %s", AverageMiddle5FL);
        exit(1);
}

fprintf (pointerAverageMiddle5FL, "Specimen\tLevel\tEndplate\tAverage Central Failure Load (N)\tNormalised
Average Central Failure Load\n");

printf ("Please enter the name of the average middle 5 stiffness data output file: ");
scanf ("%s", &AverageMiddle5ST);

/* open file and check that file opened */
if ((pointerAverageMiddle5ST = fopen (AverageMiddle5ST,"w")) == NULL)  /* open output file in write mode */
{       printf ("\nCould not open file %s", AverageMiddle5ST);
        exit(1);
```

```
}

fprintf (pointerAverageMiddle5ST, "Specimen\tLevel\tEndplate\tAverage Central Stiffness (N/mm)\tNormalised Average Central Stiffness\n");

printf ("Please enter the name of the average corner failure load data output file: ");
scanf ("%s", &AverageCornerFL);

/* open file and check that file opened */
if ((pointerAverageCornerFL = fopen (AverageCornerFL,"w")) == NULL) /* open output file in write mode */
{       printf ("\nCould not open file %s", AverageCornerFL);
        exit(1);
}
fprintf (pointerAverageCornerFL, "Specimen\tLevel\tEndplate\tAverage Corner Failure Load (N)\tNormalised Average Corner Failure Load\n");

printf ("Please enter the name of the average corner stiffness data output file: ");
scanf ("%s", AverageCornerST);

/* open file and check that file opened */
if ((pointerAverageCornerST = fopen (AverageCornerST,"w")) == NULL) /* open output file in write mode */
{       printf ("\nCould not open file %s", AverageCornerST);
        exit(1);
}

fprintf (pointerAverageCornerST, "Specimen\tLevel\tEndplate\tAverage Corner Stiffness (N/mm)\tNormalised Average Corner Stiffness\n");

printf ("Please enter the name of the DEXA failure load data output file: ");
scanf ("%s", &DEXAfl);

/* open file and check that file opened */
if ((pointerDEXAfl = fopen (DEXAfl,"w")) == NULL) /* open the output file in write mode */
{       printf ("\nCould not open file %s", DEXAfl);
        exit(1);
}

fprintf (pointerDEXAfl, "Specimen\tLevel\tEndplate\tDEXA\tfl(-30,40)\tfl(-15,40)\tfl(0,40)\tfl(15,40)\tfl(30,40)\tfl(-45,20)\tfl(-30,20)\tfl(-15,20)\tfl(0,20)\tfl(15,20)\tfl(30,20)\tfl(45,20)\tfl(-45,0)\tfl(-30,0)\tfl(-15,0)\tfl(0,0)\tfl(15,0)\tfl(30,0)\tfl(45,0)\tfl(-45,-20)\tfl(-30,-20)\tfl(-15,-20)\tfl(0,-20)\tfl(15,-20)\tfl(30,-20)\tfl(45,-20)\tfl(-45,-40)\tfl(-30,-40)\tfl(-15,-40)\tfl(0,-40)\tfl(15,-40)\tfl(30,-40)\tfl(45,-40)\n");

printf ("Please enter the name of the DEXA stiffness data output file: ");
scanf ("%s", DEXAst);

/* open file and check that file opened */
if ((pointerDEXAst = fopen (DEXAst,"w")) == NULL) /* open the output file in write mode */
{       printf ("\nCould not open file %s", DEXAst);
        exit(1);
}

fprintf (pointerDEXAst, "Specimen\tLevel\tEndplate\tDEXA\tst(-30,40)\tst(-15,40)\tst(0,40)\tst(15,40)\tst(30,40)\tst(-45,20)\tst(-30,20)\tst(-15,20)\tst(0,20)\tst(15,20)\tst(30,20)\tst(45,20)\tst(-
```

```
45,0)\tst(-30,0)\tst(-15,0)\tst(0,0)\tst(15,0)\tst(30,0)\tst(45,0)\tst(-45,-20)\tst(-30,-20)\tst(-15,-20)\tst(0,-20)\tst(15,-
20)\tst(30,-20)\tst(45,-20)\tst(-45,-40)\tst(-30,-40)\tst(-15,-40)\tst(0,-40)\tst(15,-40)\tst(30,-40)\tst(45,-40)\n");

printf ("Please enter the name of the general failure load data output file: ");
scanf ("%s", &GeneralFL);

/* open file and check that file opened */
if ((pointerGeneralFL = fopen (GeneralFL,"w")) == NULL) /* open the output file in write mode */
{       printf ("\nCould not open file %s", GeneralFL);
        exit(1);
}

fprintf (pointerGeneralFL, "Specimen\tLevel\tEndplate\tfl(-30,40)\tfl(-15,40)\tfl(0,40)\tfl(15,40)\tfl(30,40)\tfl(-
45,20)\tfl(-30,20)\tfl(-15,20)\tfl(0,20)\tfl(15,20)\tfl(30,20)\tfl(45,20)\tfl(-45,0)\tfl(-30,0)\tfl(-
15,0)\tfl(0,0)\tfl(15,0)\tfl(30,0)\tfl(45,0)\tfl(-45,-20)\tfl(-30,-20)\tfl(-15,-20)\tfl(0,-20)\tfl(15,-20)\tfl(30,-20)\tfl(45,-
20)\tfl(-45,-40)\tfl(-30,-40)\tfl(-15,-40)\tfl(0,-40)\tfl(15,-40)\tfl(30,-40)\tfl(45,-40)\n");

printf ("Please enter the name of the general stiffness data output file: ");
scanf ("%s", GeneralST);

/* open file and check that file opened */
if ((pointerGeneralST = fopen (GeneralST,"w")) == NULL) /* open the output file in write mode */
{       printf ("\nCould not open file %s", GeneralST);
        exit(1);
}

fprintf (pointerGeneralST, "Specimen\tLevel\tEndplate\tst(-30,40)\tst(-15,40)\tst(0,40)\tst(15,40)\tst(30,40)\tst(-
45,20)\tst(-30,20)\tst(-15,20)\tst(0,20)\tst(15,20)\tst(30,20)\tst(45,20)\tst(-45,0)\tst(-30,0)\tst(-
15,0)\tst(0,0)\tst(15,0)\tst(30,0)\tst(45,0)\tst(-45,-20)\tst(-30,-20)\tst(-15,-20)\tst(0,-20)\tst(15,-20)\tst(30,-20)\tst(45,-
20)\tst(-45,-40)\tst(-30,-40)\tst(-15,-40)\tst(0,-40)\tst(15,-40)\tst(30,-40)\tst(45,-40)\n");

printf ("Please enter the name of the normalised DEXA failure load data output file: ");
scanf ("%s", DEXAfl_Norm);

/* open file and check that file opened */
if ((pointerDEXAfl_Norm = fopen (DEXAfl_Norm,"w")) == NULL) /* open output file in write mode */
{       printf ("\nCould not open file %s", DEXAfl_Norm);
        exit(1);
}

fprintf (pointerDEXAfl_Norm, "Specimen\tLevel\tEndplate\tDEXA\tfl_n(-30,40)\tfl_n(-
15,40)\tfl_n(0,40)\tfl_n(15,40)\tfl_n(30,40)\tfl_n(-45,20)\tfl_n(-30,20)\tfl_n(-
15,20)\tfl_n(0,20)\tfl_n(15,20)\tfl_n(30,20)\tfl_n(45,20)\tfl_n(-45,0)\tfl_n(-30,0)\tfl_n(-
15,0)\tfl_n(0,0)\tfl_n(15,0)\tfl_n(30,0)\tfl_n(45,0)\tfl_n(-45,-20)\tfl_n(-30,-20)\tfl_n(-15,-20)\tfl_n(0,-20)\tfl_n(15,-
20)\tfl_n(30,-20)\tfl_n(45,-20)\tfl_n(-45,-40)\tfl_n(-30,-40)\tfl_n(-15,-40)\tfl_n(0,-40)\tfl_n(15,-40)\tfl_n(30,-
40)\tfl_n(45,-40)\n");

printf ("Please enter the name of the normalised DEXA stiffness data output file: ");
scanf ("%s", DEXAst_Norm);

/* open file and check that file opened */
if ((pointerDEXAst_Norm = fopen (DEXAst_Norm,"w")) == NULL) /* open output file in write mode */
{       printf ("\nCould not open file %s", DEXAst_Norm);
        exit(1);
```

```
}

fprintf (pointerDEXAst_Norm, "Specimen\tLevel\tEndplate\tDEXA\tst_n(-30,40)\tst_n(-
15,40)\tst_n(0,40)\tst_n(15,40)\tst_n(30,40)\tst_n(-45,20)\tst_n(-30,20)\tst_n(-
15,20)\tst_n(0,20)\tst_n(15,20)\tst_n(30,20)\tst_n(45,20)\tst_n(-45,0)\tst_n(-30,0)\tst_n(-
15,0)\tst_n(0,0)\tst_n(15,0)\tst_n(30,0)\tst_n(45,0)\tst_n(-45,-20)\tst_n(-30,-20)\tst_n(-15,-20)\tst_n(0,-20)\tst_n(15,-
20)\tst_n(30,-20)\tst_n(45,-20)\tst_n(-45,-40)\tst_n(-30,-40)\tst_n(-15,-40)\tst_n(0,-40)\tst_n(15,-40)\tst_n(30,-
40)\tst_n(45,-40)\n");

printf ("Please enter the name of the normalised general failure load data output file: ");
scanf ("%s", &GeneralFL_Norm);

/* open file and check that file opened */
if ((pointerGeneralFL_Norm = fopen (GeneralFL_Norm,"w")) == NULL) /* open output file in write mode */
{       printf ("\nCould not open file %s", GeneralFL_Norm);
        exit(1);
}

fprintf (pointerGeneralFL_Norm, "Specimen\tLevel\tEndplate\tfl_n(-30,40)\tfl_n(-
15,40)\tfl_n(0,40)\tfl_n(15,40)\tfl_n(30,40)\tfl_n(-45,20)\tfl_n(-30,20)\tfl_n(-
15,20)\tfl_n(0,20)\tfl_n(15,20)\tfl_n(30,20)\tfl_n(45,20)\tfl_n(-45,0)\tfl_n(-30,0)\tfl_n(-
15,0)\tfl_n(0,0)\tfl_n(15,0)\tfl_n(30,0)\tfl_n(45,0)\tfl_n(-45,-20)\tfl_n(-30,-20)\tfl_n(-15,-20)\tfl_n(0,-20)\tfl_n(15,-
20)\tfl_n(30,-20)\tfl_n(45,-20)\tfl_n(-45,-40)\tfl_n(-30,-40)\tfl_n(-15,-40)\tfl_n(0,-40)\tfl_n(15,-40)\tfl_n(30,-
40)\tfl_n(45,-40)\n");

printf ("Please enter the name of the normalised general stiffness data output file: ");
scanf ("%s", GeneralST_Norm);

/* open file and check that file opened */
if ((pointerGeneralST_Norm = fopen (GeneralST_Norm,"w")) == NULL) /* open output file in write mode */
{       printf ("\nCould not open file %s", GeneralST_Norm);
        exit(1);
}

fprintf (pointerGeneralST_Norm, "Specimen\tLevel\tEndplate\tst_n(-30,40)\tst_n(-
15,40)\tst_n(0,40)\tst_n(15,40)\tst_n(30,40)\tst_n(-45,20)\tst_n(-30,20)\tst_n(-
15,20)\tst_n(0,20)\tst_n(15,20)\tst_n(30,20)\tst_n(45,20)\tst_n(-45,0)\tst_n(-30,0)\tst_n(-
15,0)\tst_n(0,0)\tst_n(15,0)\tst_n(30,0)\tst_n(45,0)\tst_n(-45,-20)\tst_n(-30,-20)\tst_n(-15,-20)\tst_n(0,-20)\tst_n(15,-
20)\tst_n(30,-20)\tst_n(45,-20)\tst_n(-45,-40)\tst_n(-30,-40)\tst_n(-15,-40)\tst_n(0,-40)\tst_n(15,-40)\tst_n(30,-
40)\tst_n(45,-40)\n");

printf ("Please enter the name of the basic Statistica file: ");
scanf ("%s", Statistica);

/* open file and check that file opened */
if ((pointerStatistica = fopen (Statistica,"w")) == NULL) /* open the output file in write mode */
{       printf ("\nCould not open file %s", Statistica);
        exit(1);
}

fprintf (pointerStatistica, "Specimen\tLevel\tEndplate\tDEXA\tx\ty\tFailure Load (N)\tStiffness
(N/mm)\trSquared\tNormalised Failure Load\tNormalised Stiffness\n");

/***** WHILE NOT AT END OF FILE, LOOP THROUGH PROGRAM *****/
```

```
/* scan in the name of the endplate being processed (listed in data file) */

printf ("Entering while loop.\n");

while (fscanf(pointerDataFile,"%s\t%f\t%d", &MapThisData, &DEXA, &NumTests) != EOF)      /* read in the
name of the endplate currently being mapped */
{
/***** EXTRACT SPECIMEN#, SPINAL LEVEL AND ENDPLATE FROM HEADER
        Specimen#_Level_Endplate *****/

/* copy the label into GetEndplate to avoid accidentally modifying it */
strcpy(GetEndplate,MapThisData);

/* extract Specimen Number */
SpecimenNum[0] = GetEndplate[0];
SpecimenNum[1] = GetEndplate[1];
SpecimenNum[2] = GetEndplate[2];
SpecimenNum[3] = GetEndplate[3];

/* extract Spinal Level */
SpinalLevel[0] = GetEndplate[5];
SpinalLevel[1] = GetEndplate[6];

/* extract Endplate */
Endplate[0] = GetEndplate[8];

/* header for mapped data output file */
fprintf (pointerMappedData, "This is the mapped data for %s.\n\n", MapThisData);

/***** initialise arrays *****/
InitialiseIntArray (X, 35);
InitialiseIntArray (Y, 35);
InitialiseFloatArray (FailureLoad, 35);
InitialiseFloatArray (Stiffness, 35);
InitialiseFloatArray (rSquared, 35);
InitialiseFloatArray (forty, 14);
InitialiseFloatArray (twenty, 14);
InitialiseFloatArray (zero, 14);
InitialiseFloatArray (minus_twenty, 14);
InitialiseFloatArray (minus_forty, 14);

/***** read in x, y, failure load, stiffness, and r-squared *****/

/***** read in values *****/

i = 0;                  /* initialise array pointer */

LoopCheck = 0;          /* will be set to 1 when end of specimen record is reached */

while (LoopCheck != 1)
{       fscanf(pointerDataFile,"%d %d %f %f %f %f %f", &X[i],&Y[i],
&FailureLoad[i],&Stiffness[i],&rSquared[i],&NormFailureLoad, &NormStiffness);
        if (Stiffness[i] != 1) fprintf(pointerStatistica, "%s\t%s\t%s\t%f\t%d\t%d\t%f\t%f\t%f\t%f\t%f\n",
SpecimenNum, SpinalLevel, Endplate, DEXA, X[i], Y[i], FailureLoad[i], Stiffness[i], rSquared[i],
NormFailureLoad, NormStiffness);
```

```
        LoopCheck = X[i];
        i++;
}
NumPoints = i-1; /* number of data points read in from DataFile (subtract 1 because last set of data is the dummy
data denoting the end of the specimen data) */

/***** sort the failure loads by (x,y) *****/

i = 0;

while (i < NumPoints)
{       x_value = X[i];
        x_el = SortByX (x_value);

        y_value = Y[i];
        ToSort = FailureLoad[i];
        rSq = 0;

        SortByY (x_el, y_value, ToSort, rSq);
        i++;
}

/* output the central failure load */
fprintf (pointerCentrePointFL, "%s\t%s\t%s\t%f\n", SpecimenNum, SpinalLevel, Endplate, zero[3]);

/* output the average failure load of the central 5 points */

AverageMiddle = 0;
AverageMiddle += twenty[3] + zero[2] + zero[3] + zero[4] + minus_twenty[3];
NumberNonZero = 5;
if (twenty[3] == 0) NumberNonZero -= 1;
if (zero[2] == 0) NumberNonZero -= 1;
if (zero[3] == 0) NumberNonZero -= 1;
if (zero[4] == 0) NumberNonZero -= 1;
if (minus_twenty[3] == 0) NumberNonZero -= 1;
AverageMiddle /= NumberNonZero;

fprintf (pointerAverageMiddle5FL, "%s\t%s\t%s\t%f\t%f\n", SpecimenNum, SpinalLevel, Endplate,
AverageMiddle, AverageMiddle/zero[3]);

/* output the average corner failure load value */

AverageCorner = 0;
AverageCorner += twenty[1] + twenty[5] + minus_forty[1] + minus_forty[5];
NumberNonZero = 4;
if (twenty[1] == 0) NumberNonZero -= 1;
if (twenty[5] == 0) NumberNonZero -= 1;
if (minus_forty[1] == 0) NumberNonZero -= 1;
if (minus_forty[5] == 0) NumberNonZero -= 1;
AverageCorner /= NumberNonZero;

fprintf (pointerAverageCornerFL, "%s\t%s\t%s\t%f\t%f\n", SpecimenNum, SpinalLevel, Endplate, AverageCorner,
AverageCorner/zero[3]);
```

```
/* output the failure loads with DEXA */

fprintf (pointerDEXAfl, "%s\t%s\t%s\t%f\t", SpecimenNum, SpinalLevel, Endplate, DEXA);
GeneralOutput (pointerDEXAfl, forty, twenty, zero, minus_twenty, minus_forty, 1);

/* output the failure loads without DEXA */

fprintf (pointerGeneralFL, "%s\t%s\t%s\t", SpecimenNum, SpinalLevel, Endplate);
GeneralOutput (pointerGeneralFL, forty, twenty, zero, minus_twenty, minus_forty, 1);

/* output the normalised failure loads with DEXA */

fprintf (pointerDEXAfl_Norm, "%s\t%s\t%s\t%f\t", SpecimenNum, SpinalLevel, Endplate, DEXA);
GeneralOutput (pointerDEXAfl_Norm, forty, twenty, zero, minus_twenty, minus_forty, zero[3]);

/* output the normalised failure loads without DEXA */

fprintf (pointerGeneralFL_Norm, "%s\t%s\t%s\t", SpecimenNum, SpinalLevel, Endplate);
GeneralOutput (pointerGeneralFL_Norm, forty, twenty, zero, minus_twenty, minus_forty, zero[3]);

/* output the mapped failure loads to the mapped data output file */

fprintf (pointerMappedData, "Failure Load (N)\n\n");
fprintf (pointerMappedData, "x =\t -45\t -30\t -15\t 0\t 15\t 30\t 45\t\n");

fprintf (pointerMappedData, "y = 40");
SendToFile (pointerMappedData, forty, 0, 1);

fprintf (pointerMappedData, "y = 20");
SendToFile (pointerMappedData, twenty, 0, 1);

fprintf (pointerMappedData, "y = 0");
SendToFile (pointerMappedData, zero, 0, 1);

fprintf (pointerMappedData, "y = -20");
SendToFile (pointerMappedData, minus_twenty, 0, 1);

fprintf (pointerMappedData, "y = -40");
SendToFile (pointerMappedData, minus_forty, 0, 1);

/* output the normalised mapped failure loads to the mapped data output file */

fprintf (pointerMappedData, "\n\nNormalised Failure Load (N)\n\n");
fprintf (pointerMappedData, "x =\t -45\t -30\t -15\t 0\t 15\t 30\t 45\t\n");

failure_0 = zero[3];

fprintf (pointerMappedData, "y = 40");
SendToFile (pointerMappedData, forty, 0, failure_0);

fprintf (pointerMappedData, "y = 20");
SendToFile (pointerMappedData, twenty, 0, failure_0);

fprintf (pointerMappedData, "y = 0");
SendToFile (pointerMappedData, zero, 0, failure_0);

fprintf (pointerMappedData, "y = -20");
SendToFile (pointerMappedData, minus_twenty, 0, failure_0);
```

```
fprintf (pointerMappedData, "y = -40");
SendToFile (pointerMappedData, minus_forty, 0, failure_0);

/***** sort the stiffnesses by (x,y) *****/

i = 0;

while (i < NumPoints)
{       x_value = X[i];
        x_el = SortByX (x_value);

        y_value = Y[i];
        ToSort = Stiffness[i];
        rSq = rSquared[i];

        SortByY (x_el, y_value, ToSort, rSq);

        i++;
}

/* output the central stiffness */
fprintf (pointerCentrePointST, "%s\t%s\t%s\t%f\n", SpecimenNum, SpinalLevel, Endplate, zero[3]);

/* output the average stiffness of the central 5 points */

AverageMiddle = 0;
AverageMiddle += twenty[3] + zero[2] + zero[3] + zero[4] + minus_twenty[3];
NumberNonZero = 5;
if (twenty[3] == 0) NumberNonZero -= 1;
if (zero[2] == 0) NumberNonZero -= 1;
if (zero[3] == 0) NumberNonZero -= 1;
if (zero[4] == 0) NumberNonZero -= 1;
if (minus_twenty[3] == 0) NumberNonZero -= 1;
AverageMiddle /= NumberNonZero;

fprintf (pointerAverageMiddle5ST, "%s\t%s\t%s\t%f\t%f\n", SpecimenNum, SpinalLevel, Endplate,
AverageMiddle, AverageMiddle/zero[3]);

/* output the average corner stiffness value */

AverageCorner = 0;
AverageCorner += twenty[1] + twenty[5] + minus_forty[1] + minus_forty[5];
NumberNonZero = 4;
if (twenty[1] == 0) NumberNonZero -= 1;
if (twenty[5] == 0) NumberNonZero -= 1;
if (minus_forty[1] == 0) NumberNonZero -= 1;
if (minus_forty[5] == 0) NumberNonZero -= 1;
AverageCorner /= NumberNonZero;

fprintf (pointerAverageCornerST, "%s\t%s\t%s\t%f\t%f\n", SpecimenNum, SpinalLevel, Endplate, AverageCorner,
AverageCorner/zero[3]);

/* output the stiffnesses with DEXA */

fprintf (pointerDEXAst, "%s\t%s\t%s\t%f\t", SpecimenNum, SpinalLevel, Endplate, DEXA);
GeneralOutput (pointerDEXAst, forty, twenty, zero, minus_twenty, minus_forty, 1);
```

```
/* output the stiffnesses without DEXA */

fprintf (pointerGeneralST, "%s\t%s\t%s\t", SpecimenNum, SpinalLevel, Endplate);
GeneralOutput (pointerGeneralST, forty, twenty, zero, minus_twenty, minus_forty, 1);

/* output the normalised stiffnesses with DEXA */

fprintf (pointerDEXAst_Norm, "%s\t%s\t%s\t%f\t", SpecimenNum, SpinalLevel, Endplate, DEXA);
GeneralOutput (pointerDEXAst_Norm, forty, twenty, zero, minus_twenty, minus_forty, zero[3]);

/* output the normalised stiffnesses without DEXA */

fprintf (pointerGeneralST_Norm, "%s\t%s\t%s\t", SpecimenNum, SpinalLevel, Endplate);
GeneralOutput (pointerGeneralST_Norm, forty, twenty, zero, minus_twenty, minus_forty, zero[3]);

/* output the mapped stiffnesses values to the the mapped data output file */

fprintf (pointerMappedData, "\n\nStiffness (N/mm)\n\n");
fprintf (pointerMappedData, "x =\t -45\t -30\t -15\t 0\t 15\t 30\t 45\t\n");
fprintf (pointerMappedData, "y = 40");
SendToFile (pointerMappedData, forty, 0, 1);

fprintf (pointerMappedData, "y = 20");
SendToFile (pointerMappedData, twenty, 0, 1);

fprintf (pointerMappedData, "y = 0");
SendToFile (pointerMappedData, zero, 0, 1);

fprintf (pointerMappedData, "y = -20");
SendToFile (pointerMappedData, minus_twenty, 0, 1);

fprintf (pointerMappedData, "y = -40");
SendToFile (pointerMappedData, minus_forty, 0, 1);

/* output the mapped r-squared values to the the mapped data output file */

fprintf (pointerMappedData, "\n\nr-Squared\n\n");
fprintf (pointerMappedData, "x =\t -45\t -30\t -15\t 0\t 15\t 30\t 45\t\n");

fprintf (pointerMappedData, "y = 40");
SendToFile (pointerMappedData, forty, 7, 1);

fprintf (pointerMappedData, "y = 20");
SendToFile (pointerMappedData, twenty, 7, 1);

fprintf (pointerMappedData, "y = 0");
SendToFile (pointerMappedData, zero, 7, 1);

fprintf (pointerMappedData, "y = -20");
SendToFile (pointerMappedData, minus_twenty, 7, 1);

fprintf (pointerMappedData, "y = -40");
SendToFile (pointerMappedData, minus_forty, 7, 1);

/* output the normalised mapped stiffnesses to the mapped data output file */
fprintf (pointerMappedData, "\n\nNormalised Stiffness (N/mm)\n\n");
fprintf (pointerMappedData, "x =\t -45\t -30\t -15\t 0\t 15\t 30\t 45\t\n");

stiffness_0 = zero[3];
```

```
fprintf (pointerMappedData, "y = 40");
SendToFile (pointerMappedData, forty, 0, stiffness_0);

fprintf (pointerMappedData, "y = 20");
SendToFile (pointerMappedData, twenty, 0, stiffness_0);

fprintf (pointerMappedData, "y = 0");
SendToFile (pointerMappedData, zero, 0, stiffness_0);

fprintf (pointerMappedData, "y = -20");
SendToFile (pointerMappedData, minus_twenty, 0, stiffness_0);

fprintf (pointerMappedData, "y = -40");
SendToFile (pointerMappedData, minus_forty, 0, stiffness_0);

fprintf (pointerMappedData, "\n\n")
;
/***** END OF MAPPING *****/

} /* END OF WHILE LOOP */

/* close the data (input) file */
fclose (pointerDataFile);

/* close all output files */
fclose (pointerMappedData);
fclose (pointerCentrePointFL);
fclose (pointerCentrePointST);
fclose (pointerAverageMiddle5FL);
fclose (pointerAverageMiddle5ST);
fclose (pointerAverageCornerFL);
fclose (pointerAverageCornerST);
fclose (pointerDEXAfl);
fclose (pointerDEXAst);
fclose (pointerGeneralFL);
fclose (pointerGeneralST);
fclose (pointerStatistica);

return (1);

} /********** End of Main Program **********/

/********** Beginning of Functions **********/
/***** function that initialises float arrays *****/

void InitialiseFloatArray (float array_name[], int number_elements)
{       int i;
        for (i = 0; i < number_elements; i++) {array_name[i] = 0;}
        return;
}

/***** function that initialises integer arrays *****/

void InitialiseIntArray (int array_name[], int number_elements)
{       int i;
        for (i = 0; i < number_elements; i++) {array_name[i] = 0;}
```

```
        return;
}
```

***/***** function that determines the correct array location based on x value *****/***

```
int SortByX (int x_value)
{       int x_el;

        switch (x_value)
        {       case -45:
                        x_el = 0;
                        break;
                case -30:
                        x_el = 1;
                        break;
                case -15:
                        x_el = 2;
                        break;
                case 0:
                        x_el = 3;
                        break;
                case 15:
                        x_el = 4;
                        break;
                case 30:
                        x_el = 5;
                        break;
                default: /* case 45 */
                        x_el = 6;
                        break;
        }

        return x_el;
}
```

***/***** function that determines the correct array to store the failure load or stiffness value in based on y-value -> stores the value *****/***

```
void SortByY (int x_el, int y_value, float ToSort, float rSq)
{       switch (y_value)
        {       case 40:
                        forty[x_el] = ToSort;
                        forty[x_el + 7] = rSq;
                        break;
                case 20:
                        twenty[x_el] = ToSort;
                        twenty[x_el + 7] = rSq;
                        break;
                case 0:
                        zero[x_el] = ToSort;
                        zero[x_el + 7] = rSq;
```

```
                    break;
            case -20:
                    minus_twenty[x_el] = ToSort;
                    minus_twenty[x_el + 7] = rSq;
                    break;
            default: /* case -40 */
                    minus_forty[x_el] = ToSort;
                    minus_forty[x_el + 7] = rSq;
                    break;
        }
        return;
}
```

***/***** function that output data to file *****/***

```
void SendToFile (FILE *file_pointer, float array[ ], int array_pointer, float divisor)
{       int i;

        for (i = array_pointer; i < (array_pointer + 7); i++){fprintf (file_pointer, "\t%f", array[i]/divisor);}
        fprintf (file_pointer, "\n");

        return;
}
```

***/***** function to output data *****/***

```
void GeneralOutput(FILE * filepointer, float forty[], float twenty[], float zero[], float minus_twenty[], float
minus_forty[], float divisor)
{       int i;

        for (i = 1; i <= 5; i++) {fprintf(filepointer, "%f\t", forty[i]/divisor);}
        for (i = 0; i <= 6; i++) {fprintf(filepointer, "%f\t", twenty[i]/divisor);}
        for (i = 0; i <= 6; i++) {fprintf(filepointer, "%f\t", zero[i]/divisor);}
        for (i = 0; i <= 6; i++) {fprintf(filepointer, "%f\t", minus_twenty[i]/divisor);}
        for (i = 0; i <= 6; i++) {fprintf(filepointer, "%f\t", minus_forty[i]/divisor);}
        fprintf(filepointer, "\n");

        return;
}
```

## Appendix D

## *Post Hoc* Newman-Keuls Mean Comparison Tables

This appendix provides additional information on the ANOVAs used to analyse the study results in the form of Newman-Keuls *post hoc* comparison tables, which show the p-values for the comparison of each pair of means in the graphs. The "within map" comparisons show the probability that each point in a single graph (e.g. the sacral endplate failure load map) differs from the other points in the graph. The "between map" comparisons show the probability that each point in one endplate map differs from each point in another endplate map (e.g. superior lumbar versus sacral endplate failure load map).

In each case the map (or maps) being analysed is shown, followed by the *post hoc* comparison table. The two top rows and left columns show the AP and LAT test site co-ordinates as percentages of the AP and LAT endplate dimensions. The mean failure loads or stiffnesses being compared are given in the third row and column (bold font) in Newtons (failure load) or Newtons per millimetre (stiffness). The p-values indicating the probability that each pair of means is different are given in the body of the table to four decimal places. The significant p-values ($p < 0.05$) are highlighted in grey (i.e. less than 5% chance of being wrong if one states that the two means are significantly different).

### D.1 "Within Map" Comparisons

### D.1.1 Superior Lumbar Endplate Maximum AP, LAT Failure Load Map

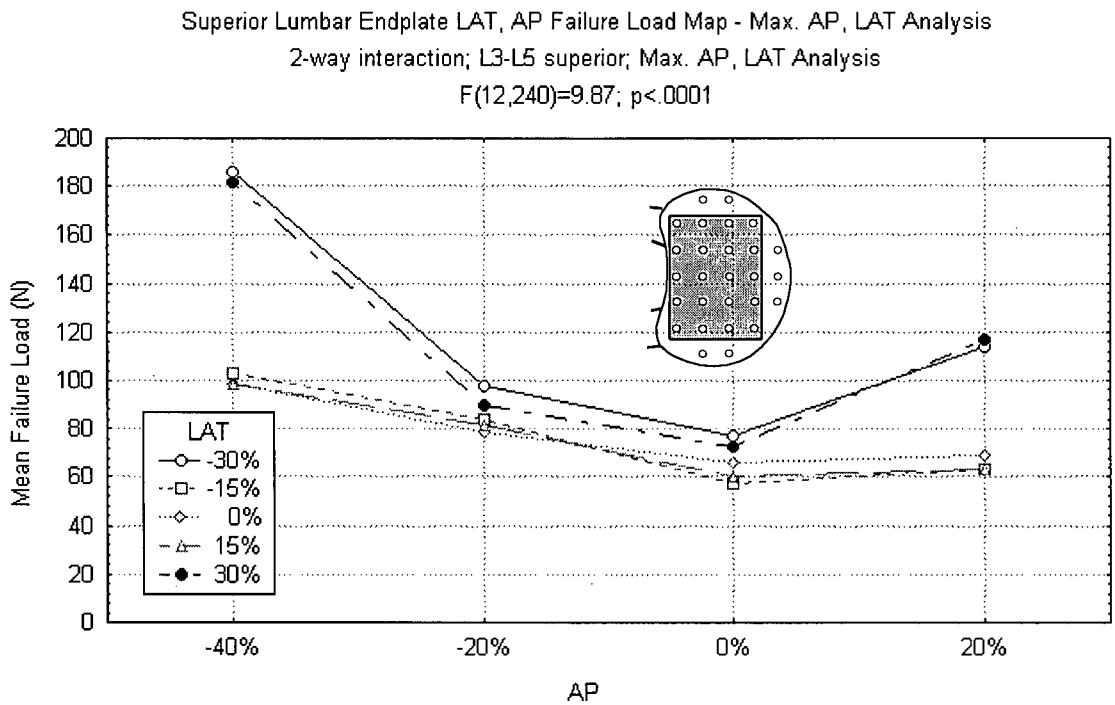


Figure D.1: Maximum AP, LAT failure load distribution in the superior lumbar endplates. This plot shows the effect of the LAT distance from the centre of the endplate on the AP failure load distribution. The p-value of < 0.0001 indicates that there are differences between the AP failure load distributions at different LAT co-ordinates. Note that curves that are equidistant from the centre (e.g. +/- 30% LAT) have the same shape, reflecting the lateral symmetry of the failure load distribution. The strongest sites are located postero-laterally (+/-40% AP, +/-30% LAT), in front of the pedicles.

Table D.1: Newman-Keuls *post hoc* comparison of the means in the superior lumbar endplate maximum AP, LAT failure load distribution (Figure D.1).

| | | AP | -40% | | | | | -20% | | | | |
|---|---|---|---|---|---|---|---|---|---|---|---|---|
| | | LAT | -30% | -15% | 0% | 15% | 30% | -30% | -15% | 0% | 15% | 30% |
| AP | LAT | Mean FL | **186.37** | **103.12** | **98.81** | **98.49** | **181.41** | **97.90** | **83.49** | **78.39** | **81.83** | **89.55** |
| -40% | -30% | **186.37** | | 0.0000 | 0.0000 | 0.0000 | 0.5590 | 0.0000 | 0.0000 | 0.0000 | 0.0000 | 0.0000 |
| | -15% | **103.12** | 0.0000 | | 0.6117 | 0.8488 | 0.0000 | 0.9275 | 0.1885 | 0.0696 | 0.1555 | 0.4977 |
| | 0% | **98.81** | 0.0000 | 0.6117 | | 0.9699 | 0.0000 | 0.9937 | 0.3701 | 0.1954 | 0.3408 | 0.6946 |
| | 15% | **98.49** | 0.0000 | 0.8488 | 0.9699 | | 0.0000 | 0.9449 | 0.2888 | 0.1671 | 0.2835 | 0.5428 |
| | 30% | **181.41** | 0.5590 | 0.0000 | 0.0000 | 0.0000 | | 0.0000 | 0.0000 | 0.0000 | 0.0000 | 0.0000 |
| -20% | -30% | **97.90** | 0.0000 | 0.9275 | 0.9937 | 0.9449 | 0.0000 | | 0.2056 | 0.1447 | 0.2299 | 0.3247 |
| | -15% | **83.49** | 0.0000 | 0.1885 | 0.3701 | 0.2888 | 0.0000 | 0.2056 | | 0.8194 | 0.8442 | 0.4752 |
| | 0% | **78.39** | 0.0000 | 0.0696 | 0.1954 | 0.1671 | 0.0000 | 0.1447 | 0.8194 | | 0.6856 | 0.5531 |
| | 15% | **81.83** | 0.0000 | 0.1555 | 0.3408 | 0.2835 | 0.0000 | 0.2299 | 0.8442 | 0.6856 | | 0.6336 |
| | 30% | **89.55** | 0.0000 | 0.4977 | 0.6946 | 0.5428 | 0.0000 | 0.3247 | 0.4752 | 0.5531 | 0.6336 | |
| 0% | -30% | **77.39** | 0.0000 | 0.0612 | 0.1847 | 0.1637 | 0.0000 | 0.1498 | 0.8894 | 0.9061 | 0.8602 | 0.6060 |
| | -15% | **57.18** | 0.0000 | 0.0000 | 0.0001 | 0.0001 | 0.0000 | 0.0001 | 0.0708 | 0.2316 | 0.1040 | 0.0076 |
| | 0% | **65.97** | 0.0000 | 0.0007 | 0.0052 | 0.0050 | 0.0000 | 0.0053 | 0.3736 | 0.5861 | 0.4217 | 0.1002 |
| | 15% | **60.30** | 0.0000 | 0.0001 | 0.0005 | 0.0005 | 0.0000 | 0.0006 | 0.1599 | 0.3934 | 0.2138 | 0.0239 |
| | 30% | **72.54** | 0.0000 | 0.0116 | 0.0508 | 0.0460 | 0.0000 | 0.0443 | 0.6969 | 0.7697 | 0.6931 | 0.3394 |
| 20% | -30% | **113.83** | 0.0000 | 0.2067 | 0.1796 | 0.2694 | 0.0000 | 0.3296 | 0.0064 | 0.0010 | 0.0040 | 0.0483 |
| | -15% | **63.59** | 0.0000 | 0.0002 | 0.0020 | 0.0019 | 0.0000 | 0.0021 | 0.2686 | 0.5021 | 0.3236 | 0.0566 |
| | 0% | **69.10** | 0.0000 | 0.0030 | 0.0167 | 0.0156 | 0.0000 | 0.0157 | 0.5337 | 0.6922 | 0.5621 | 0.1937 |
| | 15% | **63.40** | 0.0000 | 0.0003 | 0.0021 | 0.0021 | 0.0000 | 0.0024 | 0.3012 | 0.5702 | 0.3686 | 0.0635 |
| | 30% | **116.89** | 0.0000 | 0.2356 | **0.1432** | **0.1915** | 0.0000 | 0.2202 | 0.0021 | 0.0003 | 0.0012 | 0.0216 |

| | | AP | 0% | | | | | 20% | | | | |
|---|---|---|---|---|---|---|---|---|---|---|---|---|
| | | LAT | -30% | -15% | 0% | 15% | 30% | -30% | -15% | 0% | 15% | 30% |
| AP | LAT | Mean FL | **77.39** | **57.18** | **65.97** | **60.30** | **72.54** | **113.83** | **63.59** | **69.10** | **63.40** | **116.89** |
| -40% | -30% | **186.37** | 0.0000 | 0.0000 | 0.0000 | 0.0000 | 0.0000 | 0.0000 | 0.0000 | 0.0000 | 0.0000 | 0.0000 |
| | -15% | **103.12** | 0.0612 | 0.0000 | 0.0007 | 0.0001 | 0.0116 | 0.2067 | 0.0002 | 0.0030 | 0.0003 | 0.2356 |
| | 0% | **98.81** | 0.1847 | 0.0001 | 0.0052 | 0.0005 | 0.0508 | 0.1796 | 0.0020 | 0.0167 | 0.0021 | 0.1432 |
| | 15% | **98.49** | 0.1637 | 0.0001 | 0.0050 | 0.0005 | 0.0460 | 0.2694 | 0.0019 | 0.0156 | 0.0021 | 0.1915 |
| | 30% | **181.41** | 0.0000 | 0.0000 | 0.0000 | 0.0000 | 0.0000 | 0.0000 | 0.0000 | 0.0000 | 0.0000 | 0.0000 |
| -20% | -30% | **97.90** | 0.1498 | 0.0001 | 0.0053 | 0.0006 | 0.0443 | 0.3296 | 0.0021 | 0.0157 | 0.0024 | 0.2202 |
| | -15% | **83.49** | 0.8894 | 0.0708 | 0.3736 | 0.1599 | 0.6969 | 0.0064 | 0.2686 | 0.5337 | 0.3012 | 0.0021 |
| | 0% | **78.39** | 0.9061 | 0.2316 | 0.5861 | 0.3934 | 0.7697 | 0.0010 | 0.5021 | 0.6922 | 0.5702 | 0.0003 |
| | 15% | **81.83** | 0.8602 | 0.1040 | 0.4217 | 0.2138 | 0.6931 | 0.0040 | 0.3236 | 0.5621 | 0.3686 | 0.0012 |
| | 30% | **89.55** | 0.6060 | | 0.1002 | 0.0239 | 0.3394 | 0.0483 | 0.0566 | 0.1937 | 0.0635 | 0.0216 |
| 0% | -30% | **77.39** | | 0.2500 | 0.5336 | 0.4049 | 0.5677 | 0.0008 | 0.4803 | 0.5910 | 0.5655 | 0.0002 |
| | -15% | **57.18** | 0.2500 | | 0.8385 | 0.7136 | 0.5407 | 0.0000 | 0.8743 | 0.7244 | 0.7441 | 0.0000 |
| | 0% | **65.97** | 0.5336 | 0.8385 | | 0.9087 | 0.7188 | 0.0000 | 0.7789 | 0.7128 | 0.9504 | 0.0000 |
| | 15% | **60.30** | 0.4049 | 0.7136 | 0.9087 | | 0.7002 | 0.0000 | 0.9202 | 0.8380 | 0.7147 | 0.0000 |
| | 30% | **72.54** | 0.5677 | 0.5407 | 0.7188 | 0.7002 | | 0.0001 | 0.7168 | 0.6846 | 0.8179 | 0.0000 |
| 20% | -30% | **113.83** | 0.0008 | 0.0000 | 0.0000 | 0.0000 | 0.0001 | | 0.0000 | 0.0000 | 0.0000 | 0.7181 |
| | -15% | **63.59** | 0.4803 | 0.8743 | 0.7789 | 0.9202 | 0.7168 | 0.0000 | | 0.7930 | 0.9817 | 0.0000 |
| | 0% | **69.10** | 0.5910 | 0.7244 | 0.7128 | 0.8380 | 0.6846 | 0.0000 | 0.7930 | | 0.9078 | 0.0000 |
| | 15% | **63.40** | 0.5655 | 0.7441 | 0.9504 | 0.7147 | 0.8179 | 0.0000 | 0.9817 | **0.9078** | | 0.0000 |
| | 30% | **116.89** | 0.0002 | 0.0000 | 0.0000 | 0.0000 | 0.0000 | 0.7181 | 0.0000 | 0.0000 | 0.0000 | |

## D.1.2 Superior Lumbar Endplate Full AP Failure Load Map

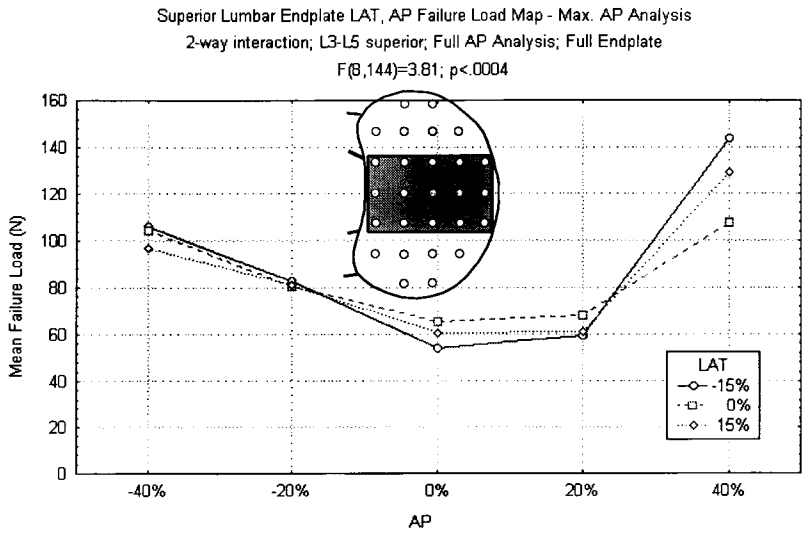


Figure D.2: Full AP failure load distribution in the superior lumbar endplates. This plot shows the effect of the LAT distance from the centre of the endplate on the AP failure load distribution using the largest complete AP data set (inset figure). The p-value of < 0.0004 indicates that there are differences between the AP failure load distributions at different LAT co-ordinates. A *post hoc* Newman-Keuls test indicates that the curves differ only at the most anterior test sites (40% AP).

Table D.2: Newman-Keuls *post hoc* comparison of the means in the superior lumbar endplate full AP, LAT failure load distribution (Figure D.2).

| | AP | -40% | | | -20% | | | 0% | | | 20% | | | 40% | | |
|---|---|---|---|---|---|---|---|---|---|---|---|---|---|---|---|---|
| | LAT | -15% | 0% | 15% | -15% | 0% | 15% | -15% | 0% | 15% | -15% | 0% | 15% | -15% | 0% | 15% |
| **AP** | **LAT** | **105.76** | **104.30** | **96.78** | **82.60** | **80.80** | **80.92** | **53.98** | **65.67** | **60.38** | **59.37** | **68.11** | **61.10** | **143.80** | **107.33** | **129.00** |
| -40% | -15% | | 0.8400 | 0.4250 | 0.0070 | 0.0069 | 0.0050 | 0.0000 | 0.0000 | 0.0000 | 0.0000 | 0.0000 | 0.0000 | 0.0000 | 0.8270 | 0.0035 |
| | 0% | 0.8400 | | 0.2956 | 0.0072 | 0.0095 | 0.0063 | 0.0000 | 0.0000 | 0.0000 | 0.0000 | 0.0000 | 0.0000 | 0.0000 | 0.9072 | 0.0033 |
| | 15% | 0.4250 | 0.2956 | | 0.0485 | 0.1170 | 0.0701 | 0.0000 | 0.0002 | 0.0000 | 0.0000 | 0.0007 | 0.0000 | 0.0000 | 0.4580 | 0.0001 |
| -20% | -15% | 0.0070 | 0.0072 | 0.0485 | | 0.9661 | 0.8154 | 0.0023 | 0.1281 | 0.0329 | 0.0271 | 0.1827 | 0.0333 | 0.0000 | 0.0053 | 0.0000 |
| | 0% | 0.0069 | 0.0095 | 0.1170 | 0.9661 | | 0.9867 | 0.0036 | 0.0889 | 0.0365 | 0.0342 | 0.0777 | 0.0313 | 0.0000 | 0.0042 | 0.0000 |
| | 15% | 0.0050 | 0.0063 | 0.0701 | 0.8154 | 0.9867 | | 0.0044 | 0.1464 | 0.0491 | 0.0434 | 0.1761 | 0.0462 | 0.0000 | 0.0033 | 0.0000 |
| 0% | -15% | 0.0000 | 0.0000 | 0.0000 | 0.0023 | 0.0036 | 0.0044 | | 0.4808 | 0.6463 | 0.4534 | 0.3620 | 0.7551 | 0.0000 | 0.0000 | 0.0000 |
| | 0% | 0.0000 | 0.0000 | 0.0002 | 0.1281 | 0.0889 | 0.1464 | 0.4808 | | 0.7425 | 0.8173 | 0.7336 | 0.5250 | 0.0000 | 0.0000 | 0.0000 |
| | 15% | 0.0000 | 0.0000 | 0.0000 | 0.0329 | 0.0365 | 0.0491 | 0.6463 | 0.7425 | | 0.8881 | 0.7045 | 0.9206 | 0.0000 | 0.0000 | 0.0000 |
| 20% | -15% | 0.0000 | 0.0000 | 0.0000 | 0.0271 | 0.0342 | 0.0434 | 0.4534 | 0.8173 | 0.8881 | | 0.7419 | 0.9687 | 0.0000 | 0.0000 | 0.0000 |
| | 0% | 0.0000 | 0.0000 | 0.0007 | 0.1827 | 0.0777 | 0.1761 | 0.3620 | 0.7336 | 0.7045 | 0.7419 | | 0.5921 | 0.0000 | 0.0000 | 0.0000 |
| | 15% | 0.0000 | 0.0000 | 0.0000 | 0.0333 | 0.0313 | 0.0462 | 0.7551 | 0.5250 | 0.9206 | 0.9687 | 0.5921 | | 0.0000 | 0.0000 | 0.0000 |
| 40% | -15% | 0.0000 | 0.0000 | 0.0000 | 0.0000 | 0.0000 | 0.0000 | 0.0000 | 0.0000 | 0.0000 | 0.0000 | 0.0000 | 0.0000 | | 0.0000 | 0.0396 |
| | 0% | 0.8270 | 0.9072 | 0.4580 | 0.0053 | 0.0042 | 0.0033 | 0.0000 | 0.0000 | 0.0000 | 0.0000 | 0.0000 | 0.0000 | 0.0000 | | 0.0026 |
| | 15% | 0.0035 | 0.0033 | 0.0001 | 0.0000 | 0.0000 | 0.0000 | 0.0000 | 0.0000 | 0.0000 | 0.0000 | 0.0000 | 0.0000 | 0.0396 | 0.0026 | |

## D.1.3 Superior Lumbar Endplate Full LAT Failure Load Map

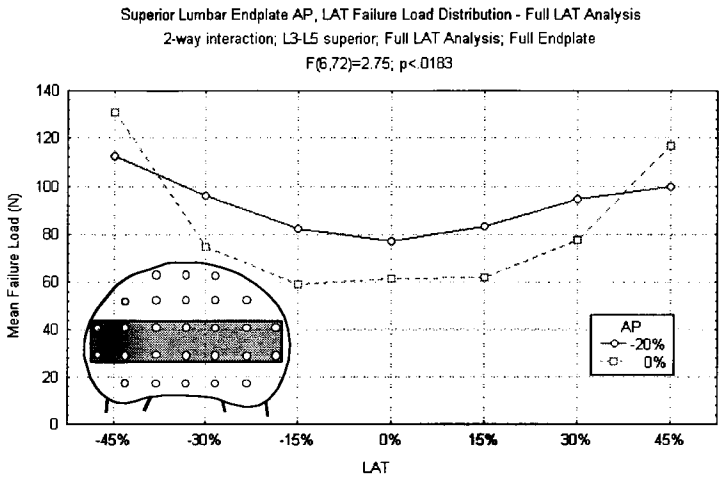


Figure D.3: Full LAT failure load distribution in the superior lumbar endplates. This plot shows the effect of the AP distance from the centre of the endplate on the LAT failure load distribution using the largest complete LAT data set (inset figure). The p-value of < 0.0183 indicates that there are differences between the LAT failure load distributions at different AP co-ordinates. A *post hoc* Newman-Keuls test indicates that the curves differ in that the five central points on the –20% AP curve are not significantly different, while only the three central points on the 0% AP curve are not significantly different.

Table D.3: Newman-Keuls *post hoc* comparison of the means in the superior lumbar endplate AP, Full LAT failure load distribution (Figure 3.43).

| | AP | -20% | | | | | | | 0% | | | | | | |
|---|---|---|---|---|---|---|---|---|---|---|---|---|---|---|---|
| | LAT | -45% | -30% | -15% | 0% | 15% | 30% | 45% | -45% | -30% | -15% | 0% | 15% | 30% | 45% |
| AP | LAT | **112.56** | **96.20** | **82.20** | **77.06** | **83.22** | **94.41** | **99.69** | **130.86** | **74.95** | **59.16** | **61.60** | **61.79** | **77.82** | **116.82** |
| -20% | -45% | | 0.3088 | 0.0802 | 0.0405 | 0.0727 | 0.3648 | 0.2496 | 0.2317 | 0.0294 | 0.0006 | 0.0010 | 0.0009 | 0.0384 | 0.7019 |
| | -30% | 0.3088 | | 0.5894 | 0.5194 | 0.4745 | 0.8721 | 0.7542 | 0.0210 | 0.4759 | 0.0408 | 0.0613 | 0.0525 | 0.4660 | 0.2546 |
| | -15% | 0.0802 | 0.5894 | | 0.8887 | 0.9269 | 0.5165 | 0.5166 | 0.0011 | 0.9137 | 0.3769 | 0.4362 | 0.3588 | 0.6938 | 0.0395 |
| | 0% | 0.0405 | 0.5194 | 0.8887 | | 0.9448 | 0.5247 | 0.3990 | 0.0004 | 0.8491 | 0.4933 | 0.5069 | 0.3581 | 0.9461 | 0.0168 |
| | 15% | 0.0727 | 0.4745 | 0.9269 | 0.9448 | | 0.3164 | 0.4517 | 0.0011 | 0.9447 | 0.3820 | 0.4550 | 0.3911 | 0.8775 | 0.0383 |
| | 30% | 0.3648 | 0.8721 | 0.5165 | 0.5247 | 0.3164 | | 0.8828 | 0.0189 | 0.5005 | 0.0526 | 0.0759 | 0.0633 | 0.4449 | 0.2664 |
| | 45% | 0.2496 | 0.7542 | 0.5166 | 0.3990 | 0.4517 | 0.8828 | | 0.0317 | 0.3458 | 0.0196 | 0.0313 | 0.0273 | 0.3680 | 0.2761 |
| 0% | -45% | 0.2317 | 0.0210 | 0.0011 | 0.0004 | 0.0011 | 0.0189 | 0.0317 | | 0.0003 | 0.0001 | 0.0001 | 0.0001 | 0.0004 | 0.2099 |
| | -30% | 0.0294 | 0.4759 | 0.9137 | 0.8491 | 0.9447 | 0.5005 | 0.3458 | 0.0003 | | 0.4892 | 0.4551 | 0.2395 | 0.9638 | 0.0114 |
| | -15% | 0.0006 | 0.0408 | 0.3769 | 0.4933 | 0.3820 | 0.0526 | 0.0196 | 0.0001 | 0.4892 | | 0.8267 | 0.9696 | 0.5478 | 0.0002 |
| | 0% | 0.0010 | 0.0613 | 0.4362 | 0.5069 | 0.4550 | 0.0759 | 0.0313 | 0.0001 | 0.4551 | 0.8267 | | 0.9864 | 0.5899 | 0.0004 |
| | 15% | 0.0009 | 0.0525 | 0.3588 | 0.3581 | 0.3911 | 0.0633 | 0.0273 | 0.0001 | 0.2395 | 0.9696 | 0.9864 | | 0.4758 | 0.0004 |
| | 30% | 0.0384 | 0.4660 | 0.6938 | 0.9461 | 0.8775 | 0.4449 | 0.3680 | 0.0004 | 0.9638 | 0.5478 | 0.5899 | 0.4758 | | 0.0165 |
| | 45% | 0.7019 | 0.2546 | 0.0395 | 0.0168 | 0.0383 | 0.2664 | 0.2761 | 0.2099 | 0.0114 | 0.0002 | 0.0004 | 0.0004 | 0.0165 | |

### D.1.4 Superior Lumbar Endplate Maximum AP, LAT Stiffness Map

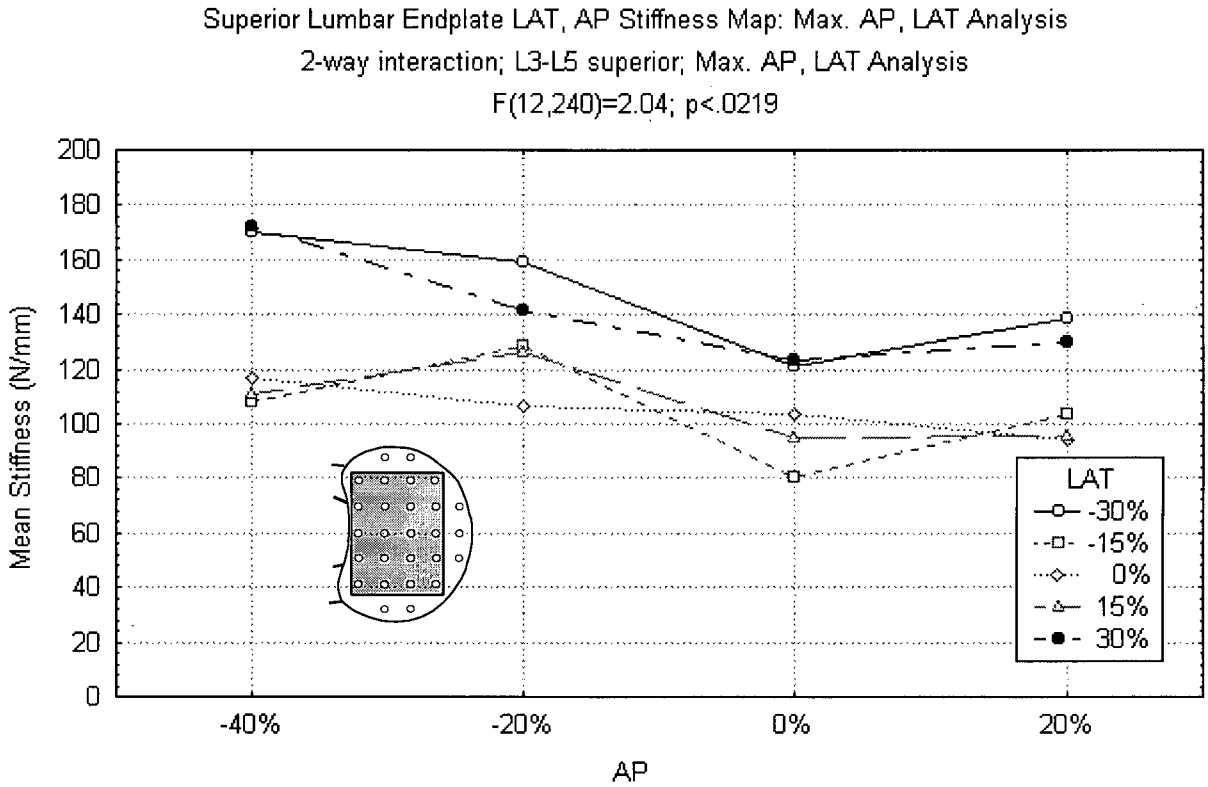


Figure D.4: Maximum AP, LAT stiffness distribution in the superior lumbar endplates. This plot shows the effect of the LAT distance from the centre of the endplate on the AP stiffness distribution. The p-value of $< 0.0219$ indicates that there are differences between the AP stiffness distributions at different LAT co-ordinates. Note that curves that are equidistant from the centre (e.g. +/- 30% LAT) have the same shape, reflecting the lateral symmetry of the failure load distribution. The stiffest sites are located postero-laterally (+/-40% AP, +/-30% LAT), in front of the pedicles.

Table D.4: Newman-Keuls *post hoc* comparison of the means in the superior lumbar endplate AP, LAT stiffness distribution (Figure D.4)

| | AP | -40% | | | | | -20% | | | | |
|---|---|---|---|---|---|---|---|---|---|---|---|
| | LAT | -30% | -15% | 0% | 15% | 30% | -30% | -15% | 0% | 15% | 30% |
| AP | LAT | **170.05** | **108.23** | **117.00** | **111.15** | **172.39** | **159.36** | **128.25** | **106.31** | **126.04** | **141.84** |
| -40% | -30% | | 0.0000 | 0.0001 | 0.0000 | 0.8318 | 0.3313 | 0.0020 | 0.0000 | 0.0012 | 0.0279 |
| | -15% | 0.0000 | | 0.7046 | 0.7907 | 0.0000 | 0.0002 | 0.5345 | 0.8615 | 0.5859 | 0.0688 |
| | 0% | 0.0001 | 0.7046 | | 0.5947 | 0.0000 | 0.0038 | 0.8451 | 0.7655 | 0.8443 | 0.3174 |
| | 15% | 0.0000 | 0.7907 | 0.5947 | | 0.0000 | 0.0005 | 0.6287 | 0.8989 | 0.6575 | 0.1183 |
| | 30% | 0.8318 | 0.0000 | 0.0000 | 0.0000 | | 0.4628 | 0.0012 | 0.0000 | 0.0007 | 0.0281 |
| -20% | -30% | **0.3313** | 0.0002 | 0.0038 | 0.0005 | 0.4628 | | 0.0378 | 0.0001 | 0.0296 | **0.1112** |
| | -15% | 0.0020 | 0.5345 | 0.8451 | 0.6287 | 0.0012 | 0.0378 | | 0.4856 | 0.8408 | 0.6044 |
| | 0% | 0.0000 | 0.8615 | 0.7655 | 0.8989 | 0.0000 | 0.0001 | 0.4856 | | 0.5525 | 0.0484 |
| | 15% | 0.0012 | 0.5859 | 0.8443 | 0.6575 | 0.0007 | 0.0296 | 0.8408 | 0.5525 | | 0.6042 |
| | 30% | 0.0279 | 0.0688 | 0.3174 | 0.1183 | 0.0281 | 0.1112 | 0.6044 | 0.0484 | 0.6042 | |
| 0% | -30% | 0.0003 | 0.6492 | 0.7134 | 0.6407 | 0.0001 | 0.0117 | 0.9138 | 0.6666 | 0.8925 | 0.4868 |
| | -15% | 0.0000 | 0.1821 | 0.0298 | 0.1161 | 0.0000 | 0.0000 | 0.0011 | 0.2171 | 0.0023 | 0.0000 |
| | 0% | 0.0000 | 0.9022 | 0.7341 | 0.8981 | 0.0000 | 0.0000 | 0.3718 | 0.7967 | 0.4472 | 0.0246 |
| | 15% | 0.0000 | 0.8281 | 0.4710 | 0.7547 | 0.0000 | 0.0000 | 0.0977 | 0.8349 | 0.1440 | 0.0018 |
| | 30% | 0.0006 | 0.6399 | 0.8289 | 0.6799 | 0.0003 | 0.0187 | 0.8993 | 0.6281 | 0.8119 | 0.5491 |
| 20% | -30% | 0.0242 | 0.1180 | 0.4190 | 0.1847 | 0.0200 | 0.1512 | 0.5955 | 0.0885 | 0.6449 | 0.7914 |
| | -15% | 0.0000 | 0.9724 | 0.8208 | 0.9563 | 0.0000 | 0.0001 | 0.4186 | 0.9631 | 0.5049 | 0.0281 |
| | 0% | 0.0000 | 0.8630 | 0.4916 | 0.7848 | 0.0000 | 0.0000 | 0.0948 | 0.8809 | 0.1424 | 0.0016 |
| | 15% | 0.0000 | 0.7767 | 0.4451 | 0.7144 | 0.0000 | 0.0000 | 0.1007 | 0.7603 | 0.1451 | 0.0021 |
| | 30% | 0.0023 | 0.5165 | 0.8593 | 0.6267 | 0.0015 | 0.0351 | 0.8968 | 0.4566 | 0.9415 | 0.5107 |

| | AP | 0% | | | | | 20% | | | | |
|---|---|---|---|---|---|---|---|---|---|---|---|
| | LAT | -30% | -15% | 0% | 15% | 30% | -30% | -15% | 0% | 15% | 30% |
| AP | LAT | **121.04** | **80.38** | **103.47** | **94.82** | **123.42** | **138.93** | **103.44** | **94.19** | **95.52** | **129.68** |
| -40% | -30% | 0.0003 | 0.0000 | 0.0000 | 0.0000 | 0.0006 | 0.0242 | 0.0000 | 0.0000 | 0.0000 | 0.0023 |
| | -15% | 0.6492 | 0.1821 | 0.9022 | 0.8281 | 0.6399 | 0.1180 | 0.9724 | 0.8630 | 0.7767 | 0.5165 |
| | 0% | 0.7134 | 0.0298 | 0.7341 | 0.4710 | 0.8289 | 0.4190 | 0.8208 | 0.4916 | 0.4451 | 0.8593 |
| | 15% | 0.6407 | 0.1161 | 0.8981 | 0.7547 | 0.6799 | 0.1847 | 0.9563 | 0.7848 | 0.7144 | 0.6267 |
| | 30% | 0.0001 | 0.0000 | 0.0000 | 0.0000 | 0.0003 | 0.0200 | 0.0000 | 0.0000 | 0.0000 | 0.0015 |
| -20% | -30% | 0.0117 | 0.0000 | 0.0000 | 0.0000 | 0.0187 | 0.1512 | 0.0001 | 0.0000 | 0.0000 | 0.0351 |
| | -15% | 0.9138 | 0.0011 | 0.3718 | 0.0977 | 0.8993 | 0.5955 | **0.4186** | **0.0948** | **0.1007** | 0.8968 |
| | 0% | 0.6666 | 0.2171 | 0.7967 | 0.8349 | 0.6281 | 0.0885 | 0.9631 | 0.8809 | 0.7603 | 0.4566 |
| | 15% | 0.8925 | 0.0023 | 0.4472 | 0.1440 | 0.8119 | 0.6449 | 0.5049 | 0.1424 | 0.1451 | 0.9415 |
| | 30% | 0.4868 | 0.0000 | 0.0246 | 0.0018 | 0.5491 | 0.7914 | 0.0281 | 0.0016 | 0.0021 | 0.5107 |
| 0% | -30% | | 0.0100 | 0.6006 | 0.2931 | 0.8288 | 0.5814 | 0.6822 | 0.3013 | 0.2823 | 0.9351 |
| | -15% | 0.0100 | | 0.2875 | 0.3878 | 0.0052 | 0.0000 | 0.2217 | 0.2094 | 0.5144 | 0.0007 |
| | 0% | 0.6006 | 0.2875 | | 0.8607 | 0.5391 | 0.0494 | 0.9973 | 0.9168 | 0.7496 | 0.3368 |
| | 15% | 0.2931 | 0.3878 | 0.8607 | | 0.2177 | 0.0048 | 0.7136 | 0.9539 | 0.9498 | 0.0773 |
| | 30% | 0.8288 | 0.0052 | 0.5391 | 0.2177 | | 0.6215 | 0.6087 | 0.2197 | 0.2144 | 0.9414 |
| 20% | -30% | 0.5814 | 0.0000 | 0.0494 | 0.0048 | 0.6215 | | 0.0568 | 0.0043 | 0.0053 | 0.4004 |
| | -15% | 0.6822 | 0.2217 | 0.9973 | 0.7136 | 0.6087 | 0.0568 | | 0.8351 | 0.4716 | 0.3761 |
| | 0% | 0.3013 | 0.2094 | 0.9168 | 0.9539 | 0.2197 | 0.0043 | 0.8351 | | 0.9920 | 0.0738 |
| | 15% | 0.2823 | 0.5144 | 0.7496 | 0.9498 | 0.2144 | 0.0053 | 0.4716 | 0.9920 | | 0.0811 |
| | 30% | 0.9351 | 0.0007 | 0.3368 | 0.0773 | 0.9414 | 0.4004 | 0.3761 | 0.0738 | 0.0811 | |

### D.1.5 Superior Lumbar Endplate Full AP Stiffness Map

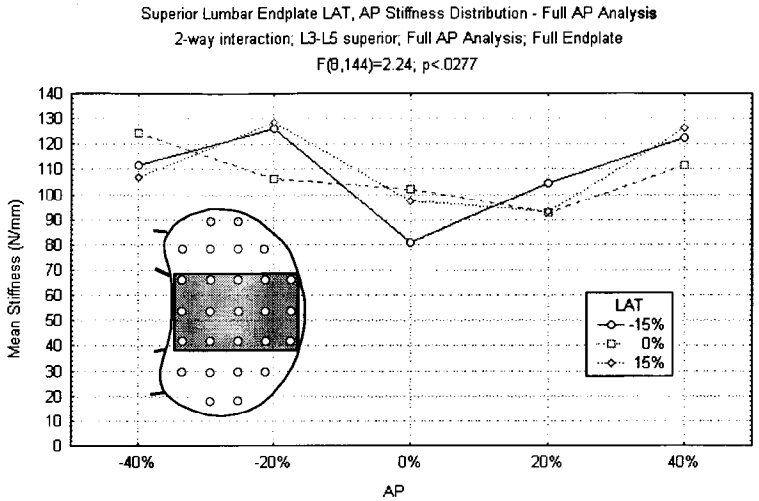


Figure D.5: Full AP stiffness distribution in the superior lumbar endplates. This plot shows the effect of the LAT distance from the centre of the endplate on the AP stiffness distribution using the largest complete AP data set (inset figure). The p-value of < 0.0277 indicates that there are differences between the AP stiffness distributions at different LAT co-ordinate.s

Table D.5: Newman-Keuls *post hoc* comparison of the means in the superior lumbar endplate full AP, LAT stiffness distribution (Figure D.5).

| | AP | -40% | | | -20% | | | 0% | | | 20% | | | 40% | | |
|---|---|---|---|---|---|---|---|---|---|---|---|---|---|---|---|---|
| | LAT | -15% | 0% | 15% | -15% | 0% | 15% | -15% | 0% | 15% | -15% | 0% | 15% | -15% | 0% | 15% |
| AP | LAT | **111.68** | **124.45** | **107.07** | **126.47** | **106.60** | **128.74** | **81.07** | **102.18** | **97.58** | **104.47** | **92.74** | **93.20** | **122.40** | **111.86** | **126.35** |
| -40% | -15% | | 0.5713 | 0.6422 | 0.6708 | 0.8655 | 0.6033 | 0.0526 | 0.8739 | 0.7139 | 0.8863 | 0.5449 | 0.5056 | 0.5264 | 0.9854 | 0.5767 |
| | 0% | 0.5713 | | 0.4023 | 0.9776 | 0.4664 | 0.9730 | 0.0008 | 0.3249 | 0.1446 | 0.4056 | 0.0536 | 0.0522 | 0.8362 | 0.4130 | 0.8483 |
| | 15% | 0.6422 | 0.4023 | | 0.4440 | 0.9622 | 0.3616 | 0.1486 | 0.9607 | 0.8743 | 0.9627 | 0.7778 | 0.7285 | 0.4106 | 0.8794 | 0.3759 |
| -20% | -15% | 0.6708 | 0.9776 | 0.4440 | | 0.4805 | 0.8188 | 0.0004 | 0.2974 | 0.1192 | 0.3944 | 0.0381 | 0.0384 | 0.9768 | 0.5811 | 0.9907 |
| | 0% | 0.8655 | 0.4664 | 0.9622 | 0.4805 | | 0.3853 | 0.1343 | 0.8963 | 0.7997 | 0.8297 | 0.7292 | 0.6596 | 0.5024 | 0.9517 | 0.4208 |
| | 15% | 0.6033 | 0.9730 | 0.3616 | 0.8188 | 0.3853 | | 0.0002 | 0.2104 | 0.0732 | 0.2984 | 0.0201 | 0.0206 | 0.9687 | 0.5313 | 0.9686 |
| 0% | -15% | 0.0526 | 0.0008 | 0.1486 | 0.0004 | 0.1343 | 0.0002 | | 0.2085 | 0.3434 | 0.1714 | 0.2395 | 0.4399 | 0.0016 | 0.0599 | 0.0004 |
| | 0% | 0.8739 | 0.3249 | 0.9607 | 0.2974 | 0.8963 | 0.2104 | 0.2085 | | 0.6428 | 0.8176 | 0.7773 | 0.6375 | 0.3905 | 0.9256 | 0.2642 |
| | 15% | 0.7139 | 0.1446 | 0.8743 | 0.1192 | 0.7997 | 0.0732 | 0.3434 | 0.6428 | | 0.7667 | 0.8775 | 0.6594 | 0.1945 | 0.7801 | 0.1055 |
| 20% | -15% | 0.8863 | 0.4056 | 0.9627 | 0.3944 | 0.8297 | 0.2984 | 0.1714 | 0.8176 | 0.7667 | | 0.7621 | 0.6677 | 0.4610 | 0.9458 | 0.3484 |
| | 0% | 0.5449 | 0.0536 | 0.7778 | 0.0381 | 0.7292 | 0.0201 | 0.2395 | 0.7773 | 0.8775 | 0.7621 | | 0.9631 | 0.0829 | 0.5949 | 0.0343 |
| | 15% | 0.5056 | 0.0522 | 0.7285 | 0.0384 | 0.6596 | 0.0206 | 0.4399 | 0.6375 | 0.6594 | 0.6677 | 0.9631 | | 0.0789 | 0.5643 | 0.0341 |
| 40% | -15% | 0.5264 | 0.8362 | 0.4106 | 0.9768 | 0.5024 | 0.9687 | 0.0016 | 0.3905 | 0.1945 | 0.4610 | 0.0829 | 0.0789 | | 0.2883 | 0.9164 |
| | 0% | 0.9854 | 0.4130 | 0.8794 | 0.5811 | 0.9517 | 0.5313 | 0.0599 | 0.9256 | 0.7801 | 0.9458 | 0.5949 | 0.5643 | 0.2883 | | 0.4620 |
| | 15% | 0.5767 | 0.8483 | 0.3759 | 0.9907 | 0.4208 | 0.9686 | 0.0004 | 0.2642 | 0.1055 | 0.3484 | 0.0343 | 0.0341 | 0.9164 | 0.4620 | |

## D.1.6 Superior Lumbar Endplate Full LAT Stiffness Map

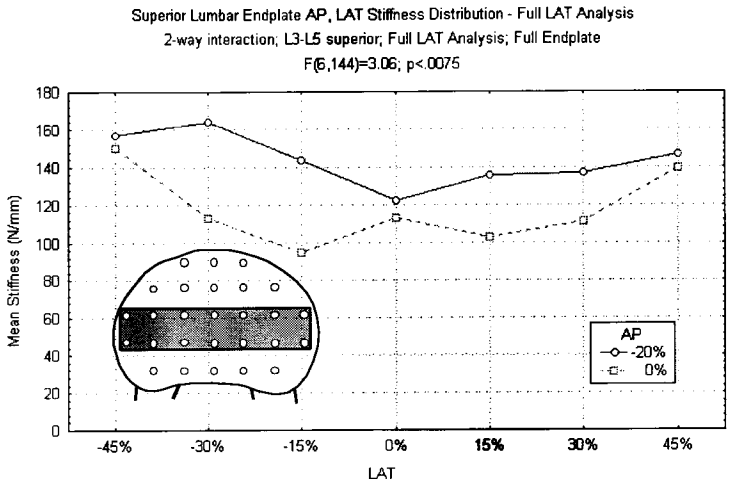


Figure D.6: Full LAT stiffness distribution in the superior lumbar endplates. This plot shows the effect of the AP distance from the centre of the endplate on the LAT stiffness distribution using the largest complete LAT data set (inset figure). The p-value of < 0.0075 indicates that there are differences between the LAT stiffness distributions at different AP co-ordinates.

Table D.6: Newman-Keuls *post hoc* comparison of the means in the superior lumbar endplate AP, Full LAT stiffness distribution (Figure D.6).

| | AP | -20% | | | | | | | 0% | | | | | | |
|---|---|---|---|---|---|---|---|---|---|---|---|---|---|---|---|
| | LAT | -45% | -30% | -15% | 0% | 15% | 30% | 45% | -45% | -30% | -15% | 0% | 15% | 30% | 45% |
| AP | LAT | **156.90** | **164.11** | **143.65** | **122.34** | **135.88** | **136.78** | **146.34** | **150.22** | **113.42** | **94.65** | **113.16** | **102.80** | **111.59** | **139.34** |
| -20% | -45% | | 0.5104 | 0.6211 | 0.0345 | 0.4680 | 0.4423 | 0.5999 | 0.5421 | 0.0024 | 0.0000 | 0.0026 | 0.0001 | 0.0018 | 0.4955 |
| | -30% | 0.5104 | | 0.3352 | 0.0044 | 0.1645 | 0.1612 | 0.3662 | 0.4134 | 0.0002 | 0.0000 | 0.0002 | 0.0000 | 0.0001 | 0.2102 |
| | -15% | 0.6211 | 0.3352 | | 0.2933 | 0.8935 | 0.8052 | 0.8062 | 0.8205 | 0.0642 | 0.0003 | 0.0790 | 0.0060 | 0.0674 | 0.6937 |
| | 0% | 0.0345 | 0.0044 | 0.2933 | | 0.2164 | 0.3850 | 0.2420 | 0.1435 | 0.4157 | 0.1161 | 0.6794 | 0.3832 | 0.7601 | 0.4067 |
| | 15% | 0.4680 | 0.1645 | 0.8935 | 0.2164 | | 0.9345 | 0.8753 | 0.7804 | 0.1005 | 0.0032 | 0.1616 | 0.0304 | 0.1731 | 0.9466 |
| | 30% | 0.4423 | 0.1612 | 0.8052 | 0.3850 | 0.9345 | | 0.8191 | 0.7359 | 0.1429 | 0.0030 | 0.1966 | 0.0317 | 0.1941 | 0.8156 |
| | 45% | 0.5999 | 0.3662 | 0.8062 | 0.2420 | 0.8753 | 0.8191 | | 0.7233 | 0.0424 | 0.0001 | 0.0504 | 0.0028 | 0.0404 | 0.7985 |
| 0% | -45% | 0.5421 | 0.4134 | 0.8205 | 0.1435 | 0.7804 | 0.7359 | 0.7233 | | 0.0179 | 0.0000 | 0.0206 | 0.0008 | 0.0154 | 0.7533 |
| | -30% | 0.0024 | 0.0002 | 0.0642 | 0.4157 | 0.1005 | 0.1429 | 0.0424 | 0.0179 | | 0.4254 | 0.9809 | 0.7668 | 0.9847 | 0.1249 |
| | -15% | 0.0000 | 0.0000 | 0.0003 | 0.1161 | 0.0032 | 0.0030 | 0.0001 | 0.0000 | 0.4254 | | 0.3291 | 0.4568 | 0.2694 | 0.0015 |
| | 0% | 0.0026 | 0.0002 | 0.0790 | 0.6794 | 0.1616 | 0.1966 | 0.0504 | 0.0206 | 0.9809 | 0.3291 | | 0.6114 | 0.8859 | 0.1598 |
| | 15% | 0.0001 | 0.0000 | 0.0060 | 0.3832 | 0.0304 | 0.0317 | 0.0028 | 0.0008 | 0.7668 | 0.4568 | 0.6114 | | 0.4225 | 0.0193 |
| | 30% | 0.0018 | 0.0001 | 0.0674 | 0.7601 | 0.1731 | 0.1941 | 0.0404 | 0.0154 | 0.9847 | 0.2694 | 0.8859 | 0.4225 | | 0.1475 |
| | 45% | 0.4955 | 0.2102 | 0.6937 | 0.4067 | 0.9466 | 0.8156 | 0.7985 | 0.7533 | 0.1249 | 0.0015 | 0.1598 | 0.0193 | 0.1475 | |

### D.1.7 Inferior Lumbar Endplate Maximum AP, LAT Failure Load Map

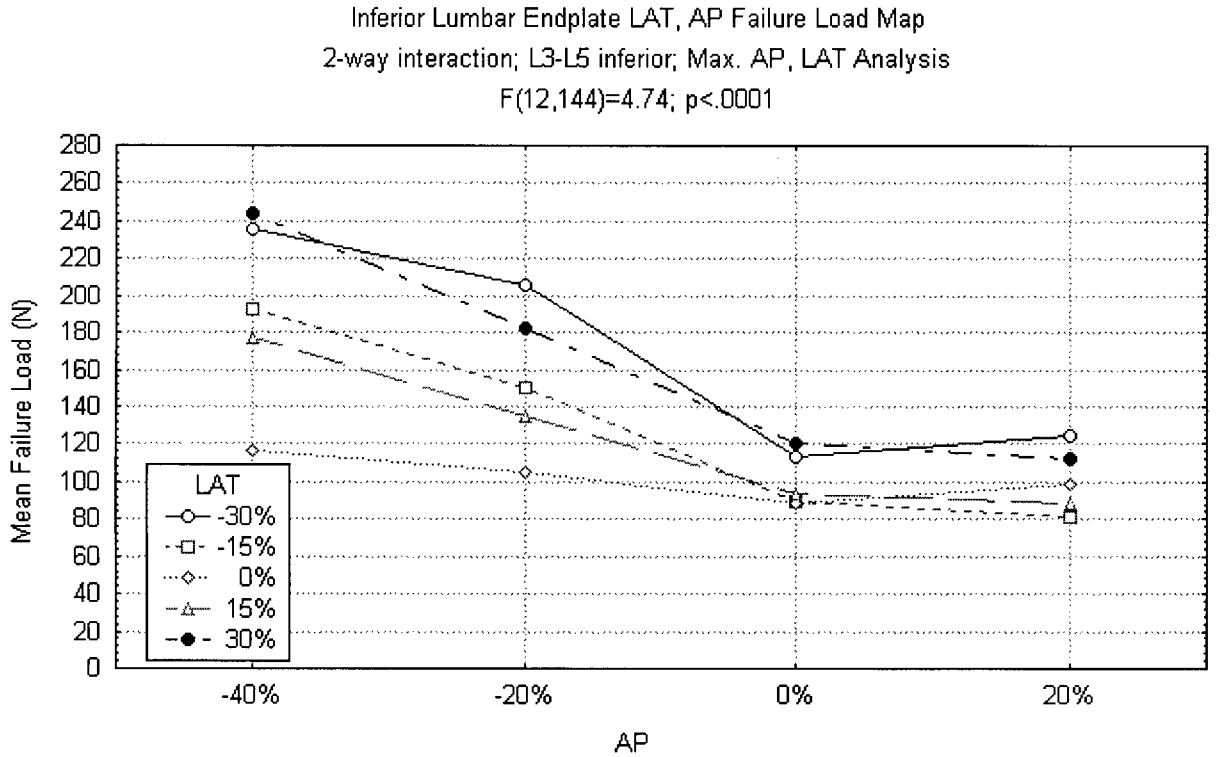


Figure D.7: Maximum AP, LAT failure load distribution in the inferior lumbar endplates. This plot shows the effect of the LAT distance from the centre of the endplate on the AP failure load distribution. The p-value of $< 0.0001$ indicates that there are differences between the AP failure load distributions at different LAT co-ordinates. Note that curves that are equidistant from the centre (e.g. +/- 30% LAT) have the same shape, reflecting the lateral symmetry of the failure load distribution. The strongest sites are located postero-laterally (+/- 40% AP, +/- 30% LAT), in front of the pedicles.

Table D.7: Newman-Keuls *post hoc* comparison of the means in the inferior lumbar endplate AP, LAT failure load distribution (Figure D.7).

| | AP | -40% | | | | | -20% | | | | |
|---|---|---|---|---|---|---|---|---|---|---|---|
| | LAT | -30% | -15% | 0% | 15% | 30% | -30% | -15% | 0% | 15% | 30% |
| AP | LAT | **235.78** | **192.42** | **115.97** | **177.09** | **243.93** | **206.30** | **150.08** | **104.58** | **134.73** | **182.10** |
| -40% | -30% | | 0.0061 | 0.0000 | 0.0003 | 0.5643 | 0.0370 | 0.0000 | 0.0000 | 0.0000 | 0.0009 |
| | -15% | 0.0061 | | 0.0000 | 0.5236 | 0.0015 | 0.3261 | 0.0146 | 0.0000 | 0.0004 | 0.4652 |
| | 0% | 0.0000 | 0.0000 | | 0.0002 | 0.0000 | 0.0000 | 0.1116 | 0.8516 | 0.5454 | 0.0001 |
| | 15% | 0.0003 | 0.5236 | 0.0002 | | 0.0001 | 0.1641 | 0.0561 | 0.0000 | 0.0077 | 0.7230 |
| | 30% | 0.5643 | 0.0015 | 0.0000 | 0.0001 | | 0.0212 | 0.0000 | 0.0000 | 0.0000 | 0.0001 |
| -20% | -30% | 0.0370 | 0.3261 | 0.0000 | 0.1641 | 0.0212 | | 0.0007 | 0.0000 | 0.0000 | 0.2005 |
| | -15% | 0.0000 | 0.0146 | 0.1116 | 0.0561 | 0.0000 | 0.0007 | | 0.0281 | 0.2774 | 0.0608 |
| | 0% | 0.0000 | 0.0000 | 0.8516 | 0.0000 | 0.0000 | 0.0000 | 0.0281 | | 0.3328 | 0.0000 |
| | 15% | 0.0000 | 0.0004 | 0.5454 | 0.0077 | 0.0000 | 0.0000 | 0.2774 | 0.3328 | | 0.0045 |
| | 30% | 0.0009 | 0.4652 | 0.0001 | 0.7230 | 0.0001 | 0.2005 | 0.0608 | 0.0000 | 0.0045 | |
| 0% | -30% | 0.0000 | 0.0000 | 0.8748 | 0.0002 | 0.0000 | 0.0000 | 0.1044 | 0.7933 | 0.5722 | 0.0001 |
| | -15% | 0.0000 | 0.0000 | 0.5198 | 0.0000 | 0.0000 | 0.0000 | 0.0011 | 0.7287 | 0.0492 | 0.0000 |
| | 0% | 0.0000 | 0.0000 | 0.5327 | 0.0000 | 0.0000 | 0.0000 | 0.0009 | 0.7960 | 0.0449 | 0.0000 |
| | 15% | 0.0000 | 0.0000 | 0.6110 | 0.0000 | 0.0000 | 0.0000 | 0.0026 | 0.7183 | 0.0865 | 0.0000 |
| | 30% | 0.0000 | 0.0000 | 0.7328 | 0.0007 | 0.0000 | 0.0000 | 0.1623 | 0.7811 | 0.5857 | 0.0002 |
| 20% | -30% | 0.0000 | 0.0000 | 0.8129 | 0.0012 | 0.0000 | 0.0000 | 0.1695 | 0.7153 | 0.4751 | 0.0005 |
| | -15% | 0.0000 | 0.0000 | 0.3087 | 0.0000 | 0.0000 | 0.0000 | 0.0001 | 0.6679 | 0.0110 | 0.0000 |
| | 0% | 0.0000 | 0.0000 | 0.7292 | 0.0000 | 0.0000 | 0.0000 | 0.0080 | 0.6659 | 0.1687 | 0.0000 |
| | 15% | 0.0000 | 0.0000 | 0.5812 | 0.0000 | 0.0000 | 0.0000 | 0.0009 | 0.8646 | 0.0491 | 0.0000 |
| | 30% | 0.0000 | 0.0000 | 0.9516 | 0.0001 | 0.0000 | 0.0000 | 0.0948 | 0.6129 | 0.5802 | 0.0000 |

| | AP | 0% | | | | | 20% | | | | |
|---|---|---|---|---|---|---|---|---|---|---|---|
| | LAT | -30% | -15% | 0% | 15% | 30% | -30% | -15% | 0% | 15% | 30% |
| AP | LAT | **113.74** | **89.95** | **88.75** | **93.62** | **120.80** | **124.64** | **81.65** | **98.48** | **88.46** | **111.73** |
| -40% | -30% | 0.0000 | 0.0000 | 0.0000 | 0.0000 | 0.0000 | 0.0000 | 0.0000 | 0.0000 | 0.0000 | 0.0000 |
| | -15% | 0.0000 | | | | | | 0.0000 | 0.0000 | 0.0000 | 0.0000 |
| | 0% | 0.8748 | 0.5198 | 0.5327 | 0.6110 | 0.7328 | 0.8129 | 0.3087 | 0.7292 | 0.5812 | 0.9516 |
| | 15% | 0.0002 | 0.0000 | 0.0000 | 0.0000 | 0.0007 | 0.0012 | 0.0000 | 0.0000 | 0.0000 | 0.0001 |
| | 30% | 0.0000 | 0.0000 | 0.0000 | 0.0000 | 0.0000 | 0.0000 | 0.0000 | 0.0000 | 0.0000 | 0.0000 |
| -20% | -30% | 0.0000 | 0.0000 | 0.0000 | 0.0000 | 0.0000 | 0.0000 | 0.0000 | 0.0000 | 0.0000 | 0.0000 |
| | -15% | 0.1044 | 0.0011 | 0.0009 | 0.0026 | 0.1623 | 0.1695 | 0.0001 | 0.0080 | 0.0009 | 0.0948 |
| | 0% | 0.7933 | 0.7287 | 0.7960 | 0.7183 | 0.7811 | 0.7153 | 0.6679 | 0.6659 | 0.8646 | 0.6129 |
| | 15% | 0.5722 | 0.0492 | 0.0449 | 0.0865 | 0.5857 | 0.4751 | 0.0110 | 0.1687 | 0.0491 | 0.5802 |
| | 30% | 0.0001 | 0.0000 | 0.0000 | 0.0000 | 0.0002 | 0.0005 | 0.0000 | 0.0000 | 0.0000 | 0.0000 |
| 0% | -30% | | 0.5426 | 0.5695 | 0.6123 | 0.8717 | 0.8676 | 0.3601 | 0.7017 | 0.6278 | 0.8867 |
| | -15% | 0.5426 | | 0.9325 | 0.7948 | 0.3621 | 0.2545 | 0.9361 | 0.8182 | 0.9939 | 0.5355 |
| | 0% | 0.5695 | 0.9325 | | 0.9366 | 0.3620 | 0.2474 | 0.8703 | 0.9016 | 0.9839 | 0.5812 |
| | 15% | 0.6123 | 0.7948 | 0.9366 | | 0.4650 | 0.3549 | 0.9158 | 0.7312 | 0.9834 | 0.5750 |
| | 30% | 0.8717 | 0.3621 | 0.3620 | 0.4650 | | 0.7858 | 0.1697 | 0.6123 | 0.3968 | 0.9185 |
| 20% | -30% | 0.8676 | 0.2545 | 0.2474 | 0.3549 | 0.7858 | | 0.0968 | 0.5132 | 0.2702 | 0.8919 |
| | -15% | 0.3601 | 0.9361 | 0.8703 | 0.9158 | 0.1697 | 0.0968 | | 0.8417 | 0.6299 | 0.3965 |
| | 0% | 0.7017 | 0.8182 | 0.9016 | 0.7312 | 0.6123 | 0.5132 | 0.8417 | | 0.9546 | 0.6164 |
| | 15% | 0.6278 | 0.9939 | 0.9839 | 0.9834 | 0.3968 | 0.2702 | 0.6299 | 0.9546 | | 0.6520 |
| | 30% | 0.8867 | 0.5355 | 0.5812 | 0.5750 | 0.9185 | 0.8919 | 0.3965 | 0.6164 | 0.6520 | |

## D.1.8 Inferior Lumbar Endplate Full AP Failure Load Map

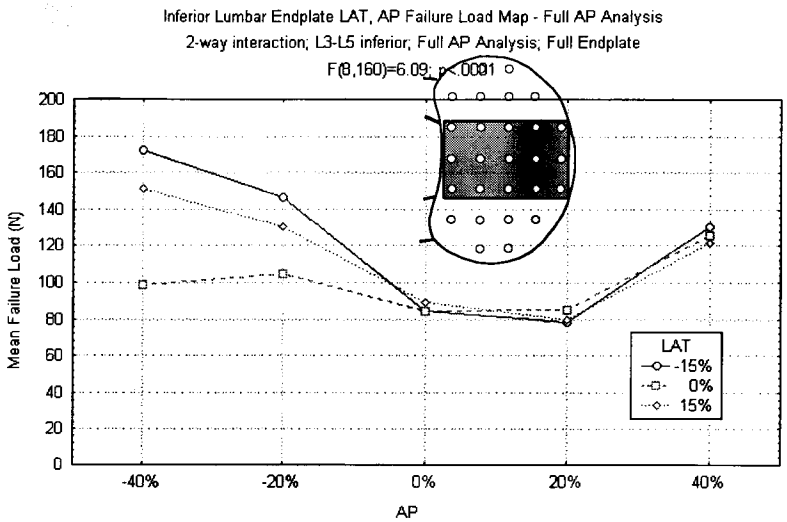


Figure D.8: Full AP failure load distribution in the inferior lumbar endplates. This plot shows the effect of the LAT distance from the centre of the endplate on the AP failure load distribution using the largest complete AP data set (inset figure). The p-value of < 0.0001 indicates that there are differences between the AP failure load distributions at different LAT co-ordinates. A *post hoc* Newman-Keuls comparison shows that this difference is due to the lower failure loads in the posterior half of the 0% LAT curve relative to the corresponding values in the +/- 15% LAT curves.

Table D.8: Newman-Keuls *post hoc* comparison of the means in the inferior lumbar endplate full AP, failure load distribution (Figure D.8).

| | AP | -40% | | | -20% | | | 0% | | | 20% | | | 40% | | |
|---|---|---|---|---|---|---|---|---|---|---|---|---|---|---|---|---|
| | LAT | -15% | 0% | 15% | -15% | 0% | 15% | -15% | 0% | 15% | -15% | 0% | 15% | -15% | 0% | 15% |
| AP | LAT | **172.32** | **98.40** | **151.67** | **146.55** | **104.63** | **130.47** | **84.37** | **84.81** | **88.92** | **78.09** | **85.02** | **80.09** | **130.12** | **125.99** | **121.58** |
| -40% | -15% | | 0.0000 | 0.0443 | 0.0324 | 0.0000 | 0.0003 | 0.0000 | 0.0000 | 0.0000 | 0.0000 | 0.0000 | 0.0000 | 0.0004 | 0.0001 | 0.0000 |
| | 0% | 0.0000 | | 0.0000 | 0.0001 | 0.5442 | 0.0221 | 0.6496 | 0.5479 | 0.3559 | 0.4292 | 0.3937 | 0.4770 | 0.0172 | 0.0363 | 0.0620 |
| | 15% | 0.0443 | 0.0000 | | 0.6183 | 0.0001 | 0.0973 | 0.0000 | 0.0000 | 0.0000 | 0.0000 | 0.0000 | 0.0000 | 0.1537 | 0.0906 | 0.0397 |
| -20% | -15% | 0.0324 | 0.0001 | 0.6183 | | 0.0006 | 0.1173 | 0.0000 | 0.0000 | 0.0000 | 0.0000 | 0.0000 | 0.0000 | 0.2457 | 0.1872 | 0.1068 |
| | 0% | 0.0000 | 0.5442 | 0.0001 | 0.0006 | | 0.0870 | 0.3582 | 0.3013 | 0.2769 | 0.1617 | 0.2241 | 0.2030 | 0.0626 | 0.0939 | 0.0989 |
| | 15% | 0.0003 | 0.0221 | 0.0973 | 0.1173 | 0.0870 | | 0.0003 | 0.0003 | 0.0010 | 0.0000 | 0.0 | 0.0001 | 0.9732 | 0.9006 | 0.8225 |
| 0% | -15% | 0.0000 | 0.6496 | 0.0000 | 0.0000 | 0.3582 | 0.0003 | | 0.9661 | 0.9710 | 0.8139 | 0.9978 | 0.6769 | 0.0003 | 0.0013 | 0.0054 |
| | 0% | 0.0000 | 0.5479 | 0.0000 | 0.0000 | 0.3013 | 0.0003 | 0.9661 | | 0.9155 | 0.9142 | 0.9833 | 0.8903 | 0.0003 | 0.0012 | 0.0046 |
| | 15% | 0.0000 | 0.3559 | 0.0000 | 0.0000 | 0.2769 | 0.0010 | 0.9710 | 0.9155 | | 0.8994 | 0.7045 | 0.9116 | 0.0009 | 0.0028 | 0.0080 |
| 20% | -15% | 0.0000 | 0.4292 | 0.0000 | 0.0000 | 0.1617 | 0.0000 | 0.8139 | 0.9142 | 0.8994 | | 0.9619 | 0.8457 | 0.0000 | 0.0001 | 0.0008 |
| | 0% | 0.0000 | 0.3937 | 0.0000 | 0.0000 | 0.2241 | 0.0003 | 0.9978 | 0.9833 | 0.7045 | 0.9619 | | 0.9635 | 0.0002 | 0.0009 | 0.0034 |
| | 15% | 0.0000 | 0.4770 | 0.0000 | 0.0000 | 0.2030 | 0.0001 | 0.6769 | 0.8903 | 0.9116 | 0.8457 | 0.9635 | | 0.0001 | 0.0003 | 0.0014 |
| 40% | -15% | 0.0004 | 0.0172 | 0.1537 | 0.2457 | 0.0626 | 0.9732 | 0.0003 | 0.0003 | 0.0009 | 0.0000 | 0.0002 | 0.0001 | | 0.6876 | 0.6829 |
| | 0% | 0.0001 | 0.0363 | 0.0906 | 0.1872 | 0.0939 | 0.9006 | 0.0013 | 0.0012 | 0.0028 | 0.0001 | 0.0009 | 0.0003 | 0.6876 | | 0.6671 |
| | 15% | 0.0000 | 0.0620 | 0.0397 | 0.1068 | 0.0989 | 0.8225 | 0.0054 | 0.0046 | 0.0080 | 0.0008 | 0.0034 | 0.0014 | 0.6829 | 0.6671 | |

## D.1.9 Inferior Lumbar Endplate Full LAT Failure Load Map

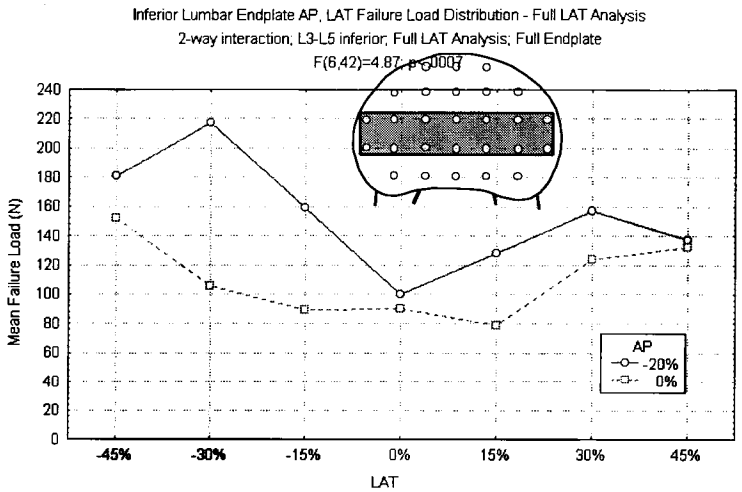


Figure D.9: Full LAT failure load distribution in the inferior lumbar endplates. This plot shows the effect of the AP distance from the centre of the endplate on the LAT failure load distribution using the largest complete LAT data set (inset figure). The p-value of < 0.0007 indicates that there are differences between the LAT failure load distributions at different AP co-ordinates.

Table D.9: Newman-Keuls *post hoc* comparison of the means in the inferior lumbar endplate AP, Full LAT failure load distribution (Figure D.9).

| | AP | -20% | | | | | | | 0% | | | | | | |
|---|---|---|---|---|---|---|---|---|---|---|---|---|---|---|---|
| | LAT | -45% | -30% | -15% | 0% | 15% | 30% | 45% | -45% | -30% | -15% | 0% | 15% | 30% | 45% |
| AP | LAT | **180.60** | **217.20** | **159.36** | **99.78** | **127.98** | **156.92** | **137.44** | **152.35** | **105.63** | **89.63** | **90.07** | **78.86** | **124.02** | **132.11** |
| -20% | -45% | | 0.0357 | 0.2149 | 0.0009 | 0.0471 | 0.3479 | 0.0968 | 0.3493 | 0.0020 | 0.0003 | 0.0003 | 0.0002 | 0.0329 | 0.0648 |
| | -30% | 0.0357 | | 0.0039 | 0.0002 | 0.0002 | 0.0049 | 0.0005 | 0.0036 | 0.0002 | 0.0001 | 0.0001 | 0.0001 | 0.0002 | 0.0003 |
| | -15% | 0.2149 | 0.0039 | | 0.0254 | 0.4393 | 0.8855 | 0.5679 | 0.9093 | 0.0502 | 0.0069 | 0.0063 | 0.0013 | 0.3734 | 0.4954 |
| | 0% | 0.0009 | 0.0002 | 0.0254 | | 0.3504 | 0.0302 | 0.2443 | 0.0473 | 0.7304 | 0.8200 | 0.5681 | 0.6051 | 0.3311 | 0.3240 |
| | 15% | 0.0471 | 0.0002 | 0.4393 | 0.3504 | | 0.4352 | 0.8414 | 0.4789 | 0.3889 | 0.2271 | 0.1823 | 0.0769 | 0.8154 | 0.8079 |
| | 30% | 0.3479 | 0.0049 | 0.8855 | 0.0302 | 0.4352 | | 0.4861 | 0.7879 | 0.0569 | 0.0088 | 0.0078 | 0.0017 | 0.3866 | 0.4633 |
| | 45% | 0.0968 | 0.0005 | 0.5679 | 0.2443 | 0.8414 | 0.4861 | | 0.3816 | 0.3399 | 0.1133 | 0.0973 | 0.0297 | 0.8558 | 0.7534 |
| 0% | -45% | 0.3493 | 0.0036 | 0.9093 | 0.0473 | 0.4789 | 0.7879 | 0.3816 | | 0.0824 | 0.0154 | 0.0134 | 0.0031 | 0.4565 | 0.4594 |
| | -30% | 0.0020 | 0.0002 | 0.0502 | 0.7304 | 0.3889 | 0.0569 | 0.3399 | 0.0824 | | 0.7788 | 0.6293 | 0.5134 | 0.2816 | 0.4059 |
| | -15% | 0.0003 | 0.0001 | 0.0069 | 0.8200 | 0.2271 | 0.0088 | 0.1133 | 0.0154 | 0.7788 | | 0.9793 | 0.5265 | 0.2654 | 0.1785 |
| | 0% | 0.0003 | 0.0001 | 0.0063 | 0.5681 | 0.1823 | 0.0078 | 0.0973 | 0.0134 | 0.6293 | 0.9793 | | 0.7850 | 0.1994 | 0.1493 |
| | 15% | 0.0002 | 0.0001 | 0.0013 | 0.6051 | 0.0769 | 0.0017 | 0.0297 | 0.0031 | 0.5134 | 0.5265 | 0.7850 | | 0.1012 | 0.0538 |
| | 30% | 0.0329 | 0.0002 | 0.3734 | 0.3311 | 0.8154 | 0.3866 | 0.8558 | 0.4565 | 0.2816 | 0.2654 | 0.1994 | 0.1012 | | 0.8812 |
| | 45% | 0.0648 | 0.0003 | 0.4954 | 0.3240 | 0.8079 | 0.4633 | 0.7534 | 0.4594 | 0.4059 | 0.1785 | 0.1493 | 0.0538 | 0.8812 | |

### D.1.10 Inferior Lumbar Endplate Maximum AP, LAT Stiffness Map

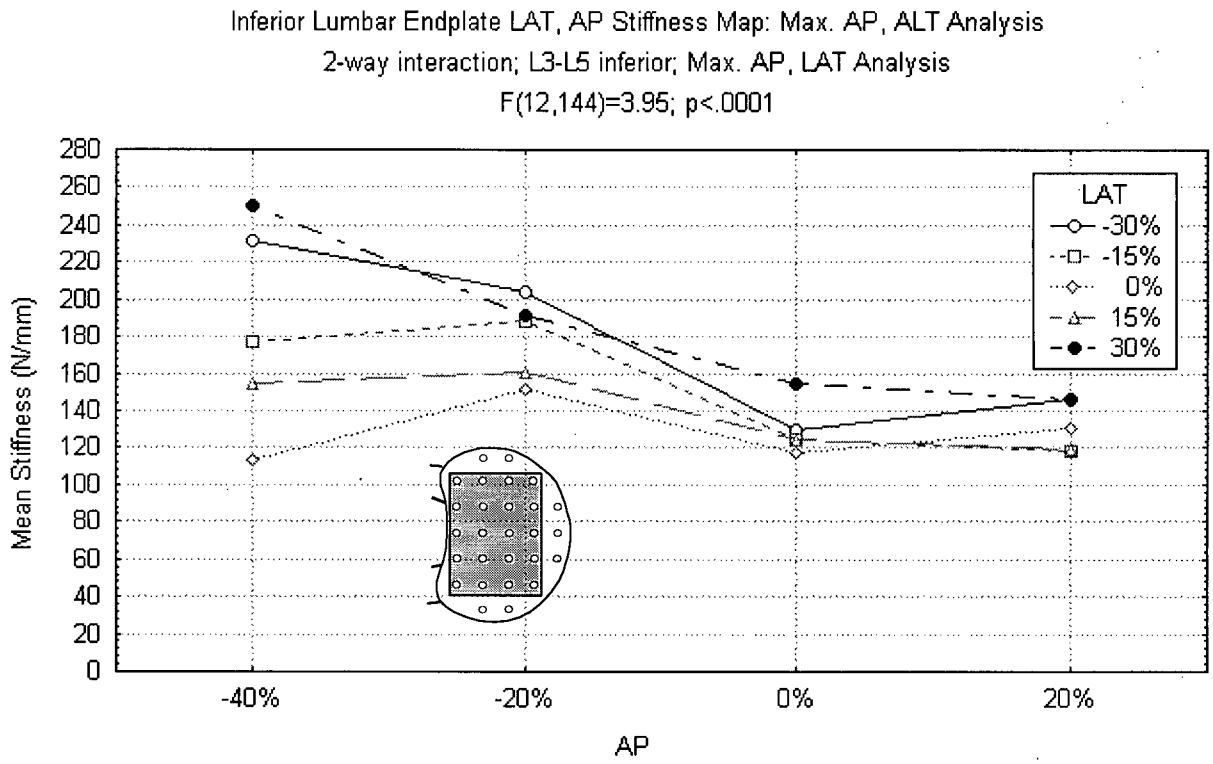


Figure D.10: Maximum LAT, AP stiffness distribution in the inferior lumbar endplates. This plot shows the effect of the LAT distance from the centre of the endplate on the AP stiffness distribution. The p-value of $< 0.0001$ indicates that there are differences between the AP stiffness distributions at different LAT co-ordinates. Note that curves that are equidistant from the centre (e.g. +/- 30% LAT) have the same shape, reflecting the lateral symmetry of the failure load distribution. The stiffest sites are located postero-laterally (+/- 40% AP, +/- 30% LAT), in front of the pedicles.

Table D.10: Newman-Keuls *post hoc* comparison of the means in the inferior lumbar endplate AP, LAT stiffness distribution (Figure D.10).

| | AP | -40% | | | | | -20% | | | | |
|---|---|---|---|---|---|---|---|---|---|---|---|
| | LAT | -30% | -15% | 0% | 15% | 30% | -30% | -15% | 0% | 15% | 30% |
| AP | LAT | **231.30** | **177.27** | **112.80** | **154.26** | **250.51** | **203.98** | **188.06** | **150.90** | **161.09** | **191.57** |
| -40% | -30% | | 0.0103 | 0.0000 | 0.0001 | 0.2482 | 0.1007 | 0.0462 | 0.0001 | 0.0004 | 0.0447 |
| | -15% | 0.0103 | | 0.0092 | 0.5101 | 0.0002 | 0.3753 | 0.5166 | 0.5071 | 0.3309 | 0.6658 |
| | 0% | 0.0000 | 0.0092 | | 0.3450 | 0.0000 | | | 0.4410 | 0.1764 | 0.0003 |
| | 15% | 0.0001 | 0.5101 | 0.3450 | | 0.0000 | | **0.2508** | 0.8399 | 0.9113 | 0.2183 |
| | 30% | 0.2482 | | 0.0000 | 0.0000 | | | | 0.0000 | 0.0000 | 0.0023 |
| -20% | -30% | 0.1007 | 0.3753 | 0.0000 | 0.0445 | 0.0143 | | 0.6041 | 0.0308 | **0.0744** | **0.4556** |
| | -15% | 0.0462 | 0.5166 | 0.0007 | 0.2508 | 0.0016 | 0.6041 | | 0.2223 | 0.2368 | 0.8329 |
| | 0% | 0.0001 | 0.5071 | 0.4410 | 0.8399 | 0.0000 | 0.0308 | 0.2223 | | 0.9281 | 0.1801 |
| | 15% | 0.0004 | 0.3309 | 0.1764 | 0.9113 | 0.0000 | **0.0744** | 0.2368 | 0.9281 | | 0.2582 |
| | 30% | 0.0447 | 0.6658 | 0.0003 | 0.2183 | 0.0023 | 0.4556 | 0.8329 | 0.1801 | 0.2582 | |
| 0% | -30% | 0.0000 | 0.0950 | 0.9541 | 0.6699 | 0.0000 | 0.0005 | 0.0155 | 0.6979 | 0.5496 | 0.0087 |
| | -15% | 0.0000 | 0.0528 | 0.9784 | 0.5737 | 0.0000 | 0.0002 | 0.0069 | 0.6248 | 0.4235 | 0.0036 |
| | 0% | 0.0000 | **0.0241** | 0.7643 | 0.5107 | 0.0000 | 0.0001 | 0.0022 | 0.6063 | 0.3086 | 0.0010 |
| | 15% | 0.0000 | 0.0553 | 0.9589 | 0.6185 | 0.0000 | 0.0002 | 0.0070 | 0.6822 | 0.4477 | 0.0036 |
| | 30% | 0.0001 | 0.3665 | 0.3592 | 0.9753 | 0.0000 | **0.0366** | 0.1877 | 0.9705 | 0.7043 | 0.1753 |
| 20% | -30% | 0.0000 | 0.4953 | 0.5455 | 0.9603 | 0.0000 | 0.0178 | 0.1843 | 0.9539 | 0.9453 | 0.1348 |
| | -15% | 0.0000 | **0.0218** | 0.9486 | 0.4691 | 0.0000 | 0.0001 | 0.0020 | 0.5573 | 0.2836 | 0.0009 |
| | 0% | 0.0000 | **0.1019** | 0.9567 | 0.6342 | 0.0000 | 0.0006 | 0.0181 | 0.6346 | 0.5477 | 0.0105 |
| | 15% | 0.0000 | | 0.9736 | 0.4991 | 0.0000 | 0.0001 | 0.0029 | 0.5781 | 0.3203 | 0.0014 |
| | 30% | 0.0000 | **0.4375** | 0.5770 | 0.8896 | 0.0000 | 0.0164 | 0.1619 | 0.7958 | 0.9075 | 0.1214 |

| | AP | 0% | | | | | 20% | | | | |
|---|---|---|---|---|---|---|---|---|---|---|---|
| | LAT | -30% | -15% | 0% | 15% | 30% | -30% | -15% | 0% | 15% | 30% |
| AP | LAT | **129.45** | **124.94** | **117.79** | **124.27** | **154.77** | **146.03** | **117.95** | **131.14** | **119.94** | **146.59** |
| -40% | -30% | 0.0000 | 0.0000 | 0.0000 | 0.0000 | 0.0001 | 0.0000 | 0.0000 | 0.0000 | 0.0000 | 0.0000 |
| | -15% | 0.0950 | 0.0528 | 0.0241 | 0.0553 | 0.3665 | 0.4953 | 0.0218 | 0.1019 | 0.0283 | 0.4375 |
| | 0% | 0.9541 | 0.9784 | 0.7643 | 0.9589 | 0.3592 | 0.5455 | 0.9486 | 0.9567 | 0.9736 | 0.5770 |
| | 15% | 0.6699 | 0.5737 | 0.5107 | 0.6185 | 0.9753 | 0.9603 | 0.4691 | 0.6342 | 0.4991 | 0.8896 |
| | 30% | 0.0000 | 0.0000 | 0.0000 | 0.0000 | 0.0000 | 0.0000 | 0.0000 | 0.0000 | 0.0000 | 0.0000 |
| -20% | -30% | 0.0005 | 0.0002 | 0.0001 | 0.0002 | 0.0366 | 0.0178 | 0.0001 | 0.0006 | 0.0001 | 0.0164 |
| | -15% | 0.0155 | 0.0069 | 0.0022 | 0.0070 | 0.1877 | 0.1843 | 0.0020 | 0.0181 | 0.0029 | 0.1619 |
| | 0% | 0.6979 | 0.6248 | 0.6063 | 0.6822 | 0.9705 | 0.9539 | 0.5573 | 0.6346 | 0.5781 | 0.7958 |
| | 15% | 0.5496 | 0.4235 | 0.3086 | 0.4477 | 0.7043 | 0.9453 | 0.2836 | 0.5477 | 0.3203 | 0.9075 |
| | 30% | 0.0087 | 0.0036 | 0.0010 | 0.0036 | 0.1753 | 0.1348 | 0.0009 | 0.0105 | 0.0014 | 0.1214 |
| 0% | -30% | | 0.7863 | 0.9819 | 0.9481 | 0.7315 | 0.5790 | 0.9585 | 0.9192 | 0.9406 | 0.7316 |
| | -15% | 0.7863 | | 0.9929 | 0.9681 | 0.6247 | 0.5836 | 0.9751 | 0.9264 | 0.9515 | 0.6903 |
| | 0% | 0.9819 | 0.9929 | | 0.9800 | 0.5329 | 0.6893 | 0.9924 | 0.9849 | 0.9909 | 0.7275 |
| | 15% | 0.9481 | 0.9681 | 0.9800 | | 0.6598 | 0.6865 | 0.9235 | 0.9763 | 0.7945 | 0.7618 |
| | 30% | 0.7315 | 0.6247 | 0.5329 | 0.6598 | | 0.9848 | 0.4952 | 0.7144 | 0.5319 | 0.9610 |
| 20% | -30% | 0.5790 | 0.5836 | 0.6893 | 0.6865 | 0.9848 | | 0.6245 | 0.3707 | 0.6198 | 0.9730 |
| | -15% | 0.9585 | 0.9751 | 0.9924 | 0.9235 | 0.4952 | 0.6245 | | 0.9689 | 0.9049 | 0.6732 |
| | 0% | 0.9192 | 0.9264 | 0.9849 | 0.9763 | 0.7144 | 0.3707 | 0.9689 | | 0.9623 | 0.6219 |
| | 15% | 0.9406 | 0.9515 | 0.9909 | 0.7945 | 0.5319 | 0.6198 | 0.9049 | 0.9623 | | 0.6811 |
| | 30% | 0.7316 | 0.6903 | 0.7275 | 0.7618 | 0.9610 | 0.9730 | 0.6732 | 0.6219 | 0.6811 | |

## D.1.11 Inferior Lumbar Endplate Full AP Stiffness Map

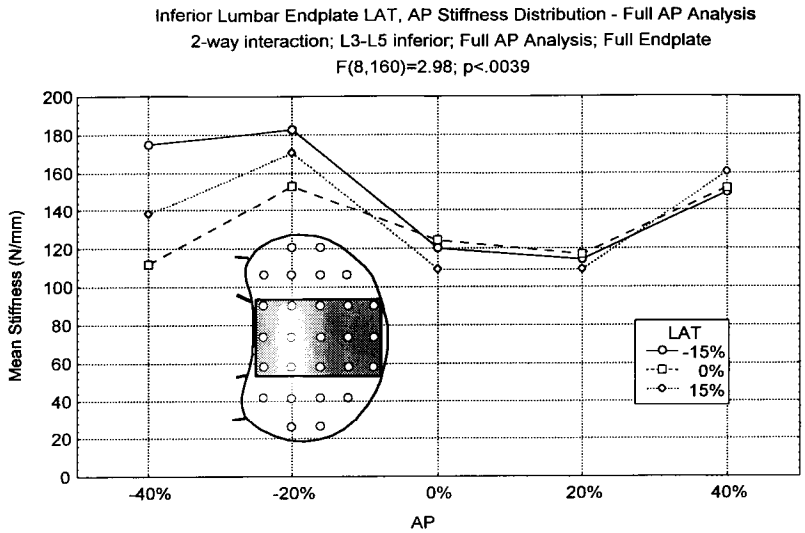


Figure D.11: Full AP stiffness distribution in the inferior lumbar endplates. This plot shows the effect of the LAT distance from the centre of the endplate on the AP stiffness distribution using the largest complete AP data set (inset figure). The p-value of < 0.0039 indicates that there are differences between the AP stiffness distributions at different LAT co-ordinates.

Table D.11: Newman-Keuls *post hoc* comparison of the means in the inferior lumbar endplate full AP, LAT stiffness distribution (Figure D.11

| | AP | -40% | | | -20% | | | 0% | | | 20% | | | 40% | | |
|---|---|---|---|---|---|---|---|---|---|---|---|---|---|---|---|---|
| | LAT | -15% | 0% | 15% | -15% | 0% | 15% | -15% | 0% | 15% | -15% | 0% | 15% | -15% | 0% | 15% |
| AP | LAT | **174.58** | **111.86** | **138.25** | **182.65** | **152.75** | **170.13** | **119.88** | **124.26** | **108.83** | **114.27** | **116.93** | **108.86** | **149.74** | **152.08** | **160.49** |
| -40% | -15% | | 0.0001 | 0.0672 | 0.5277 | 0.3189 | 0.7280 | 0.0006 | 0.0021 | 0.0000 | 0.0001 | 0.0003 | 0.0000 | 0.3753 | 0.3966 | 0.5126 |
| | 0% | 0.0001 | | 0.3054 | 0.0000 | 0.0371 | 0.0003 | 0.9231 | 0.8686 | 0.9694 | 0.8505 | 0.9169 | 0.8141 | 0.0476 | 0.0352 | 0.0055 |
| | 15% | 0.0672 | 0.3054 | | 0.0120 | 0.6683 | 0.1253 | 0.3215 | 0.2733 | 0.2917 | 0.3296 | 0.3401 | 0.2434 | 0.3685 | 0.5252 | 0.4088 |
| -20% | -15% | 0.5277 | 0.0000 | 0.0120 | | 0.1322 | 0.5900 | 0.0000 | 0.0002 | 0.0000 | 0.0000 | 0.0000 | 0.0000 | 0.1335 | 0.1587 | 0.3060 |
| | 0% | 0.3189 | 0.0371 | 0.6683 | 0.1322 | | 0.3615 | 0.1042 | 0.1687 | 0.0248 | 0.0529 | 0.0749 | 0.0210 | 0.9700 | 0.9584 | 0.5442 |
| | 15% | 0.7280 | 0.0003 | 0.1253 | 0.5900 | 0.3615 | | 0.0021 | 0.0061 | 0.0001 | 0.0005 | 0.0011 | 0.0001 | 0.4999 | 0.4910 | 0.4505 |
| 0% | -15% | 0.0006 | 0.9231 | 0.3215 | 0.0000 | 0.1042 | 0.0021 | | 0.7321 | 0.9547 | 0.8990 | 0.8171 | 0.9103 | 0.0897 | 0.0862 | 0.0249 |
| | 0% | 0.0021 | 0.8686 | 0.2733 | 0.0002 | 0.1687 | 0.0061 | 0.7321 | | 0.8915 | 0.8628 | 0.8342 | 0.8344 | 0.1135 | 0.1295 | 0.0519 |
| | 15% | 0.0000 | 0.9694 | 0.2917 | 0.0000 | 0.0248 | 0.0001 | 0.9547 | 0.8915 | | 0.9741 | 0.9696 | 0.9983 | 0.0368 | 0.0248 | 0.0031 |
| 20% | -15% | 0.0001 | 0.8505 | 0.3296 | 0.0000 | 0.0529 | 0.0005 | 0.8990 | 0.8628 | 0.9741 | | 0.8351 | 0.9058 | 0.0612 | 0.0484 | 0.0091 |
| | 0% | 0.0003 | 0.9169 | 0.3401 | 0.0000 | 0.0749 | 0.0011 | 0.8171 | 0.8342 | 0.9696 | 0.8351 | | 0.9218 | 0.0763 | 0.0656 | 0.0150 |
| | 15% | 0.0000 | 0.8141 | 0.2434 | 0.0000 | 0.0210 | 0.0001 | 0.9103 | 0.8344 | 0.9983 | 0.9058 | 0.9218 | | 0.0299 | 0.0206 | 0.0026 |
| 40% | -15% | 0.3753 | 0.0476 | 0.3685 | 0.1335 | 0.9700 | 0.4999 | 0.0897 | 0.1135 | 0.0368 | 0.0612 | 0.0763 | 0.0299 | | 0.8550 | 0.8347 |
| | 0% | 0.3966 | 0.0352 | 0.5252 | 0.1587 | 0.9584 | 0.4910 | 0.0862 | 0.1295 | 0.0248 | 0.0484 | 0.0656 | 0.0206 | 0.8550 | | 0.7874 |
| | 15% | 0.5126 | 0.0055 | 0.4088 | 0.3060 | 0.5442 | 0.4505 | 0.0249 | 0.0519 | 0.0031 | 0.0091 | 0.0150 | 0.0026 | 0.8347 | 0.7874 | |

## D.1.12 Inferior Lumbar Endplate Full LAT Stiffness Map

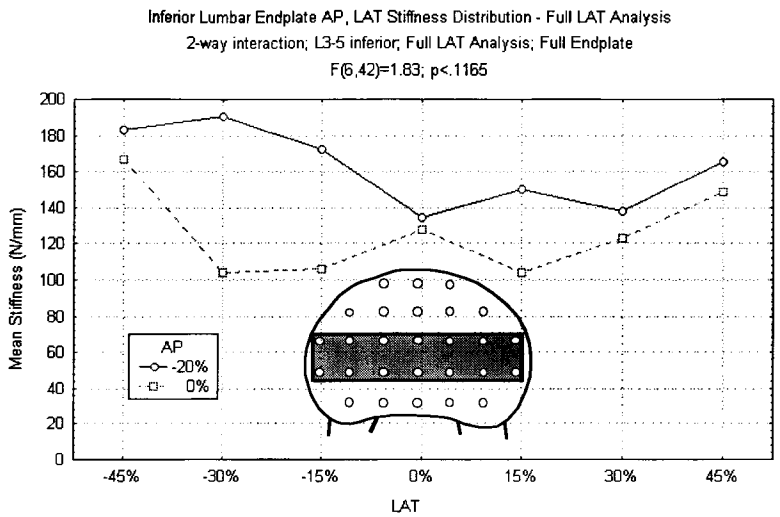


Figure D.12: Full LAT stiffness distribution in the inferior lumbar endplates. This plot shows the effect of the AP distance from the centre of the endplate on the LAT stiffness distribution using the largest complete LAT data set (inset figure). The p-value of < 0.1165 indicates that there are no significant differences between the LAT stiffness distributions at these two AP co-ordinates.

Table D.12: Newman-Keuls *post hoc* comparison of the means in the inferior lumbar endplate AP, Full LAT stiffness distribution (Figure D.12).

| | AP | -20% | | | | | | | 0% | | | | | | |
|---|---|---|---|---|---|---|---|---|---|---|---|---|---|---|---|
| | LAT | -45% | -30% | -15% | 0% | 15% | 30% | 45% | -45% | -30% | -15% | 0% | 15% | 30% | 45% |
| AP | LAT | **182.90** | **190.33** | **172.02** | **134.19** | **149.73** | **137.65** | **165.90** | **166.94** | **104.06** | **106.41** | **127.93** | **103.94** | **122.93** | **148.95** |
| -20% | -45% | | 0.7440 | 0.6327 | 0.3980 | 0.5884 | 0.4281 | 0.8751 | 0.7612 | 0.0462 | 0.0521 | 0.2936 | 0.0519 | 0.2255 | 0.6644 |
| | -30% | 0.7440 | | 0.6987 | 0.2683 | 0.4787 | 0.3012 | 0.8150 | 0.7300 | 0.0224 | 0.0259 | 0.1830 | 0.0250 | 0.1324 | 0.5351 |
| | -15% | 0.6327 | 0.6987 | | 0.6362 | 0.7580 | 0.6528 | 0.9604 | 0.8234 | 0.1255 | 0.1367 | 0.5251 | 0.1406 | 0.4410 | 0.8442 |
| | 0% | 0.3980 | 0.2683 | 0.6362 | | 0.9012 | 0.8792 | 0.6290 | 0.6970 | 0.6721 | 0.6121 | 0.7832 | 0.7619 | 0.8725 | 0.7917 |
| | 15% | 0.5884 | 0.4787 | 0.7580 | 0.9012 | | 0.8546 | 0.4785 | 0.7283 | 0.4802 | 0.4807 | 0.8692 | 0.5342 | 0.8408 | 0.9725 |
| | 30% | 0.4281 | 0.3012 | 0.6528 | 0.8792 | 0.8546 | | 0.5990 | 0.6946 | 0.6744 | 0.6421 | 0.9034 | 0.7479 | 0.9145 | 0.6197 |
| | 45% | 0.8751 | 0.8150 | 0.9604 | 0.6290 | 0.4785 | 0.5990 | | 0.9633 | 0.1661 | 0.1731 | 0.5519 | 0.1903 | 0.4905 | 0.7352 |
| 0% | -45% | 0.7612 | 0.7300 | 0.8234 | 0.6970 | 0.7283 | 0.6946 | 0.9633 | | 0.1753 | 0.1864 | 0.6026 | 0.1976 | 0.5273 | 0.8556 |
| | -30% | 0.0462 | 0.0224 | 0.1255 | 0.6721 | 0.4802 | 0.6744 | 0.1661 | 0.1753 | | 0.9175 | 0.7174 | 0.9959 | 0.6834 | 0.4378 |
| | -15% | 0.0521 | 0.0259 | 0.1367 | 0.6121 | 0.4807 | 0.6421 | 0.1731 | 0.1864 | 0.9175 | | 0.6108 | 0.9935 | 0.4689 | 0.4267 |
| | 0% | 0.2936 | 0.1830 | 0.5251 | 0.7832 | 0.8692 | 0.9034 | 0.5519 | 0.6026 | 0.7174 | 0.6108 | | 0.8248 | 0.8261 | 0.7889 |
| | 15% | 0.0519 | 0.0250 | 0.1406 | 0.7619 | 0.5342 | 0.7479 | 0.1903 | 0.1976 | 0.9959 | 0.9935 | 0.8248 | | 0.8348 | 0.4990 |
| | 30% | 0.2255 | 0.1324 | 0.4410 | 0.8725 | 0.8408 | 0.9145 | 0.4905 | 0.5273 | 0.6834 | 0.4689 | 0.8261 | 0.8348 | | 0.7783 |
| | 45% | 0.6644 | 0.5351 | 0.8442 | 0.7917 | 0.9725 | 0.6197 | 0.7352 | 0.8556 | 0.4378 | 0.4267 | 0.7889 | 0.4990 | 0.7783 | |

### D.1.13 Sacral Endplate Maximum AP, LAT Failure Load Map

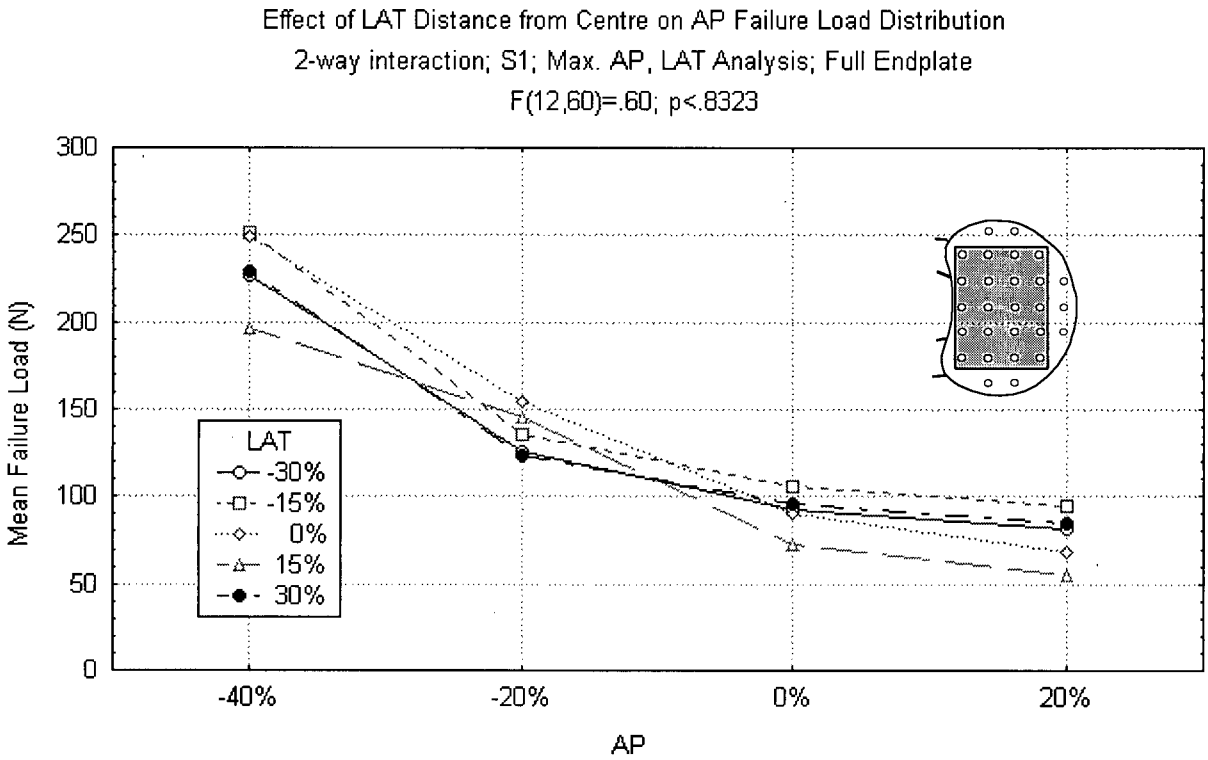


Figure D.13: Maximum AP, LAT failure load distribution in the sacral endplates. This plot shows the effect of the LAT distance from the centre of the endplate on the AP failure load distribution. The p-value of < 0.8323 indicates that there are no differences between the AP failure load curves at different LAT co-ordinates. Note that the strongest test sites lie along the posterior margin of the endplate (-40% AP).

Table D.13: Newman-Keuls *post hoc* comparison of the means in the sacral endplate AP, LAT failure load distribution (Figure D.13).

| | AP | -40% | | | | | -20% | | | | |
|---|---|---|---|---|---|---|---|---|---|---|---|
| | LAT | -30% | -15% | 0% | 15% | 30% | -30% | -15% | 0% | 15% | 30% |
| AP | LAT | **227.71** | **251.24** | **249.50** | **196.82** | **229.36** | **125.24** | **135.81** | **154.76** | **145.53** | **123.98** |
| -40% | -30% | | 0.7763 | 0.6534 | 0.2157 | 0.9471 | 0.0015 | 0.0040 | 0.0123 | 0.0080 | 0.0018 |
| | -15% | 0.7763 | | 0.9440 | 0.1922 | 0.6510 | 0.0002 | 0.0005 | 0.0032 | 0.0014 | 0.0003 |
| | 0% | 0.6534 | 0.9440 | | 0.1543 | 0.4180 | 0.0002 | 0.0005 | 0.0028 | 0.0013 | 0.0003 |
| | 15% | 0.2157 | 0.1922 | 0.1543 | | 0.3908 | 0.0402 | 0.0749 | 0.0937 | 0.1032 | 0.0492 |
| | 30% | 0.9471 | 0.6510 | 0.4180 | 0.3908 | | 0.0017 | 0.0046 | 0.0189 | 0.0104 | 0.0018 |
| -20% | -30% | 0.0015 | 0.0002 | 0.0002 | 0.0402 | 0.0017 | | 0.6703 | 0.6319 | 0.6911 | 0.9594 |
| | -15% | 0.0040 | 0.0005 | 0.0005 | 0.0749 | 0.0046 | 0.6703 | | 0.7242 | 0.6952 | 0.8814 |
| | 0% | 0.0123 | 0.0032 | 0.0028 | 0.0937 | 0.0189 | 0.6319 | 0.7242 | | 0.7099 | 0.7241 |
| | 15% | 0.0080 | 0.0014 | 0.0013 | 0.1032 | 0.0104 | 0.6911 | 0.6952 | 0.7099 | | 0.8188 |
| | 30% | 0.0018 | 0.0003 | 0.0003 | 0.0492 | 0.0018 | 0.9594 | 0.8814 | 0.7241 | 0.8188 | |
| 0% | -30% | 0.0002 | 0.0001 | 0.0001 | 0.0032 | 0.0002 | 0.7719 | 0.5862 | 0.2447 | 0.4000 | 0.7100 |
| | -15% | 0.0003 | 0.0002 | 0.0002 | 0.0080 | 0.0003 | 0.7011 | 0.6083 | 0.3539 | 0.4862 | 0.4538 |
| | 0% | 0.0002 | 0.0001 | 0.0001 | 0.0029 | 0.0002 | 0.7959 | 0.5993 | 0.2392 | 0.4011 | 0.7526 |
| | 15% | 0.0001 | 0.0002 | 0.0002 | 0.0005 | 0.0001 | 0.5202 | 0.2981 | 0.0706 | 0.1523 | 0.5026 |
| | 30% | 0.0002 | 0.0001 | 0.0002 | 0.0034 | 0.0002 | 0.6516 | 0.5082 | 0.2339 | 0.3624 | 0.5100 |
| 20% | -30% | 0.0001 | 0.0002 | 0.0001 | 0.0012 | 0.0002 | 0.6931 | 0.4613 | 0.1410 | 0.2699 | 0.6673 |
| | -15% | 0.0002 | 0.0001 | 0.0001 | 0.0035 | 0.0002 | 0.7356 | 0.5660 | 0.2494 | 0.3957 | 0.6441 |
| | 0% | 0.0001 | 0.0002 | 0.0002 | 0.0004 | 0.0002 | 0.4471 | 0.2382 | 0.0499 | 0.1139 | 0.4363 |
| | 15% | 0.0002 | 0.0002 | 0.0002 | 0.0002 | 0.0002 | 0.1938 | 0.0818 | 0.0123 | 0.0325 | 0.1912 |
| | 30% | 0.0001 | 0.0001 | 0.0001 | 0.0016 | 0.0001 | 0.7187 | 0.4979 | 0.1665 | 0.3048 | 0.6840 |

| | AP | 0% | | | | | 20% | | | | |
|---|---|---|---|---|---|---|---|---|---|---|---|
| | LAT | -30% | -15% | 0% | 15% | 30% | -30% | -15% | 0% | 15% | 30% |
| AP | LAT | **92.61** | **105.36** | **90.50** | **72.87** | **96.50** | **81.24** | **94.94** | **68.45** | **55.36** | **84.52** |
| -40% | -30% | 0.0002 | 0.0003 | 0.0002 | 0.0001 | 0.0002 | 0.0001 | 0.0002 | 0.0001 | 0.0002 | 0.0001 |
| | -15% | 0.0001 | 0.0002 | 0.0001 | 0.0002 | 0.0001 | 0.0002 | 0.0001 | 0.0002 | 0.0002 | 0.0001 |
| | 0% | 0.0001 | 0.0002 | 0.0001 | 0.0002 | 0.0002 | 0.0001 | 0.0001 | 0.0002 | 0.0002 | 0.0001 |
| | 15% | 0.0032 | 0.0080 | 0.0029 | 0.0005 | 0.0034 | 0.0012 | 0.0035 | 0.0004 | 0.0002 | 0.0016 |
| | 30% | 0.0002 | 0.0003 | 0.0002 | 0.0001 | 0.0002 | 0.0002 | 0.0002 | 0.0002 | 0.0002 | 0.0001 |
| -20% | -30% | 0.7719 | 0.7011 | 0.7959 | 0.5202 | 0.6516 | 0.6931 | 0.7356 | 0.4471 | 0.1938 | 0.7187 |
| | -15% | 0.5862 | 0.6083 | 0.5993 | 0.2981 | 0.5082 | 0.4613 | 0.5660 | 0.2382 | 0.0818 | 0.4979 |
| | 0% | 0.2447 | 0.3539 | 0.2392 | 0.0706 | 0.2339 | 0.1410 | 0.2494 | 0.0499 | 0.0123 | 0.1665 |
| | 15% | 0.4000 | 0.4862 | 0.4011 | 0.1523 | 0.3624 | 0.2699 | 0.3957 | 0.1139 | 0.0325 | 0.3048 |
| | 30% | 0.7100 | 0.4538 | 0.7526 | 0.5026 | 0.5100 | 0.6673 | 0.6441 | 0.4363 | 0.1912 | 0.6840 |
| 0% | -30% | | 0.9549 | 0.9324 | 0.9297 | 0.9865 | 0.9673 | 0.9252 | 0.9230 | 0.7384 | 0.9427 |
| | -15% | 0.9549 | | 0.9744 | 0.8892 | 0.7213 | 0.9571 | 0.9068 | 0.8535 | 0.5853 | 0.9579 |
| | 0% | 0.9324 | 0.9744 | | 0.8910 | 0.9950 | 0.9255 | 0.9824 | 0.8983 | 0.7127 | 0.8095 |
| | 15% | 0.9297 | 0.8892 | 0.8910 | | 0.9610 | 0.7358 | 0.9465 | 0.8588 | 0.7591 | 0.8846 |
| | 30% | 0.9865 | 0.7213 | 0.9950 | 0.9610 | | 0.9893 | 0.9498 | 0.9460 | 0.7637 | 0.9885 |
| 20% | -30% | 0.9673 | 0.9571 | 0.9255 | 0.7358 | 0.9893 | | 0.9809 | 0.8629 | 0.7219 | 0.8947 |
| | -15% | 0.9252 | 0.9068 | 0.9824 | 0.9465 | 0.9498 | 0.9809 | | 0.9336 | 0.7464 | 0.9746 |
| | 0% | 0.9230 | 0.8535 | 0.8983 | 0.8588 | 0.9460 | 0.8629 | 0.9336 | | 0.5979 | 0.9148 |
| | 15% | 0.7384 | 0.5853 | 0.7127 | 0.7591 | 0.7637 | 0.7219 | 0.7464 | 0.5979 | | 0.7619 |
| | 30% | 0.9427 | 0.9579 | 0.8095 | 0.8846 | 0.9885 | 0.8947 | 0.9746 | 0.9148 | 0.7619 | |

## D.1.14 Sacral Endplate Full AP Failure Load Map

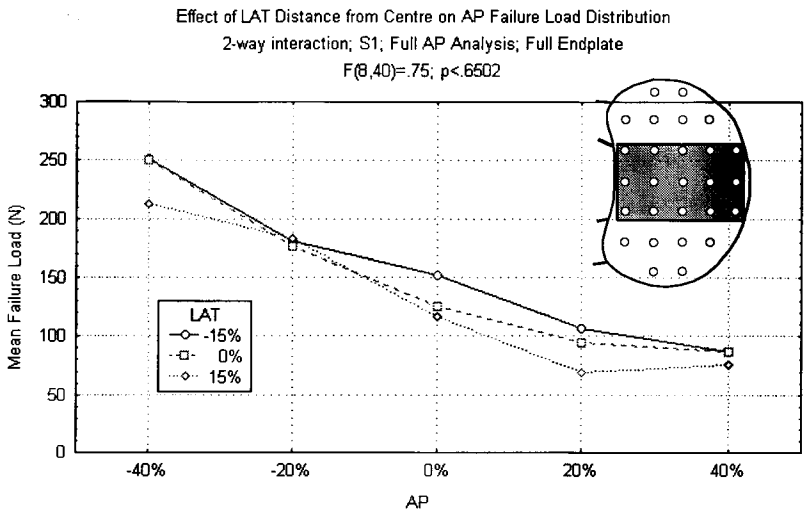


Figure D.14: Full AP failure load distribution in the sacral endplates. This plot shows the effect of the LAT distance from the centre of the endplate on the AP failure load distribution using the largest complete AP data set (inset figure). The p-value of < 0.6502 indicates that there are no significant differences between the AP failure load curves at different LAT co-ordinates.

Table D.14: Newman-Keuls post hoc comparison of the means in the sacral endplate full AP failure load distribution (Figure D.14).

| | AP | -40% | | | -20% | | | 0% | | | 20% | | | 40% | | |
|---|---|---|---|---|---|---|---|---|---|---|---|---|---|---|---|---|
| | LAT | -15% | 0% | 15% | -15% | 0% | 15% | -15% | 0% | 15% | -15% | 0% | 15% | -15% | 0% | 15% |
| AP | LAT | **251.63** | **249.93** | **212.92** | **181.07** | **176.14** | **183.66** | **152.65** | **125.85** | **117.47** | **107.55** | **95.30** | **69.58** | **86.70** | **86.74** | **76.57** |
| -40% | -15% | | 0.9274 | 0.1057 | 0.0043 | 0.0029 | 0.0040 | 0.0002 | 0.0001 | 0.0001 | 0.0002 | 0.0002 | 0.0001 | 0.0001 | 0.0001 | 0.0001 |
| | 0% | 0.9274 | | 0.0531 | 0.0035 | 0.0026 | 0.0028 | 0.0002 | 0.0001 | 0.0001 | 0.0001 | 0.0002 | 0.0001 | 0.0001 | 0.0002 | 0.0001 |
| | 15% | 0.1057 | 0.0531 | | 0.2120 | 0.2122 | 0.1229 | 0.0190 | 0.0006 | 0.0003 | 0.0002 | 0.0001 | 0.0001 | 0.0002 | 0.0002 | 0.0001 |
| -20% | -15% | 0.0043 | 0.0035 | 0.2120 | | 0.7922 | 0.8900 | 0.2875 | 0.0246 | 0.0119 | 0.0039 | 0.0008 | 0.0002 | 0.0004 | 0.0003 | 0.0002 |
| | 0% | 0.0029 | 0.0026 | 0.2122 | 0.7922 | | 0.9139 | 0.2130 | 0.0263 | 0.0153 | 0.0057 | 0.0013 | 0.0002 | 0.0006 | 0.0005 | 0.0002 |
| | 15% | 0.0040 | 0.0028 | 0.1229 | 0.8900 | 0.9139 | | 0.3524 | 0.0267 | 0.0116 | 0.0035 | 0.0007 | 0.0001 | 0.0004 | 0.0003 | 0.0002 |
| 0% | -15% | 0.0002 | 0.0002 | 0.0190 | 0.2875 | 0.2130 | 0.3524 | | 0.1567 | 0.1534 | 0.0877 | 0.0284 | 0.0020 | 0.0159 | 0.0121 | 0.0045 |
| | 0% | 0.0001 | 0.0001 | 0.0006 | 0.0246 | 0.0263 | 0.0267 | 0.1567 | | 0.6542 | 0.5898 | 0.3654 | 0.0740 | 0.3031 | 0.2371 | 0.1369 |
| | 15% | 0.0001 | 0.0001 | 0.0003 | 0.0119 | 0.0153 | 0.0116 | 0.1534 | 0.6542 | | 0.5959 | 0.4634 | 0.1595 | 0.4706 | 0.3601 | 0.2587 |
| 20% | -15% | 0.0002 | 0.0001 | 0.0002 | 0.0039 | 0.0057 | 0.0035 | 0.0877 | 0.5898 | 0.5959 | | 0.5133 | 0.3360 | 0.6774 | 0.5069 | 0.4640 |
| | 0% | 0.0002 | 0.0002 | 0.0001 | 0.0008 | 0.0013 | 0.0007 | 0.0284 | 0.3654 | 0.4634 | 0.5133 | | 0.6402 | 0.8886 | 0.6471 | 0.7450 |
| | 15% | 0.0001 | 0.0001 | 0.0001 | 0.0002 | 0.0002 | 0.0001 | 0.0020 | 0.0740 | 0.1595 | 0.3360 | 0.6402 | | 0.6299 | 0.7921 | 0.7088 |
| 40% | -15% | 0.0001 | 0.0001 | 0.0002 | 0.0004 | 0.0006 | 0.0004 | 0.0159 | 0.3031 | 0.4706 | 0.6774 | 0.8886 | 0.6299 | | 0.9982 | 0.5885 |
| | 0% | 0.0001 | 0.0002 | 0.0002 | 0.0003 | 0.0005 | 0.0003 | 0.0121 | 0.2371 | 0.3601 | 0.5069 | 0.6471 | 0.7921 | 0.9982 | | 0.8482 |
| | 15% | 0.0001 | 0.0001 | 0.0001 | 0.0002 | 0.0002 | 0.0002 | 0.0045 | 0.1369 | 0.2587 | 0.4640 | 0.7450 | 0.7088 | 0.5885 | 0.8482 | |

## D.1.15 Sacral Endplate Full LAT Failure Load Map

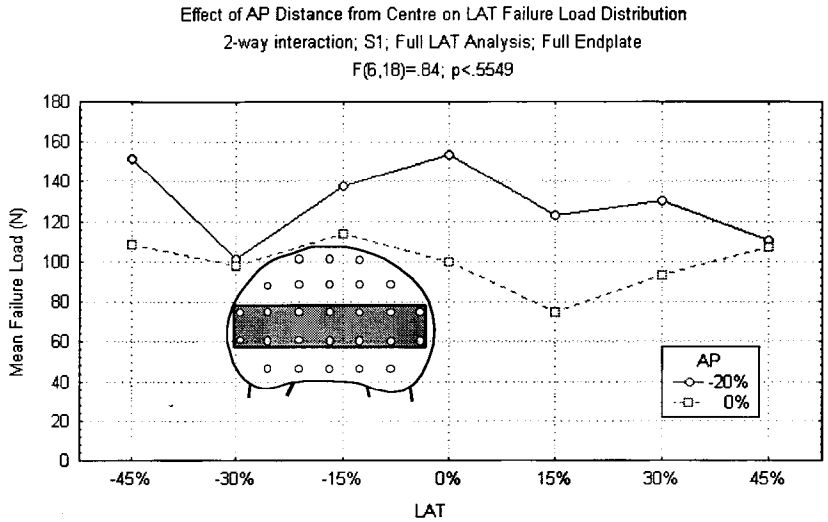


Figure D.15: Full LAT failure load distribution in the sacral endplates. This plot shows the effect of the AP distance from the centre of the endplate on the LAT failure load distribution using the largest complete LAT data set (inset figure). The p-value of < 0.5549 indicates that there are no significant differences between the LAT failure load curves at different AP co-ordinates. A Newman-Keuls *post hoc* comparison showed that the apparent lateral variation in these curves is not significant (i.e. they should be interpreted as straight, horizontal lines).

Table D.15: Newman-Keuls *post hoc* comparison of the means in the sacral endplate Full LAT failure load distribution (Figure D.15).

| | AP | -20% | | | | | | | 0% | | | | | | |
|---|---|---|---|---|---|---|---|---|---|---|---|---|---|---|---|
| | LAT | -45% | -30% | -15% | 0% | 15% | 30% | 45% | -45% | -30% | -15% | 0% | 15% | 30% | 45% |
| AP | LAT | **151.23** | **101.39** | **137.61** | **153.55** | **122.85** | **130.42** | **110.64** | **108.78** | **98.25** | **113.97** | **99.67** | **74.98** | **93.16** | **106.98** |
| -20% | -45% | | 0.4362 | 0.5525 | 0.9192 | 0.5975 | 0.6318 | 0.4872 | 0.5124 | 0.4413 | 0.4831 | 0.4375 | 0.1046 | 0.3552 | 0.5272 |
| | -30% | 0.4362 | | 0.7391 | 0.4229 | 0.9266 | 0.8477 | 0.9760 | 0.9426 | 0.9894 | 0.9794 | 0.9399 | 0.7655 | 0.9828 | 0.8069 |
| | -15% | 0.5525 | 0.7391 | | 0.7617 | 0.7913 | 0.7530 | 0.7519 | 0.7909 | 0.7556 | 0.7225 | 0.7469 | 0.2636 | 0.6658 | 0.8141 |
| | 0% | 0.9192 | 0.4229 | 0.7617 | | 0.6563 | 0.7354 | 0.5004 | 0.5137 | 0.4191 | 0.5134 | 0.4193 | 0.0956 | 0.3327 | 0.5197 |
| | 15% | 0.5975 | 0.9266 | 0.7913 | 0.6563 | | 0.7404 | 0.8515 | 0.9226 | 0.9502 | 0.6978 | 0.9400 | 0.5325 | 0.9125 | 0.9526 |
| | 30% | 0.6318 | 0.8477 | 0.7530 | 0.7354 | 0.7404 | | 0.8155 | 0.8685 | 0.8719 | 0.7485 | 0.8604 | 0.3825 | 0.8048 | 0.8973 |
| | 45% | 0.4872 | 0.9760 | 0.7519 | 0.5004 | 0.8515 | 0.8155 | | 0.9352 | 0.9931 | 0.8841 | 0.9876 | 0.7529 | 0.9845 | 0.9856 |
| 0% | -45% | 0.5124 | 0.9426 | 0.7909 | 0.5137 | 0.9226 | 0.8685 | 0.9352 | | 0.9894 | 0.9712 | 0.9770 | 0.7400 | 0.9803 | 0.9371 |
| | -30% | 0.4413 | 0.9894 | 0.7556 | 0.4191 | 0.9502 | 0.8719 | 0.9931 | 0.9894 | | 0.9910 | 0.9504 | 0.5654 | 0.8237 | 0.9796 |
| | -15% | 0.4831 | 0.9794 | 0.7225 | 0.5134 | 0.6978 | 0.7485 | 0.8841 | 0.9712 | 0.9910 | | 0.9867 | 0.7207 | 0.9794 | 0.9893 |
| | 0% | 0.4375 | 0.9399 | 0.7469 | 0.4193 | 0.9400 | 0.8604 | 0.9876 | 0.9770 | 0.9504 | 0.9867 | | 0.6955 | 0.9551 | 0.9438 |
| | 15% | 0.1046 | 0.7655 | 0.2636 | 0.0956 | 0.5325 | 0.3825 | 0.7529 | 0.7400 | 0.5654 | 0.7207 | 0.6955 | | 0.4296 | 0.7139 |
| | 30% | 0.3552 | 0.9828 | 0.6658 | 0.3327 | 0.9125 | 0.8048 | 0.9845 | 0.9803 | 0.8237 | 0.9794 | 0.9551 | 0.4296 | | 0.9710 |
| | 45% | 0.5272 | 0.8069 | 0.8141 | 0.5197 | 0.9526 | 0.8973 | 0.9856 | 0.9371 | 0.9796 | 0.9893 | 0.9438 | 0.7139 | 0.9710 | |

### D.1.16 Sacral Endplate Maximum AP, LAT Stiffness Map

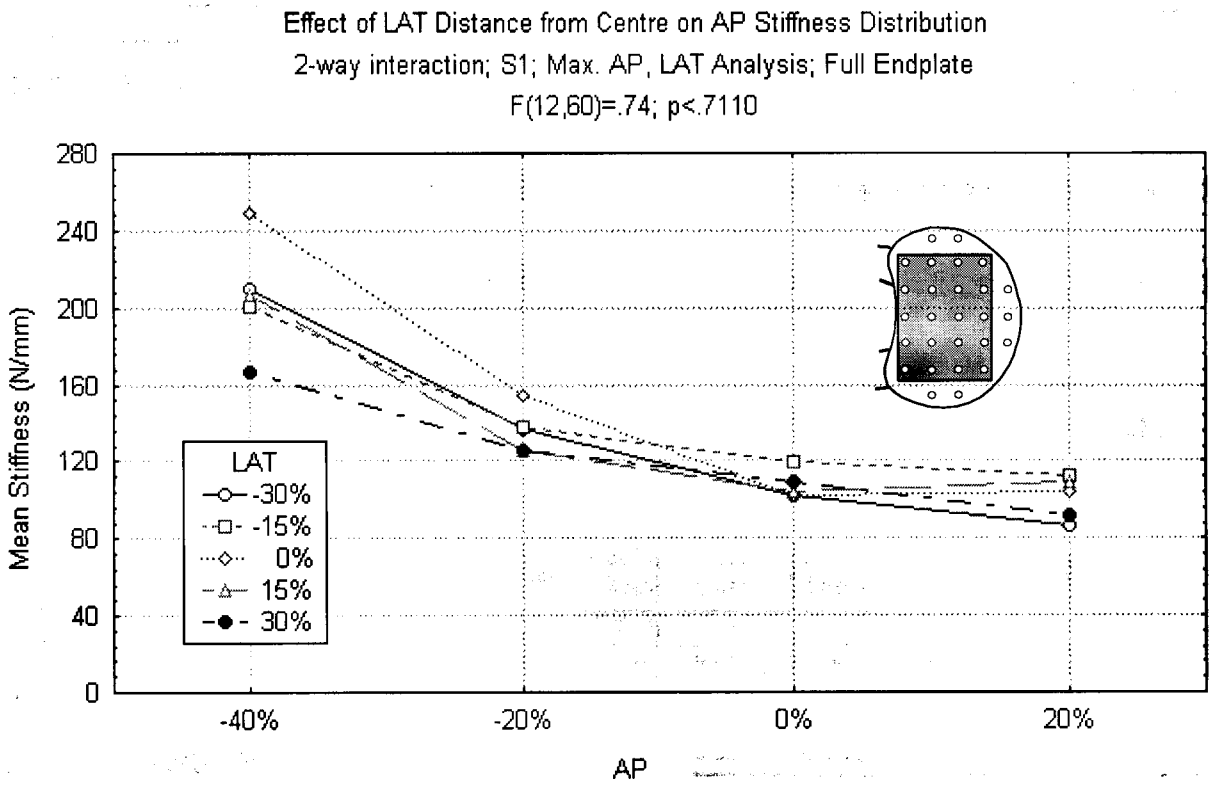


Figure D.16: Maximum LAT, AP stiffness distribution in the sacral endplates. This plot shows the effect of the LAT distance from the centre of the endplate on the AP stiffness distribution. The p-value of $< 0.7110$ indicates that there are no significant differences between the AP stiffness curves at different LAT co-ordinates. The stiffest sites are located along the posterior margin of the endplate.

Table D.16: Newman-Keuls *post hoc* comparison of the means in the sacral endplate AP, LAT stiffness distribution (Figure D.16).

| | AP | -40% | | | | | -20% | | | | |
|---|---|---|---|---|---|---|---|---|---|---|---|
| | LAT | -30% | -15% | 0% | 15% | 30% | -30% | -15% | 0% | 15% | 30% |
| AP | LAT | **210.39** | **200.58** | **249.59** | **206.81** | **166.67** | **136.50** | **138.36** | **154.37** | **125.21** | **125.44** |
| -40% | -30% | | 0.9229 | 0.1321 | 0.8894 | 0.3312 | 0.0768 | 0.0703 | 0.2005 | 0.0384 | 0.0320 |
| | -15% | 0.9229 | | 0.2353 | 0.8094 | 0.1916 | 0.1052 | 0.0835 | 0.1783 | 0.0667 | 0.0522 |
| | 0% | 0.1321 | 0.2353 | | 0.2264 | 0.0166 | 0.001 | | 0059 | 0.0005 | 0.0004 |
| | 15% | 0.8894 | 0.8094 | 0.2264 | | 0.2694 | 0.0825 | 0.0713 | 0.1842 | 0.0454 | 0.0367 |
| | 30% | 0.3312 | 0.1916 | 0.0166 | 0.2694 | | 0.6447 | 0.5161 | 0.6336 | 0.5922 | 0.4995 |
| -20% | -30% | 0.0768 | 0.1052 | 0.0012 | 0.0825 | 0.6447 | | 0.9427 | 0.7668 | 0.8992 | 0.6683 |
| | -15% | 0.0703 | 0.0835 | 0.0012 | 0.0713 | 0.5161 | 0.9427 | | 0.5353 | 0.9560 | 0.8701 |
| | 0% | 0.2005 | 0.1783 | 0.0059 | 0.1842 | 0.6336 | 0.7668 | 0.5353 | | 0.7871 | 0.6746 |
| | 15% | 0.0384 | 0.0667 | 0.0005 | 0.0454 | 0.5922 | 0.8992 | 0.9560 | 0.7871 | | 0.9931 |
| | 30% | 0.0320 | 0.0522 | 0.0004 | 0.0367 | 0.4995 | 0.6683 | 0.8701 | 0.6746 | 0.9931 | |
| 0% | -30% | 0.0073 | 0.0183 | 0.0002 | 0.0100 | 0.3746 | 0.9358 | 0.9365 | 0.6578 | 0.9835 | 0.9907 |
| | -15% | 0.0257 | 0.0490 | 0.0004 | 0.0315 | 0.5353 | 0.9144 | 0.9500 | 0.7570 | 0.8325 | 0.9734 |
| | 0% | 0.0080 | 0.0205 | 0.0002 | 0.0111 | 0.4036 | 0.9536 | 0.9525 | 0.6936 | 0.9911 | 0.9949 |
| | 15% | 0.0078 | 0.0188 | 0.0002 | 0.0105 | 0.3656 | 0.9114 | 0.9190 | 0.6351 | 0.9636 | 0.9815 |
| | 30% | 0.0118 | 0.0269 | 0.0002 | 0.0156 | 0.4345 | 0.9326 | 0.9428 | 0.6993 | 0.9684 | 0.9870 |
| 20% | -30% | 0.0015 | 0.0041 | 0.0002 | 0.0021 | 0.1508 | 0.7561 | 0.7443 | 0.3588 | 0.9087 | 0.9277 |
| | -15% | 0.0125 | 0.0264 | 0.0002 | 0.0159 | 0.4058 | 0.8723 | 0.9056 | 0.6480 | 0.8623 | 0.9520 |
| | 0% | 0.0084 | 0.0206 | 0.0002 | 0.0114 | 0.3923 | 0.9356 | 0.9388 | 0.6710 | 0.9806 | 0.9899 |
| | 15% | 0.0106 | 0.0235 | 0.0002 | 0.0137 | 0.3932 | 0.8926 | 0.9133 | 0.6469 | 0.9230 | 0.9686 |
| | 30% | 0.0024 | 0.0066 | 0.0002 | 0.0034 | 0.2078 | 0.8291 | 0.8222 | 0.4503 | 0.9433 | 0.9585 |

| | AP | 0% | | | | | 20% | | | | |
|---|---|---|---|---|---|---|---|---|---|---|---|
| | LAT | -30% | -15% | 0% | 15% | 30% | -30% | -15% | 0% | 15% | 30% |
| AP | LAT | **101.72** | **119.76** | **101.63** | **104.28** | **108.86** | **86.30** | **111.89** | **103.85** | **109.12** | **91.16** |
| -40% | -30% | 0.0073 | 0.0257 | 0.0080 | 0.0078 | 0.0118 | 0.0015 | 0.0125 | 0.0084 | 0.0106 | 0.0024 |
| | -15% | 0.0183 | 0.0490 | 0.0205 | 0.0188 | 0.0269 | 0.0041 | 0.0264 | 0.0206 | 0.0235 | 0.0066 |
| | 0% | 0.0002 | 0.0004 | 0.0002 | 0.0002 | 0.0002 | 0.0002 | 0.0002 | 0.0002 | 0.0002 | 0.0002 |
| | 15% | 0.0100 | 0.0315 | 0.0111 | 0.0105 | 0.0156 | 0.0021 | 0.0159 | 0.0114 | 0.0137 | 0.0034 |
| | 30% | 0.3746 | 0.5353 | 0.4036 | 0.3656 | 0.4345 | 0.1508 | 0.4058 | 0.3923 | 0.3932 | 0.2078 |
| -20% | -30% | 0.9358 | 0.9144 | 0.9536 | 0.9114 | 0.9326 | 0.7561 | 0.8723 | 0.9356 | 0.8926 | 0.8291 |
| | -15% | 0.9365 | 0.9500 | 0.9525 | 0.9190 | 0.9428 | 0.7443 | 0.9056 | 0.9388 | 0.9133 | 0.8222 |
| | 0% | 0.6578 | 0.7570 | 0.6936 | 0.6351 | 0.6993 | 0.3588 | 0.6480 | 0.6710 | 0.6469 | 0.4503 |
| | 15% | 0.9835 | 0.8325 | 0.9911 | 0.9636 | 0.9684 | 0.9087 | 0.8623 | 0.9806 | 0.9230 | 0.9433 |
| | 30% | 0.9907 | 0.9734 | 0.9949 | 0.9815 | 0.9870 | 0.9277 | 0.9520 | 0.9899 | 0.9686 | 0.9585 |
| 0% | -30% | | 0.9920 | 0.9973 | 0.9946 | 0.9925 | 0.9316 | 0.9987 | 0.9341 | 0.9985 | 0.9111 |
| | -15% | 0.9920 | | 0.9965 | 0.9742 | 0.9741 | 0.9491 | 0.7604 | 0.9892 | 0.9099 | 0.9699 |
| | 0% | 0.9973 | 0.9965 | | 0.9997 | 0.9986 | 0.8223 | 0.9997 | 0.9959 | 0.9997 | 0.6849 |
| | 15% | 0.9946 | 0.9742 | 0.9997 | | 0.8591 | 0.9813 | 0.9909 | 0.9869 | 0.9807 | 0.9860 |
| | 30% | 0.9925 | 0.9741 | 0.9986 | 0.8591 | | 0.9745 | 0.9924 | 0.9793 | 0.9922 | 0.9825 |
| 20% | -30% | 0.9316 | 0.9491 | 0.8223 | 0.9813 | 0.9745 | | 0.9849 | 0.9593 | 0.9861 | 0.8507 |
| | -15% | 0.9987 | 0.7604 | 0.9997 | 0.9909 | 0.9924 | 0.9849 | | 0.9979 | 0.9145 | 0.9921 |
| | 0% | 0.9341 | 0.9892 | 0.9959 | 0.9869 | 0.9793 | 0.9593 | 0.9979 | | 0.9970 | 0.9601 |
| | 15% | 0.9985 | 0.9099 | 0.9997 | 0.9807 | 0.9922 | 0.9861 | 0.9145 | 0.9970 | | 0.9922 |
| | 30% | 0.9111 | 0.9699 | 0.6849 | 0.9860 | 0.9825 | 0.8507 | 0.9921 | 0.9601 | 0.9922 | |

## D.1.17 Sacral Endplate Full AP Stiffness Map

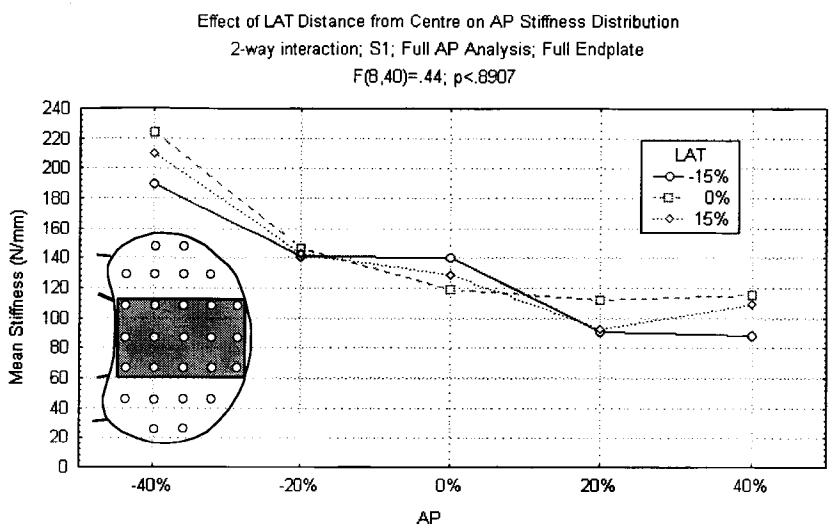


Figure D.17: Full AP stiffness distribution in the sacral endplates. This plot shows the effect of the LAT distance from the centre of the endplate on the AP stiffness distribution using the largest complete AP data set (inset figure). The p-value of < 0.8907 indicates that there are no significant differences between the AP stiffness distributions at different LAT co-ordinates.

Table D.17: Newman-Keuls *post hoc* comparison of the means in the sacral endplate full AP stiffness distribution (Figure D.17).

| | AP | -40% | | | -20% | | | 0% | | | 20% | | | 40% | | |
|---|---|---|---|---|---|---|---|---|---|---|---|---|---|---|---|---|
| | LAT | -15% | 0% | 15% | -15% | 0% | 15% | -15% | 0% | 15% | -15% | 0% | 15% | -15% | 0% | 15% |
| AP | LAT | **189.81** | **223.72** | **210.21** | **141.08** | **146.49** | **143.29** | **140.43** | **118.89** | **128.86** | **90.88** | **112.39** | **92.46** | **88.08** | **115.23** | **109.11** |
| -40% | -15% | | 0.3685 | 0.4164 | 0.2194 | 0.0889 | 0.1599 | 0.2903 | 0.0891 | 0.1628 | 0.0130 | 0.0733 | 0.0133 | 0.0110 | 0.0791 | 0.0635 |
| | 0% | 0.3685 | | 0.5896 | 0.0217 | 0.0175 | 0.0195 | 0.0269 | 0.0040 | 0.0099 | 0.0004 | 0.0028 | 0.0004 | 0.0004 | 0.0032 | 0.0022 |
| | 15% | 0.4164 | 0.5896 | | 0.0594 | 0.0370 | 0.0485 | 0.0766 | 0.0146 | 0.0328 | 0.0015 | 0.0107 | 0.0015 | 0.0012 | 0.0121 | 0.0088 |
| -20% | -15% | 0.2194 | 0.0217 | 0.0594 | | 0.9743 | 0.9294 | 0.9795 | 0.8085 | 0.8757 | 0.5385 | 0.8551 | 0.5218 | 0.5162 | 0.8350 | 0.8538 |
| | 0% | 0.0889 | 0.0175 | 0.0370 | 0.9743 | | 0.8985 | 0.9949 | 0.8740 | 0.9532 | 0.4926 | 0.8640 | 0.4892 | 0.4599 | 0.8663 | 0.8467 |
| | 15% | 0.1599 | 0.0195 | 0.0485 | 0.9294 | 0.8985 | | 0.9928 | 0.8616 | 0.9373 | 0.5313 | 0.8724 | 0.5219 | 0.5030 | 0.8660 | 0.8625 |
| 0% | -15% | 0.2903 | 0.0269 | 0.0766 | 0.9795 | 0.9949 | 0.9928 | | 0.6639 | 0.6440 | 0.4977 | 0.7904 | 0.4725 | 0.4828 | 0.7419 | 0.8039 |
| | 0% | 0.0891 | 0.0040 | 0.0146 | 0.8085 | 0.8740 | 0.8616 | 0.6639 | | 0.6904 | 0.8668 | 0.9630 | 0.8235 | 0.8739 | 0.8836 | 0.9791 |
| | 15% | 0.1628 | 0.0099 | 0.0328 | 0.8757 | 0.9532 | 0.9373 | 0.6440 | 0.6904 | | 0.7259 | 0.9103 | 0.6874 | 0.7228 | 0.8477 | 0.9305 |
| 20% | -15% | 0.0130 | 0.0004 | 0.0015 | 0.5385 | 0.4926 | 0.5313 | 0.4977 | 0.8668 | 0.7259 | | 0.8222 | 0.9496 | 0.9112 | 0.8625 | 0.7449 |
| | 0% | 0.0733 | 0.0028 | 0.0107 | 0.8551 | 0.8640 | 0.8724 | 0.7904 | 0.9630 | 0.9103 | 0.8222 | | 0.7037 | 0.8633 | 0.9097 | 0.8957 |
| | 15% | 0.0133 | 0.0004 | 0.0015 | 0.5218 | 0.4892 | 0.5219 | 0.4725 | 0.8235 | 0.6874 | 0.9496 | 0.7037 | | 0.9831 | 0.7961 | 0.5066 |
| 40% | -15% | 0.0110 | 0.0004 | 0.0012 | 0.5162 | 0.4599 | 0.5030 | 0.4828 | 0.8739 | 0.7228 | 0.9112 | 0.8633 | 0.9831 | | 0.8813 | 0.8320 |
| | 0% | 0.0791 | 0.0032 | 0.0121 | 0.8350 | 0.8663 | 0.8660 | 0.7419 | 0.8836 | 0.8477 | 0.8625 | 0.9097 | 0.7961 | 0.8813 | | 0.9672 |
| | 15% | 0.0635 | 0.0022 | 0.0088 | 0.8538 | 0.8467 | 0.8625 | 0.8039 | 0.9791 | 0.9305 | 0.7449 | 0.8957 | 0.5066 | 0.8320 | 0.9672 | |

## D.1.18 Sacral Endplate Full LAT Stiffness Map

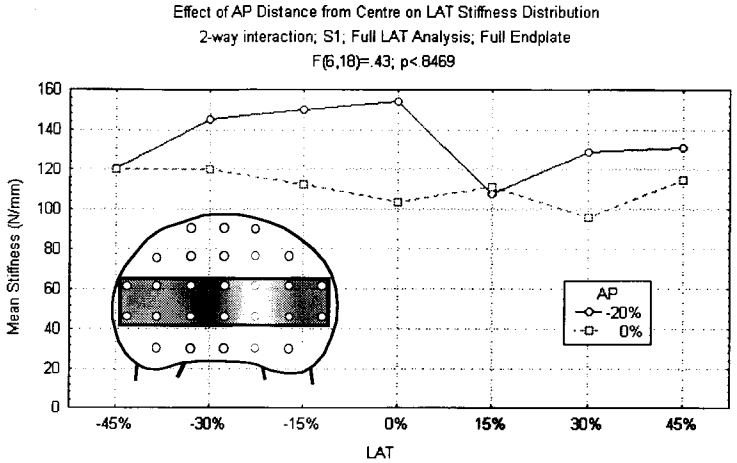


Figure D.18: Full LAT stiffness distribution in the sacral endplates. This plot shows the effect of the AP distance from the centre of the endplate on the LAT stiffness distribution using the largest complete LAT data set (inset figure). The p-value of < 0.8469 indicates that there are no significant differences between the LAT stiffness distributions at these two AP co-ordinates. A Newman-Keuls *post hoc* comparison showed that the apparent lateral variation in these curves is not significant (i.e. they should be interpreted as straight, horizontal lines).

Table D.18: Newman-Keuls *post hoc* comparison of the means in the sacral endplate Full LAT stiffness distribution (Figure D.18).

| | AP | -20% | | | | | | | 0% | | | | | | |
|---|---|---|---|---|---|---|---|---|---|---|---|---|---|---|---|
| | LAT | -45% | -30% | -15% | 0% | 15% | 30% | 45% | -45% | -30% | -15% | 0% | 15% | 30% | 45% |
| AP | LAT | **120.38** | **145.60** | **149.89** | **153.85** | **107.92** | **129.01** | **131.23** | **119.85** | **120.29** | **112.35** | **103.66** | **111.45** | **95.77** | **114.77** |
| -20% | -45% | | 0.8319 | 0.8565 | 0.8657 | 0.9995 | 0.7755 | 0.9299 | 0.9999 | 0.9979 | 0.9988 | 0.9990 | 0.9996 | 0.9944 | 0.9976 |
| | -30% | 0.8319 | | 0.8874 | 0.9589 | 0.9499 | 0.8446 | 0.6358 | 0.9505 | 0.9116 | 0.9450 | 0.9313 | 0.9584 | 0.8594 | 0.9390 |
| | -15% | 0.8565 | 0.8874 | | 0.8959 | 0.9310 | 0.8957 | 0.8081 | 0.9457 | 0.9144 | 0.9309 | 0.9060 | 0.9439 | 0.8195 | 0.9283 |
| | 0% | 0.8657 | 0.9589 | 0.8959 | | 0.9094 | 0.9168 | 0.8719 | 0.9387 | 0.9119 | 0.9147 | 0.8778 | 0.9269 | 0.7782 | 0.9154 |
| | 15% | 0.9995 | 0.9499 | 0.9310 | 0.9094 | | 0.9957 | 0.9961 | 0.9942 | 0.9982 | 0.9880 | 0.8881 | 0.9071 | 0.9130 | 0.9956 |
| | 30% | 0.7755 | 0.8446 | 0.8957 | 0.9168 | 0.9957 | | 0.9416 | 0.9897 | 0.9542 | 0.9926 | 0.9932 | 0.9964 | 0.9765 | 0.9885 |
| | 45% | 0.9299 | 0.6358 | 0.8081 | 0.8719 | 0.9961 | 0.9416 | | 0.9951 | 0.9826 | 0.9947 | 0.9933 | 0.9971 | 0.9758 | 0.9930 |
| 0% | -45% | 0.9999 | 0.9505 | 0.9457 | 0.9387 | 0.9942 | 0.9897 | 0.9951 | | 0.9885 | 0.9658 | 0.9935 | 0.9920 | 0.9811 | 0.8667 |
| | -30% | 0.9979 | 0.9116 | 0.9144 | 0.9119 | 0.9982 | 0.9542 | 0.9826 | 0.9885 | | 0.9932 | 0.9974 | 0.9982 | 0.9894 | 0.9814 |
| | -15% | 0.9988 | 0.9450 | 0.9309 | 0.9147 | 0.9880 | 0.9926 | 0.9947 | 0.9658 | 0.9932 | | 0.9912 | 0.9765 | 0.9798 | 0.9362 |
| | 0% | 0.9990 | 0.9313 | 0.9060 | 0.8778 | 0.8881 | 0.9932 | 0.9933 | 0.9935 | 0.9974 | 0.9912 | | 0.9632 | 0.7943 | 0.9956 |
| | 15% | 0.9996 | 0.9584 | 0.9439 | 0.9269 | 0.9071 | 0.9964 | 0.9971 | 0.9920 | 0.9982 | 0.9765 | 0.9632 | | 0.9517 | 0.9933 |
| | 30% | 0.9944 | 0.8594 | 0.8195 | 0.7782 | 0.9130 | 0.9765 | 0.9758 | 0.9811 | 0.9894 | 0.9798 | 0.7943 | 0.9517 | | 0.9865 |
| | 45% | 0.9976 | 0.9390 | 0.9283 | 0.9154 | 0.9956 | 0.9885 | 0.9930 | 0.8667 | 0.9814 | 0.9362 | 0.9956 | 0.9933 | 0.9865 | |

## D.2 "Between Map" Comparisons

### D.2.1 Superior and Inferior Lumbar Endplate Maximum AP, LAT Failure Load Maps

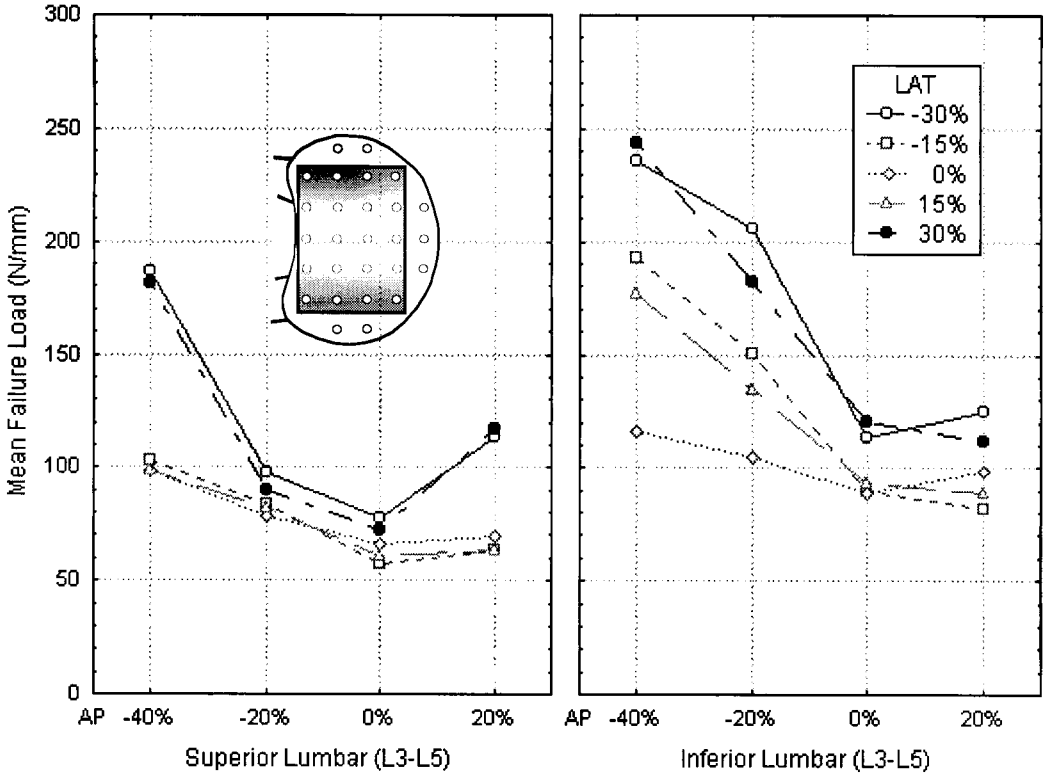


Figure D.19: Comparison of the superior and inferior lumbar endplate maximum AP, LAT failure load distributions. The p-value of $< 0.0001$ indicates that there are significant differences between the shapes of the superior and inferior lumbar endplate maps. These differences are mainly in the posterior half of the endplate. In both endplate groups the strongest test sites are located postero-laterally (+/- 40% AP, +/- 30% LAT), in front of the pedicles. The *post hoc* Newman-Keuls comparison of these graphs is given in Table D.19.

Table D.19: Newman-Keuls *post hoc* comparison of the means in the superior and inferior lumbar endplate maximum AP, LAT failure load distributions (Figure D.19). The "within endplate" comparisons for the superior and inferior lumbar endplate maximum AP, LAT failure load maps can be found in Tables D.1 and D.7, respectively.

| | inferior | AP | -40% | | | | | -20% | | | | |
|---|---|---|---|---|---|---|---|---|---|---|---|---|
| superior | | LAT | -30% | -15% | 0% | 15% | 30% | -30% | -15% | 0% | 15% | 30% |
| AP | LAT | Mean FL | **235.78** | **192.42** | **115.97** | **177.09** | **243.93** | **206.30** | **150.08** | **104.58** | **134.73** | **182.10** |
| -40% | -30% | **186.37** | 0.0000 | 0.5798 | 0.0000 | 0.8309 | 0.0000 | 0.1618 | 0.0080 | 0.0000 | 0.0001 | 0.6960 |
| | -15% | **103.12** | 0.0000 | 0.0000 | 0.8484 | 0.0000 | 0.0000 | 0.0000 | 0.0009 | 0.8936 | 0.1075 | 0.0000 |
| | 0% | **98.81** | 0.0000 | 0.0000 | 0.7016 | 0.0000 | 0.0000 | 0.0000 | 0.0002 | 0.8577 | 0.0405 | 0.0000 |
| | 15% | **98.49** | 0.0000 | 0.0000 | 0.7509 | 0.0000 | 0.0000 | 0.0000 | 0.0002 | 0.9447 | 0.0430 | 0.0000 |
| | 30% | **181.41** | 0.0000 | 0.7452 | 0.0000 | 0.6924 | 0.0000 | 0.1523 | 0.0116 | 0.0000 | 0.0001 | 0.9500 |
| -20% | -30% | **97.90** | 0.0000 | 0.0000 | 0.8216 | 0.0000 | 0.0000 | 0.0000 | 0.0002 | 0.9903 | 0.0475 | 0.0000 |
| | -15% | **83.49** | 0.0000 | 0.0000 | 0.1809 | 0.0000 | 0.0000 | 0.0000 | 0.0000 | 0.7409 | 0.0005 | 0.0000 |
| | 0% | **78.39** | 0.0000 | 0.0000 | 0.0642 | 0.0000 | 0.0000 | 0.0000 | 0.0000 | 0.5177 | 0.0001 | 0.0000 |
| | 15% | **81.83** | 0.0000 | 0.0000 | 0.1338 | 0.0000 | 0.0000 | 0.0000 | 0.0000 | 0.6771 | 0.0003 | 0.0000 |
| | 30% | **89.55** | 0.0000 | 0.0000 | 0.4313 | 0.0000 | 0.0000 | 0.0000 | 0.0000 | 0.9074 | 0.0042 | 0.0000 |
| 0% | -30% | **77.39** | 0.0000 | 0.0000 | 0.0523 | 0.0000 | 0.0000 | 0.0000 | 0.0000 | 0.4808 | 0.0001 | 0.0000 |
| | -15% | **57.18** | 0.0000 | 0.0000 | 0.0000 | 0.0000 | 0.0000 | 0.0000 | 0.0000 | 0.0032 | 0.0000 | 0.0000 |
| | 0% | **65.97** | 0.0000 | 0.0000 | 0.0011 | 0.0000 | 0.0000 | 0.0000 | 0.0000 | 0.0476 | 0.0000 | 0.0000 |
| | 15% | **60.30** | 0.0000 | 0.0000 | 0.0001 | 0.0000 | 0.0000 | 0.0000 | 0.0000 | 0.0094 | 0.0000 | 0.0000 |
| | 30% | **72.54** | 0.0000 | 0.0000 | 0.0118 | 0.0000 | 0.0000 | 0.0000 | 0.0000 | 0.2173 | 0.0000 | 0.0000 |
| 20% | -30% | **113.83** | 0.0000 | 0.0000 | 0.8445 | 0.0000 | 0.0000 | 0.0000 | 0.0159 | 0.8323 | 0.3942 | 0.0000 |
| | -15% | **63.59** | 0.0000 | 0.0000 | 0.0005 | 0.0000 | 0.0000 | 0.0000 | 0.0000 | 0.0247 | 0.0000 | 0.0000 |
| | 0% | **69.10** | 0.0000 | 0.0000 | 0.0036 | 0.0000 | 0.0000 | 0.0000 | 0.0000 | 0.1044 | 0.0000 | 0.0000 |
| | 15% | **63.40** | 0.0000 | 0.0000 | 0.0005 | 0.0000 | 0.0000 | 0.0000 | 0.0000 | 0.0253 | 0.0000 | 0.0000 |
| | 30% | **116.89** | 0.0000 | 0.0000 | 0.9330 | 0.0000 | 0.0000 | 0.0000 | 0.0202 | 0.8706 | 0.3602 | 0.0000 |

| | inferior | AP | 0% | | | | | 20% | | | | |
|---|---|---|---|---|---|---|---|---|---|---|---|---|
| superior | | LAT | -30% | -15% | 0% | 15% | 30% | -30% | -15% | 0% | 15% | 30% |
| AP | LAT | Mean FL | **113.74** | **89.95** | **88.75** | **93.62** | **120.80** | **124.64** | **81.65** | **98.48** | **88.46** | **111.73** |
| -40% | -30% | **186.37** | 0.0000 | 0.0000 | 0.0000 | 0.0000 | 0.0000 | 0.0000 | 0.0000 | 0.0000 | 0.0000 | 0.0000 |
| | -15% | **103.12** | 0.7653 | 0.8925 | 0.9273 | 0.9539 | 0.7398 | 0.5651 | **0.7565** | 0.9743 | 0.9442 | 0.7104 |
| | 0% | **98.81** | 0.6494 | 0.9656 | 0.9842 | 0.9896 | 0.5350 | 0.3482 | 0.9200 | 0.9995 | 0.9902 | 0.6382 |
| | 15% | **98.49** | 0.7298 | 0.9360 | 0.9740 | 0.9705 | 0.5697 | 0.3713 | 0.9062 | 0.9990 | 0.9845 | 0.7448 |
| | 30% | **181.41** | 0.0000 | 0.0000 | 0.0000 | 0.0000 | 0.0000 | 0.0000 | 0.0000 | 0.0000 | 0.0000 | 0.0000 |
| -20% | -30% | **97.90** | 0.8341 | 0.7468 | 0.9189 | 0.6952 | 0.6267 | 0.4111 | 0.8620 | 0.9582 | 0.9550 | 0.8679 |
| | -15% | **83.49** | 0.2409 | 0.9766 | 0.8804 | 0.9397 | 0.0635 | 0.0214 | 0.9845 | 0.8706 | 0.6494 | 0.3201 |
| | 0% | **78.39** | 0.0986 | 0.9654 | 0.9340 | 0.9007 | 0.0168 | 0.0045 | 0.7655 | 0.7576 | 0.8888 | 0.1483 |
| | 15% | **81.83** | 0.1866 | 0.9765 | 0.9213 | 0.9343 | 0.0426 | 0.0133 | 0.9873 | 0.8448 | 0.8162 | 0.2581 |
| | 30% | **89.55** | 0.4949 | 0.9711 | 0.9416 | 0.9263 | 0.2157 | 0.0959 | 0.9792 | 0.9256 | 0.9946 | 0.5780 |
| 0% | -30% | **77.39** | 0.0828 | 0.9666 | 0.9450 | 0.8984 | 0.0129 | 0.0033 | 0.9197 | 0.7409 | 0.9138 | 0.1276 |
| | -15% | **57.18** | 0.0001 | 0.1696 | 0.1826 | 0.0736 | 0.0000 | 0.0000 | 0.4299 | 0.0204 | 0.1744 | 0.0002 |
| | 0% | **65.97** | 0.0023 | 0.5545 | 0.5391 | 0.3546 | 0.0002 | 0.0000 | 0.7060 | 0.1637 | 0.5028 | 0.0046 |
| | 15% | **60.30** | 0.0003 | 0.2968 | 0.3081 | 0.1488 | 0.0000 | 0.0000 | 0.5760 | 0.0493 | 0.2927 | 0.0006 |
| | 30% | **72.54** | 0.0210 | 0.8523 | 0.8170 | 0.6984 | 0.0022 | 0.0005 | 0.8386 | 0.4634 | 0.7706 | 0.0363 |
| 20% | -30% | **113.83** | 0.9939 | 0.5155 | 0.5208 | 0.7038 | 0.9198 | 0.8603 | 0.2108 | 0.8556 | 0.5392 | 0.9799 |
| | -15% | **63.59** | 0.0010 | 0.4358 | 0.4326 | 0.2518 | 0.0001 | 0.0000 | 0.6481 | 0.1011 | 0.4051 | 0.0020 |
| | 0% | **69.10** | 0.0069 | 0.7125 | 0.6837 | 0.5173 | 0.0006 | 0.0001 | 0.7805 | 0.2855 | 0.6393 | 0.0129 |
| | 15% | **63.40** | 0.0010 | 0.4588 | 0.4625 | 0.2658 | 0.0001 | 0.0000 | 0.7068 | 0.1059 | 0.4384 | 0.0020 |
| | 30% | **116.89** | 0.9917 | 0.3978 | 0.3868 | 0.6017 | 0.7208 | 0.7582 | 0.1209 | 0.8044 | 0.3975 | 0.9898 |

## D.2.2 Superior and Inferior Lumbar Endplate Full AP Failure Load Maps

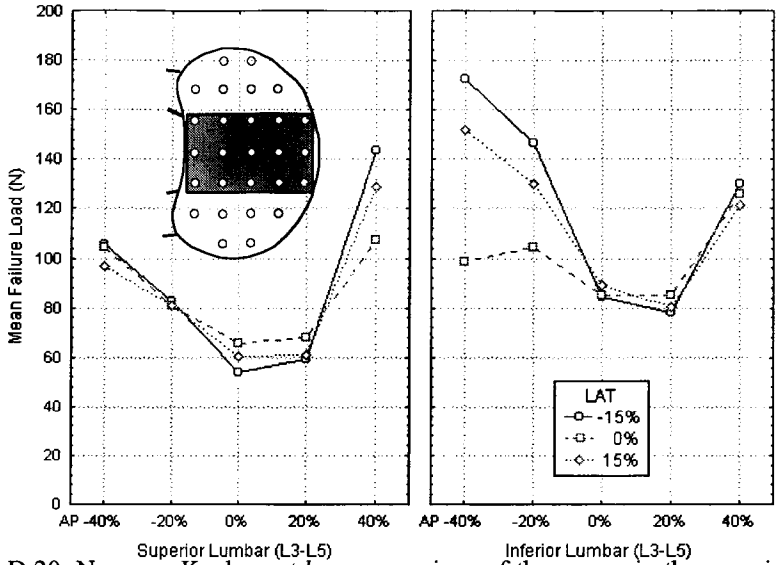


Figure D.20: Comparison of the superior and inferior lumbar endplate full AP failure load distributions. The p-value of < 0.0001 indicates that there are significant differences in the shapes of the maps. Note that the inferior lumbar endplates are stronger posteriorly than anteriorly, while the reverse is true in the superior endplates. The *post hoc* Newman-Keuls comparison of these graphs is given in Table D.20.

Table D.20: Newman-Keuls *post hoc* comparison of the means in the superior and inferior lumbar endplate full AP failure load distributions (Figure D.20). The "within endplate" comparisons for the superior and inferior lumbar endplate full AP failure load maps can be found in Tables D.2 and D.8, respectively.

| inferior | | AP | -40% | | | -20% | | | 0% | | | 20% | | | 40% | | |
|---|---|---|---|---|---|---|---|---|---|---|---|---|---|---|---|---|---|
| superior | | LAT | -15% | 0% | 15% | -15% | 0% | 15% | -15% | 0% | 15% | -15% | 0% | 15% | -15% | 0% | 15% |
| AP | LAT | Mean FL | **172.32** | **98.40** | **151.67** | **146.55** | **104.63** | **130.47** | **84.37** | **84.81** | **88.92** | **78.09** | **85.02** | **80.09** | **130.12** | **125.99** | **121.58** |
| -40% | -15% | **105.76** | 0.0000 | 0.8481 | 0.0000 | 0.0002 | 0.9008 | 0.0901 | 0.3034 | 0.2842 | 0.4257 | 0.1180 | 0.2472 | 0.1846 | 0.0762 | 0.1130 | 0.1868 |
| | 0% | **104.30** | 0.0000 | 0.5138 | 0.0000 | 0.0002 | 0.9714 | 0.0901 | 0.2929 | 0.2586 | 0.3228 | 0.1411 | 0.2063 | 0.2099 | 0.0819 | 0.1565 | 0.3116 |
| | 15% | **96.78** | 0.0000 | 0.8581 | 0.0000 | 0.0000 | 0.8215 | 0.0090 | 0.6453 | 0.5473 | 0.3844 | 0.5511 | 0.3948 | 0.6512 | 0.0086 | 0.0271 | 0.0880 |
| -20% | -15% | **82.60** | 0.0000 | 0.5836 | 0.0000 | 0.0000 | 0.2638 | 0.0000 | 0.8443 | 0.9675 | 0.9567 | 0.9876 | 0.9932 | 0.9926 | 0.0000 | 0.0001 | 0.0010 |
| | 0% | **80.80** | 0.0000 | 0.5809 | 0.0000 | 0.0000 | 0.2302 | 0.0000 | 0.9791 | 0.9920 | 0.9729 | 0.9519 | 0.9972 | 0.9379 | 0.0000 | 0.0001 | 0.0006 |
| | 15% | **80.92** | 0.0000 | 0.5276 | 0.0000 | 0.0000 | 0.2069 | 0.0000 | 0.9227 | 0.9733 | 0.9502 | 0.9895 | 0.9912 | 0.9954 | 0.0000 | 0.0001 | 0.0005 |
| 0% | -15% | **53.98** | 0.0000 | 0.0001 | 0.0000 | 0.0000 | 0.0000 | 0.0000 | 0.0372 | 0.0367 | 0.0096 | 0.1066 | 0.0387 | 0.0749 | 0.0000 | 0.0000 | 0.0000 |
| | 0% | **65.67** | 0.0000 | 0.0180 | 0.0000 | 0.0000 | 0.0016 | 0.0000 | 0.4353 | 0.4614 | 0.2636 | 0.3543 | 0.4982 | 0.3811 | 0.0000 | 0.0000 | 0.0000 |
| | 15% | **60.38** | 0.0000 | 0.0024 | 0.0000 | 0.0000 | 0.0002 | 0.0000 | 0.1929 | 0.1987 | 0.0799 | 0.2862 | 0.2134 | 0.2469 | 0.0000 | 0.0000 | 0.0000 |
| 20% | -15% | **59.37** | 0.0000 | 0.0017 | 0.0000 | 0.0000 | 0.0001 | 0.0000 | 0.1714 | 0.1739 | 0.0650 | 0.3024 | 0.1849 | 0.2476 | 0.0000 | 0.0000 | 0.0000 |
| | 0% | **68.11** | 0.0000 | 0.0387 | 0.0000 | 0.0000 | 0.0042 | 0.0000 | 0.5492 | 0.5880 | 0.3881 | 0.2696 | 0.6345 | 0.3813 | 0.0000 | 0.0000 | 0.0000 |
| | 15% | **61.10** | 0.0000 | 0.0030 | 0.0000 | 0.0000 | 0.0002 | 0.0000 | 0.1973 | 0.2068 | 0.0877 | 0.2366 | 0.2249 | 0.2195 | 0.0000 | 0.0000 | 0.0000 |
| 40% | -15% | **143.80** | 0.0087 | 0.0000 | 0.6592 | 0.7610 | 0.0005 | 0.1403 | 0.0000 | 0.0000 | 0.0000 | 0.0000 | 0.0000 | 0.0000 | 0.2849 | 0.2810 | 0.1368 |
| | 0% | **107.33** | 0.0000 | 0.8611 | 0.0000 | 0.0004 | 0.9521 | 0.1074 | 0.2477 | 0.2364 | 0.3917 | 0.0809 | 0.2098 | 0.1337 | 0.0859 | 0.0973 | 0.1150 |
| | 15% | **129.00** | 0.0001 | 0.0164 | 0.1220 | 0.2956 | 0.0760 | 0.9856 | 0.0001 | 0.0001 | 0.0004 | 0.0000 | 0.0001 | 0.0000 | 0.9013 | 0.7394 | 0.6898 |

### D.2.3 Superior and Inferior Lumbar Endplate Full LAT Failure Load Maps

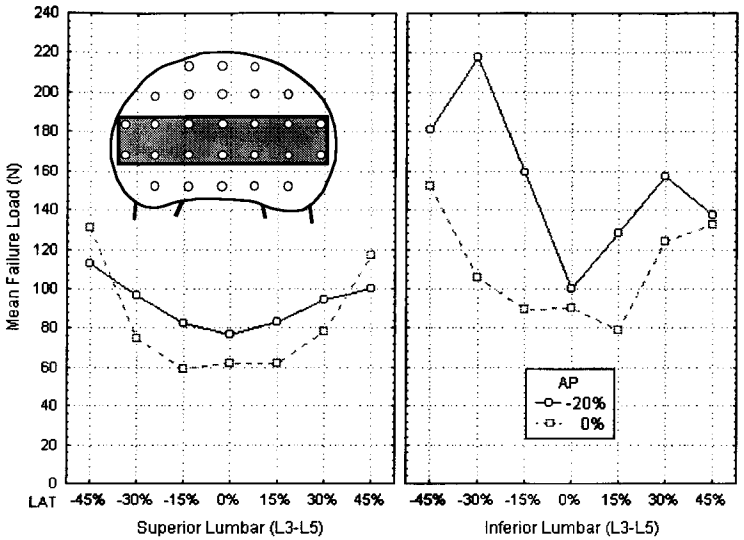


Figure D.21: Comparison of the superior and inferior endplate full LAT failure load distributions. The p-value of < 0.0271 indicates that there are significant differences between the shapes of the superior and inferior lumbar endplate maps. This difference is mainly due to the larger posterior failure loads in the inferior endplate map. The *post hoc* Newman-Keuls comparison of these graphs is given in Table D.21.

Table D.21: Newman-Keuls *post hoc* comparison of the means in the superior and inferior lumbar endplate full LAT failure load distributions (Figure D.21). The **"within** endplate" comparisons for the superior and inferior lumbar endplate full LAT failure load maps can be found in Tables D.3 and D.9, respectively.

| | inferior | AP | -20% | | | | | | | 0% | | | | | | |
|---|---|---|---|---|---|---|---|---|---|---|---|---|---|---|---|---|
| superior | | LAT | -45% | -30% | -15% | 0% | 15% | 30% | 45% | -45% | -30% | -15% | 0% | 15% | 30% | 45% |
| AP | LAT | Mean FL | **180.60** | **217.20** | **159.36** | **99.78** | **127.98** | **156.92** | **137.44** | **152.35** | **105.63** | **89.63** | **90.07** | **78.86** | **124.02** | **132.11** |
| -20% | -45% | **112.56** | 0.0003 | 0.0001 | 0.0281 | 0.6185 | 0.6724 | 0.0393 | 0.5363 | 0.0794 | 0.6126 | 0.7005 | 0.6523 | 0.3345 | 0.6797 | 0.7079 |
| | -30% | **96.20** | 0.0001 | 0.0001 | 0.0009 | 0.9631 | 0.2883 | 0.0015 | 0.1017 | 0.0042 | 0.9008 | 0.9631 | 0.8950 | 0.8641 | 0.3977 | 0.2165 |
| | -15% | **82.20** | 0.0002 | 0.0002 | 0.0002 | 0.9020 | 0.0548 | 0.0002 | 0.0090 | 0.0003 | 0.7360 | 0.8498 | 0.9391 | 0.8072 | 0.1047 | 0.0285 |
| | 0% | **77.06** | 0.0002 | 0.0002 | 0.0002 | 0.8507 | 0.0253 | 0.0002 | 0.0033 | 0.0002 | 0.6298 | 0.9407 | 0.9629 | 0.9906 | 0.0544 | 0.0116 |
| | 15% | **83.22** | 0.0002 | 0.0002 | 0.0002 | 0.8882 | 0.0592 | 0.0002 | 0.0103 | 0.0003 | 0.7248 | 0.6400 | 0.8708 | 0.9454 | 0.1103 | 0.0319 |
| | 30% | **94.41** | 0.0001 | 0.0002 | 0.0006 | 0.9794 | 0.2637 | 0.0011 | 0.0833 | 0.0031 | 0.9237 | 0.9348 | 0.7513 | 0.8641 | 0.3789 | 0.1872 |
| | 45% | **99.69** | 0.0001 | 0.0001 | 0.0020 | 0.9951 | 0.3765 | 0.0032 | 0.1616 | 0.0085 | 0.9013 | 0.9475 | 0.8952 | 0.7922 | 0.4817 | 0.3084 |
| 0% | -45% | **130.86** | 0.0074 | 0.0001 | 0.3012 | 0.2648 | 0.8338 | 0.3188 | 0.8799 | 0.3975 | 0.4398 | 0.1167 | 0.1105 | 0.0176 | 0.8711 | 0.9272 |
| | -30% | **74.95** | 0.0002 | 0.0002 | 0.0002 | 0.8046 | 0.0171 | 0.0002 | 0.0020 | 0.0002 | 0.5599 | 0.9341 | 0.9540 | 0.9918 | 0.0384 | 0.0075 |
| | -15% | **59.16** | 0.0002 | 0.0002 | 0.0002 | 0.1803 | 0.0005 | 0.0002 | 0.0002 | 0.0002 | 0.0669 | 0.4422 | 0.4660 | 0.7776 | 0.0010 | 0.0002 |
| | 0% | **61.60** | 0.0002 | 0.0002 | 0.0002 | 0.2420 | 0.0007 | 0.0002 | 0.0002 | 0.0002 | 0.0978 | 0.5107 | 0.5419 | 0.8039 | 0.0017 | 0.0003 |
| | 15% | **61.79** | 0.0002 | 0.0002 | 0.0002 | 0.2257 | 0.0007 | 0.0002 | 0.0002 | 0.0002 | 0.0911 | 0.4610 | 0.4983 | 0.7222 | 0.0016 | 0.0003 |
| | 30% | **77.82** | 0.0002 | 0.0002 | 0.0002 | 0.8417 | 0.0269 | 0.0002 | 0.0036 | 0.0002 | 0.6243 | 0.9091 | 0.9465 | 0.9394 | 0.0568 | 0.0127 |
| | 45% | **116.82** | 0.0005 | 0.0002 | 0.0570 | 0.5975 | 0.6933 | 0.0749 | 0.6588 | 0.1353 | 0.6914 | 0.5525 | 0.5138 | 0.2028 | 0.5995 | 0.7962 |

### D.2.4 Superior and Inferior Lumbar Endplate Maximum AP, LAT Stiffness Maps

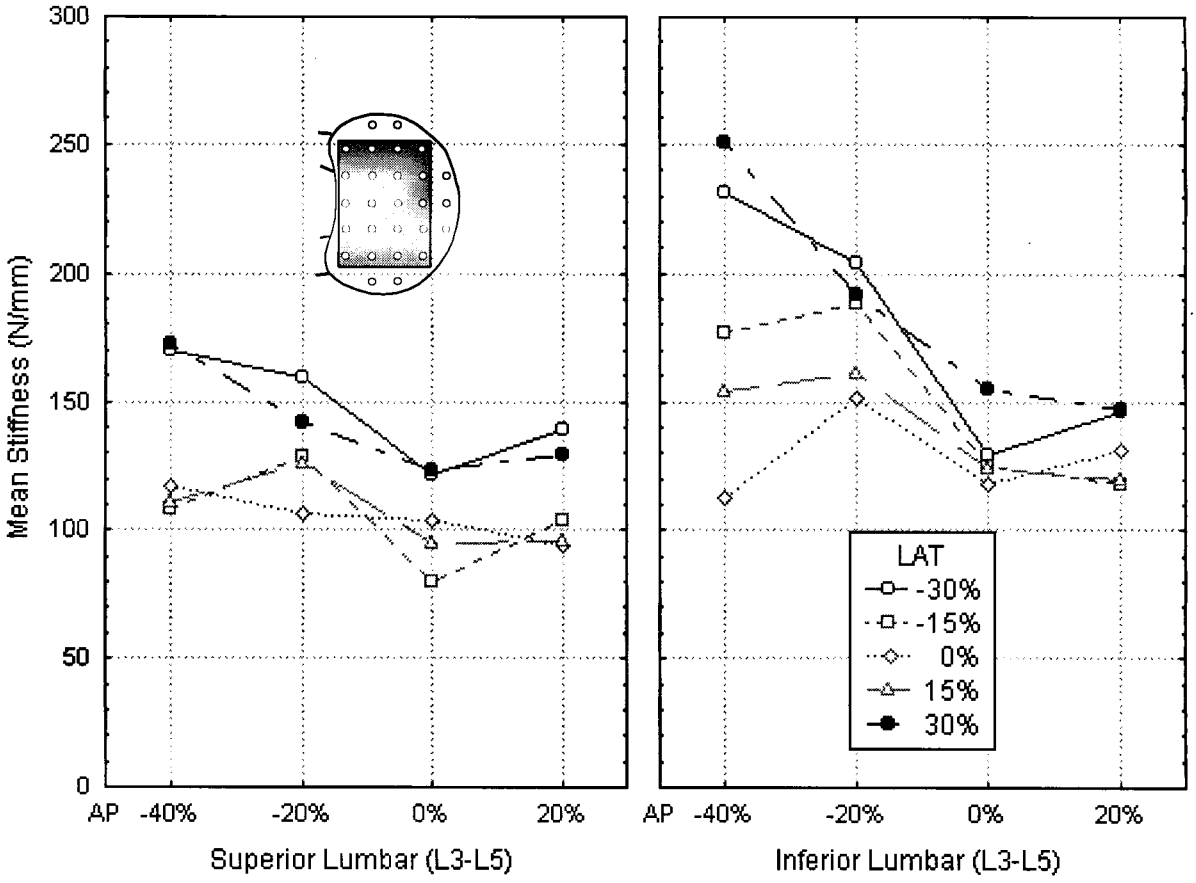


Figure D.22: Comparison of the superior and inferior lumbar endplate maximum AP, LAT stiffness distributions. The p-value of $< 0.0248$ indicates that there are significant differences between the shapes of the superior and inferior lumbar endplate stiffness maps. In both endplate groups the stiffest test sites are located postero-laterally (+/- 40% AP, +/- 30% LAT), in front of the pedicles. The *post hoc* Newman-Keuls comparison of these graphs is given in Table D.22.

Table D.22: Newman-Keuls *post hoc* comparison of the means in the superior and inferior lumbar endplate maximum AP, LAT stiffness distributions (Figure D.22). The "within endplate" comparisons for the superior and inferior lumbar endplate maximum AP, LAT stiffness maps can be found in Tables D.4 and D.10, respectively.

| inferior | | AP | -40% | | | | | -20% | | | | |
|---|---|---|---|---|---|---|---|---|---|---|---|---|
| superior | | LAT | -30% | -15% | 0% | 15% | 30% | -30% | -15% | 0% | 15% | 30% |
| AP | LAT | Mean ST | **231.30** | **177.27** | **112.80** | **154.26** | **250.51** | **203.98** | **188.06** | **150.90** | **161.09** | **191.57** |
| -40% | -30% | **170.05** | 0.0001 | 0.8548 | 0.0053 | 0.7700 | 0.0000 | 0.1215 | 0.5429 | 0.7174 | 0.5077 | 0.5032 |
| | -15% | **108.23** | 0.0000 | 0.0001 | 0.9388 | 0.0909 | 0.0000 | 0.0000 | 0.0000 | 0.1693 | 0.0207 | 0.0000 |
| | 0% | **117.00** | 0.0000 | 0.0022 | 0.7564 | 0.3653 | 0.0000 | 0.0000 | 0.0001 | 0.5255 | 0.1371 | 0.0000 |
| | 15% | **111.15** | 0.0000 | 0.0003 | 0.9025 | 0.1554 | 0.0000 | 0.0000 | 0.0000 | 0.2660 | 0.0415 | 0.0000 |
| | 30% | **172.39** | 0.0002 | 0.7182 | 0.0028 | 0.7625 | 0.0000 | 0.1336 | 0.4781 | 0.6897 | 0.6811 | 0.4879 |
| -20% | -30% | **159.36** | 0.0000 | 0.6764 | 0.0808 | 0.9245 | 0.0000 | 0.0218 | 0.2760 | 0.9238 | 0.8984 | 0.2065 |
| | -15% | **128.25** | 0.0000 | 0.0259 | 0.9881 | 0.6534 | 0.0000 | 0.0000 | 0.0012 | 0.7624 | 0.4239 | 0.0004 |
| | 0% | **106.31** | 0.0000 | 0.0001 | 0.9635 | 0.0629 | 0.0000 | 0.0000 | 0.0000 | 0.1237 | 0.0129 | 0.0000 |
| | 15% | **126.04** | 0.0000 | 0.0161 | 0.9935 | 0.5872 | 0.0000 | 0.0000 | 0.0007 | 0.7110 | 0.3458 | 0.0002 |
| | 30% | **141.84** | 0.0000 | 0.2385 | 0.7347 | 0.8900 | 0.0000 | 0.0004 | 0.0311 | 0.9085 | 0.8468 | 0.0147 |
| 0% | -30% | **121.04** | 0.0000 | 0.0057 | 0.9904 | 0.4728 | 0.0000 | 0.0000 | 0.0002 | 0.6242 | 0.2195 | 0.0001 |
| | -15% | **80.38** | 0.0000 | 0.0000 | 0.3272 | 0.0000 | 0.0000 | 0.0000 | 0.0000 | 0.0001 | 0.0000 | 0.0000 |
| | 0% | **103.47** | 0.0000 | 0.0000 | 0.9588 | 0.0335 | 0.0000 | 0.0000 | 0.0000 | 0.0712 | 0.0059 | 0.0000 |
| | 15% | **94.82** | 0.0000 | 0.0000 | 0.8879 | 0.0033 | 0.0000 | 0.0000 | 0.0000 | 0.0088 | 0.0004 | 0.0000 |
| | 30% | **123.42** | 0.0000 | 0.0104 | 0.9865 | 0.5700 | 0.0000 | 0.0000 | 0.0004 | 0.7121 | 0.3001 | 0.0001 |
| 20% | -30% | **138.93** | 0.0000 | 0.1655 | 0.8376 | 0.8675 | 0.0000 | 0.0002 | 0.0172 | 0.9026 | 0.7836 | 0.0076 |
| | -15% | **103.44** | 0.0000 | 0.0000 | 0.9828 | 0.0356 | 0.0000 | 0.0000 | 0.0000 | 0.0756 | 0.0063 | 0.0000 |
| | 0% | **94.19** | 0.0000 | 0.0000 | 0.9070 | 0.0029 | 0.0000 | 0.0000 | 0.0000 | 0.0078 | 0.0003 | 0.0000 |
| | 15% | **95.52** | 0.0000 | 0.0000 | 0.8622 | 0.0039 | 0.0000 | 0.0000 | 0.0000 | 0.0101 | 0.0005 | 0.0000 |
| | 30% | **129.68** | 0.0000 | 0.0292 | 0.9904 | 0.6081 | 0.0000 | 0.0000 | 0.0015 | 0.7023 | 0.4183 | 0.0005 |

| inferior | | AP | 0% | | | | | 20% | | | | |
|---|---|---|---|---|---|---|---|---|---|---|---|---|
| superior | | LAT | -30% | -15% | 0% | 15% | 30% | -30% | -15% | 0% | 15% | 30% |
| AP | LAT | Mean ST | **129.45** | **124.94** | **117.79** | **124.27** | **154.77** | **146.03** | **117.95** | **131.14** | **119.94** | **146.59** |
| -40% | -30% | **170.05** | 0.1224 | 0.0664 | 0.0194 | 0.0631 | 0.6713 | 0.6365 | 0.0186 | 0.1303 | 0.0290 | 0.5928 |
| | -15% | **108.23** | 0.9541 | 0.9785 | 0.9549 | 0.9746 | 0.0870 | 0.3378 | 0.9797 | 0.9490 | 0.9775 | 0.3307 |
| | 0% | **117.00** | 0.9979 | 0.9990 | 0.9532 | 0.9983 | 0.3606 | 0.7350 | 0.9973 | 0.9981 | 0.9964 | 0.7355 |
| | 15% | **111.15** | 0.9807 | 0.9912 | 0.9611 | 0.9885 | 0.1504 | 0.4695 | 0.9871 | 0.9794 | 0.9871 | 0.4639 |
| | 30% | **172.39** | 0.0856 | 0.0426 | 0.0109 | 0.0400 | 0.6899 | 0.5795 | 0.0105 | 0.0946 | 0.0169 | 0.5460 |
| -20% | -30% | **159.36** | 0.4963 | 0.3766 | 0.1939 | 0.3735 | 0.7345 | 0.9226 | 0.1856 | 0.4823 | 0.2441 | 0.8796 |
| | -15% | **128.25** | 0.9294 | 0.9675 | 0.9976 | 0.9912 | 0.6763 | 0.8455 | 0.9950 | 0.9966 | 0.9964 | 0.8770 |
| | 0% | **106.31** | 0.9303 | 0.9680 | 0.9582 | 0.9641 | 0.0597 | 0.2673 | 0.9782 | 0.9203 | 0.9735 | 0.2596 |
| | 15% | **126.04** | 0.9656 | 0.9351 | 0.9988 | 0.9906 | 0.6051 | 0.8195 | 0.9969 | 0.9957 | 0.9977 | 0.8468 |
| | 30% | **141.84** | 0.8909 | 0.9169 | 0.8865 | 0.9321 | 0.9315 | 0.7567 | 0.8666 | 0.7084 | 0.9025 | 0.9342 |
| 0% | -30% | **121.04** | 0.9962 | 0.9917 | 0.9951 | 0.9691 | 0.4761 | 0.7916 | 0.9716 | 0.9981 | 0.9350 | 0.8023 |
| | -15% | **80.38** | 0.0411 | 0.0909 | 0.1946 | 0.0957 | 0.0000 | 0.0004 | 0.2124 | 0.0313 | 0.1669 | 0.0003 |
| | 0% | **103.47** | 0.8670 | 0.9344 | 0.9400 | 0.9303 | 0.0314 | 0.1731 | 0.9629 | 0.8472 | 0.9530 | 0.1662 |
| | 15% | **94.82** | 0.5108 | 0.6785 | 0.7969 | 0.6815 | 0.0030 | 0.0300 | 0.8309 | 0.4629 | 0.7860 | 0.0278 |
| | 30% | **123.42** | 0.9978 | 0.9931 | 0.9937 | 0.9498 | 0.5769 | 0.8504 | 0.9777 | 0.9992 | 0.9641 | 0.8627 |
| 20% | -30% | **138.93** | 0.8968 | 0.9462 | 0.9412 | 0.9604 | 0.9049 | 0.8591 | 0.9262 | 0.5646 | 0.9478 | 0.9420 |
| | -15% | **103.44** | 0.8861 | 0.9492 | 0.9646 | 0.9470 | 0.0333 | 0.1837 | 0.9781 | 0.8654 | 0.9694 | 0.1760 |
| | 0% | **94.19** | 0.4997 | 0.6746 | 0.8120 | 0.6800 | 0.0026 | 0.0272 | 0.8413 | 0.4488 | 0.7936 | 0.0251 |
| | 15% | **95.52** | 0.5235 | 0.6830 | 0.7786 | 0.6833 | [illegible] | [illegible] | 0.8187 | 0.4789 | 0.7772 | [illegible] |
| | 30% | **129.68** | 0.9865 | 0.9968 | 0.9986 | 0.9987 | 0.6446 | 0.7462 | 0.9974 | 0.9141 | 0.9985 | 0.8117 |

### D.2.5 Superior and Inferior Lumbar Endplate Full AP Stiffness Maps

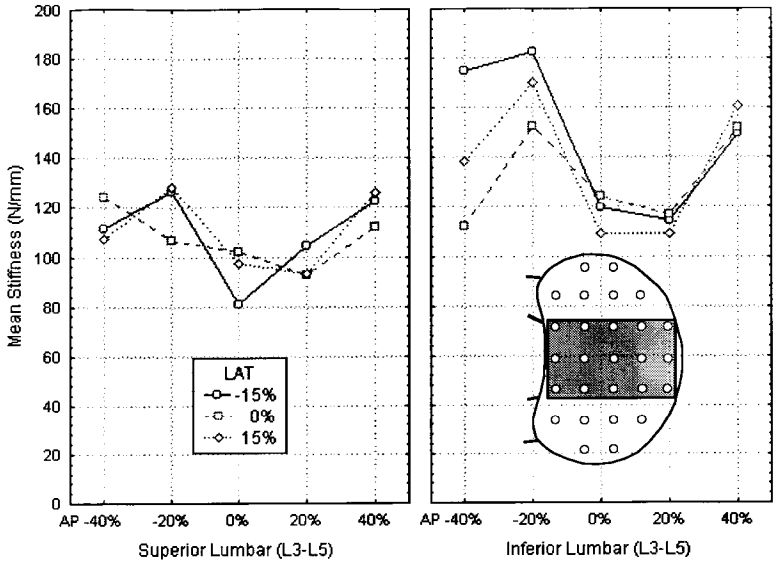


Figure D.23: Comparison of the superior and inferior lumbar endplate full AP stiffness distributions. The p-value of < 0.0068 indicates that there are significant differences in the shapes of the superior and inferior lumbar endplate stiffness maps. The *post hoc* Newman-Keuls comparison of these graphs is given in Table D.23.

Table D.23: Newman-Keuls *post hoc* comparison of the means in the superior and inferior lumbar endplate maximum full AP stiffness distributions (Figure D.23). The "within endplate" comparisons for the superior and inferior lumbar endplate maximum AP, LAT stiffness maps can be found in Tables D.5 and D.11, respectively.

| inferior | | AP | -40% | | | -20% | | | 0% | | | 20% | | | 40% | | |
|---|---|---|---|---|---|---|---|---|---|---|---|---|---|---|---|---|---|
| superior | | LAT | -15% | 0% | 15% | -15% | 0% | 15% | -15% | 0% | 15% | -15% | 0% | 15% | -15% | 0% | 15% |
| AP | LAT | Mean ST | **174.58** | **111.86** | **138.25** | **182.65** | **152.75** | **170.13** | **119.88** | **124.26** | **108.83** | **114.27** | **116.93** | **108.86** | **149.74** | **152.08** | **160.49** |
| -40% | -15% | **111.68** | 0.0000 | 0.9877 | 0.5256 | 0.0000 | 0.0349 | 0.0001 | 0.9813 | 0.9605 | 0.9673 | 0.9961 | 0.9914 | 0.8078 | 0.0632 | 0.0377 | 0.0031 |
| | 0% | **124.45** | 0.0008 | 0.9603 | 0.7580 | 0.0000 | 0.2236 | 0.0033 | 0.9794 | 0.9867 | 0.9608 | 0.9521 | 0.9671 | 0.9437 | 0.2480 | 0.2073 | 0.0497 |
| | 15% | **107.07** | 0.0000 | 0.9939 | 0.3399 | 0.0000 | 0.0114 | 0.0001 | 0.9739 | 0.9267 | 0.8797 | 0.9962 | 0.9902 | 0.9871 | 0.0241 | 0.0129 | 0.0008 |
| -20% | -15% | **126.47** | 0.0012 | 0.9627 | 0.5673 | 0.0001 | 0.2093 | 0.0042 | 0.9931 | 0.9976 | 0.9523 | 0.9666 | 0.9829 | 0.9365 | 0.1862 | 0.1775 | 0.0527 |
| | 0% | **106.60** | 0.0000 | 0.9976 | 0.3382 | 0.0000 | 0.0107 | 0.0000 | 0.9801 | 0.9353 | 0.9799 | 0.9979 | 0.9936 | 0.9974 | 0.0232 | 0.0122 | 0.0007 |
| | 15% | **128.74** | 0.0020 | 0.9347 | 0.4126 | 0.0002 | 0.2343 | 0.0067 | 0.9884 | 0.9953 | 0.9114 | 0.9462 | 0.9721 | 0.8903 | 0.1666 | 0.1842 | 0.0686 |
| 0% | -15% | **81.07** | 0.0000 | 0.2511 | 0.0002 | 0.0000 | 0.0000 | 0.0000 | 0.0650 | 0.0229 | 0.2892 | 0.1958 | 0.1217 | 0.3301 | 0.0000 | 0.0000 | 0.0000 |
| | 0% | **102.18** | 0.0000 | 0.9912 | 0.1656 | 0.0000 | 0.0027 | 0.0000 | 0.9341 | 0.8263 | 0.9790 | 0.9897 | 0.9738 | 0.9927 | 0.0066 | 0.0031 | 0.0001 |
| | 15% | **97.58** | 0.0000 | 0.9500 | 0.0571 | 0.0000 | 0.0005 | 0.0000 | 0.7833 | 0.5923 | 0.9278 | 0.9391 | 0.8834 | 0.9601 | 0.0013 | 0.0006 | 0.0000 |
| 20% | -15% | **104.47** | 0.0000 | 0.9956 | 0.2470 | 0.0000 | 0.0056 | 0.0000 | 0.9642 | 0.8935 | 0.9819 | 0.9955 | 0.9873 | 0.9957 | 0.0130 | 0.0065 | 0.0003 |
| | 0% | **92.74** | 0.0000 | 0.8623 | 0.0158 | 0.0000 | 0.0001 | 0.0000 | 0.5623 | 0.3461 | 0.8643 | 0.8221 | 0.7136 | 0.9029 | 0.0003 | 0.0001 | 0.0000 |
| | 15% | **93.20** | 0.0000 | 0.8453 | 0.0168 | 0.0000 | 0.0001 | 0.0000 | 0.5567 | 0.3472 | 0.8303 | 0.8106 | 0.7041 | 0.8803 | 0.0003 | 0.0001 | 0.0000 |
| 40% | -15% | **122.40** | 0.0005 | 0.9447 | 0.8204 | 0.0000 | 0.2112 | 0.0023 | 0.8285 | 0.8729 | 0.9630 | 0.8971 | 0.8849 | 0.9415 | 0.2640 | 0.2056 | 0.0413 |
| | 0% | **111.86** | 0.0000 | 0.9998 | 0.4529 | 0.0000 | 0.0290 | 0.0001 | 0.9007 | 0.8944 | 0.9990 | 0.8359 | 0.9005 | 0.9939 | 0.0509 | 0.0308 | 0.0026 |
| | 15% | **126.35** | 0.0014 | 0.9458 | 0.7347 | 0.0001 | 0.2571 | 0.0051 | 0.9811 | 0.9823 | 0.9386 | 0.9447 | 0.9656 | 0.9182 | 0.2589 | 0.2304 | 0.0648 |

### D.2.6 Superior and Inferior Lumbar Endplate Full LAT Stiffness Maps

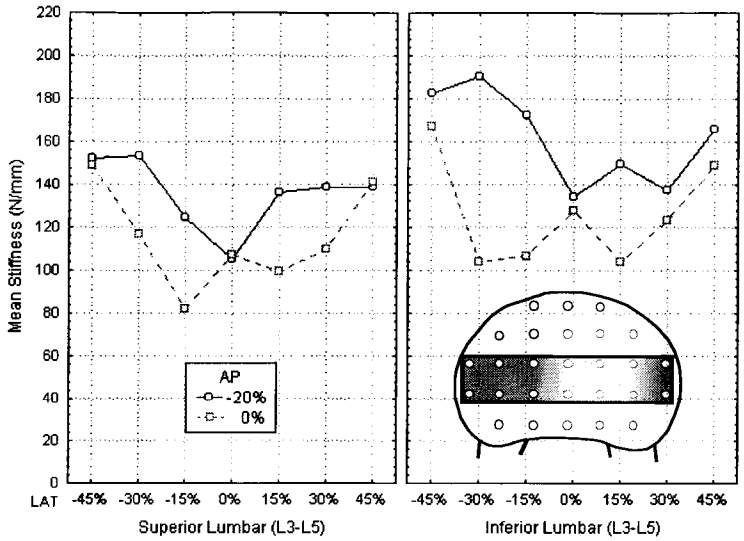


Figure D.24: Figure 3.13: Comparison of the superior and inferior lumbar endplate full LAT stiffness distributions. The p-value of < 0.7113 indicates that there are no significant differences in the shapes of the superior and inferior lumbar endplate stiffness maps. The *post hoc* Newman-Keuls comparison of these graphs is given in Table D.24.

Table D.24: Newman-Keuls *post hoc* comparison of the means in the superior and inferior lumbar endplate maximum full LAT stiffness distributions (Figure D.24). The "within endplate" comparisons for the superior and inferior lumbar endplate maximum AP, LAT stiffness maps can be found in Tables D.6 and D.12, respectively.

| | inferior | AP | -20% | | | | | | | 0% | | | | | | |
|---|---|---|---|---|---|---|---|---|---|---|---|---|---|---|---|---|
| superior | | LAT | -45% | -30% | -15% | 0% | 15% | 30% | 45% | -45% | -30% | -15% | 0% | 15% | 30% | 45% |
| AP | LAT | Mean ST | **182.90** | **190.33** | **172.02** | **134.19** | **149.73** | **137.65** | **165.90** | **166.94** | **104.06** | **106.41** | **127.93** | **103.94** | **122.93** | **148.95** |
| -20% | -45% | **152.13** | 0.4841 | 0.3000 | 0.7799 | 0.9894 | 0.8903 | 0.9906 | 0.7067 | 0.8275 | 0.3638 | 0.4078 | 0.9465 | 0.3804 | 0.8958 | 0.9978 |
| | -30% | **153.66** | 0.4447 | 0.2853 | 0.7141 | 0.9885 | 0.9721 | 0.9911 | 0.4812 | 0.7238 | 0.3275 | 0.3728 | 0.9413 | 0.3420 | 0.8823 | 0.9988 |
| | -15% | **124.27** | 0.0769 | 0.0235 | 0.3083 | 0.8349 | 0.9263 | 0.9381 | 0.4835 | 0.4734 | 0.9393 | 0.9063 | 0.8333 | 0.9602 | 0.9382 | 0.8858 |
| | 0% | **105.35** | 0.0037 | 0.0009 | 0.0296 | 0.7657 | 0.4617 | 0.7379 | 0.0731 | 0.0665 | 0.9404 | 0.9514 | 0.8956 | 0.9964 | 0.9120 | 0.4361 |
| | 15% | **135.96** | 0.2861 | 0.1208 | 0.6751 | 0.9188 | 0.9931 | 0.9227 | 0.8171 | 0.8199 | 0.7517 | 0.7410 | 0.8883 | 0.7865 | 0.9434 | 0.9750 |
| | 30% | **138.64** | 0.3166 | 0.1424 | 0.6974 | 0.9941 | 0.9877 | 0.9543 | 0.8165 | 0.8280 | 0.7318 | 0.7402 | 0.9719 | 0.7613 | 0.9707 | 0.9333 |
| | 45% | **138.95** | 0.2937 | 0.1319 | 0.6620 | 0.9988 | 0.9712 | 0.9969 | 0.7747 | 0.7935 | 0.7543 | 0.7689 | 0.9880 | 0.7804 | 0.9830 | 0.8325 |
| 0% | -45% | **149.27** | 0.5246 | 0.3092 | 0.8439 | 0.9881 | 0.9786 | 0.9848 | 0.8721 | 0.9100 | 0.4279 | 0.4659 | 0.9475 | 0.4489 | 0.9096 | 0.9854 |
| | -30% | **117.08** | 0.0270 | 0.0070 | 0.1456 | 0.8600 | 0.7995 | 0.8972 | 0.2730 | 0.2607 | 0.9748 | 0.9268 | 0.9233 | 0.9883 | 0.7360 | 0.7529 |
| | -15% | **81.97** | 0.0002 | 0.0002 | 0.0004 | 0.1323 | 0.0223 | 0.0996 | 0.0011 | 0.0009 | 0.5800 | 0.7195 | 0.2625 | 0.4155 | 0.3558 | 0.0218 |
| | 0% | **107.00** | 0.0044 | 0.0010 | 0.0340 | 0.7009 | 0.4707 | 0.7011 | 0.0805 | 0.0742 | 0.9983 | 0.9732 | 0.8316 | 0.9998 | 0.7940 | 0.4355 |
| | 15% | **99.44** | 0.0013 | 0.0004 | 0.0119 | 0.6875 | 0.3034 | 0.6252 | 0.0332 | 0.0295 | 0.9617 | 0.9944 | 0.8589 | 0.7957 | 0.9113 | 0.2921 |
| | 30% | **109.48** | 0.0068 | 0.0016 | 0.0482 | 0.7102 | 0.5399 | 0.7329 | 0.1080 | 0.1006 | 0.9979 | 0.9829 | 0.8236 | 0.9996 | 0.7179 | 0.4965 |
| | 45% | **140.98** | 0.3231 | 0.1527 | 0.6865 | 0.9988 | 0.9577 | 0.9975 | 0.7793 | 0.8060 | 0.7099 | 0.7324 | 0.9887 | 0.7353 | 0.9807 | 0.6464 |

### D.2.7 Superior Lumbar and Sacral Endplate Maximum AP, LAT Failure Load Maps

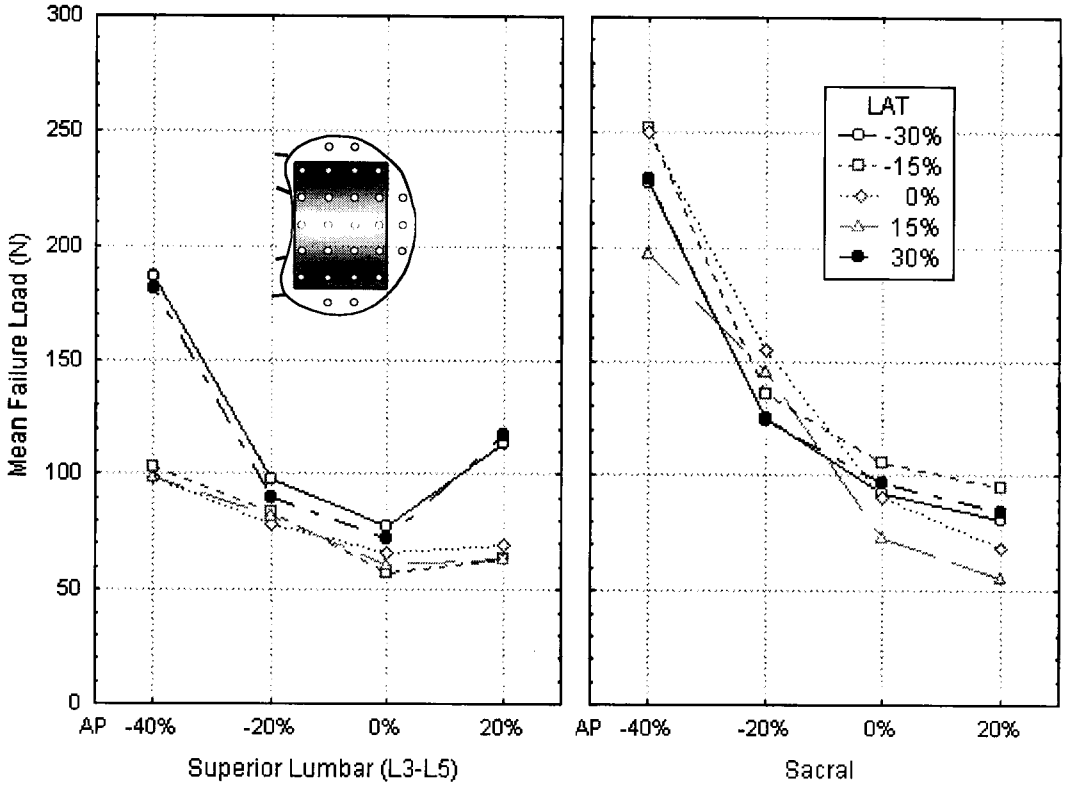


Figure D.25: Comparison of the superior lumbar and sacral endplate maximum AP, LAT failure load distributions. The p-value of $< 0.0077$ indicates that there are significant shape differences between the two failure load maps. The *post hoc* Newman Keuls results for this comparison are given in Table D.25.

Table D.25: Newman-Keuls *post hoc* comparison of the means in the superior lumbar and sacral endplate maximum AP, LAT failure load distributions (Figure D.25). The "within endplate" comparisons for the superior lumbar and sacral endplate maximum AP, LAT failure load maps can be found in Tables D.1 and D.13, respectively.

| sacrum | | AP | -40% | | | | | -20% | | | | |
|---|---|---|---|---|---|---|---|---|---|---|---|---|
| superior L | | LAT | -30% | -15% | 0% | 15% | 30% | -30% | -15% | 0% | 15% | 30% |
| AP | LAT | Mean FL | **227.71** | **251.24** | **249.50** | **196.82** | **229.36** | **125.24** | **135.81** | **154.76** | **145.53** | **123.98** |
| -40% | -30% | **186.37** | 0.0115 | 0.0001 | 0.0001 | 0.4684 | 0.0152 | 0.0003 | 0.0042 | 0.0725 | 0.0239 | 0.0003 |
| | -15% | **103.12** | 0.0000 | 0.0000 | 0.0000 | 0.0000 | 0.0000 | 0.6419 | 0.2600 | 0.0103 | 0.0646 | 0.5973 |
| | 0% | **98.81** | 0.0000 | 0.0000 | 0.0000 | 0.0000 | 0.0000 | 0.5254 | 0.1684 | 0.0041 | 0.0327 | 0.5016 |
| | 15% | **98.49** | 0.0000 | 0.0000 | 0.0000 | 0.0000 | 0.0000 | 0.5819 | 0.1914 | 0.0046 | 0.0369 | 0.5701 |
| | 30% | **181.41** | 0.0072 | 0.0001 | 0.0001 | 0.5335 | 0.0079 | 0.0009 | 0.0085 | 0.0645 | 0.0343 | 0.0010 |
| -20% | -30% | **97.90** | 0.0000 | 0.0000 | 0.0000 | 0.0000 | 0.0000 | 0.6165 | 0.2040 | 0.0046 | 0.0384 | 0.6144 |
| | -15% | **83.49** | 0.0000 | 0.0000 | 0.0000 | 0.0000 | 0.0000 | 0.2170 | 0.0284 | 0.0002 | 0.0023 | 0.2423 |
| | 0% | **78.39** | 0.0000 | 0.0000 | 0.0000 | 0.0000 | 0.0000 | 0.1127 | 0.0104 | 0.0000 | 0.0006 | 0.1321 |
| | 15% | **81.83** | 0.0000 | 0.0000 | 0.0000 | 0.0000 | 0.0000 | 0.1791 | 0.0209 | 0.0001 | 0.0015 | 0.2032 |
| | 30% | **89.55** | 0.0000 | 0.0000 | 0.0000 | 0.0000 | 0.0000 | 0.4252 | 0.0869 | 0.0008 | 0.0101 | 0.4526 |
| 0% | -30% | **77.39** | 0.0000 | 0.0000 | 0.0000 | 0.0000 | 0.0000 | 0.1001 | 0.0087 | 0.0000 | 0.0005 | 0.1186 |
| | -15% | **57.18** | 0.0000 | 0.0000 | 0.0000 | 0.0000 | 0.0000 | 0.0009 | 0.0000 | 0.0000 | 0.0000 | 0.0012 |
| | 0% | **65.97** | 0.0000 | 0.0000 | 0.0000 | 0.0000 | 0.0000 | 0.0095 | 0.0004 | 0.0000 | 0.0000 | 0.0124 |
| | 15% | **60.30** | 0.0000 | 0.0000 | 0.0000 | 0.0000 | 0.0000 | 0.0022 | 0.0001 | 0.0000 | 0.0000 | 0.0030 |
| | 30% | **72.54** | 0.0000 | 0.0000 | 0.0000 | 0.0000 | 0.0000 | 0.0406 | 0.0025 | 0.0000 | 0.0001 | 0.0503 |
| 20% | -30% | **113.83** | 0.0000 | 0.0000 | 0.0000 | 0.0000 | 0.0000 | 0.8583 | 0.5465 | 0.0680 | 0.2382 | 0.7612 |
| | -15% | **63.59** | 0.0000 | 0.0000 | 0.0000 | 0.0000 | 0.0000 | 0.0052 | 0.0002 | 0.0000 | 0.0000 | 0.0069 |
| | 0% | **69.10** | 0.0000 | 0.0000 | 0.0000 | 0.0000 | 0.0000 | 0.0187 | 0.0009 | 0.0000 | 0.0000 | 0.0239 |
| | 15% | **63.40** | 0.0000 | 0.0000 | 0.0000 | 0.0000 | 0.0000 | 0.0052 | 0.0002 | 0.0000 | 0.0000 | 0.0070 |
| | 30% | **116.89** | 0.0000 | 0.0000 | 0.0000 | 0.0000 | 0.0000 | 0.8313 | 0.5552 | 0.0909 | 0.2726 | 0.6232 |

| sacrum | | AP | 0% | | | | | 20% | | | | |
|---|---|---|---|---|---|---|---|---|---|---|---|---|
| superior L | | LAT | -30% | -15% | 0% | 15% | 30% | -30% | -15% | 0% | 15% | 30% |
| AP | LAT | Mean FL | **92.61** | **105.36** | **90.50** | **72.87** | **96.50** | **81.24** | **94.94** | **68.45** | **55.36** | **84.52** |
| -40% | -30% | **186.37** | 0.0000 | 0.0000 | 0.0000 | 0.0000 | 0.0000 | 0.0000 | 0.0000 | 0.0000 | 0.0000 | 0.0000 |
| | -15% | **103.12** | 0.9909 | 0.8767 | 0.9883 | 0.7666 | 0.9909 | 0.9525 | 0.9931 | 0.6322 | 0.1435 | 0.9562 |
| | 0% | **98.81** | 0.9981 | 0.8927 | 0.9975 | 0.8989 | 0.9985 | 0.9876 | 0.9989 | 0.8134 | 0.2851 | 0.9868 |
| | 15% | **98.49** | 0.9942 | 0.9644 | 0.9938 | 0.8866 | 0.9896 | 0.9830 | 0.9948 | 0.8026 | 0.2836 | 0.9788 |
| | 30% | **181.41** | 0.0000 | 0.0000 | 0.0000 | 0.0000 | 0.0000 | 0.0000 | 0.0000 | 0.0000 | 0.0000 | 0.0000 |
| -20% | -30% | **97.90** | 0.9831 | 0.9857 | 0.9861 | 0.8798 | 0.9226 | 0.9787 | 0.9770 | 0.8011 | 0.2929 | 0.9682 |
| | -15% | **83.49** | 0.9699 | 0.9365 | 0.9622 | 0.9773 | 0.9723 | 0.9866 | 0.9686 | 0.9816 | 0.8267 | 0.9430 |
| | 0% | **78.39** | 0.9765 | 0.8682 | 0.9807 | 0.9222 | 0.9630 | 0.8435 | 0.9668 | 0.9832 | 0.9104 | 0.9932 |
| | 15% | **81.83** | 0.9758 | 0.9202 | 0.9748 | 0.9717 | 0.9719 | 0.9675 | 0.9712 | 0.9835 | 0.8600 | 0.9809 |
| | 30% | **89.55** | 0.9755 | 0.9852 | 0.9473 | 0.9438 | 0.9890 | 0.9785 | 0.9822 | 0.9317 | 0.6005 | 0.7274 |
| 0% | -30% | **77.39** | 0.9802 | 0.8576 | 0.9853 | 0.7536 | 0.9646 | 0.9615 | 0.9698 | 0.9719 | 0.9107 | 0.9964 |
| | -15% | **57.18** | 0.5636 | 0.1326 | 0.6465 | 0.9761 | 0.4077 | 0.8827 | 0.4652 | 0.9707 | 0.8992 | 0.8556 |
| | 0% | **65.97** | 0.8544 | 0.4270 | 0.8947 | 0.9894 | 0.7541 | 0.9651 | 0.7934 | 0.8636 | 0.9774 | 0.9713 |
| | 15% | **60.30** | 0.6979 | 0.2201 | 0.7687 | 0.9885 | 0.5489 | 0.9349 | 0.6058 | 0.9800 | 0.9373 | 0.9232 |
| | 30% | **72.54** | 0.9507 | 0.7012 | 0.9649 | 0.9822 | 0.9098 | 0.9747 | 0.9254 | 0.9566 | 0.9584 | 0.9914 |
| 20% | -30% | **113.83** | 0.8689 | 0.5567 | 0.8398 | 0.2868 | 0.8938 | 0.6203 | 0.8954 | 0.1725 | 0.0135 | 0.6710 |
| | -15% | **63.59** | 0.7913 | 0.3285 | 0.8448 | 0.9877 | 0.6677 | 0.9515 | 0.7156 | 0.9393 | 0.9793 | 0.9531 |
| | 0% | **69.10** | 0.8980 | 0.5460 | 0.9252 | 0.9631 | 0.8265 | 0.9596 | 0.8540 | 0.9643 | 0.9807 | 0.9785 |
| | 15% | **63.40** | 0.8109 | 0.3373 | 0.8635 | 0.9948 | 0.6864 | 0.9664 | 0.7355 | 0.9852 | 0.9445 | 0.9636 |
| | 30% | **116.89** | 0.8048 | 0.7029 | 0.7622 | 0.1893 | 0.8511 | 0.4919 | 0.8453 | 0.1033 | 0.0061 | 0.5578 |

### D.2.8 Superior Lumbar and Sacral Endplate Full AP Failure Load Maps

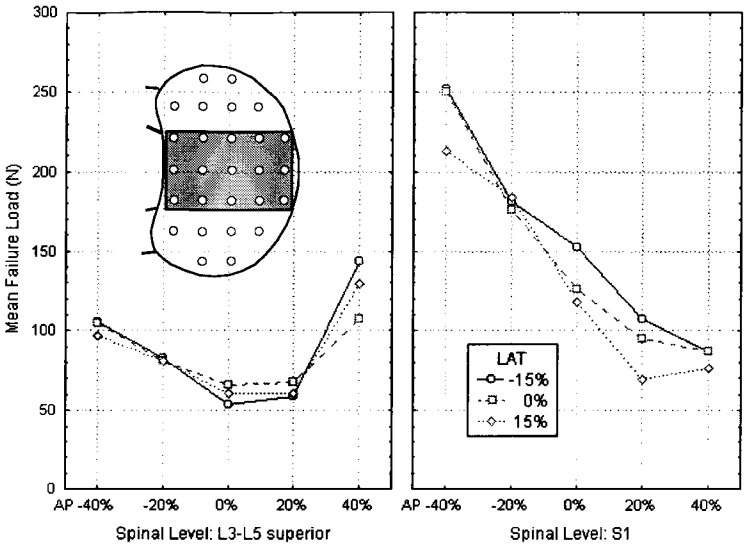


Figure D.26: Comparison of the LAT, full AP failure load distribution in the superior lumbar and sacral endplates. The p-value of < 0.0482 indicates that there are significant shape differences between these two failure load maps.

Table D.26: Newman-Keuls *post hoc* comparison of the means in the superior lumbar and sacral endplate full AP failure load distributions (Figure D.26). The "within endplate" comparisons for the superior lumbar and sacral endplate full AP failure load maps can be found in Tables D.2 and D.14, respectively.

| sacrum | | AP | -40% | | | -20% | | | 0% | | | 20% | | | 40% | | |
|---|---|---|---|---|---|---|---|---|---|---|---|---|---|---|---|---|---|
| superior L | | LAT | -15% | 0% | 15% | -15% | 0% | 15% | -15% | 0% | 15% | -15% | 0% | 15% | -15% | 0% | 15% |
| AP | LAT | Mean FL | **251.63** | **249.93** | **212.92** | **181.07** | **176.14** | **183.66** | **152.65** | **125.85** | **117.47** | **107.55** | **95.30** | **69.58** | **86.70** | **86.74** | **76.57** |
| -40% | -15% | **105.76** | 0.0000 | 0.0000 | 0.0000 | 0.0000 | 0.0000 | 0.0000 | 0.0013 | 0.4099 | 0.7413 | 0.9868 | 0.8025 | 0.0652 | 0.5657 | 0.4682 | 0.2546 |
| | 0% | **104.30** | 0.0000 | 0.0000 | 0.0000 | 0.0000 | 0.0000 | 0.0000 | 0.0010 | 0.4242 | 0.7855 | 0.9923 | 0.7161 | 0.0794 | 0.5470 | 0.4255 | 0.2838 |
| | 15% | **96.78** | 0.0000 | 0.0000 | 0.0000 | 0.0000 | 0.0000 | 0.0000 | 0.0001 | 0.1536 | 0.4720 | 0.8848 | 0.8981 | 0.3101 | 0.8189 | 0.6598 | 0.6547 |
| -20% | -15% | **82.60** | 0.0000 | 0.0000 | 0.0000 | 0.0000 | 0.0000 | 0.0000 | 0.0000 | 0.0084 | 0.0765 | 0.4329 | 0.6899 | 0.7928 | 0.7229 | 0.9317 | 0.9539 |
| | 0% | **80.80** | 0.0000 | 0.0000 | 0.0000 | 0.0000 | 0.0000 | 0.0000 | 0.0000 | 0.0064 | 0.0665 | 0.4236 | 0.8094 | 0.5957 | 0.9567 | 0.9860 | 0.7144 |
| | 15% | **80.92** | 0.0000 | 0.0000 | 0.0000 | 0.0000 | 0.0000 | 0.0000 | 0.0000 | 0.0057 | 0.0591 | 0.3860 | 0.7250 | 0.7605 | 0.8714 | 0.9583 | 0.9249 |
| 0% | -15% | **53.98** | 0.0000 | 0.0000 | 0.0000 | 0.0000 | 0.0000 | 0.0000 | 0.0000 | 0.0000 | 0.0000 | 0.0006 | 0.0240 | 0.8280 | 0.1669 | 0.1862 | 0.5129 |
| | 0% | **65.67** | 0.0000 | 0.0000 | 0.0000 | 0.0000 | 0.0000 | 0.0000 | 0.0000 | 0.0001 | 0.0008 | 0.0231 | 0.2347 | 0.9387 | 0.6067 | 0.6667 | 0.7815 |
| | 15% | **60.38** | 0.0000 | 0.0000 | 0.0000 | 0.0000 | 0.0000 | 0.0000 | 0.0000 | 0.0000 | 0.0001 | 0.0052 | 0.1022 | 0.9318 | 0.4041 | 0.4472 | 0.7267 |
| 20% | -15% | **59.37** | 0.0000 | 0.0000 | 0.0000 | 0.0000 | 0.0000 | 0.0000 | 0.0000 | 0.0000 | 0.0001 | 0.0040 | 0.0913 | 0.9505 | 0.3898 | 0.4279 | 0.7520 |
| | 0% | **68.11** | 0.0000 | 0.0000 | 0.0000 | 0.0000 | 0.0000 | 0.0000 | 0.0000 | 0.0001 | 0.0018 | 0.0415 | 0.3106 | 0.8989 | 0.6774 | 0.7436 | 0.7448 |
| | 15% | **61.10** | 0.0000 | 0.0000 | 0.0000 | 0.0000 | 0.0000 | 0.0000 | 0.0000 | 0.0000 | 0.0002 | 0.0059 | 0.1050 | 0.8833 | 0.3957 | 0.4437 | 0.6669 |
| 40% | -15% | **143.80** | 0.0000 | 0.0000 | 0.0000 | 0.0069 | 0.0142 | 0.0051 | 0.4439 | 0.2664 | 0.1032 | 0.0147 | 0.0011 | 0.0000 | 0.0001 | 0.0001 | 0.0000 |
| | 0% | **107.33** | 0.0000 | 0.0000 | 0.0000 | 0.0000 | 0.0000 | 0.0000 | 0.0017 | 0.3769 | 0.6543 | 0.9847 | 0.8366 | 0.0503 | 0.5581 | 0.4778 | 0.2176 |
| | 15% | **129.00** | 0.0000 | 0.0000 | 0.0000 | 0.0001 | 0.0003 | 0.0001 | 0.1014 | 0.7853 | 0.5784 | 0.2471 | 0.0849 | 0.0001 | 0.0114 | 0.0096 | 0.0006 |

## D.2.9 Superior Lumbar and Sacral Endplate Full LAT Failure Load Maps

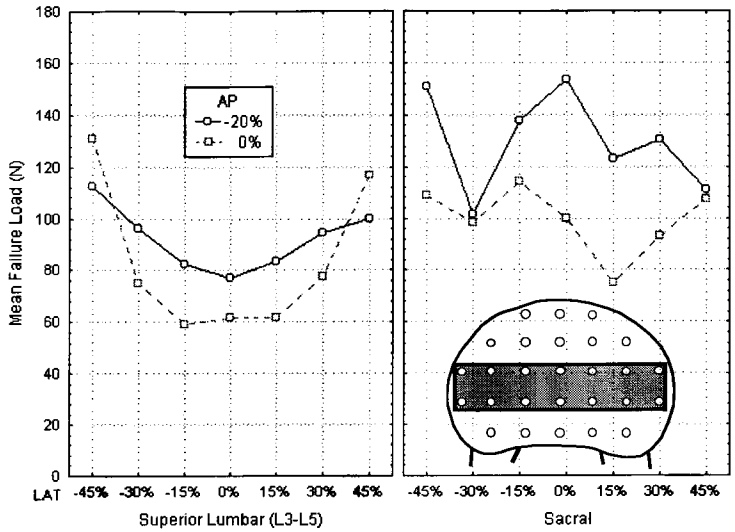


Figure D.27: Comparison of the full LAT failure load distribution in the superior lumbar and sacral endplates. The p-value of < 0.3303 indicates that there are no significant shape differences between these two failure load maps. The *post hoc* Newman-Keuls results for this comparison are given in Table D.27, Appendix D.

Table D.27: Newman-Keuls *post hoc* comparison of the means in the superior lumbar and sacral endplate full LAT failure load distributions (Figure D.27). The **"within** endplate" comparisons for the superior lumbar and sacral endplate full LAT failure load maps can be found in Tables D.3 and D.15, respectively.

| sacrum | | AP | -20% | | | | | | | 0% | | | | | | |
|---|---|---|---|---|---|---|---|---|---|---|---|---|---|---|---|---|
| superior L | | LAT | -45% | -30% | -15% | 0% | 15% | 30% | 45% | -45% | -30% | -15% | 0% | 15% | 30% | 45% |
| AP | LAT | Mean FL | **151.23** | **101.39** | **137.61** | **153.55** | **122.85** | **130.42** | **110.64** | **108.78** | **98.25** | **113.97** | **99.67** | **74.98** | **93.16** | **106.98** |
| -20% | -45% | **112.56** | 0.2886 | 0.9617 | 0.7381 | 0.2602 | 0.9255 | 0.8182 | 0.9079 | 0.9718 | 0.9886 | 0.9328 | 0.9866 | 0.6490 | 0.9843 | 0.9868 |
| | -30% | **96.20** | 0.0882 | 0.9979 | 0.4538 | 0.0668 | 0.9024 | 0.6890 | 0.9880 | 0.9883 | 0.9022 | 0.9864 | 0.9763 | 0.9041 | 0.9817 | 0.9868 |
| | -15% | **82.20** | 0.0102 | 0.9633 | 0.1080 | 0.0069 | 0.5165 | 0.2516 | 0.8570 | 0.8774 | 0.9270 | 0.8129 | 0.9398 | 0.9722 | 0.7868 | 0.8914 |
| | 0% | **77.06** | 0.0042 | 0.9268 | 0.0544 | 0.0028 | 0.3568 | 0.1468 | 0.7487 | 0.7841 | 0.9050 | 0.6778 | 0.9086 | 0.9003 | 0.8678 | 0.8120 |
| | 15% | **83.22** | 0.0114 | 0.9563 | 0.1164 | 0.0078 | 0.5297 | 0.2639 | 0.8549 | 0.8720 | 0.8940 | 0.8170 | 0.9196 | 0.9875 | 0.5507 | 0.8825 |
| | 30% | **94.41** | 0.0728 | 0.9983 | 0.4092 | 0.0541 | 0.8837 | 0.6509 | 0.9870 | 0.9884 | 0.9710 | 0.9833 | 0.9890 | 0.9030 | 0.9402 | 0.9883 |
| | 45% | **99.69** | 0.1095 | 0.9186 | 0.4940 | 0.0861 | 0.8966 | 0.7002 | 0.9644 | 0.9470 | 0.9959 | 0.9774 | 0.9991 | 0.9195 | 0.9988 | 0.8993 |
| 0% | -45% | **130.86** | 0.4397 | 0.7481 | 0.6850 | 0.5225 | 0.8796 | 0.9791 | 0.8851 | 0.8846 | 0.7517 | 0.8464 | 0.7681 | 0.1164 | 0.6444 | 0.8793 |
| | -30% | **74.95** | 0.0031 | 0.9272 | 0.0434 | 0.0021 | 0.3184 | 0.1239 | 0.7270 | 0.7693 | 0.9227 | 0.6440 | 0.9193 | 0.9985 | 0.9271 | 0.8040 |
| | -15% | **59.16** | 0.0003 | 0.4490 | 0.0023 | 0.0002 | 0.0362 | 0.0090 | 0.1910 | 0.2271 | 0.4837 | 0.1369 | 0.4594 | 0.8751 | 0.5672 | 0.2643 |
| | 0% | **61.60** | 0.0003 | 0.5224 | 0.0036 | 0.0003 | 0.0519 | 0.0136 | 0.2444 | 0.2852 | 0.5475 | 0.1813 | 0.5267 | 0.8514 | 0.6138 | 0.3258 |
| | 15% | **61.79** | 0.0003 | 0.4974 | 0.0035 | 0.0003 | 0.0498 | 0.0131 | 0.2326 | 0.2706 | 0.5125 | 0.1735 | 0.4958 | 0.7072 | 0.5606 | 0.3082 |
| | 30% | **77.82** | 0.0045 | 0.9174 | 0.0573 | 0.0030 | 0.3626 | 0.1515 | 0.7437 | 0.7762 | 0.8799 | 0.6783 | 0.8900 | 0.9841 | 0.7916 | 0.8010 |
| | 45% | **116.82** | 0.3101 | 0.9667 | 0.7203 | 0.2986 | 0.7176 | 0.6921 | 0.9822 | 0.9886 | 0.9815 | 0.8636 | 0.9815 | 0.5201 | 0.9673 | 0.9913 |

### D.2.10 Superior Lumbar and Sacral Endplate Maximum AP, LAT Stiffness Maps

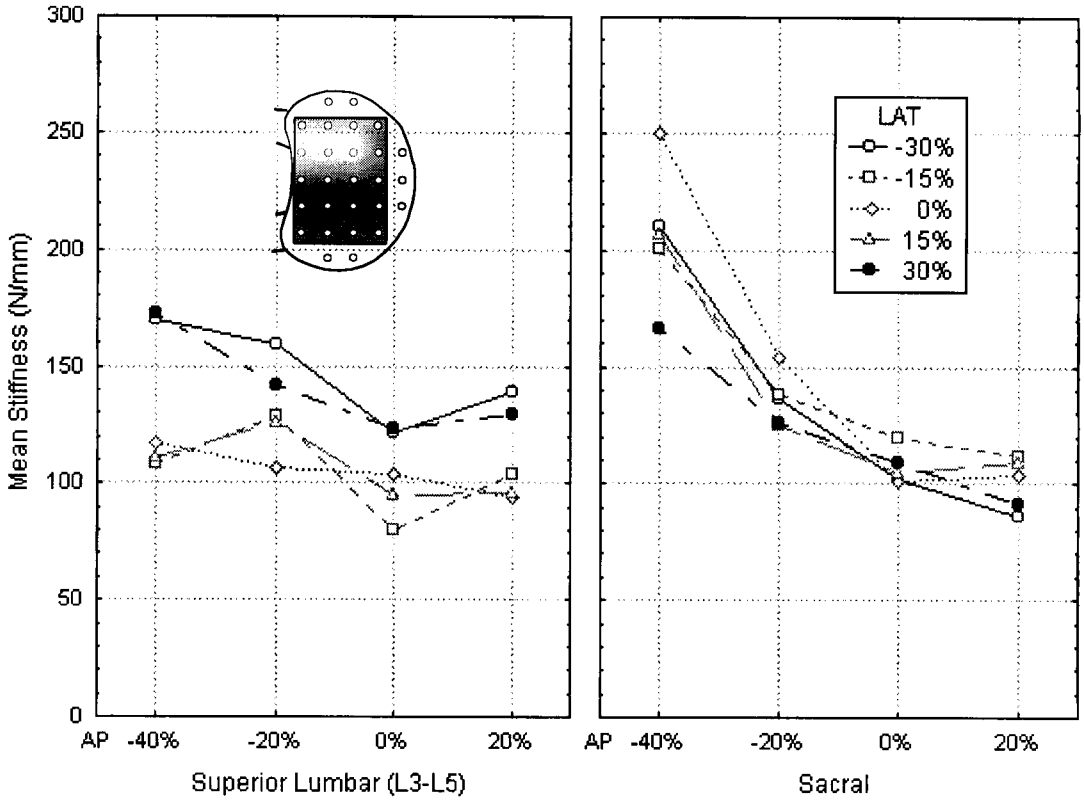


Figure D.28: Comparison of the maximum AP, LAT stiffness distribution in the superior lumbar and sacral endplates. The p-value of $< 0.0702$ indicates that the superior and inferior lumbar endplate stiffness maps are not significantly different. The *post hoc* Newman-Keuls results for this comparison are given in Table D.28.

Table D.28: Newman-Keuls *post hoc* comparison of the means in the superior lumbar and sacral endplate maximum AP, LAT stiffness distributions (Figure D.28). The "within endplate" comparisons for the superior lumbar and sacral endplate maximum AP, LAT stiffness maps can be found in Tables D.4 and D.16, respectively.

| sacrum | | AP | -40% | | | | | -20% | | | | |
|---|---|---|---|---|---|---|---|---|---|---|---|---|
| superior L | | LAT | -30% | -15% | 0% | 15% | 30% | -30% | -15% | 0% | 15% | 30% |
| AP | LAT | Mean ST | **210.39** | **200.58** | **249.59** | **206.81** | **166.67** | **136.50** | **138.36** | **154.37** | **125.21** | **125.44** |
| -40% | -30% | **170.05** | 0.1387 | 0.1849 | 0.0001 | 0.1489 | 0.8459 | 0.5309 | 0.5330 | 0.8040 | 0.3239 | 0.3000 |
| | -15% | **108.23** | 0.0000 | 0.0000 | 0.0000 | 0.0000 | 0.0960 | 0.9535 | 0.9386 | 0.4397 | 0.9936 | 0.9962 |
| | 0% | **117.00** | 0.0001 | 0.0003 | 0.0000 | 0.0001 | 0.2379 | 0.9827 | 0.9795 | 0.6675 | 0.9898 | 0.9967 |
| | 15% | **111.15** | [illegible]0 | 0.0001 | 0.0000 | 0.0000 | 0.1216 | 0.9517 | 0.9408 | 0.4831 | 0.9842 | 0.9920 |
| | 30% | **172.39** | 0.1274 | 0.1050 | 0.0001 | 0.1175 | 0.9422 | 0.4989 | 0.5118 | 0.8387 | 0.2717 | 0.2530 |
| -20% | -30% | **159.36** | 0.0522 | 0.1237 | 0.0000 | 0.0699 | 0.6744 | 0.7773 | 0.7470 | 0.7740 | 0.6748 | 0.6343 |
| | -15% | **128.25** | 0.0002 | 0.0019 | 0.0000 | 0.0005 | 0.3998 | 0.8834 | 0.9378 | 0.7442 | 0.9981 | 0.9857 |
| | 0% | **106.31** | 0.0000 | 0.0000 | 0.0000 | 0.0000 | 0.0741 | 0.9376 | 0.9179 | 0.3818 | 0.9919 | 0.9948 |
| | 15% | **126.04** | 0.0001 | 0.0013 | 0.0000 | 0.0003 | 0.3656 | 0.9317 | 0.9547 | 0.7331 | 0.9988 | 0.9725 |
| | 30% | **141.84** | 0.0026 | 0.0130 | 0.0000 | 0.0047 | 0.4821 | 0.9900 | 0.9782 | 0.4714 | 0.9896 | 0.9819 |
| 0% | -30% | **121.04** | 0.0001 | 0.0006 | 0.0000 | 0.0001 | 0.3254 | 0.9871 | 0.9864 | 0.7496 | 0.9688 | 0.9943 |
| | -15% | **80.38** | 0.0000 | 0.0000 | 0.0000 | 0.0000 | 0.0004 | 0.2119 | 0.1687 | 0.0083 | 0.5935 | 0.6046 |
| | 0% | **103.47** | 0.0000 | 0.0000 | 0.0000 | 0.0000 | 0.0543 | 0.9268 | 0.9011 | **0.3266** | 0.9937 | 0.9955 |
| | 15% | **94.82** | 0.0000 | 0.0000 | 0.0000 | 0.0000 | 0.0122 | 0.7529 | 0.6942 | 0.1247 | 0.9658 | 0.9704 |
| | 30% | **123.42** | 0.0001 | 0.0010 | 0.0000 | 0.0002 | 0.3835 | 0.9892 | 0.9895 | 0.7929 | 0.9179 | 0.9926 |
| 20% | -30% | **138.93** | 0.0017 | 0.0094 | 0.0000 | 0.0031 | 0.5007 | 0.9893 | 0.9738 | 0.6482 | 0.9938 | 0.9873 |
| | -15% | **103.44** | 0.0000 | 0.0000 | 0.0000 | 0.0000 | 0.0576 | 0.9379 | 0.9139 | 0.3423 | 0.9959 | 0.9970 |
| | 0% | **94.19** | 0.0000 | 0.0000 | 0.0000 | 0.0000 | 0.0112 | 0.7460 | 0.6855 | 0.1183 | 0.9662 | 0.9704 |
| | 15% | **95.52** | 0.0000 | 0.0000 | 0.0000 | 0.0000 | 0.0134 | 0.7609 | 0.7044 | 0.1322 | 0.9656 | 0.9706 |
| | 30% | **129.68** | 0.0003 | 0.0023 | 0.0000 | 0.0006 | 0.3975 | 0.6949 | 0.8718 | 0.7153 | 0.9990 | 0.9949 |

| sacrum | | AP | 0% | | | | | 20% | | | | |
|---|---|---|---|---|---|---|---|---|---|---|---|---|
| superior L | | LAT | -30% | -15% | 0% | 15% | 30% | -30% | -15% | 0% | 15% | 30% |
| AP | LAT | Mean ST | **101.72** | **119.76** | **101.63** | **104.28** | **108.86** | **86.30** | **111.89** | **103.85** | **109.12** | **91.16** |
| -40% | -30% | **170.05** | 0.0234 | 0.2191 | 0.0244 | 0.0305 | 0.0590 | 0.0008 | 0.0785 | 0.0300 | 0.0570 | 0.0026 |
| | -15% | **108.23** | 0.9998 | 0.9945 | 0.9999 | 0.9720 | 0.9711 | 0.9894 | 0.9996 | 0.9944 | 0.9986 | 0.9981 |
| | 0% | **117.00** | 0.9993 | 0.8742 | 0.9996 | 0.9961 | 0.9902 | 0.9533 | 0.7687 | 0.9979 | 0.9690 | 0.9886 |
| | 15% | **111.15** | 0.9999 | 0.9603 | 1.0000 | 0.9988 | 0.9905 | 0.9893 | 0.9662 | 0.9996 | 0.9070 | 0.9983 |
| | 30% | **172.39** | 0.0150 | 0.1728 | 0.0156 | 0.0201 | 0.0410 | 0.0004 | 0.0567 | 0.0197 | 0.0398 | 0.0015 |
| -20% | -30% | **159.36** | 0.1516 | 0.5722 | 0.1580 | 0.1755 | 0.2690 | 0.0103 | 0.3114 | 0.1757 | 0.2588 | 0.0287 |
| | -15% | **128.25** | 0.9919 | 0.9990 | 0.9938 | 0.9892 | 0.9941 | 0.7606 | 0.9906 | 0.9911 | 0.9911 | 0.9017 |
| | 0% | **106.31** | 0.9998 | 0.9945 | 1.0000 | 0.9070 | 0.9882 | 0.9923 | 0.9996 | 0.9891 | 0.9985 | 0.9987 |
| | 15% | **126.04** | 0.9958 | 0.9992 | 0.9970 | 0.9936 | 0.9962 | 0.8249 | 0.9924 | 0.9950 | 0.9937 | 0.9367 |
| | 30% | **141.84** | 0.8117 | 0.9828 | 0.8251 | 0.8251 | 0.8975 | 0.2524 | 0.9086 | 0.8305 | 0.8849 | 0.4361 |
| 0% | -30% | **121.04** | 0.9980 | 0.9410 | 0.9988 | 0.9942 | 0.9926 | 0.9043 | 0.9527 | 0.9962 | 0.9836 | 0.9710 |
| | -15% | **80.38** | 0.9242 | 0.7598 | 0.8860 | 0.9685 | 0.9506 | 0.7335 | 0.9413 | 0.9600 | 0.9586 | 0.8094 |
| | 0% | **103.47** | 0.9944 | 0.9976 | 0.9996 | 0.9988 | 0.9996 | 0.9871 | 0.9999 | 0.9827 | 0.9999 | 0.9968 |
| | 15% | **94.82** | 0.9789 | 0.9889 | 0.9192 | 0.9994 | 0.9993 | 0.9614 | 0.9995 | 0.9986 | 0.9996 | 0.9758 |
| | 30% | **123.42** | 0.9960 | 0.9758 | 0.9973 | 0.9910 | 0.9910 | 0.8575 | 0.9642 | 0.9936 | 0.9827 | 0.9505 |
| 20% | -30% | **138.93** | 0.8858 | 0.9909 | 0.8966 | 0.8912 | 0.9396 | 0.3510 | 0.9433 | 0.8964 | 0.9294 | 0.5555 |
| | -15% | **103.44** | 0.9213 | 0.9987 | 0.9941 | 1.0000 | 0.9999 | 0.9766 | 1.0000 | 0.9997 | 1.0000 | 0.9923 |
| | 0% | **94.19** | 0.9927 | 0.9898 | 0.9738 | 0.9997 | 0.9995 | 0.8929 | 0.9996 | 0.9993 | 0.9997 | 0.8616 |
| | 15% | **95.52** | 0.9324 | 0.9880 | 0.7254 | 0.9988 | 0.9990 | 0.9843 | 0.9993 | 0.9969 | 0.9995 | 0.9945 |
| | 30% | **129.68** | 0.9889 | 0.9992 | 0.9912 | 0.9867 | 0.9933 | 0.7200 | 0.9910 | 0.9887 | 0.9904 | 0.8774 |

## D.2.11 Superior Lumbar and Sacral Endplate Full AP Stiffness Maps

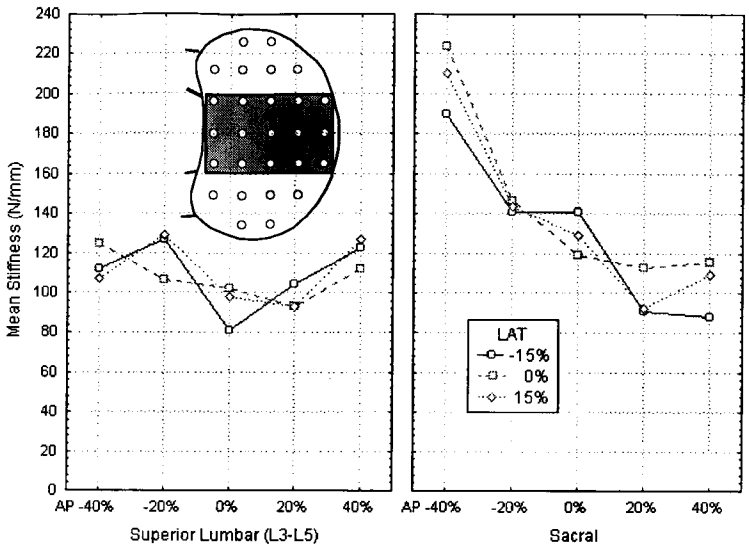


Figure D.29: Comparison of the full AP stiffness distribution in the superior lumbar and sacral endplates. The p-value of < 0.2888 indicates that the shapes of the two maps are not significantly different. The *post hoc* Newman-Keuls results for this comparison are given in Table D.29.

Table D.29: Newman-Keuls *post hoc* comparison of the means in the superior lumbar and sacral endplate maximum full AP stiffness distributions (Figure D.23). The "within endplate" comparisons for the superior lumbar and sacral endplate full AP stiffness maps can be found in Tables D.5 and D.17, respectively.

| sacrum | | AP | -40% | | | -20% | | | 0% | | | 20% | | | 40% | | |
|---|---|---|---|---|---|---|---|---|---|---|---|---|---|---|---|---|---|
| superior L | | LAT | -15% | 0% | 15% | -15% | 0% | 15% | -15% | 0% | 15% | -15% | 0% | 15% | -15% | 0% | 15% |
| AP | LAT | Mean ST | **189.81** | **223.72** | **210.21** | **141.08** | **146.49** | **143.29** | **140.43** | **118.89** | **128.86** | **90.88** | **112.39** | **92.46** | **88.08** | **115.23** | **109.11** |
| -40% | -15% | **111.68** | 0.0001 | 0.0000 | 0.0000 | 0.8167 | 0.6602 | 0.7654 | 0.8058 | 0.9910 | 0.9917 | 0.9657 | 0.9989 | 0.9696 | 0.9420 | 0.9960 | 0.8704 |
| | 0% | **124.45** | 0.0014 | 0.0000 | 0.0000 | 0.9412 | 0.8994 | 0.9337 | 0.9138 | 0.9338 | 0.9987 | 0.7745 | 0.9407 | 0.8095 | 0.6792 | 0.9367 | 0.9783 |
| | 15% | **107.07** | 0.0001 | 0.0000 | 0.0000 | 0.6966 | 0.5023 | 0.6264 | 0.6911 | 0.9894 | 0.9771 | 0.9834 | 0.9972 | 0.9836 | 0.9720 | 0.9955 | 0.8973 |
| -20% | -15% | **126.47** | 0.0015 | 0.0000 | 0.0000 | 0.8868 | 0.8661 | 0.8945 | 0.8125 | 0.9892 | 0.9874 | 0.7408 | 0.9738 | 0.7826 | 0.6358 | 0.9805 | 0.9848 |
| | 0% | **106.60** | 0.0001 | 0.0000 | 0.0000 | 0.7075 | 0.5079 | 0.6349 | 0.7045 | 0.9942 | 0.9809 | 0.9750 | 0.9991 | 0.9732 | 0.9620 | 0.9981 | 0.9862 |
| | 15% | **128.74** | 0.0021 | 0.0000 | 0.0000 | 0.8626 | 0.8711 | 0.8882 | 0.7389 | 0.9893 | 0.9938 | 0.6610 | 0.9689 | 0.7100 | 0.5471 | 0.9787 | 0.9773 |
| 0% | -15% | **81.07** | 0.0000 | 0.0000 | 0.0000 | 0.0301 | 0.0094 | 0.0193 | 0.0325 | 0.5803 | 0.2602 | 0.8084 | 0.8074 | 0.8885 | 0.6568 | 0.7216 | 0.8306 |
| | 0% | **102.18** | 0.0001 | 0.0000 | 0.0000 | 0.5565 | 0.3491 | 0.4744 | 0.5591 | 0.9884 | 0.9494 | 0.9800 | 0.9982 | 0.9726 | 0.9736 | 0.9961 | 0.9923 |
| | 15% | **97.58** | 0.0000 | 0.0000 | 0.0000 | 0.3629 | 0.1940 | 0.2904 | 0.3682 | 0.9596 | 0.8577 | 0.9932 | 0.9907 | 0.9882 | 0.9909 | 0.9829 | 0.9781 |
| 20% | -15% | **104.47** | 0.0001 | 0.0000 | 0.0000 | 0.6390 | 0.4309 | 0.5600 | 0.6387 | 0.9922 | 0.9693 | 0.9780 | 0.9988 | 0.9739 | 0.9685 | 0.9975 | 0.9911 |
| | 0% | **92.74** | 0.0000 | 0.0000 | 0.0000 | 0.2122 | 0.0963 | 0.1588 | 0.2189 | 0.9112 | 0.7174 | 0.9923 | 0.9772 | 0.9855 | 0.9910 | 0.9588 | 0.9688 |
| | 15% | **93.20** | 0.0000 | 0.0000 | 0.0000 | 0.2128 | 0.0978 | 0.1602 | 0.2185 | 0.8988 | 0.7119 | 0.9989 | 0.9700 | 0.9988 | 0.9976 | 0.9496 | 0.9523 |
| 40% | -15% | **122.40** | 0.0010 | 0.0000 | 0.0000 | 0.9367 | 0.8816 | 0.9242 | 0.9147 | 0.8240 | 0.9985 | 0.8264 | 0.9209 | 0.8545 | 0.7436 | 0.8923 | 0.9804 |
| | 0% | **111.86** | 0.0001 | 0.0000 | 0.0000 | 0.7888 | 0.6332 | 0.7380 | 0.7738 | 0.9705 | 0.9869 | 0.9752 | 0.9734 | 0.9792 | 0.9548 | 0.9752 | 0.9833 |
| | 15% | **126.35** | 0.0019 | 0.0000 | 0.0000 | 0.9379 | 0.9077 | 0.9357 | 0.8997 | 0.9651 | 0.9986 | 0.7201 | 0.9502 | 0.7615 | 0.6153 | 0.9554 | 0.9754 |

## D.2.12 Superior Lumbar and Sacral Endplate Full LAT Stiffness Maps

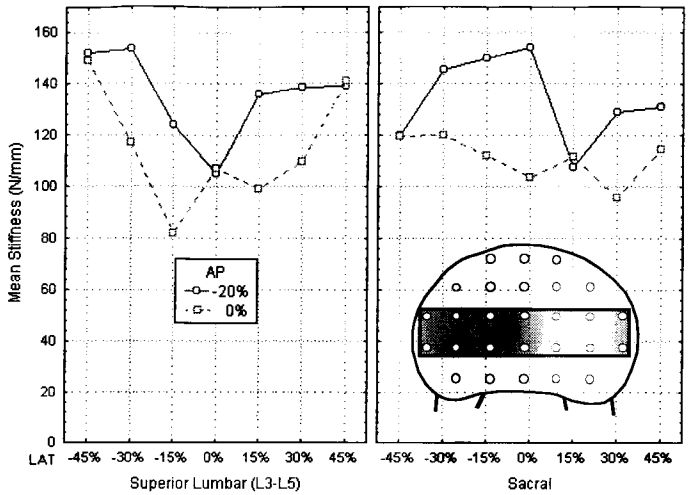


Figure D.30: Comparison of the full LAT stiffness distribution in the superior lumbar and sacral lumbar endplates. The p-value of < 0.4651 indicates that there are no significant differences between the shapes of the maps. The *post hoc* Newman-Keuls results for this comparison are given in Table D.30.

Table D.30: Newman-Keuls *post hoc* comparison of the means in the superior lumbar and sacral endplate maximum full LAT stiffness distributions (Figure D.30). The "within endplate" comparisons for the superior lumbar and sacral endplate full LAT stiffness maps can be found in Tables D.6 and D.18, respectively.

| sacrum | | AP | -20% | | | | | | | 0% | | | | | | |
|---|---|---|---|---|---|---|---|---|---|---|---|---|---|---|---|---|
| superior L | | LAT | -45% | -30% | -15% | 0% | 15% | 30% | 45% | -45% | -30% | -15% | 0% | 15% | 30% | 45% |
| AP | LAT | Mean ST | **120.38** | **145.60** | **149.89** | **153.85** | **107.92** | **129.01** | **131.23** | **119.85** | **120.29** | **112.35** | **103.66** | **111.45** | **95.77** | **114.77** |
| -20% | -45% | **152.13** | 0.9215 | 0.9888 | 0.9130 | 0.9962 | 0.8160 | 0.9804 | 0.9829 | 0.9477 | 0.9386 | 0.8690 | 0.7455 | 0.8674 | 0.5038 | 0.9006 |
| | -30% | **153.66** | 0.9170 | 0.9949 | 0.9815 | 0.9930 | 0.7916 | 0.9805 | 0.9840 | 0.9417 | 0.9333 | 0.8525 | 0.7135 | 0.8494 | 0.4664 | 0.8881 |
| | -15% | **124.27** | 0.8495 | 0.9667 | 0.9616 | 0.9641 | 0.9985 | 0.8177 | 0.9385 | 0.9965 | 0.9794 | 0.9972 | 0.9985 | 0.9985 | 0.9861 | 0.9973 |
| | 0% | **105.35** | 0.9997 | 0.8933 | 0.8257 | 0.7628 | 0.9915 | 0.9943 | 0.9917 | 0.9986 | 0.9993 | 0.9994 | 0.9343 | 0.9983 | 0.9659 | 0.9993 |
| | 15% | **135.96** | 0.9410 | 0.9898 | 0.9934 | 0.9969 | 0.9762 | 0.9386 | 0.8179 | 0.9858 | 0.9726 | 0.9774 | 0.9684 | 0.9813 | 0.8782 | 0.9814 |
| | 30% | **138.64** | 0.9475 | 0.9865 | 0.9939 | 0.9980 | 0.9642 | 0.9654 | 0.9305 | 0.9836 | 0.9723 | 0.9693 | 0.9506 | 0.9732 | 0.8326 | 0.9757 |
| | 45% | **138.95** | 0.9705 | 0.9437 | 0.9836 | 0.9960 | 0.9707 | 0.9886 | 0.9817 | 0.9905 | 0.9843 | 0.9772 | 0.9567 | 0.9796 | 0.8431 | 0.9831 |
| 0% | -45% | **149.27** | 0.9206 | 0.8583 | 0.9761 | 0.9995 | 0.8517 | 0.9749 | 0.9746 | 0.9528 | 0.9414 | 0.8906 | 0.7956 | 0.8918 | 0.5693 | 0.9158 |
| | -30% | **117.08** | 0.9986 | 0.9620 | 0.9410 | 0.9262 | 0.9977 | 0.9920 | 0.9928 | 0.8926 | 0.9866 | 0.9711 | 0.9992 | 0.9928 | 0.9935 | 0.9107 |
| | -15% | **81.97** | 0.8584 | 0.2422 | 0.1689 | 0.1228 | 0.8647 | 0.6554 | 0.6050 | 0.8185 | 0.8357 | 0.8950 | 0.7149 | 0.8790 | 0.5021 | 0.8773 |
| | 0% | **107.00** | 0.9997 | 0.9096 | 0.8505 | 0.7954 | 0.9642 | 0.9951 | 0.9930 | 0.9984 | 0.9993 | 0.9990 | 0.9855 | 0.9964 | 0.9819 | 0.9990 |
| | 15% | **99.44** | 0.9982 | 0.7794 | 0.6791 | 0.5938 | 0.9938 | 0.9806 | 0.9725 | 0.9954 | 0.9969 | 0.9984 | 0.8374 | 0.9971 | 0.8580 | 0.9979 |
| | 30% | **109.48** | 0.9995 | 0.9223 | 0.8735 | 0.8300 | 0.9396 | 0.9941 | 0.9924 | 0.9959 | 0.9984 | 0.9893 | 0.9986 | 0.9235 | 0.9940 | 0.9940 |
| | 45% | **140.98** | 0.9724 | 0.8222 | 0.9724 | 0.9958 | 0.9615 | 0.9919 | 0.9894 | 0.9895 | 0.9840 | 0.9719 | 0.9419 | 0.9739 | 0.8068 | 0.9796 |

### D.2.13 Inferior Lumbar and Sacral Endplate Maximum AP, LAT Failure Load Maps

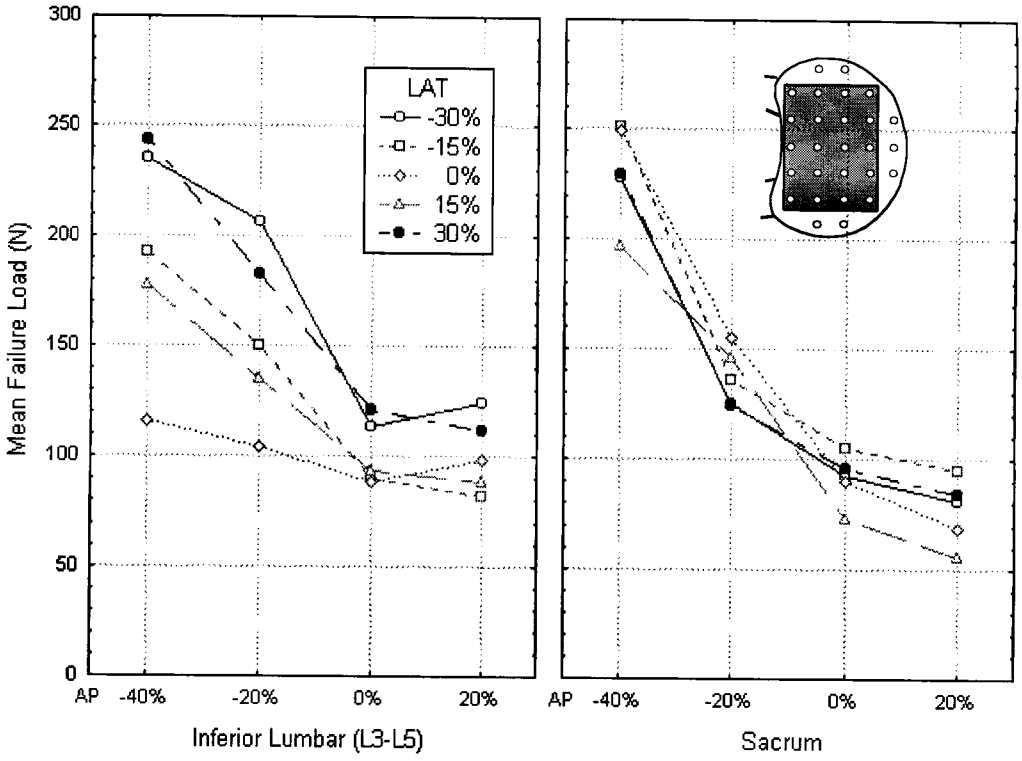


Figure D.31: Comparison of the maximum AP, LAT failure load distribution in the inferior lumbar and sacral endplates. The p-value of $< 0.0014$ indicates that there are significant differences between the shapes of the two failure load maps. The *post hoc* Newman-Keuls comparison of these maps is given in Table D.31.

.

Table D.31: Newman-Keuls *post hoc* comparison of the means in the inferior lumbar and sacral endplate maximum AP, LAT failure load distributions (Figure D.31). The "within endplate" comparisons for the inferior lumbar and sacral endplate maximum AP, LAT failure load maps can be found in Tables D.7 and D.13, respectively.

| sacrum | | AP | -40% | | | | | -20% | | | | |
|---|---|---|---|---|---|---|---|---|---|---|---|---|
| inferior L | | LAT | -30% | -15% | 0% | 15% | 30% | -30% | -15% | 0% | 15% | 30% |
| AP | LAT | Mean FL | **227.71** | **251.24** | **249.50** | **196.82** | **229.36** | **125.24** | **135.81** | **154.76** | **145.53** | **123.98** |
| -40% | -30% | **235.78** | 0.9036 | 0.8444 | 0.7464 | 0.2331 | 0.7329 | 0.0000 | 0.0000 | 0.0006 | 0.0001 | 0.0000 |
| | -15% | **192.42** | 0.2387 | 0.0466 | 0.0497 | 0.8150 | 0.2843 | 0.0108 | 0.0420 | 0.1876 | 0.1266 | 0.0124 |
| | 0% | **115.97** | 0.0000 | 0.0000 | 0.0000 | 0.0014 | 0.0000 | 0.9881 | 0.9412 | 0.5555 | 0.7682 | 0.9051 |
| | 15% | **177.09** | 0.0772 | 0.0039 | 0.0047 | 0.7208 | 0.0802 | 0.0852 | 0.1821 | 0.2355 | 0.3360 | 0.1089 |
| | 30% | **243.93** | 0.8246 | 0.9202 | 0.7674 | 0.1231 | 0.7189 | 0.0000 | 0.0000 | 0.0001 | 0.0000 | 0.0000 |
| -20% | -30% | **206.30** | 0.2552 | 0.2035 | 0.1958 | 0.6146 | 0.4381 | 0.0009 | 0.0056 | 0.0679 | 0.0273 | 0.0009 |
| | -15% | **150.08** | 0.0010 | 0.0000 | 0.0000 | 0.1290 | 0.0009 | 0.6787 | 0.7284 | 0.8039 | 0.8088 | 0.8089 |
| | 0% | **104.58** | 0.0000 | 0.0000 | 0.0000 | 0.0002 | 0.0000 | 0.9747 | 0.8562 | 0.2987 | 0.5674 | 0.9471 |
| | 15% | **134.73** | 0.0001 | 0.0000 | 0.0000 | 0.0271 | 0.0000 | 0.6140 | 0.9545 | 0.8250 | 0.8342 | 0.9406 |
| | 30% | **182.10** | 0.1090 | 0.0090 | 0.0103 | 0.7139 | 0.1207 | 0.0515 | 0.1364 | 0.3141 | 0.2946 | 0.0626 |
| 0% | -30% | **113.74** | 0.0000 | 0.0000 | 0.0000 | 0.0010 | 0.0000 | 0.9903 | 0.9399 | 0.5198 | 0.7537 | 0.9483 |
| | -15% | **89.95** | 0.0000 | 0.0000 | 0.0000 | 0.0000 | 0.0000 | 0.8875 | 0.5795 | 0.0745 | 0.2405 | 0.8731 |
| | 0% | **88.75** | 0.0000 | 0.0000 | 0.0000 | 0.0000 | 0.0000 | 0.8790 | 0.5574 | 0.0659 | 0.2223 | 0.8675 |
| | 15% | **93.62** | 0.0000 | 0.0000 | 0.0000 | 0.0000 | 0.0000 | 0.9030 | 0.6345 | 0.1038 | 0.2937 | 0.8774 |
| | 30% | **120.80** | 0.0000 | 0.0000 | 0.0000 | 0.0037 | 0.0000 | 0.9954 | 0.9680 | 0.6794 | 0.8457 | 0.8660 |
| 20% | -30% | **124.64** | 0.0000 | 0.0000 | 0.0000 | 0.0059 | 0.0000 | 0.9746 | 0.9341 | 0.6822 | 0.8014 | 0.9719 |
| | -15% | **81.65** | 0.0000 | 0.0000 | 0.0000 | 0.0000 | 0.0000 | 0.7236 | 0.3416 | 0.0226 | 0.1002 | 0.7205 |
| | 0% | **98.48** | 0.0000 | 0.0000 | 0.0000 | 0.0001 | 0.0000 | 0.9207 | 0.7050 | 0.1570 | 0.3743 | 0.8775 |
| | 15% | **88.46** | 0.0000 | 0.0000 | 0.0000 | 0.0000 | 0.0000 | 0.8907 | 0.5716 | 0.0676 | 0.2293 | 0.8824 |
| | 30% | **111.73** | 0.0000 | 0.0000 | 0.0000 | 0.0007 | 0.0000 | 0.9916 | 0.9376 | 0.4865 | 0.7382 | 0.9666 |

| sacrum | | AP | 0% | | | | | 20% | | | | |
|---|---|---|---|---|---|---|---|---|---|---|---|---|
| inferior L | | LAT | -30% | -15% | 0% | 15% | 30% | -30% | -15% | 0% | 15% | 30% |
| AP | LAT | Mean FL | **92.61** | **105.36** | **90.50** | **72.87** | **96.50** | **81.24** | **94.94** | **68.45** | **55.36** | **84.52** |
| -40% | -30% | **235.78** | 0.0000 | 0.0000 | 0.0000 | 0.0000 | 0.0000 | 0.0000 | 0.0000 | 0.0000 | 0.0000 | 0.0000 |
| | -15% | **192.42** | 0.0000 | 0.0004 | 0.0000 | 0.0000 | 0.0001 | 0.0000 | 0.0001 | 0.0000 | 0.0000 | 0.0000 |
| | 0% | **115.97** | 0.9657 | 0.9427 | 0.9592 | 0.6906 | 0.9462 | 0.9168 | 0.9532 | 0.5382 | 0.1321 | 0.9420 |
| | 15% | **177.09** | 0.0012 | 0.0103 | 0.0008 | 0.0000 | 0.0022 | 0.0001 | 0.0017 | 0.0000 | 0.0000 | 0.0003 |
| | 30% | **243.93** | 0.0000 | 0.0000 | 0.0000 | 0.0000 | 0.0000 | 0.0000 | 0.0000 | 0.0000 | 0.0000 | 0.0000 |
| -20% | -30% | **206.30** | 0.0000 | 0.0000 | 0.0000 | 0.0000 | 0.0000 | 0.0000 | 0.0000 | 0.0000 | 0.0000 | 0.0000 |
| | -15% | **150.08** | 0.1750 | 0.4221 | 0.1418 | 0.0105 | 0.2219 | 0.0500 | 0.2001 | 0.0043 | 0.0002 | 0.0764 |
| | 0% | **104.58** | 0.9883 | 0.9671 | 0.9895 | 0.9216 | 0.9035 | 0.9908 | 0.9562 | 0.8437 | 0.3876 | 0.9930 |
| | 15% | **134.73** | 0.6370 | 0.8260 | 0.5858 | 0.1359 | 0.6719 | 0.3663 | 0.6539 | 0.0727 | 0.0061 | 0.4524 |
| | 30% | **182.10** | 0.0004 | 0.0041 | 0.0003 | 0.0000 | 0.0008 | 0.0001 | 0.0006 | 0.0000 | 0.0000 | 0.0001 |
| 0% | -30% | **113.74** | 0.9710 | 0.8963 | 0.9669 | 0.7462 | 0.9426 | 0.9400 | 0.9544 | 0.6029 | 0.1675 | 0.9577 |
| | -15% | **89.95** | 0.9890 | 0.9964 | 0.9764 | 0.9715 | 0.9993 | 0.9974 | 0.9989 | 0.9475 | 0.6568 | 0.9917 |
| | 0% | **88.75** | 0.9969 | 0.9970 | 0.9952 | 0.9593 | 0.9996 | 0.9947 | 0.9995 | 0.9346 | 0.6378 | 0.9726 |
| | 15% | **93.62** | 0.9571 | 0.9893 | 0.9850 | 0.9846 | 0.9872 | 0.9992 | 0.9442 | 0.9624 | 0.6707 | 0.9991 |
| | 30% | **120.80** | 0.9211 | 0.9244 | 0.9061 | 0.5210 | 0.9026 | 0.8157 | 0.9078 | 0.3686 | 0.0672 | 0.8636 |
| 20% | -30% | **124.64** | 0.8945 | 0.9485 | 0.8705 | 0.4124 | 0.8947 | 0.7306 | 0.8919 | 0.2715 | 0.0401 | 0.7980 |
| | -15% | **81.65** | 0.9973 | 0.9895 | 0.9971 | 0.8868 | 0.9987 | 0.9825 | 0.9987 | 0.8966 | 0.6296 | 0.8787 |
| | 0% | **98.48** | 0.9980 | 0.9290 | 0.9983 | 0.9798 | 0.9165 | 0.9990 | 0.9807 | 0.9478 | 0.5973 | 0.9992 |
| | 15% | **88.46** | 0.9995 | 0.9983 | 0.9995 | 0.9218 | 0.9999 | 0.9808 | 0.9999 | 0.8960 | 0.5761 | 0.8342 |
| | 30% | **111.73** | 0.9722 | 0.7348 | 0.9702 | 0.7876 | 0.9280 | 0.9547 | 0.9485 | 0.6552 | 0.2022 | 0.9672 |

### D.2.14 Inferior Lumbar and Sacral Endplate Full AP Failure Load Maps

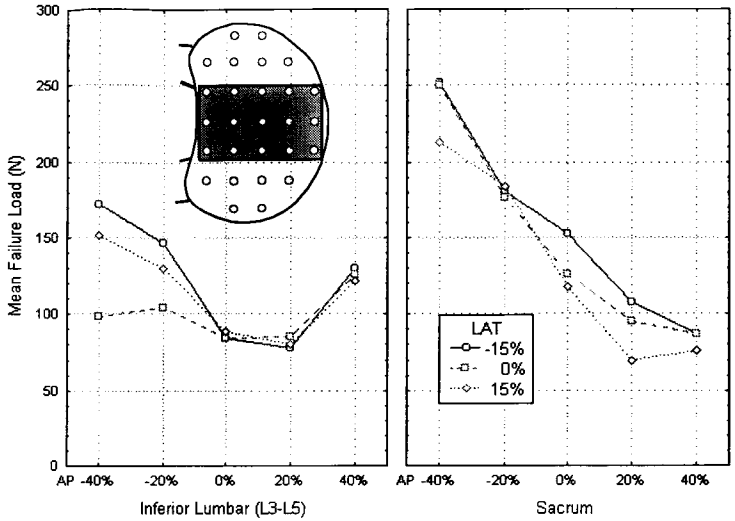


Figure D.32: Comparison of the LAT, full AP failure load distribution in the inferior lumbar and sacral endplates. The p-value of < 0.0127 indicates that there are significant shape differences between these two failure load maps. The results of a *post hoc* comparison of these graphs is given in Table D.32.

Table D.32: Newman-Keuls *post hoc* comparison of the means in the inferior lumbar and sacral endplate full AP failure load distributions (Figure D.32). The "within endplate" comparisons for the inferior lumbar and sacral endplate full AP failure load maps can be found in Tables D.8 and D.14, respectively.

| sacrum | | AP | -40% | | | -20% | | | 0% | | | 20% | | | 40% | | |
|---|---|---|---|---|---|---|---|---|---|---|---|---|---|---|---|---|---|
| inferior L | | LAT | -15% | 0% | 15% | -15% | 0% | 15% | -15% | 0% | 15% | -15% | 0% | 15% | -15% | 0% | 15% |
| AP | LAT | Mean FL | **251.63** | **249.93** | **212.92** | **181.07** | **176.14** | **183.66** | **152.65** | **125.85** | **117.47** | **107.55** | **95.30** | **69.58** | **86.70** | **86.74** | **76.57** |
| -40% | -15% | **172.32** | 0.0000 | 0.0000 | 0.0612 | 0.8352 | 0.8027 | 0.8806 | 0.1985 | 0.0491 | 0.0125 | 0.0012 | 0.0001 | 0.0000 | 0.0000 | 0.0000 | 0.0000 |
| | 0% | **98.40** | 0.0000 | 0.0000 | 0.0000 | 0.0000 | 0.0001 | 0.0000 | 0.0202 | 0.4694 | 0.5971 | 0.8212 | 0.8396 | 0.7699 | 0.9406 | 0.8714 | 0.9420 |
| | 15% | **151.67** | 0.0000 | 0.0000 | 0.0012 | 0.3057 | 0.3788 | 0.2920 | 0.9489 | 0.5403 | 0.3307 | 0.0926 | 0.0123 | 0.0000 | 0.0020 | 0.0018 | 0.0002 |
| -20% | -15% | **146.55** | 0.0000 | 0.0000 | 0.0004 | 0.2124 | 0.2991 | 0.1879 | 0.9162 | 0.6580 | 0.4799 | 0.1750 | 0.0332 | 0.0001 | 0.0070 | 0.0061 | 0.0008 |
| | 0% | **104.63** | 0.0000 | 0.0000 | 0.0000 | 0.0001 | 0.0002 | 0.0000 | 0.0636 | 0.6359 | 0.6784 | 0.8487 | 0.8149 | 0.5239 | 0.8503 | 0.7690 | 0.7994 |
| | 15% | **130.47** | 0.0000 | 0.0000 | 0.0000 | 0.0164 | 0.0337 | 0.0119 | 0.4683 | 0.9905 | 0.9581 | 0.7462 | 0.3899 | 0.0105 | 0.1748 | 0.1562 | 0.0491 |
| 0% | -15% | **84.37** | 0.0000 | 0.0000 | 0.0000 | 0.0000 | 0.0000 | 0.0000 | 0.0013 | 0.2464 | 0.5312 | 0.8868 | 0.9918 | 0.8702 | 0.9988 | 0.9999 | 0.9567 |
| | 0% | **84.81** | 0.0000 | 0.0000 | 0.0000 | 0.0000 | 0.0000 | 0.0000 | 0.0013 | 0.2348 | 0.5025 | 0.8624 | 0.9836 | 0.9197 | 0.9917 | 0.9993 | 0.9833 |
| | 15% | **88.92** | 0.0000 | 0.0000 | 0.0000 | 0.0000 | 0.0000 | 0.0000 | 0.0025 | 0.2344 | 0.4232 | 0.7412 | 0.6765 | 0.9615 | 0.9884 | 0.8867 | 0.9967 |
| 20% | -15% | **78.09** | 0.0000 | 0.0000 | 0.0000 | 0.0000 | 0.0000 | 0.0000 | 0.0002 | 0.1111 | 0.3263 | 0.7437 | 0.9707 | 0.8432 | 0.9934 | 0.9977 | 0.9205 |
| | 0% | **85.02** | 0.0000 | 0.0000 | 0.0000 | 0.0000 | 0.0000 | 0.0000 | 0.0012 | 0.2142 | 0.4589 | 0.8225 | 0.9625 | 0.9521 | 0.9130 | 0.9931 | 0.9939 |
| | 15% | **80.09** | 0.0000 | 0.0000 | 0.0000 | 0.0000 | 0.0000 | 0.0000 | 0.0004 | 0.1413 | 0.3767 | 0.7839 | 0.9754 | 0.9021 | 0.9928 | 0.9981 | 0.9712 |
| 40% | -15% | **130.12** | 0.0000 | 0.0000 | 0.0000 | 0.0197 | 0.0420 | 0.0138 | 0.5807 | 0.9580 | 0.9224 | 0.6801 | 0.3569 | 0.0104 | 0.1639 | 0.1446 | 0.0482 |
| | 0% | **125.99** | 0.0000 | 0.0000 | 0.0000 | 0.0097 | 0.0233 | 0.0063 | 0.5037 | 0.9927 | 0.9447 | 0.7482 | 0.4778 | 0.0256 | 0.2653 | 0.2341 | 0.0998 |
| | 15% | **121.58** | 0.0000 | 0.0000 | 0.0000 | 0.0048 | 0.0133 | 0.0029 | 0.4608 | 0.7799 | 0.7886 | 0.6296 | 0.5203 | 0.0546 | 0.3544 | 0.3063 | 0.1773 |

## D.2.15 Inferior Lumbar and Sacral Endplate Full LAT Failure Load Maps

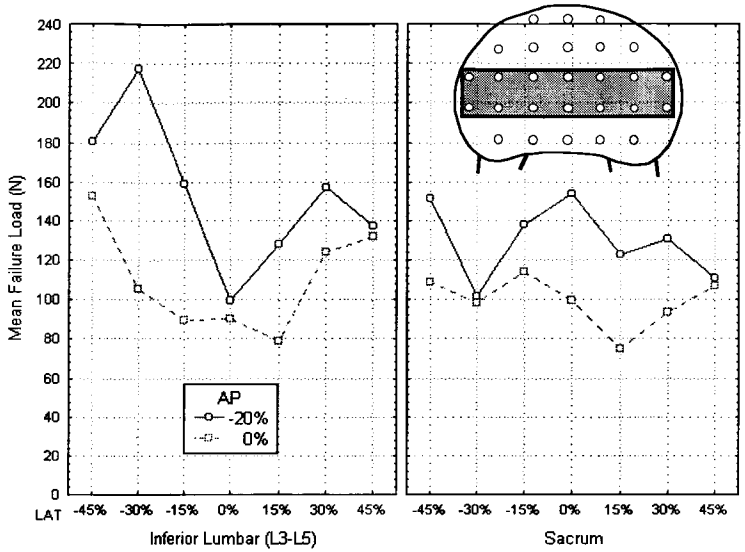


Figure D.33: Comparison of the AP, full LAT failure load distribution in the inferior lumbar and sacral endplates. The p-value of $< 0.0128$ indicates that the shapes of these two failure load maps are significantly different. The results of a *post hoc* Newman-Keuls comparison of these two maps is given in Table D.33.

Table D.33: Newman-Keuls *post hoc* comparison of the means in the inferior lumbar and sacral endplate full LAT failure load distributions (Figure D.33). The "within endplate" comparisons for the inferior lumbar and sacral endplate full LAT failure load maps can be found in Tables D.9 and D.15, respectively.

| sacrum | | AP | -20% | | | | | | | 0% | | | | | | |
|---|---|---|---|---|---|---|---|---|---|---|---|---|---|---|---|---|
| inferior L | | LAT | -45% | -30% | -15% | 0% | 15% | 30% | 45% | -45% | -30% | -15% | 0% | 15% | 30% | 45% |
| AP | LAT | Mean FL | **151.23** | **101.39** | **137.61** | **153.55** | **122.85** | **130.42** | **110.64** | **108.78** | **98.25** | **113.97** | **99.67** | **74.98** | **93.16** | **106.98** |
| -20% | -45% | **180.60** | 0.6990 | 0.0267 | 0.3564 | 0.5466 | 0.2100 | 0.3047 | 0.0636 | 0.0554 | 0.0216 | 0.0867 | 0.0246 | 0.0009 | 0.0109 | 0.0481 |
| | -30% | **217.20** | 0.0297 | 0.0002 | 0.0054 | 0.0216 | 0.0015 | 0.0033 | 0.0004 | 0.0003 | 0.0002 | 0.0005 | 0.0002 | 0.0002 | 0.0002 | 0.0003 |
| | -15% | **159.36** | 0.9945 | 0.3084 | 0.8908 | 0.9559 | 0.8123 | 0.8834 | 0.4924 | 0.4619 | 0.2760 | 0.5702 | 0.2978 | 0.0211 | 0.1741 | 0.4312 |
| | 0% | **99.78** | 0.4332 | 0.9369 | 0.8372 | 0.4122 | 0.9460 | 0.9110 | 0.9946 | 0.9919 | 0.9970 | 0.9922 | 0.9960 | 0.9224 | 0.9880 | 0.9846 |
| | 15% | **127.98** | 0.8604 | 0.9246 | 0.9895 | 0.9100 | 0.9654 | 0.9050 | 0.9122 | 0.9328 | 0.9444 | 0.9005 | 0.9451 | 0.4374 | 0.8807 | 0.9438 |
| | 30% | **156.92** | 0.9923 | 0.3577 | 0.8756 | 0.8689 | 0.8405 | 0.8934 | 0.5401 | 0.5122 | 0.3266 | 0.6141 | 0.3491 | 0.0283 | 0.2124 | 0.4833 |
| | 45% | **137.44** | 0.7765 | 0.8245 | 0.9934 | 0.9316 | 0.9790 | 0.9363 | 0.8876 | 0.8890 | 0.8284 | 0.9075 | 0.8388 | 0.2279 | 0.7062 | 0.8868 |
| 0% | -45% | **152.35** | 0.9563 | 0.4495 | 0.7491 | 0.9532 | 0.8720 | 0.8874 | 0.6128 | 0.5932 | 0.4260 | 0.6751 | 0.4481 | 0.0468 | 0.2939 | 0.5710 |
| | -30% | **105.63** | 0.5631 | 0.8357 | 0.9112 | 0.5522 | 0.9571 | 0.9486 | 0.9947 | 0.9869 | 0.9963 | 0.9939 | 0.9912 | 0.8831 | 0.9897 | 0.9473 |
| | -15% | **89.63** | 0.2482 | 0.9972 | 0.6613 | 0.2215 | 0.9111 | 0.8107 | 0.9935 | 0.9943 | 0.9741 | 0.9872 | 0.9876 | 0.7517 | 0.9835 | 0.9945 |
| | 0% | **90.07** | 0.2434 | 0.9934 | 0.6515 | 0.2185 | 0.8970 | 0.7975 | 0.9904 | 0.9909 | 0.9146 | 0.9828 | 0.9648 | 0.8792 | 0.8796 | 0.9905 |
| | 15% | **78.86** | 0.0786 | 0.9522 | 0.3243 | 0.0669 | 0.6538 | 0.4858 | 0.9147 | 0.9228 | 0.8740 | 0.8747 | 0.9078 | 0.8491 | 0.8950 | 0.9272 |
| | 30% | **124.02** | 0.8301 | 0.9512 | 0.9847 | 0.8714 | 0.9542 | 0.9468 | 0.9120 | 0.9435 | 0.9706 | 0.8740 | 0.9698 | 0.5442 | 0.9292 | 0.9589 |
| | 45% | **132.11** | 0.7825 | 0.9098 | 0.9604 | 0.8966 | 0.9909 | 0.9340 | 0.9379 | 0.9428 | 0.9190 | 0.9467 | 0.9238 | 0.3527 | 0.8346 | 0.9446 |

### D.2.16 Inferior Lumbar and Sacral Endplate Maximum AP, LAT Stiffness Maps

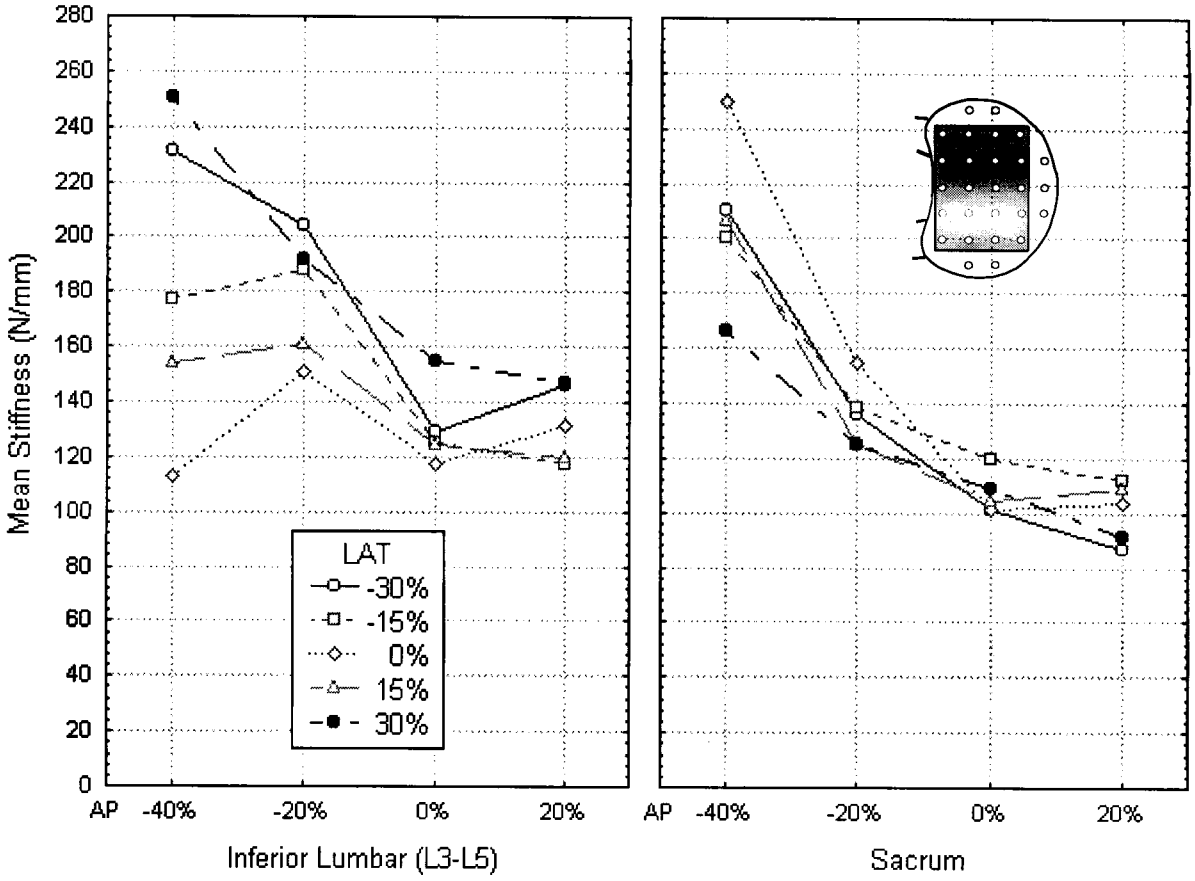


Figure D.34: Comparison of the maximum AP, LAT stiffness distribution in the inferior lumbar and sacral endplates. The p-value of $< 0.0017$ indicates that the shapes of the superior and inferior lumbar endplate stiffness maps are significantly different. The results of the Newman-Keuls *post hoc* comparison of these two graphs is given in Table D.34

Table D.34: Newman-Keuls *post hoc* comparison of the means in the inferior lumbar and sacral endplate maximum AP, LAT stiffness distributions (Figure D.34). The "within endplate" comparisons for the superior lumbar and sacral endplate maximum AP, LAT stiffness maps can be found in Tables D.10 and D.16, respectively.

| sacrum | | AP | -40% | | | | | -20% | | | | |
|---|---|---|---|---|---|---|---|---|---|---|---|---|
| inferior L | | LAT | -30% | -15% | 0% | 15% | 30% | -30% | -15% | 0% | 15% | 30% |
| AP | LAT | Mean ST | **210.39** | **200.58** | **249.59** | **206.81** | **166.67** | **136.50** | **138.36** | **154.37** | **125.21** | **125.44** |
| -40% | -30% | **231.30** | 0.3249 | 0.5976 | 0.3890 | 0.4813 | 0.0594 | 0.0011 | 0.0015 | 0.0154 | 0.0002 | 0.0002 |
| | -15% | **177.27** | 0.7082 | 0.6908 | 0.0191 | 0.7327 | 0.6178 | 0.7045 | 0.7147 | 0.8178 | 0.4763 | 0.4505 |
| | 0% | **112.80** | 0.0015 | 0.0086 | 0.0000 | 0.0029 | 0.5800 | 0.9941 | 0.9930 | 0.8894 | 0.9991 | 0.9996 |
| | 15% | **154.26** | 0.2555 | 0.4179 | 0.0006 | 0.3197 | 0.9774 | 0.9608 | 0.9449 | 0.9960 | 0.9371 | 0.9137 |
| | 30% | **250.51** | 0.2327 | 0.2199 | 0.9655 | 0.2386 | 0.0038 | 0.0001 | 0.0001 | 0.0005 | 0.0000 | 0.0000 |
| -20% | -30% | **203.98** | 0.9510 | 0.8728 | 0.2001 | 0.8943 | 0.4939 | 0.0950 | 0.1085 | 0.3201 | 0.0261 | 0.0246 |
| | -15% | **188.06** | 0.9003 | 0.8256 | 0.0731 | 0.9034 | 0.5724 | 0.3870 | 0.4061 | 0.6076 | 0.1865 | 0.1743 |
| | 0% | **150.90** | 0.2013 | 0.3632 | 0.0003 | 0.2613 | 0.9766 | 0.9612 | 0.9350 | 0.9854 | 0.9547 | 0.9326 |
| | 15% | **161.09** | 0.3289 | 0.4274 | 0.0016 | 0.3810 | 0.7928 | 0.9650 | 0.9629 | 0.9463 | 0.8994 | 0.8783 |
| | 30% | **191.57** | 0.9021 | 0.6713 | 0.0904 | 0.8902 | 0.6443 | 0.3143 | 0.3361 | 0.5809 | 0.1337 | 0.1254 |
| 0% | -30% | **129.45** | 0.0180 | 0.0635 | 0.0000 | 0.0299 | 0.8434 | 0.9410 | 0.9752 | 0.9621 | 0.9783 | 0.8503 |
| | -15% | **124.94** | 0.0105 | 0.0432 | 0.0000 | 0.0184 | 0.8191 | 0.9943 | 0.9958 | 0.9665 | 0.9896 | 0.9997 |
| | 0% | **117.79** | 0.0039 | 0.0199 | 0.0000 | 0.0073 | 0.7339 | 0.9986 | 0.9983 | 0.9532 | 0.9999 | 1.0000 |
| | 15% | **124.27** | 0.0101 | 0.0425 | 0.0000 | 0.0178 | 0.8278 | 0.9975 | 0.9979 | 0.9720 | 0.9989 | 0.9999 |
| | 30% | **154.77** | 0.2086 | 0.3193 | 0.0005 | 0.2569 | 0.8413 | 0.9894 | 0.9875 | 0.9847 | 0.9653 | 0.9531 |
| 20% | -30% | **146.03** | 0.1416 | 0.2975 | 0.0002 | 0.1944 | 0.9784 | 0.8950 | 0.7179 | 0.9950 | 0.9584 | 0.9276 |
| | -15% | **117.95** | 0.0037 | 0.0190 | 0.0000 | 0.0070 | 0.7145 | 0.9972 | 0.9970 | 0.9435 | 0.9994 | 0.9998 |
| | 0% | **131.14** | 0.0218 | 0.0726 | 0.0000 | 0.0355 | 0.8495 | 0.8006 | 0.9383 | 0.9583 | 0.9924 | 0.9611 |
| | 15% | **119.94** | 0.0048 | 0.0227 | 0.0000 | 0.0088 | 0.7267 | 0.9942 | 0.9946 | 0.9410 | 0.9946 | 0.9990 |
| | 30% | **146.59** | 0.1365 | 0.2799 | 0.0002 | 0.1859 | 0.9651 | 0.9646 | 0.9205 | 0.9832 | 0.9736 | 0.9550 |

| sacrum | | AP | 0% | | | | | 20% | | | | |
|---|---|---|---|---|---|---|---|---|---|---|---|---|
| inferior L | | LAT | -30% | -15% | 0% | 15% | 30% | -30% | -15% | 0% | 15% | 30% |
| AP | LAT | Mean ST | **101.72** | **119.76** | **101.63** | **104.28** | **108.86** | **86.30** | **111.89** | **103.85** | **109.12** | **91.16** |
| -40% | -30% | **231.30** | 0.0000 | 0.0001 | 0.0000 | 0.0000 | 0.0000 | 0.0000 | 0.0000 | 0.0000 | 0.0000 | 0.0000 |
| | -15% | **177.27** | 0.0833 | 0.3985 | 0.0869 | 0.1069 | 0.1832 | 0.0069 | 0.2323 | 0.1068 | 0.1783 | 0.0164 |
| | 0% | **112.80** | 0.9985 | 0.9879 | 0.9995 | 0.9945 | 0.9977 | 0.9645 | 0.9655 | 0.9983 | 0.9835 | 0.9842 |
| | 15% | **154.26** | 0.6749 | 0.9400 | 0.6927 | 0.7201 | 0.8373 | 0.2043 | 0.8721 | 0.7280 | 0.8239 | 0.3287 |
| | 30% | **250.51** | 0.0000 | 0.0000 | 0.0000 | 0.0000 | 0.0000 | 0.0000 | 0.0000 | 0.0000 | 0.0000 | 0.0000 |
| -20% | -30% | **203.98** | 0.0007 | 0.0143 | 0.0007 | 0.0011 | 0.0026 | 0.0000 | 0.0043 | 0.0010 | 0.0026 | 0.0001 |
| | -15% | **188.06** | 0.0148 | 0.1337 | 0.0155 | 0.0206 | 0.0420 | 0.0008 | 0.0590 | 0.0204 | 0.0409 | 0.0021 |
| | 0% | **150.90** | 0.7681 | 0.9634 | 0.7850 | 0.8038 | 0.8965 | 0.2823 | 0.9198 | 0.8120 | 0.8848 | 0.4267 |
| | 15% | **161.09** | 0.4784 | 0.8756 | 0.4934 | 0.5362 | 0.6861 | 0.0983 | 0.7460 | 0.5405 | 0.6732 | 0.1785 |
| | 30% | **191.57** | 0.0081 | 0.0900 | 0.0085 | 0.0116 | 0.0249 | 0.0004 | 0.0362 | 0.0115 | 0.0243 | 0.0010 |
| 0% | -30% | **129.45** | 0.9958 | 0.9993 | 0.9971 | 0.9962 | 0.9991 | 0.8732 | 0.9992 | 0.9972 | 0.9985 | 0.9435 |
| | -15% | **124.94** | 0.9971 | 0.9949 | 0.9982 | 0.9967 | 0.9991 | 0.9099 | 0.9987 | 0.9979 | 0.9981 | 0.9610 |
| | 0% | **117.79** | 0.9951 | 0.9953 | 0.9978 | 0.9883 | 0.9935 | 0.9258 | 0.9582 | 0.9948 | 0.9770 | 0.9633 |
| | 15% | **124.27** | 0.9961 | 0.9754 | 0.9977 | 0.9951 | 0.9984 | 0.9034 | 0.9973 | 0.9970 | 0.9966 | 0.9563 |
| | 30% | **154.77** | 0.6975 | 0.9593 | 0.7133 | 0.7459 | 0.8597 | 0.2130 | 0.8951 | 0.7515 | 0.8491 | 0.3429 |
| 20% | -30% | **146.03** | 0.8643 | 0.9783 | 0.8788 | 0.8855 | 0.9462 | 0.4078 | 0.9574 | 0.8938 | 0.9369 | 0.5658 |
| | -15% | **117.95** | 0.9977 | 0.9323 | 0.9990 | 0.9953 | 0.9982 | 0.9436 | 0.9919 | 0.9979 | 0.9937 | 0.9750 |
| | 0% | **131.14** | 0.9946 | 0.9995 | 0.9961 | 0.9954 | 0.9989 | 0.8516 | 0.9991 | 0.9965 | 0.9983 | 0.9319 |
| | 15% | **119.94** | 0.9988 | 0.9931 | 0.9994 | 0.9983 | 0.9996 | 0.9506 | 0.9990 | 0.9991 | 0.9987 | 0.9805 |
| | 30% | **146.59** | 0.8681 | 0.9834 | 0.8816 | 0.8910 | 0.9504 | 0.4070 | 0.9623 | 0.8981 | 0.9423 | 0.5670 |

## D.2.17 Inferior Lumbar and Sacral Endplate Full AP Stiffness Maps

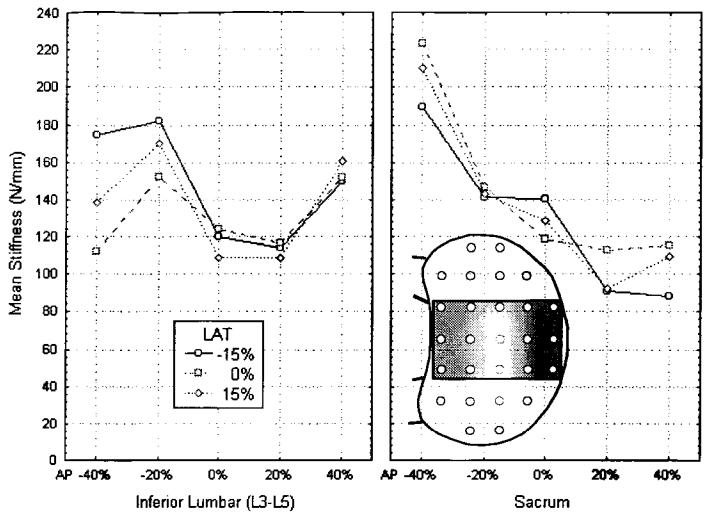


Figure D.35: Comparison of the full AP stiffness distribution in the inferior lumbar and sacral endplates. The p-value of < 0.2237 indicates that the shapes of the two maps are not significantly different. The *post hoc* comparison of the two maps is given in Table D.35.

Table D.35: Newman-Keuls *post hoc* comparison of the means in the inferior lumbar and sacral endplate maximum full AP stiffness distributions (Figure D.35). The "within endplate" comparisons for the inferior lumbar and sacral endplate full AP stiffness maps can be found in Tables D.11 and D.17, respectively.

| sacrum | | AP | -40% | | | -20% | | | 0% | | | 20% | | | 40% | | |
|---|---|---|---|---|---|---|---|---|---|---|---|---|---|---|---|---|---|
| inferior L | | LAT | -15% | 0% | 15% | -15% | 0% | 15% | -15% | 0% | 15% | -15% | 0% | 15% | -15% | 0% | 15% |
| AP | LAT | Mean ST | **189.81** | **223.72** | **210.21** | **141.08** | **146.49** | **143.29** | **140.43** | **118.89** | **128.86** | **90.88** | **112.39** | **92.46** | **88.08** | **115.23** | **109.11** |
| -40% | -15% | **174.58** | 0.7102 | 0.0812 | 0.2525 | 0.7252 | 0.7718 | 0.7386 | 0.7556 | 0.2041 | 0.4289 | 0.0037 | 0.1225 | 0.0049 | 0.0022 | 0.1533 | 0.0879 |
| | 0% | **111.86** | 0.0101 | 0.0000 | 0.0001 | 0.9376 | 0.8801 | 0.9218 | 0.9270 | 0.9992 | 0.9940 | 0.8870 | 0.9782 | 0.8534 | 0.8822 | 0.9981 | 0.8867 |
| | 15% | **138.25** | 0.2695 | 0.0009 | 0.0141 | 0.9883 | 0.9931 | 0.9938 | 0.9103 | 0.8544 | 0.6268 | 0.4750 | 0.9197 | 0.5018 | 0.4002 | 0.8974 | 0.9174 |
| -20% | -15% | **182.65** | 0.7108 | 0.1447 | 0.3270 | 0.4903 | 0.5703 | 0.5170 | 0.5152 | 0.0737 | 0.2093 | 0.0006 | 0.0366 | 0.0008 | 0.0003 | 0.0498 | 0.0238 |
| | 0% | **152.75** | 0.3905 | 0.0058 | 0.0463 | 0.9908 | 0.9882 | 0.9884 | 0.9956 | 0.8434 | 0.9485 | 0.1597 | 0.7724 | 0.1845 | 0.1146 | 0.8032 | 0.7132 |
| | 15% | **170.13** | 0.7386 | 0.0617 | 0.2311 | 0.8054 | 0.8251 | 0.8077 | 0.8378 | 0.3067 | 0.5506 | 0.0090 | 0.2050 | 0.0115 | 0.0054 | 0.2448 | 0.1557 |
| 0% | -15% | **119.88** | 0.0262 | 0.0000 | 0.0004 | 0.8828 | 0.8679 | 0.8899 | 0.8252 | 0.9590 | 0.8878 | 0.9405 | 0.9989 | 0.9438 | 0.9153 | 0.9951 | 0.9993 |
| | 0% | **124.26** | 0.0496 | 0.0001 | 0.0010 | 0.9077 | 0.9122 | 0.9227 | 0.8367 | 0.9583 | 0.8116 | 0.8835 | 0.9964 | 0.8919 | 0.8415 | 0.9902 | 0.9973 |
| | 15% | **108.83** | 0.0068 | 0.0000 | 0.0001 | 0.9424 | 0.8742 | 0.9224 | 0.9369 | 0.9999 | 0.9969 | 0.6216 | 0.9997 | 0.3967 | 0.7054 | 0.9999 | 0.9999 |
| 20% | -15% | **114.27** | 0.0137 | 0.0000 | 0.0002 | 0.9313 | 0.8830 | 0.9195 | 0.9146 | 0.9952 | 0.9889 | 0.9289 | 0.9225 | 0.9193 | 0.9141 | 0.9605 | 0.9933 |
| | 0% | **116.93** | 0.0188 | 0.0000 | 0.0002 | 0.9168 | 0.8804 | 0.9110 | 0.8880 | 0.9191 | 0.9723 | 0.9421 | 0.9954 | 0.9409 | 0.9225 | 0.9298 | 0.9986 |
| | 15% | **108.86** | 0.0063 | 0.0000 | 0.0001 | 0.9272 | 0.8534 | 0.9054 | 0.9193 | 0.9996 | 0.9945 | 0.7882 | 0.9978 | 0.6725 | 0.8192 | 0.9995 | 0.9897 |
| 40% | -15% | **149.74** | 0.4318 | 0.0050 | 0.0459 | 0.9699 | 0.8660 | 0.9404 | 0.9890 | 0.8500 | 0.9338 | 0.2065 | 0.8081 | 0.2337 | 0.1534 | 0.8256 | 0.7631 |
| | 0% | **152.08** | 0.4449 | 0.0065 | 0.0533 | 0.9795 | 0.9548 | 0.9687 | 0.9909 | 0.8266 | 0.9316 | 0.1633 | 0.7650 | 0.1876 | 0.1181 | 0.7913 | 0.7098 |
| | 15% | **160.49** | 0.5510 | 0.0184 | 0.1037 | 0.9530 | 0.9507 | 0.9489 | 0.9686 | 0.6253 | 0.8298 | 0.0519 | 0.5089 | 0.0629 | 0.0342 | 0.5576 | 0.4338 |

## D.2.18 Inferior Lumbar and Sacral Endplate Full LAT Stiffness Maps

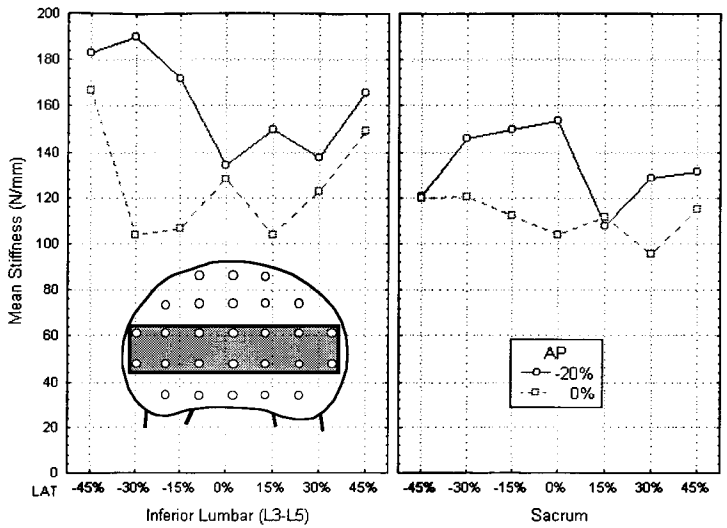


Figure D.36: Comparison of the full LAT stiffness distribution in the inferior lumbar and sacral lumbar endplates. The p-value of < 0.4778 indicates that there are no significant shape differences between the inferior lumbar and sacral lumbar endplate stiffness maps. The *post hoc* Newman-Keuls comparison of the two maps is given in Table D.36.

Table D.36: Newman-Keuls *post hoc* comparison of the means in the inferior lumbar and sacral endplate maximum full LAT stiffness distributions (Figure D.36). The "within endplate" comparisons for the inferior lumbar and sacral endplate full LAT stiffness maps can be found in Tables D.12 and D.18, respectively.

| sacrum | | AP | -20% | | | | | | | 0% | | | | | | |
|---|---|---|---|---|---|---|---|---|---|---|---|---|---|---|---|---|
| inferior L | | LAT | -45% | -30% | -15% | 0% | 15% | 30% | 45% | -45% | -30% | -15% | 0% | 15% | 30% | 45% |
| AP | LAT | Mean ST | **120.38** | **145.60** | **149.89** | **153.85** | **107.92** | **129.01** | **131.23** | **119.85** | **120.29** | **112.35** | **103.66** | **111.45** | **95.77** | **114.77** |
| -20% | -45% | **182.90** | 0.6218 | 0.9028 | 0.8269 | 0.8206 | 0.4449 | 0.7371 | 0.7516 | 0.6634 | 0.6481 | 0.5167 | 0.4082 | 0.5154 | 0.2496 | 0.5565 |
| | -30% | **190.33** | 0.4588 | 0.8184 | 0.7490 | 0.7589 | 0.2910 | 0.5890 | 0.6098 | 0.4953 | 0.4822 | 0.3538 | 0.2583 | 0.3512 | 0.1437 | 0.3908 |
| | -15% | **172.02** | 0.8419 | 0.9765 | 0.9248 | 0.9081 | 0.7064 | 0.9076 | 0.9129 | 0.8744 | 0.8624 | 0.7685 | 0.6756 | 0.7694 | 0.4844 | 0.7996 |
| | 0% | **134.19** | 0.9957 | 0.9073 | 0.9921 | 0.9906 | 0.9979 | 0.9802 | 0.9136 | 0.9995 | 0.9986 | 0.9983 | 0.9988 | 0.9989 | 0.9906 | 0.9984 |
| | 15% | **149.73** | 0.9847 | 0.9874 | 0.9957 | 0.9875 | 0.9725 | 0.9875 | 0.9833 | 0.9935 | 0.9906 | 0.9810 | 0.9730 | 0.9831 | 0.9069 | 0.9845 |
| | 30% | **137.65** | 0.9953 | 0.7705 | 0.9913 | 0.9909 | 0.9962 | 0.9888 | 0.9697 | 0.9992 | 0.9982 | 0.9972 | 0.9975 | 0.9980 | 0.9833 | 0.9975 |
| | 45% | **165.90** | 0.8956 | 0.9749 | 0.8260 | 0.6586 | 0.8053 | 0.9345 | 0.9339 | 0.9257 | 0.9145 | 0.8509 | 0.7879 | 0.8541 | 0.6111 | 0.8725 |
| 0% | -45% | **166.94** | 0.9017 | 0.9855 | 0.9224 | 0.8797 | 0.8030 | 0.9442 | 0.9459 | 0.9282 | 0.9185 | 0.8514 | 0.7813 | 0.8534 | 0.6017 | 0.8744 |
| | -30% | **104.06** | 0.9996 | 0.9740 | 0.9685 | 0.9449 | 0.9890 | 0.9987 | 0.9984 | 0.9971 | 0.9988 | 0.9981 | 0.9999 | 0.9929 | 0.9901 | 0.9988 |
| | -15% | **106.41** | 0.9996 | 0.9793 | 0.9761 | 0.9570 | 0.9560 | 0.9989 | 0.9987 | 0.9962 | 0.9986 | 0.9963 | 0.9997 | 0.9812 | 0.9949 | 0.9980 |
| | 0% | **127.93** | 0.9583 | 0.9865 | 0.9962 | 0.9937 | 0.9981 | 0.9684 | 0.9920 | 0.9983 | 0.9922 | 0.9974 | 0.9995 | 0.9987 | 0.9951 | 0.9966 |
| | 15% | **103.94** | 0.9998 | 0.9794 | 0.9737 | 0.9522 | 0.9989 | 0.9993 | 0.9990 | 0.9990 | 0.9996 | 0.9996 | 0.9920 | 0.9987 | 0.9514 | 0.9997 |
| | 30% | **122.93** | 0.9254 | 0.9802 | 0.9916 | 0.9864 | 0.9993 | 0.9728 | 0.9900 | 0.9995 | 0.9949 | 0.9988 | 0.9999 | 0.9996 | 0.9984 | 0.9982 |
| | 45% | **148.95** | 0.9786 | 0.9023 | 0.9994 | 0.9979 | 0.9695 | 0.9768 | 0.9655 | 0.9914 | 0.9871 | 0.9777 | 0.9718 | 0.9806 | 0.9053 | 0.9811 |